PB-235 841

WORKBOOK OF THERMAL PLUME PREDICTION. VOLUME 2. SURFACE DISCHARGE

Mostafa A. Shirazi, et al

Pacific Northwest Environmental Research
Laboratory
Corvallis, Oregon

May 1974

DISTRIBUTED BY:

NTIS
National Technical Information Service
U. S. DEPARTMENT OF COMMERCE

RESEARCH REPORTING SERIES

Research reports of the Office of Research and Monitoring, Environmental Protection Agency, have been grouped into five series. These five broad categories were established to facilitate further development and application of environmental technology. Elimination of traditional grouping was consciously planned to foster technology transfer and a maximum interface in related fields. The five series are:

1. Environmental Health Effects Research
2. Environmental Protection Technology
3. Ecological Research
4. Environmental Monitoring
5. Socioeconomic Environmental Studies

This report has been assigned to the ENVIRONMENTAL PROTECTION TECHNOLOGY series. This series describes research performed to develop and demonstrate instrumentation, equipment and methodology to repair or prevent environmental degradation from point and non-point sources of pollution. This work provides the new or improved technology required for the control and treatment of pollution sources to meet environmental quality standards.

√

SELECTED WATER RESOURCES ABSTRACTS

INPUT TRANSACTION FORM

[redacted]

PB 235 841

W74-12212

[redacted]

4. Title Workbook of Thermal Plume Prediction, Volume 2, Surface Discharges,

7. Author(s) ~~Dr.~~ Mostafa A. Shirazi
~~Dr.~~ Lorin R. Davis

9. Organization Environmental Protection Agency
~~Thermal Pollution Branch~~, Pacific Northwest Environmental Research Laboratory. ~~NERC~~ Corvallis, Oregon,

10. Project No. EPA Project 16130 FHH,

~~11. Contract/Grant~~ No. Program Element 1BA032,

[redacted]

15. Supplementary Notes

Environmental Protection Agency, Technology Series report ~~number~~, EPA-R2-72-005b, May 1974
430p, 8 fig, 8 tab, 3 ref, 6 append.

16. Abstract In a continuing effort to present current knowledge on heated plume prediction ~~to the public~~, nomograms are presented ~~in this second volume~~ that describe the behavior of surface jets for a wide range of ambient and initial discharge conditions encountered in practice. An attempt is made to present the material in a concise manner and in a format that is clear and accessible to a nonspecialist user. Many fundamental derivations are ~~left outside the body of the workbook and~~ retained for further reading in the appendix. These undoubtedly would be of use to the specialist researcher. ~~who seeks to advance the status of knowledge.~~

The nomograms provide qualitative results describing the surface plume trajectory, width, temperature, depth, surface area and time of travel along the plume centerline. The nomograms are not intended to be used as exclusive design tools for surface discharge problems nor for use in a precise prediction of any specific surface plume condition.

The nomograms are generated predominately from an idealized mathematical model of a plume. Some field and laboratory data have been used to adjust the performance of the model so that more realistic predcitions are obtained. However, the class of problems that can be handled this way are limited due to the limitations in the model itself. ~~We have made an earnest attempt to help the nonspecialist user by pointing out~~ the main restrictions included in the model, both in a special chapter ~~in the workbook as well as~~ in example problems. (See also W74-05111) (EPA) Src

17a. Descriptors
are described
*Thermal Pollution, *Discharge (Water), Water Quality, Water Quality Control, Water Pollution, Water Pollution Control, Surface Waters, *Forecasting

17b. Identifiers
*Surface Discharge, *Thermal Plumes

C[illegible] GPO Sup Doc
as EP1.23/2:72-005b, $ ~~4.45~~ 8.05
microfiche from NTIS as PB
$ 2.25

17c. COWRR Field & Group ~~Field~~ 05B, ~~Group~~ 5G

18. Availability 441P

[redacted]

Send To:

WATER RESOURCES SCIENTIFIC INFORMATION CENTER
U.S. DEPARTMENT OF THE INTERIOR
WASHINGTON, D. C. 20240

Abstractor Lorin R. Davis | *Institution*

WRSIC 102 (REV. JUNE 1971)

i

Reproduced by
NATIONAL TECHNICAL
INFORMATION SERVICE
U.S. Department of Commerce
Springfield VA 22151

EPA-R2-72-005b
May 1974

WORKBOOK OF THERMAL PLUME PREDICTION

Volume 2

SURFACE DISCHARGE

By

Mostafa A. Shirazi
Lorin R. Davis
Thermal Pollution Branch
Pacific Northwest Environmental Research Laboratory

Project 16130 FHH
Program Element 1BA032

NATIONAL ENVIRONMENTAL RESEARCH CENTER
OFFICE OF RESEARCH AND DEVELOPMENT
U.S. ENVIRONMENTAL PROTECTION AGENCY
CORVALLIS, OREGON 97330

For sale by the Superintendent of Documents, U.S. Government Printing Office, Washington, D.C. 20402 - Price $4.75

441

PREFACE

In a continuing effort to present current knowledge on heated plume prediction to the public, nomograms are presented in this second volume that describe the behavior of surface jets for a wide range of ambient and initial discharge conditions encountered in practice. As in the first volume, an attempt is made to present the material in a concise manner and in a format that is clear and accessible to a nonspecialist user. Many fundamental derivations are left outside the body of the workbook and retained for further reading in the appendix. These undoubtedly would be of use to the specialist researcher who seeks to advance the status of knowledge.

The nomograms provide qualitative results describing the surface plume trajectory, width, temperature, depth, surface area and time of travel along the plume centerline. The nomograms are not intended to be used as exclusive design tools for surface discharge problems nor for use in a precise prediction of any specific surface plume condition.

The nomograms are generated predominately from an idealized mathematical model of a plume. Some field and laboratory data have been used to adjust the performance of the model so that more realistic predictions are obtained. However, the class of problems that can be handled this way are limited due to the limitations in the model itself. We have made an earnest attempt to help the nonspecialist user by pointing out the main restrictions included in the model both in a special chapter in the workbook as well as in example problems.

CONTENTS

Page

Preface iii
List of Symbols and Dimensionless Numbers v - vii
List of Figures viii
List of Tables ix

Sections

I Introduction 1-14

II Nomogram Organization 15
A - (TTWD) Working Nomograms 16-17
B - (TA) Working Nomograms 18
C - (Tt) Working Nomograms 18-20
D - (TTWD) Supplementary Nomograms 20-22

III Analytical Considerations 23
A - Model Description 23
1. Model Idealization 24-25
2. Other Limitations 25-28
B - Model Applicability 28-29

IV Example Problems 30

V Acknowledgement 42

VI References 43

VII Appendices
A - (TTWD) Working Nomograms 44-177
B - (TA) Working Nomograms 178-251
C - (Tt) Working Nomograms 252-325
D - (TTWD) Supplementary Nomograms 326-354
E - Temperature Density Nomograms and Computational Aids 355-365
F - Further Analytical Considerations and Computer Program 366-430

SYMBOLS

$A = \frac{2B_o}{H_o} = \frac{W_o}{H_o}$	Channel (or jet) aspect ration
B	Characteristic (half) plume width = $\sqrt{2}\,\sigma_n$
$2B_o$	Channel (or jet) full width
C_p	Specific heat of water
D/H_o	Dimensionless plume depth = $\sqrt{2}\ H/H_o$
E, or E_o	Jet entrainment coefficient
E_h, E_v	Horizontal and vertical turbulent exchange coefficients
F	Jet densimetric Froude number, $U_o/ (\frac{\Delta\rho}{\rho_o} gH_o)^{1/2}$
g	Acceleration of gravity
H	Characteristic plume depth = $\sqrt{2}\,\sigma_z$
H_o	Channel (or jet) depth
K	Dimensionless surface heat exchange coefficient $K_E/\rho C_p U_o$
K_E	Absolute surface heat exchange coefficient commonly given in $\frac{\text{Btu}}{\text{Ft}^2\text{-day}}\ ^\circ\text{F}$,
R	U_a/U_o, ambient to jet velocity ratio
S	Length along plume centerline trajectory
$T = \Delta T_c/\Delta T_o$	Dimensionless excess centerline temperature ratio

T_a	Ambient temperature
(TA)	(Temperature, Area) Nomogram
$T_c = T_s$	Surface tmperature on centerline
T_o	Jet temperature
$TH = \Theta_o$	Initial discharge angle
(Tt)	(Temperature, time) nomogram
(TTWD)	(Temperature, Trajectory, Width, Depth) Nomogram
$U_a = V$	Ambient velocity
U_o	Jet velocity
W	Dimensionless plume full width = $2\sqrt{2}\ B/H_o$
W_o	Channel full width = $2\ B_o$
X	Longitudinal coordinate of plume centerline - along the shoreline or direction of the uniform ambient current
Y	Lateral coordinate of plume centerline - perpendicular to the shoreline or direction of the uniform ambient current
Θ_o	Angle of jet discharge with respect to ambient current expressed in degrees and measured relative to the direction of ambient current
ΔT_c	Centerline excess temperature = $T_c - T_a = T_s - T_a$

ΔT_o	Discharge excess temperature = $T_o - T_a$
$\Delta\rho$	$\rho_a - \rho_o$
ν	Kinematic viscosity
ρ_a	Ambient water density
ρ_o	Jet discharge density
σ_n	Standard deviation of horizontal temperature distribution at surface
σ_z	Standard deviation of vertical temperature distribution on plume centerline

FIGURES

No.		Page
1	Plume Trajectory for Surface Jet Showing Effects of Ambient Current.	4
2	Plume Trajectory for Surface Jet Showing Effects of Jet Densimetric Froude Number.	6
3	Plume Trajectory for Surface Jet Showing Effects of Jet Aspect Ratio.	7
4	Plume Trajectory for Surface Jet Showing Effects of Discharge Angle.	8
5	Plume Trajectory, Temperature, Width and Depth for Surface Jet Showing Effects of Ambient Current.	10
6	Plume Trajectory, Temperature, Width and Depth for Surface Jet Showing Effects of Jet Densimetric Froude Number.	11
7	Plume Trajectory, Temperature, Width and Depth for Surface Jet Showing Effects of Jet Aspect Ratio.	13
8	Plume Trajectory, Temperature, Width and Depth for Surface Jet Showing Effects of Discharge Angle.	14

TABLES

Table — Page

1 Figure numbers for (TTWD) working Nomograms of Appendix A, $\Theta_o = 90°$ and $K = 10^{-5}$ — 17 & 45

2 Summary of Figure Numbers for (TTWD) Working Nomograms of Appendix A — 17 & 45

3 Figure Numbers for (TA) Working Nomograms of Appendix B, $\Theta_o = 90°$, $K = 10^{-5}$ — 19 & 179

4 Summary of Figure Numbers for (TA) Working Nomograms of Appendix B — 19 & 179

5 Figure Numbers for (Tt) Working Nomograms of Appendix C, $\Theta_o = 90°$, $K = 10^{-5}$ — 21 & 253

6 Summary of Figure Numbers for (Tt) Working Nomograms of Appendix C — 21 & 253

7 Figure Numbers for (TTWD) Supplementary Nomograms of Appendix D, $\Theta_o = 90°$, $K = 10^{-5}$, $F = 4$, $A = 5$ — 22 & 327

8 Summary of Figure Numbers for (TTWD) Supplementary Nomograms of Appendix D — 22 & 327

I. INTRODUCTION

The surface discharge of heated water is often chosen over the submerged discharge because it affects a greater rate of heat transfer to the atmosphere due to normally higher surface temperatures and it is more economical due to the relatively simple discharge structure.

The specific plume behavior from a surface discharge is a result of a complex interaction of such factors as (a) the jet discharge characteristics, (b) the ambient water current and turbulence level, (c) the atmospheric conditions, and (d) the bottom and shoreline geometries. Since the precise effects of all factors and their mutual interaction on a plume in a natural environment are not well understood, only solutions to idealized situations can be obtained. Briefly, solutions presented in this workbook are limited to a uniform and constant (steady) surface discharge of heated water from a rectangular channel into a large and deep body of water that is either at rest or moving at a uniform and constant velocity. Details of these and other limitations are given in Section II and in Appendix F which the reader is urged to review before using the results.

Meanwhile, we will give an overview of the material in the workbook with the objective to familiarize the prospective user with (a) the manner with which the plume characteristics are presented and (b) the physical interpretation of the results.

The plume characteristics in this book are presented for several values each of the initial jet discharge, ambient flow, and atmospheric conditions. However, for the sake of convenience let us limit our attention in this introductory section to only a few of the physical factors involved. These are: the jet velocity, U_o; the jet temperature, T_o (or density, ρ_o); the jet depth, H_o; the jet half width, B_o; the ambient velocity, U_a; and the ambient temperature T_a (or density, ρ_a).

Since information on all four plume characteristics, namely, trajectory, centerline temperature, plume width and plume depth is needed, plots of these characteristics must be presented for each variation in U_o, T_o, H_o, B_o, U_a, and T_a. Clearly, a handbook containing such expanded information is difficult to use and a modest number of parametric representations of the above information may run into several thousand pages. Considerations of other factors such as angle of discharge (Θ_o), ambient turbulence, etc., would add considerably more pages to the book. However, by using appropriate dimensionless numbers and by combining information on all four plume characteristics on a single plot, it becomes possible to present the same material in less than two hundred pages.

The six parameters U_o, T_o, H_o, B_o, U_a and T_a can all be collected in three dimensionless numbers defined by $R = U_a/U_o$ for the velocity ratio, $A = 2B_o/H_o$ for the channel aspect ratio, and $F = U_o/\sqrt{\Delta\rho/\rho_o H_o g}$ for the jet densimetric Froude number. Note that the water densities ρ_a and ρ_o (with $\Delta\rho = \rho_a - \rho_o$) are related to the temperature T_a and T_o respectively, and g denotes the acceleration of gravity.

The jet densimetric Froude number represents the relative strength of two forces imparted initially to the discharged water, one due to the combined water mass and its initial velocity (inertia forces) and the other due to the initial density difference of the discharged water volume with respect to the ambient (buoyancy forces).

Consider as a first example the plots shown in Figure 1 for F=4, A=5 representing a surface discharge at ninety degrees into an ambient current. The plots are made for a typical dimensionless surface heat exchange coefficient K. Its value will be kept constant for all calculations given in this chapter. The curves marked R=0.01, 0.05, 0.1, ... etc., are the spatial coordinates (also called trajectories) of the plume centerlines whose initial jet discharge velocities (U_0) are, respectively, one hundred times, twenty times, ten times, ... etc., the ambient current velocities. The trajectory of the plume initially discharging into a zero ambient current (i.e., R=0) is coincident with the ordinate (Y) of the plot. Note also that both coordinates (X and Y) are presented in terms of dimensionless numbers, consistent with other uses in the plot.

The important physical observation drawn from Figure 1 is that plume penetration across a weak ambient current, say on the order of 5 to 10 percent of the initial jet velocity, is substantial. However, plume penetration is inhibited considerably by an incremental relative increase in the ambient current. A more specific observation related to those just mentioned is that the plume trajectory bends over more sharply in a strong ambient current than in a weak current. The cross current momentum of the jet, while initially at a maximum, is forced by the strong ambient current to change direction rapidly thus causing a relatively small initial plume penetration. At some distance from the source the plume is eventually carried along the general direction of the ambient current even if the latter is small.

Figure 1 shows plume trajectories for only the stated initial jet flow characteristics, namely for F=4 and A=5. In general, the degree of penetration depends upon the magnitude and the distribution of the initial plume momentum in the cross current direction as well as on the momentum of the ambient flow field. Since the initial

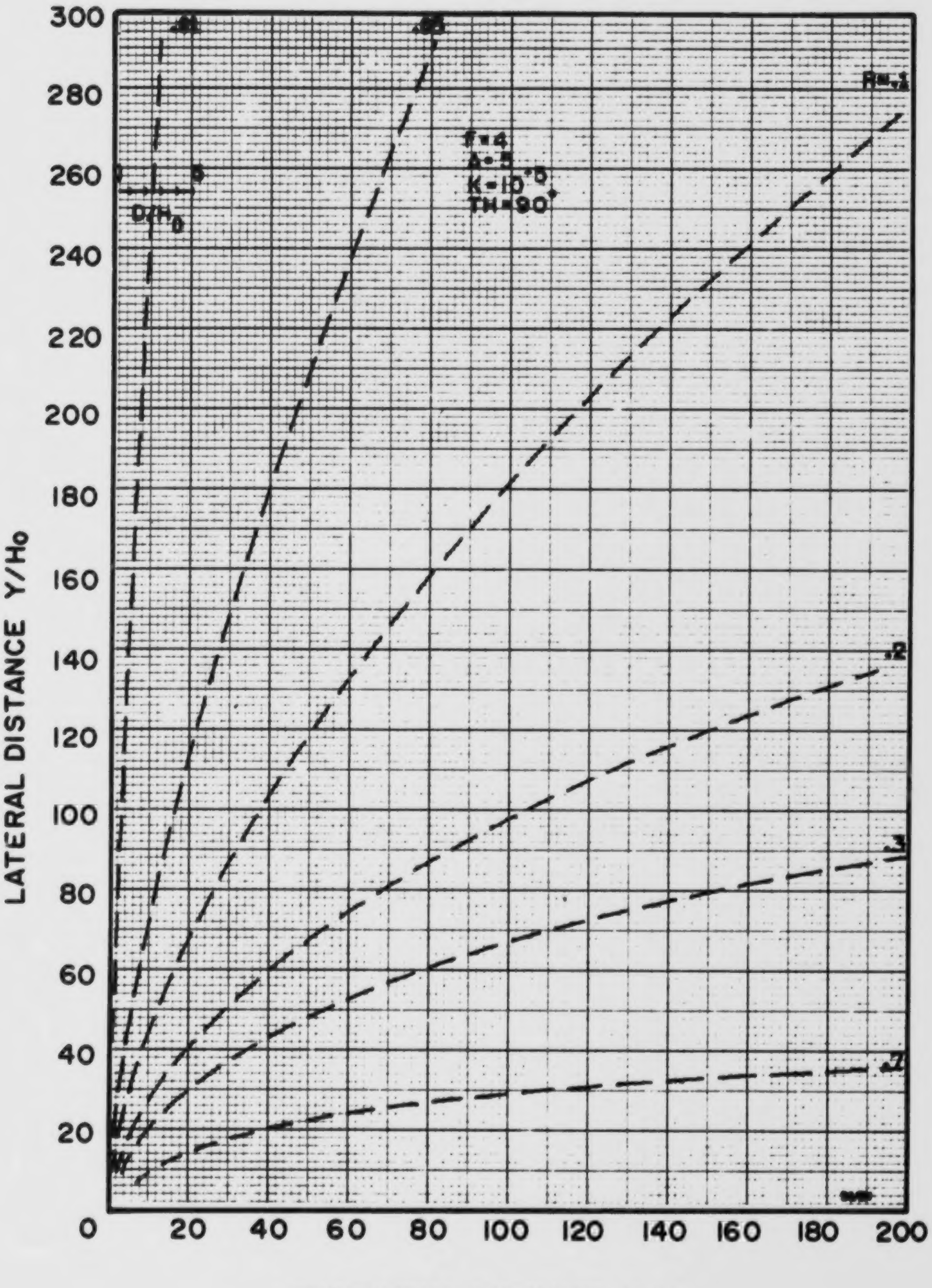

Figure 1 Plume Trajectory for Surface Jet Showing Effects of Ambient Current.

magnitude and distribution of jet momentum depend on A, F, and Θ_0, it follows, therefore, that the degree of plume penetration across the current and thus the trend shown in the above figure is modified with changes in these factors. These trends are shown in Figures 2, 3 and 4 as discussed below.

In Figure 2 the Froude number is varied while other parameters are held constant. The trajectories show a substantial influence of the jet discharge Froude number on plume penetration. The plume penetration across ambient current is greater for small Froude numbers than with large ones.

A physical explanation for this phenomenon can be attempted by reasoning that (a) the buoyancy force adds cross current momentum to the initial inertia forces thus providing a forward driving force in that direction, and (b) the same buoyancy forces cause the plume to float on top of the cooler ambient water and to "thin out" vertically thereby reducing jet-current interaction and increasing plume penetration. In this particular case penetration was further enhanced because the jet is initially five times as wide as it is deep. For larger channel aspect ratios, we should expect even less interaction with the cross current and a greater plume penetration, as shown by the plots in Figure 3. Conversely, for a small aspect ratio where the plume tends to block the flow of the ambient water, the interaction is large and the plume penetration is small.

The effects of the initial discharge angle on plume trajectory for F = 6, A = 10, and R = 0.1 are shown in Figure 4. The results support the common intuition that a plume with a shallow initial discharge angle, say 60 degrees, does not penetrate as effectively into an ambient current as one with an angle of 90 or 120 degrees.

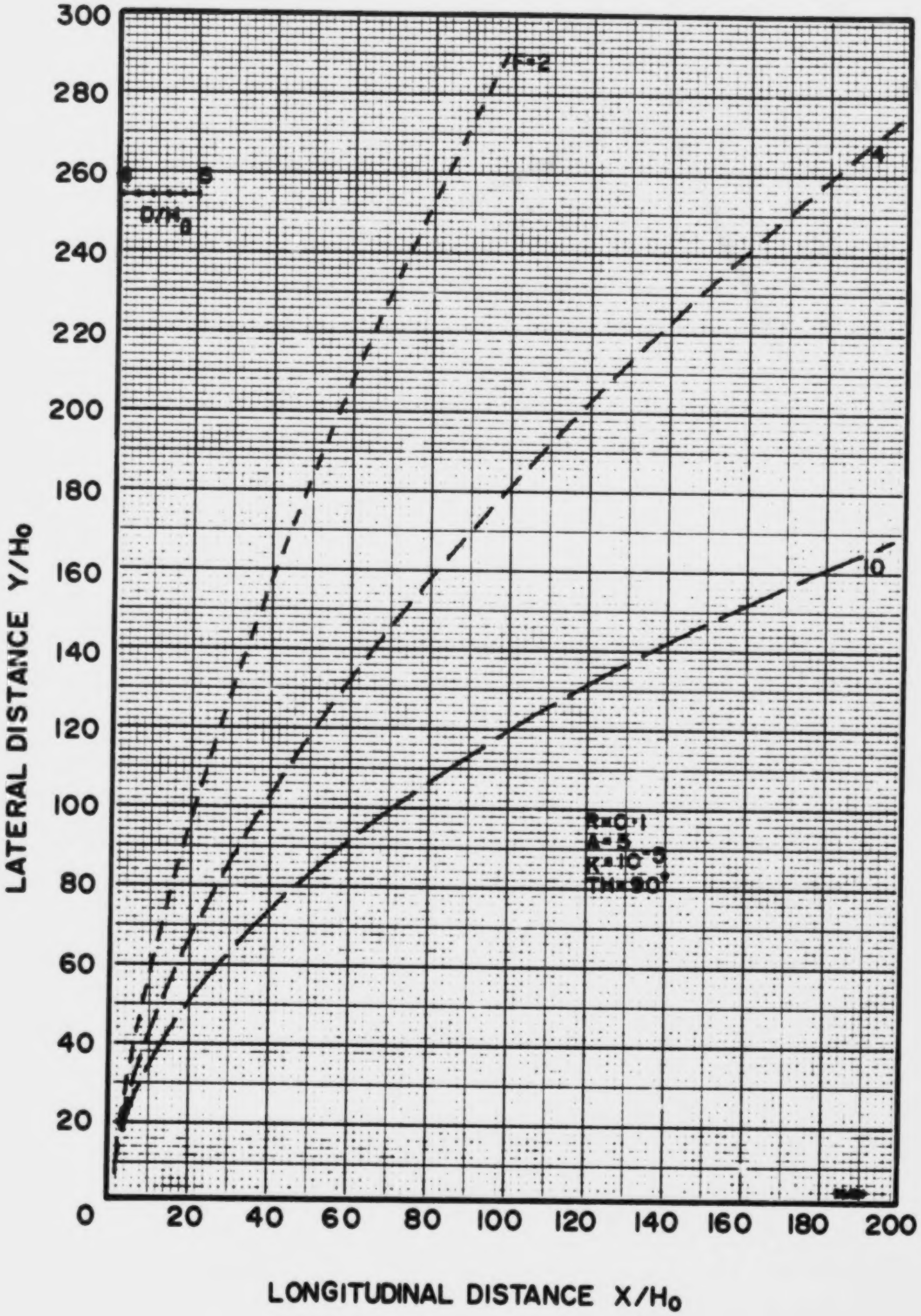

Figure 2 Plume Trajectory for Surface Jet Showing Effects of Jet Densimetric Froude Number.

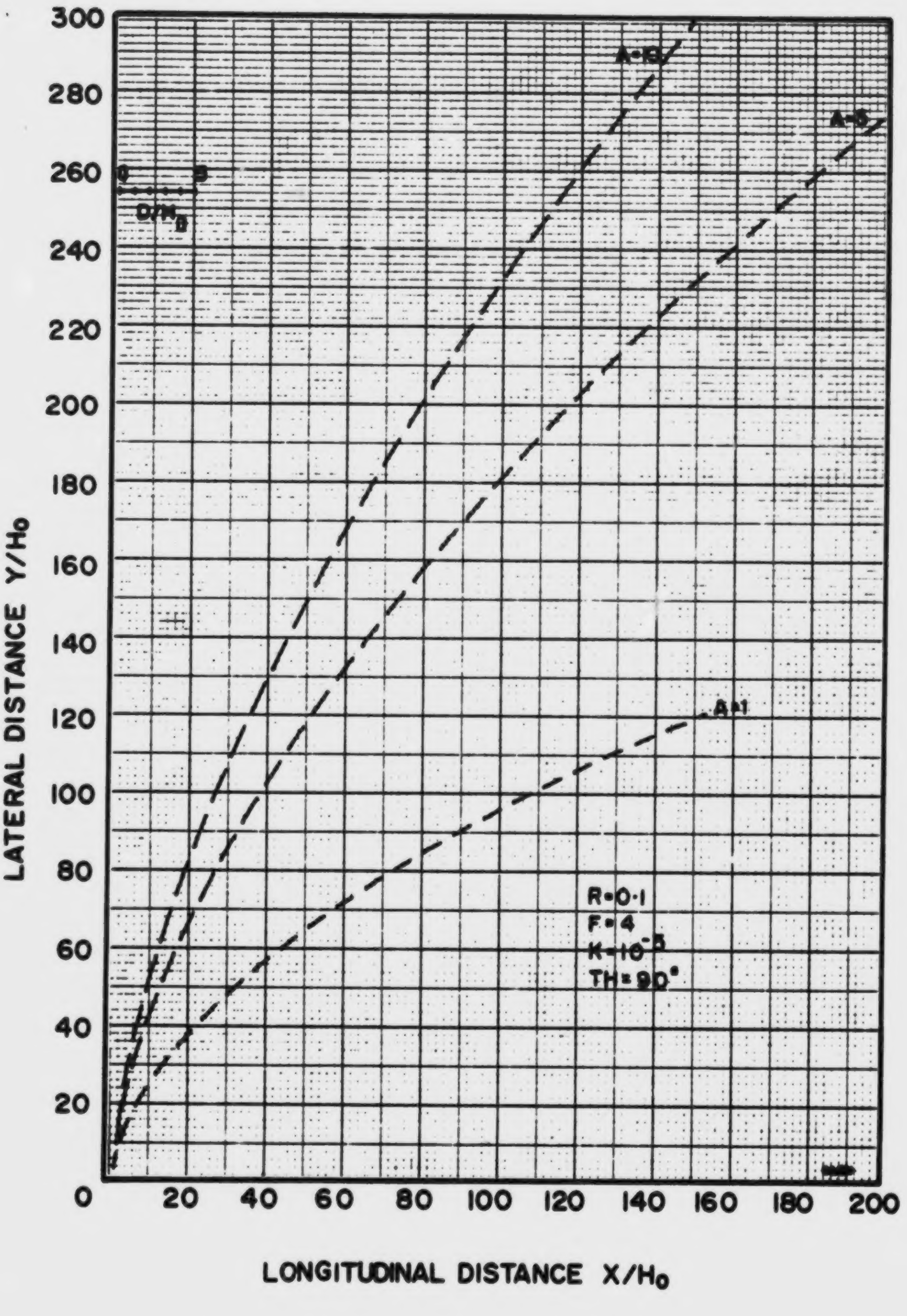

Figure 3 Plume Trajectory for Surface Jet Showing Effects of Jet Aspect Ratio.

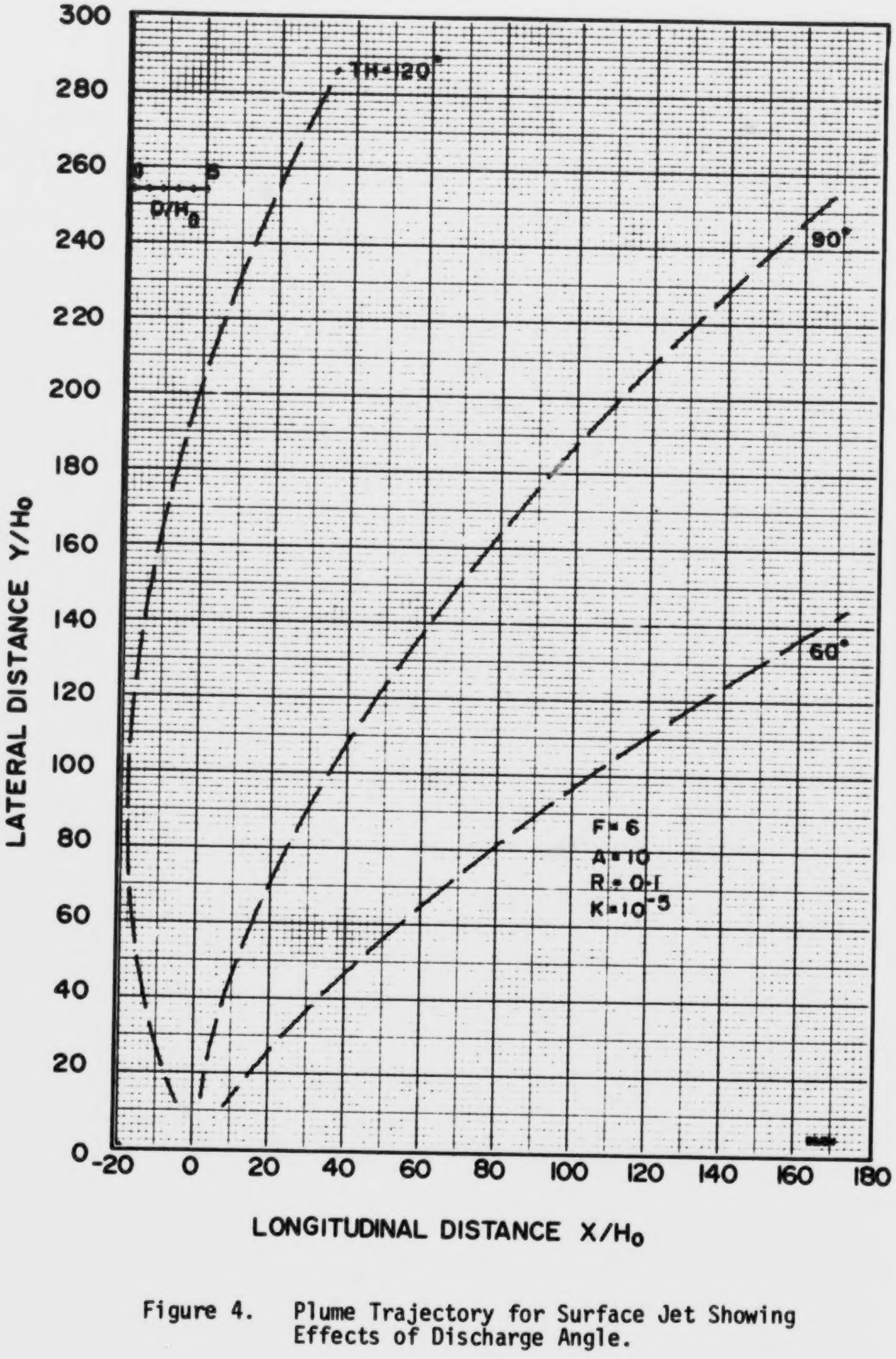

Figure 4. Plume Trajectory for Surface Jet Showing Effects of Discharge Angle.

In addition to the plume trajectory, Figures 1, 2, 3, and 4 provide information on the local plume depth D/H_o. Note that centerline plume trajectories are plotted in broken lines. The length of each broken line segment along the plume trajectory is a measure of the local plume depth as shown by the accompanying D/H_o scale in each Figure. Referring now to Figures 1, 2, 3 and 4, one can see from variations in the lengths of these segments the effects; respectively of the ambient current, Froude number, aspect ratio and discharge angle on the plume depth. These effects are most evident in Figures 2 and 3.

The plume depth generally increases rather rapidly at first, then it either becomes small and remains essentially constant because of stratification or it continues thickening (at a low rate) due to jet and ambient mixing. Plumes with lower Froude numbers tend to become thin and stratified while those with higher Froude numbers tend to thicken.

It is important when attempting to explain these results in physical terms to make a mental note of the actual problem being solved. Moving from one trajectory to another of Figures 2 and 3, in practice, may require a change in the channel depth, relative to which magnitude all plume coordinates and local depth are measured. Consequently, a direct comparision of the relative magnitudes may not be meaningful.

The foregoing figures contain information on the plume trajectory and depth. It is possible to superimpose on these figures other plume characterisitics such as centerline temperature and plume width, thereby eliminating the need for presenting additional figures as well as providing at once a more complete picture of the plume in a single plot. Examples of this manner of presentation are given in Figures 5, 6, 7, and 8 corresponding respectively, to Figures 1, 2, 3 and 4.

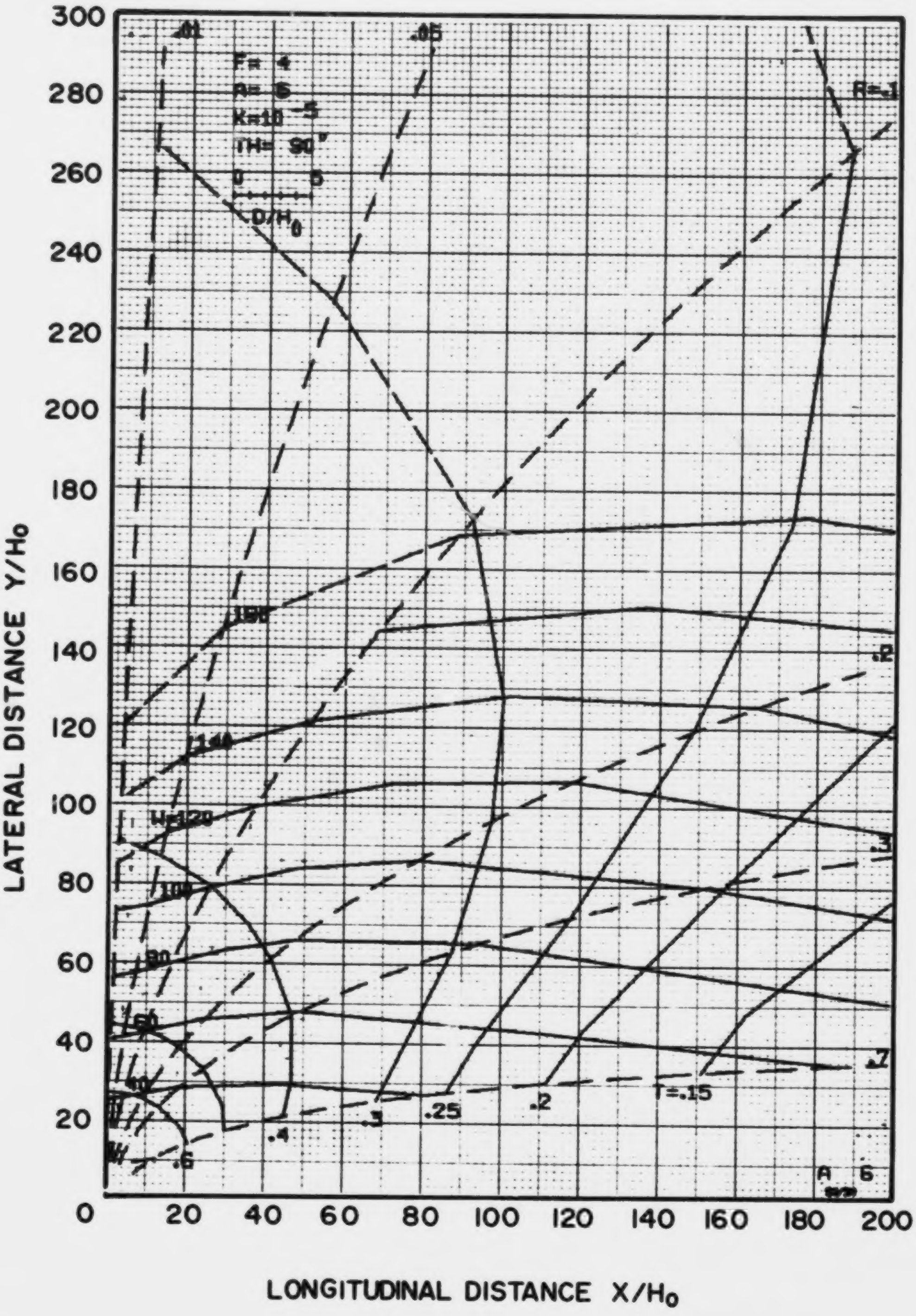

Figure 5 Plume Trajectory, Temperature, Width and Depth for Surface Jet Showing Effects of Ambient Current.

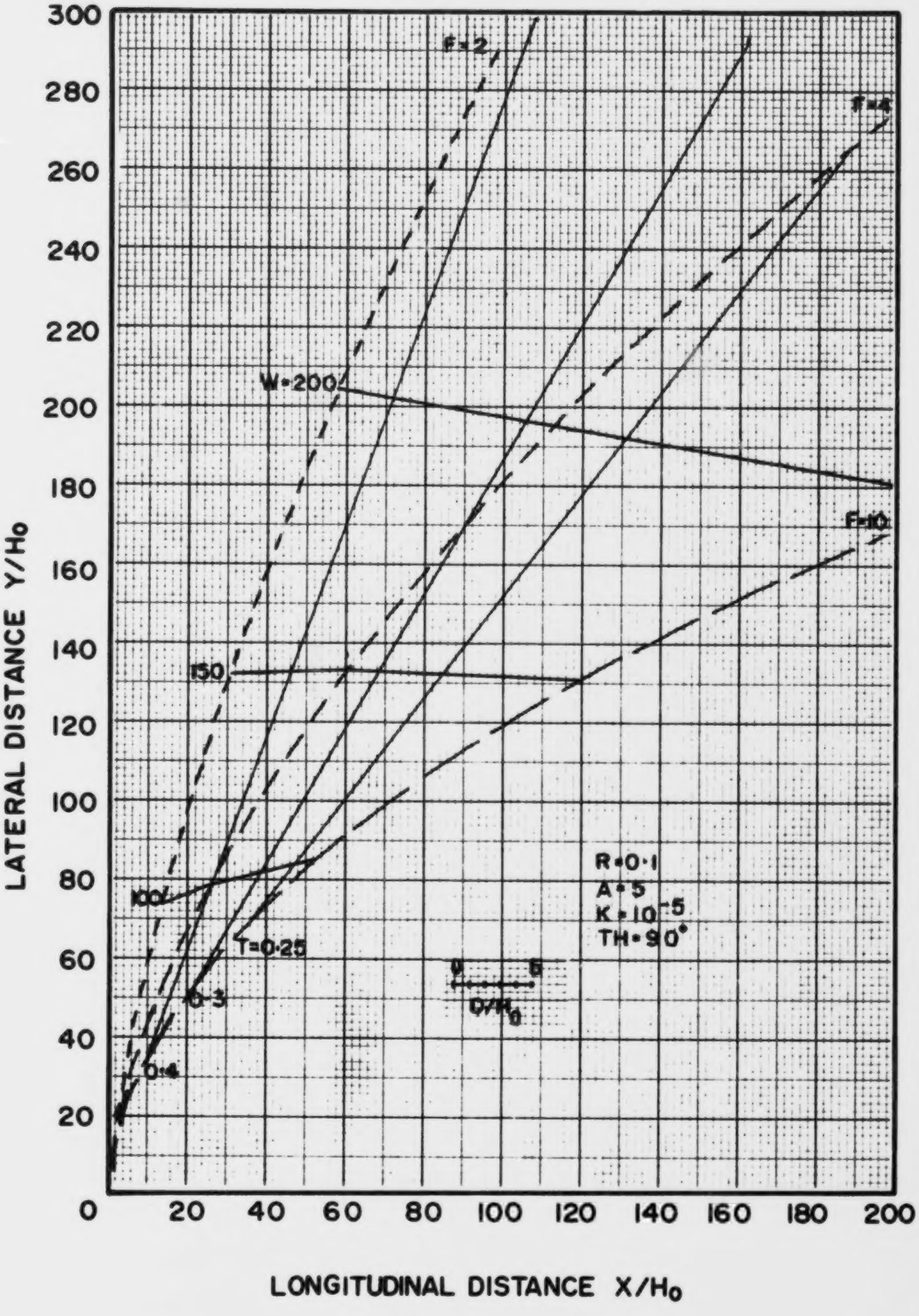

Figure 6 Plume Trajectory, Temperature, Width and Depth for Surface Jet Showing Effects of Jet Densimetric Froude Number.

The local excess centerline temperature ΔT_c, is plotted in Figure 5 as a fraction of the initial excess temperature ΔT_o. The local plume width W is also plotted in this figure as a dimensionless number. The local width is taken equal to four standard deviations of the temperature distribution when such distribution is assumed Gaussian.

The following observations are based on the analysis of Figure 5. (1) The effect of a high ambient current is to reduce the centerline plume temperature by causing additional entrainment. (2) The plume width generally varies inversely with changes in the ambient current. Thus when the ambient water is nearly stagnant one expects to find a hot and wide plume. Figures 6, 7, and 8 show that hot and wide plumes are also caused by low discharge Froude numbers, large aspect ratio and large discharge angle.

A general physical interpretation of the above can be presented as follows. We have discussed the process of interaction with respect to plume trajectories in Figures 1 through 4. Jet interaction is greatest at a high Froude number and low aspect ratio. Figures 6 and 7 are plotted to demonstrate this effect. They show a narrow and cool plume when there is a strong interaction and a wide and warm plume when there is a weak interaction. The effect of the discharge angle is somewhat complicated as shown in Figure 8. It shows that the plume is wider and hotter for a discharge angle of 120° than for 90 or 60°. This is true at least near the source. If calculations are allowed to continue, as will in the working nomograms, this trend is shown to be reversed.

The four plume characterisitics, namely, trajectory, temperature, width and depth, are combined in generalized nomograms similar to Figure 5. Their discussion and other plume characteristics such as surface area and time of travel are presented in the next section.

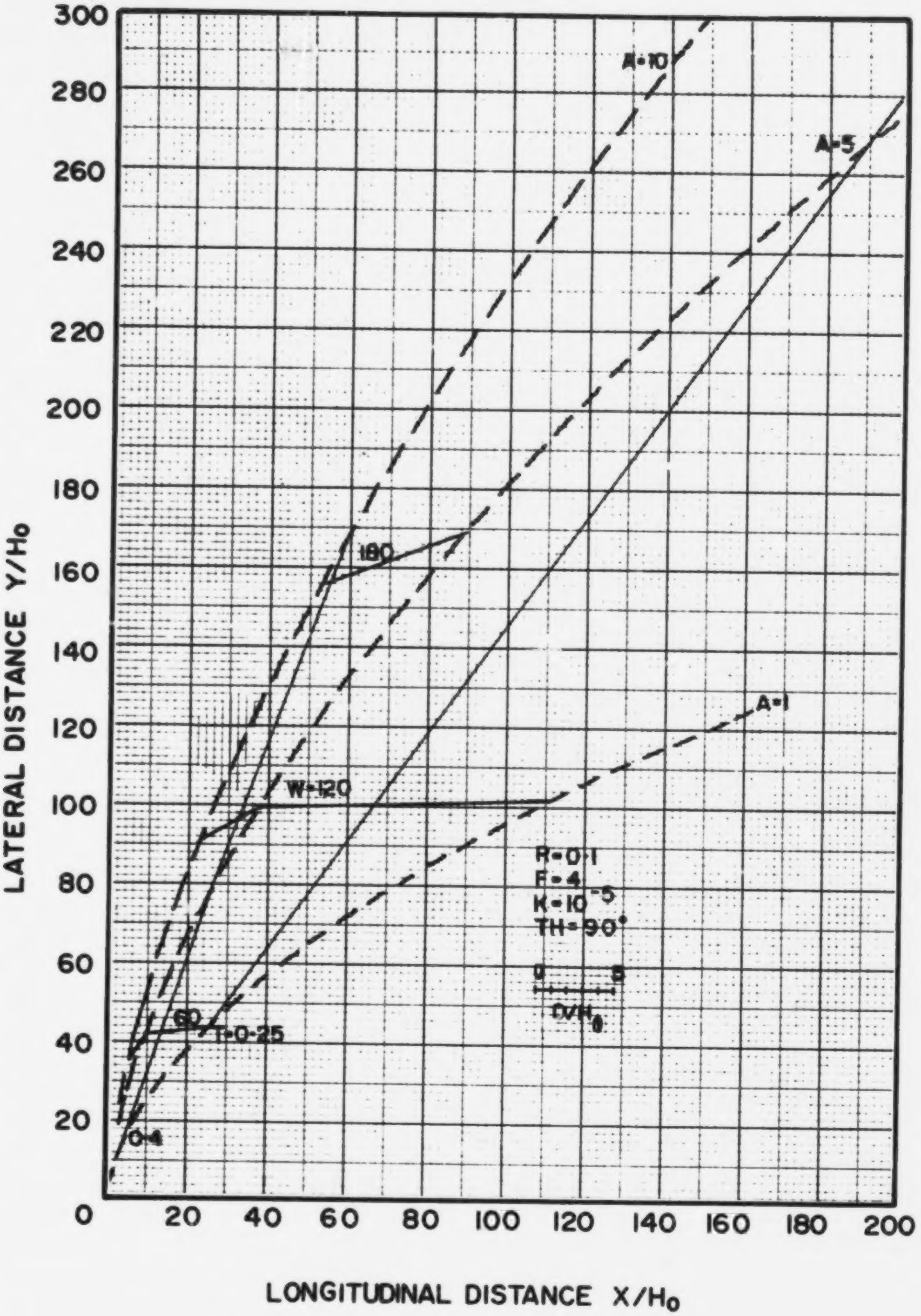

Figure 7 Plume Trajectory, Temperature, Width and Depth for Surface Jet Showing Effects of Jet Aspect Ratio.

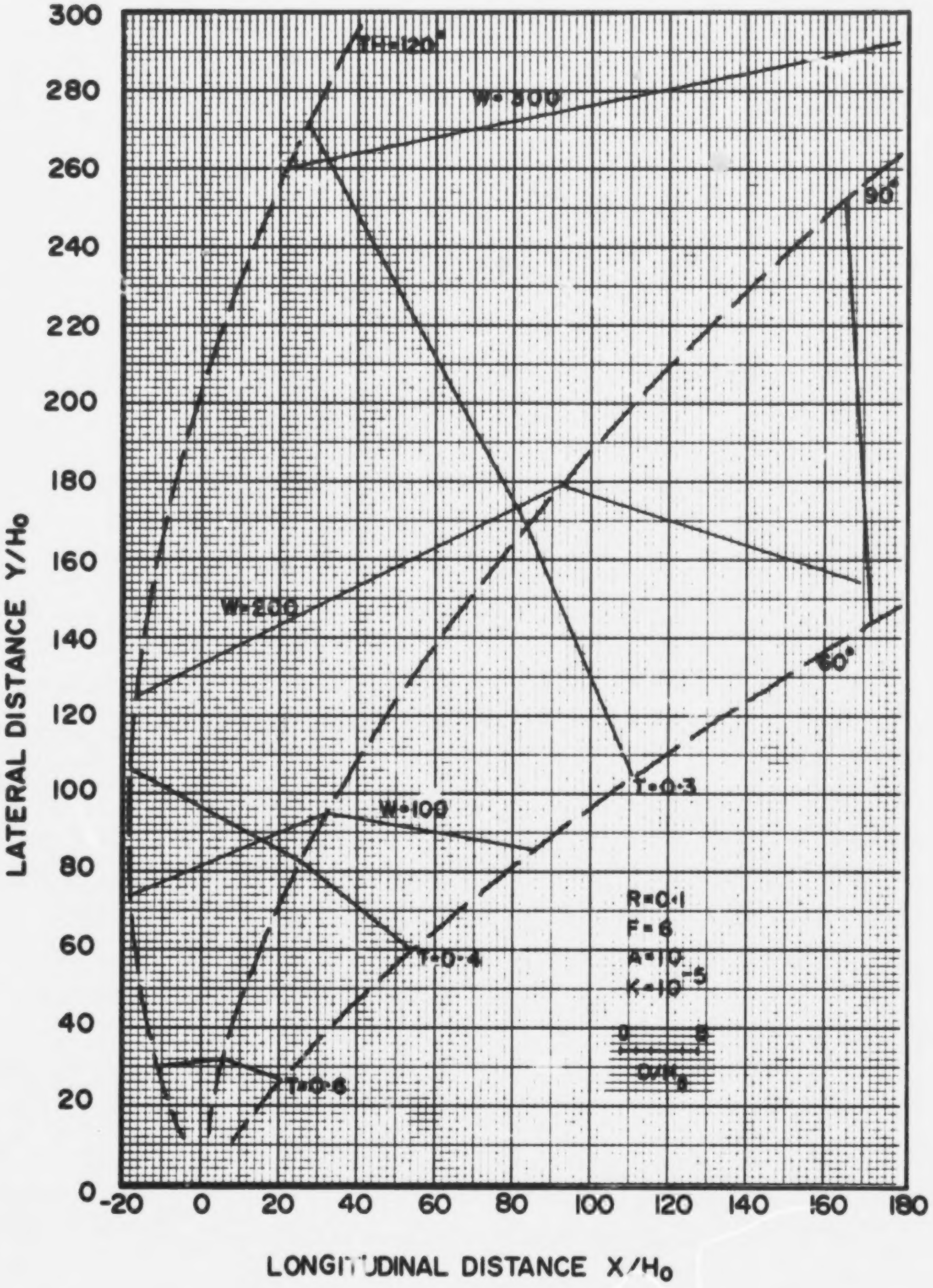

Figure 8 Plume Trajectory, Temperature, Width and Depth for Surface Jet Showing Effects of Discharge Angle.

II NOMOGRAM ORGANIZATION

Nomograms are presented in two distinct functional groups. The first group given in Appendices A, B and C are representative of typical situations encountered in practice. They do not represent extreme conditions according to our judgment. This group of nomograms constitutes the main body of the workbook. The second group of nomograms is given in Appendix D to show the variations in the results due to changes in certain of the input parameters. Ordinarily these are of little concern to the prospective user seeking qualitative results.

There are at least three reasons for presenting the additional nomograms of Appendix D. First, the user might have a problem that he considers an extreme situation. In this case he will identify a possible variation of one or more input parameters to his problem and thus use the appropriate nomogram. Second, a researcher seeking information on the sensitivity of the model to possible variations of the input parameters can make direct use of the nomograms and thus spare himself the ordeal of obtaining an operational computer program of the model for that purpose. The third reason for providing the supplementary material in Appendix D is for the sake of completeness and an admission of the fact on our part that the results presented in Appendices A, B, and C for general use, while reasonable according to present information, are not the final word. This is because the resolution of the available data is not sufficiently good to support a firm stand on details.

A - (TTWD) WORKING NOMOGRAMS

Parametric information on the local plume width, depth and centerline temperature and trajectory is given in Appendix A. A typical plot of trajectory, temperature, width, and depth (TTWD) is given in Figure 5 and discussed at considerable length in the introductory section.

A summary of the entire set of nomograms in Appendix A is listed in Tables 1 and 2. The (TTWD)-plots are subgrouped conveniently in a 4 by 4 matrix of aspect ratio and Froude number variations, respectively, as shown in Table 1. The matrix elements A1, A2,..., A16 refer to the appropriate figure numbers in Appendix A. Each subgroup of 16 plots provides plume information for a fixed initial discharge angle and heat exchange coefficient. The numerical values of these variables are $\Theta_o = 90°$ and $K = 10^{-5}$ for all the 16 plots referred to in Table 1.

Table 2 is a 3 by 3 matrix showing variations of Θ_o and K, respectively. Note that each of the entries in this matrix refer to subgroups of plots similar to Table 1. Note also that Table 1 is the first matrix entry of Table 2. Since it is likely that plots of the intermediate values of Θ_o and K receive greater use, we have placed them as the first entry for convenience.

In order for the user to locate a specific plot, some cross-referencing of the formats in Tables 1 and 2 is required. It is helpful to illustrate this by an example. The figure that gives the plume characteristics for F=4, A=5, θ_o=60° and $K = 10^{-4}$ is Figure A70. Seventy is the sum of two numbers, namely, 64 (from Table 2) plus 6 (from Table 1) where 64 is the highest figure number in the preceding matrix element.

TABLE 1
Figure numbers for (TTWD) Working Nomograms of Appendix A, Θ_o = 90° and K = 10^{-5}

F → ↓A	2	4	6	10
1	A1	A2	A3	A4
5	A5	A6	A7	A8
10	A9	A10	A11	A12
15	A13	A14	A15	A16

TABLE 2
Summary of Figure Numbers for (TTWD) Working Nomograms of Appendix A

Θ_o → ↓K	90°	60°	120°
10^{-5}	A1-A16	A17-A32	A33-A48
10^{-4}	A49-A64	A65-A80	A81-A96
10^{-6}	A97-A112	A113-A128	A128-A144

NOTE: Figures A-37, 41, 45, 46, 85, 89, 93, 94, 133, 137, 141, 142 are not included due to computational difficulties.

B - (TA) WORKING NOMOGRAMS

The nomograms of Appendix B contain information on water surface area within the plume that equals or exceeds the designated excess temperature contour namely, temperature-area (TA)-plots. The areas plotted are normalized by the square of the discharge depth. There are nine sets of plots subgrouped as 8 plots to a set as shown in Table 4. The format for each subgroup is detailed in Table 3. The combined use of Tables 3 and 4 is identical to the previous example for the use of Tables 1 and 2. For instance, if we require information on area for Figure A70 alone, we must refer to Figure B35 (i.e., 32 + 3). Note also from Table 3 that Figure B35 contains information on plumes for F=2, A=5.

C - (Tt) WORKING NOMOGRAMS

The nomograms of Appendix C contain information on the time of travel of a parcel of water along the trajectory of the plume. Since the plume temperature is not constant, the parcel of water is exposed to continually varying temperature levels. The time of exposure has been calculated in these nomograms for the centerline temperature and plotted in terms of the total exposure time, t, to a temperature excess ratio equal to or greater than $\Delta T_c/\Delta T_o$. For instance, the total time of exposure of a parcel of water that is entrained near the discharge (say, when $\Delta T_c/\Delta T_o \approx 1$) to a point along the plume trajectory whose temperature ratio is, say, 0.1, can be read directly from the plots. However, since entrainment could take place anywhere along the plume trajectory, say at a point where the temperature ratio is 0.3, the total exposure time to temperature ratios between 0.3 and 0.1 is the difference between two direct readings of the times. Note also that in these plots, the exposure time t is made dimensionless by multiplying by U_o/H_o.

TABLE 3
Figure Numbers for (TA) Working Nomograms of Appendix B, $\theta_o = 90°$, $K = 10^{-5}$

F→ ↓A	2	4	6	10
1	B1	B1	B2	B2
5	B3	B3	B4	B4
10	B5	B5	B6	B6
15	B7	B7	B8	B8

TABLE 4
Summary of Figure Numbers for (TA) Working Nomograms of Appendix B

Θ_o→ ↓K	90°	60°	120°
10^{-5}	B1-B8	B9-B16	B17-B24
10^{-4}	B25-B32	B33-B40	B41-B48
10^{-6}	B49-B56	B57-64	B65-B72

There are nine sets of plots subgrouped as 8 plots to a set as shown in Table 6. The format for each subgroup is detailed in Table 5. The combined use of Tables 5 and 6 is identical to the use of Tables 3 and 4 just explained. Thus the (Tt)-plots corresponding to Figure A70 are found in Figure C35.

D - (TTWD) SUPPLEMENTARY NOMOGRAMS

The nomograms of Appendices A, B, and C are plotted for fixed values of entrainment coefficient, horizontal and vertical eddy diffusivities, drag and shear coefficients. Some variations on these inputs (both for lower and higher magnitudes) are calculated for fixed values of typical Froude number, F=4, aspect ratio, A=5 discharge angle, Θ_o = 90° and surface heat transfer coefficient K = 10^{-5}. These results are given in Appendix D in the form of (TTWD)-plots. The summary of the plots is given in Tables 7 and 8.

TABLE 5
Figure Numbers for (Tt) Working Nomograms
of Appendix C, $\Theta_o = 90°$, $K = 10^{-5}$

F→ ↓A	2	4	6	10
1	C1	C1	C2	C2
5	C3	C3	C4	C4
10	C5	C5	C6	C6
15	C7	C7	C8	C8

TABLE 6
Summary of Figure Numbers for (Tt) Working
Nomograms of Appendix C

Θ_o → ↓K	90°	60°	120°
10^{-5}	C1-8	C9-C16	C17-C24
10^{-4}	C25-C32	C33-C40	C41-C48
10^{-6}	C49-C56	C57-C64	C65-C72

TABLE 7
Figure Numbers for (TTWD) Supplementary Nomograms of Appendix D, $\Theta_o = 90°$, $K = 10^{-5}$, $F = 4$, $A = 5$

E_h → ↓ E_v/E_h	.005	.02	.1
.001	D1	D2	D3
.01	D4	D5	D6
.2	D7	D8	D9

TABLE 8
Summary of Figure Numbers for (TTWD) Supplementary Nomograms of Appendix D

E_o	.01	D1-D9
	.05	D10-18
	.15	D19-D27

III ANALYTICAL CONSIDERATIONS

The nomograms in this volume were generated predominately from a modification to the surface jet model of Reference 1. The reader should consult References 1 and 3 for the original derivations and Appendix F for the analysis, verification, and a Fortran listing of the full modified model with an example input and output.

A - MODEL DESCRIPTION

The mathematical model describes the three dimensional behavior of a heated jet discharged from a rectangular channel at the surface of a deep and wide body of homogeneous water that is either at rest or moving with a uniform and constant (steady) velocity. The magnitudes of the discharge angle, channel dimensions, discharge velocity and temperature are arbitrary. The jet velocity and temperature distributions at the outlet are assumed uniform and constant.

The mathematical model is greatly idealized, that is, it describes the behavior of a plume whose discharge characteristics and ambient environment are closely controlled. Furthermore, the model is subjected to considerable limitations in the process of arriving at a mathematical solution. These two aspects of the model are discussed further.

1. Model Idealizations

While we need to discuss model idealizations and limitations for the benefit of the prospective user, we must also hasten to add that these shortcomings are not necessarily unique to this model. An exact simulation of a real plume in the natural environment has not been achieved. The difficulties confronting this level of effort are too numerous to enable a general solution at a reasonable cost. Some of the more obvious difficulties can be readily outlined. For example, surface discharges are not confined to open rectangular channels; the jet is usually discharged over a sloping beach; the ambient current is neither uniform, nor constant; a natural water body is often stratified, or nearly so; there will always be some wind; the discharge velocity and temperature profiles are usually nonuniform and not always constant; the natural water body is not infinite giving rise to shoreline effects and obstruction, etc.

Consequently, the nomograms do not provide a precise description of a real plume. They do, however, describe a plume realistically if one or more of the real factors that have been ignored or idealized in the model do not become dominant. Following this line of reasoning, the utility of the idealized model can, sometimes, be rightfully defended. Here are some examples: (1) The effect of wind can enter indirectly in the wind induced ambient current. In rivers, its effect may be overshadowed by the high river current; (2) The ambient water need be homogeneous only in a thin top layer with a thickness on the order of channel depth; (3) Slowly changing ambient conditions may be assumed nearly constant when compared with the plume response. However, time dependent back and forth motion of tidal currents cannot be handled with the steady state model used in this workbook; (4) The effects of discharge geometry, velocity and temperature profiles are felt mainly near the discharge and, in general, the model does not treat the development portion in a precise way thus leaving some doubts as to the need for a precise specification of these conditions; (5) The model may still provide meaningful results if the initial plume depth is small compared with the ambient water depth, regardless of beach slopes.

These are only a few comments regarding the possible adequacy of the idealized model for application to real situations. Clearly, there is considerable judgment involved on the part of the user. The difficult problem is that the assumptions can be stated and introduced in the model rather precisely, but matching these with a specific problem cannot be done with nearly as much precision. The degree of accuracy and successful prediction is principally dictated by the close agreement one finds between the stated idealizations in the model and the conditions of the real problem. This is an important fact not to be overlooked by the prospective user.

2. Other Limitations

Other limitations imposed mainly in the process of arriving at an analytical solution to the problem are important to mention though more difficult to discuss in depth without the resort to mathematical formalism. The most significant among these limitations will be discussed very briefly.

Development Calculations- The turbulent mixing of the discharged fluid with the ambient water begins immediately at the point of discharge. However, turbulent mixing penetrates both the jet region and the ambient surrounding only gradually. Thus, the width and depth of the turbulent mixing region are zero at the point of discharge but grow gradually downstream of this point until at a short distance from it the zone occupies the entire interior of the jet. The turbulent jet is then called fully developed. Obtaining a complete mathematical solution to describe the characteristics of this so called development portion of the jet is very difficult. Consequently, a partial solution is obtained by resorting to experimental data which provide estimates of the development length. Then, following the procedure outlined in Reference 1 other required information at the end of development zone is calculated from the governing equations of motion. The reader is referred to Reference 3 for a more thorough analytical treatment of this zone.

Similarity - Once the turbulent mixing is fully developed it is assumed that the mean profiles of the temperature, velocity and density do not change throughout the plume trajectory. In the present study, these profiles are assumed to be Gaussian even when there is a cross current that disturbs the symmetry within the plume. The symmetric Gaussian profile assumption can lead to reasonable results for a very small or no ambient current. Such a model is inapplicable when there is a very strong ambient current.

Additionally, in a strong current the plume may be forced against the shoreline thereby confining entrainment mainly to one side of the plume. Again, the present analysis cannot handle this complication. In this Workbook nomograms are provided for a minimum discharge angle of 60°. Even then, the velocity ratio is limited to 0.7 to avoid conditions where the edge of the plume comes into contact with the shoreline. If in a particular application this condition is violated, the user should treat the results with caution.

Entrainment - The plume expands by entraining ambient water at its outer boundaries, that is, along the plume edge. The forward motion of the jet establishes a lateral mean ambient fluid velocity into the jet. This entrainment velocity is assumed proportional to the local mean velocity at the jet centerline relative to the ambient fluid. The entrainment velocity is also affected by the jet temperature but only in the vertical direction. The proportionality factor, known as entrainment coefficient, must be prespecified in the model. Its value must be based on experimental data.

In addition to the mean convective velocity at the edge of the plume, there are large scale turbulent fluctuations that cause the turbulent diffusion of heat and momentum. In the model this turbulent entrainment is assumed to be due to the ambient contribution only. Since the turbulence scale in the ambient water is generally different in the horizontal and vertical directions, separate information on diffusivities in these directions must be provided for the model in terms of appropriate coefficients. These diffusivity coefficients must be prespecified. Their values must be based on experimental data.

Buoyant Spreading - The plume from a heated jet spreads in directions due to buoyant forces. Ordinarily the spreading of the plume, whether due to jet inertia forces or buoyant forces, must be predicted from the governing equations of motion. However, due to excessive simplification of the equations, the mechanism for generating this information from the original equations is bypassed. Consequently additional information on buoyant spreading of the plume must be provided independently of the original equations. The analysis due to Reference 1 was retained in the model but with a slight modification introduced in the spreading function.

Singularity - The original, as well as the modified model, runs into computational difficulties (singularity) at a local plume densimetric Froude number of unity. Once this value is reached computations based on the model are questionable.

Singularities occur in two equations: (a) the equation for calculating the plume depth and (b) the equation for the lateral buoyant spreading. The two equations are independent of one another and in the modified model, the first singularity occurs before the second. Unfortunately, the model becomes inoperative due to these singularities for many problems of practical interest. Greatest difficulty is noted at small values of R and F as well as large values of A. Since for these conditions the plume trajectory is nearly coincident with the Y axis, little deviation of calculated trajectory from data was noted even for calculations beyond the first singularity. Therefore, trajectories calculated by the program were used in the nomograms. However, the information on temperature and width given in (TTWD) nomograms beyond the first singularity are based on an extrapolation of previously calculated values of temperature and width for higher R. In order to clearly identify these extrapolations the plume width and temperature curves are continued with broken lines. These values should be used with caution.

B - MODEL APPLICABILITY

The foregoing discussion of the idealizations and model limitations should provide the reader with some understanding of the model, particularly with respect to its applicability to practical problems. In order to be useful, the model must be verified against laboratory and field data. If the magnitude of the plume characteristics are in reasonable agreement with data and if the trends of these characteristics are likewise reasonable, the model can be used to predict similar situations with confidence.

It is true the present surface discharge model has many shortcomings, but we have made a careful attempt to choose all the free input coefficients to the model in order to produce the best fit with the available data. Consequently, we consider the results both reasonable and of considerable practical utility. The procedure for producing the best fit to the data is contained in Appendix F.

In all cases, we have avoided presenting information on R = 0. Instead, whenever extrapolation was meaningful, calculations were extended to R = 0.01 which, in reality, may be interpreted as R = 0. For nomograms with $\theta_0 = 120°$, $R \geq 0.1$. In several instances a complete set of nomograms was omitted because of computational difficulties.

The words of caution given earlier concerning the use of the extrapolated portion of the nomograms might have escaped the avid user. They should not. The presence of the broken temperature and width lines should signal not only difficulties in the mathematical model used, but also a similar difficulty in obtaining good experimental data in a stagnant water body.

IV. EXAMPLE PROBLEMS

Examples are given in this section to demonstrate the use of the nomograms. Even though an attempt was made to develop more or less realistic problem statements, the examples should not be construed as representing a preferred design or recommended temperature zone. Numbers in these examples have been conveniently rounded off. Problems 4, 5, and 6 are presented to show example cases where using the nomograms would lead to questionable results.

Example Problem #1

Given:

A 500 MWe nuclear power plant is located on a large freshwater lake. The cooling water is discharged at the surface through a rectangular open channel. The following design data apply:

a. Waste heat to cooling water = 8.1×10^8 kcal/hr
b. Condenser ΔT (ΔT_o) = 12°C
c. Discharge angle (θ_o) = 90°
d. Discharge velocity (U_o) = 1 m/sec
e. Channel width ($W_o = 2 B_o$) = 10 m
f. Ambient water temperature (T_a) = 15°C
g. Offshore current of .05 m/sec
h. Dimensionless surface heat transfer coefficient $K = 10^{-5}$

Determine:

1. The location along the centerline of the plume where the surface temperature is 4°C above ambient.

2. The width and depth of the plume at this point.

3. The plume area enclosed by the 4°C ΔT isotherm.

4. The time of travel for a water parcel following the plume centerline from the discharge structure to the 4°C ΔT isotherm.

Solution:

1. Determine A (Aspect ratio) = $2B_o/H_o$

$$\text{Discharge rate } Q = \frac{\text{Heat load (kcal/hr)}}{\Delta T_o \times 3600\ \text{(sec/hr)} \times 1000\ (\text{kcal/m}^3\text{-°C})}$$

$$= \frac{8.1 \times 10^8}{12 \times 3600 \times 1000} = 18.8\ \text{m}^3/\text{sec}$$

$Q = 2\ B_oH_oU_o$

$H_o = Q/2\ B_oU_o = 18.8/10 \times 1$

$H_o = 1.88$ m

$A = 2\ B_o/H_o = 10/1.88 = 5.3 \sim 5$

2. Determine F (Froude Number)

$F = U_o\ /\sqrt{(\Delta\rho_o/\rho)\ gH_o}$

From Figure E1, $\Delta\rho/\rho = 0.0026$

$F = (1\ \text{m/sec})/[(0.0026)\ (9.8\ \text{m/sec}^2)\ (1.88\text{m})]^{1/2} = 4.6$

3. Location of 4°C ΔT_c isotherm:
For $\Theta_o = 90°$, $K = 10^{-5}$, $A = 5$ and $F = 4$, use nomogram A6. At $\Delta T_c/\Delta T_o = 4/12 = 0.333$ and $R = 0.05$, $X/H_o = 40$ and $Y/H_o = 180$. For Θ_o, K, and A unchanged with $F = 6$, use nomogram A7, where $X/H_o = 16$ and $Y/H_o = 82$. Interpolating to $F = 4.6$ gives $X/H_o = 33$ and $Y/H_o = 151$. Since $H_o = 1.88$ m, the 4°C ΔT isotherm will be located at (151) (1.88 m) = 283 m offshore and (33) (1.88 m) = 62 m downstream from the discharge. It should be noted that we have used the nomograms of Figure A6 in an extrapolated region. The answer is, therefore, approximate.

4. The width of the plume at the 4°C ΔT isotherm:
Using nomograms A6 and A7, W/H_o values of 200 and 170 are obtained. Interpolation for $F = 4.6$, gives $W/H_o = 190$. Thus, the width at this point is (1.88 m) (190) = 357 m.

5. The centerline depth of the plume at 4°C excess temperature:
Using nomograms A6 and A7, D/H_o values are scaled from the length of the dashes at the desired location to be 2.0 and 3.0 for $F = 4$, and 6, respectively. Interpolating to $F = 4.6$, gives $D/H_o = 2.3$. Thus, $D = (2.3)\ (1.88\ \text{m}) = 4.3$ m.

6. The area within the 4°C ΔT isotherm:
Using nomograms B3 and B4, A/H_o^2 values of 6×10^3 and 1.1×10^3 are obtained. Interpolating for $F = 4.6$ we obtain $A/H_o^2 = 4.5 \times 10^3$. Thus the area equals $(4.5 \times 10^3)\ (1.88\ \text{m})^2 = 1.6 \times 10^4\ \text{m}^2$ or about 4 acres.

7. The time for a water parcel to travel along the plume centerline from the outlet to the 4°C ΔT isotherm:
Using nomograms C3 and C4, $tU/_o/H_o$ values of 7×10^2 and 2×10^2 are obtained. Interpolating to $F = 4.6$, gives $tU_o/H_o = 550$. Thus, t = (550) (1.88 m/1 m/sec)= 1034 sec, or about 17 minutes.

Example Problem #2

Given:

A 1000 MWe fossil fueled power plant is located on a large fresh water lake. The cooling water is discharged through a one kilometer long rectangular discharge canal. The following design data apply:

a. Waste heat to cooling water = 1.08×10^9 kcal/hr

b. Condenser ΔT (ΔT_{con}) = 16.3°C

c. Discharge angle (θ_o) = 60°

d. Discharge velocity = 0.8 m/sec

e. Depth of water in channel at outlet = 1.25 m

f. Ambient water is stagnant with an ambient temperature of 20°C. Assume $K = 10^{-4}$.

Determine:

1. The location of the plume centerline where the temperature is 23°C
2. The thickness of the water layer at this point that is 21°C or warmer.
3. The plume width at this point.
4. The surface plume area having a temperature equal to or warmer than 23°C.

5. The time required for a water parcel to travel from the condenser outlet to the 23°C isotherm.

Solution:

1. Determine the water temperature at the end of the discharge canal.

The temperature distributions in a constant width canal with mixed flowing fluids is given by

$$\frac{T - T_E}{T_{con} - T_E} = \mathrm{EXP}[-K_E 2B_o X/\rho Q C_p]$$

where K_E is the surface heat transfer coefficient, $2B_o$ is the canal width, X is the distance from the beginning of the canal to the point desired, ρ is the density of water, Q is the volumetric flow rate in the canal, C_p is the heat capacity of the water, T_{con} is the condenser outlet temperature, and T_E is the equilibrium temperature of the water. Given $Q = U_o H_o 2B_o$ and $K = K_E/\rho C_p U_o$, the above equation for canal temperature can be simplified to yield the canal dischage temperatures. This expression is:

$$\frac{\Delta T_o}{\Delta T_{con}} = \mathrm{EXP}[-K\ L/H_o]$$

if T_E is taken as the ambient receiving water temperature and L is the total canal length.

Thus, for this problem $\frac{\Delta T_o}{\Delta T_{con}} = \mathrm{EXP}[-(10^{-4})(1000)/(1.25)] = .923$

Therefore $\Delta T_o = .923 \times 16.3 = 15°C$

2. Determine $A = 2B_o/H_o$

   $Q = (1.08\text{x}10^9)/[(16.3)\ (1000)\ (3600)] = 18.5\ m^2/sec$

   $2B_o = Q/H_oU_o = 18.5/(.8)(1.25) = 18.5\ m$

   $A = 2B_o/H_o = 18.5/1.25 = 14.8 \simeq 15$

3. Determine F

   From Figure E3, $G = .5\ \frac{sec}{cm^{1/2}}$

   $$F = \frac{GU_o}{\sqrt{H_o}} = \frac{(.5)\text{x}(.8)(10)}{\sqrt{1.25}} = 3.6$$

   F = 3.6, use F = 4

4. $\Delta T_c/\Delta T_o = (23\text{-}20)/15 = 0.2$
   Use R = 0.01 as an approximation for R = 0, $\theta_o = 60°$, $K = 10^{-4}$, A = 15, and F = 4, to enter nomogram A78. At $\Delta T_c/\Delta T_o = 0.2$, X/H = 380 and $Y/H_o = 620$. This gives a distance $S/H_o = 727$ as measured along the trajectory. Thus, 23°C occurs approximately on the plume centerline at (727) (1.25 m) = 909 m from the discharge.

5. The Gaussian distribution curve, Figure E5, is used to find the plume depth where the temperature is 21°C at a cross section located 909 m offshore. $(T_n\text{-}T_a)(T_c\text{-}T_a) = (21\text{-}20)/(23\text{-}20) = .333$. At this value on Figure E5, $Z/\sigma_z = 1.48$. The standard deviation σ_z can be found from knowing that the depth $D = 2\sigma_z$. Therefore, the depth

to the 21°C point is 1.48(D)/2 from the surface. The value of D for this problem is found from the length of the dash at the desired point on Figure A78 to be 2.8 H_o = (2.8)(1.25) = 3.5 m. This gives a thickness of the desired layer to be (1.48)(3.5)/(2) = 2.6 m.

6. Width of the plume at the 23°C centerline temperature:
Using nomogram A78, W/H_o is found to be greater than 450. Thus the plume is over (450) (1.25m) = 562 m wide. A gross extrapolation of the data on Figure A78 indicates the width to be more like 900 meters wide.

7. The plume area warmer than 23°C:
Using nomogram B39, a value of A/H_o^2 slightly greater than 1.5×10^5 is read off. Thus, the plume area enclosed by the 23°C isotherm is $(1.5 \times 10^5)\ (1.25\ m)^2 = 2.34 \times 10^5 m^2$, or 58 acres.

8. The time for a water parcel to travel from the condenser to the 23°C isotherm:
Assuming a constant cross section in the rectangular channel, the water parcel will take (1000m)/(0.8m/sec) = 1250 seconds to travel through the canal to the point of discharge. Using nomogram C39, tU_o/H_o is found to be approximately 5.2×10^3. Thus, $t = (5.2 \times 10^3)\ (1.25/0.8)$ = 8120 sec. Adding this value to 1250 sec gives a total travel time of 9370 sec ≃ 2.6 hr.

Example Problem #3

An 800 MWe nuclear power plant is located on an open coastline. Condenser cooling water is discharged through an open rectangular channel. The following design data apply:

a. Waste heat to cooling water = 1.3×10^9 kcal/hr
b. Discharge velocity = 1.0 m/sec
c. Offshore current along coastline = .2 m/sec
d. Condenser $\Delta T = 12°C$
e. Total width of channel = 14 m
f. Ambient water temperature and salinity are respectively 10°C and 30 ppt.
g. Surface heat transfer coefficient $K = 10^{-5}$

Determine:

1. The location on the plume centerline where $T_c = 16°C$

2. The plume width and depth at this point.

3. The surface area that has a temperature between 14 and 16°C

Solution:

1. Determine A

$$Q = (1.3 \times 10^9)/(10^3)\ (1)\ (10)\ (3.6 \times 10^3) = 36\ m^3/sec$$

$$H_o = Q/2B_oU_o = (36)/(1)(14) = 2.6\ m$$

$$A = 14/2.6 = 5.4 \sim 5$$

2. From Figure E2

$$\frac{\Delta\rho}{\rho_o} = 0.0024$$

$$F = (1)/[(0.0024)\ (9.8)\ (2.6)]^{\frac{1}{2}} = 4.04$$

3. Location of 16°C isotherm

$\Delta T_c/\Delta T_o = (16-10)/12 = .5$

$R = U_a/U_o = 0.2/1 = 0.2$

Use nomogram A6 for Θ_o=90°, K = 10^{-5}, A=5 and F=4 at R = .2 and T = .5 to find X/H_o = 18 and Y/H_o = 38. Thus, the 16°C isotherm is encountered at the centerline (18) (2.6 m) = 47 m down current and (38) (2.6 m) = 99 m away from shore.

4. The width of the plume at the 16°C centerline temperature. Using nomogram A6, W/H_o = 52. Thus, the plume width is (52)· (2.6 m) = 135 m.

5. The plume depth at this point is scaled off Figure A6 from the length of dashes. $D/H_o \approx 2$, $D = 2 \times 2.6 = 5.2$ m

6. The plume area between 4 and 6°C. For $\Delta T/\Delta T_o$ = 0.333 and 0.5, nomogram B3 gives A/H_o^2 values of 2.2×10^3 and 4.3×10^2 at R = 0.2. The difference between the two is 1.77×10^3 giving the appropriate area as (1770) $(2.6\text{m})^2 = 1.2 \times 10^4$ m^2 (3 acres).

Example Problem 4

Repeat Problem #1 for discharge at 60° into a deep river whose velocity is .7 m/sec.

Solution:

From Problem #1, F = 4.5, A = 5, K = 10^{-5}, H_o = 1.88 m.

1. Location at 4°C ΔT isotherm:

For Θ_o = 60°, K = 10^{-5}, F = 4 and A = 5 use nomogram A22. For R = .7/1.0 = 0.7 and $\Delta T_c/\Delta T_o$ = 0.333, X/H_o = 68 and Y/H_o = 18. From Figure A23 for F = 6, X/H_o = 67 and Y/H_o = 18 (nearly the same). The total width at this point is found from the same two nomograms to be about 30 or a half width of 15. Since Y/H_o is only about 18 this places the edge of the plume very near the shore. Due to uncertainties in the model, this plume could well be attached to the shore, limiting entrainment from that side. This is especially true if the bottom near the shore is not deep. The results from the nomograms for this case are therefore, to be used with caution. Hydraulic modeling or field data could be used to obtain more reliable information.

Example Problem #5

Repeat Problem 1 for a channel width of 20 m and a discharge velocity of 0.25 m/sec.

Solution:

1. Determine A

Q is given Problem #1 to be 18.8 m^3/sec
H_o = 18.8/(20 x .25)= 3.76 m
A = 20/3.76 = 5.3

2. Determine F

Since the discharge ΔT_o is the same as Problem #1.

$$F = 0.25/[(.0026)(9.8)(3.76)]^{1/2} = 0.81$$

For a discharge Froude number less than 1.0, a cold water wedge probably exists which means the actual discharge velocity is greater than that indicated and the depth is less than estimated from calculations. The nomograms cannot handle this type of problem. Hydraulic modeling or field measurements could be used to find the actual values.

Example Problem #6

Repeat Problem #1 for the case where the bottom of the lake slopes away from the shore with a 5 meter drop for every 100 meters offshore. The bottom of the discharge channel is flush with the bottom of the lake.

Solution:

The problem with a sloping bottom is whether there is sufficient ambient water between the bottom of the plume and the bottom of the lake to ensure adequate entrainment as calculated by the model. To determine this, the depth of lake is compared with plume depth. If the plume depth is close to or greater than the bottom depth, the model fails and alternate methods of analysis or hydraulic modeling would have to be used.

The plume depth at various distances from discharge for Problem #1 can be found using nomogram A6 and A7 with R = .05 and interpolating to F = 4.6. The results are tabulated below along with the lake depth for selected values of S/H_0.

S/H_o	D/H_o	Lake Bottom 5:100 slope
10	1.5	1.5
20	2.1	2.0
30	2.25	2.5

Since the plume depth exceeds the lake depth, the analysis fails.

ACKNOWLEDGEMENT

The nomograms in this workbook were plotted by the computer. A program was prepared specially for this task by Mr. Kenneth V. Byram of the National Environmental Research Center in Corvallis. His valuable assistance is acknowledged with appreciation.

REFERENCES

1. Prych, Edmund A. "A Warm Water Effluent Analyzed as a Buoyant Surface Jet" Swedish Meteorological and Hydrological Institute, Series Hydology Report, No. 21, 1972, Stockholm.

2. Shirazi, Mostafa A., "Some Results from Experimental Data on Surface Jet Discharge of Heated Water" Proceedings of the International Water Resources Association, Chicago, 1973.

3. Stolzenbach, K. D., Harleman, D. R. F. "An Analytical and Experimental Investigation of Surface Discharges of Heated Water." Water Pollution Control Series 16130 DJV 02/71, Feb. 1971.

APPENDIX A
(TTWD) WORKING NOMOGRAMS

TABLE 1
Figure numbers for (TTWD) Working Nomograms
of Appendix A, $\Theta_o = 90°$ and $K = 10^{-5}$

F→ ↓A	2	4	6	10
1	A1	A2	A3	A4
5	A5	A6	A7	A8
10	A9	A10	A11	A12
15	A13	A14	A15	A16

TABLE 2
Summary of Figure Numbers for (TTWD)
Working Nomograms of Appendix A

Θ_o→ ↓K	90°	60°	120°
10^{-5}	A1-A16	A17-A32	A33-A48
10^{-4}	A49-A64	A65-A80	A81-A96
10^{-6}	A97-A112	A113-A128	A128-A144

NOTE: Figures A-37, 41, 45, 46, 85, 89, 93, 94, 133, 137, 141, 142 are not included due to computational difficulties.

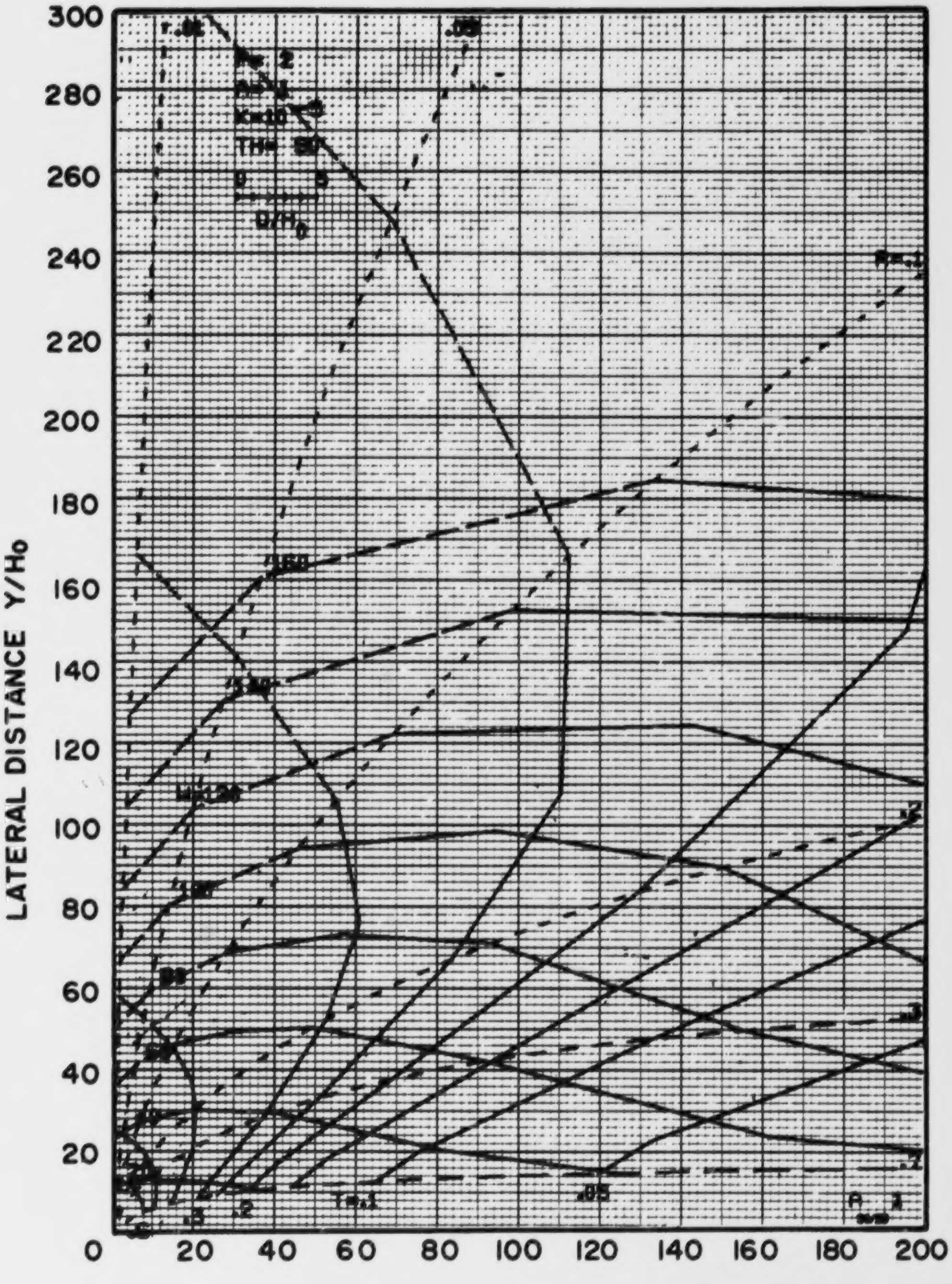

FIG(A1) TEMPERATURE, TRAJECTORY, WIDTH, AND DEPTH (TTWD)-PLOTS FOR SURFACE JET DISCHARGE

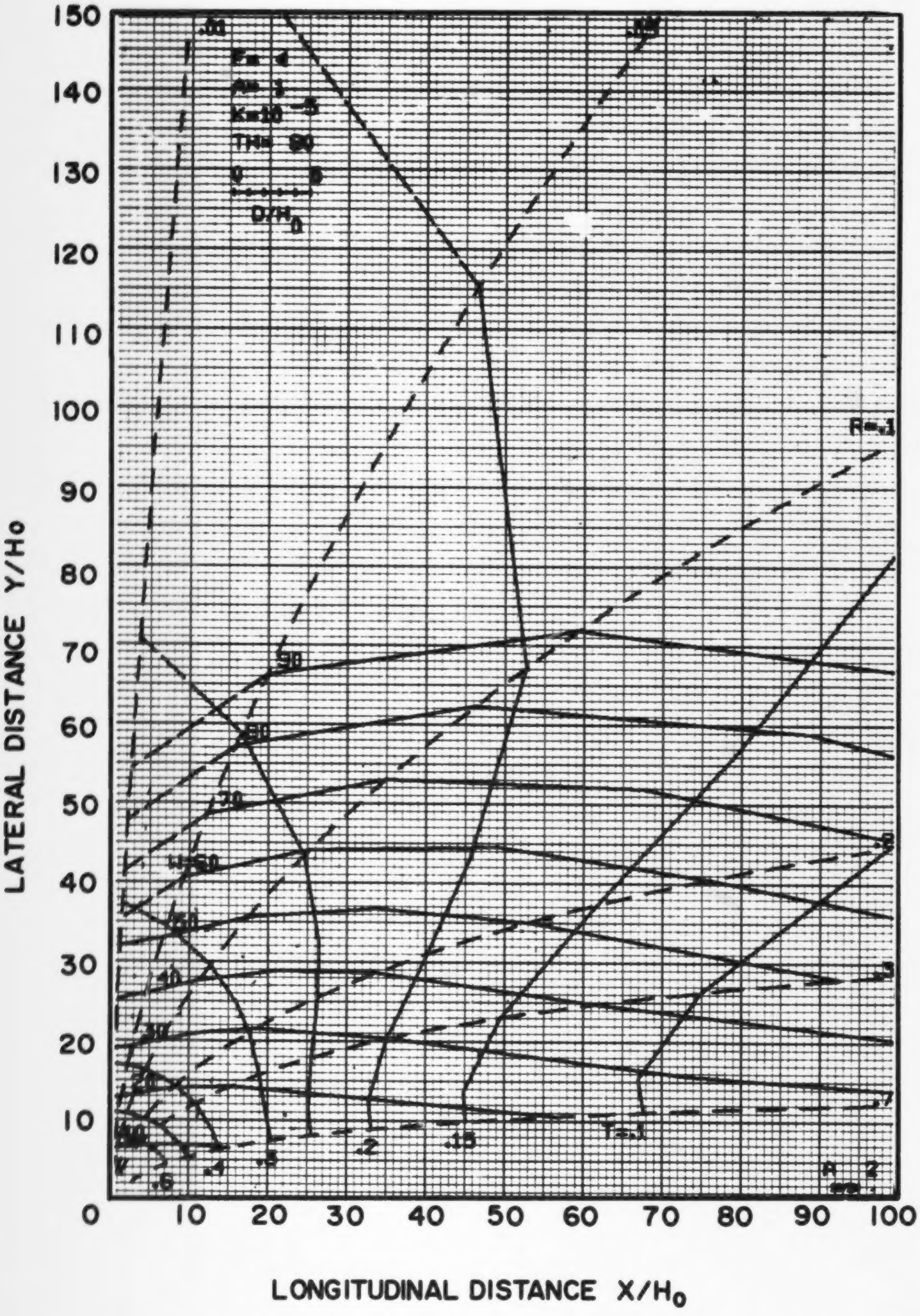

FIG(A2) TEMPERATURE, TRAJECTORY, WIDTH, AND DEPTH (TTWD)-PLOTS FOR SURFACE JET DISCHARGE

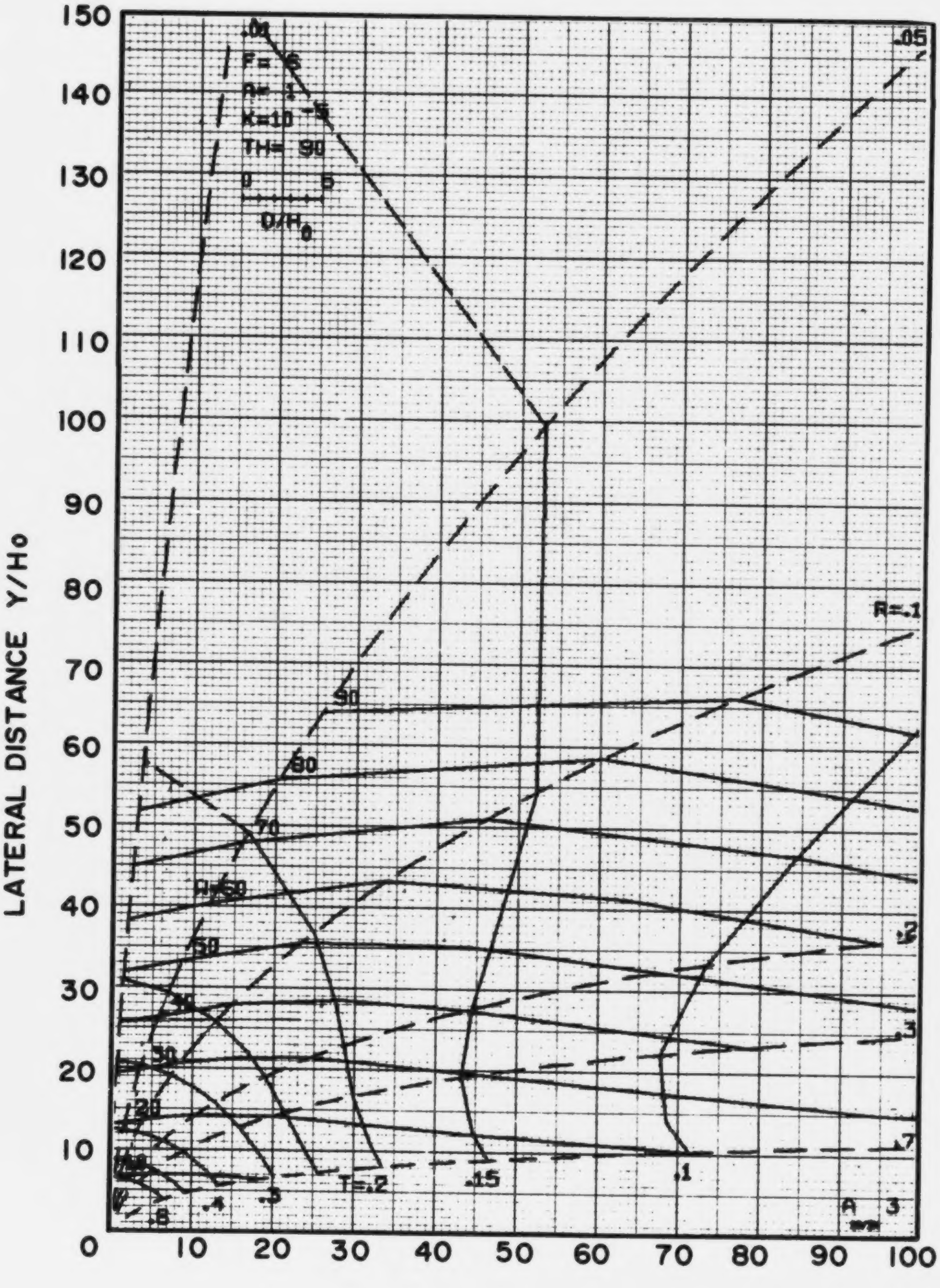

FIG(A3) TEMPERATURE, TRAJECTORY, WIDTH, AND DEPTH (TTWD)-PLOTS FOR SURFACE JET DISCHARGE

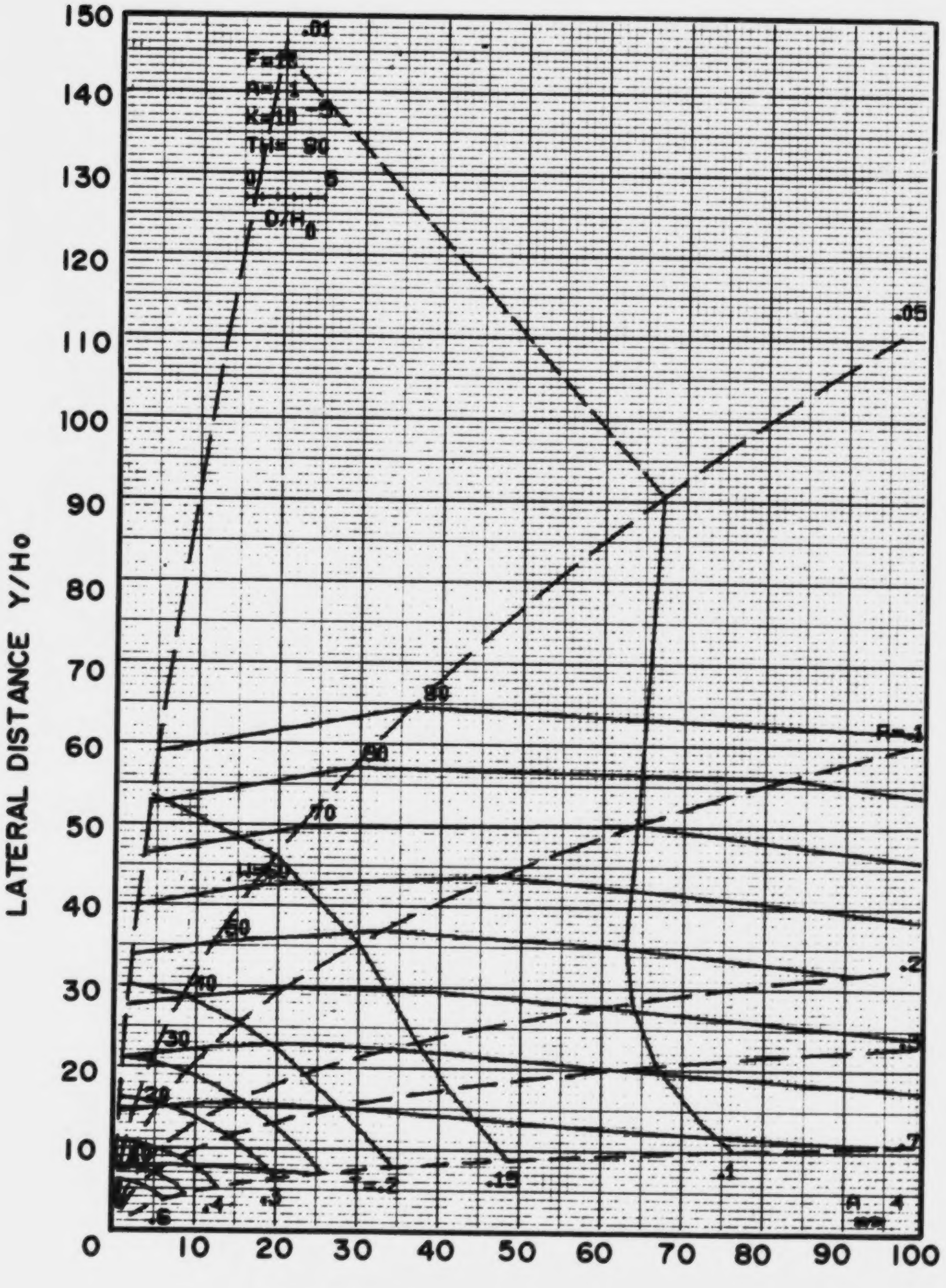

FIG(A4) TEMPERATURE, TRAJECTORY, WIDTH, AND DEPTH (TTWD)-PLOTS FOR SURFACE JET DISCHARGE

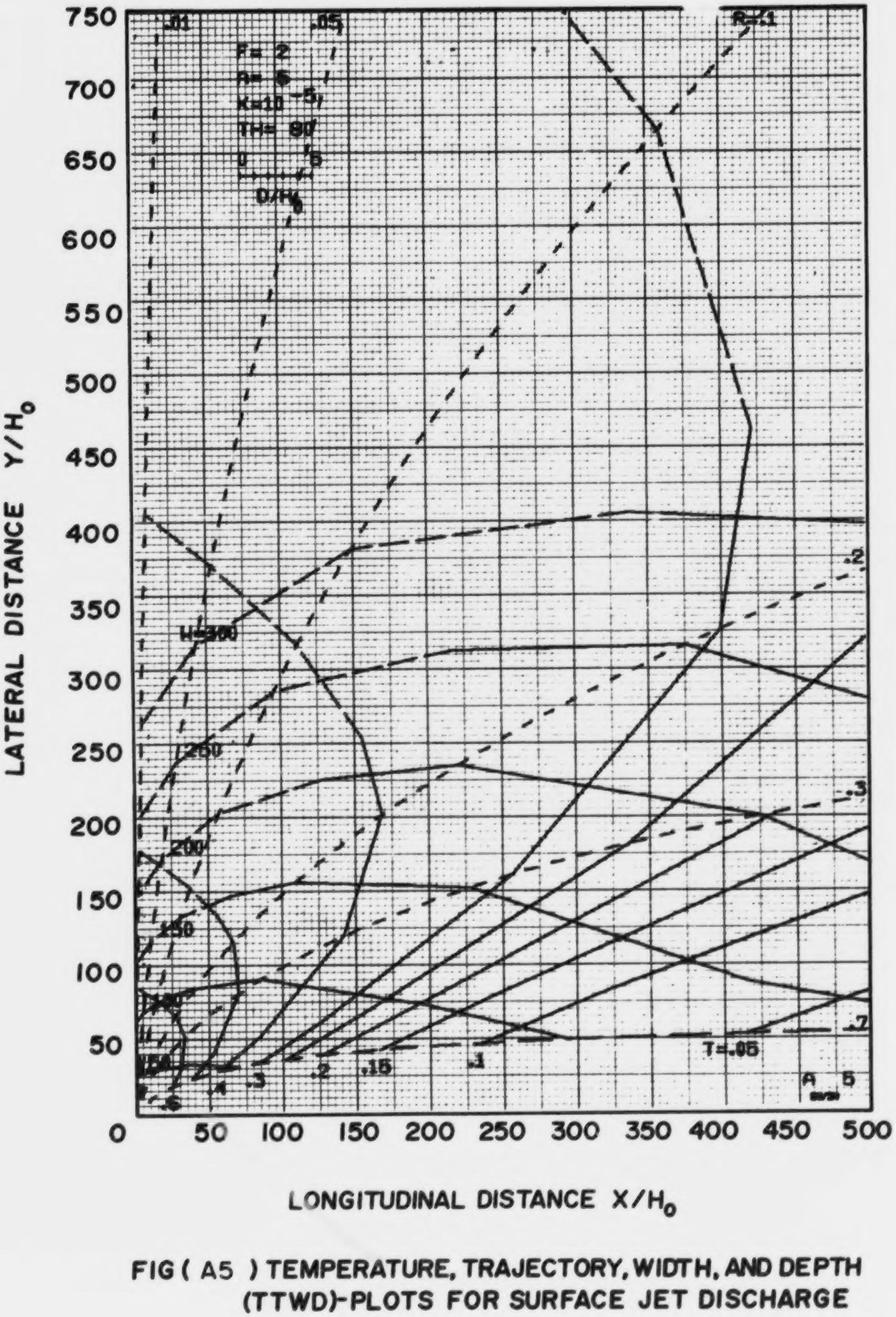

FIG (A5) TEMPERATURE, TRAJECTORY, WIDTH, AND DEPTH (TTWD)-PLOTS FOR SURFACE JET DISCHARGE

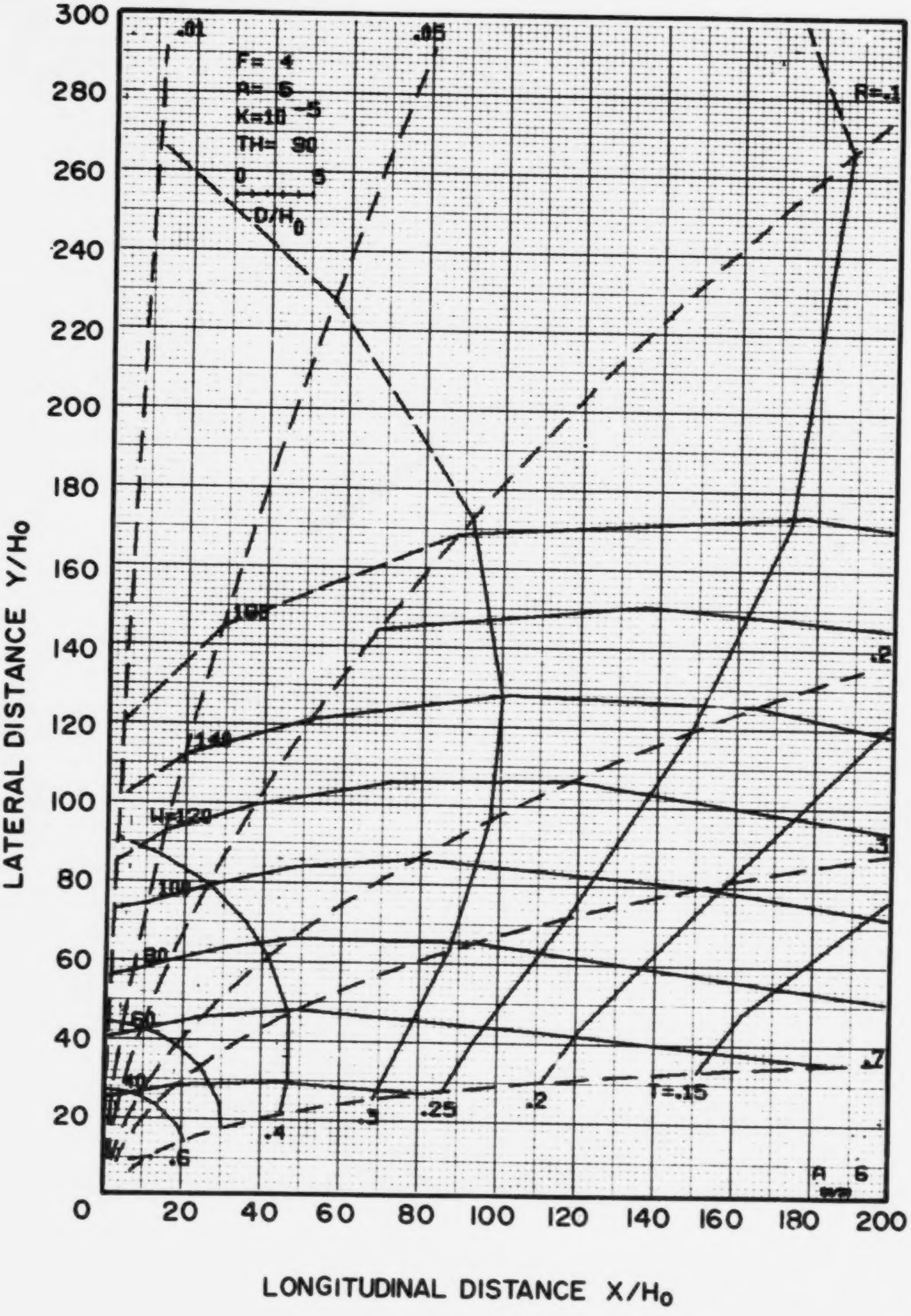

FIG(A6) TEMPERATURE, TRAJECTORY, WIDTH, AND DEPTH (TTWD)-PLOTS FOR SURFACE JET DISCHARGE

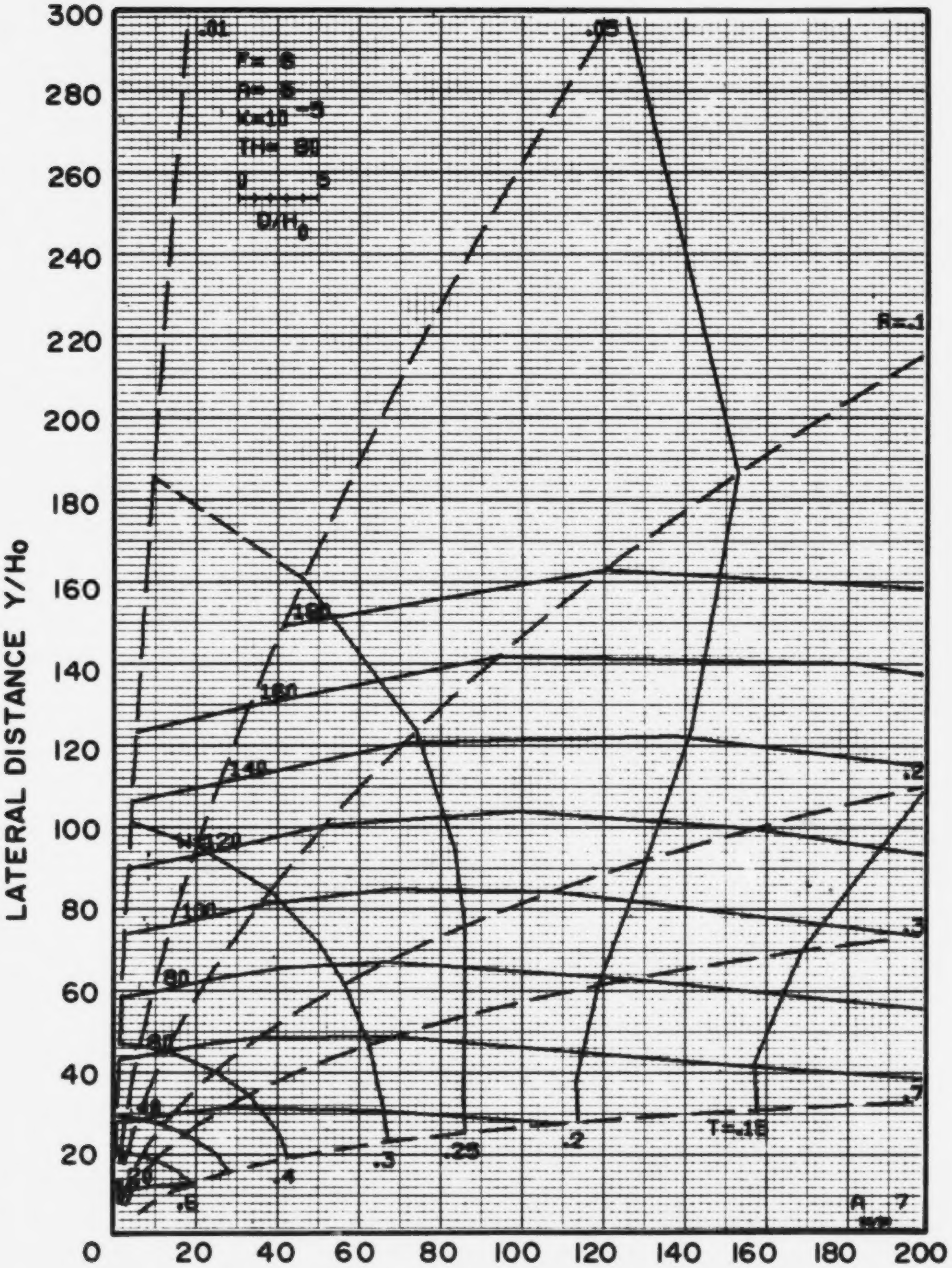

FIG(A7) TEMPERATURE, TRAJECTORY, WIDTH, AND DEPTH (TTWD)-PLOTS FOR SURFACE JET DISCHARGE

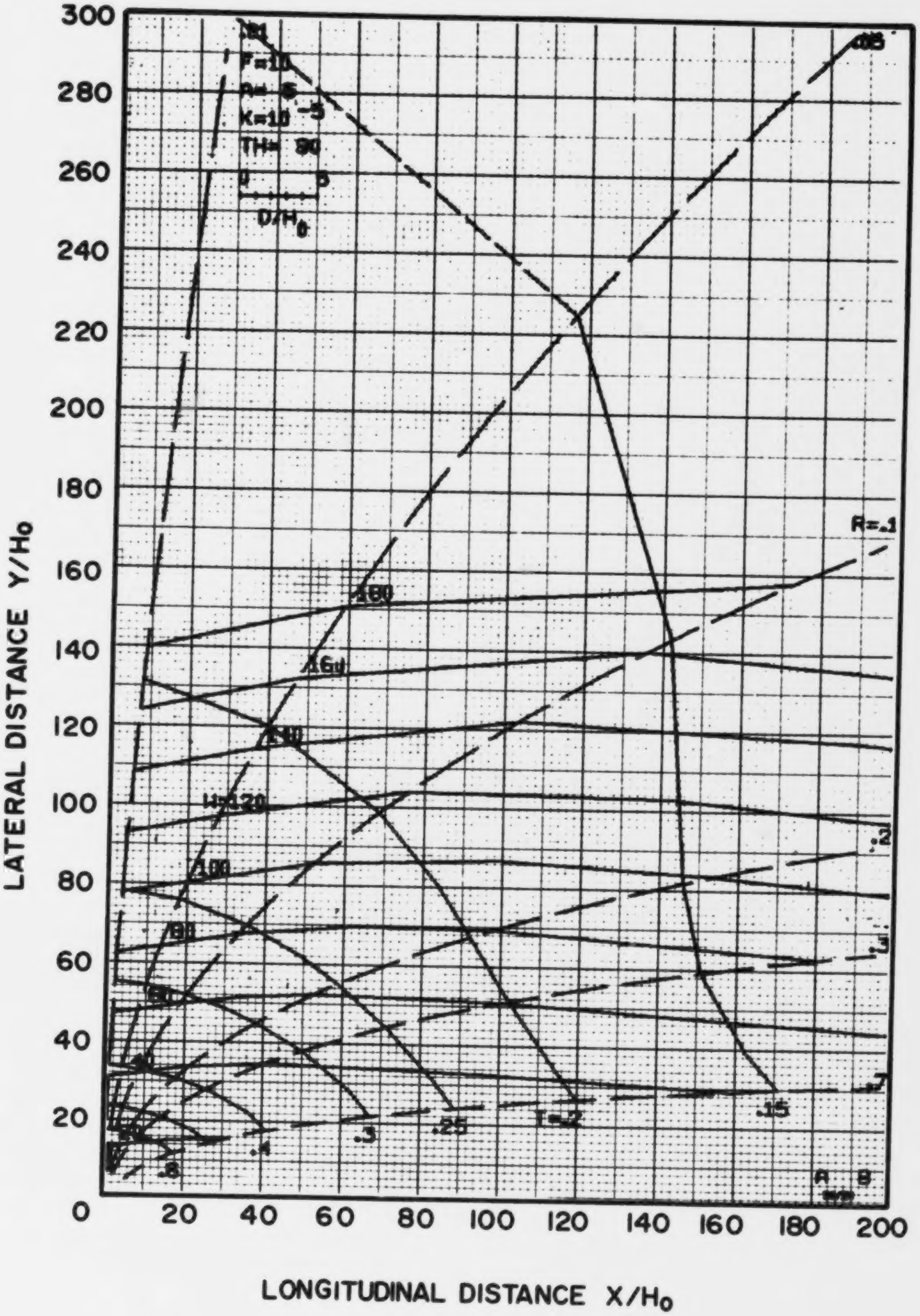

FIG(A8) TEMPERATURE, TRAJECTORY, WIDTH, AND DEPTH (TTWD)-PLOTS FOR SURFACE JET DISCHARGE

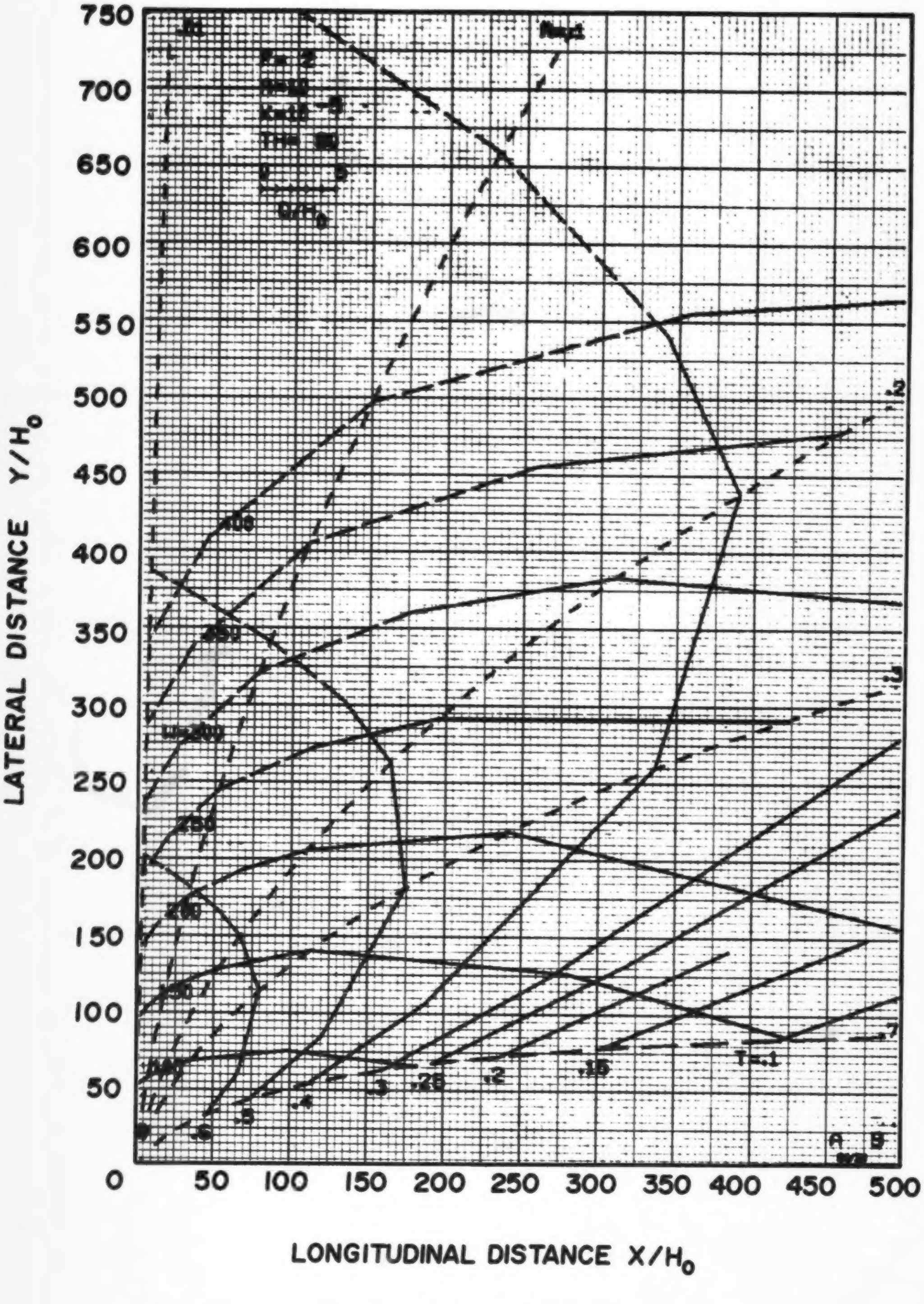

FIG (A9) TEMPERATURE, TRAJECTORY, WIDTH, AND DEPTH (TTWD)-PLOTS FOR SURFACE JET DISCHARGE

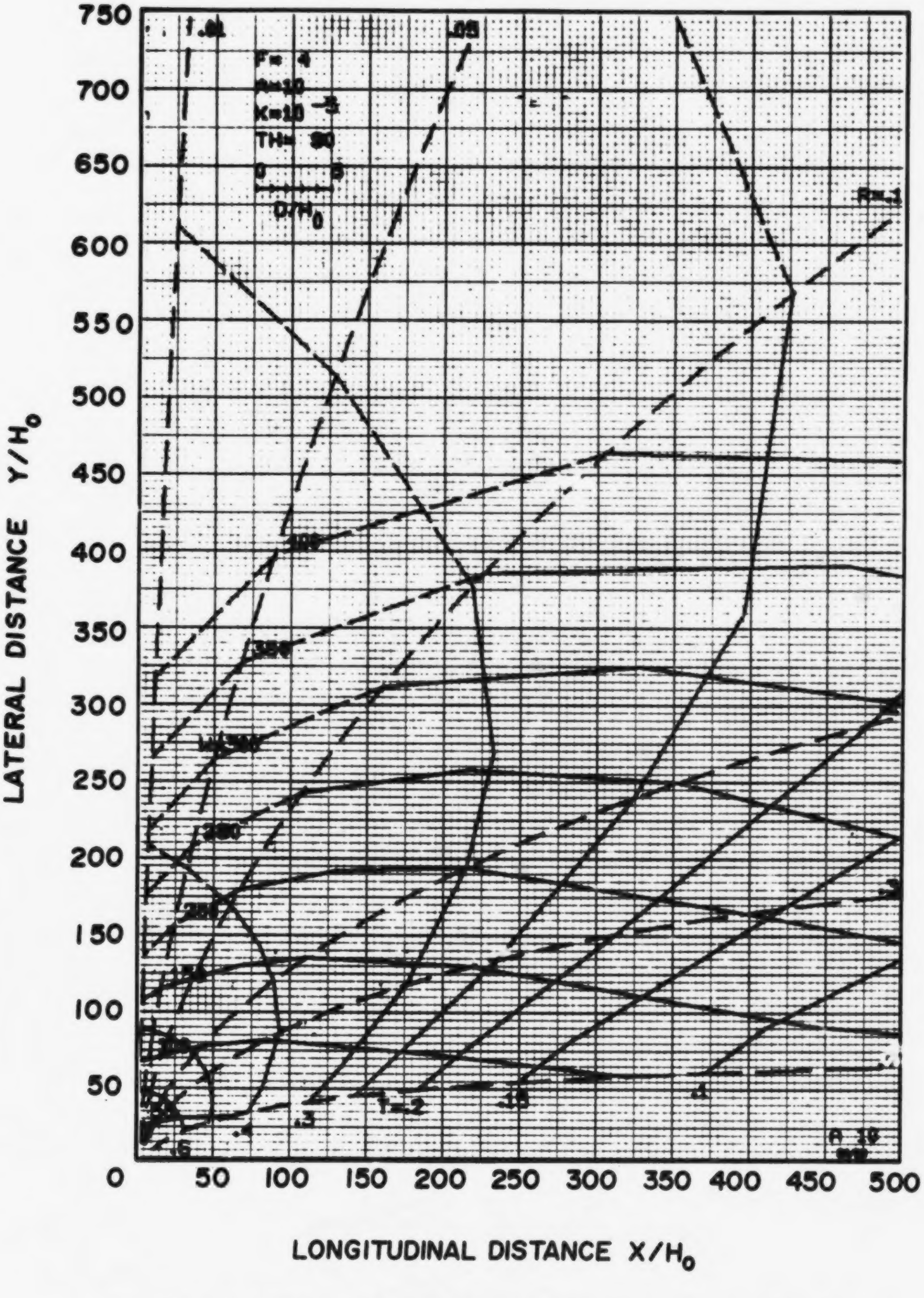

FIG (A10) TEMPERATURE, TRAJECTORY, WIDTH, AND DEPTH (TTWD)-PLOTS FOR SURFACE JET DISCHARGE

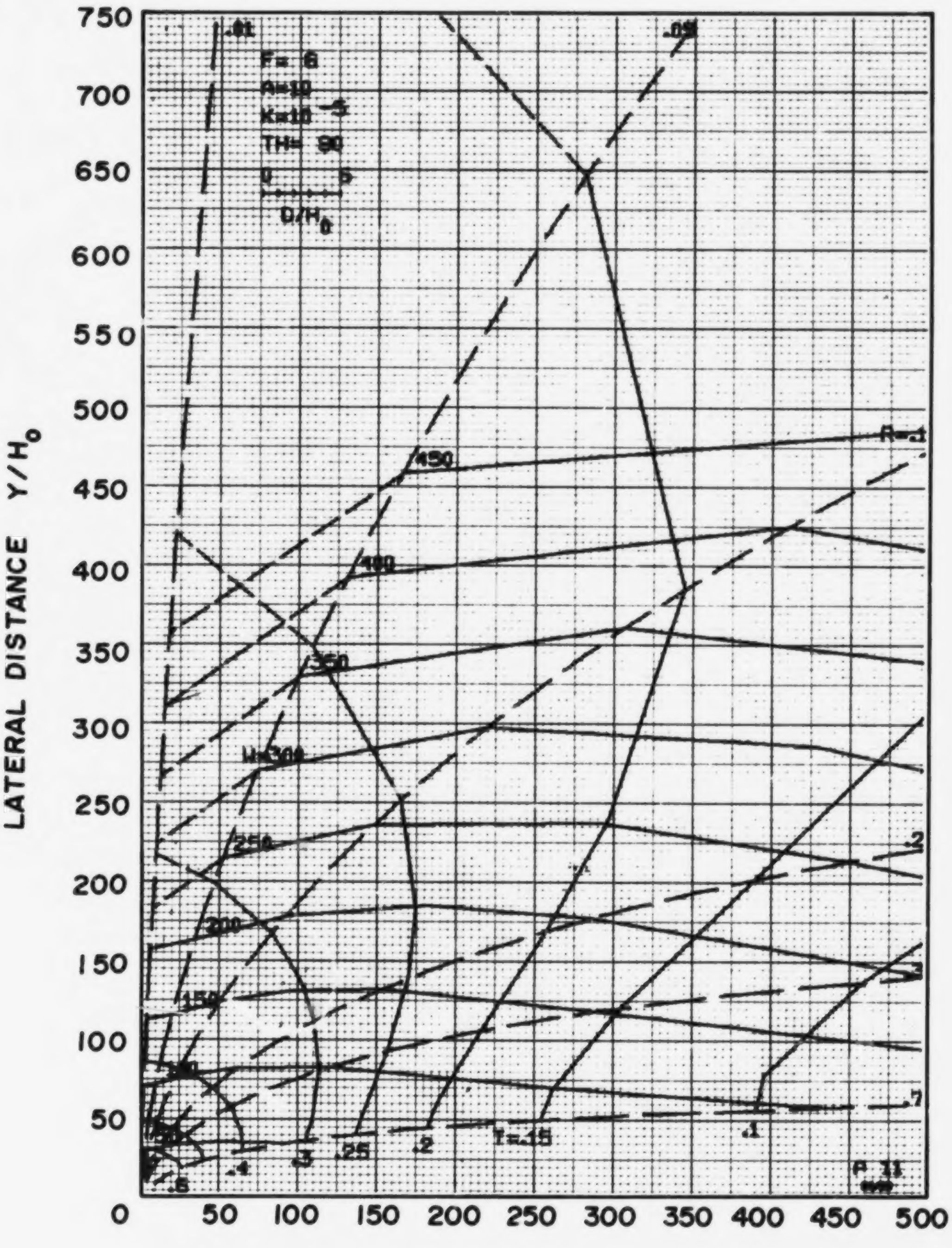

FIG (AII) TEMPERATURE, TRAJECTORY, WIDTH, AND DEPTH (TTWD)-PLOTS FOR SURFACE JET DISCHARGE

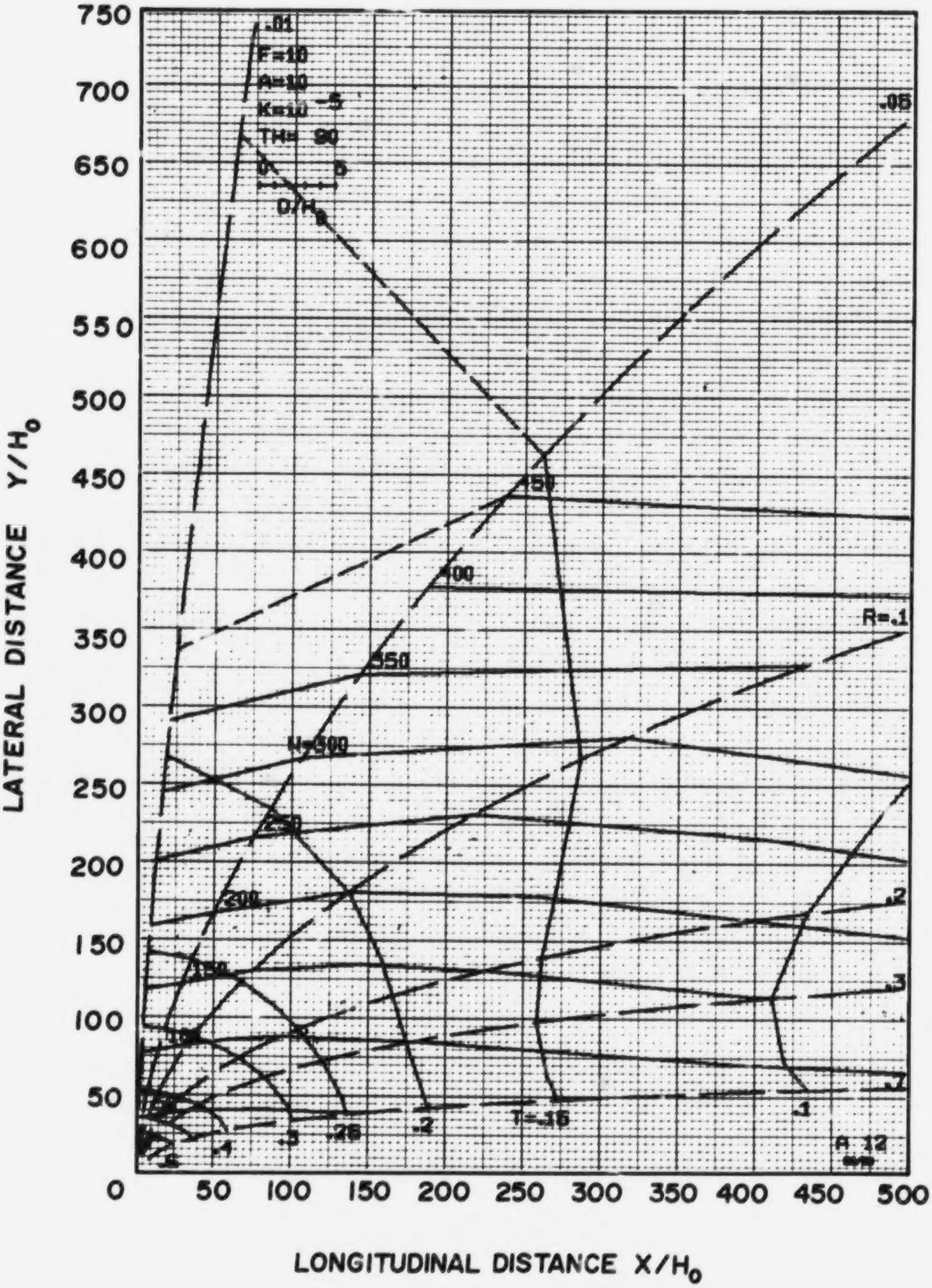

FIG (A12) TEMPERATURE, TRAJECTORY, WIDTH, AND DEPTH (TTWD)-PLOTS FOR SURFACE JET DISCHARGE

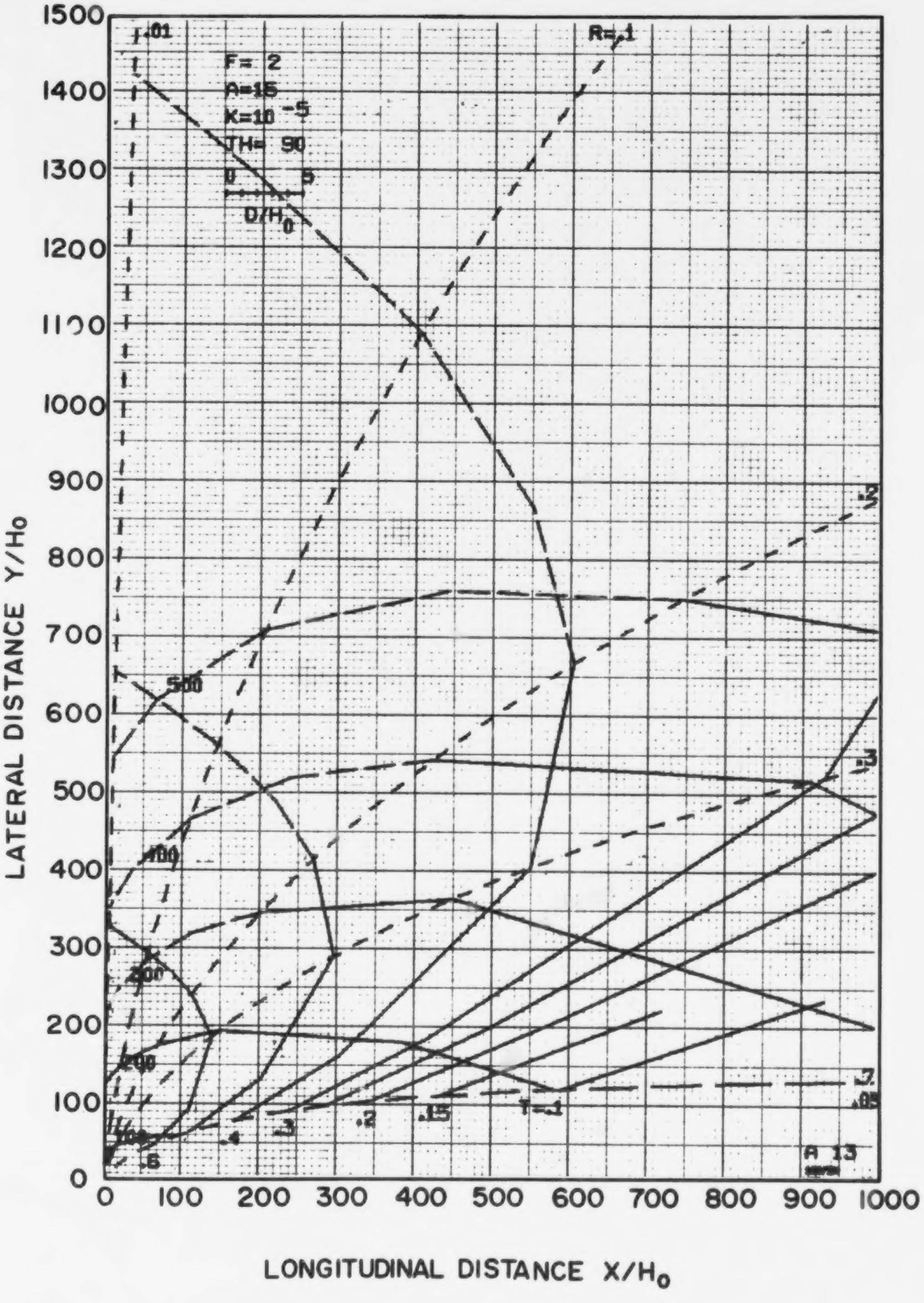

FIG (A13) TEMPERATURE, TRAJECTORY, WIDTH, AND DEPTH (TTWD)-PLOTS FOR SURFACE JET DISCHARGE

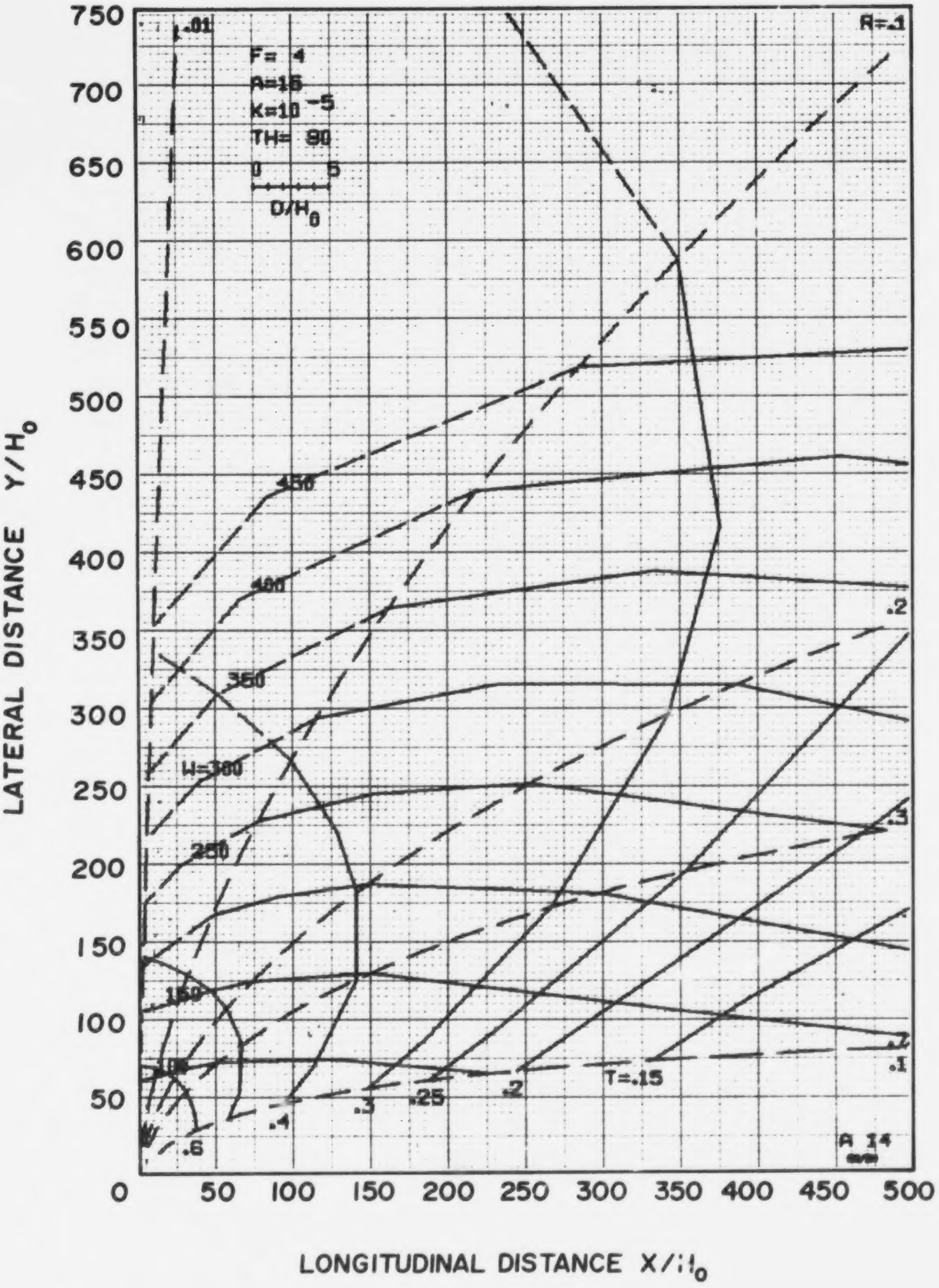

FIG (A14) TEMPERATURE, TRAJECTORY, WIDTH, AND DEPTH (TTWD)-PLOTS FOR SURFACE JET DISCHARGE

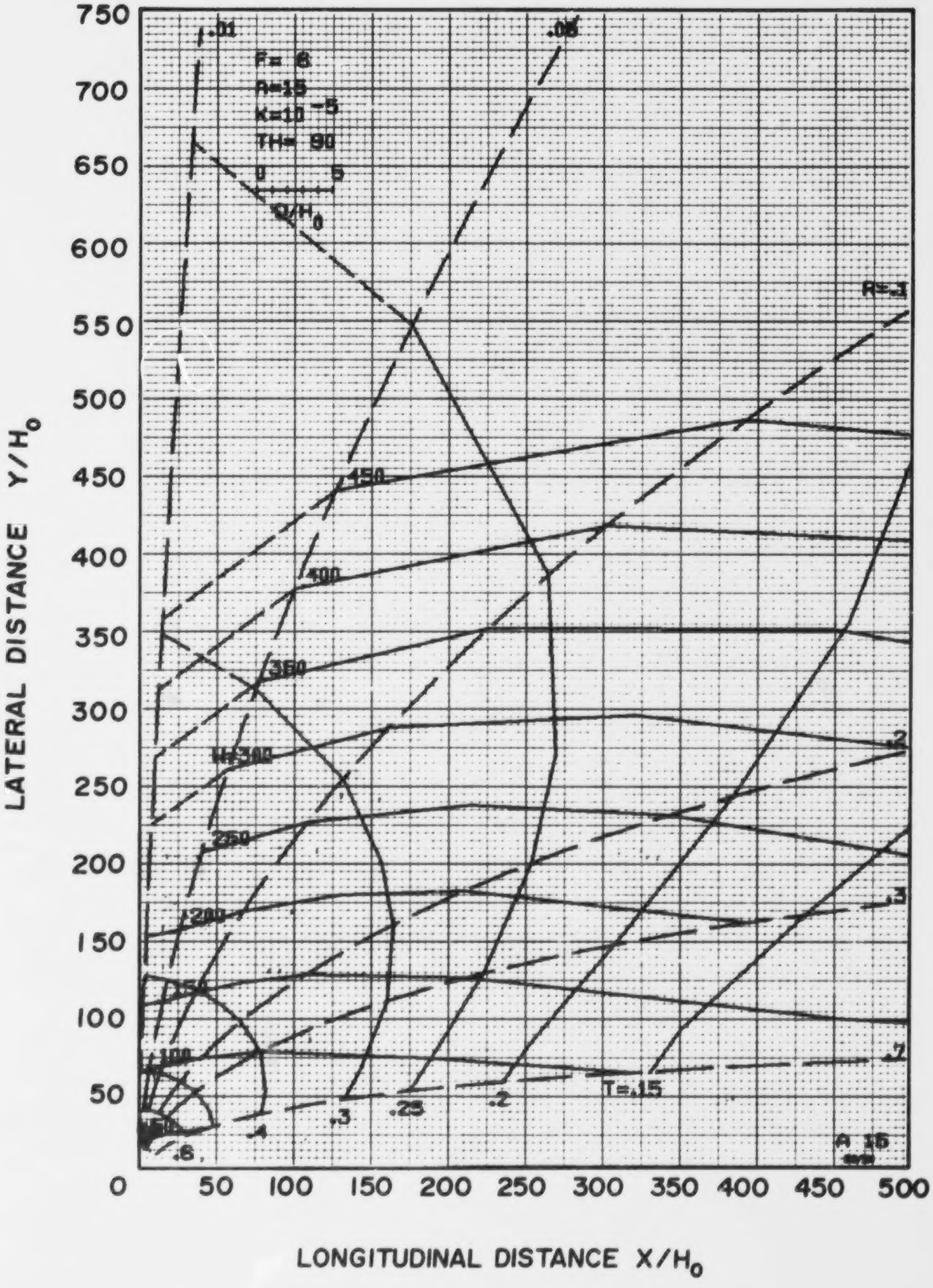

FIG (A15) TEMPERATURE, TRAJECTORY, WIDTH, AND DEPTH (TTWD)-PLOTS FOR SURFACE JET DISCHARGE

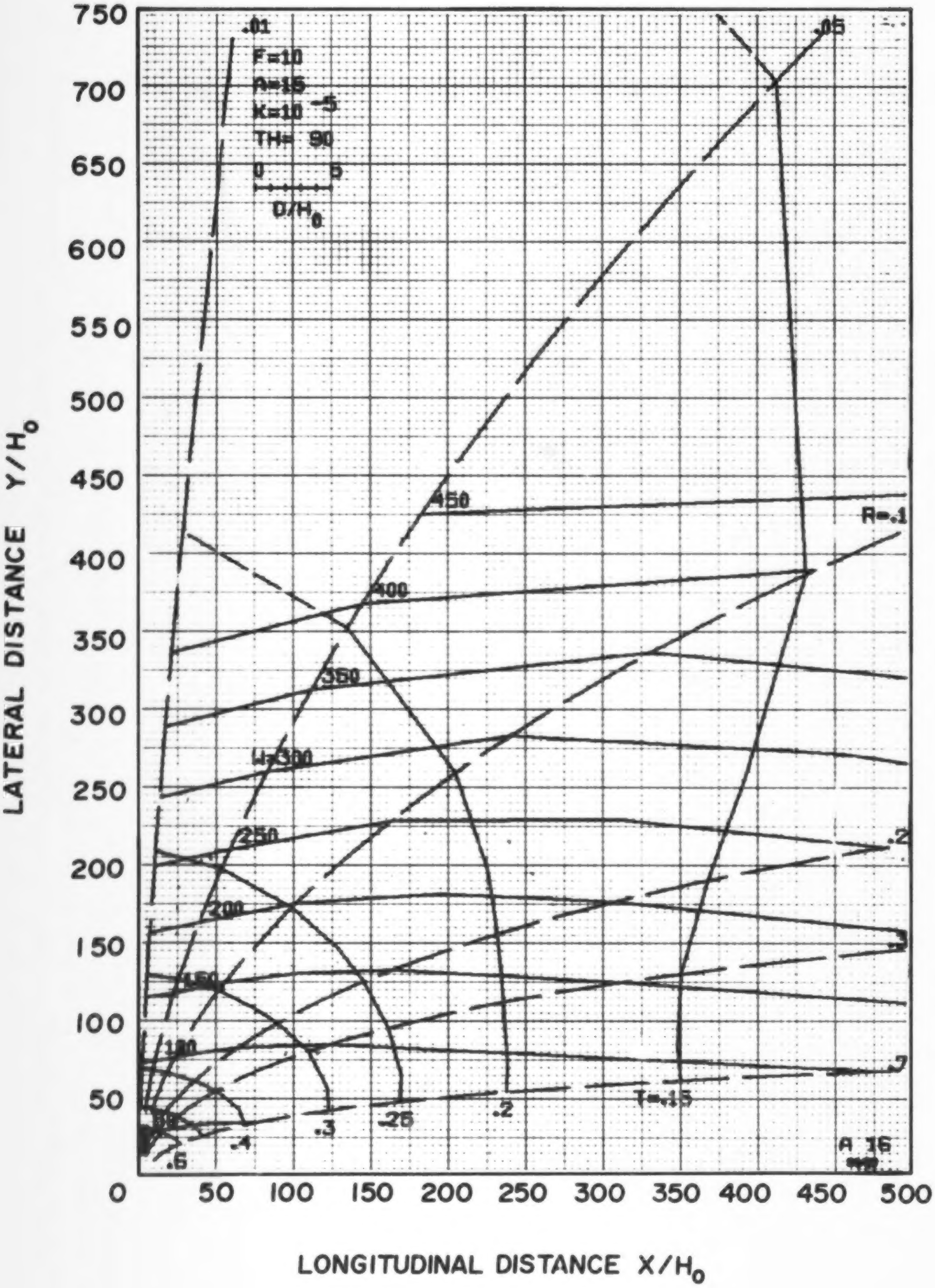

FIG (A16) TEMPERATURE, TRAJECTORY, WIDTH, AND DEPTH (TTWD)-PLOTS FOR SURFACE JET DISCHARGE

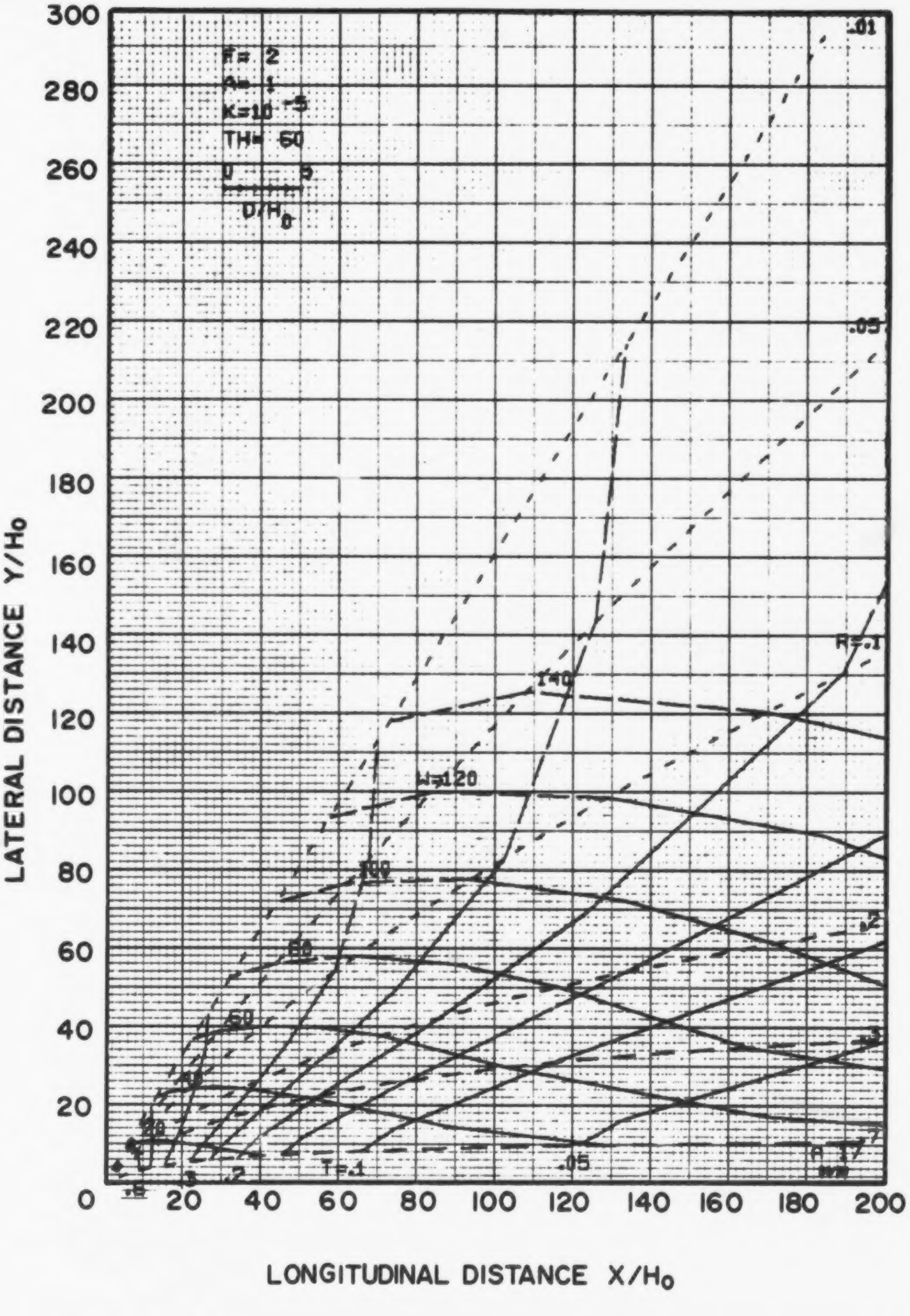

FIG(A17) TEMPERATURE, TRAJECTORY, WIDTH, AND DEPTH (TTWD)-PLOTS FOR SURFACE JET DISCHARGE

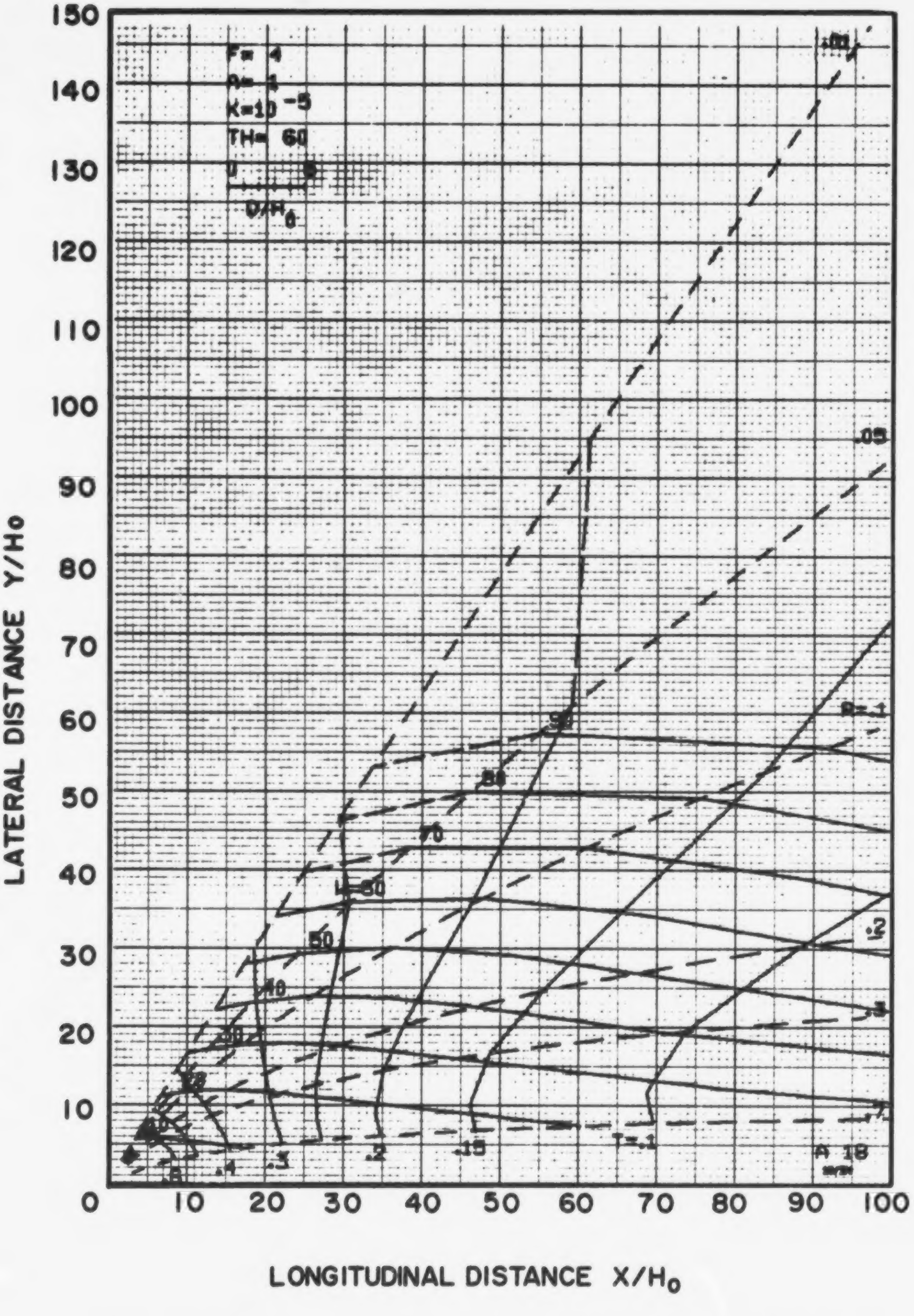

FIG(A18) TEMPERATURE, TRAJECTORY, WIDTH, AND DEPTH (TTWD)-PLOTS FOR SURFACE JET DISCHARGE

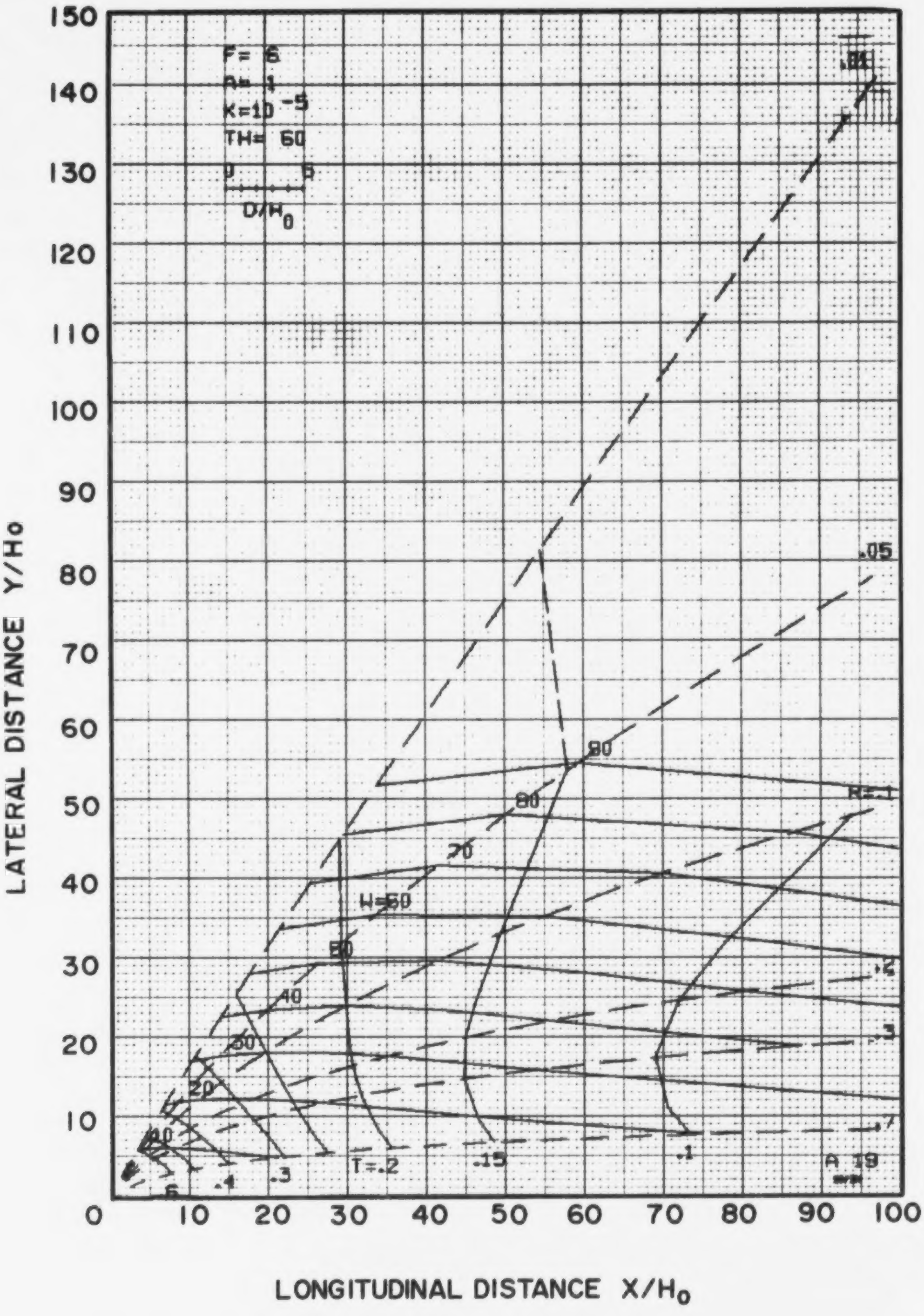

FIG(A19) TEMPERATURE, TRAJECTORY, WIDTH, AND DEPTH (TTWD)-PLOTS FOR SURFACE JET DISCHARGE

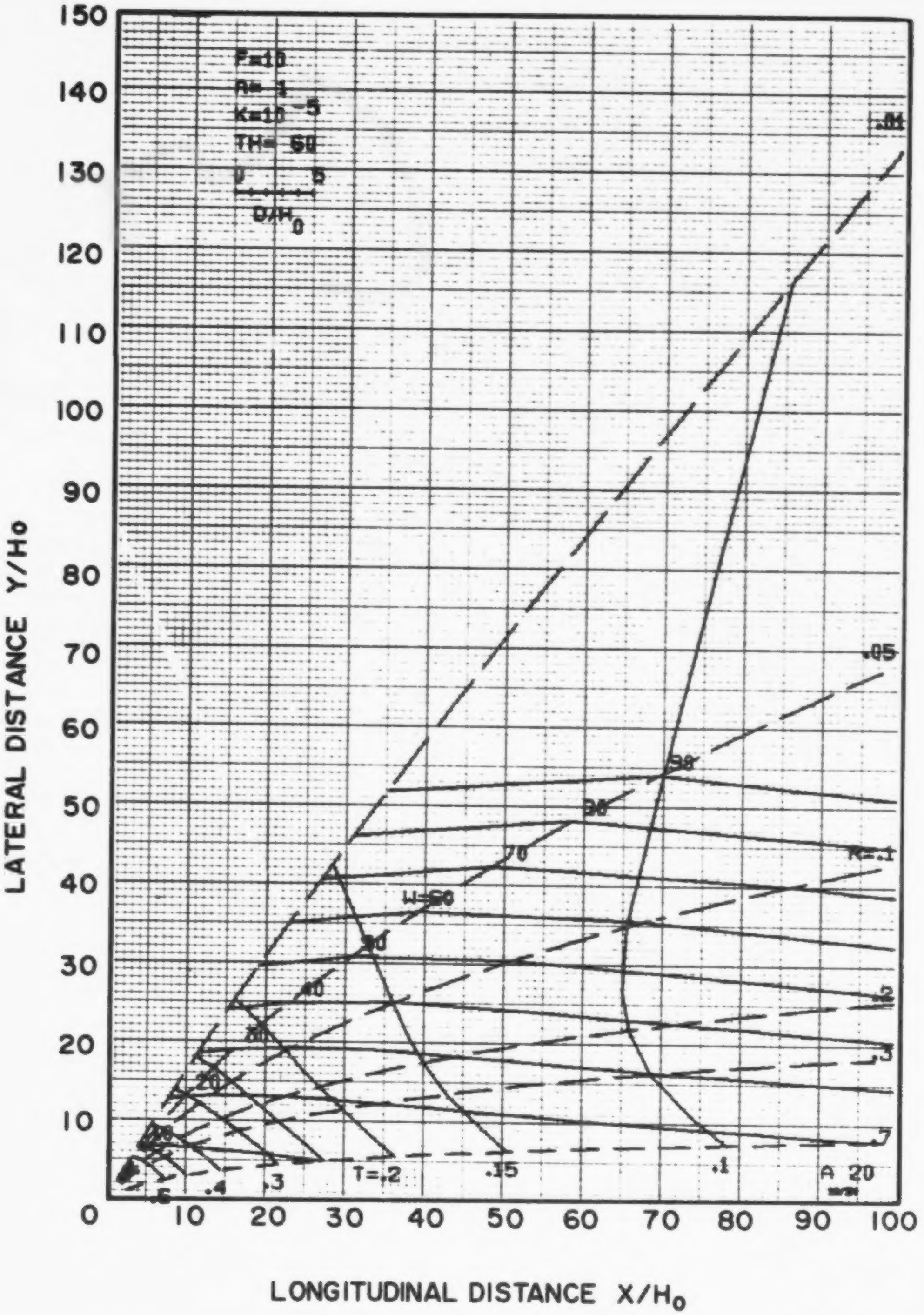

FIG(A20) TEMPERATURE, TRAJECTORY, WIDTH, AND DEPTH (TTWD)-PLOTS FOR SURFACE JET DISCHARGE

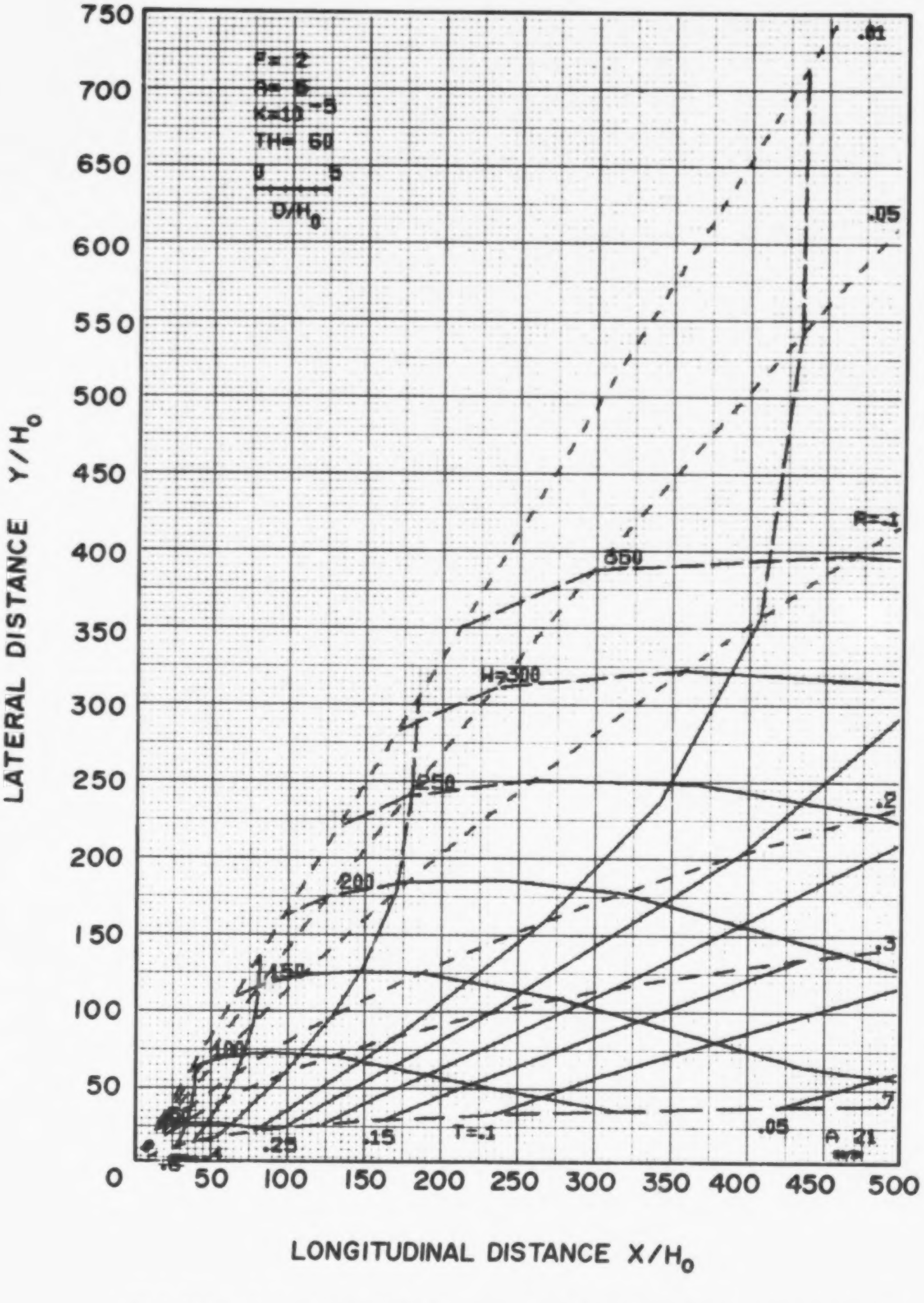

FIG (A21) TEMPERATURE, TRAJECTORY, WIDTH, AND DEPTH (TTWD)-PLOTS FOR SURFACE JET DISCHARGE

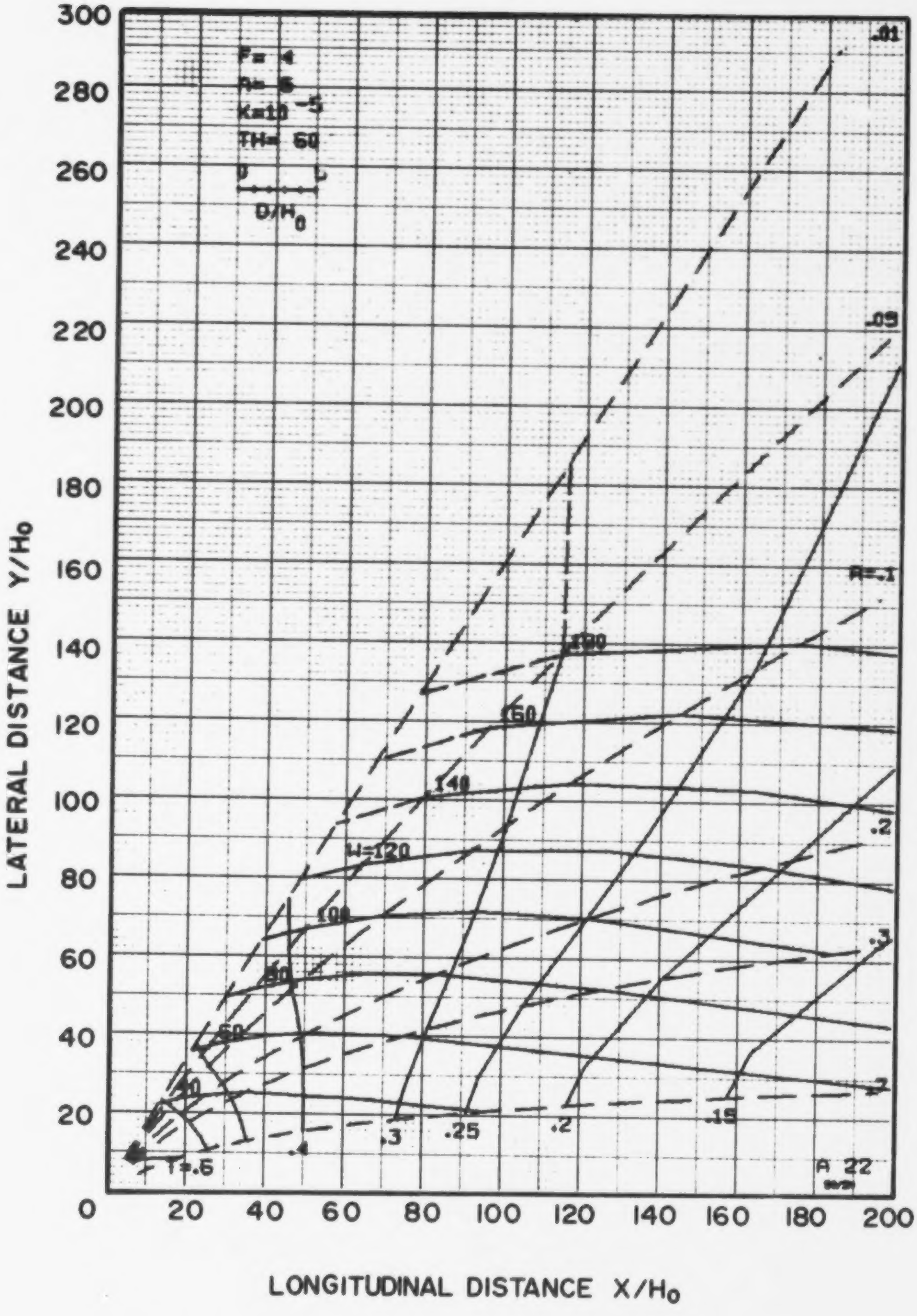

FIG (A22) TEMPERATURE, TRAJECTORY, WIDTH, AND DEPTH (TTWD)-PLOTS FOR SURFACE JET DISCHARGE

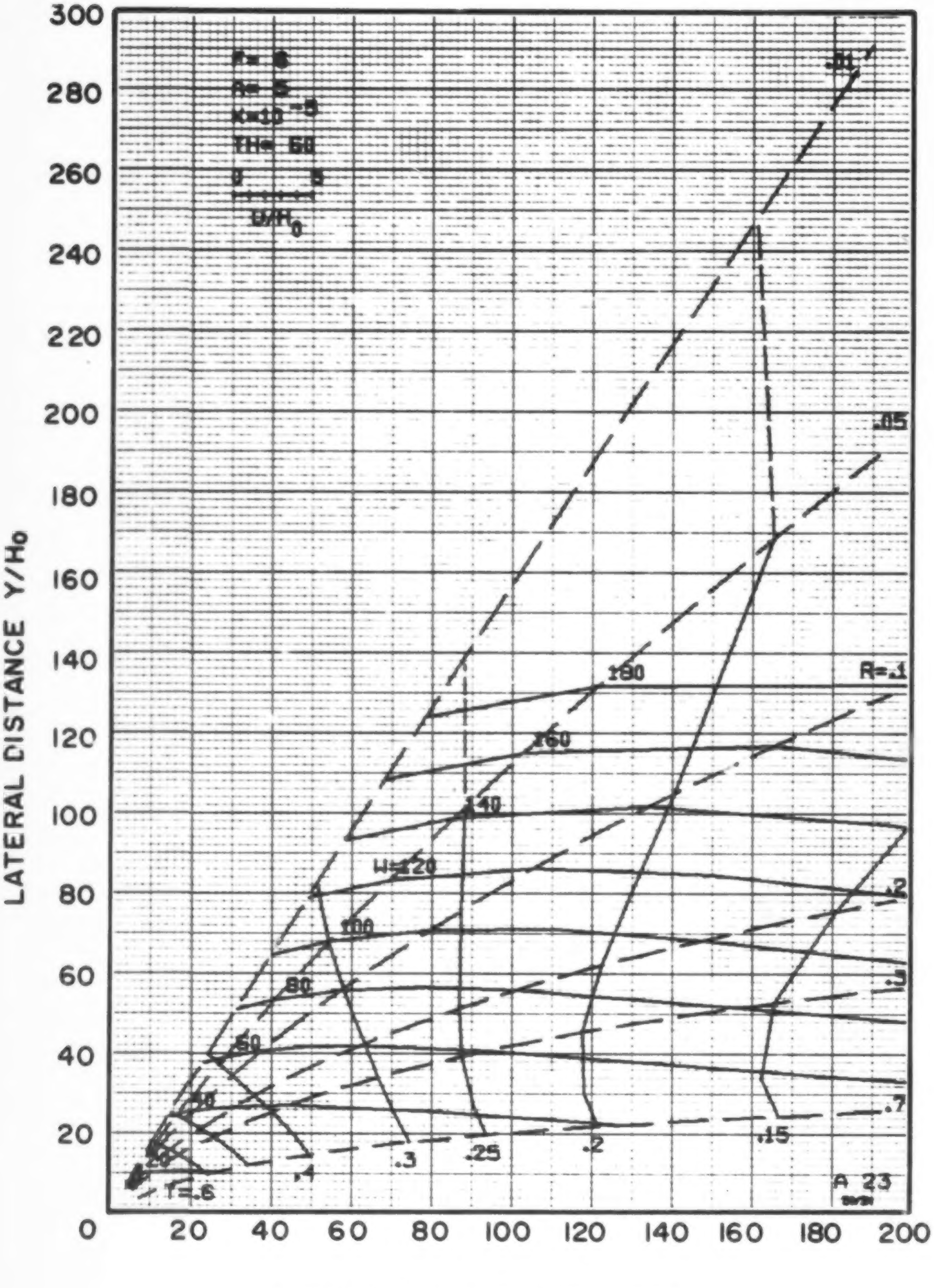

FIG (A23) TEMPERATURE, TRAJECTORY, WIDTH, AND DEPTH (TTWD)-PLOTS FOR SURFACE JET DISCHARGE

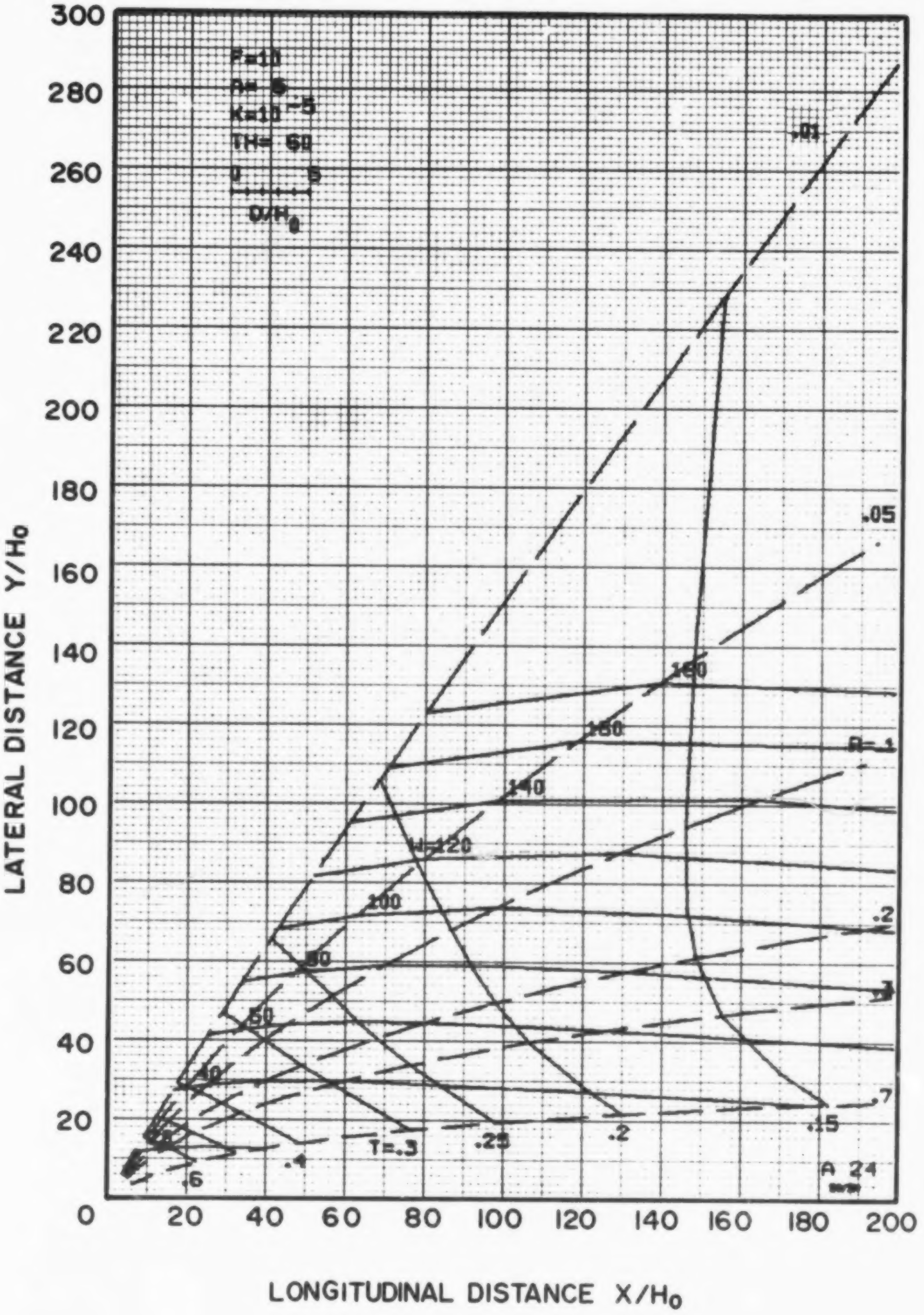

FIG (A24) TEMPERATURE, TRAJECTORY, WIDTH, AND DEPTH (TTWD)-PLOTS FOR SURFACE JET DISCHARGE

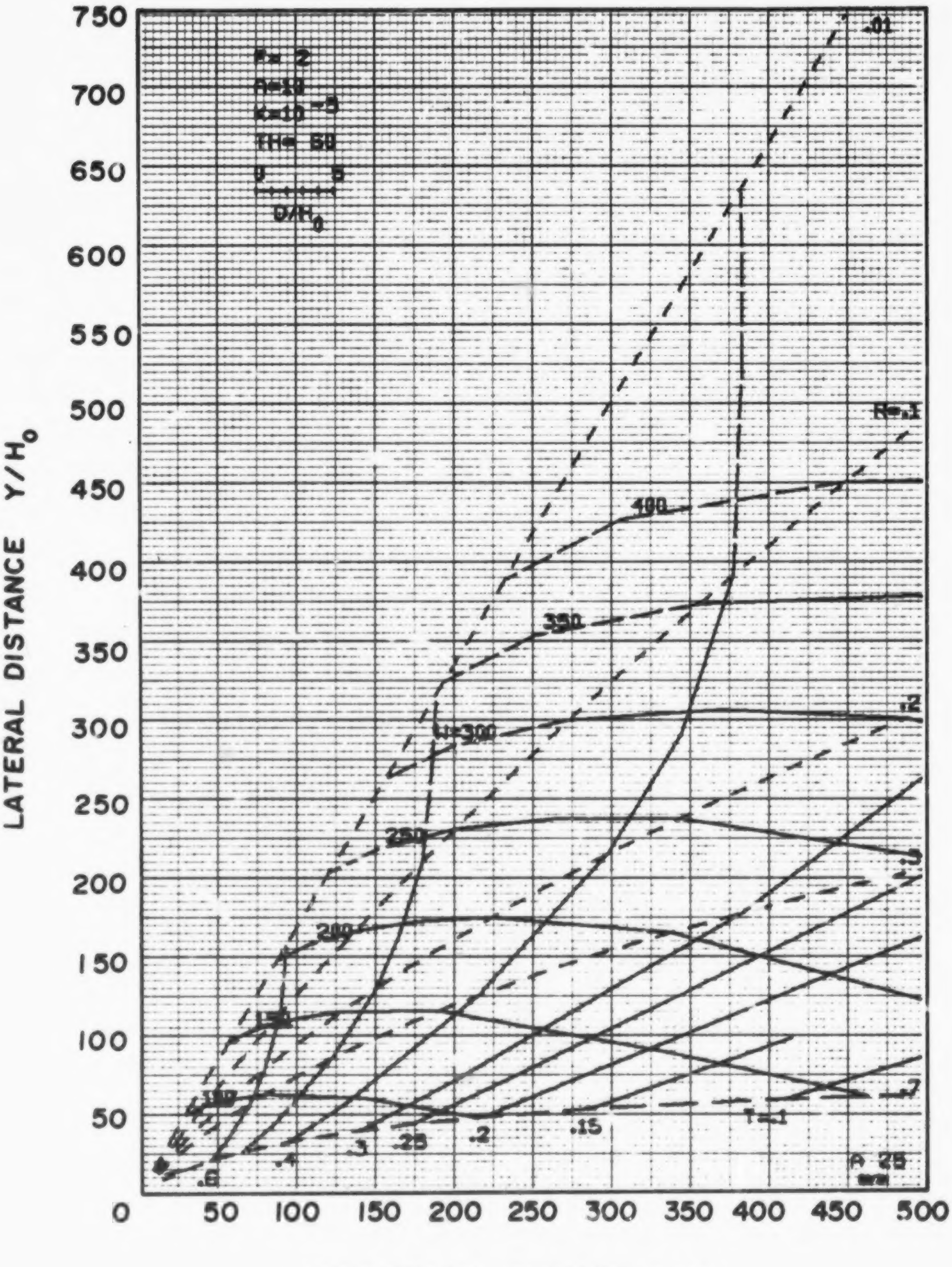

FIG (A25) TEMPERATURE, TRAJECTORY, WIDTH, AND DEPTH (TTWD)-PLOTS FOR SURFACE JET DISCHARGE

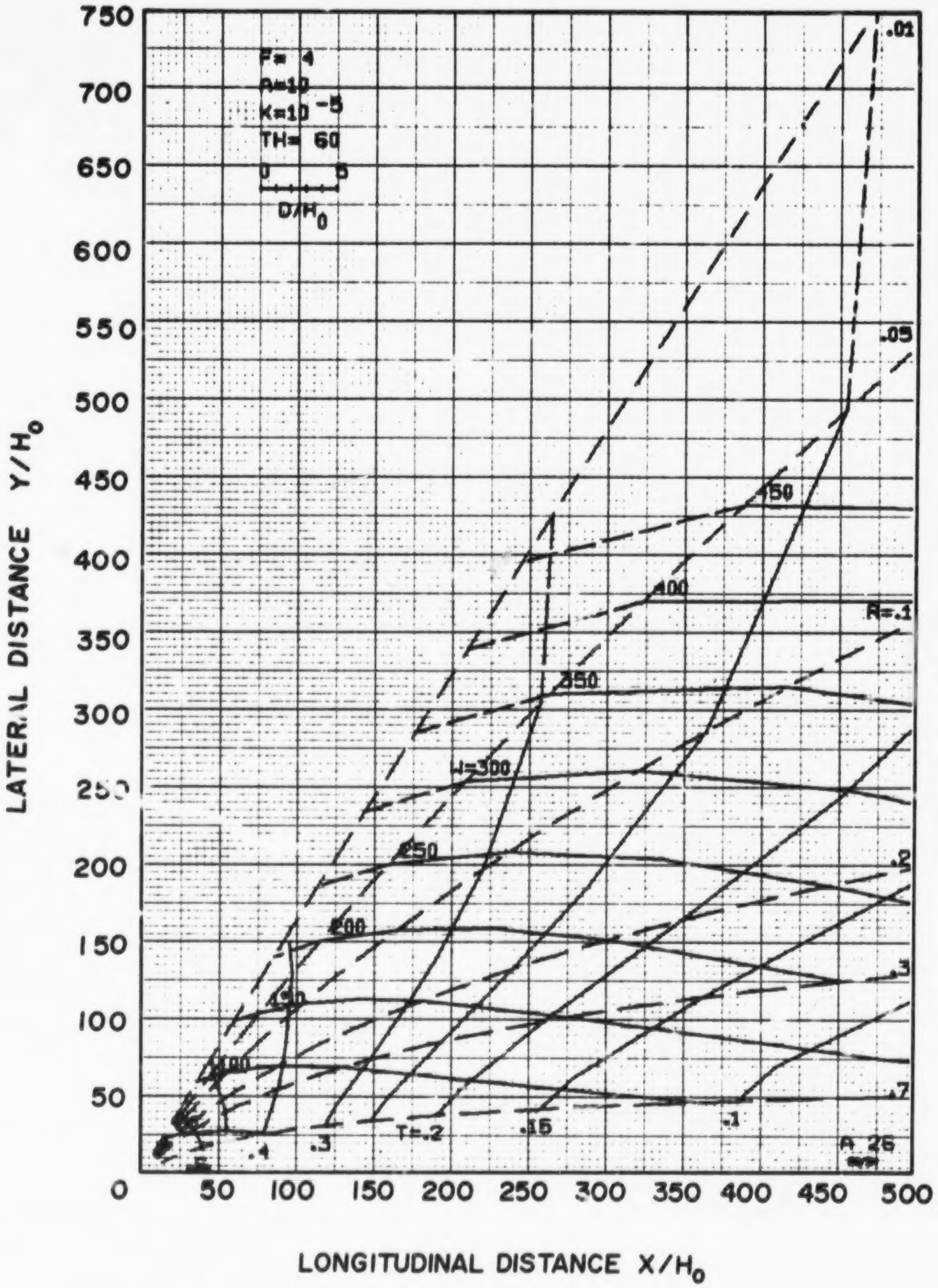

FIG (A26) TEMPERATURE, TRAJECTORY, WIDTH, AND DEPTH (TTWD)-PLOTS FOR SURFACE JET DISCHARGE

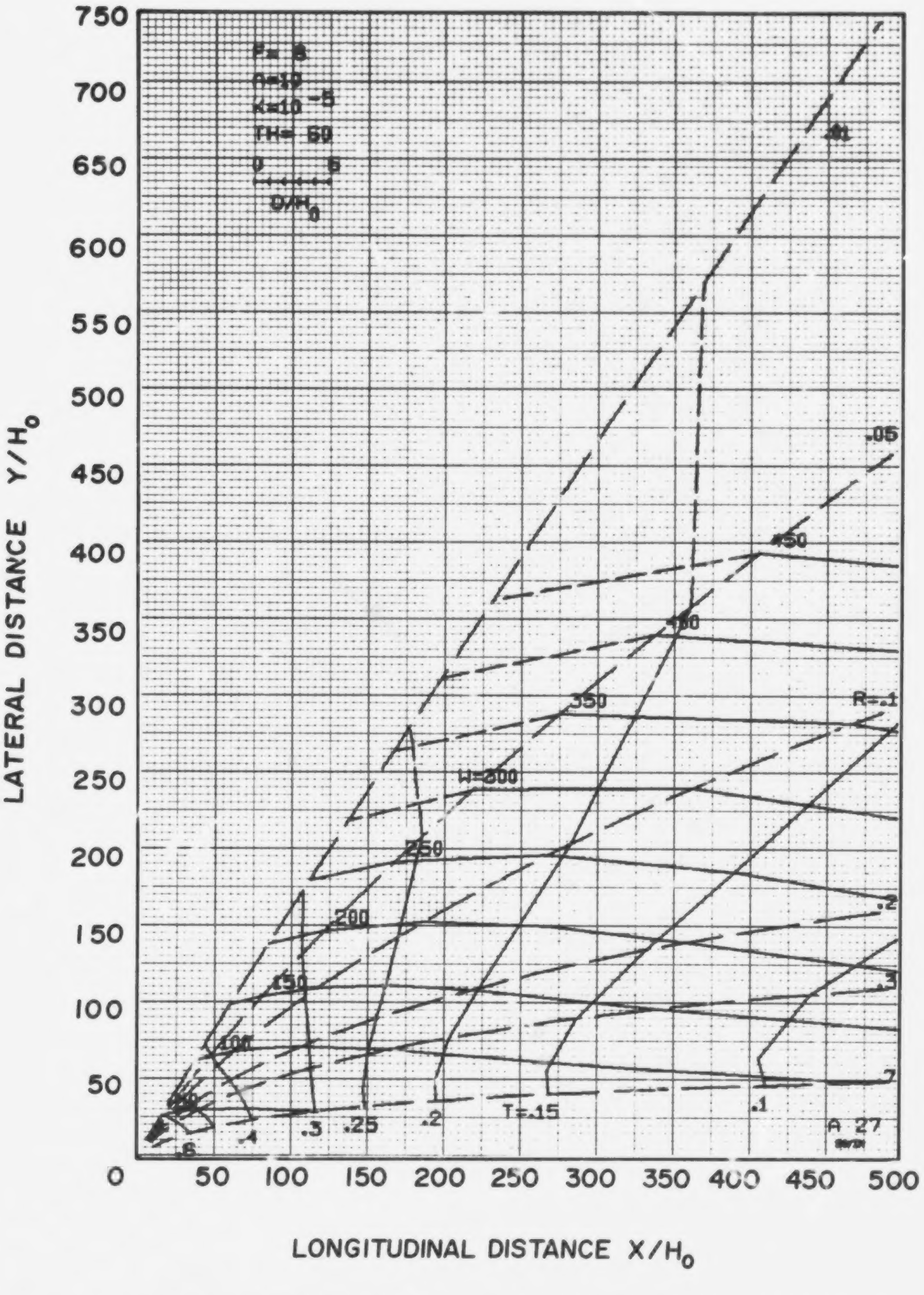

FIG (A27) TEMPERATURE, TRAJECTORY, WIDTH, AND DEPTH (TTWD)-PLOTS FOR SURFACE JET DISCHARGE

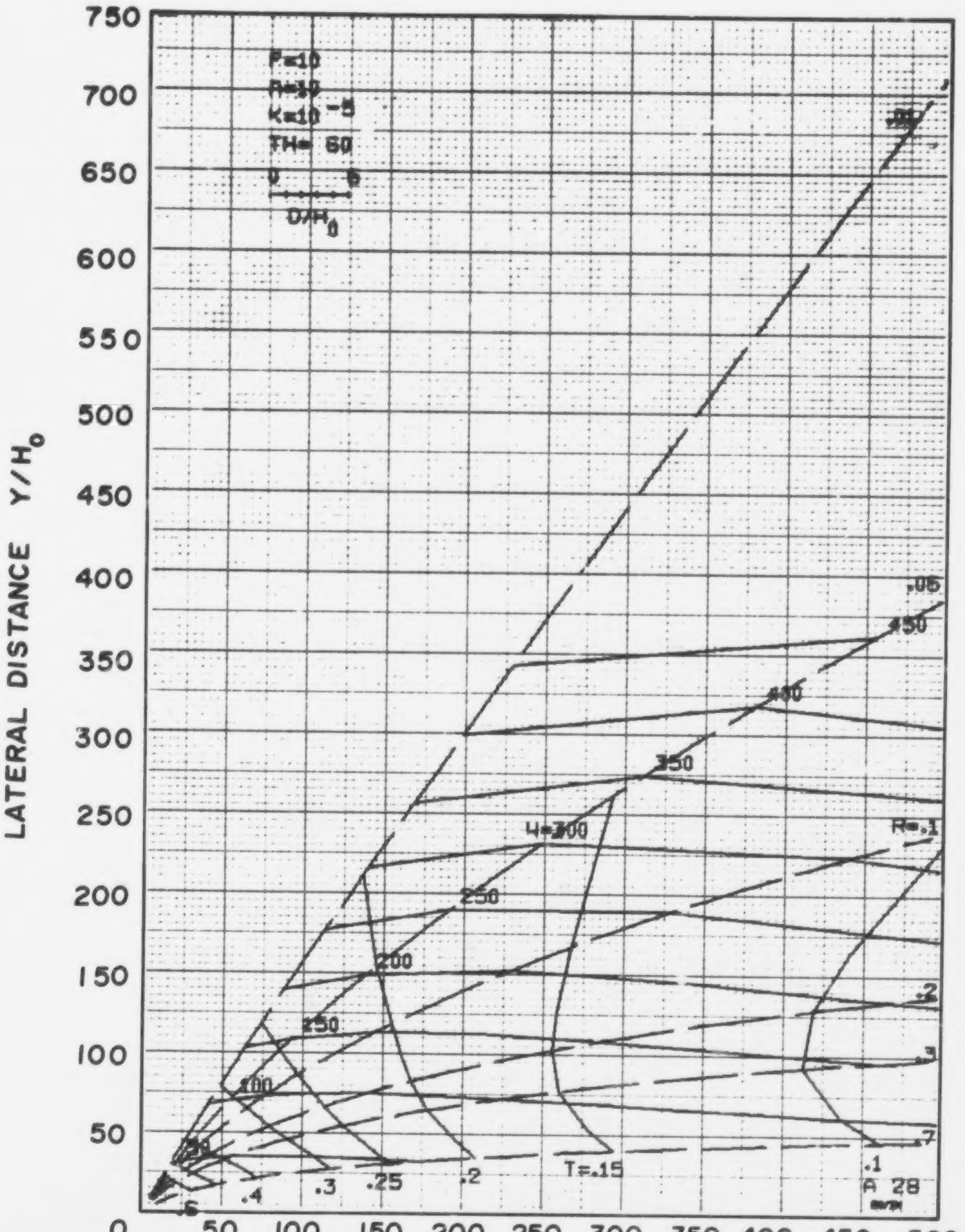

FIG (A28) TEMPERATURE, TRAJECTORY, WIDTH, AND DEPTH (TTWD)-PLOTS FOR SURFACE JET DISCHARGE

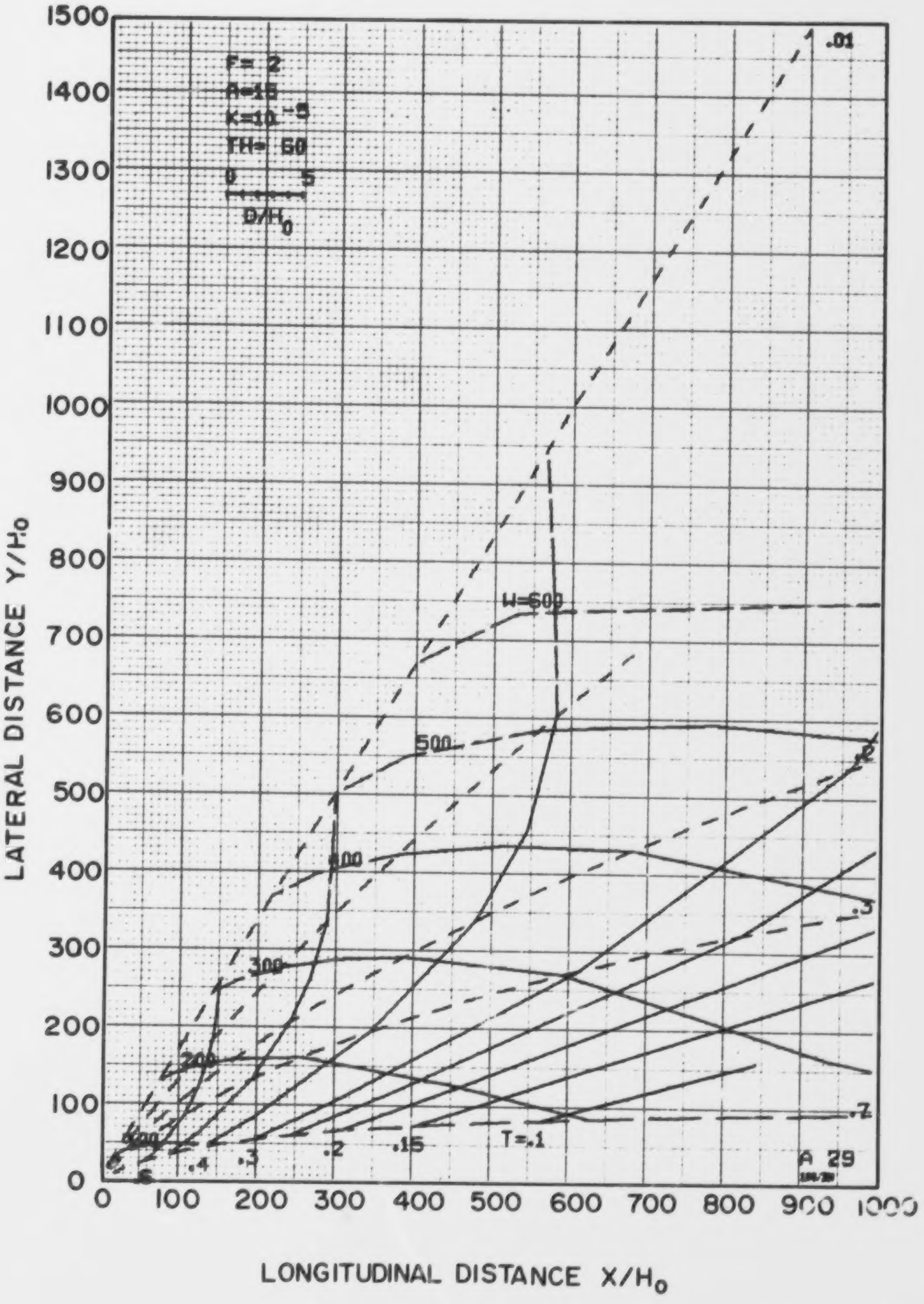

FIG (A29) TEMPERATURE, TRAJECTORY, WIDTH, AND DEPTH (TTWD)-PLOTS FOR SURFACE JET DISCHARGE

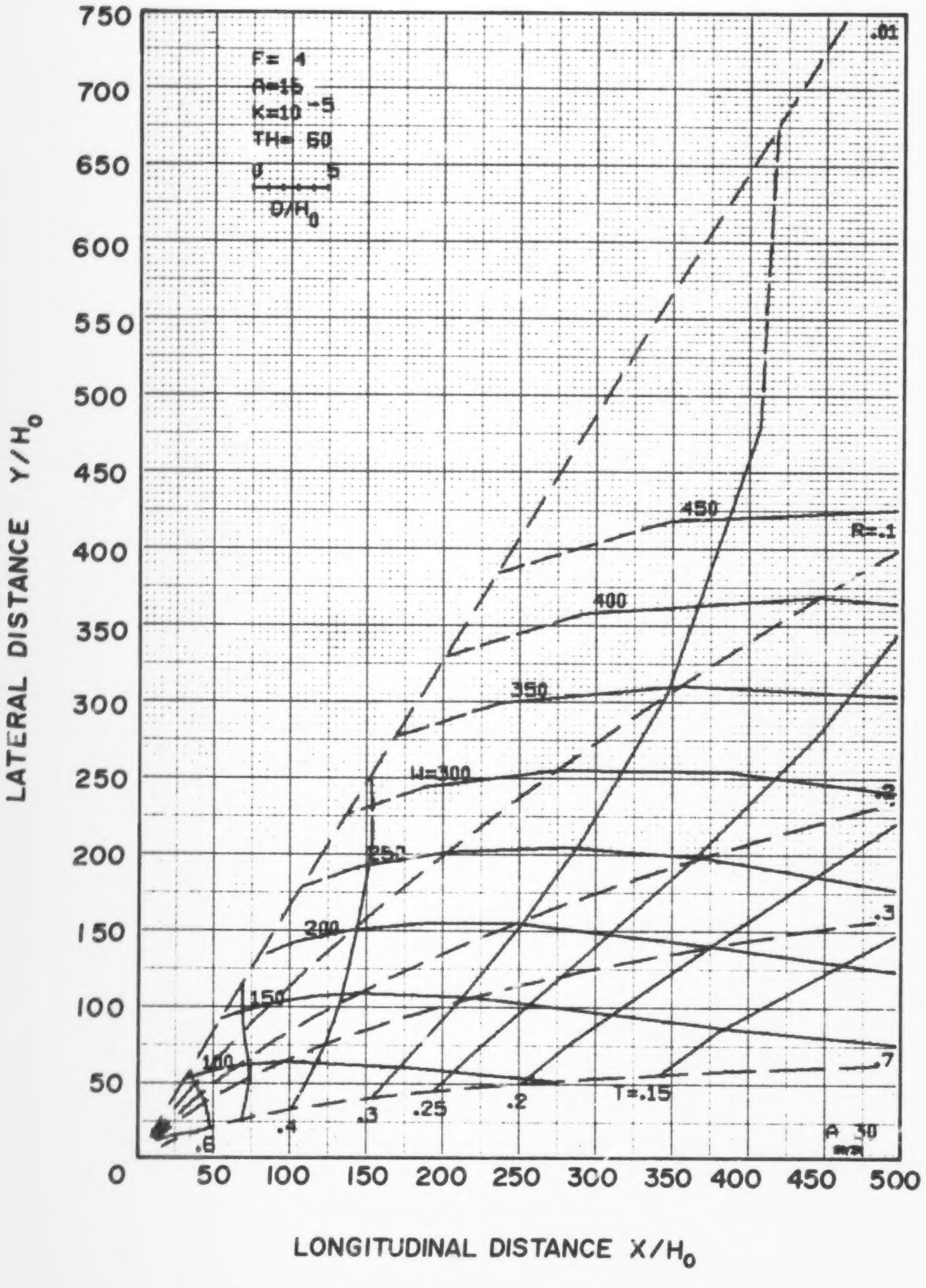

FIG (A30) TEMPERATURE, TRAJECTORY, WIDTH, AND DEPTH (TTWD)-PLOTS FOR SURFACE JET DISCHARGE

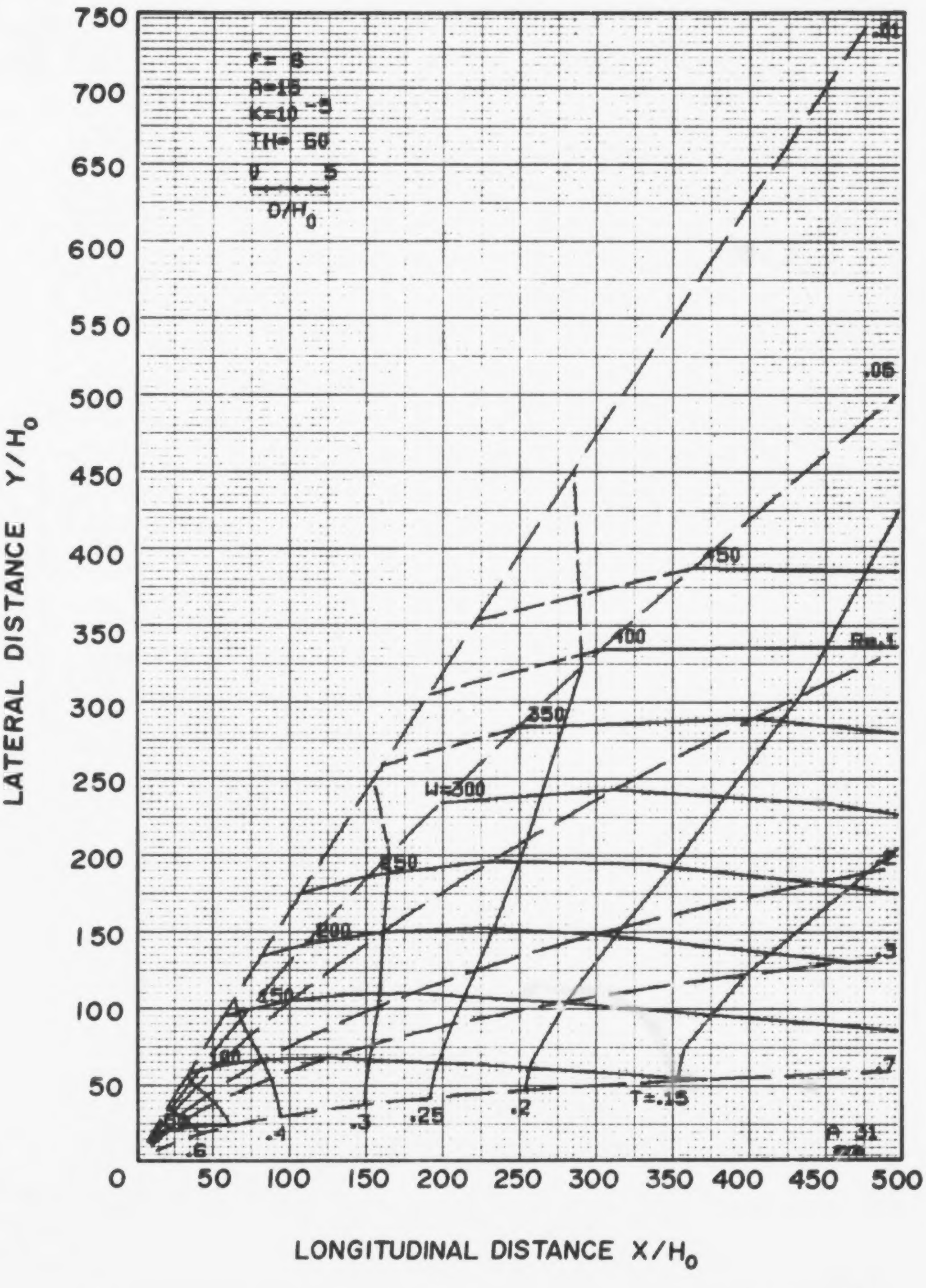

FIG (A31) TEMPERATURE, TRAJECTORY, WIDTH, AND DEPTH (TTWD)-PLOTS FOR SURFACE JET DISCHARGE

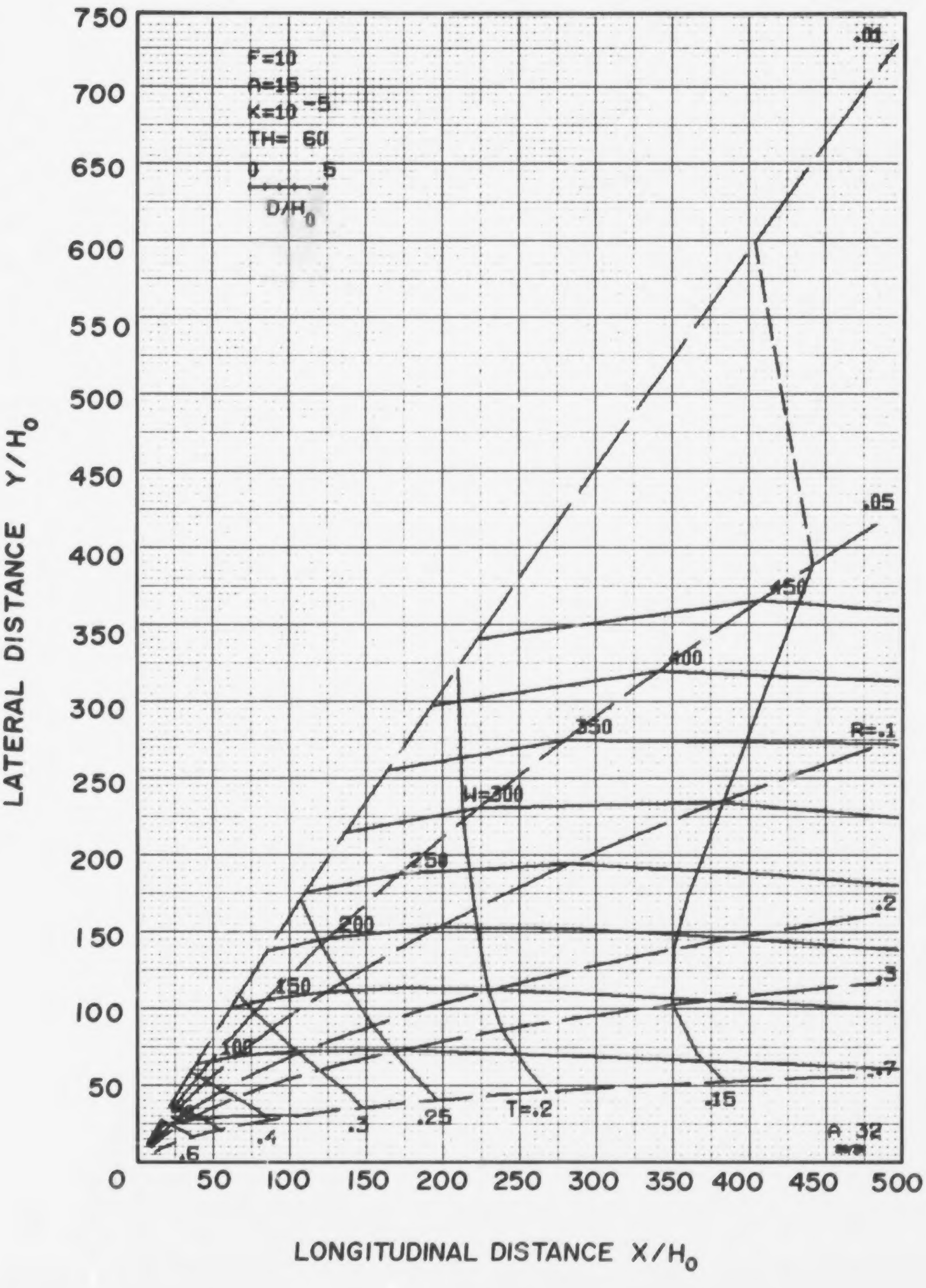

FIG (A32) TEMPERATURE, TRAJECTORY, WIDTH, AND DEPTH (TTWD)-PLOTS FOR SURFACE JET DISCHARGE

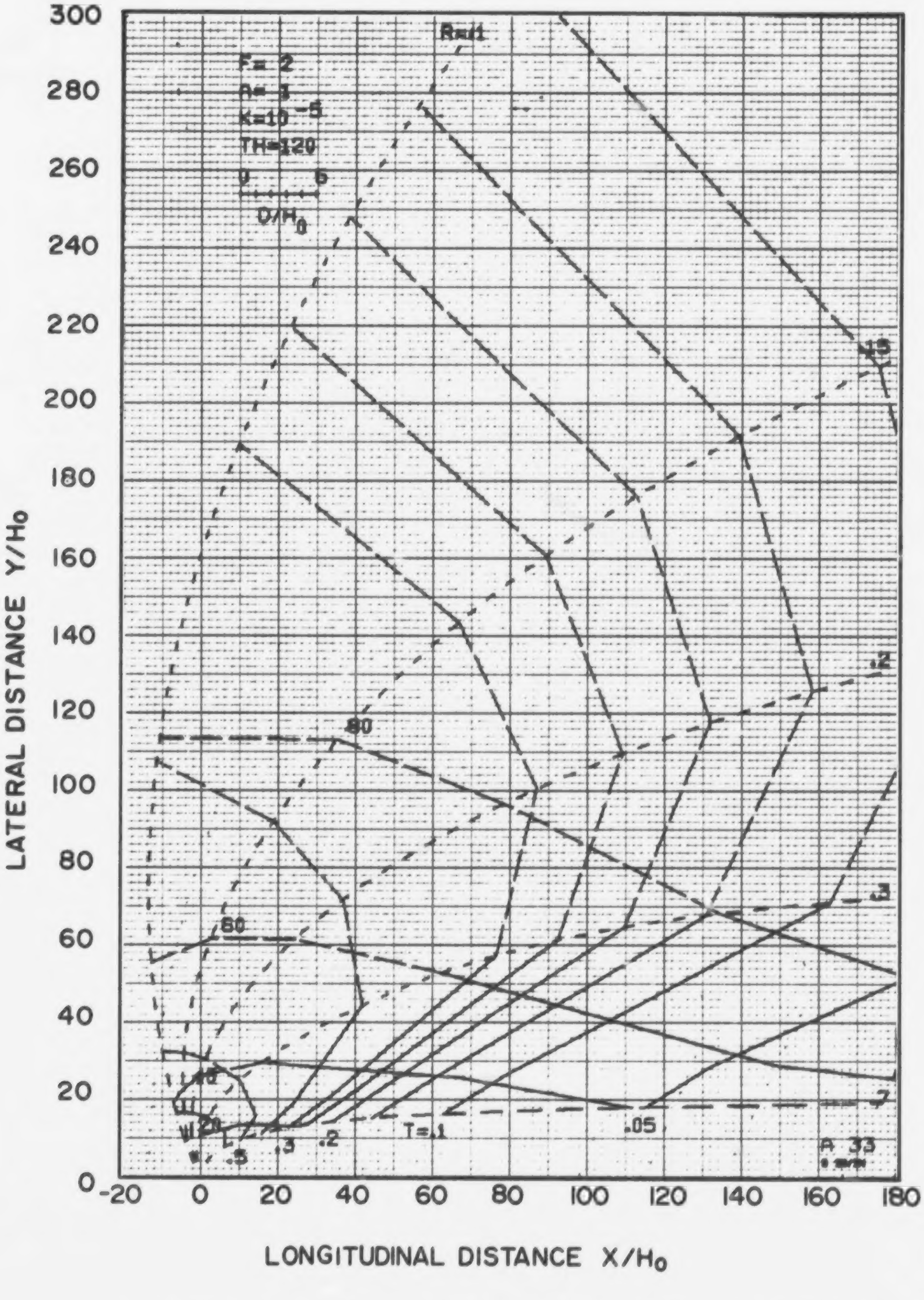

FIG (A 33) TEMPERATURE, TRAJECTORY, WIDTH, AND DEPTH (TTWD)-PLOTS FOR SURFACE JET DISCHARGE

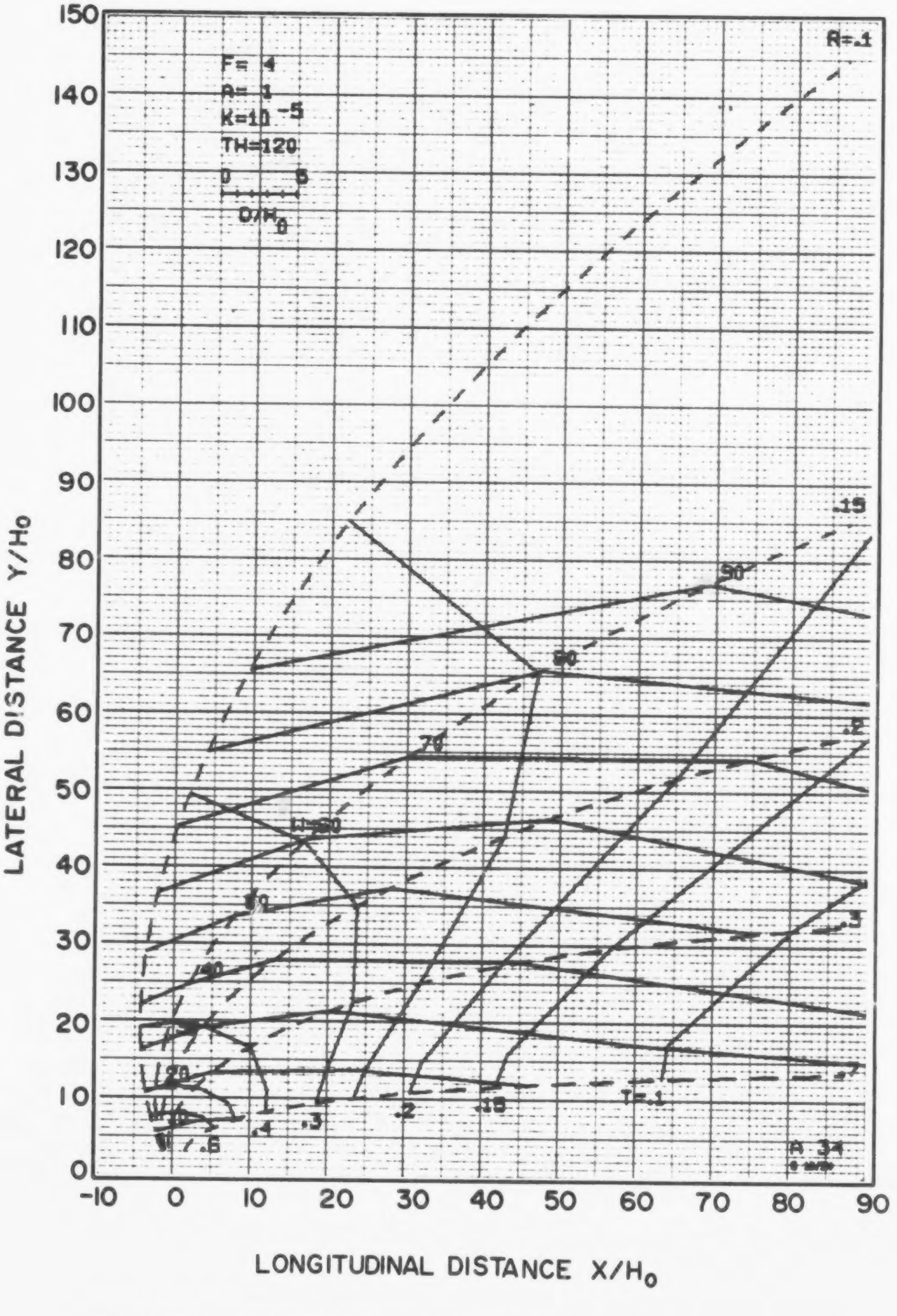

FIG (A34) TEMPERATURE, TRAJECTORY, WIDTH, AND DEPTH (TTWD)-PLOTS FOR SURFACE JET DISCHARGE

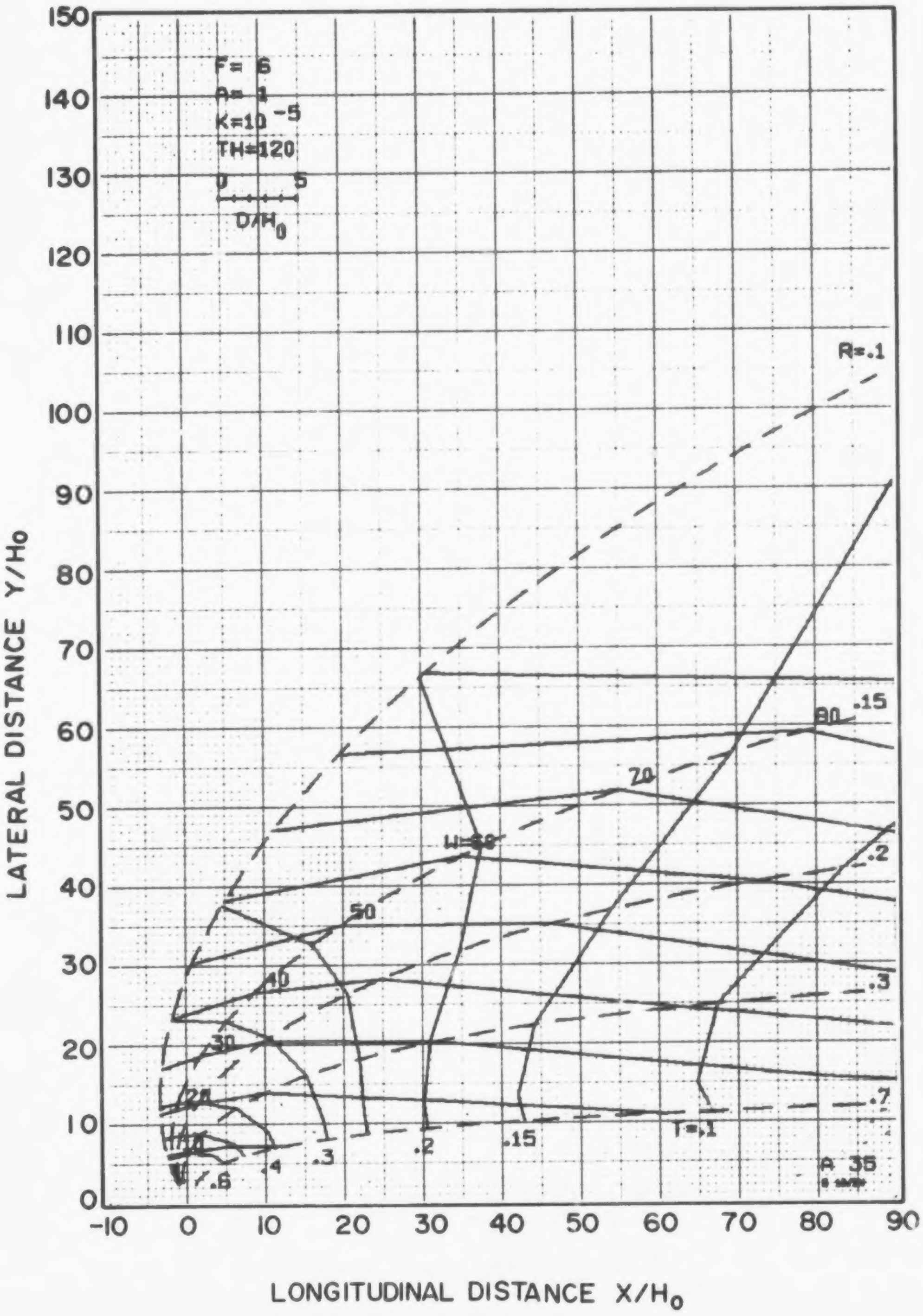

FIG (A35) TEMPERATURE, TRAJECTORY, WIDTH, AND DEPTH (TTWD)-PLOTS FOR SURFACE JET DISCHARGE

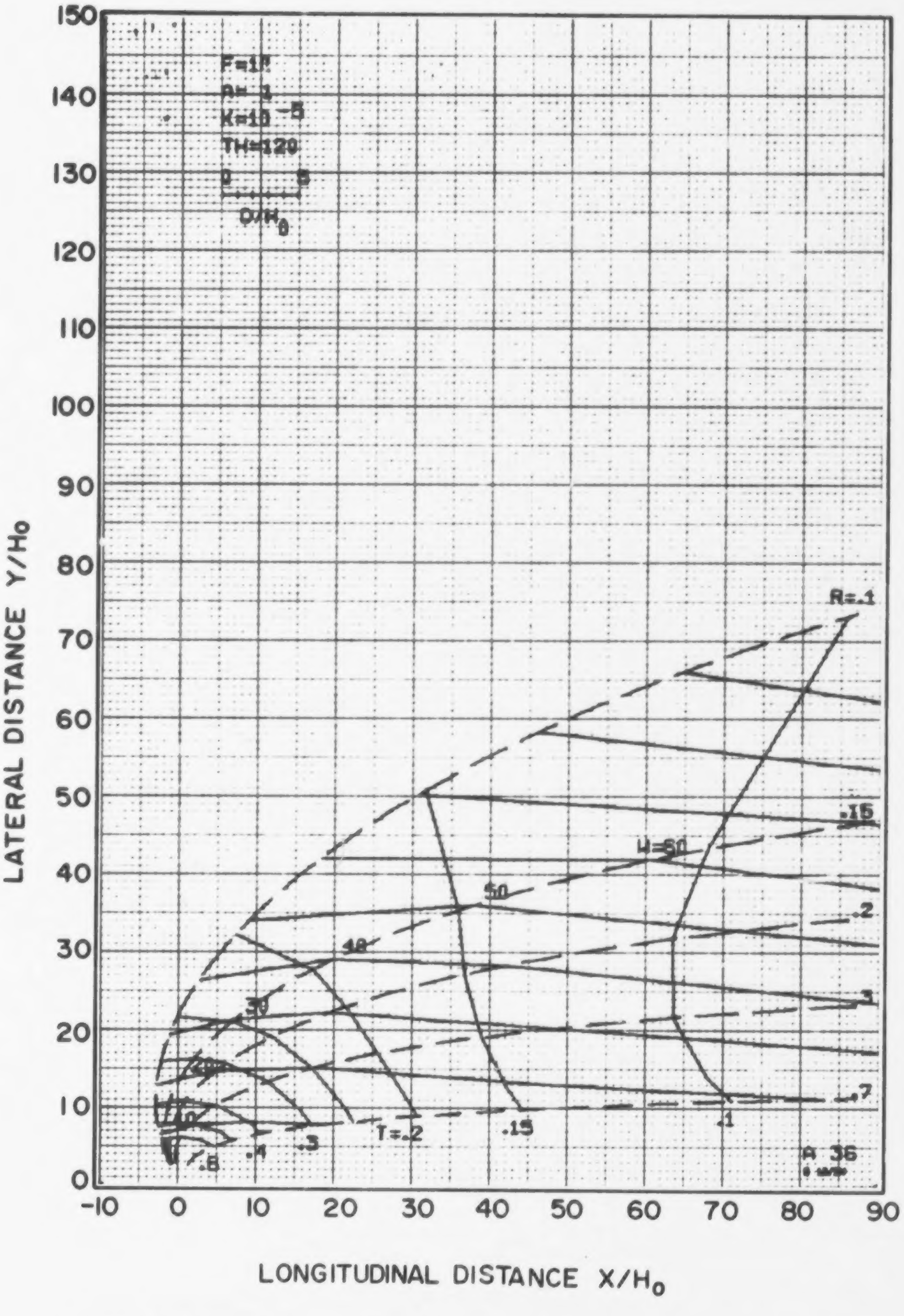

FIG (A36) TEMPERATURE, TRAJECTORY, WIDTH, AND DEPTH (TTWD)-PLOTS FOR SURFACE JET DISCHARGE

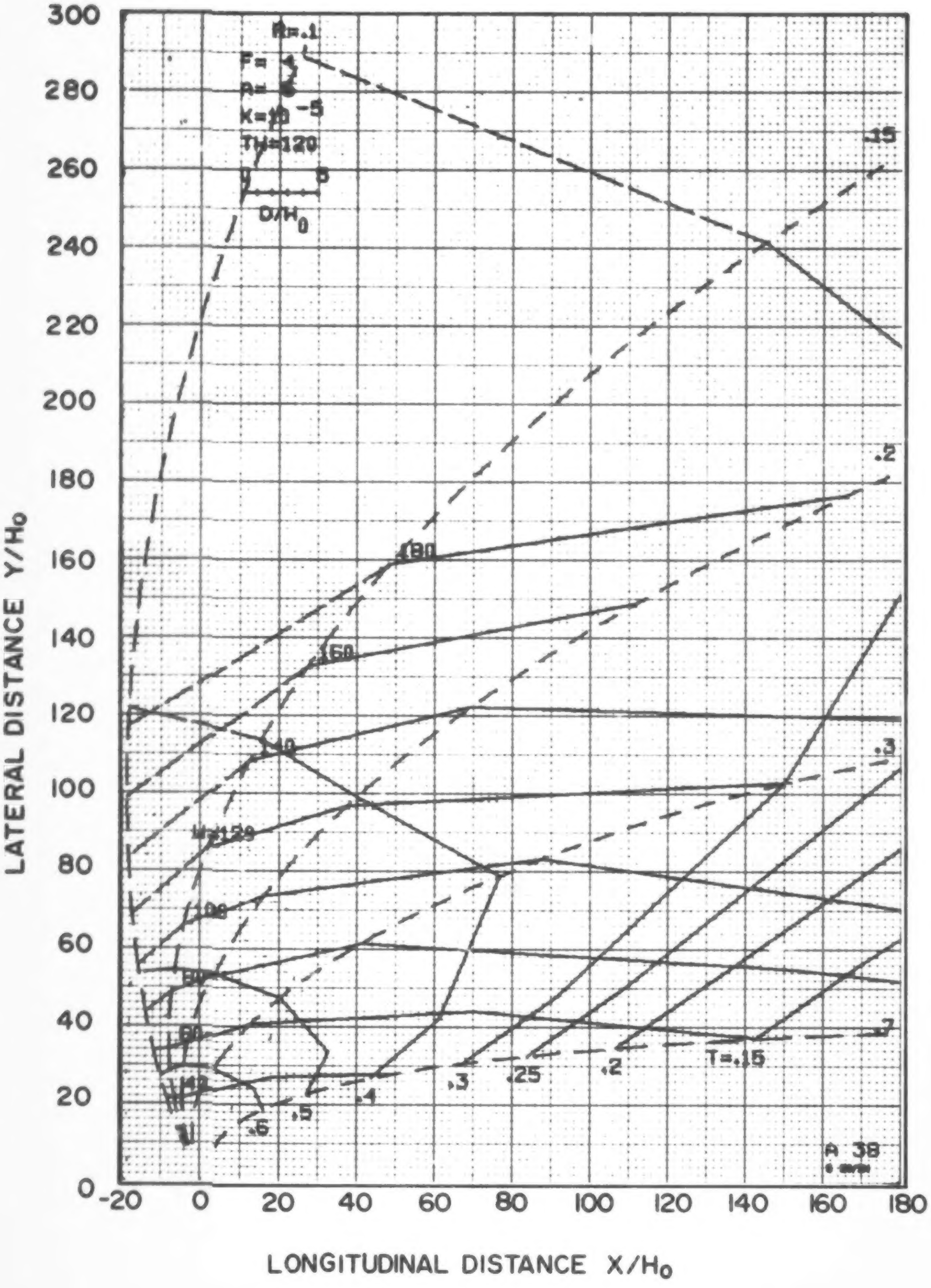

FIG (A38) TEMPERATURE, TRAJECTORY, WIDTH, AND DEPTH (TTWD)-PLOTS FOR SURFACE JET DISCHARGE

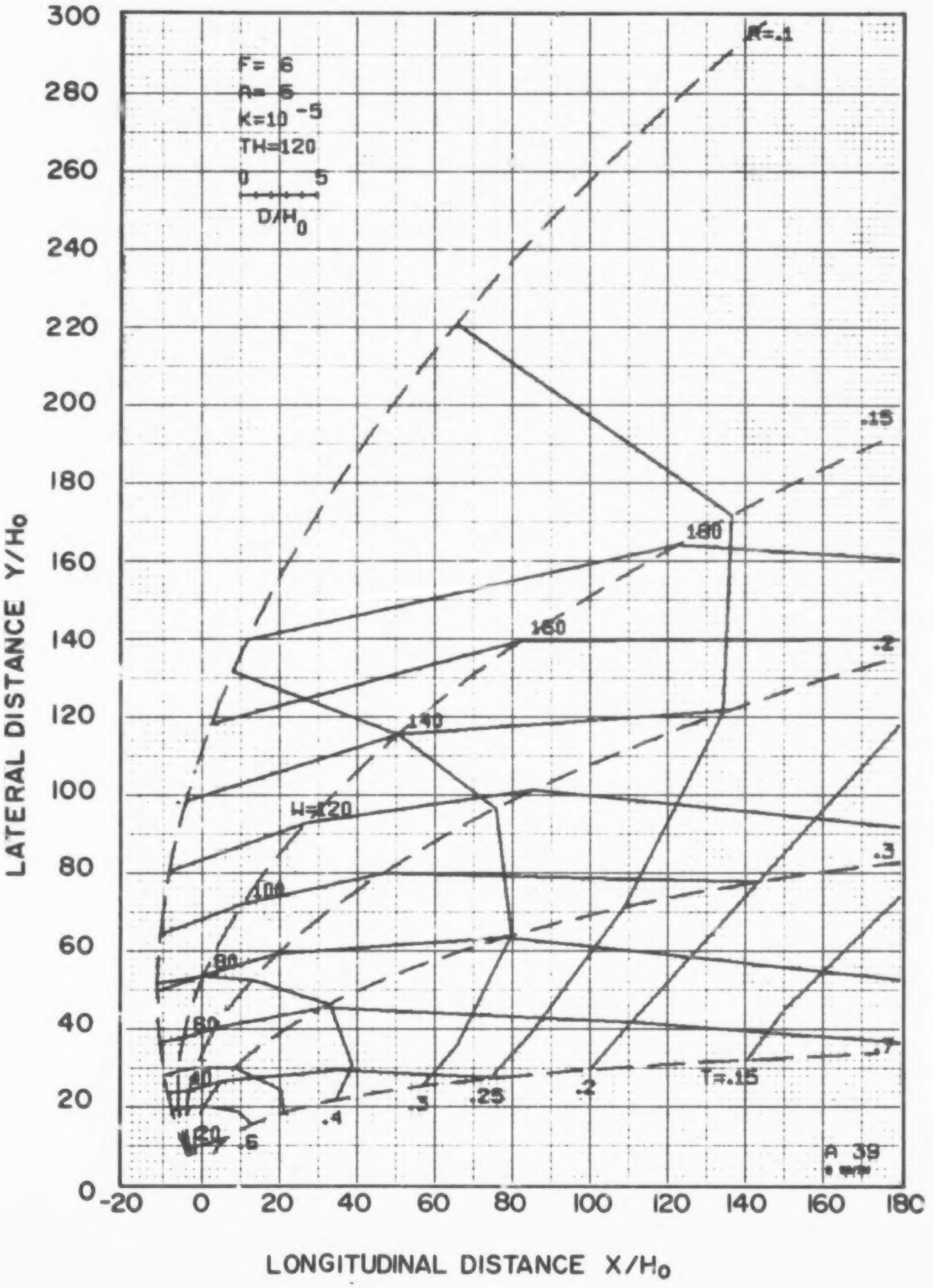

FIG (A 39) TEMPERATURE, TRAJECTORY, WIDTH, AND DEPTH (TTWD)-PLOTS FOR SURFACE JET DISCHARGE

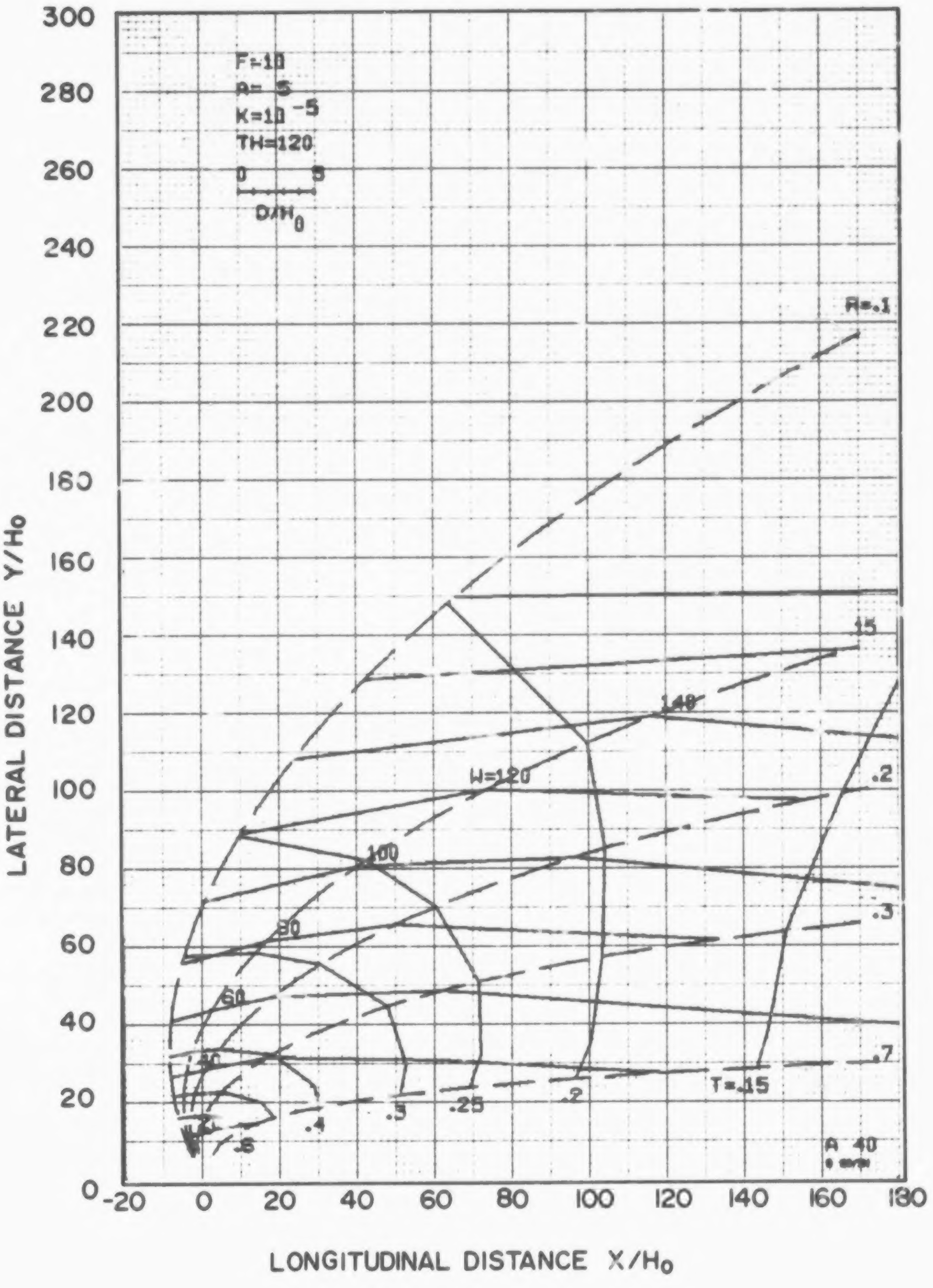

FIG (A40) TEMPERATURE, TRAJECTORY, WIDTH, AND DEPTH (TTWD)-PLOTS FOR SURFACE JET DISCHARGE

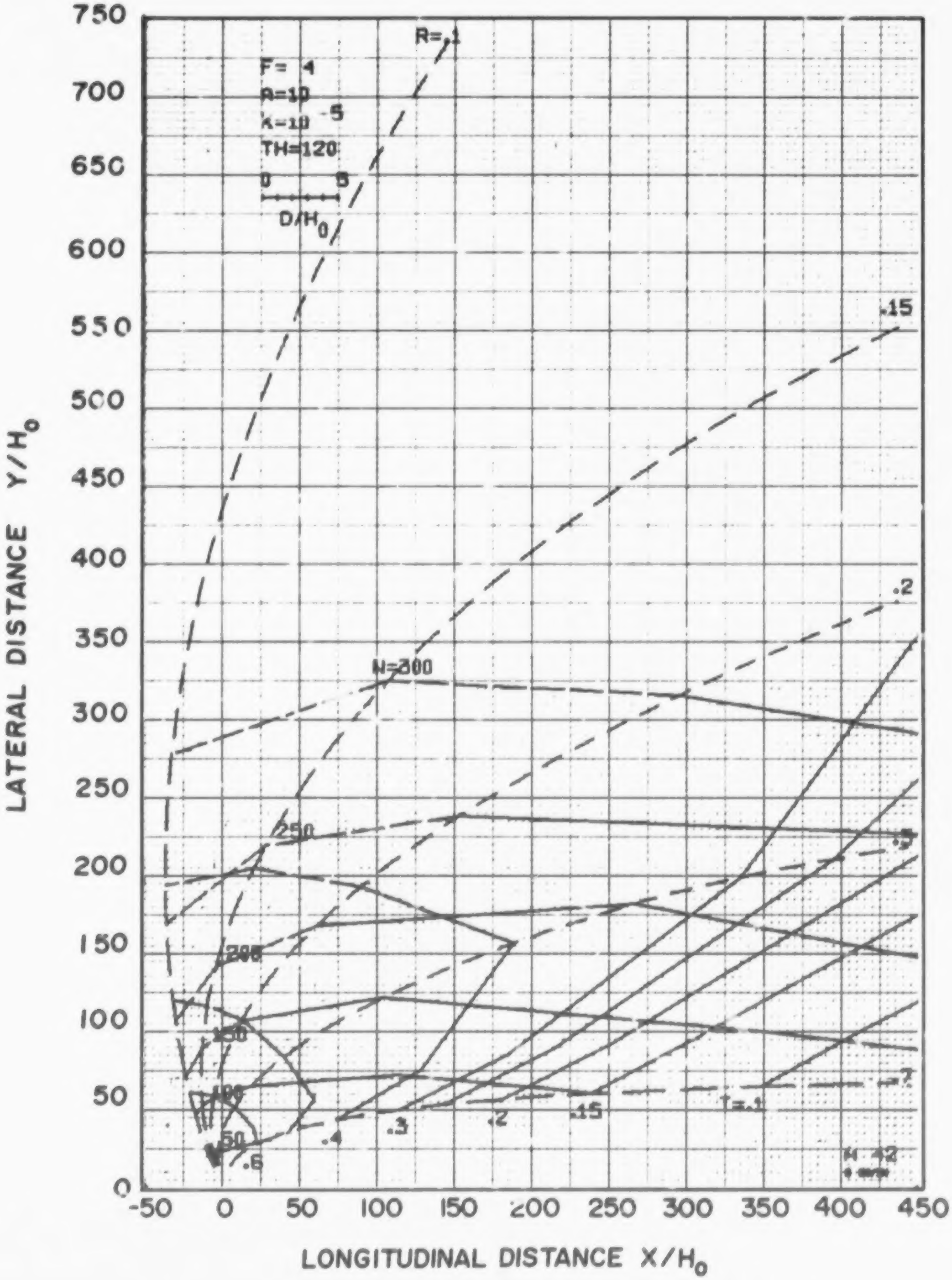

FIG (A42) TEMPERATURE. TRAJECTORY, WIDTH, AND DEPTH (TTWD)-PLOTS FOR SURFACE JET DISCHARGE

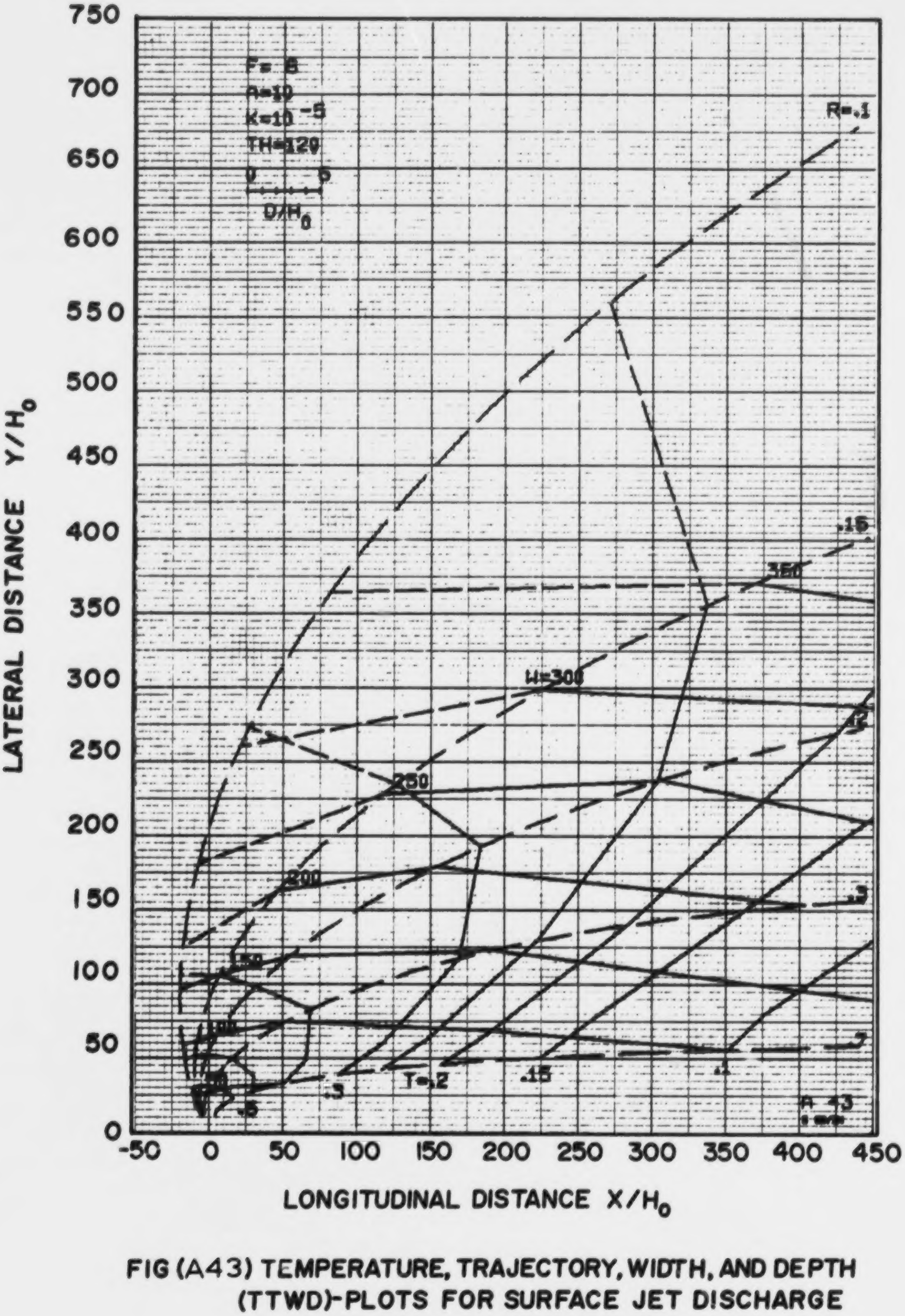

FIG (A43) TEMPERATURE, TRAJECTORY, WIDTH, AND DEPTH (TTWD)-PLOTS FOR SURFACE JET DISCHARGE

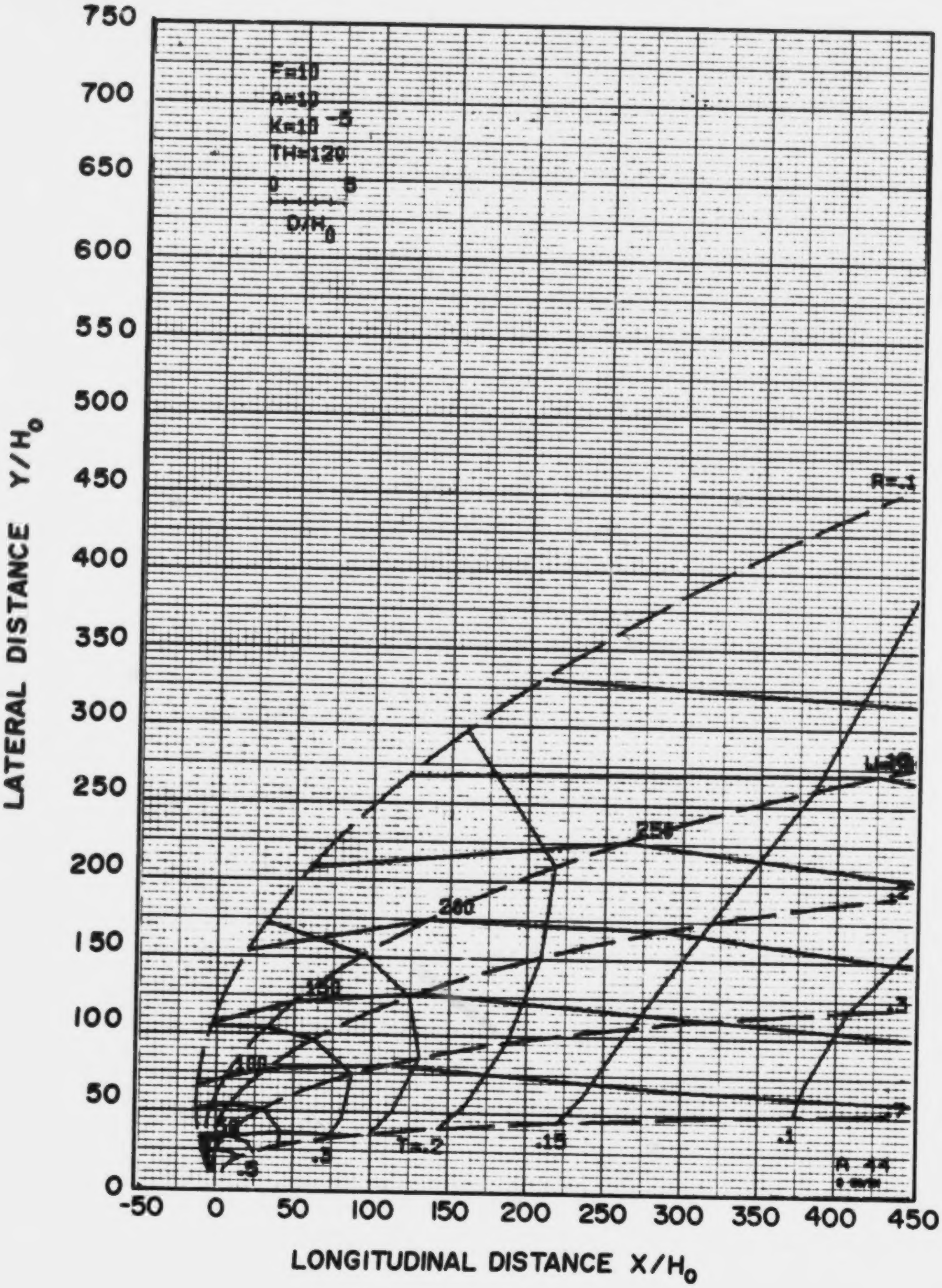

FIG (A44) TEMPERATURE, TRAJECTORY, WIDTH, AND DEPTH (TTWD)-PLOTS FOR SURFACE JET DISCHARGE

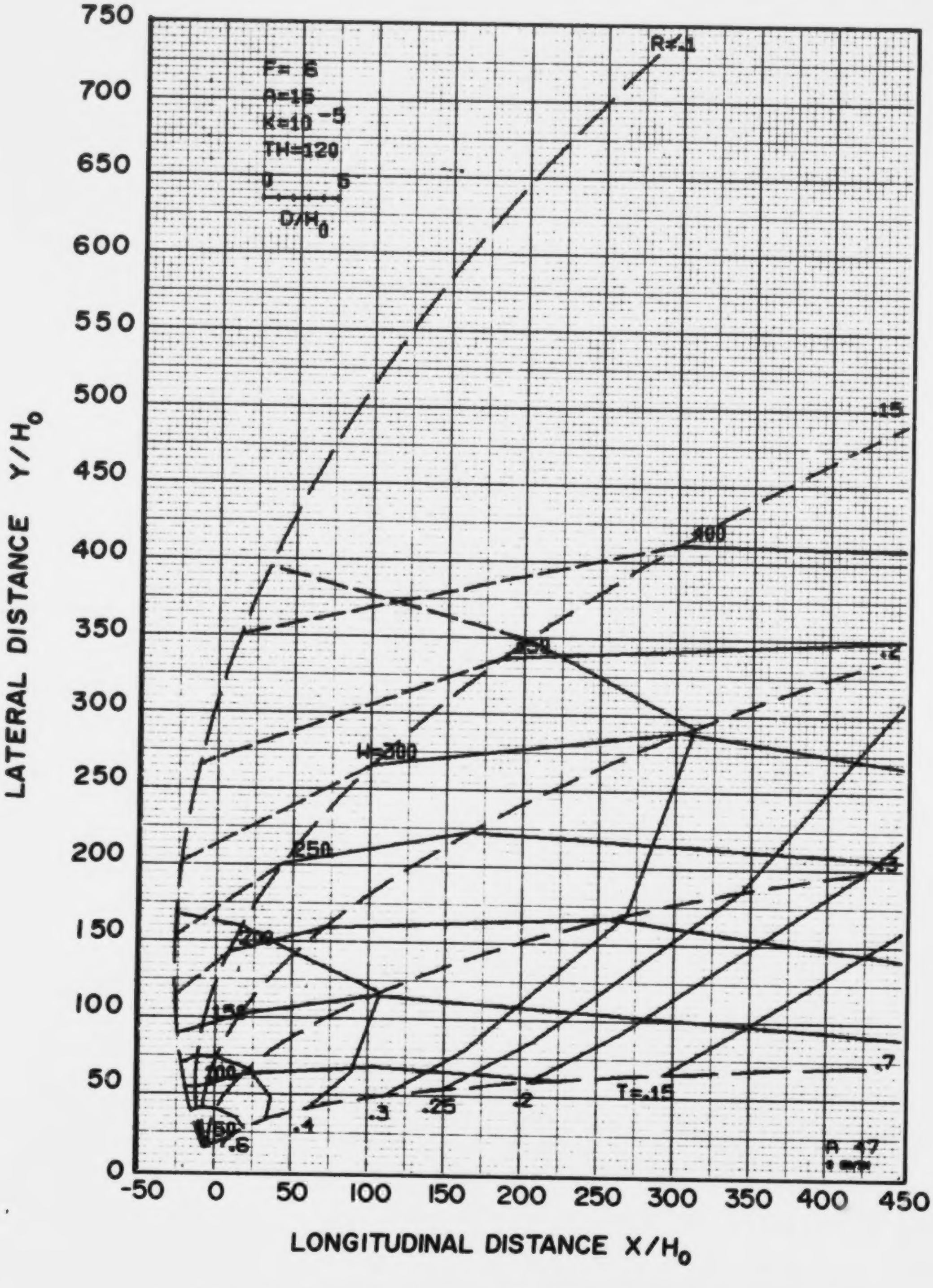

FIG (A47) TEMPERATURE, TRAJECTORY, WIDTH, AND DEPTH (TTWD)-PLOTS FOR SURFACE JET DISCHARGE

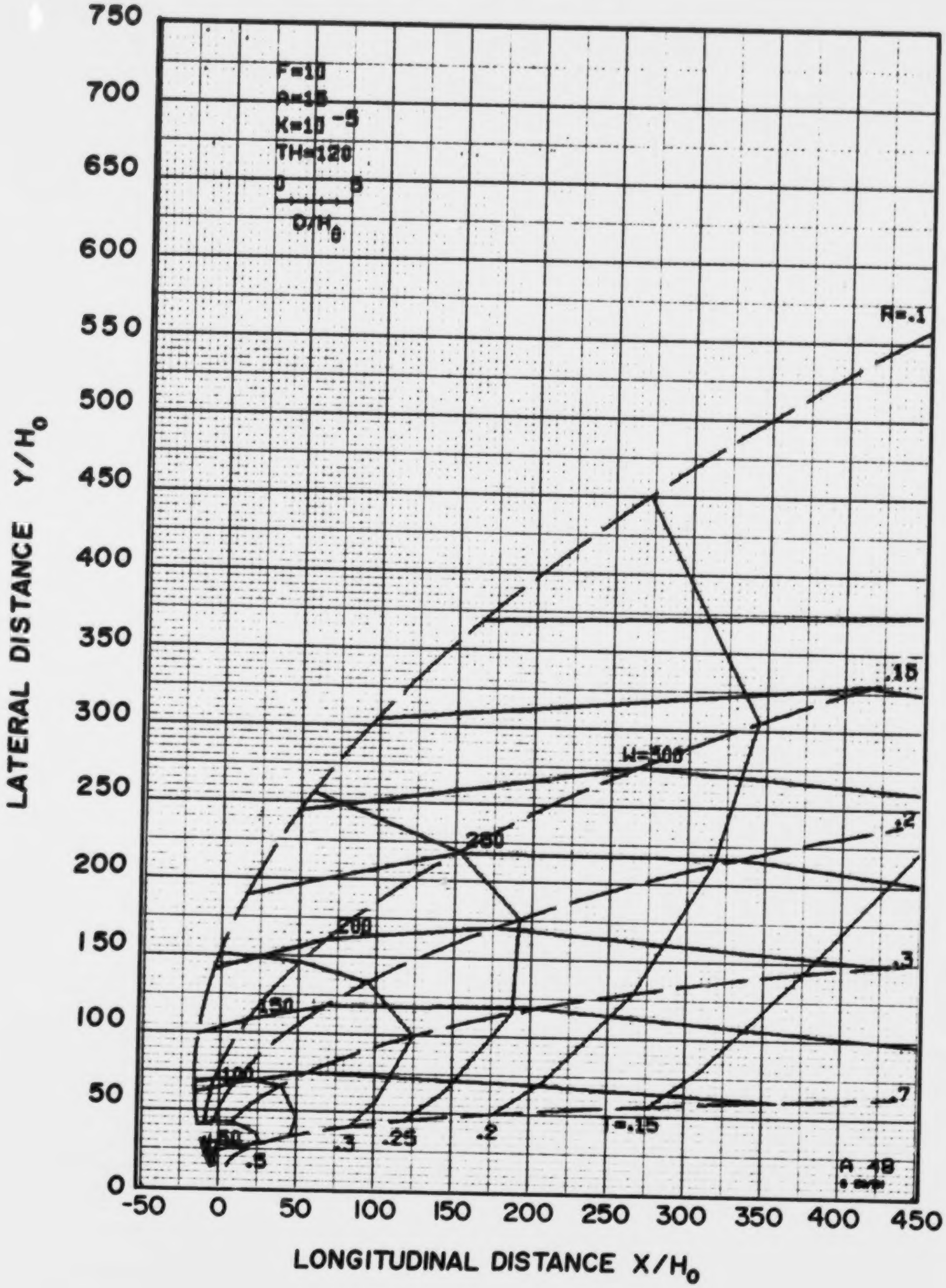

FIG (A48) TEMPERATURE, TRAJECTORY, WIDTH, AND DEPTH (TTWD)-PLOTS FOR SURFACE JET DISCHARGE

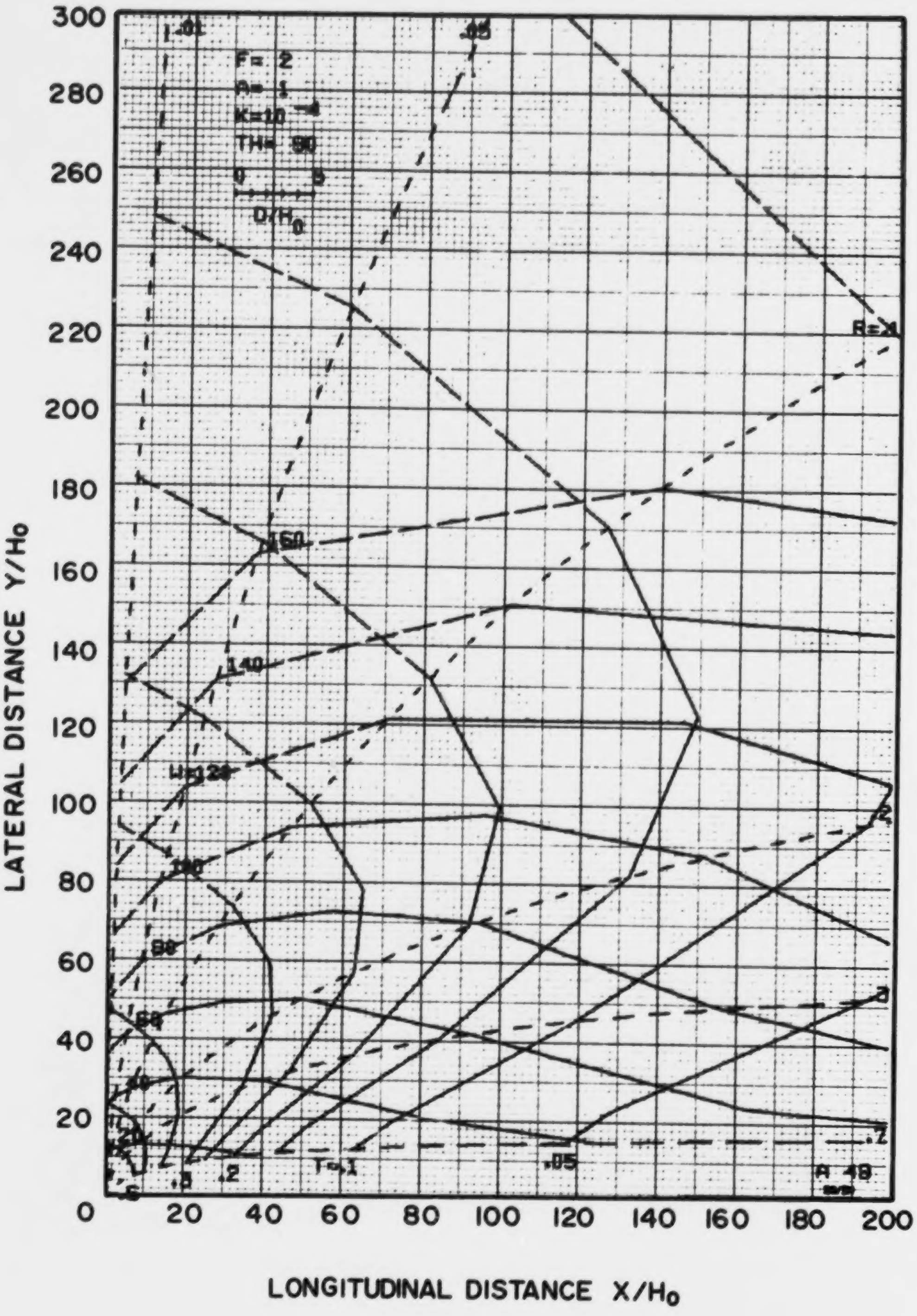

FIG (A49) TEMPERATURE, TRAJECTORY, WIDTH, AND DEPTH (TTWD)-PLOTS FOR SURFACE JET DISCHARGE

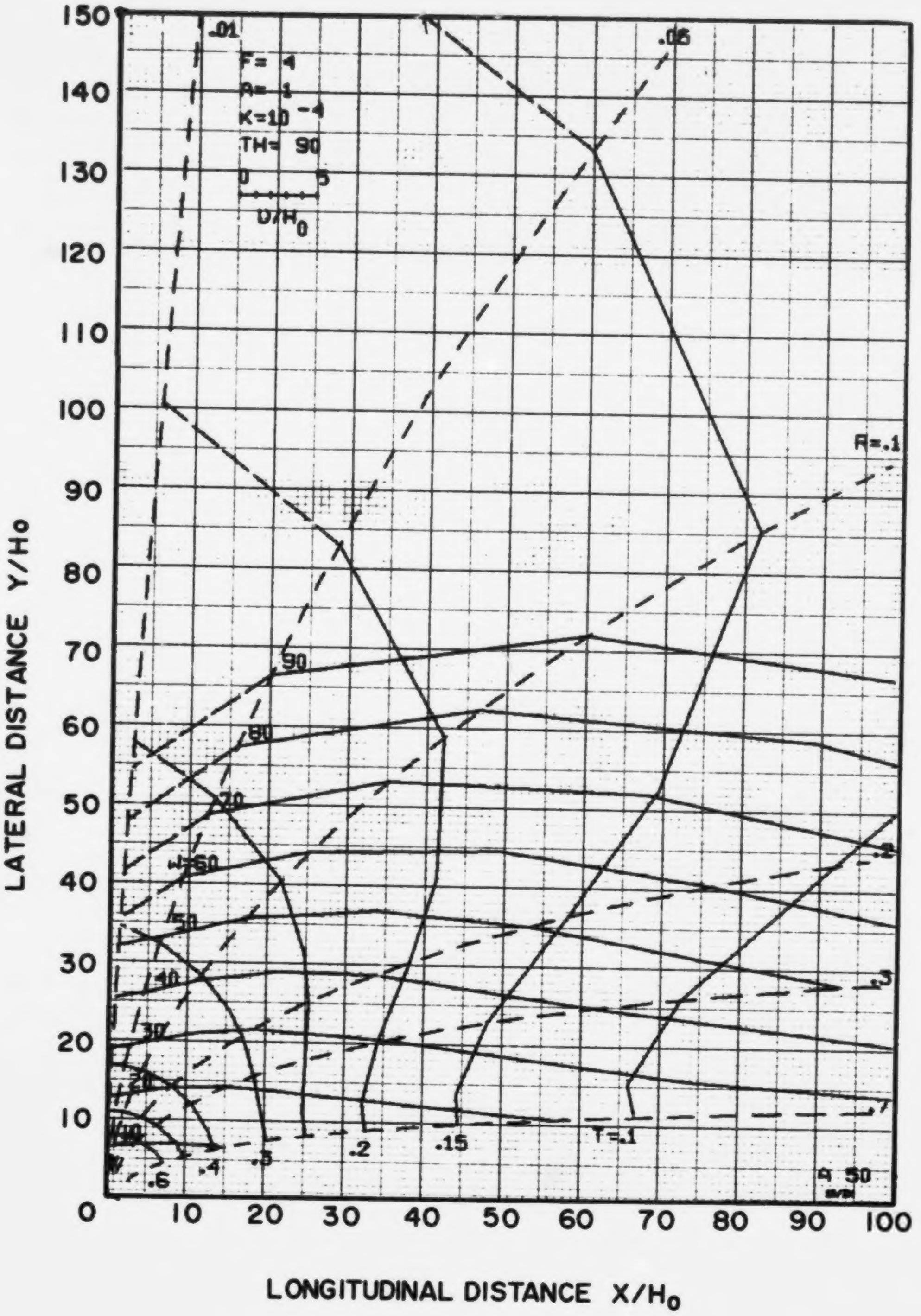

FIG(A50) TEMPERATURE, TRAJECTORY, WIDTH, AND DEPTH (TTWD)-PLOTS FOR SURFACE JET DISCHARGE

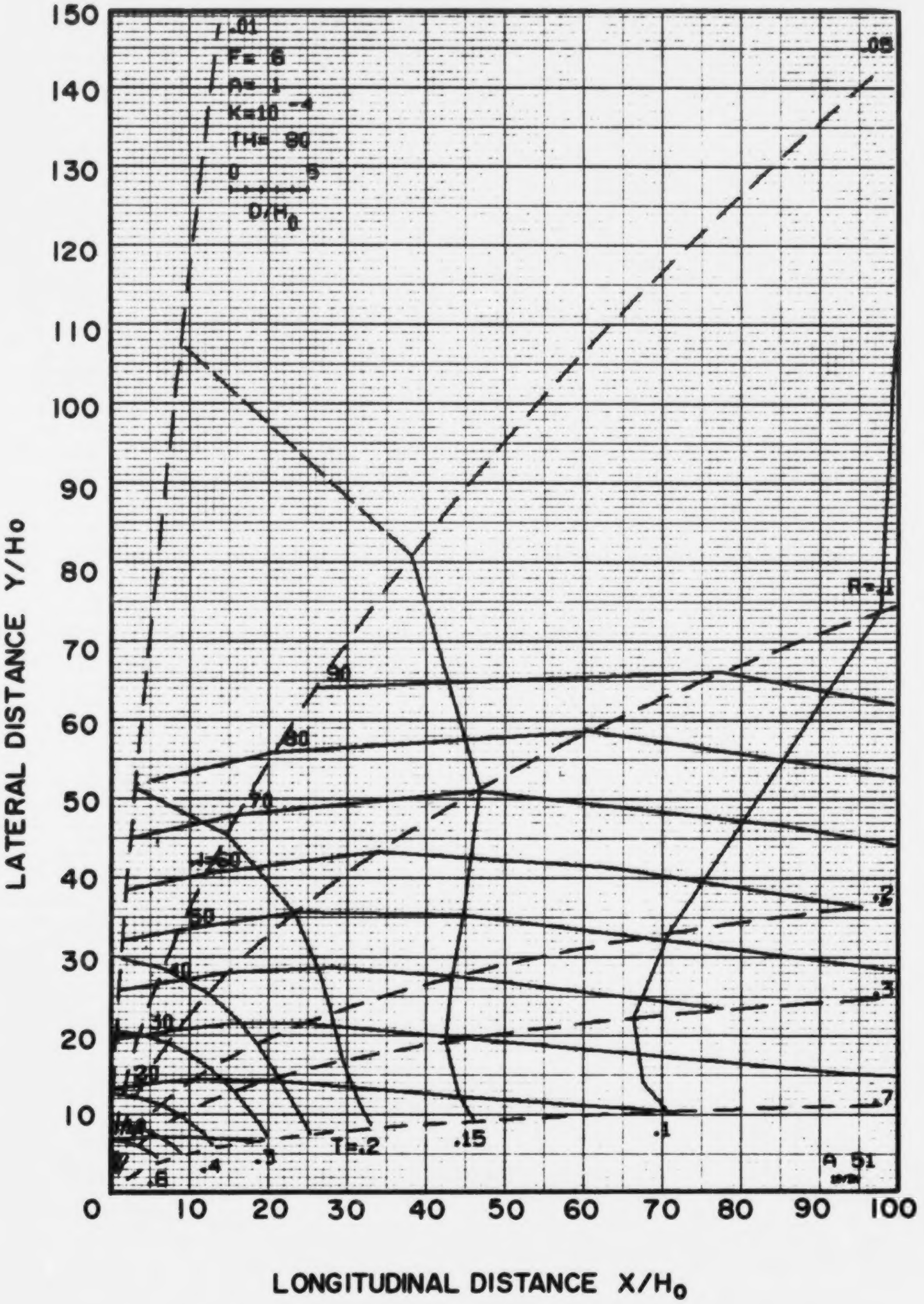

FIG(A51) TEMPERATURE, TRAJECTORY, WIDTH, AND DEPTH (TTWD)-PLOTS FOR SURFACE JET DISCHARGE

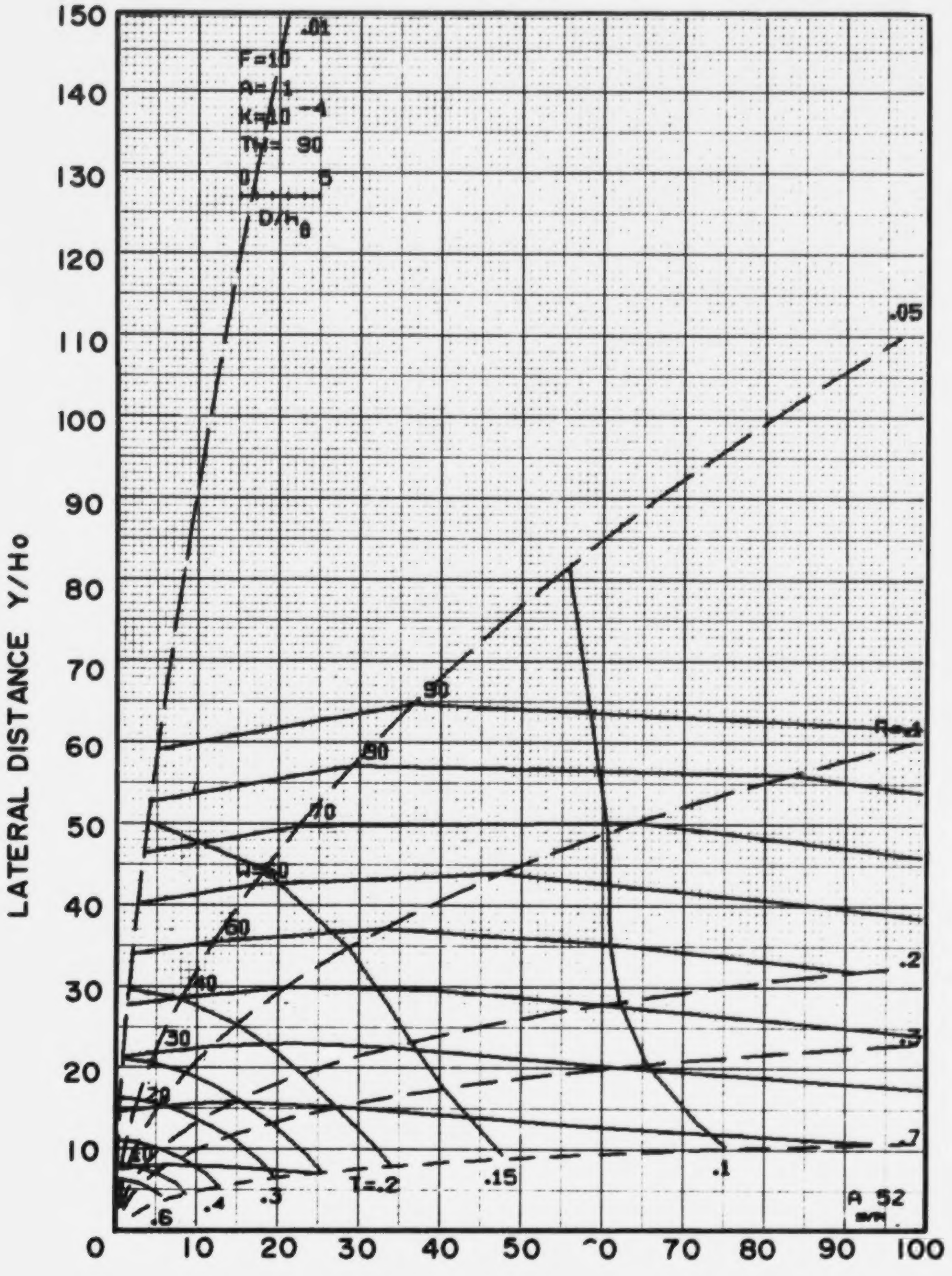

FIG(A52) TEMPERATURE, TRAJECTORY, WIDTH, AND DEPTH (TTWD)-PLOTS FOR SURFACE JET DISCHARGE

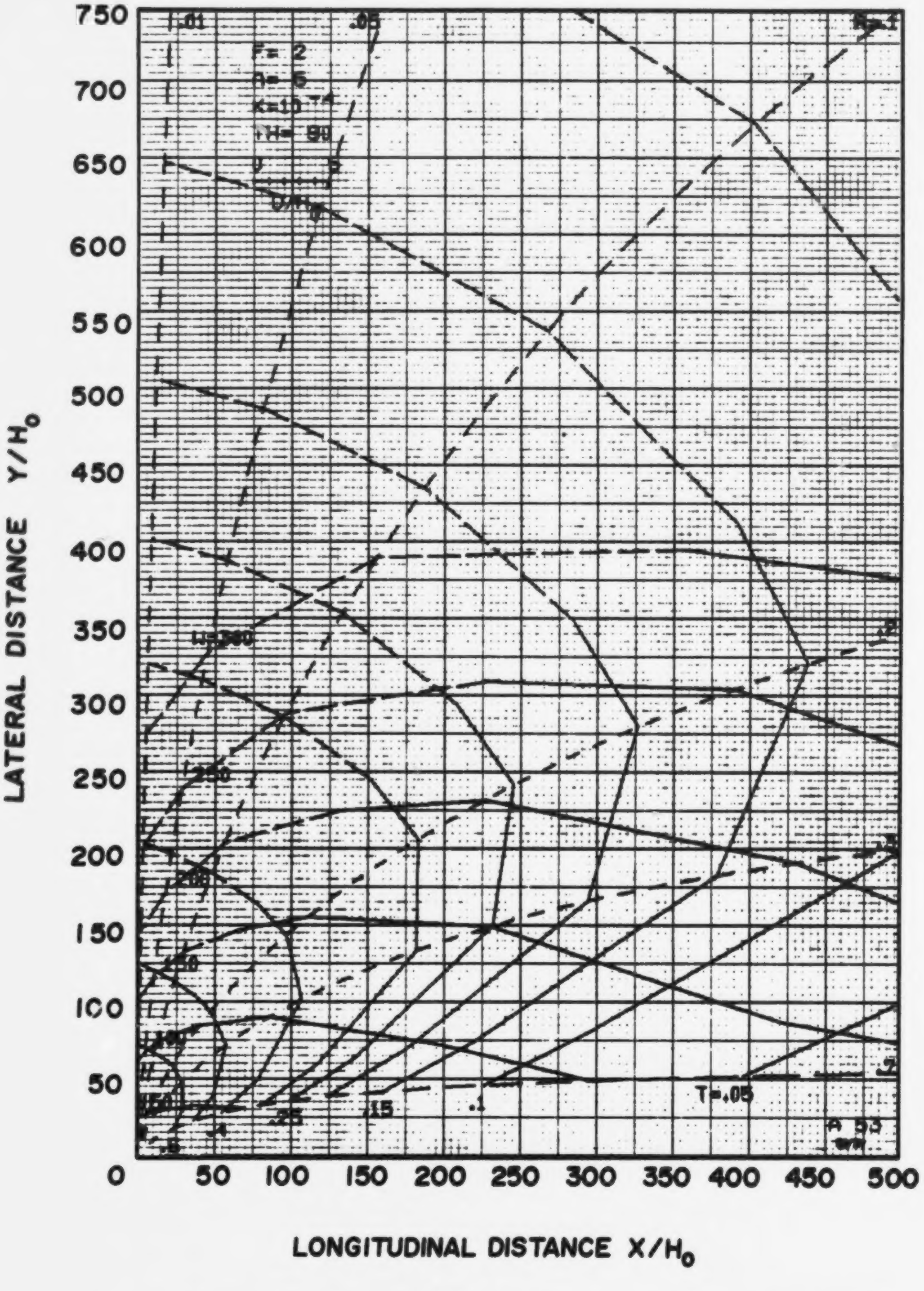

FIG (A53) TEMPERATURE, TRAJECTORY, WIDTH, AND DEPTH (TTWD)-PLOTS FOR SURFACE JET DISCHARGE

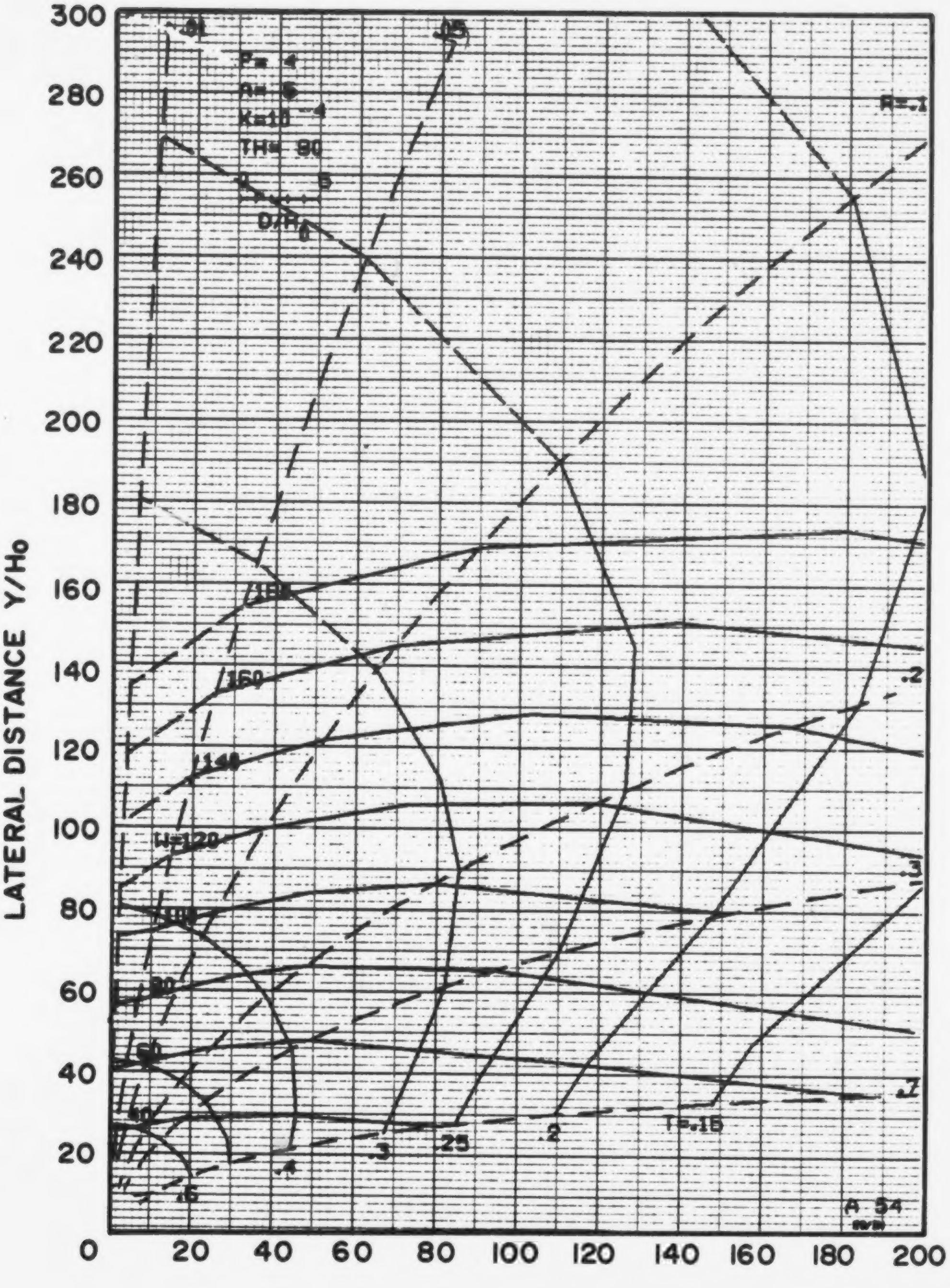

FIG (A 54) TEMPERATURE, TRAJECTORY, WIDTH, AND DEPTH (TTWD)-PLOTS FOR SURFACE JET DISCHARGE

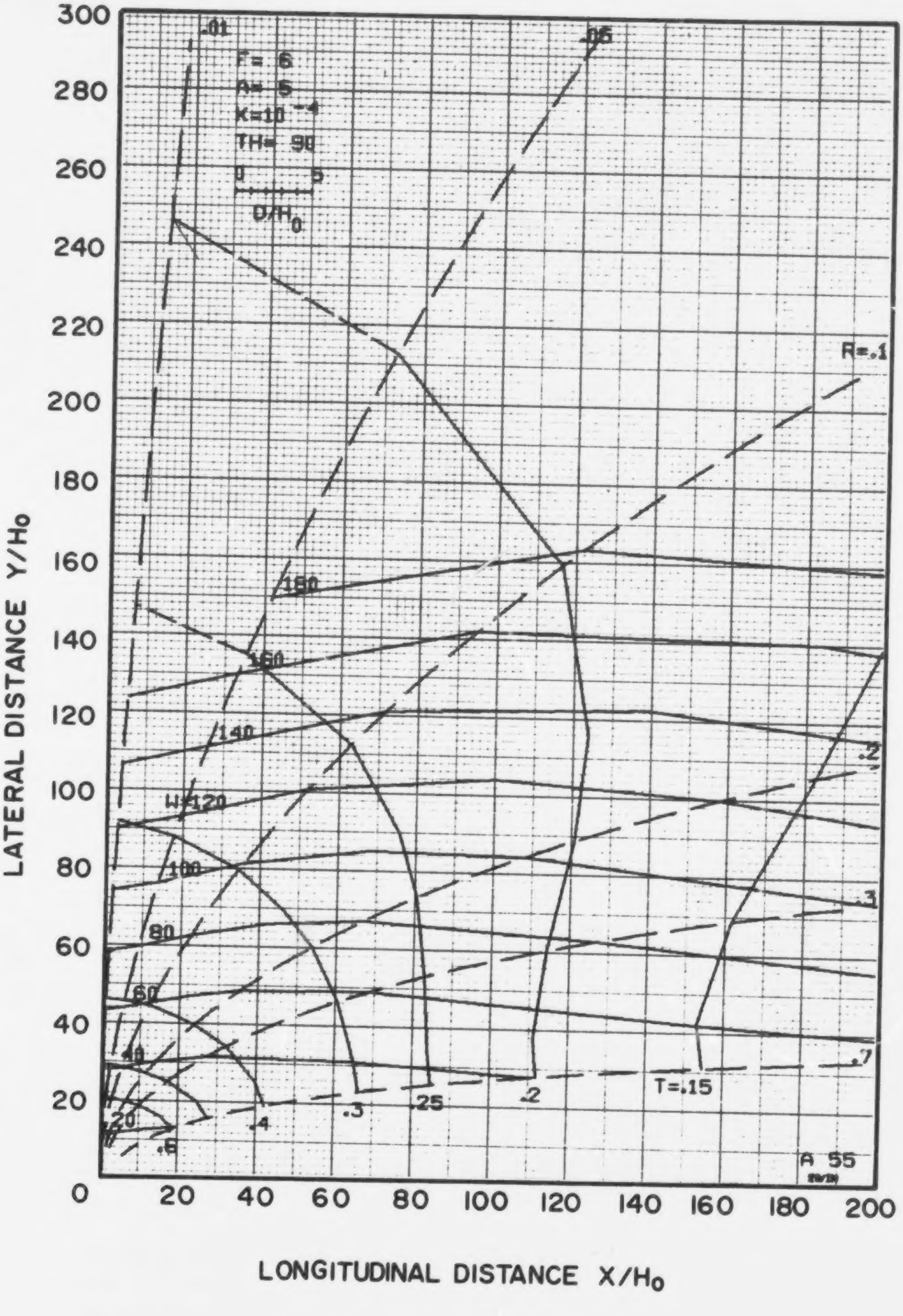

FIG(A55) TEMPERATURE, TRAJECTORY, WIDTH, AND DEPTH (TTWD)-PLOTS FOR SURFACE JET DISCHARGE

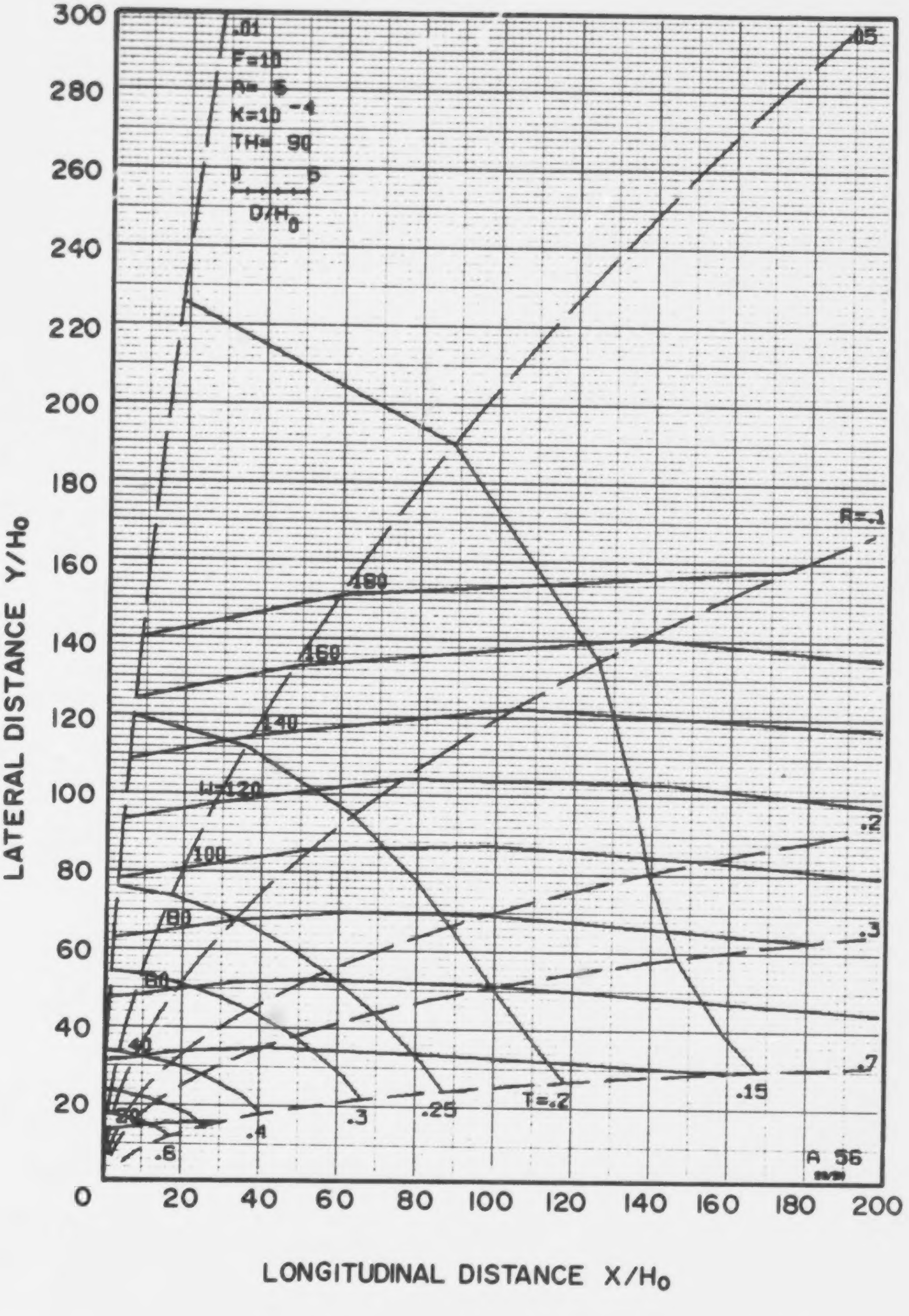

FIG (A56) TEMPERATURE, TRAJECTORY, WIDTH, AND DEPTH (TTWD)-PLOTS FOR SURFACE JET DISCHARGE

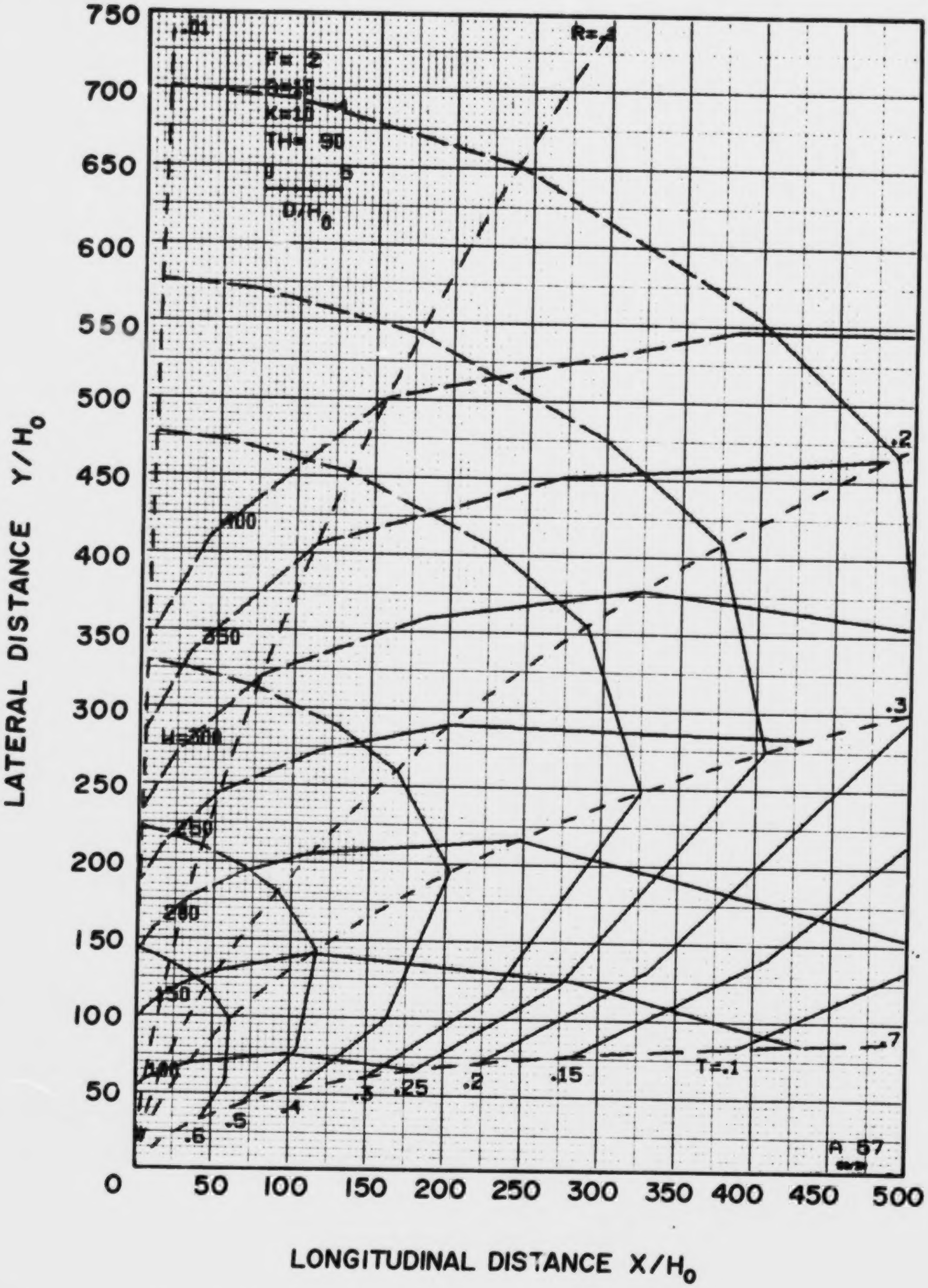

FIG (A57) TEMPERATURE, TRAJECTORY, WIDTH, AND DEPTH (TTWD)-PLOTS FOR SURFACE JET DISCHARGE

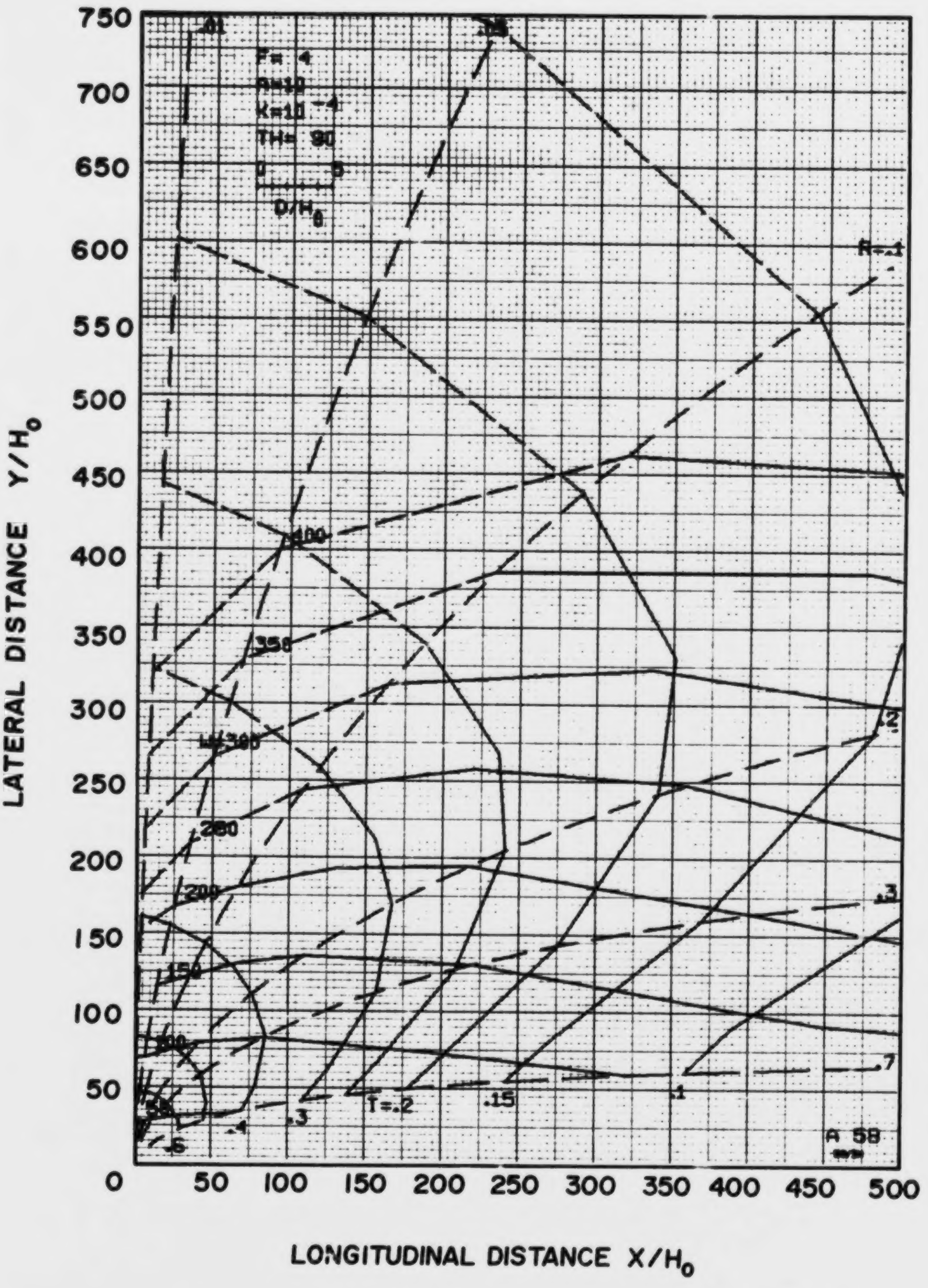

FIG (A 58) TEMPERATURE, TRAJECTORY, WIDTH, AND DEPTH (TTWD)-PLOTS FOR SURFACE JET DISCHARGE

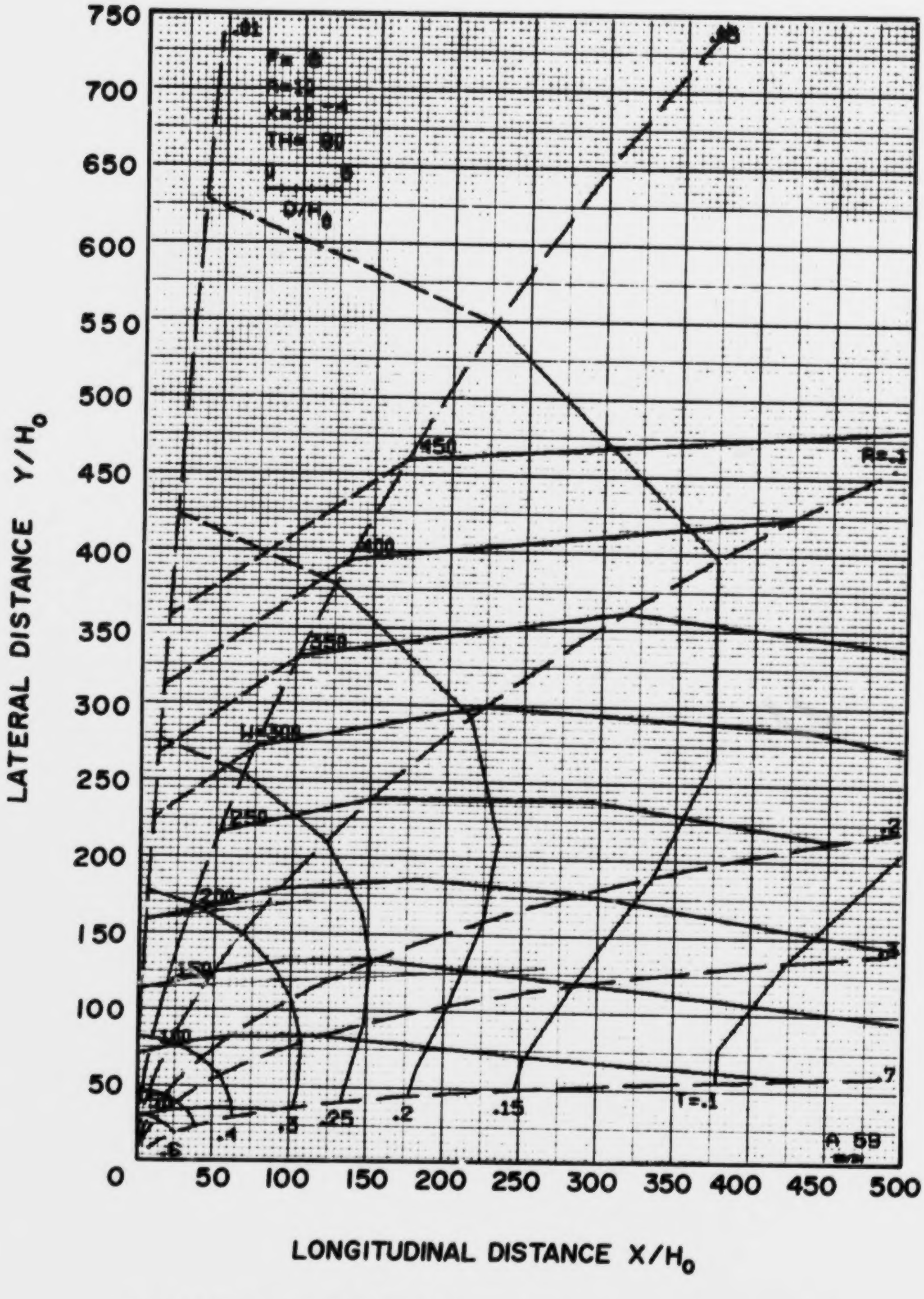

FIG (A59) TEMPERATURE, TRAJECTORY, WIDTH, AND DEPTH (TTWD)-PLOTS FOR SURFACE JET DISCHARGE

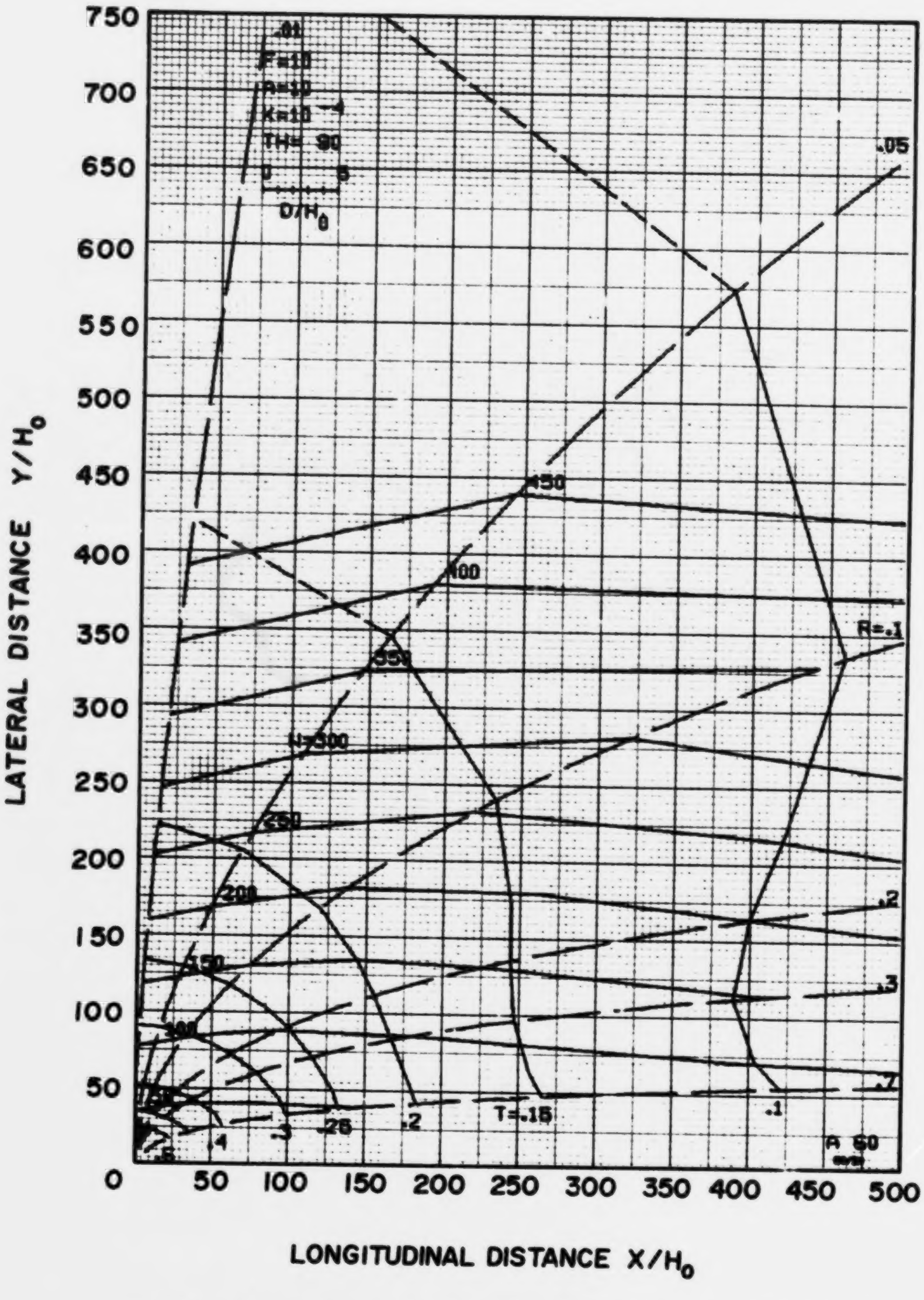

FIG (A 60) TEMPERATURE, TRAJECTORY, WIDTH, AND DEPTH (TTWD)-PLOTS FOR SURFACE JET DISCHARGE

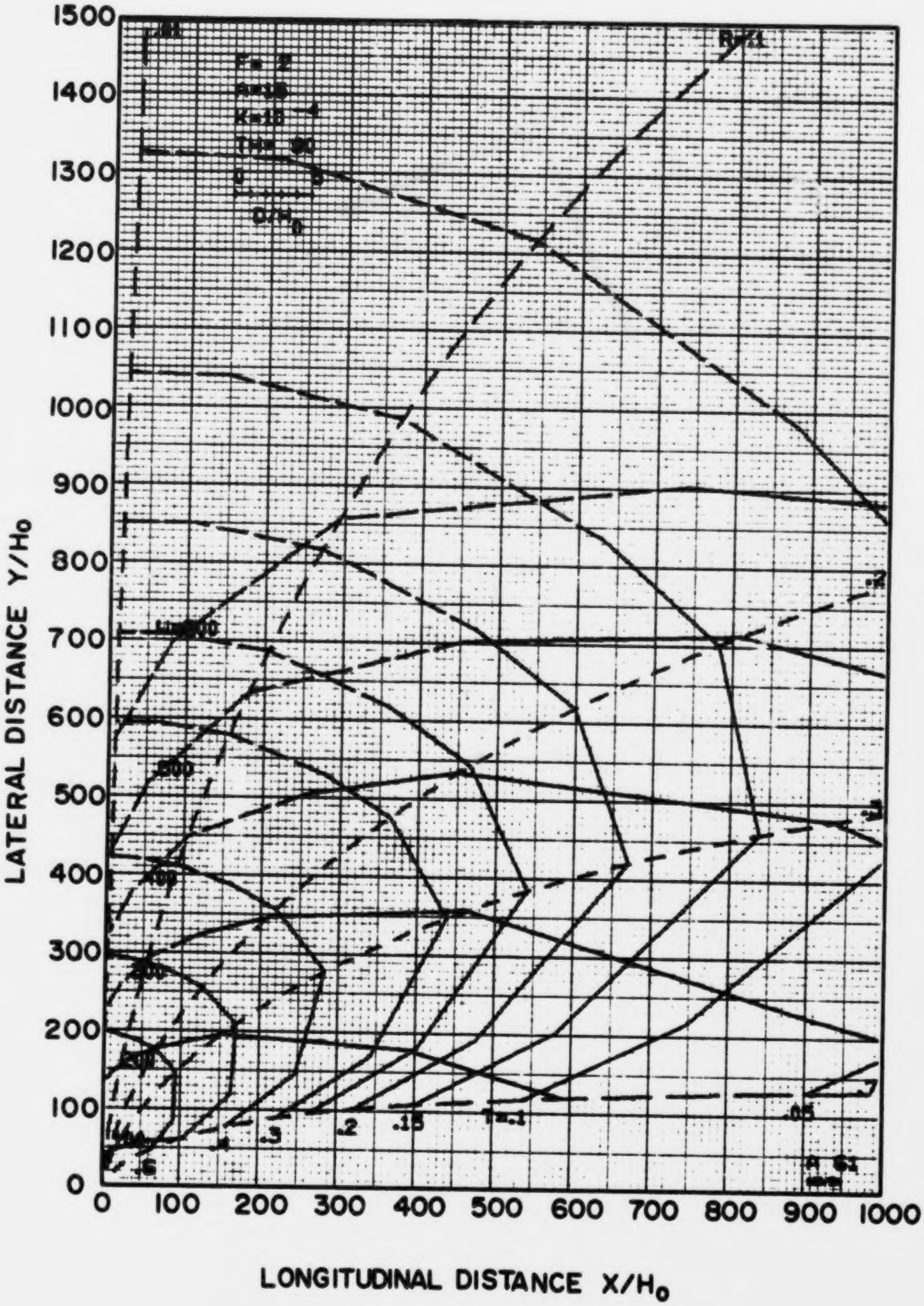

FIG (A 6 1) TEMPERATURE, TRAJECTORY, WIDTH, AND DEPTH
(TTWD)-PLOTS FOR SURFACE JET DISCHARGE

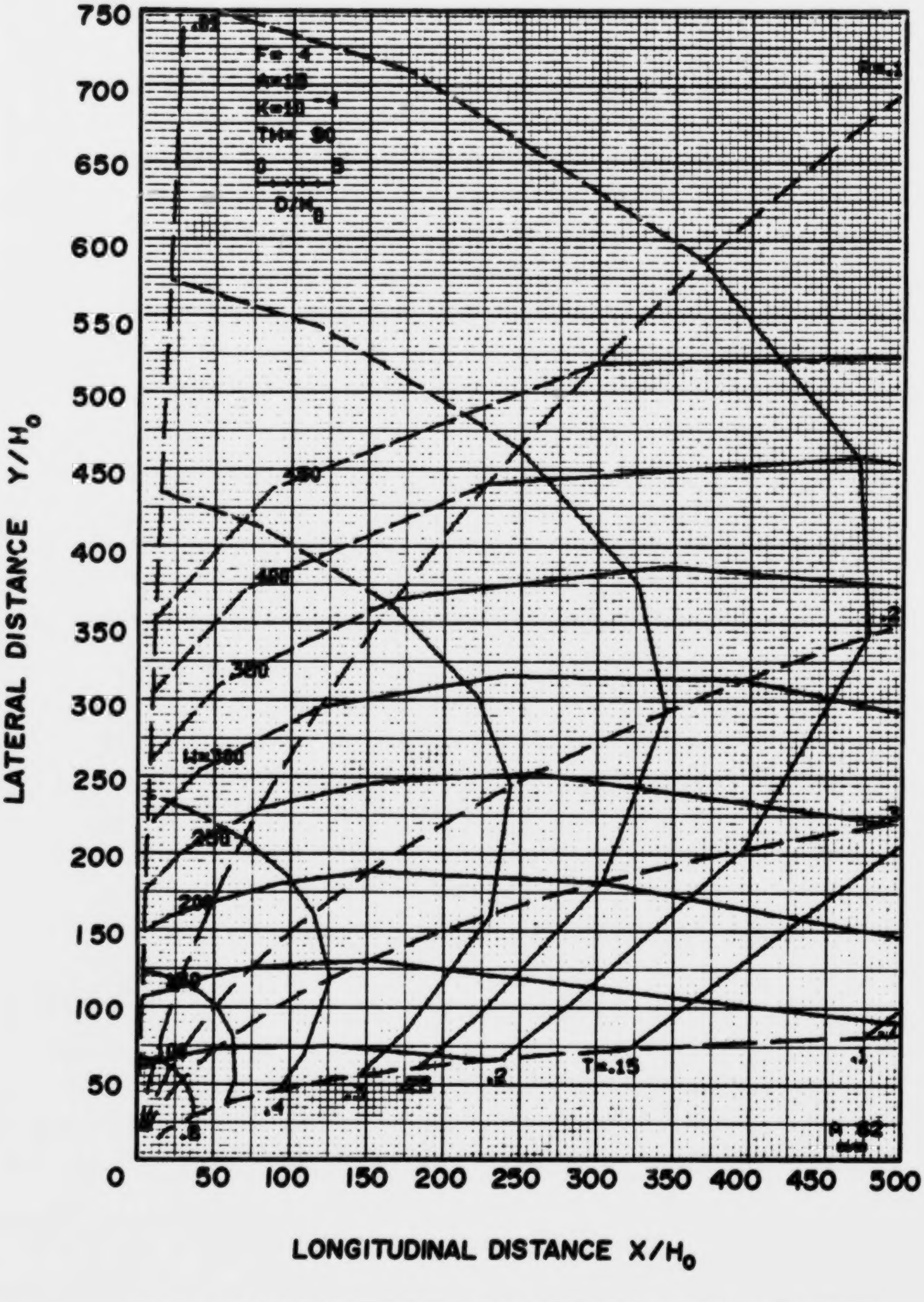

FIG (A 62) TEMPERATURE, TRAJECTORY, WIDTH, AND DEPTH (TTWD)-PLOTS FOR SURFACE JET DISCHARGE

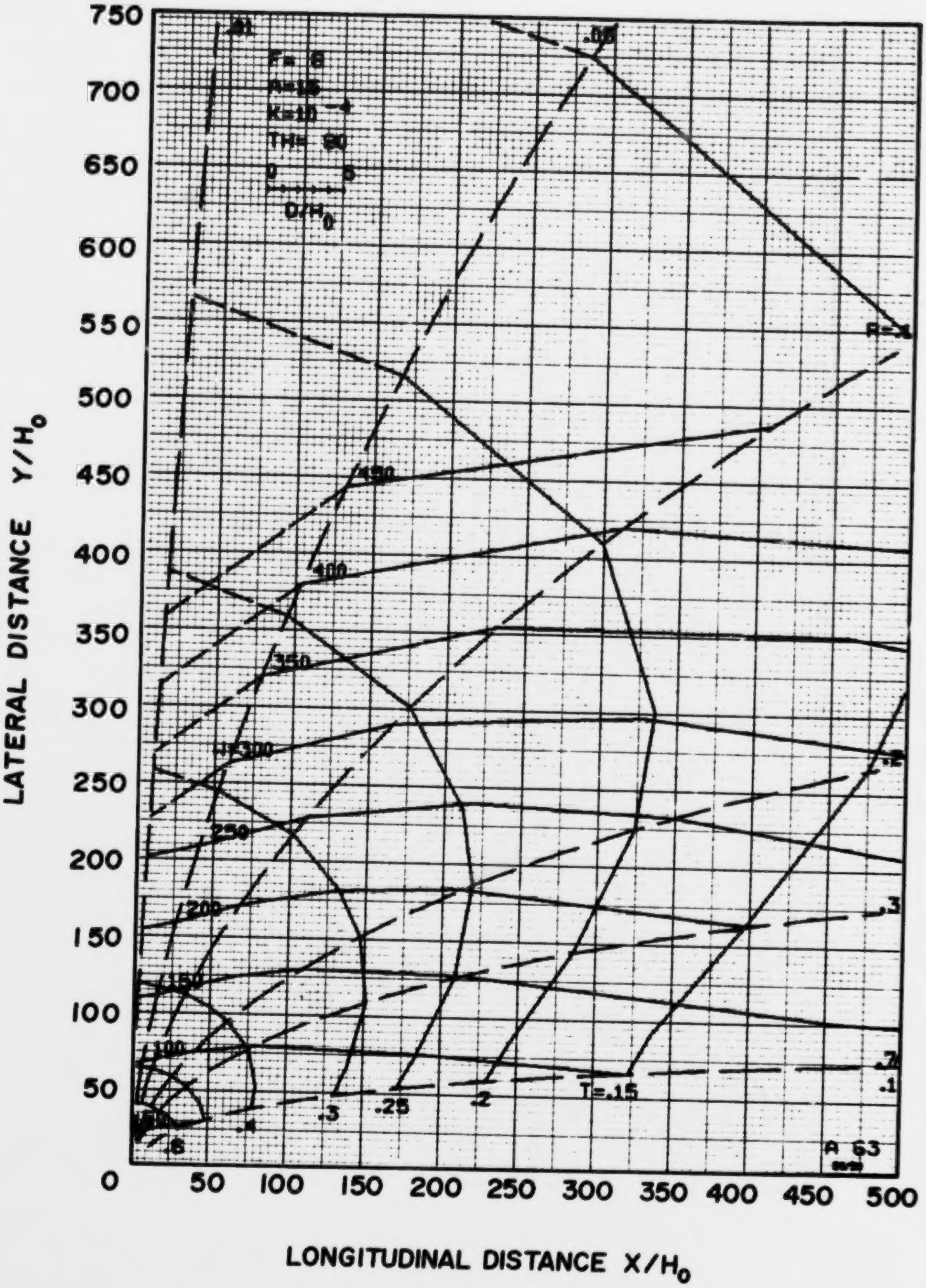

FIG (A63) TEMPERATURE, TRAJECTORY, WIDTH, AND DEPTH (TTWD)-PLOTS FOR SURFACE JET DISCHARGE

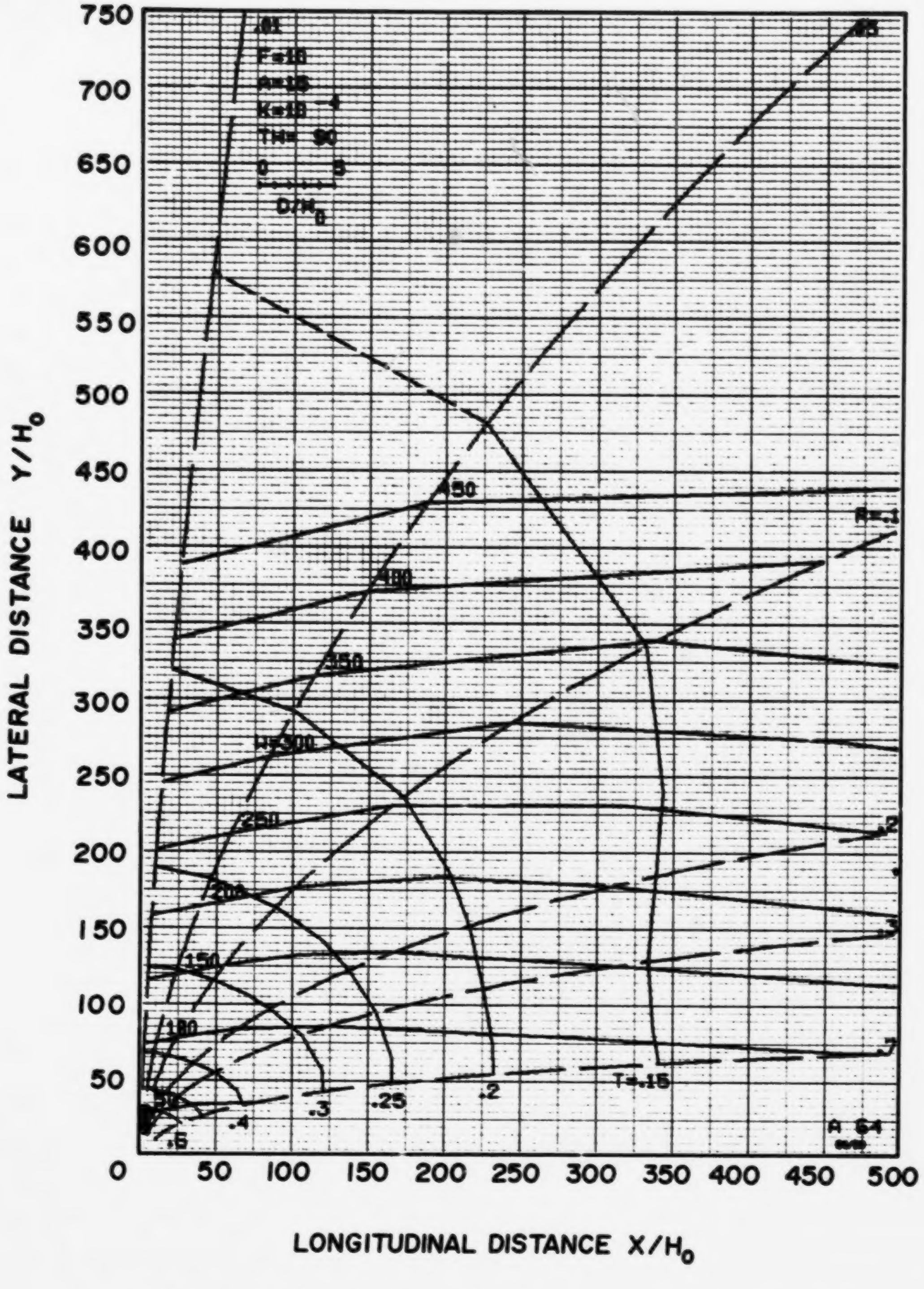

FIG (A64) TEMPERATURE, TRAJECTORY, WIDTH, AND DEPTH (TTWD)-PLOTS FOR SURFACE JET DISCHARGE

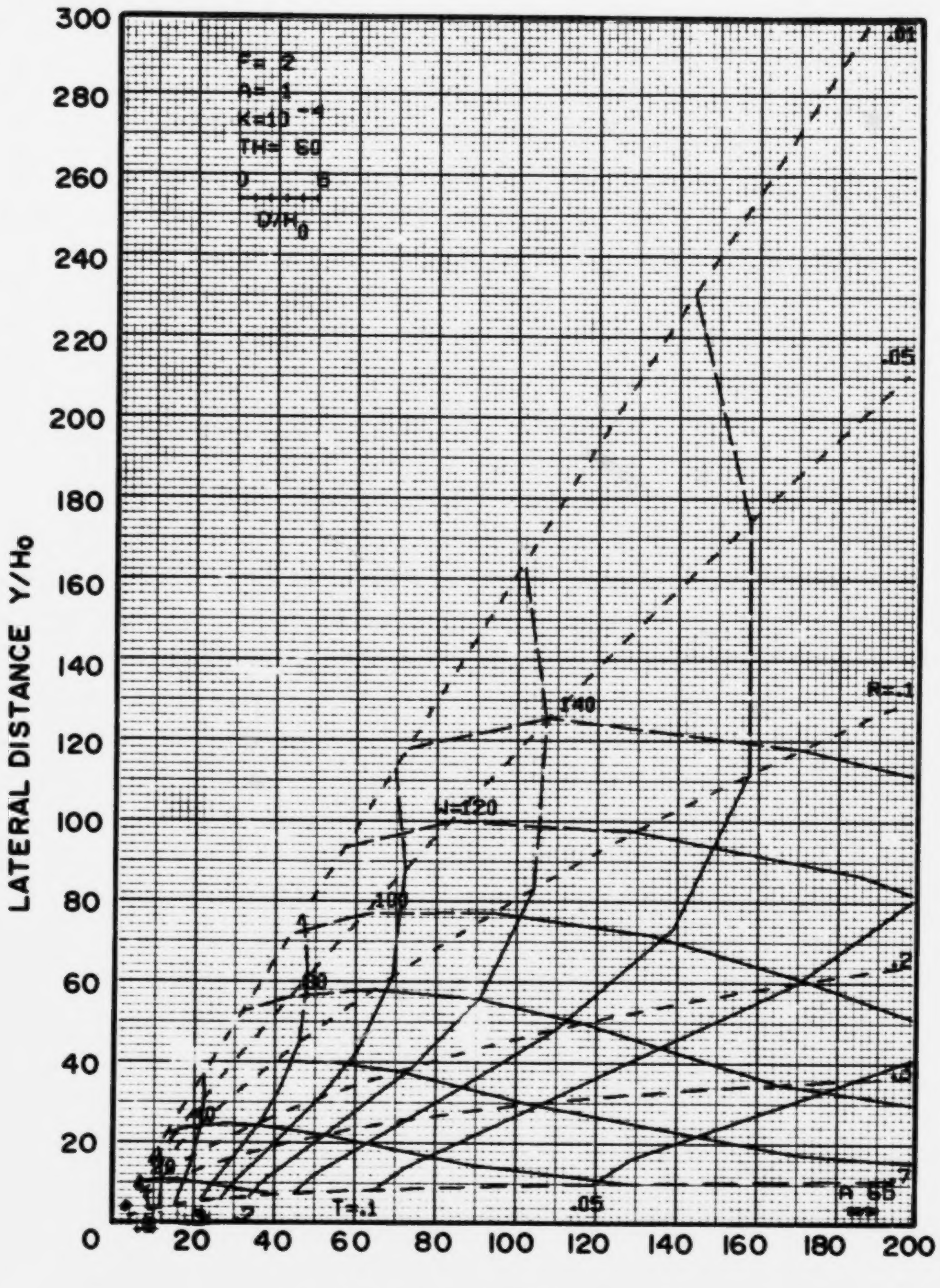

FIG (A65) TEMPERATURE, TRAJECTORY, WIDTH, AND DEPTH (TTWD)-PLOTS FOR SURFACE JET DISCHARGE

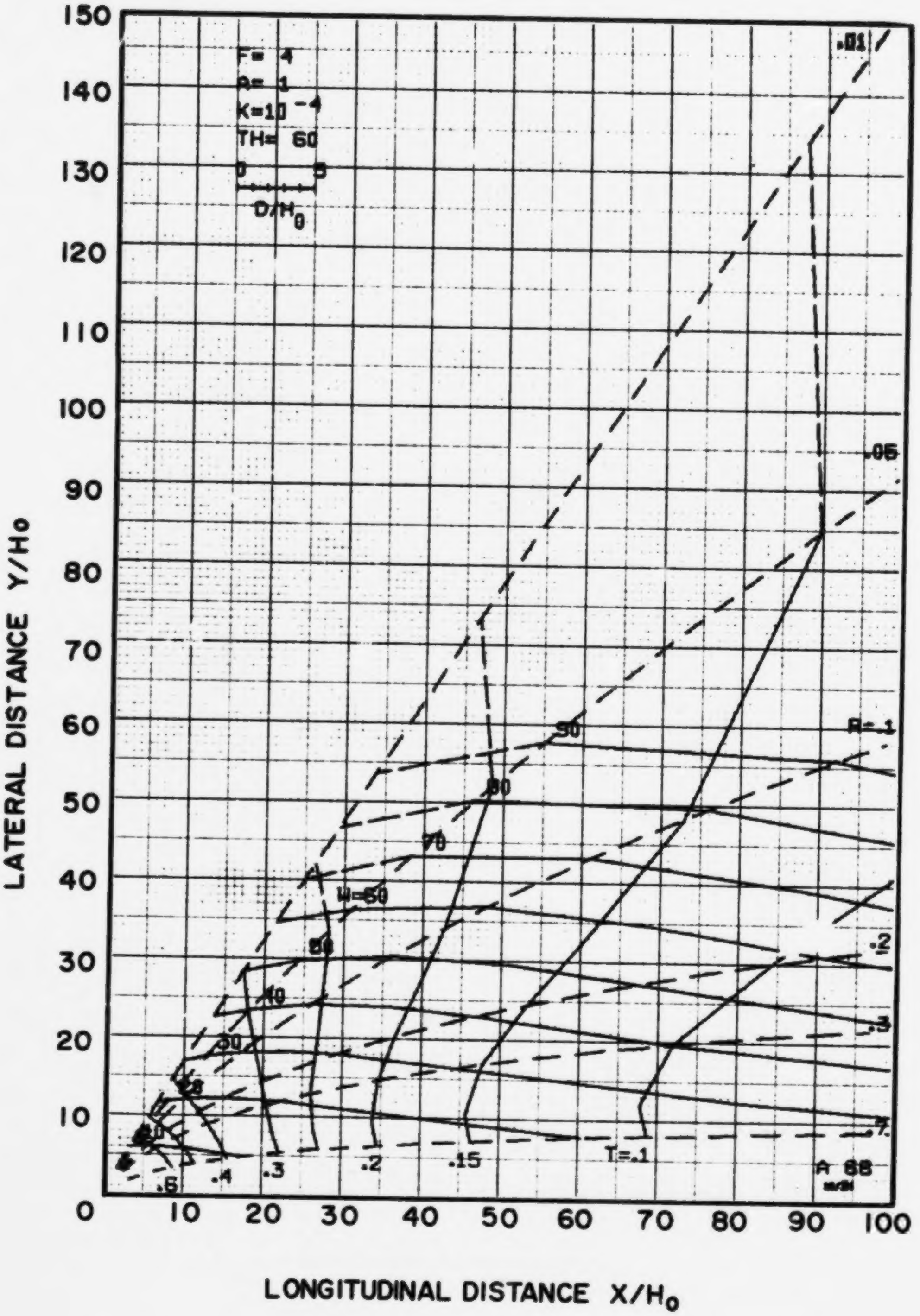

FIG(A66) TEMPERATURE, TRAJECTORY, WIDTH, AND DEPTH (TTWD)-PLOTS FOR SURFACE JET DISCHARGE

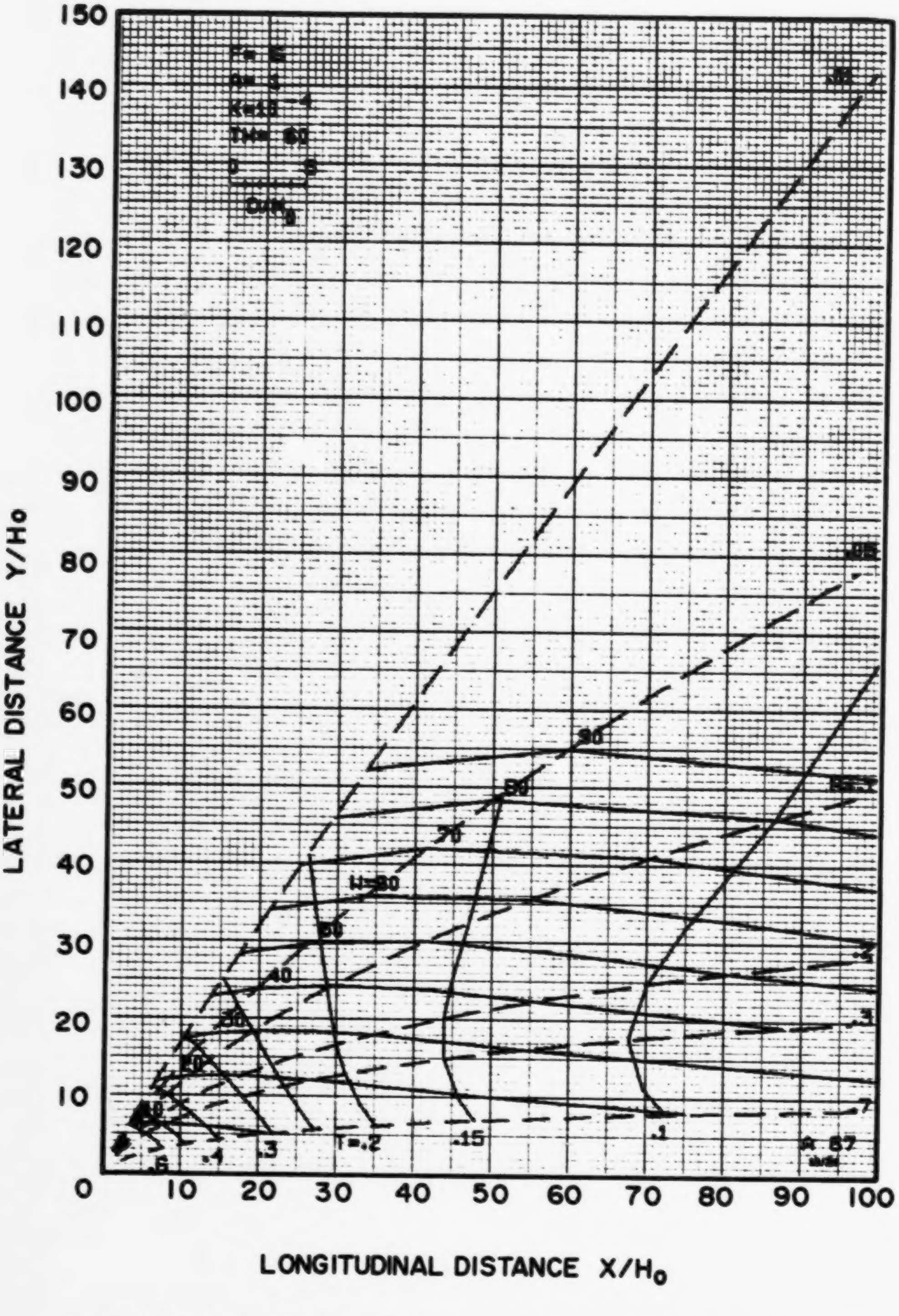

FIG(A67) TEMPERATURE, TRAJECTORY, WIDTH, AND DEPTH (TTWD)-PLOTS FOR SURFACE JET DISCHARGE

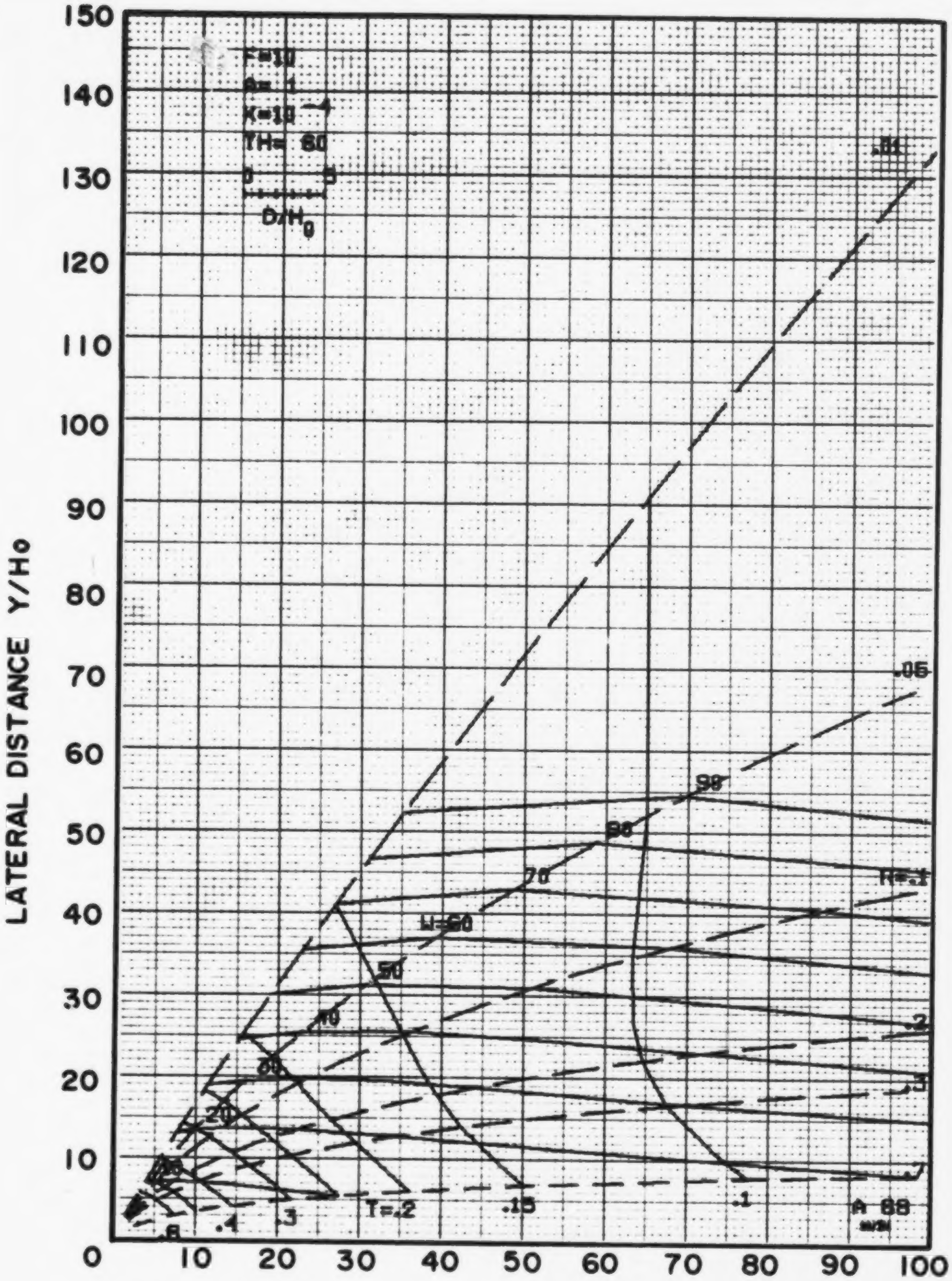

FIG(A68) TEMPERATURE, TRAJECTORY, WIDTH, AND DEPTH (TTWD)-PLOTS FOR SURFACE JET DISCHARGE

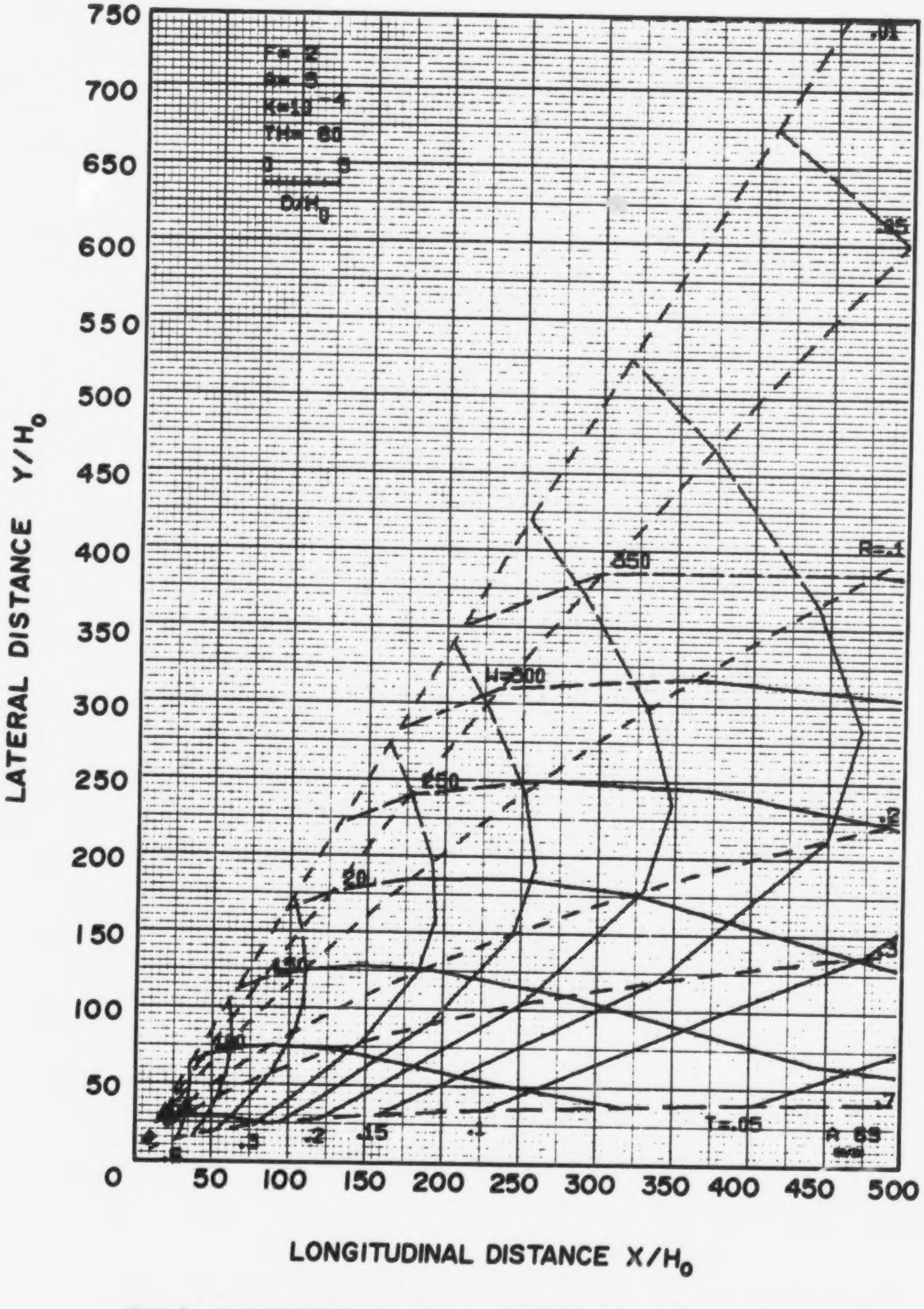

FIG (A69) TEMPERATURE, TRAJECTORY, WIDTH, AND DEPTH (TTWD)-PLOTS FOR SURFACE JET DISCHARGE

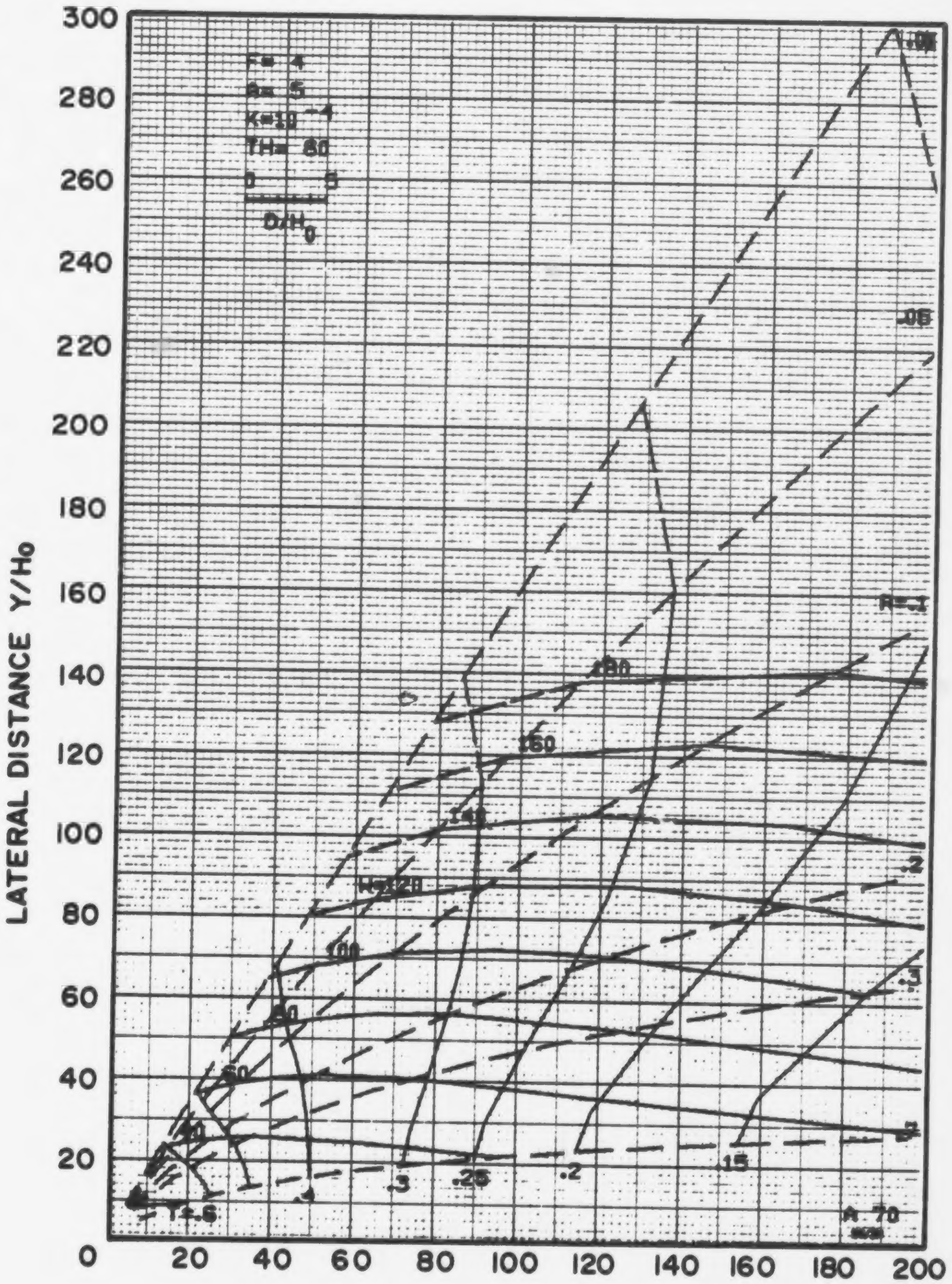

FIG (A70) TEMPERATURE, TRAJECTORY, WIDTH, AND DEPTH (TTWD)-PLOTS FOR SURFACE JET DISCHARGE

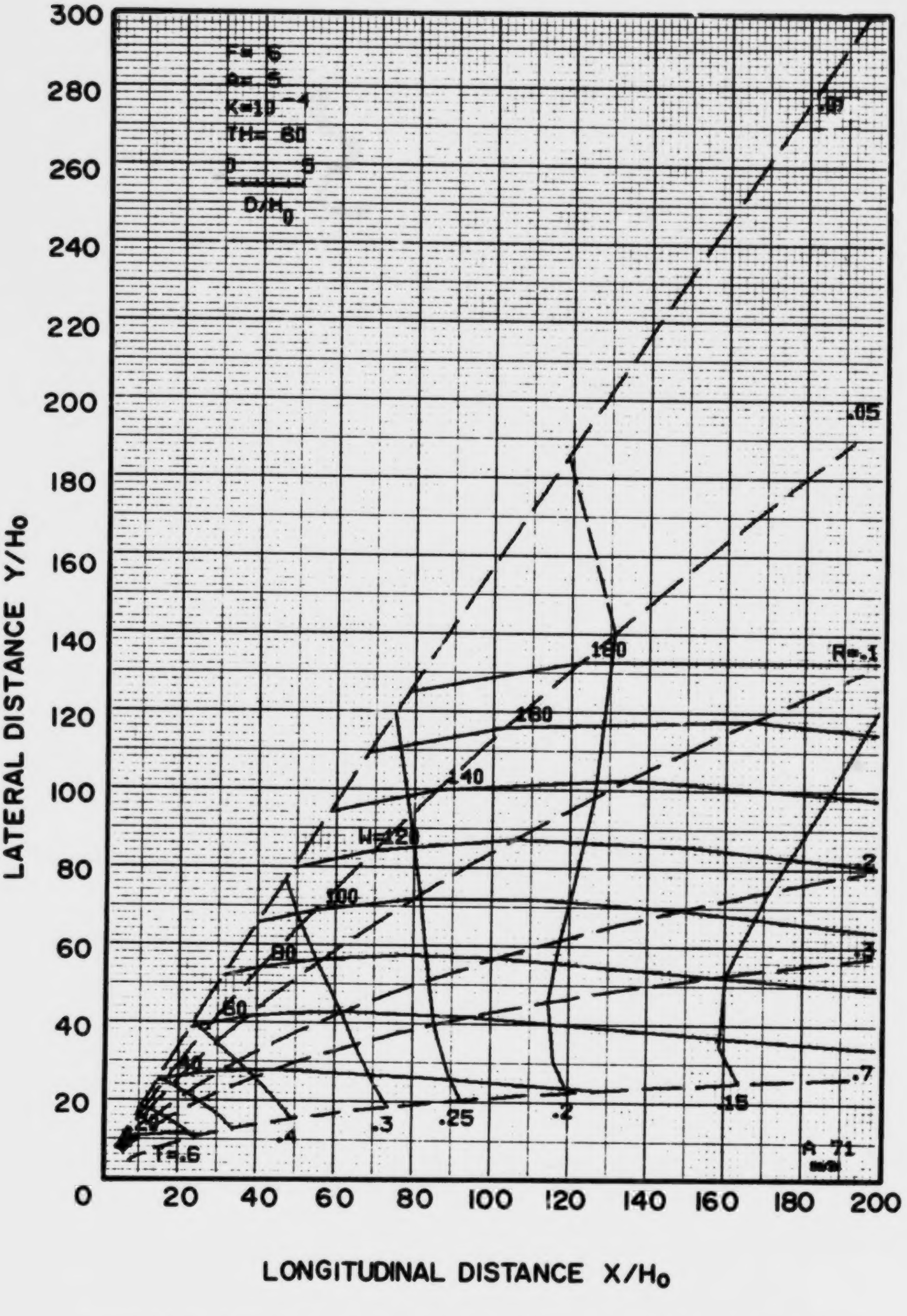

FIG (A71) TEMPERATURE, TRAJECTORY, WIDTH, AND DEPTH (TTWD)-PLOTS FOR SURFACE JET DISCHARGE

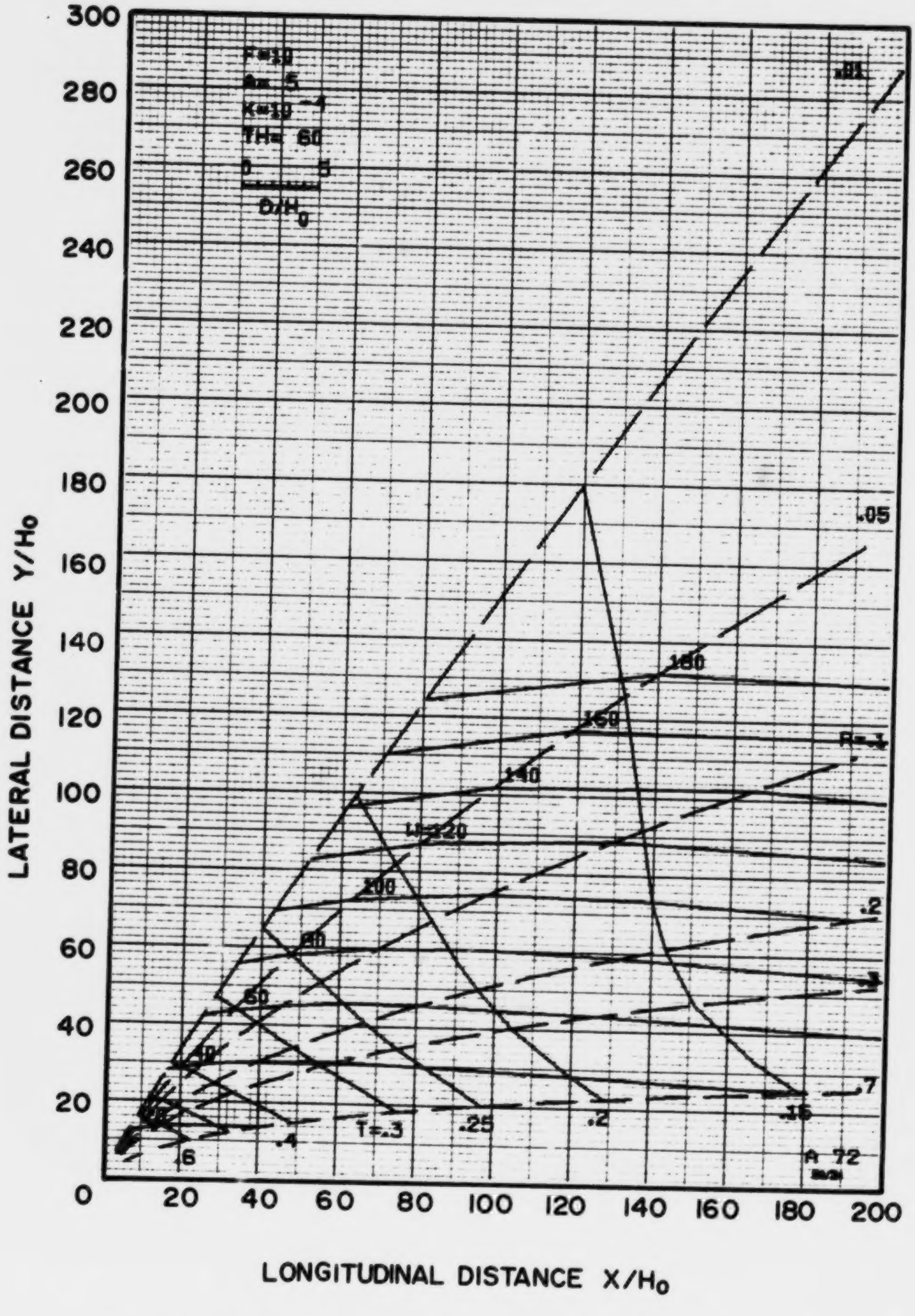

FIG (A72) TEMPERATURE, TRAJECTORY, WIDTH, AND DEPTH (TTWD)-PLOTS FOR SURFACE JET DISCHARGE

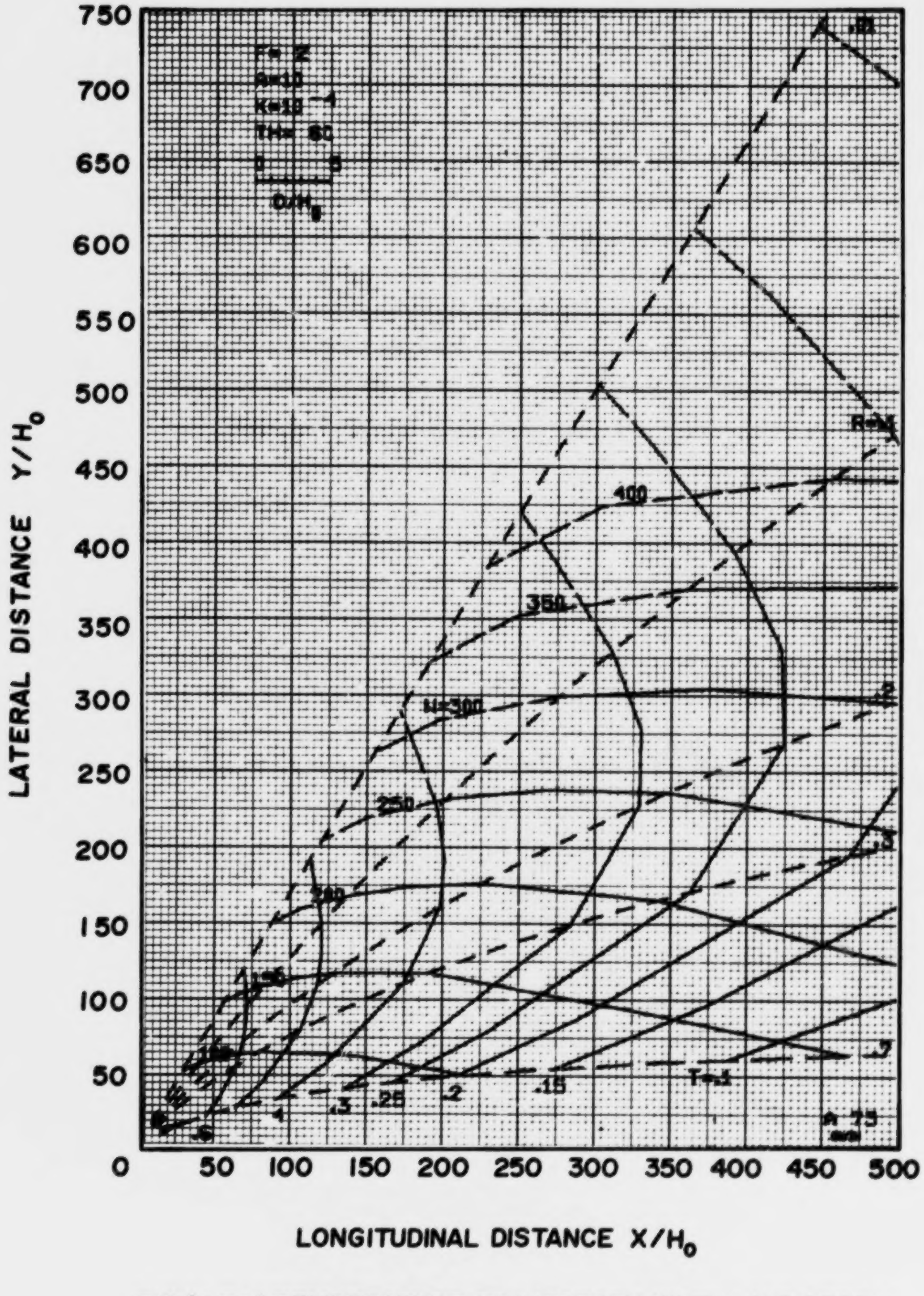

FIG (A73) TEMPERATURE, TRAJECTORY, WIDTH, AND DEPTH (TTWD)-PLOTS FOR SURFACE JET DISCHARGE

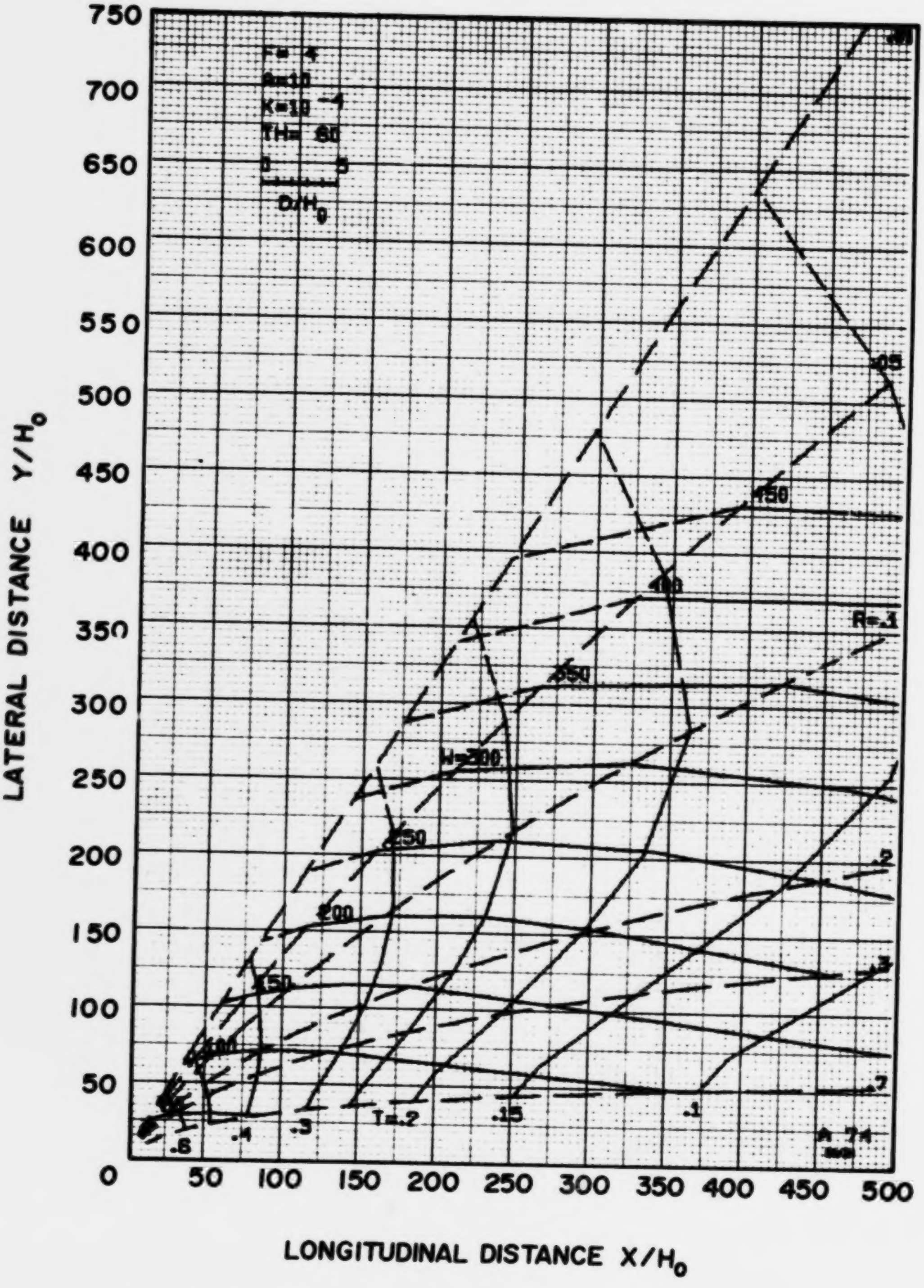

FIG (A74) TEMPERATURE, TRAJECTORY, WIDTH, AND DEPTH (TTWD)-PLOTS FOR SURFACE JET DISCHARGE

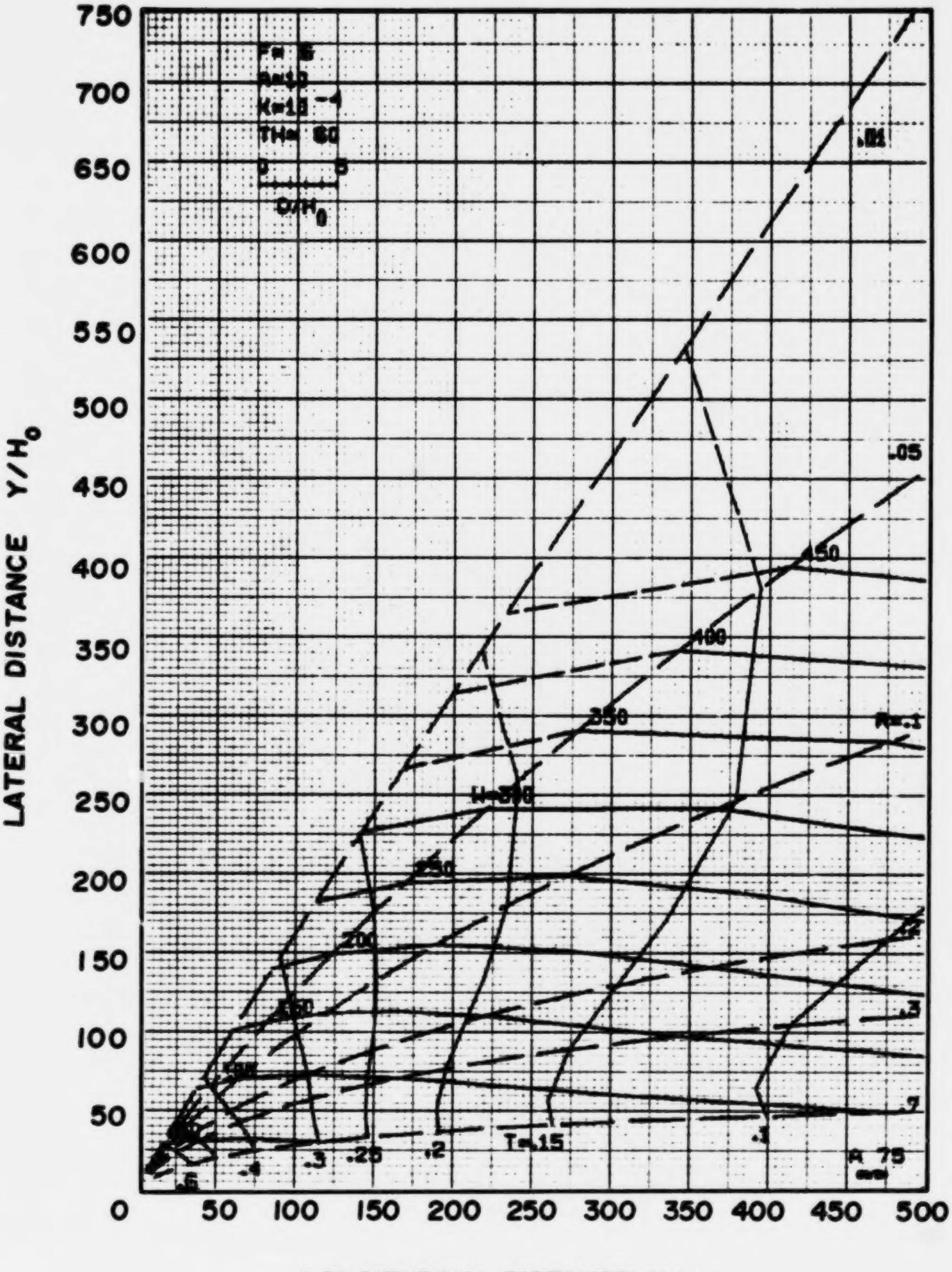

FIG (A75) TEMPERATURE, TRAJECTORY, WIDTH, AND DEPTH (TTWD)-PLOTS FOR SURFACE JET DISCHARGE

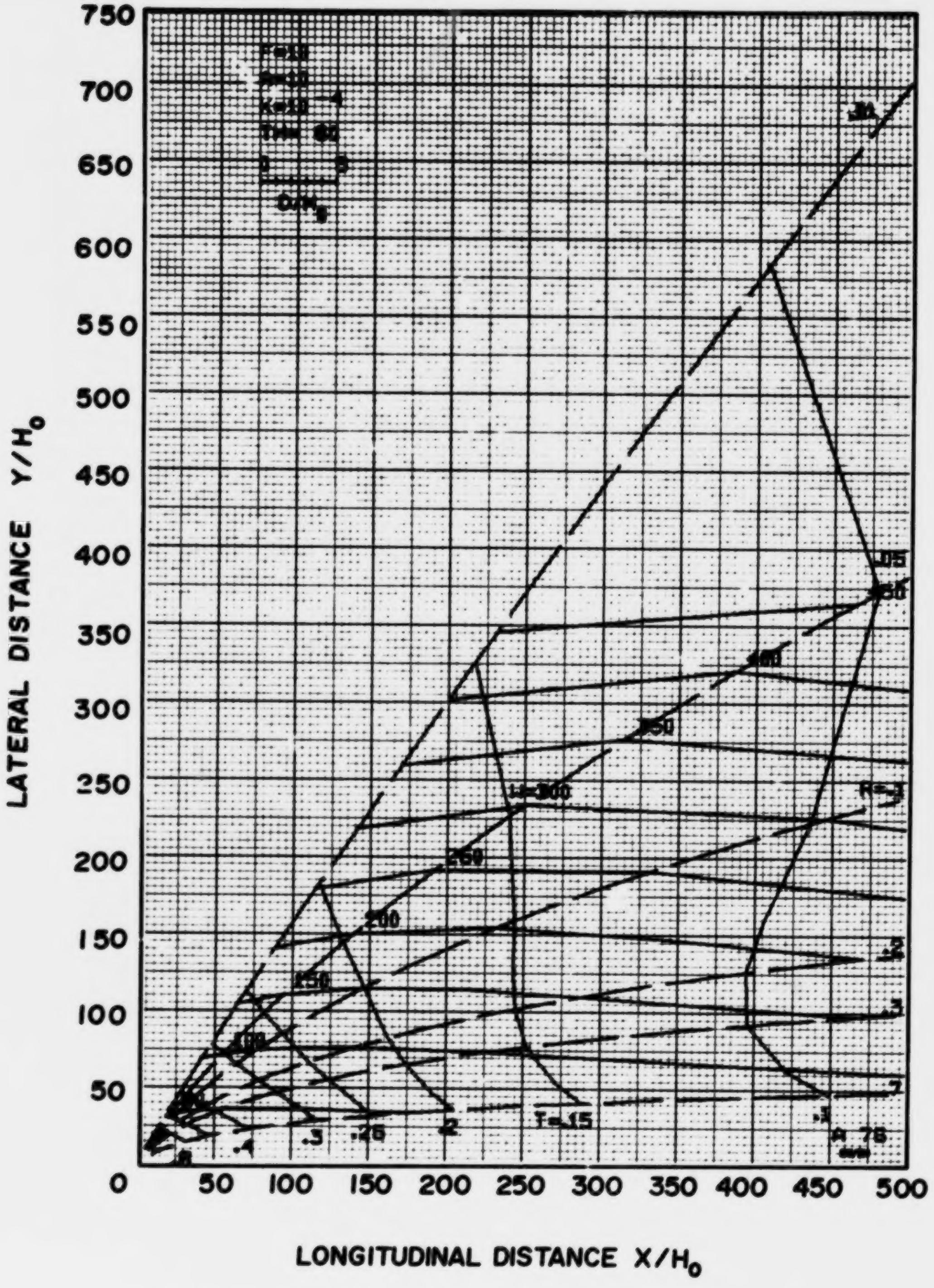

FIG (A76) TEMPERATURE, TRAJECTORY, WIDTH, AND DEPTH (TTWD)-PLOTS FOR SURFACE JET DISCHARGE

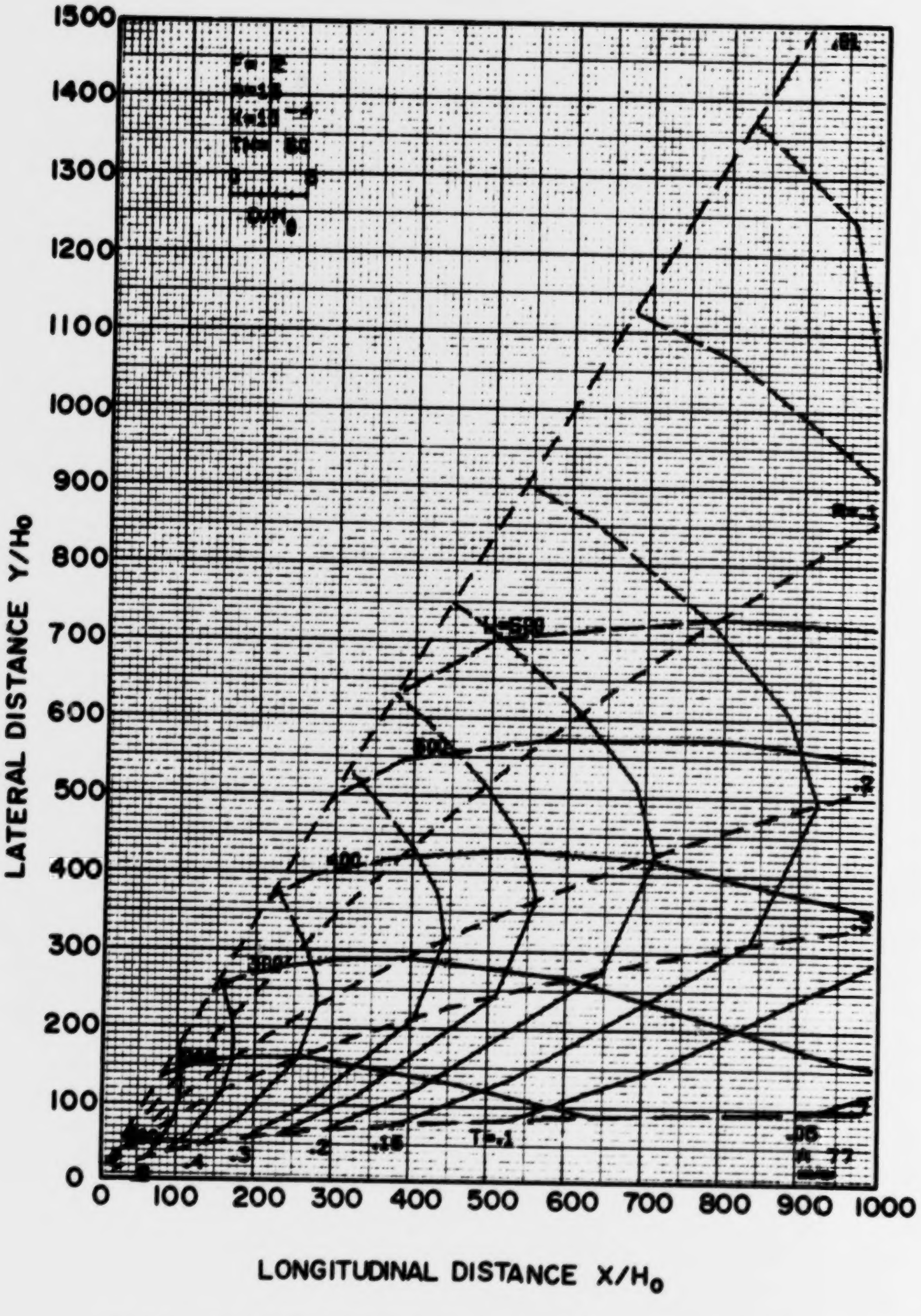

FIG (A 77) TEMPERATURE, TRAJECTORY, WIDTH, AND DEPTH (TTWD)-PLOTS FOR SURFACE JET DISCHARGE

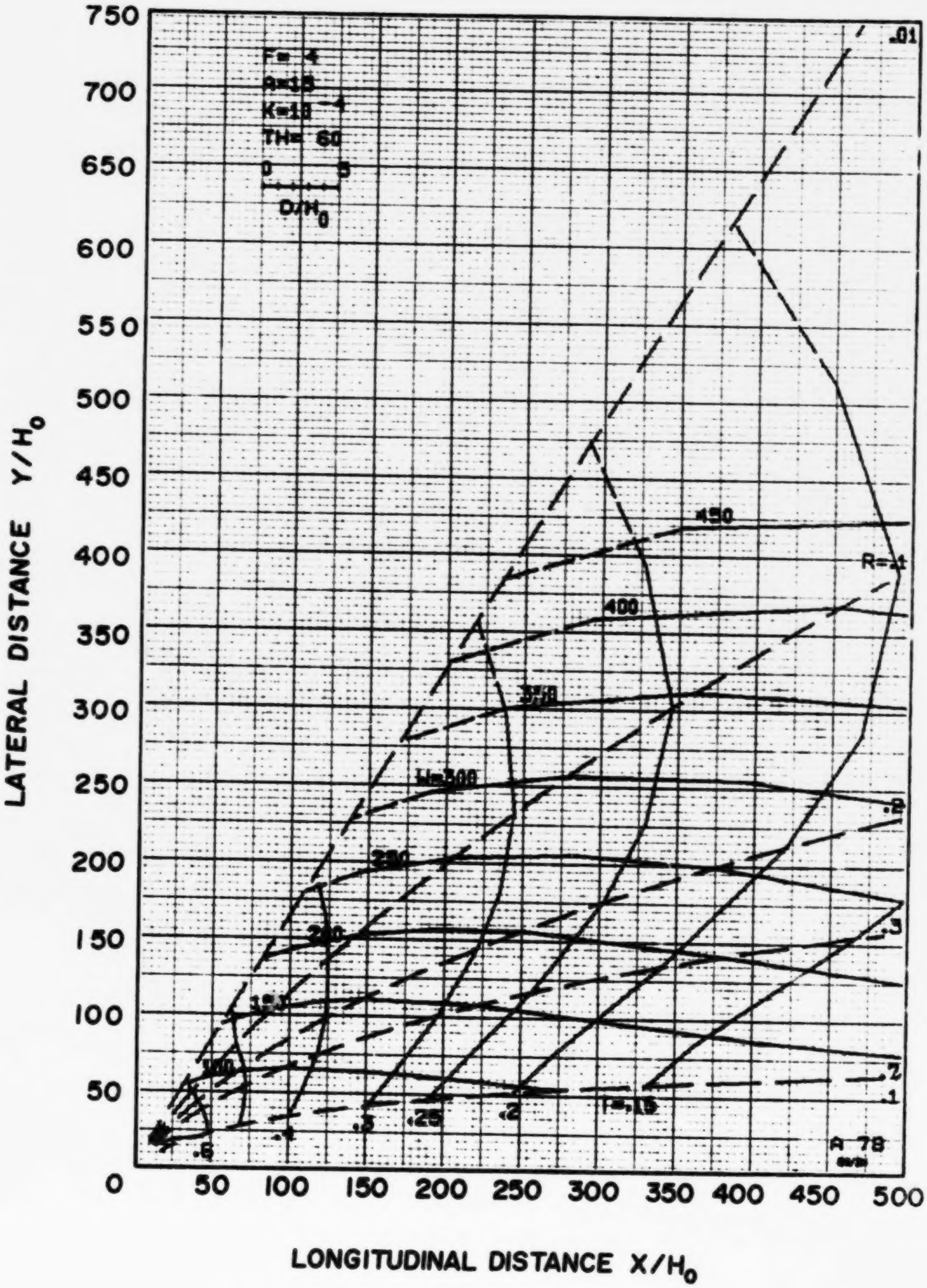

FIG (A78) TEMPERATURE, TRAJECTORY, WIDTH, AND DEPTH (TTWD)-PLOTS FOR SURFACE JET DISCHARGE

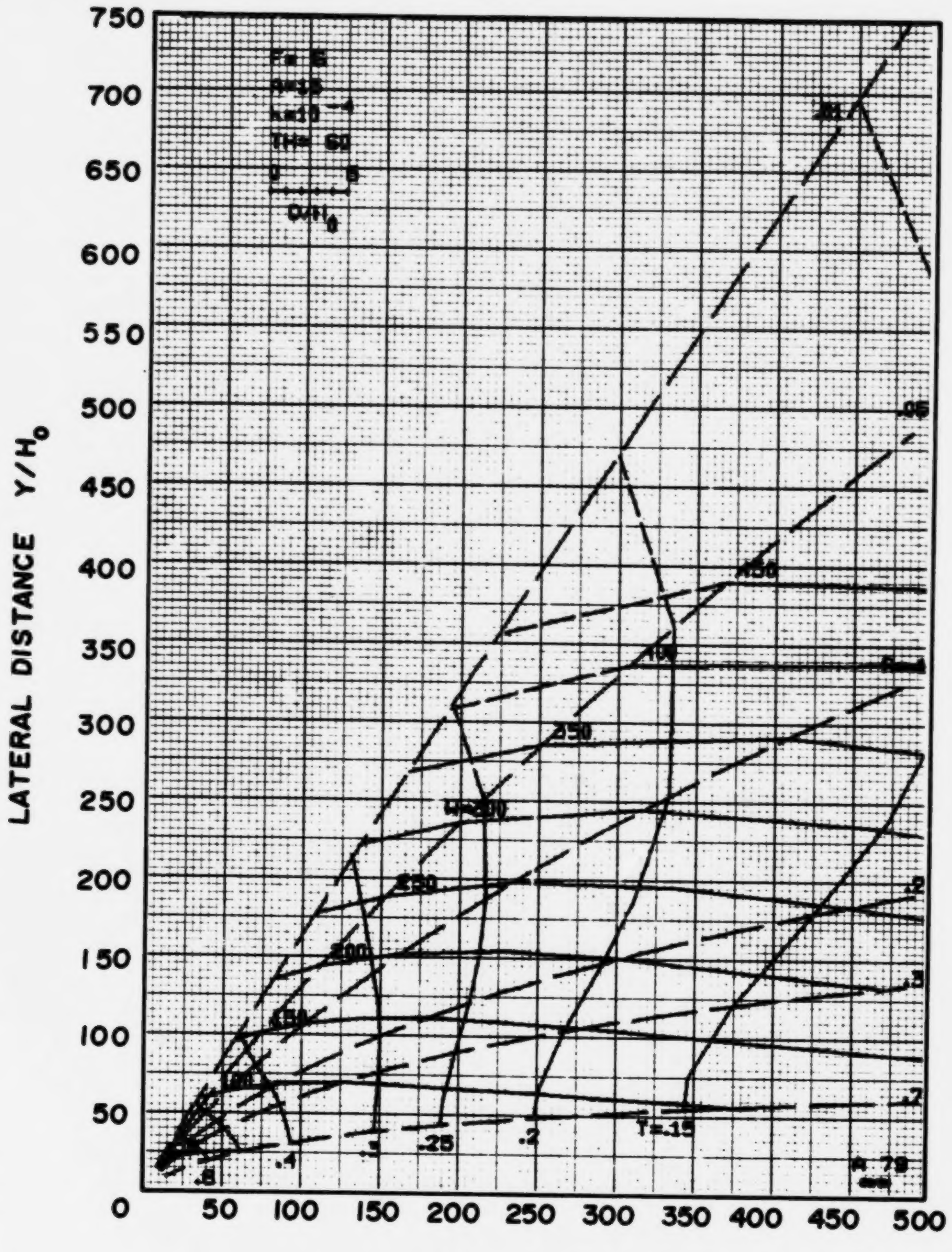

FIG (A79) TEMPERATURE, TRAJECTORY, WIDTH, AND DEPTH (TTWD)-PLOTS FOR SURFACE JET DISCHARGE

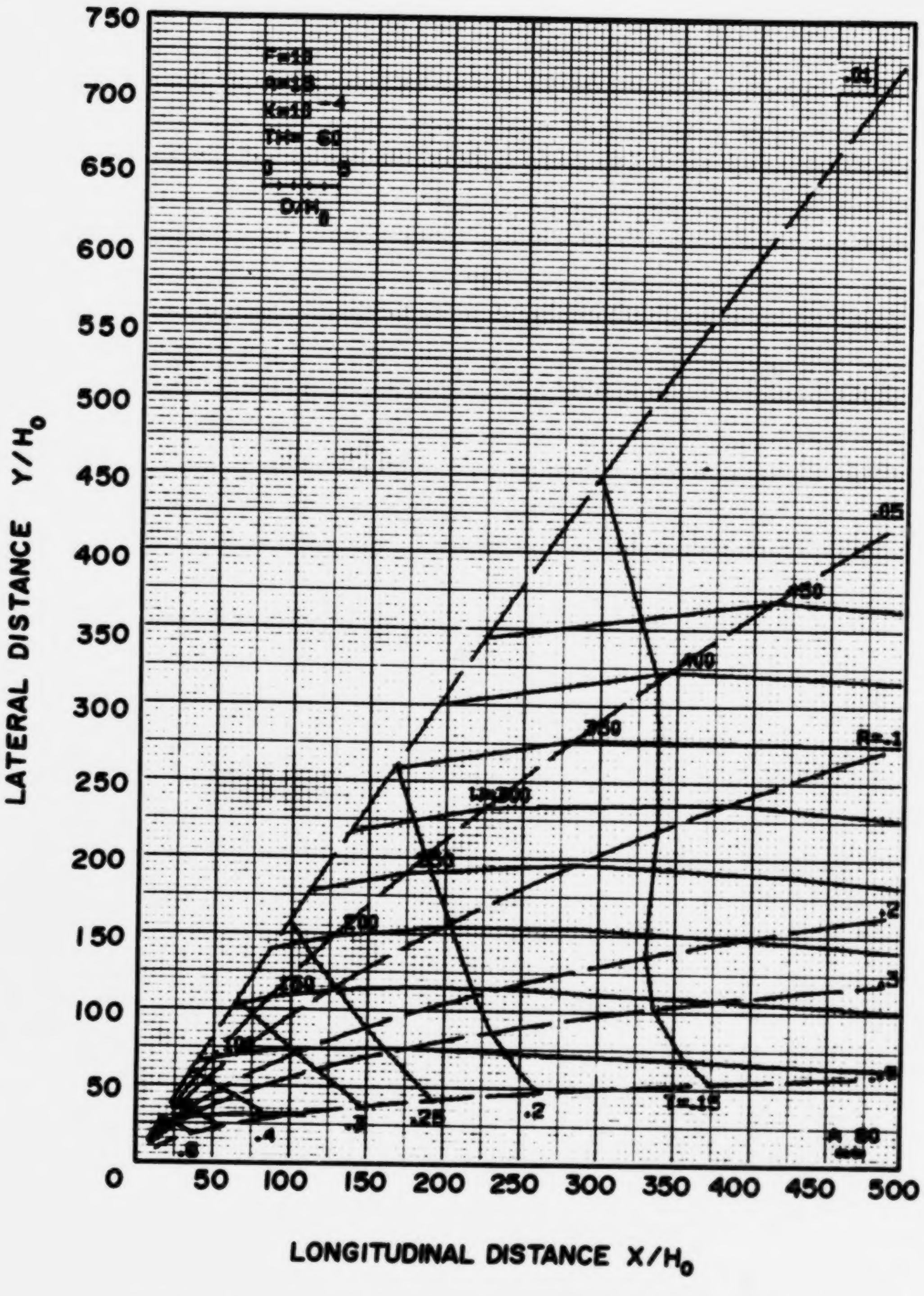

FIG (A80) TEMPERATURE, TRAJECTORY, WIDTH, AND DEPTH (TTWD)-PLOTS FOR SURFACE JET DISCHARGE

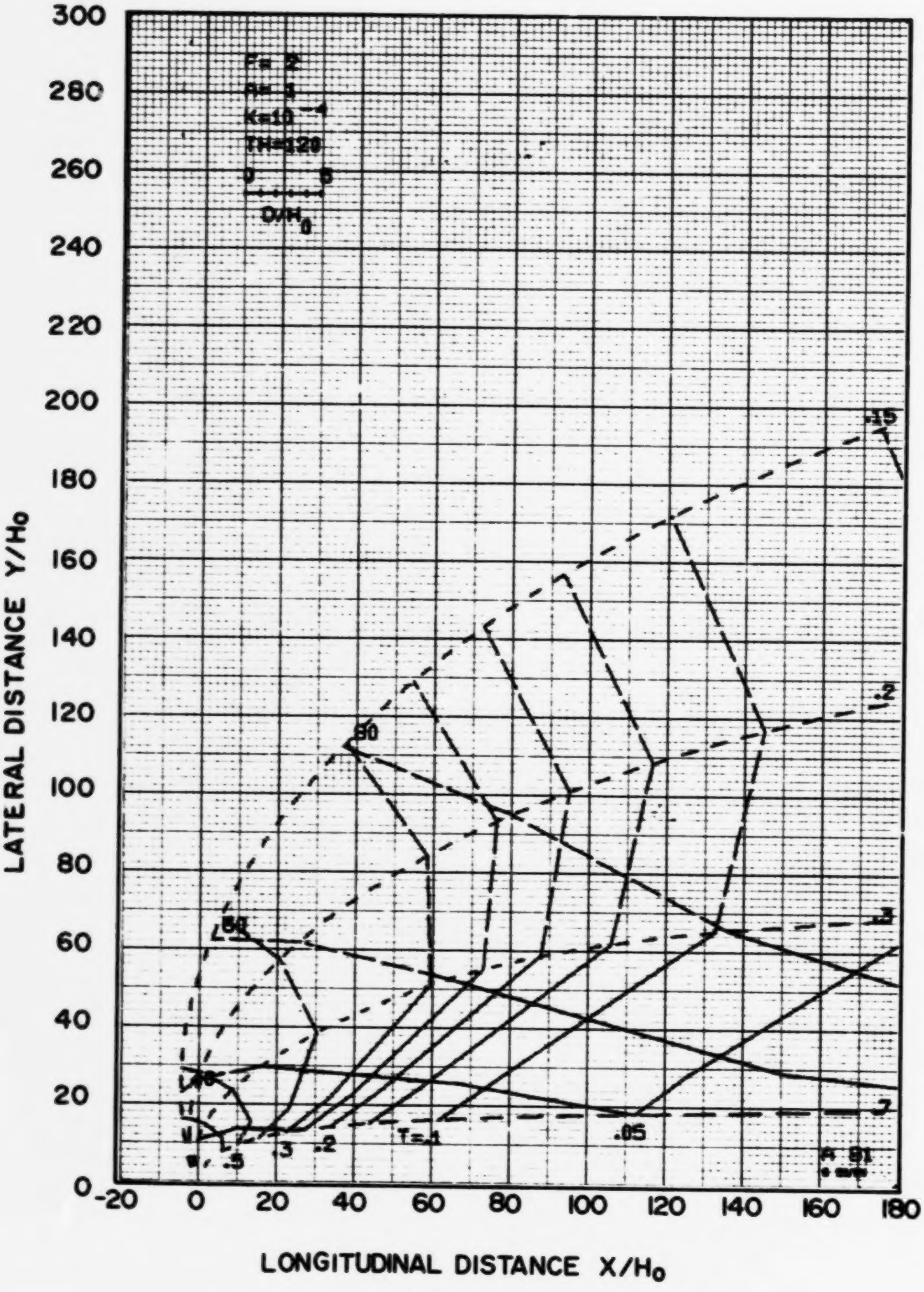

FIG (A81) TEMPERATURE, TRAJECTORY, WIDTH, AND DEPTH (TTWD)-PLOTS FOR SURFACE JET DISCHARGE

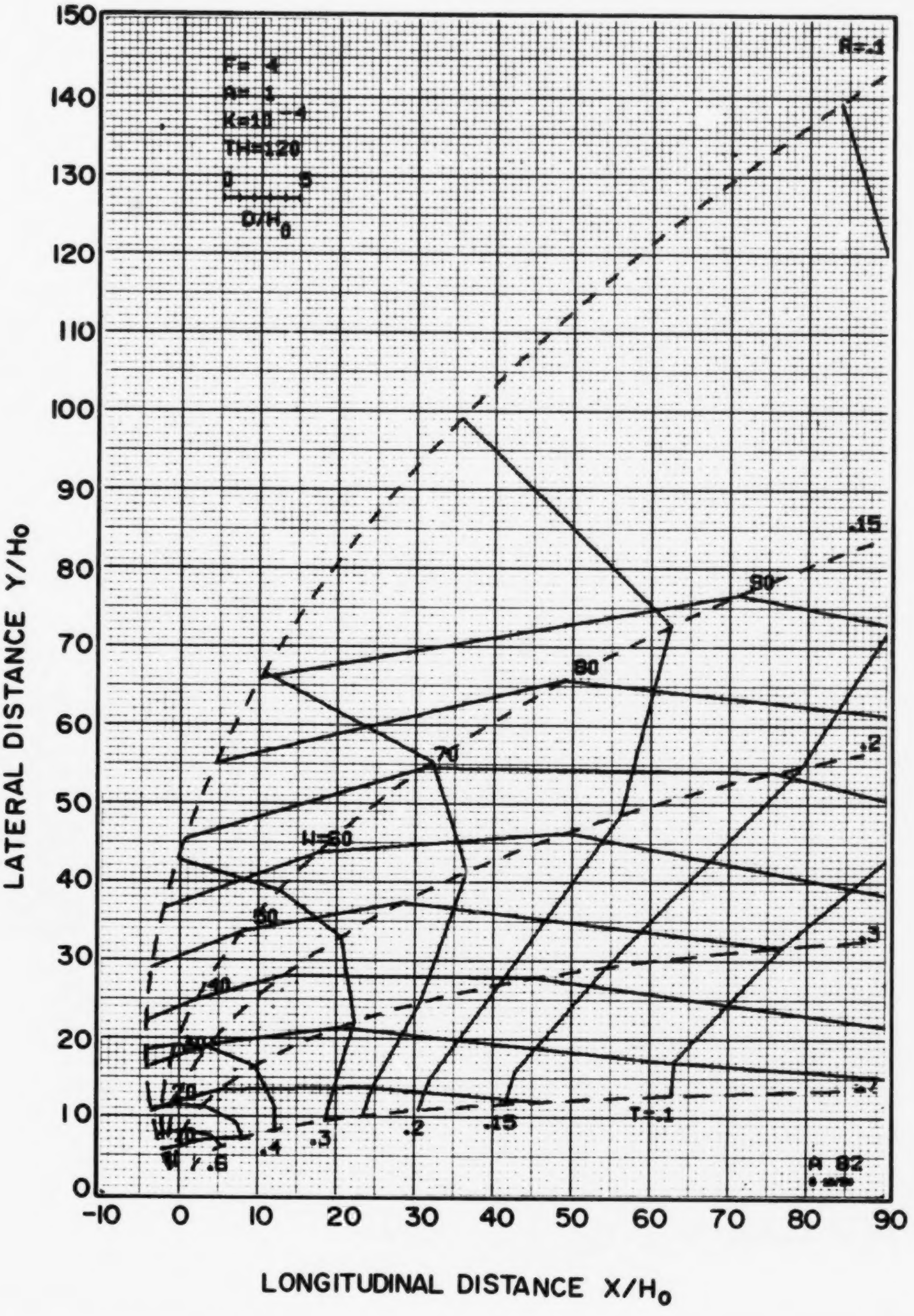

FIG (A82) TEMPERATURE, TRAJECTORY, WIDTH, AND DEPTH (TTWD)-PLOTS FOR SURFACE JET DISCHARGE

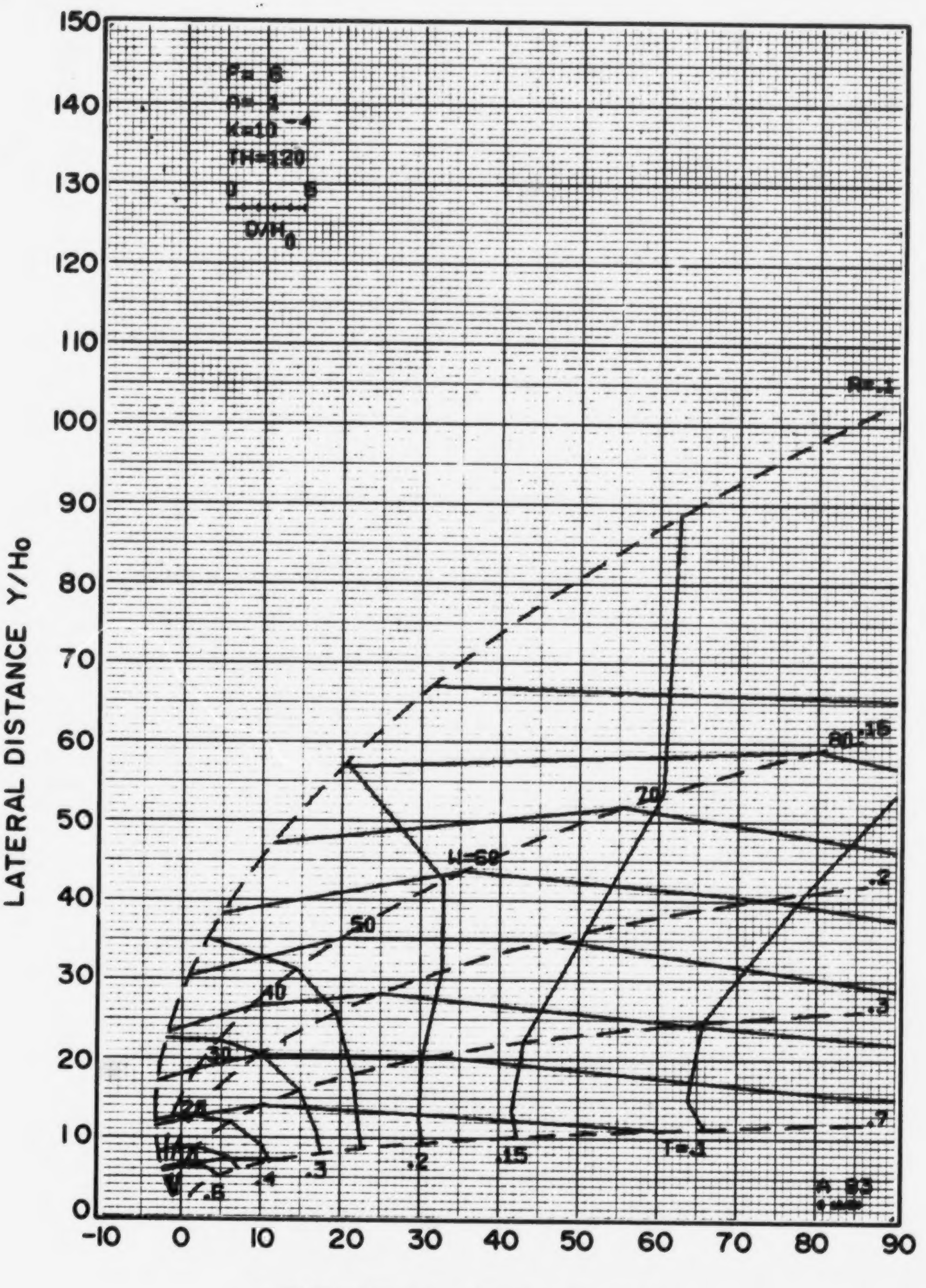

FIG (A83) TEMPERATURE, TRAJECTORY, WIDTH, AND DEPTH (TTWD)-PLOTS FOR SURFACE JET DISCHARGE

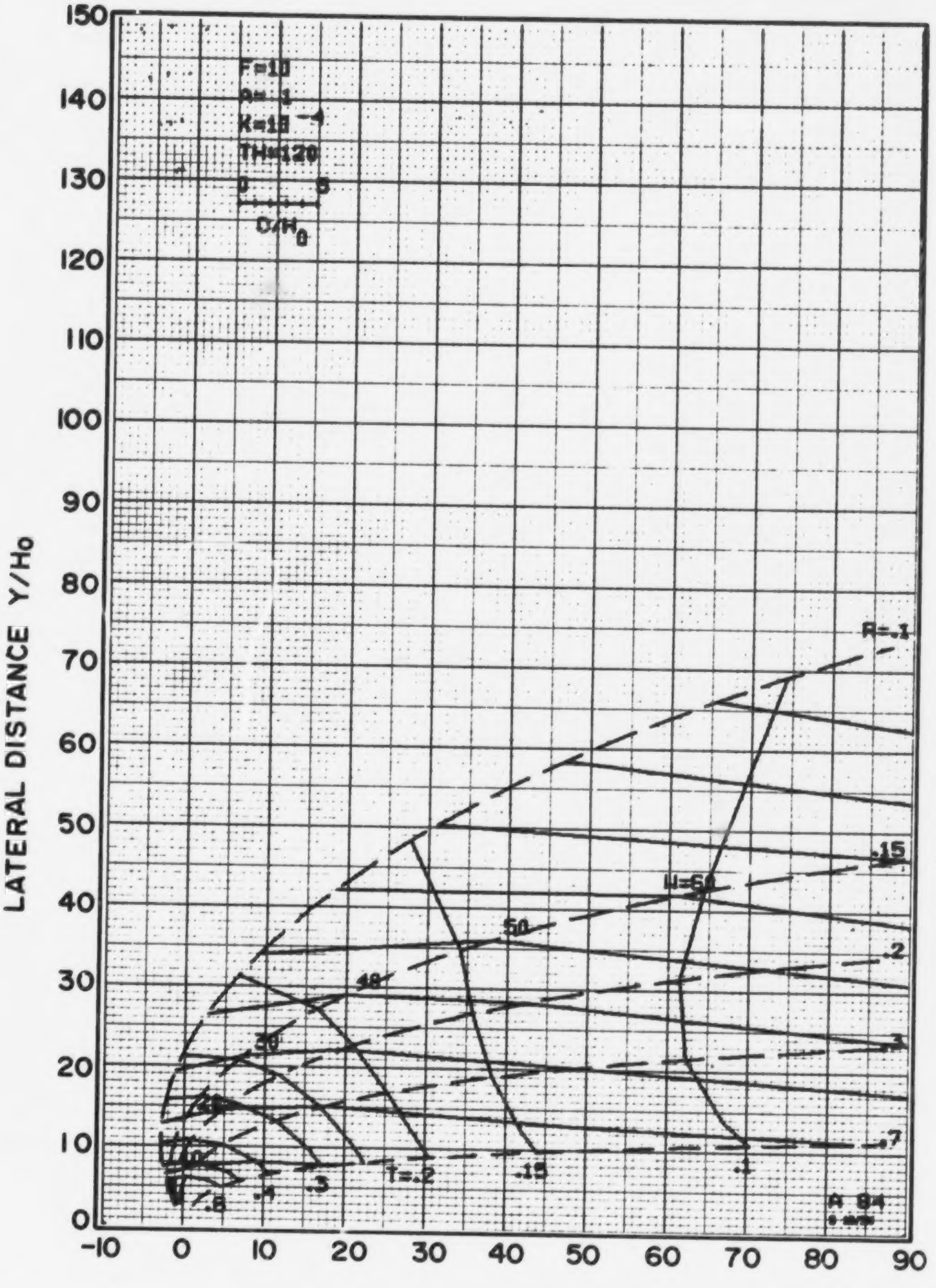

FIG (A84) TEMPERATURE, TRAJECTORY, WIDTH, AND DEPTH (TTWD)-PLOTS FOR SURFACE JET DISCHARGE

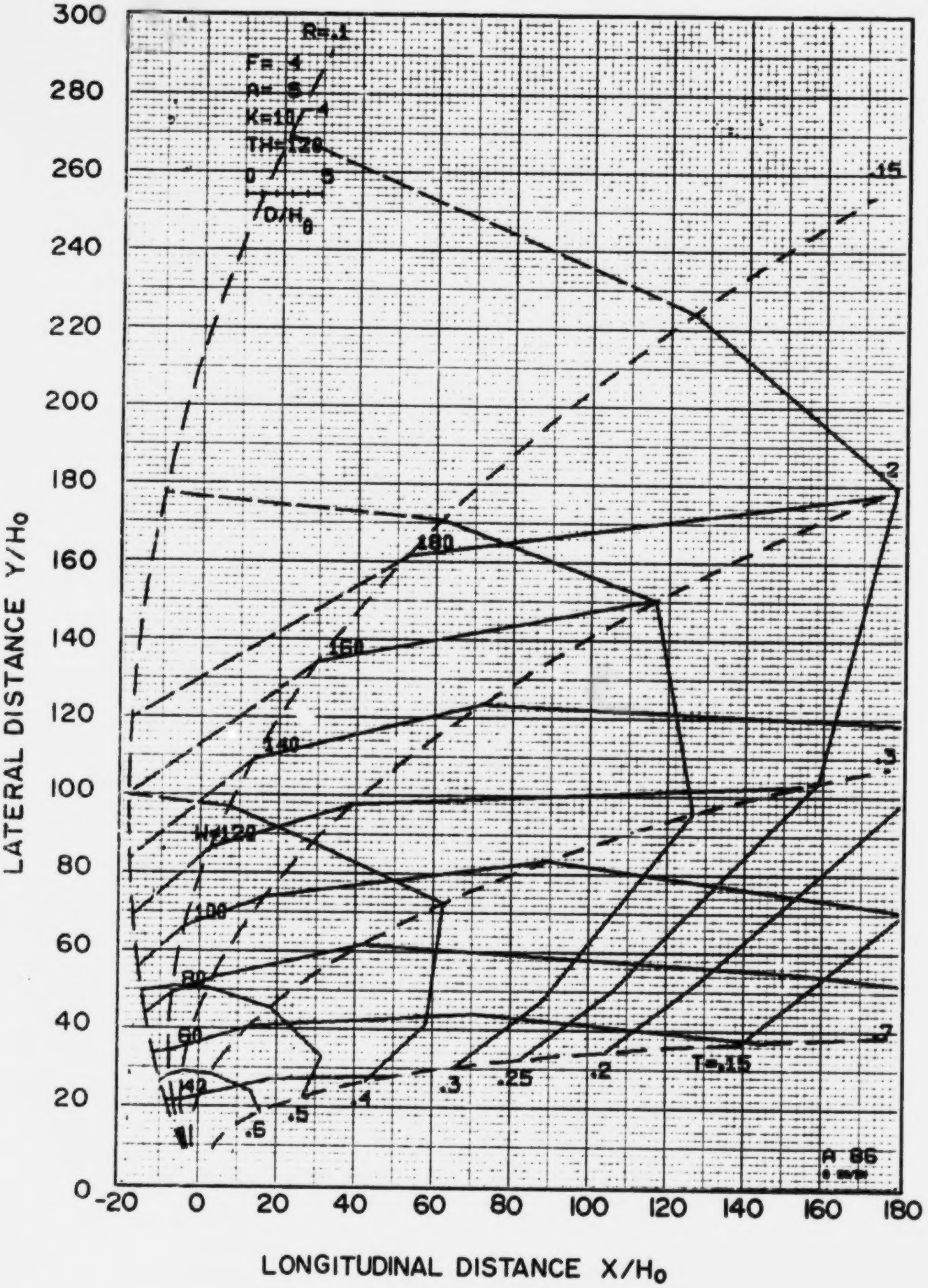

FIG (A86) TEMPERATURE, TRAJECTORY, WIDTH, AND DEPTH (TTWD)-PLOTS FOR SURFACE JET DISCHARGE

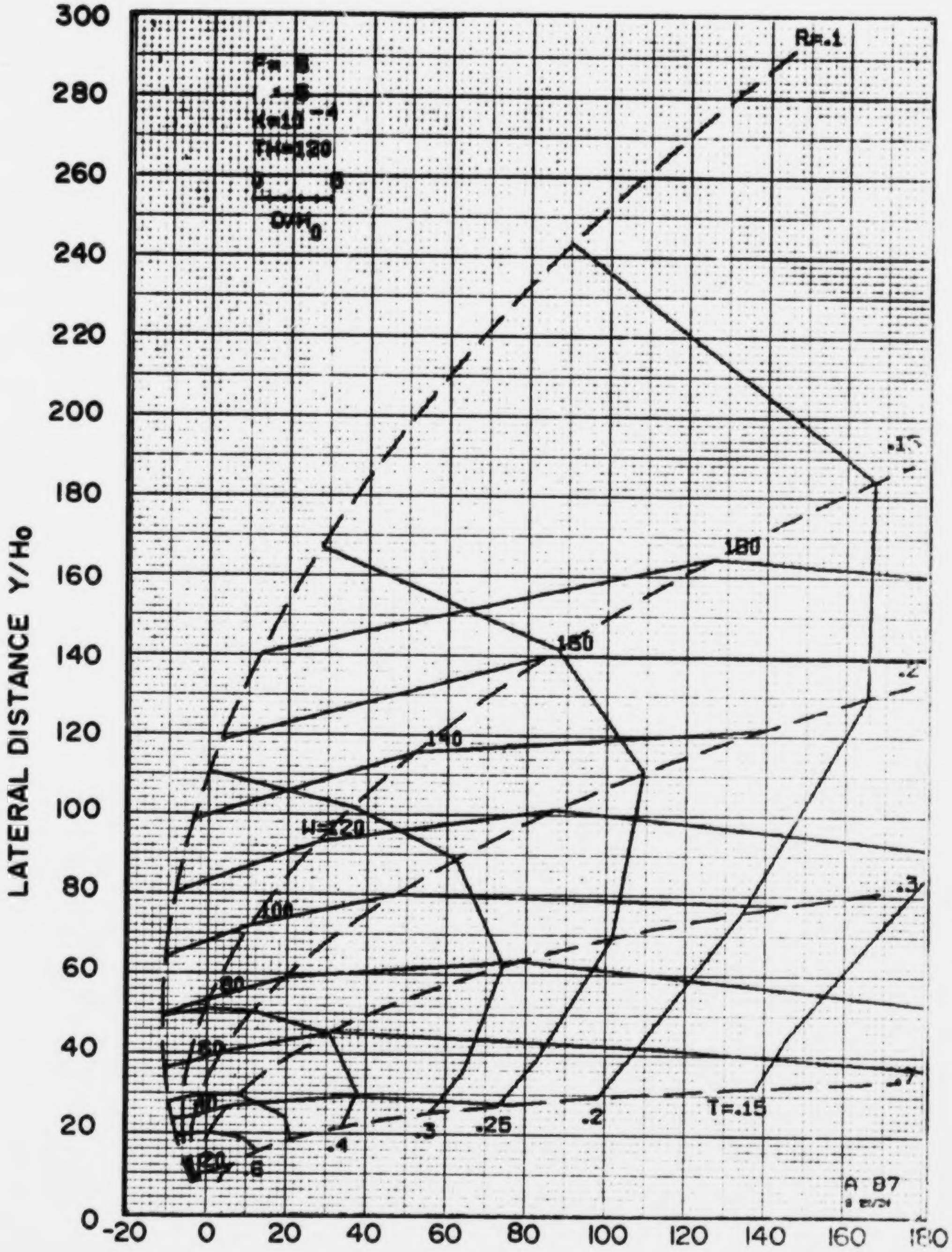

FIG (A87) TEMPERATURE, TRAJECTORY, WIDTH, AND DEPTH (TTWD)-PLOTS FOR SURFACE JET DISCHARGE

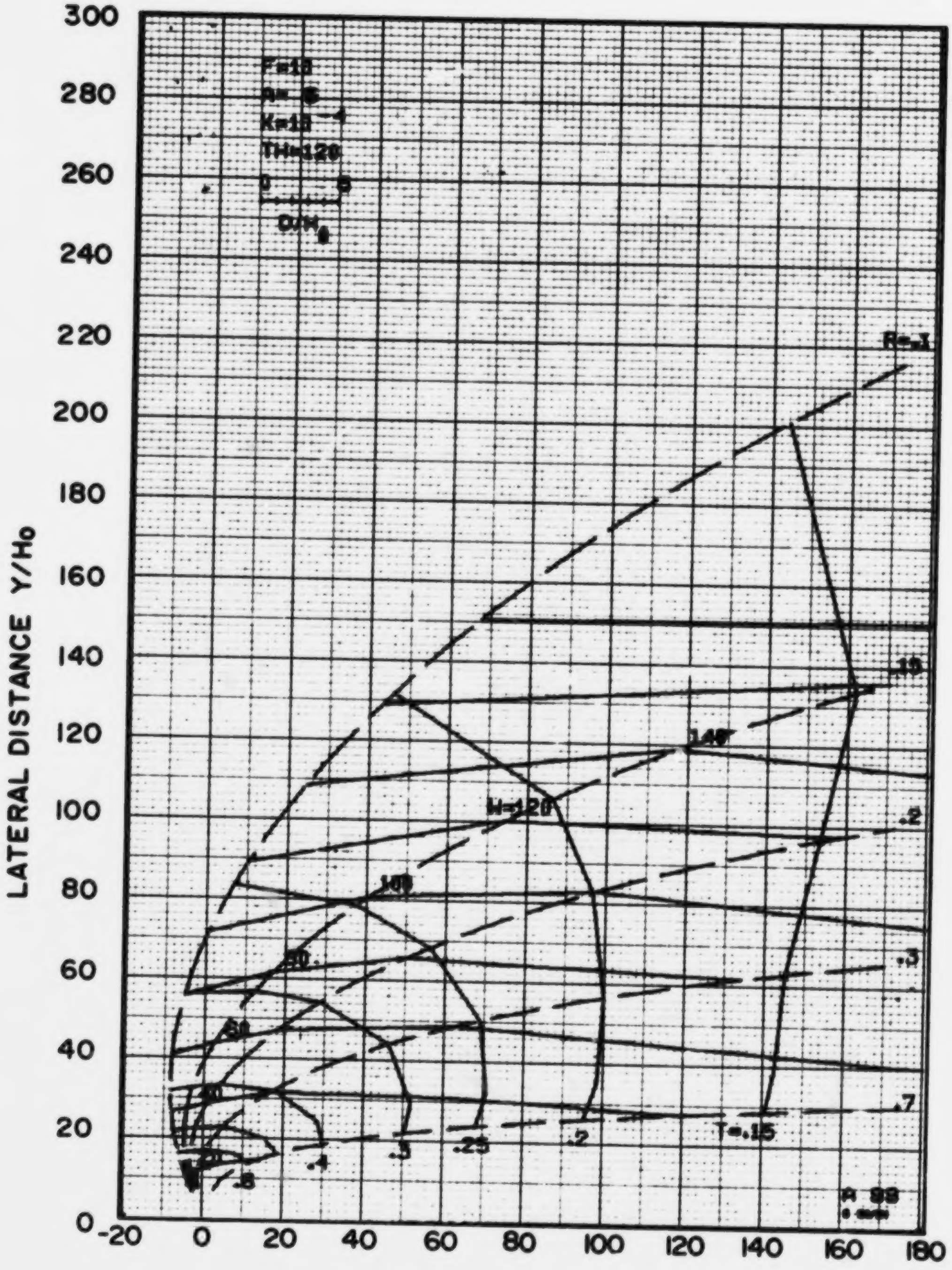

FIG (A88) TEMPERATURE, TRAJECTORY, WIDTH, AND DEPTH (TTWD)-PLOTS FOR SURFACE JET DISCHARGE

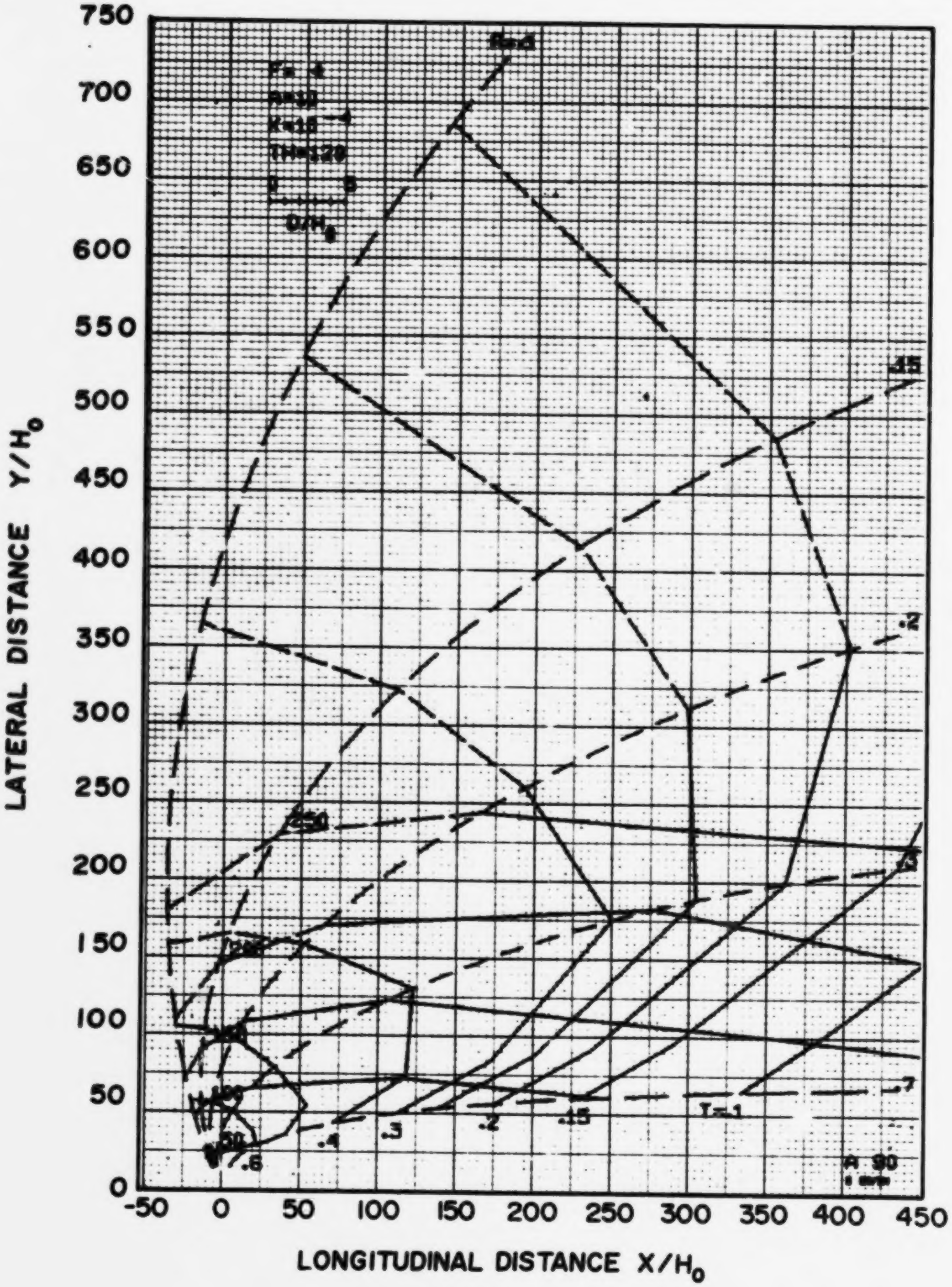

FIG (A90) TEMPERATURE, TRAJECTORY, WIDTH, AND DEPTH (TTWD)-PLOTS FOR SURFACE JET DISCHARGE

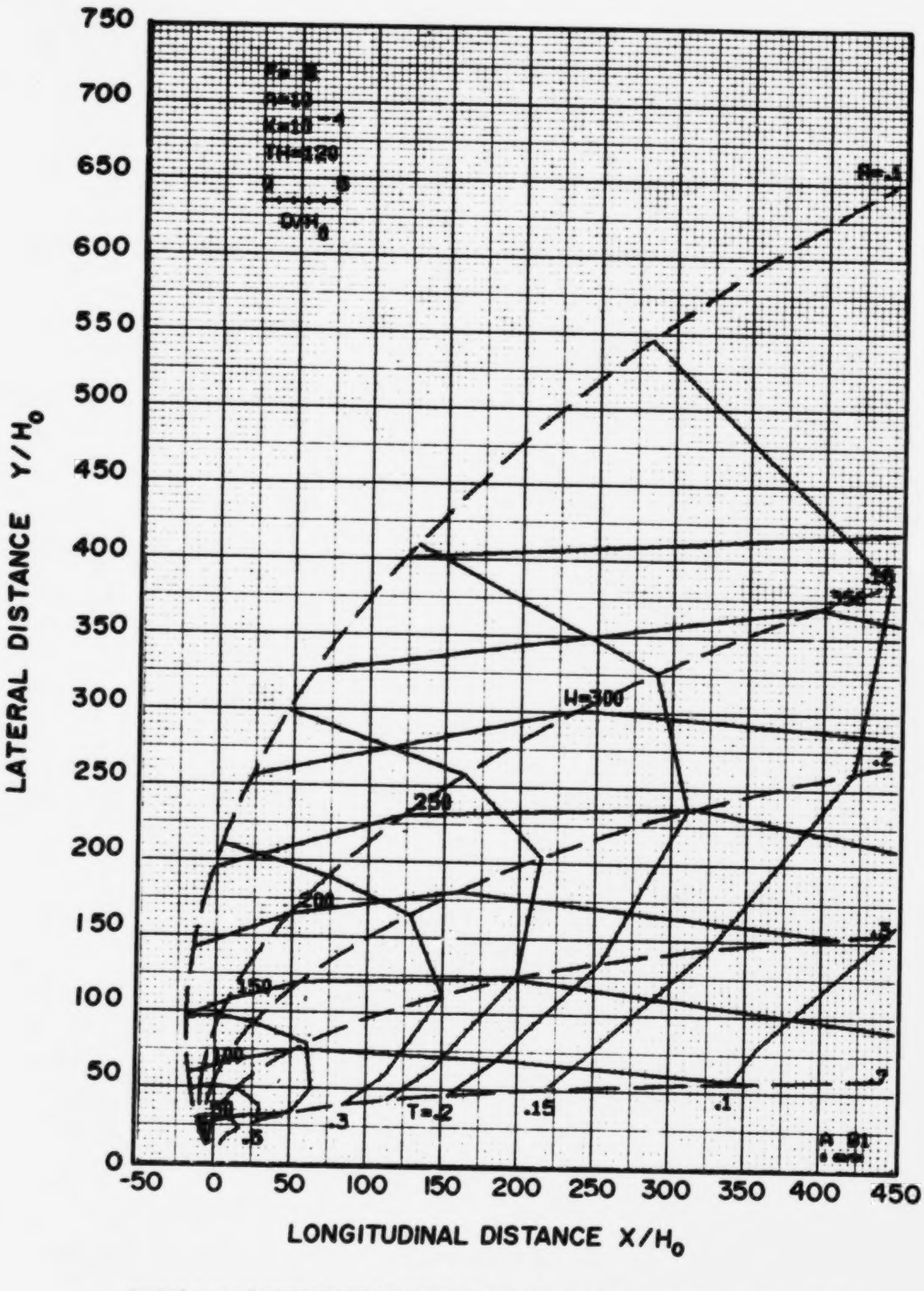

FIG (A91) TEMPERATURE, TRAJECTORY, WIDTH, AND DEPTH (TTWD)-PLOTS FOR SURFACE JET DISCHARGE

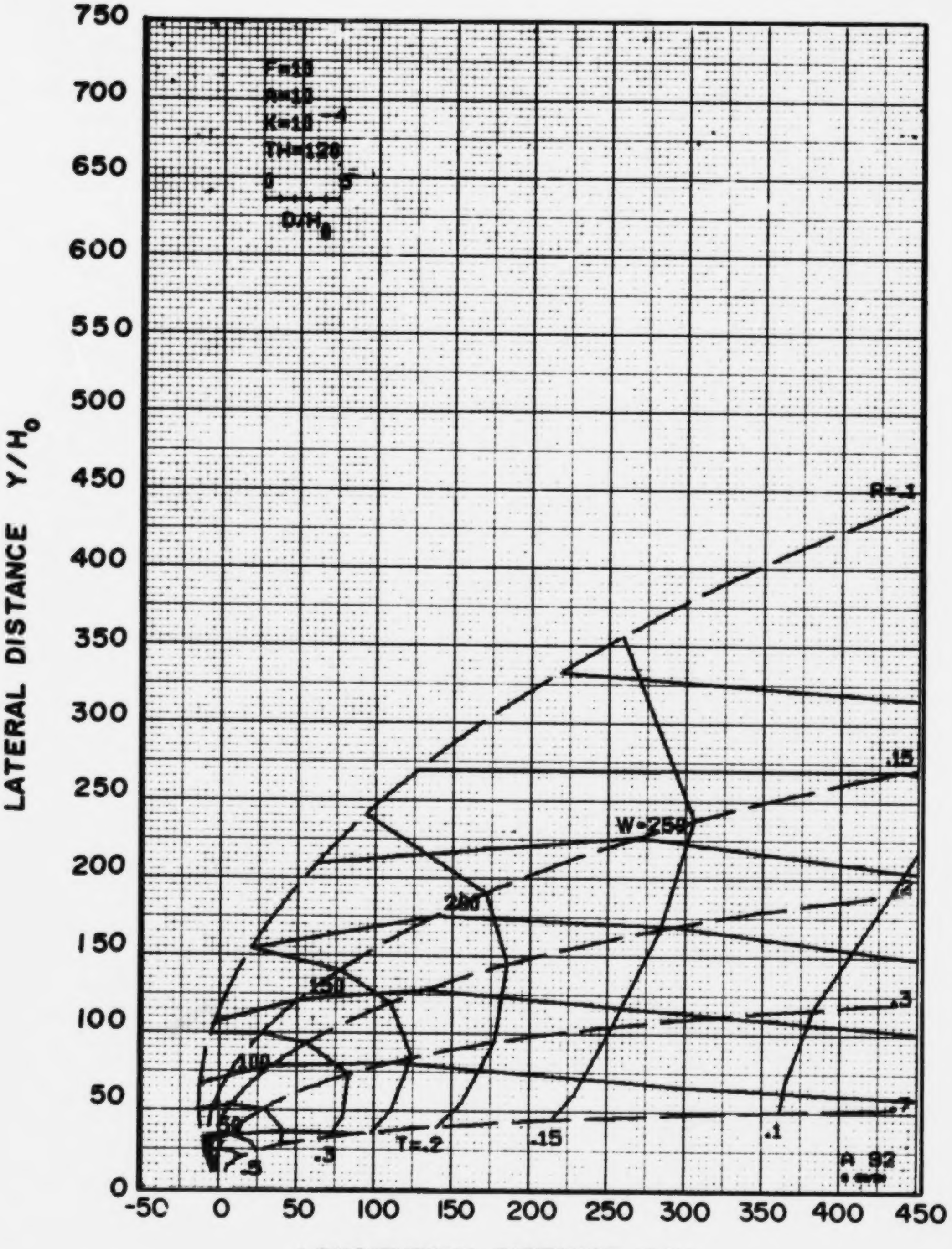

FIG (A92) TEMPERATURE, TRAJECTORY, WIDTH, AND DEPTH (TTWD)-PLOTS FOR SURFACE JET DISCHARGE

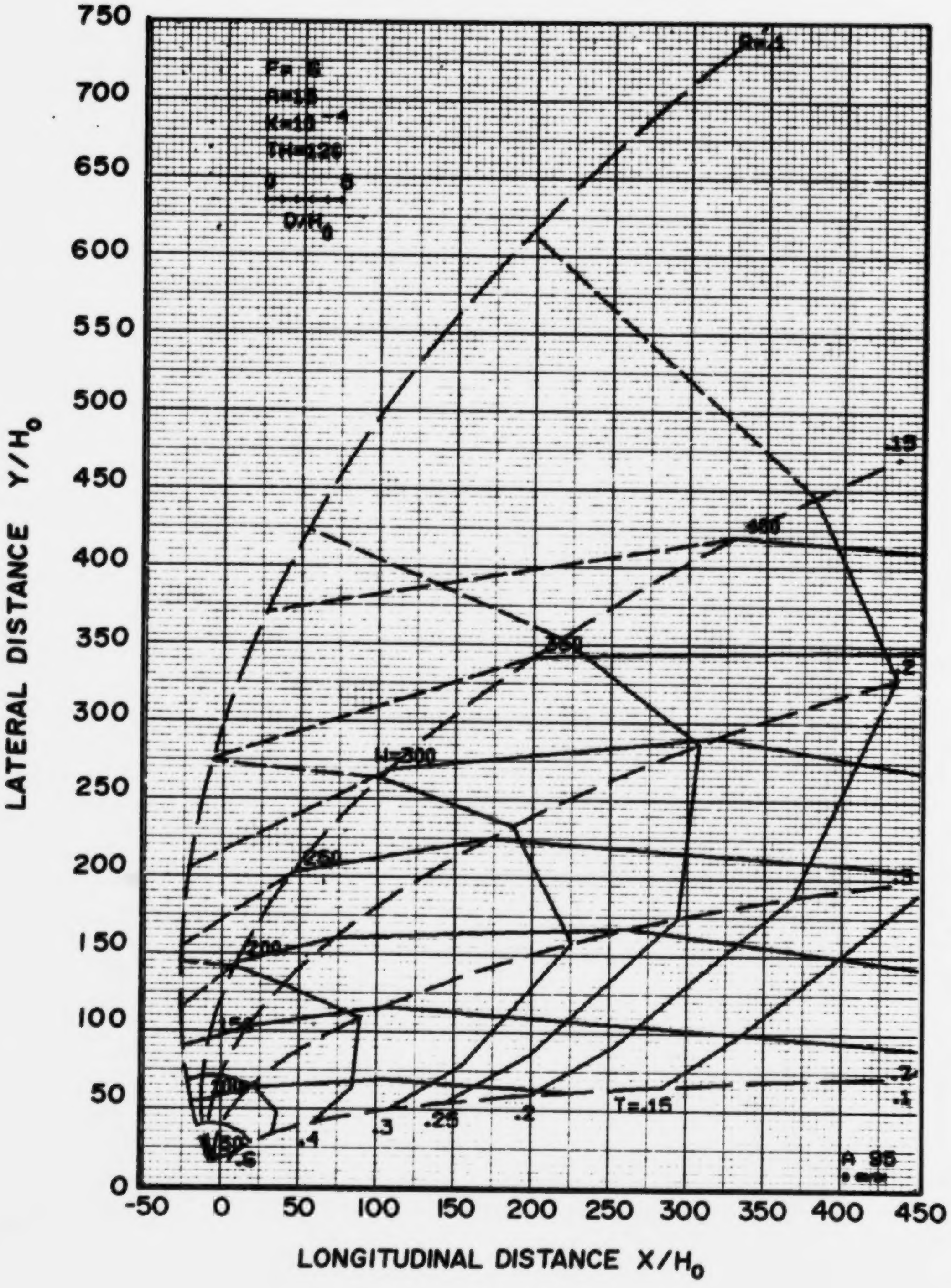

FIG (A95) TEMPERATURE, TRAJECTORY, WIDTH, AND DEPTH (TTWD)-PLOTS FOR SURFACE JET DISCHARGE

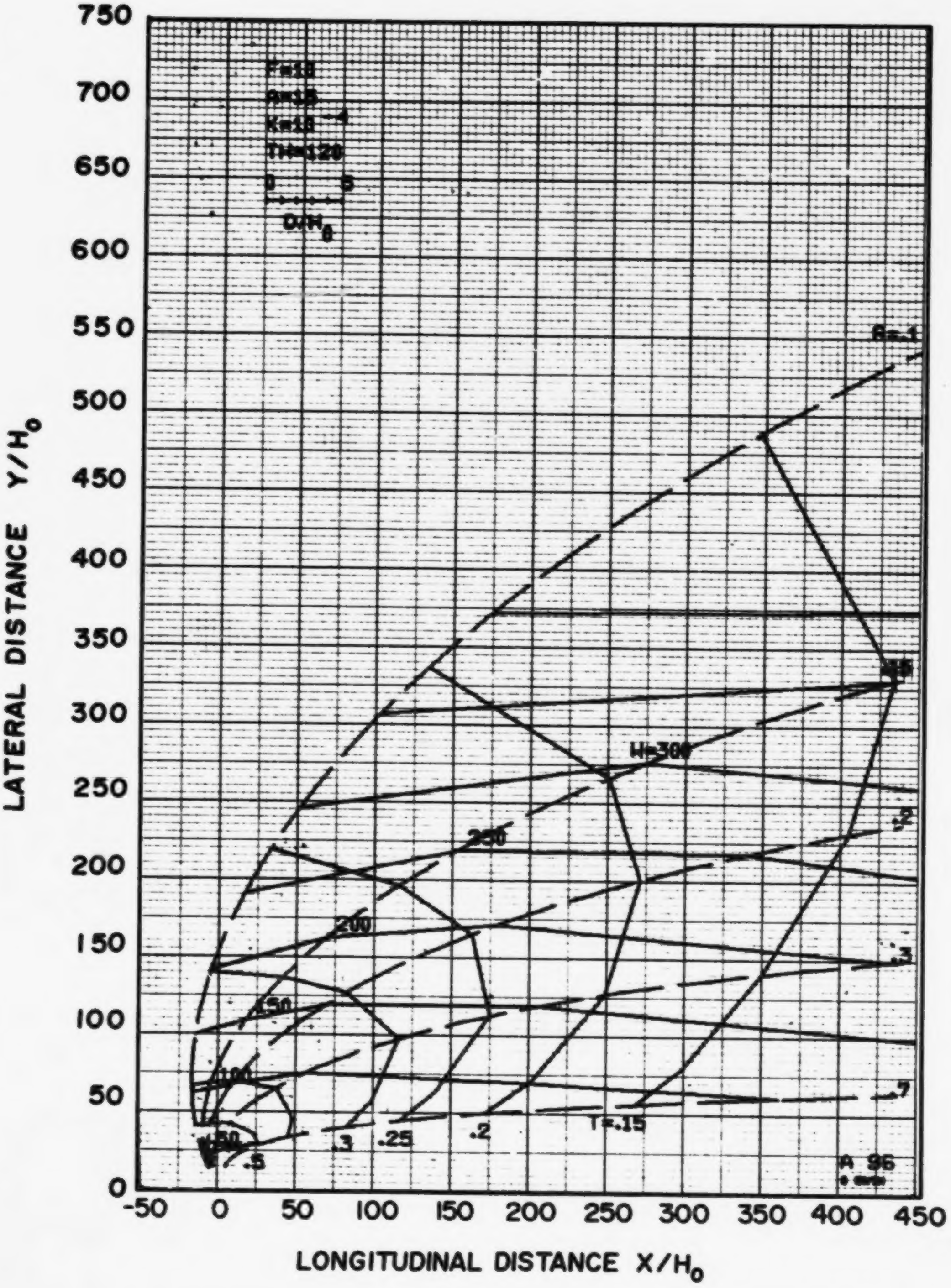

FIG (A96) TEMPERATURE, TRAJECTORY, WIDTH, AND DEPTH (TTWD)-PLOTS FOR SURFACE JET DISCHARGE

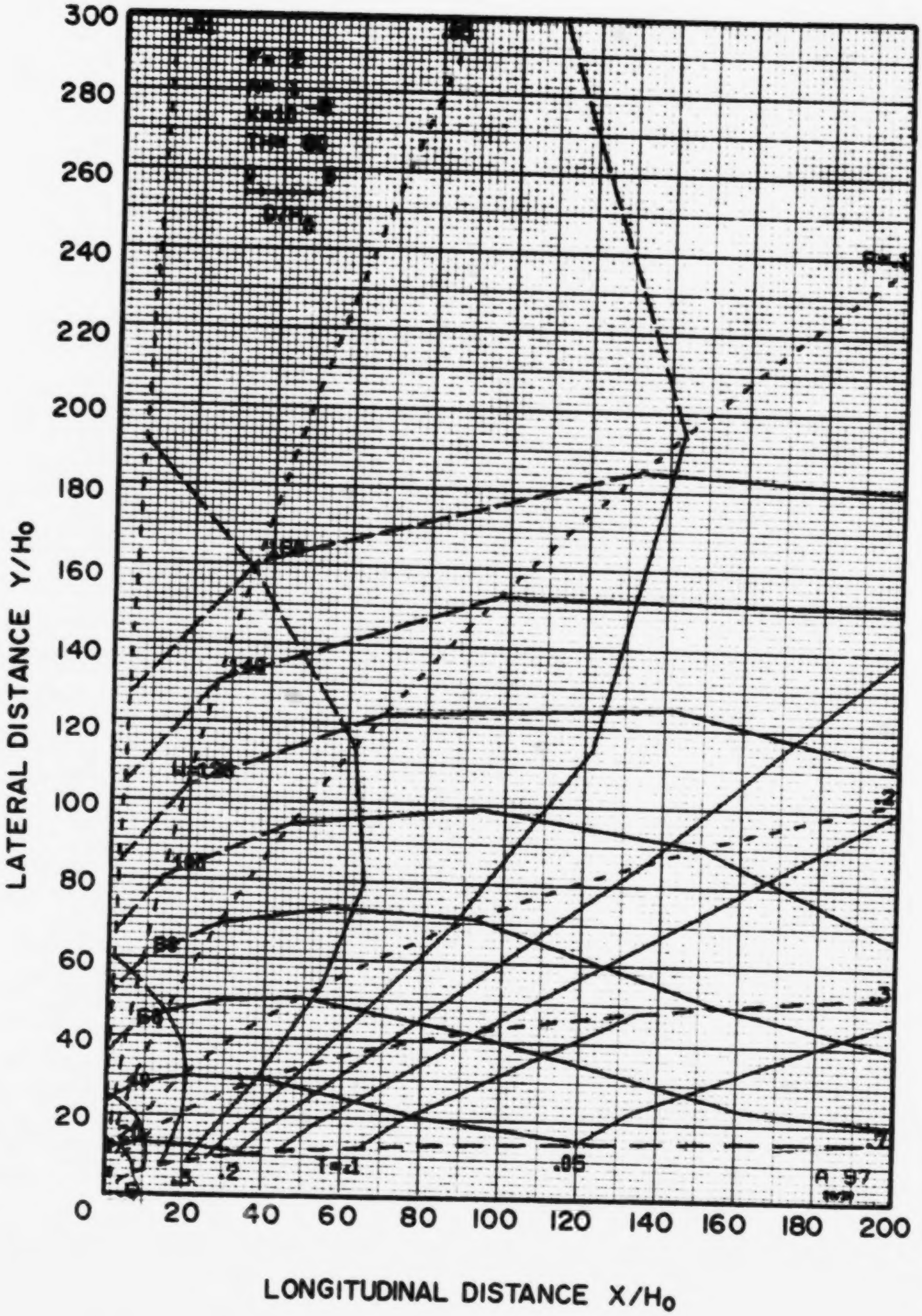

FIG (A97) TEMPERATURE, TRAJECTORY, WIDTH, AND DEPTH (TTWD)-PLOTS FOR SURFACE JET DISCHARGE

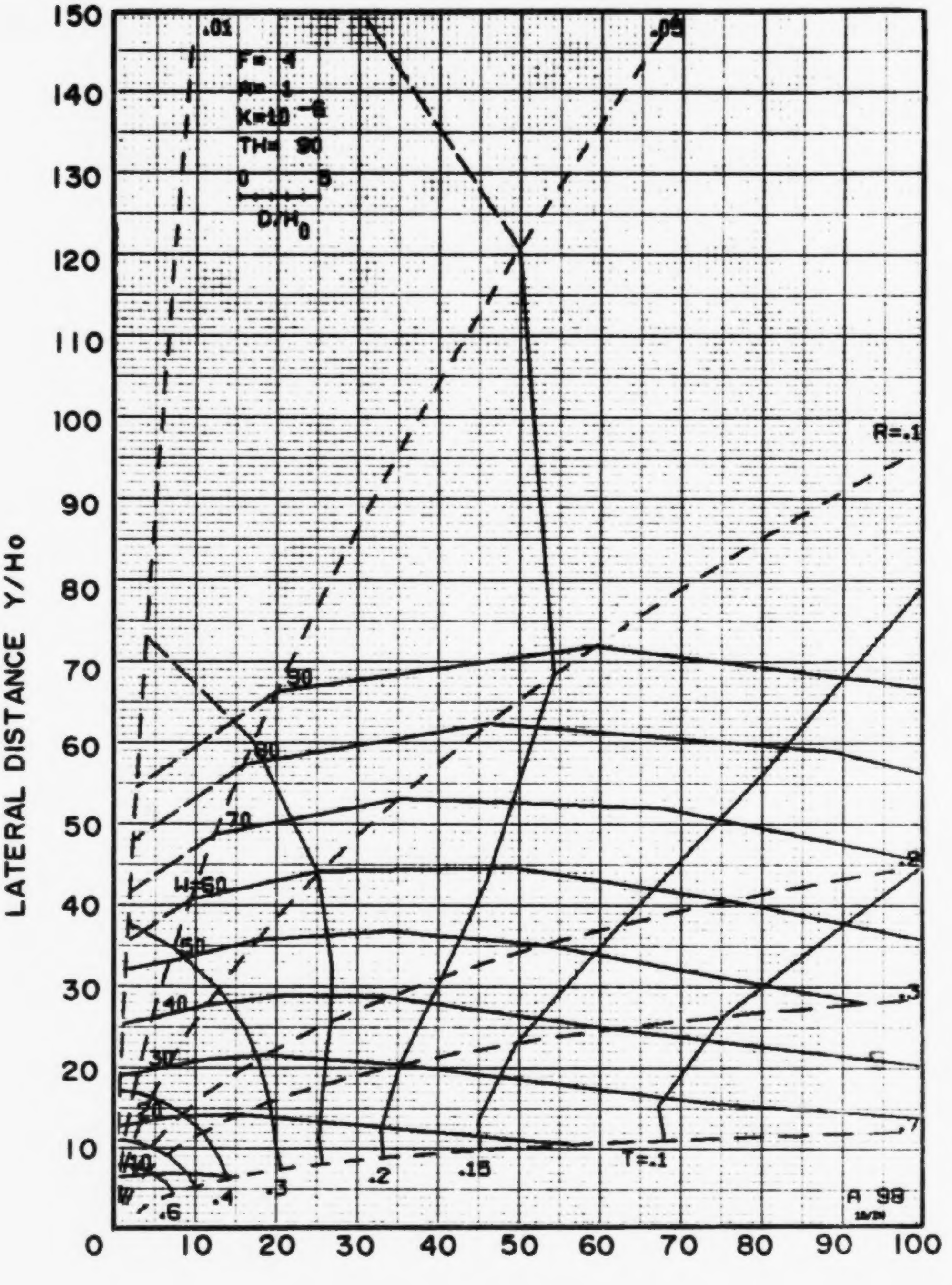

FIG(A98) TEMPERATURE, TRAJECTORY, WIDTH, AND DEPTH (TTWD)-PLOTS FOR SURFACE JET DISCHARGE

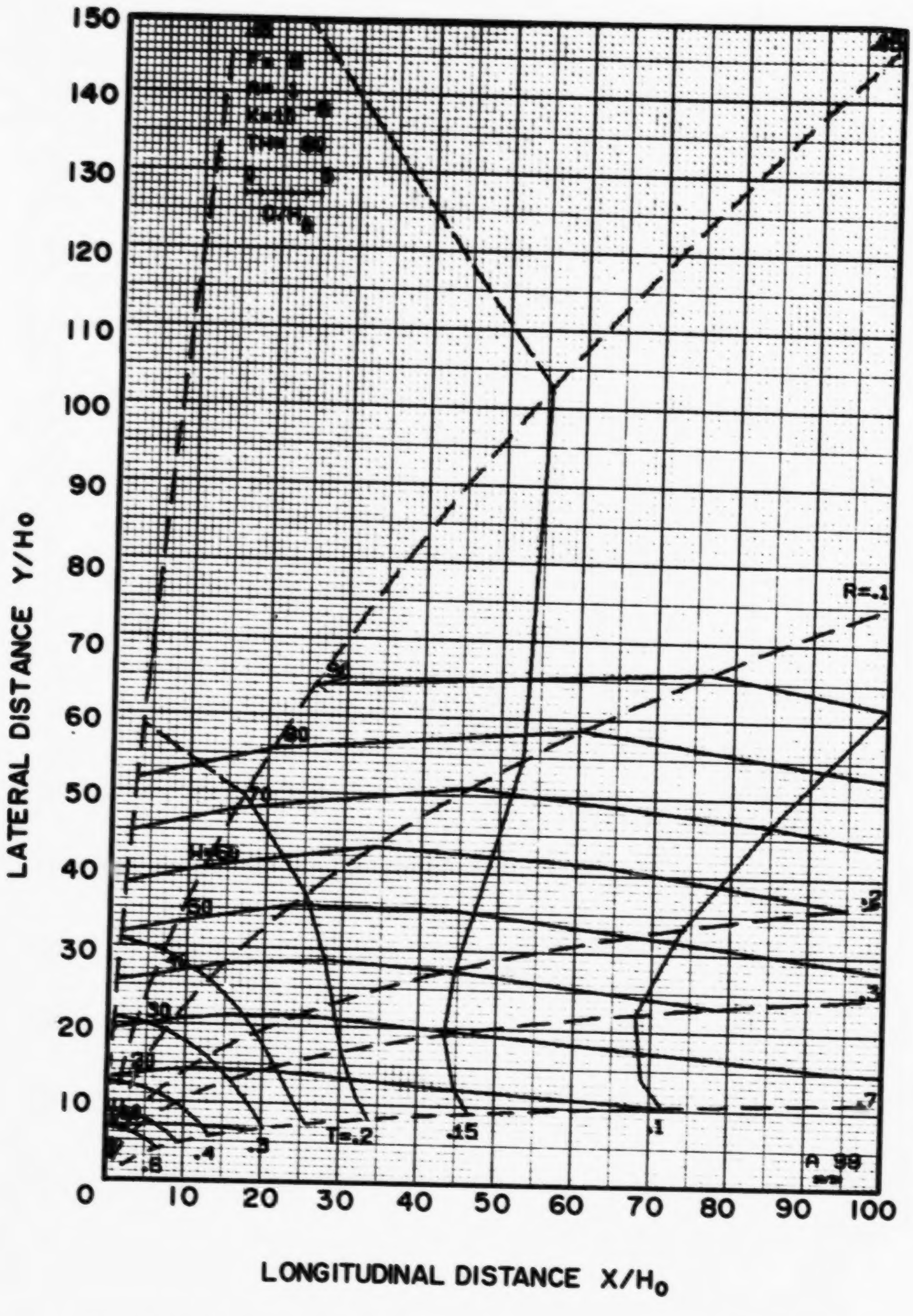

FIG(A99) TEMPERATURE, TRAJECTORY, WIDTH, AND DEPTH (TTWD)-PLOTS FOR SURFACE JET DISCHARGE

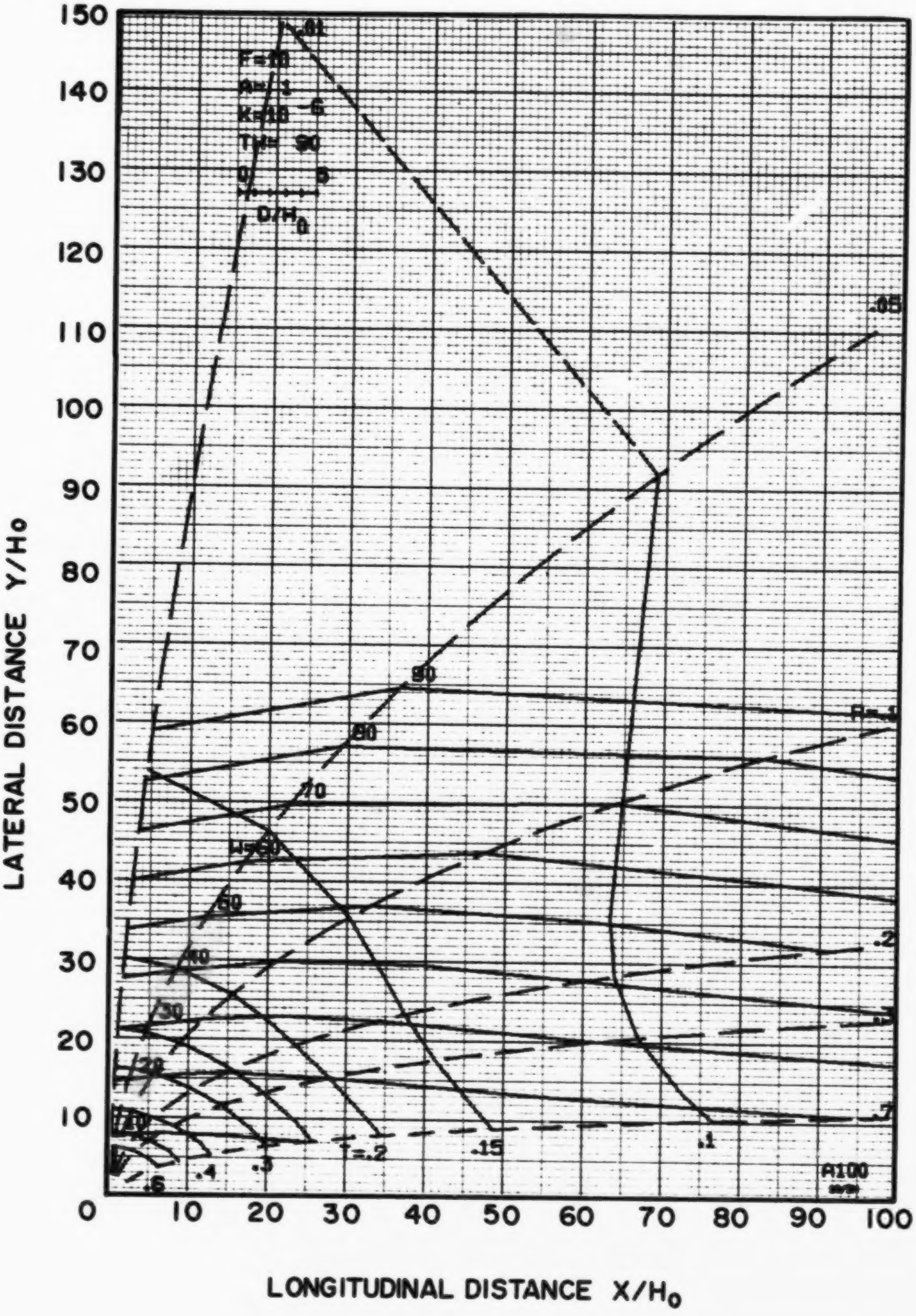

FIG(A100) TEMPERATURE, TRAJECTORY, WIDTH, AND DEPTH (TTWD)-PLOTS FOR SURFACE JET DISCHARGE

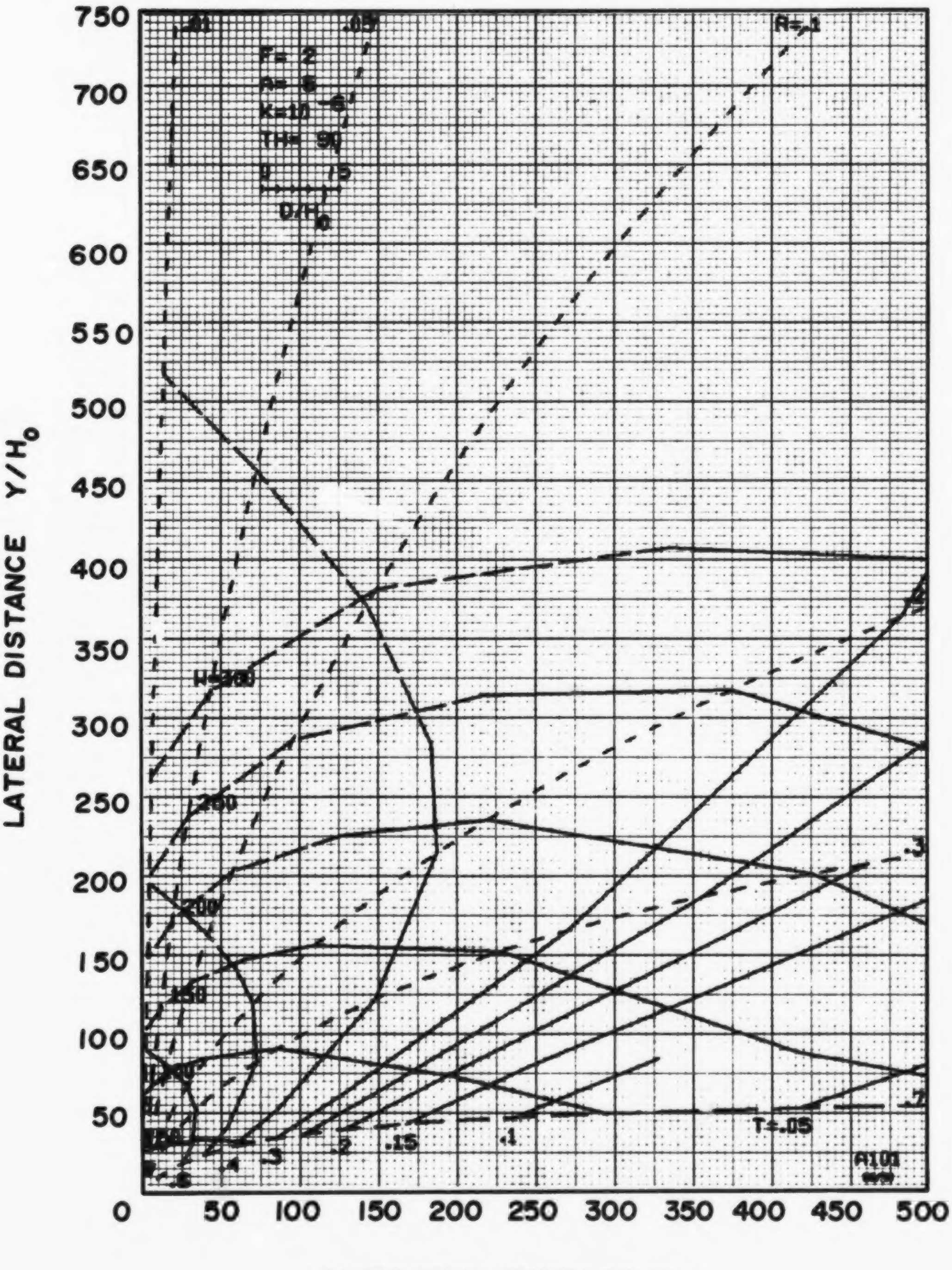

FIG (A101) TEMPERATURE, TRAJECTORY, WIDTH, AND DEPTH (TTWD)-PLOTS FOR SURFACE JET DISCHARGE

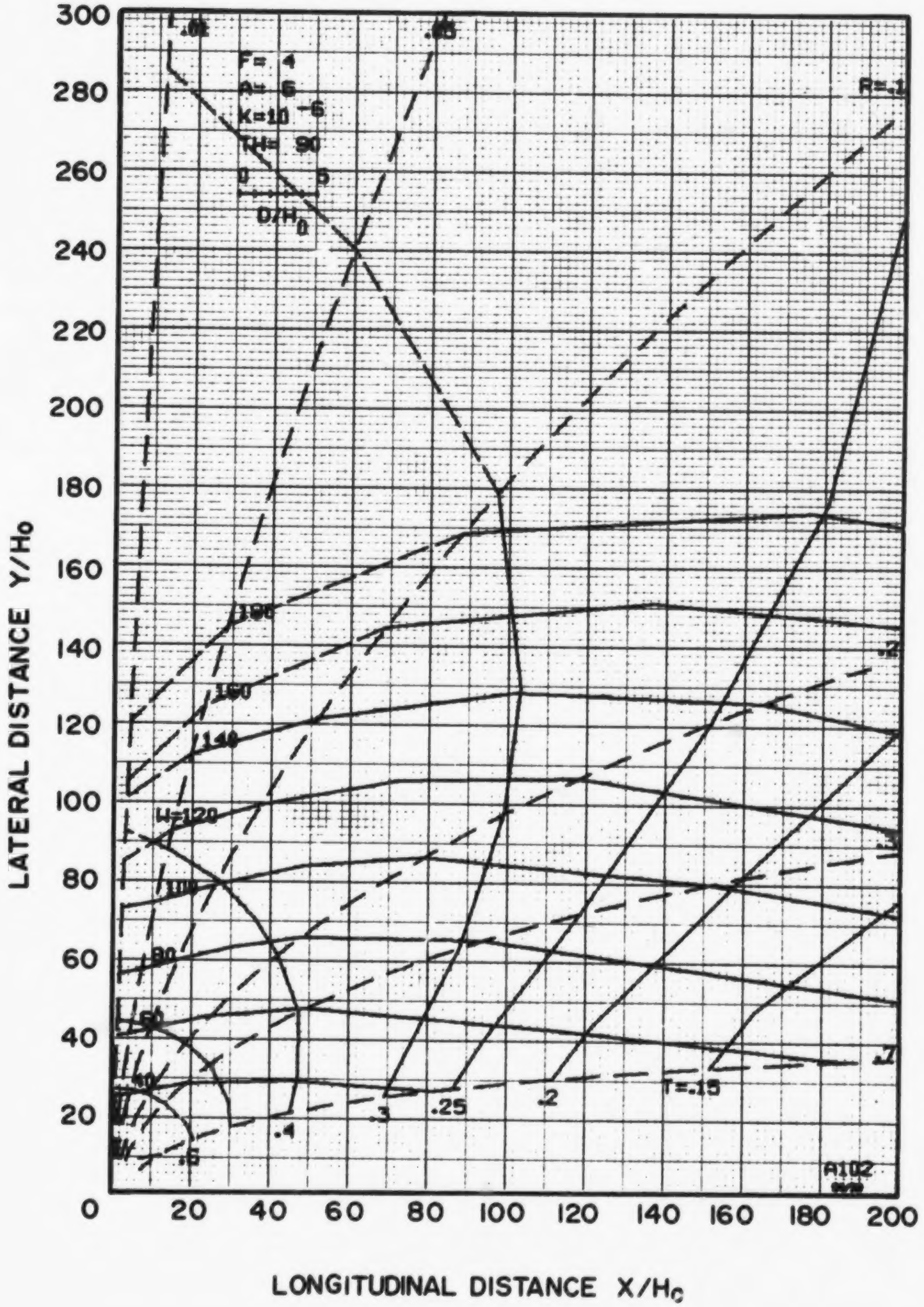

FIG (A102) TEMPERATURE, TRAJECTORY, WIDTH, AND DEPTH (TTWD)-PLOTS FOR SURFACE JET DISCHARGE

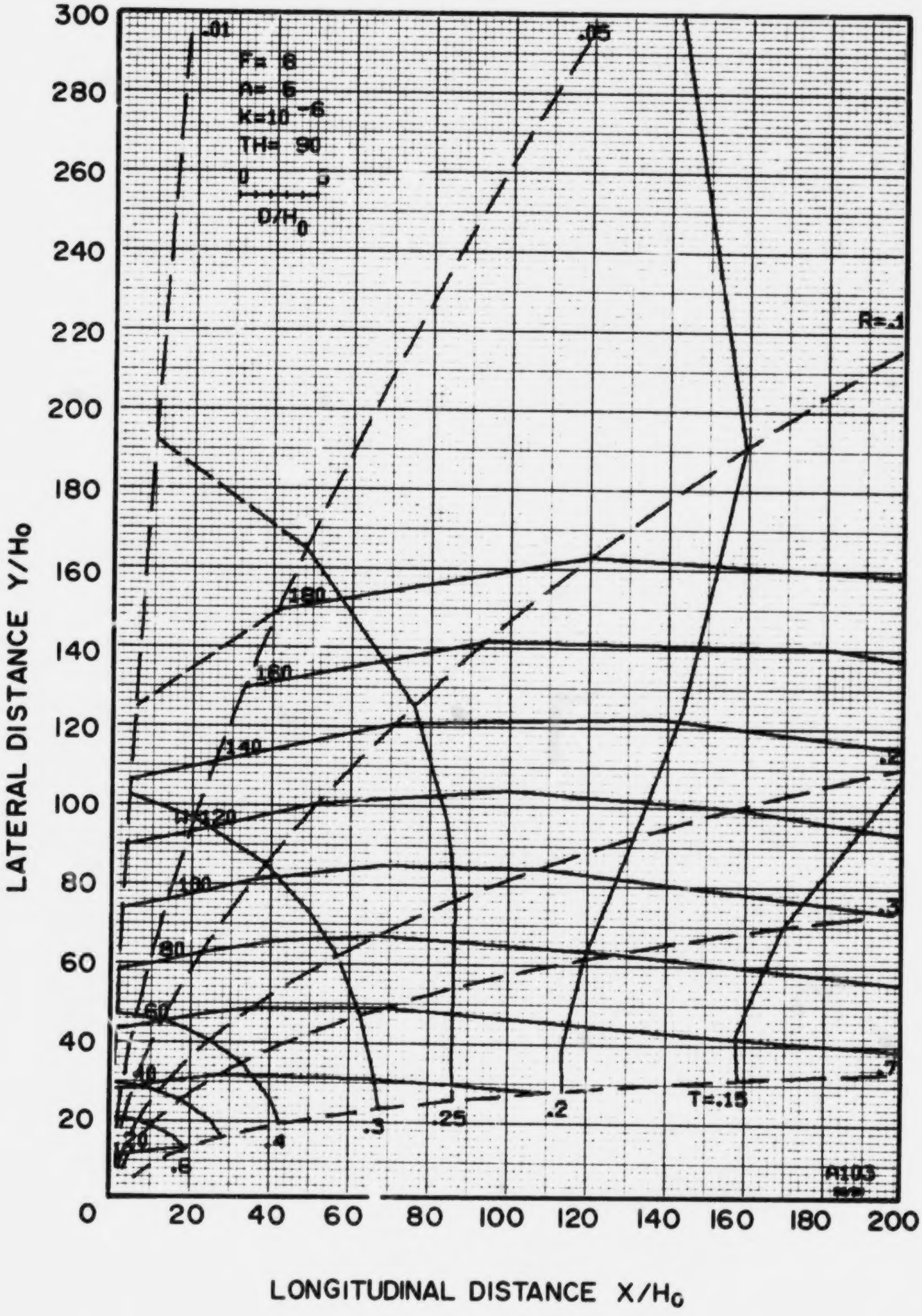

FIG (A103) TEMPERATURE, TRAJECTORY, WIDTH, AND DEPTH (TTWD)-PLOTS FOR SURFACE JET DISCHARGE

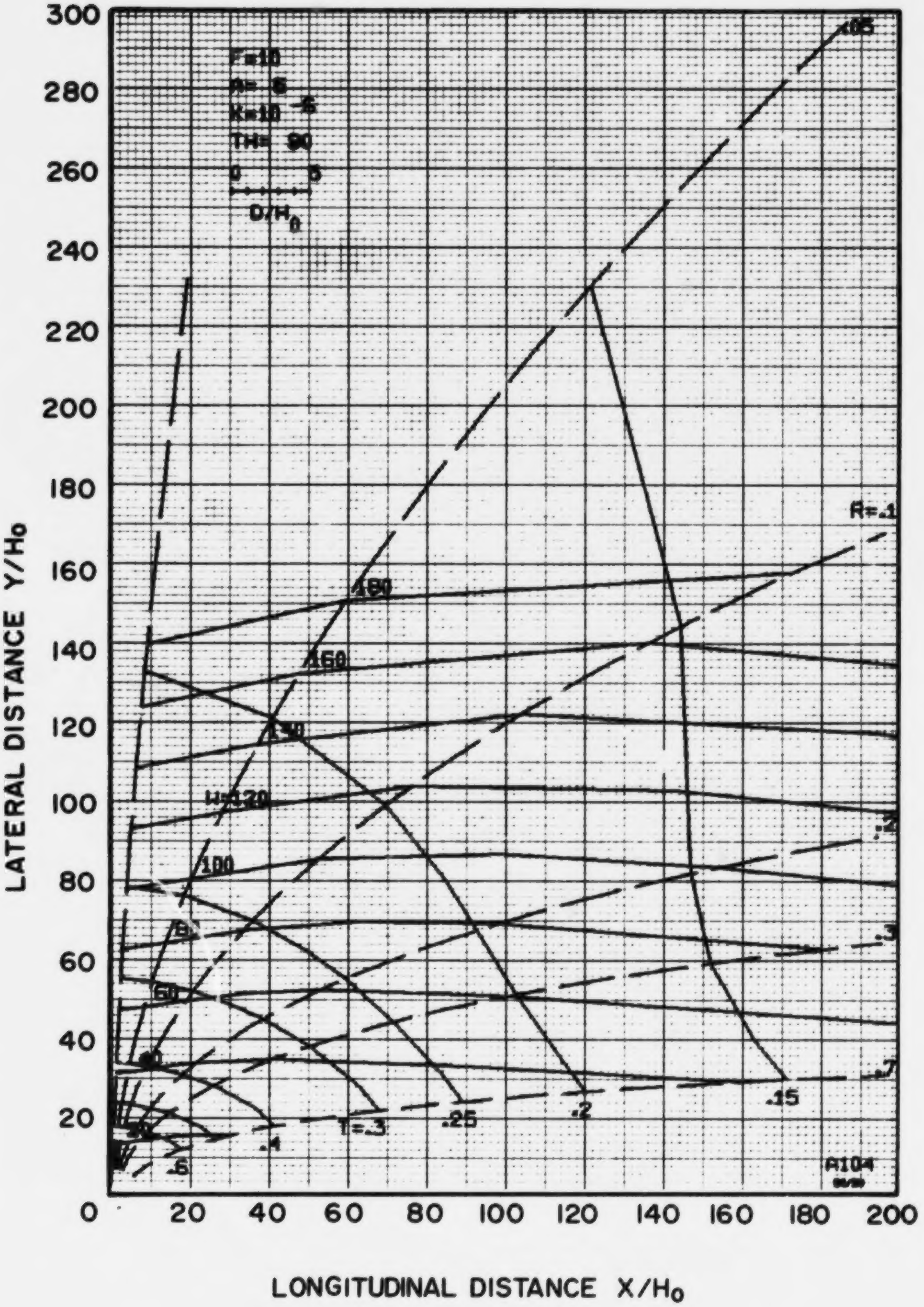

FIG (A104) TEMPERATURE, TRAJECTORY, WIDTH, AND DEPTH (TTWD)-PLOTS FOR SURFACE JET DISCHARGE

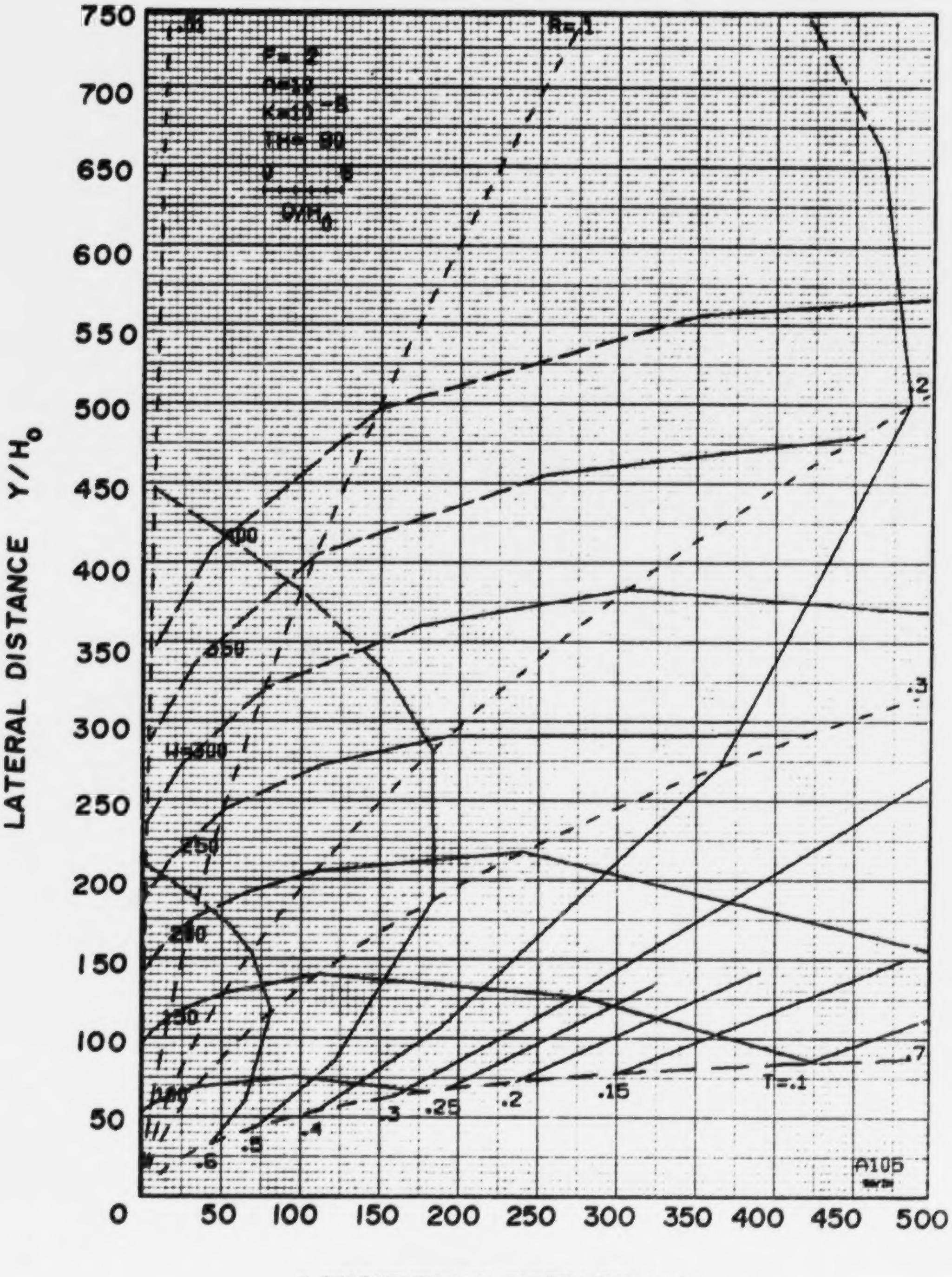

FIG (A105) TEMPERATURE, TRAJECTORY, WIDTH, AND DEPTH (TTWD)-PLOTS FOR SURFACE JET DISCHARGE

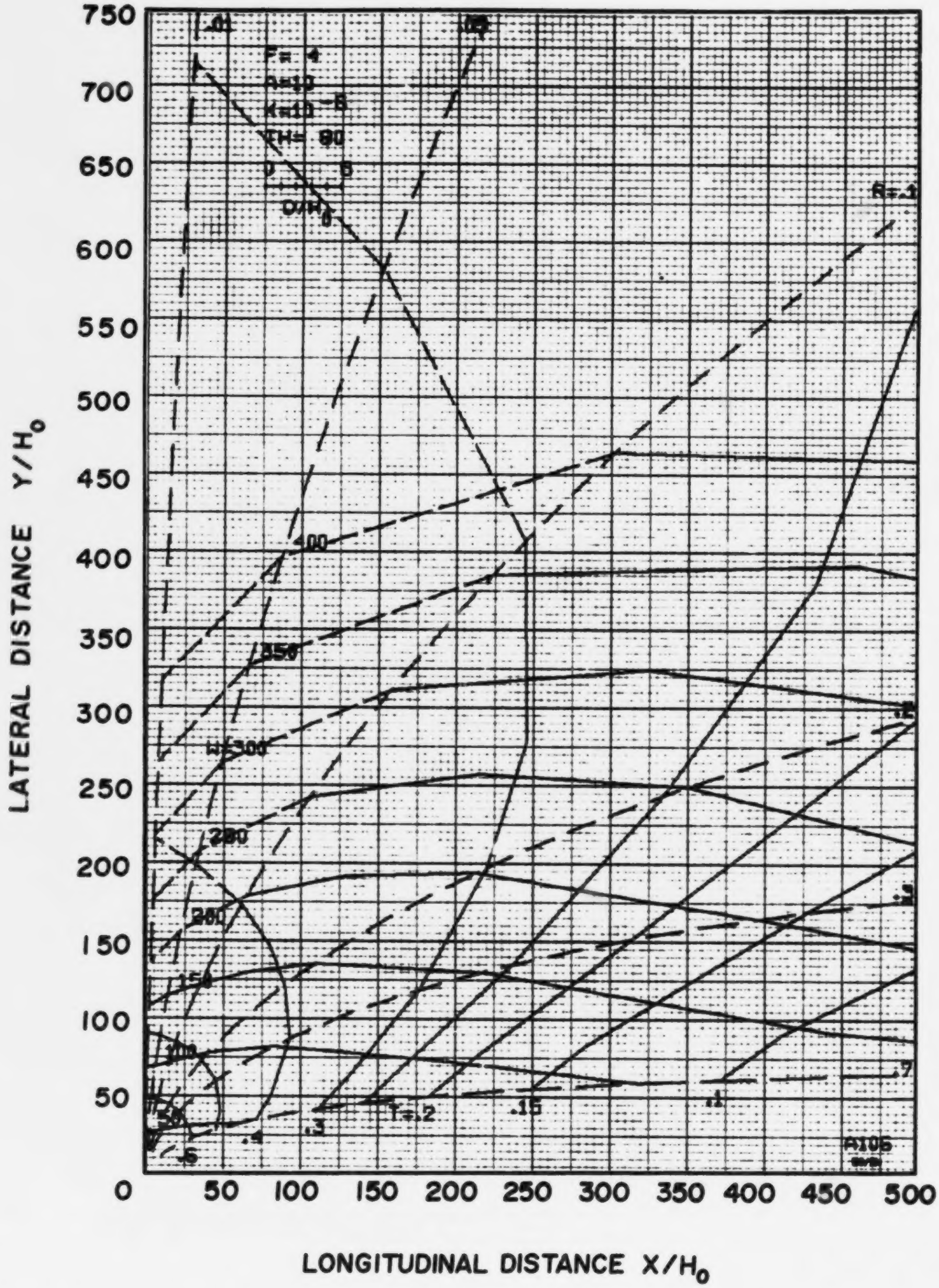

FIG (A106) TEMPERATURE, TRAJECTORY, WIDTH, AND DEPTH (TTWD)-PLOTS FOR SURFACE JET DISCHARGE

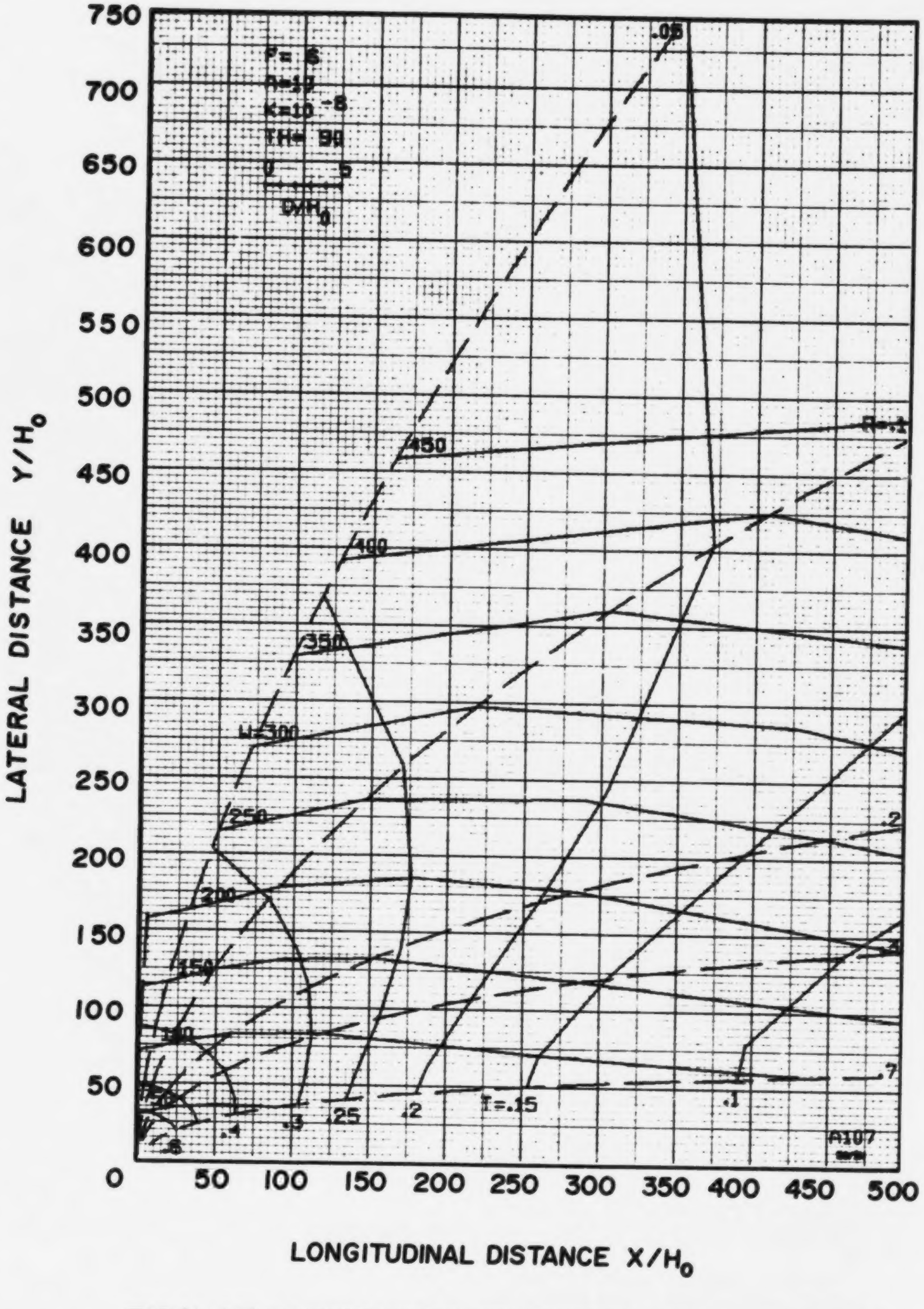

FIG (A107) TEMPERATURE, TRAJECTORY, WIDTH, AND DEPTH (TTWD)-PLOTS FOR SURFACE JET DISCHARGE

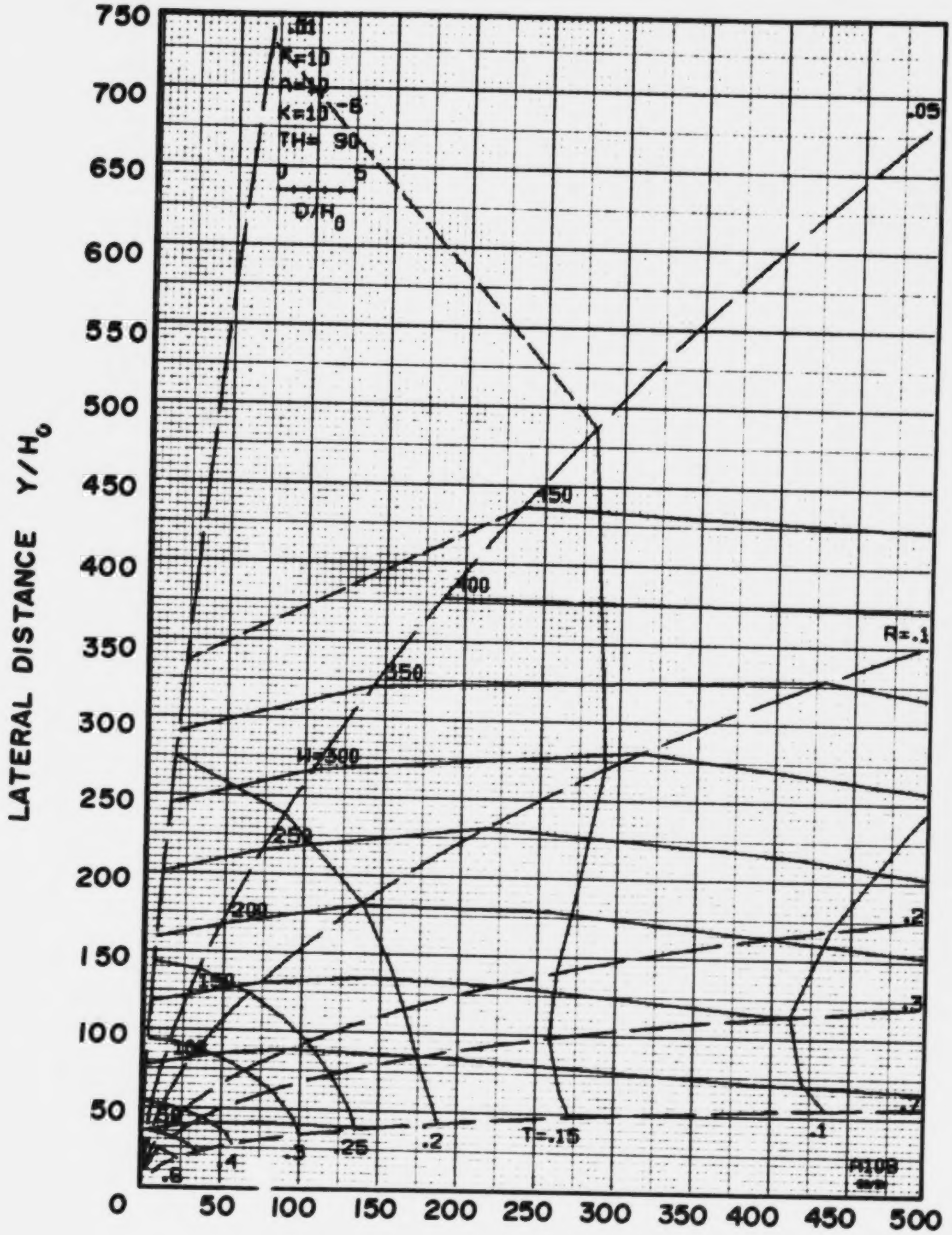

FIG (A108) TEMPERATURE, TRAJECTORY, WIDTH, AND DEPTH (TTWD)-PLOTS FOR SURFACE JET DISCHARGE

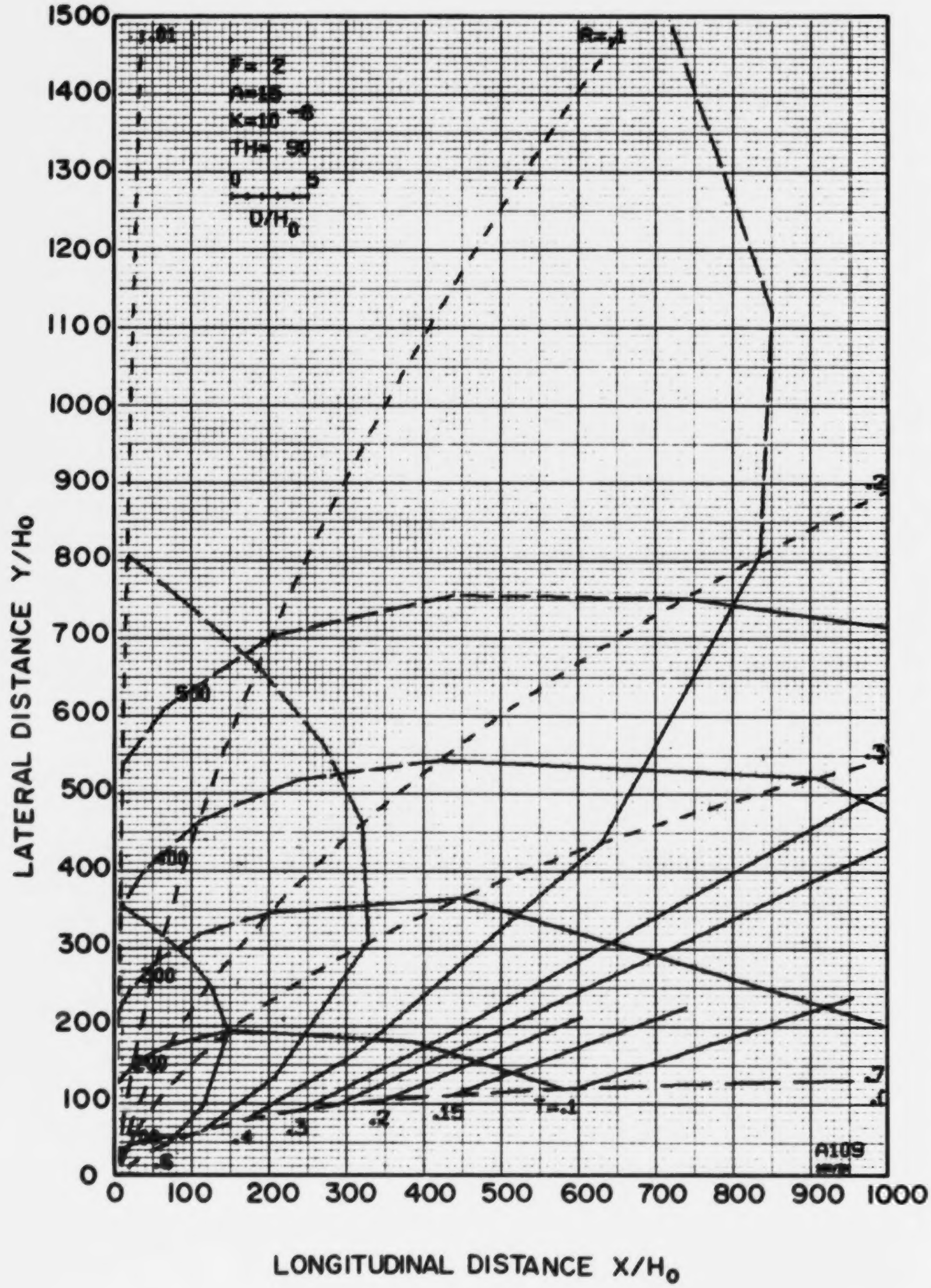

FIG (A109) TEMPERATURE, TRAJECTORY, WIDTH, AND DEPTH (TTWD)-PLOTS FOR SURFACE JET DISCHARGE

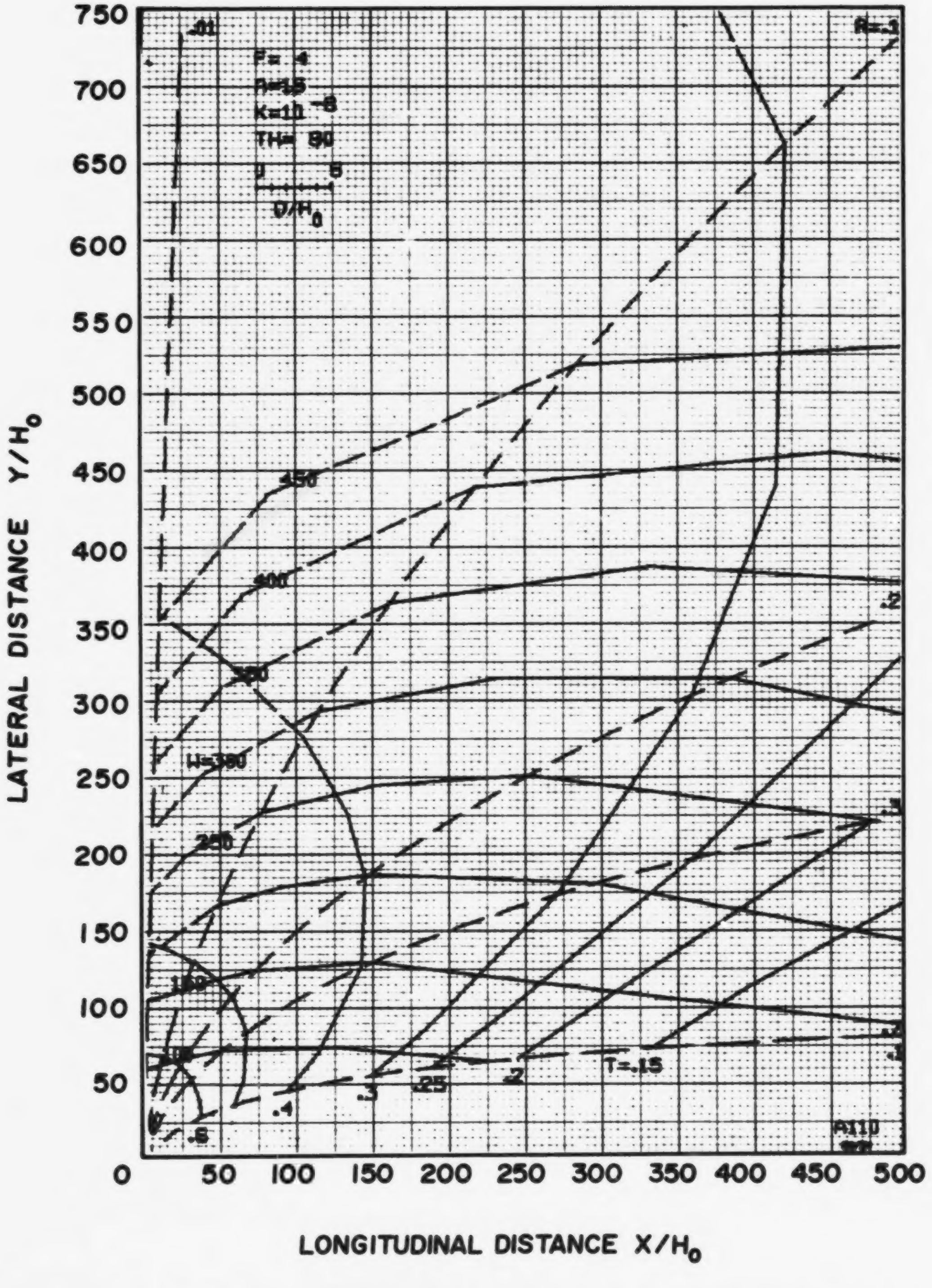

FIG (A110) TEMPERATURE, TRAJECTORY, WIDTH, AND DEPTH (TTWD)-PLOTS FOR SURFACE JET DISCHARGE

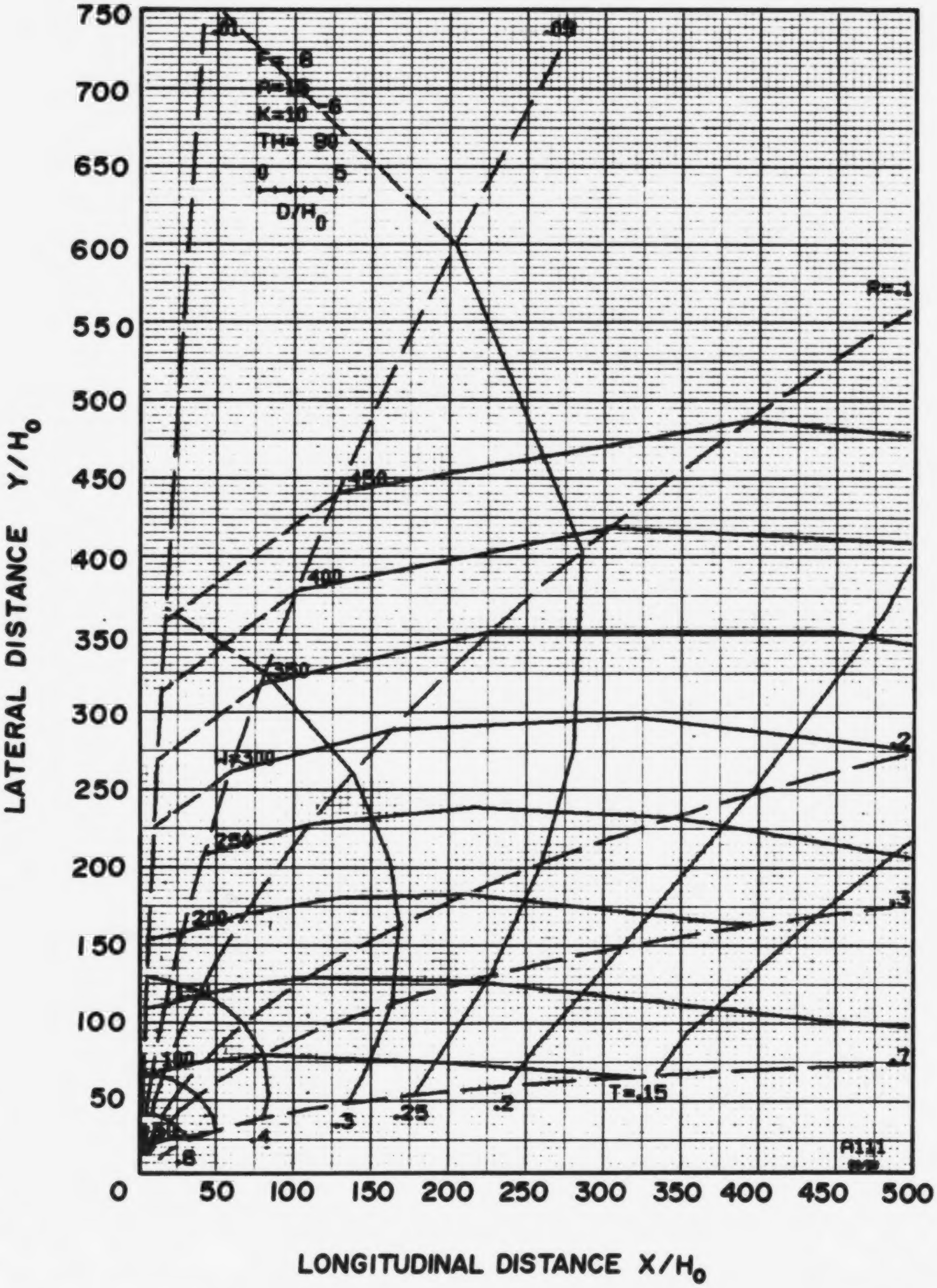

FIG (A111) TEMPERATURE, TRAJECTORY, WIDTH, AND DEPTH (TTWD)-PLOTS FOR SURFACE JET DISCHARGE

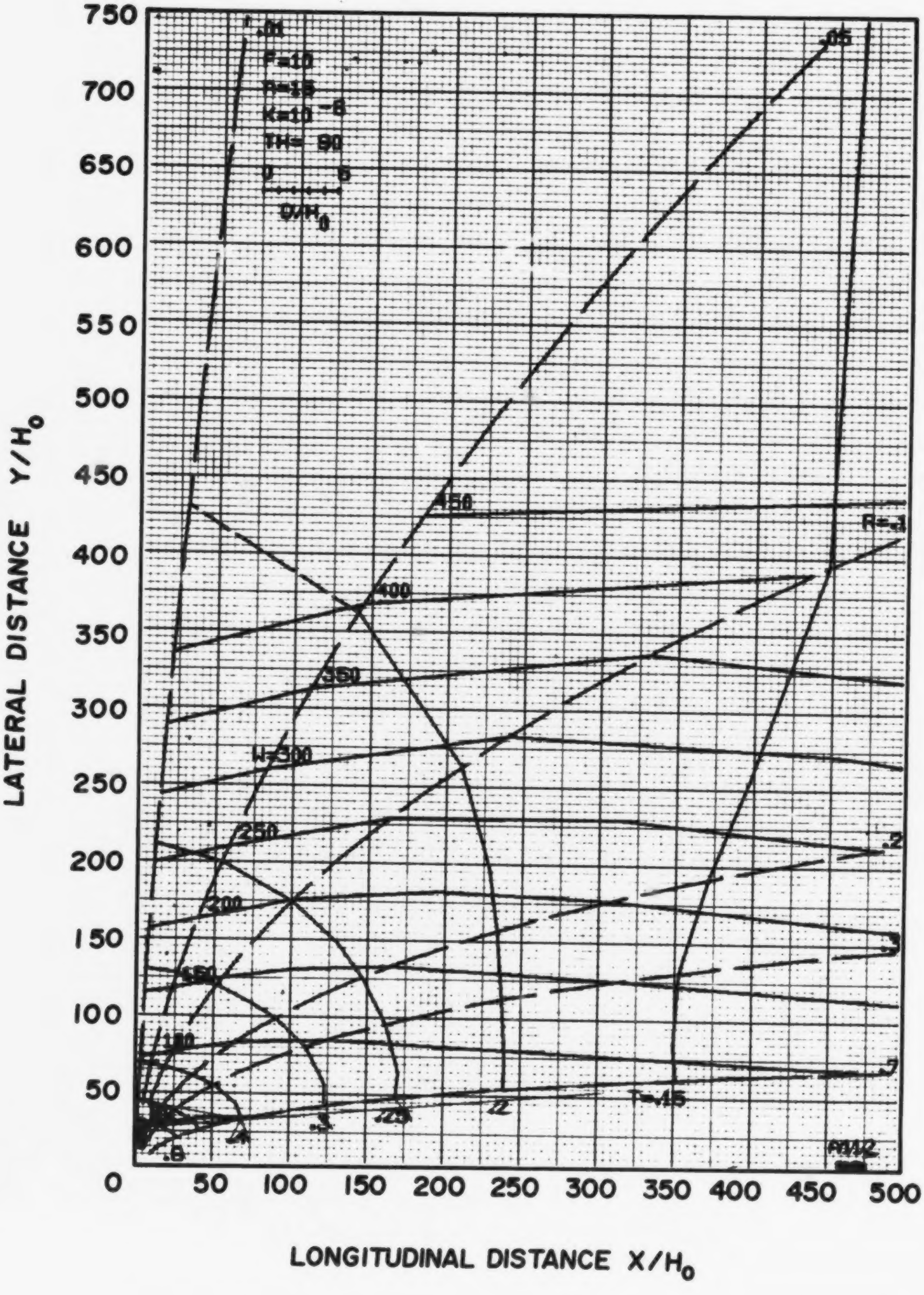

FIG (A112) TEMPERATURE, TRAJECTORY, WIDTH, AND DEPTH (TTWD)-PLOTS FOR SURFACE JET DISCHARGE

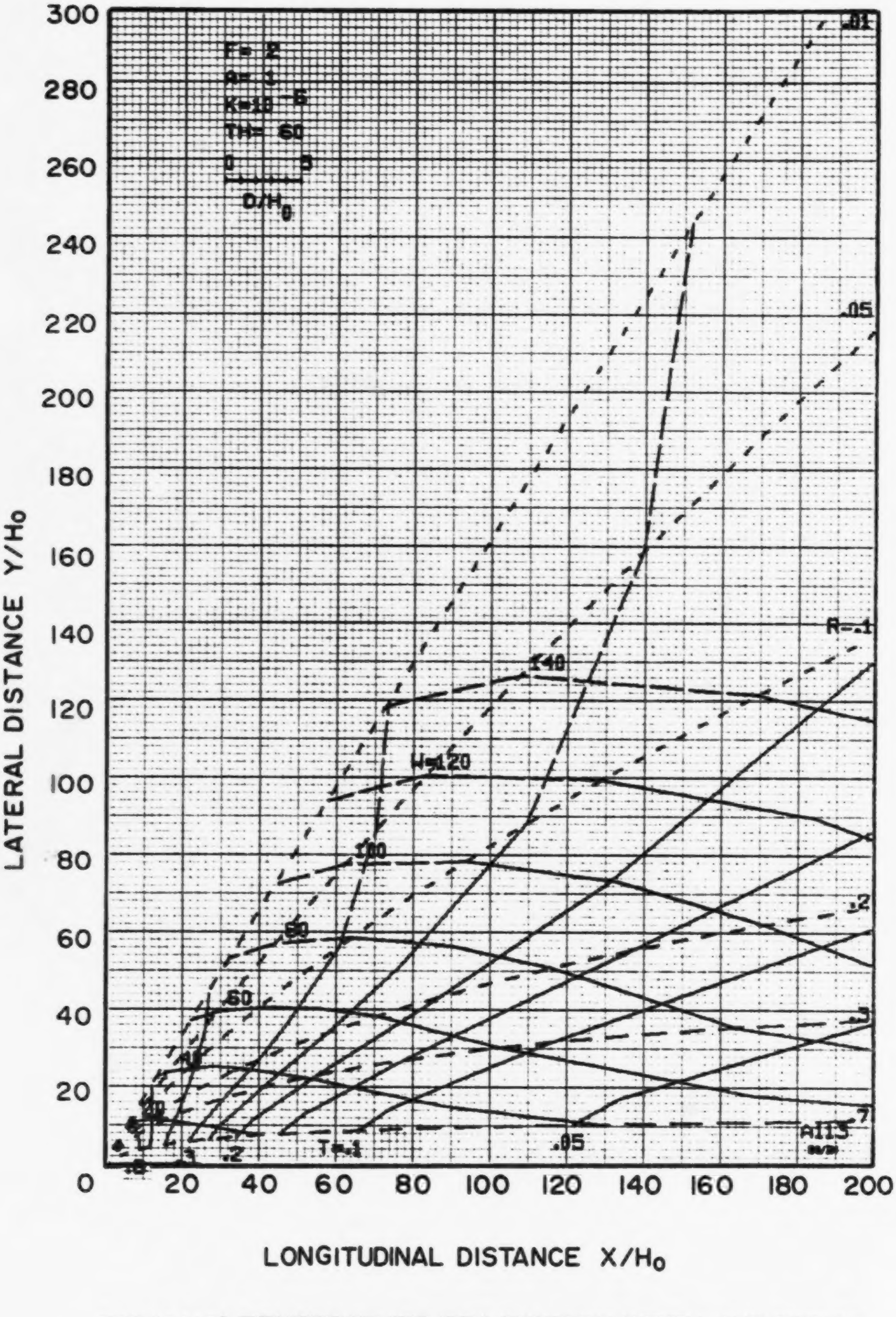

FIG (A113) TEMPERATURE, TRAJECTORY, WIDTH, AND DEPTH (TTWD)-PLOTS FOR SURFACE JET DISCHARGE

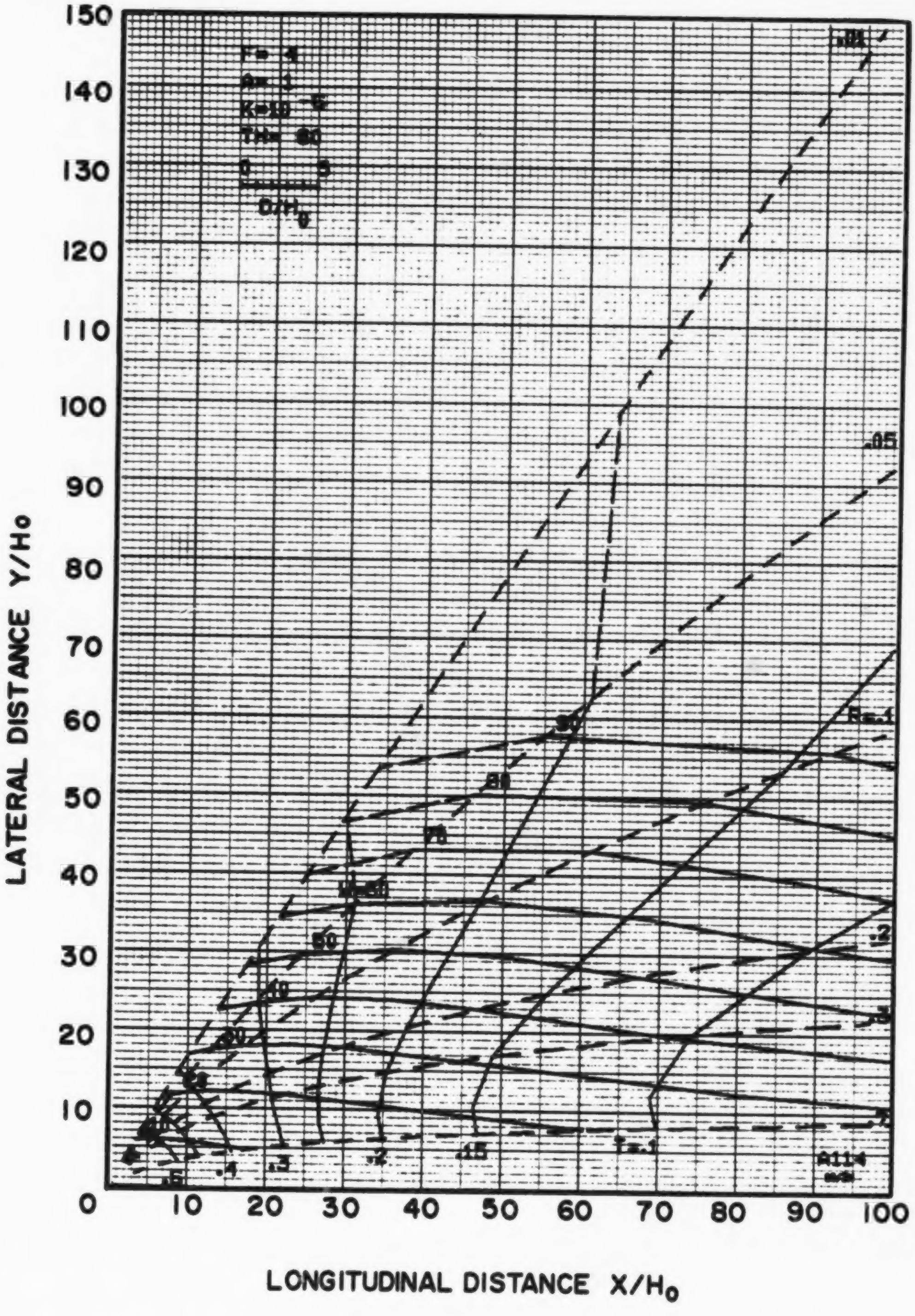

FIG(A114) TEMPERATURE, TRAJECTORY, WIDTH, AND DEPTH (TTWD)-PLOTS FOR SURFACE JET DISCHARGE

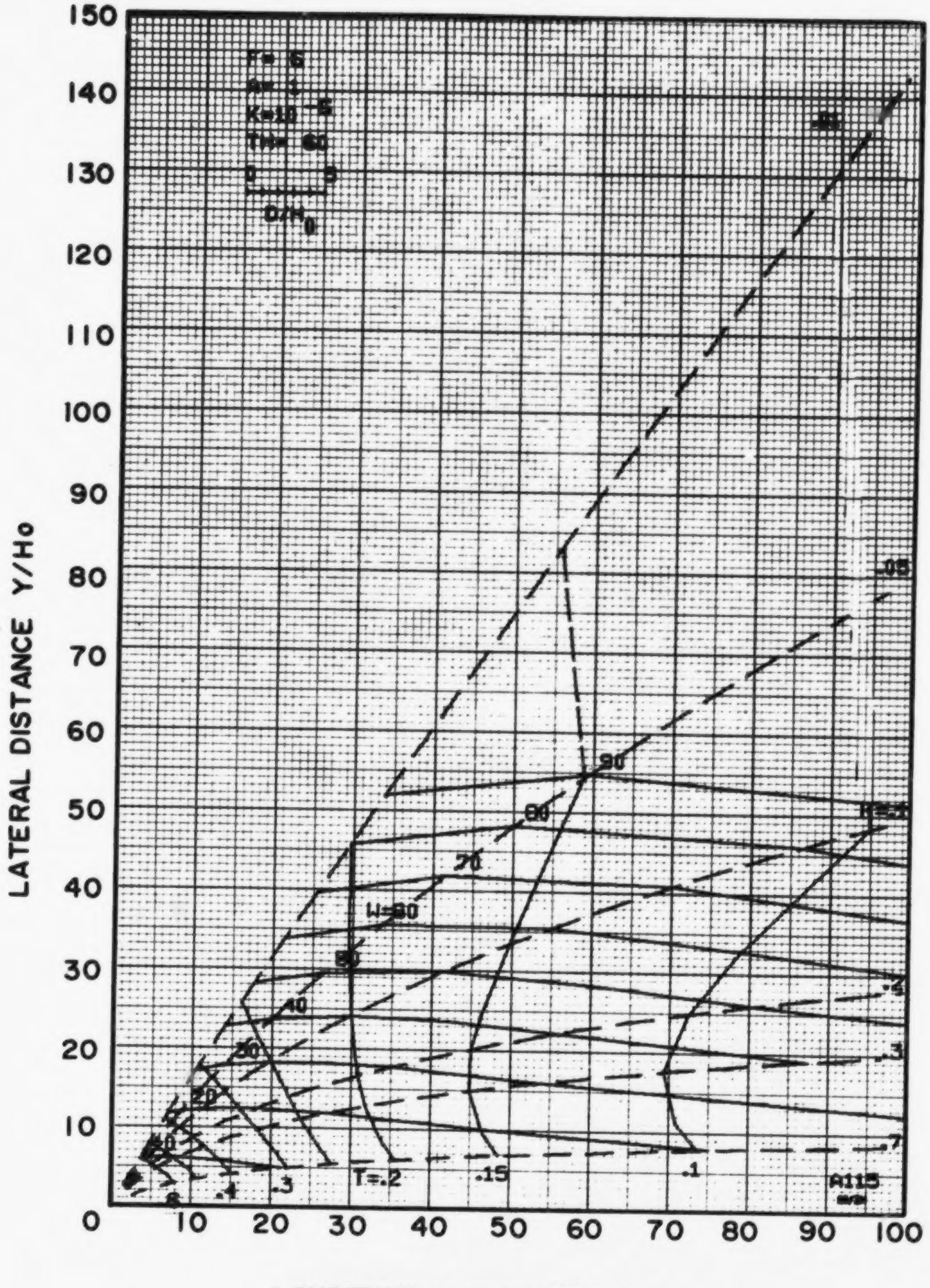

FIG(A115) TEMPERATURE, TRAJECTORY, WIDTH, AND DEPTH (TTWD)-PLOTS FOR SURFACE JET DISCHARGE

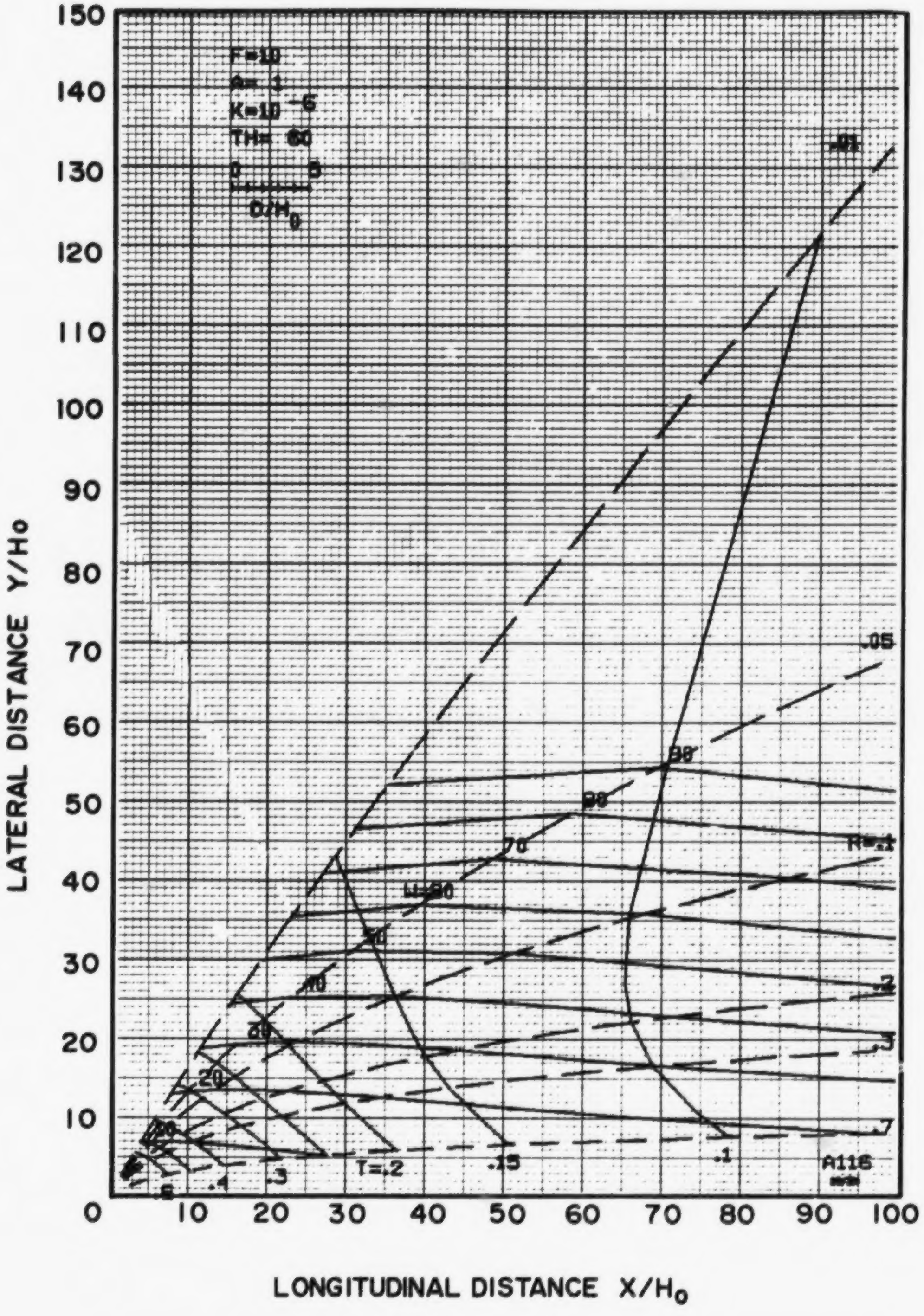

FIG(A116) TEMPERATURE, TRAJECTORY, WIDTH, AND DEPTH (TTWD)-PLOTS FOR SURFACE JET DISCHARGE

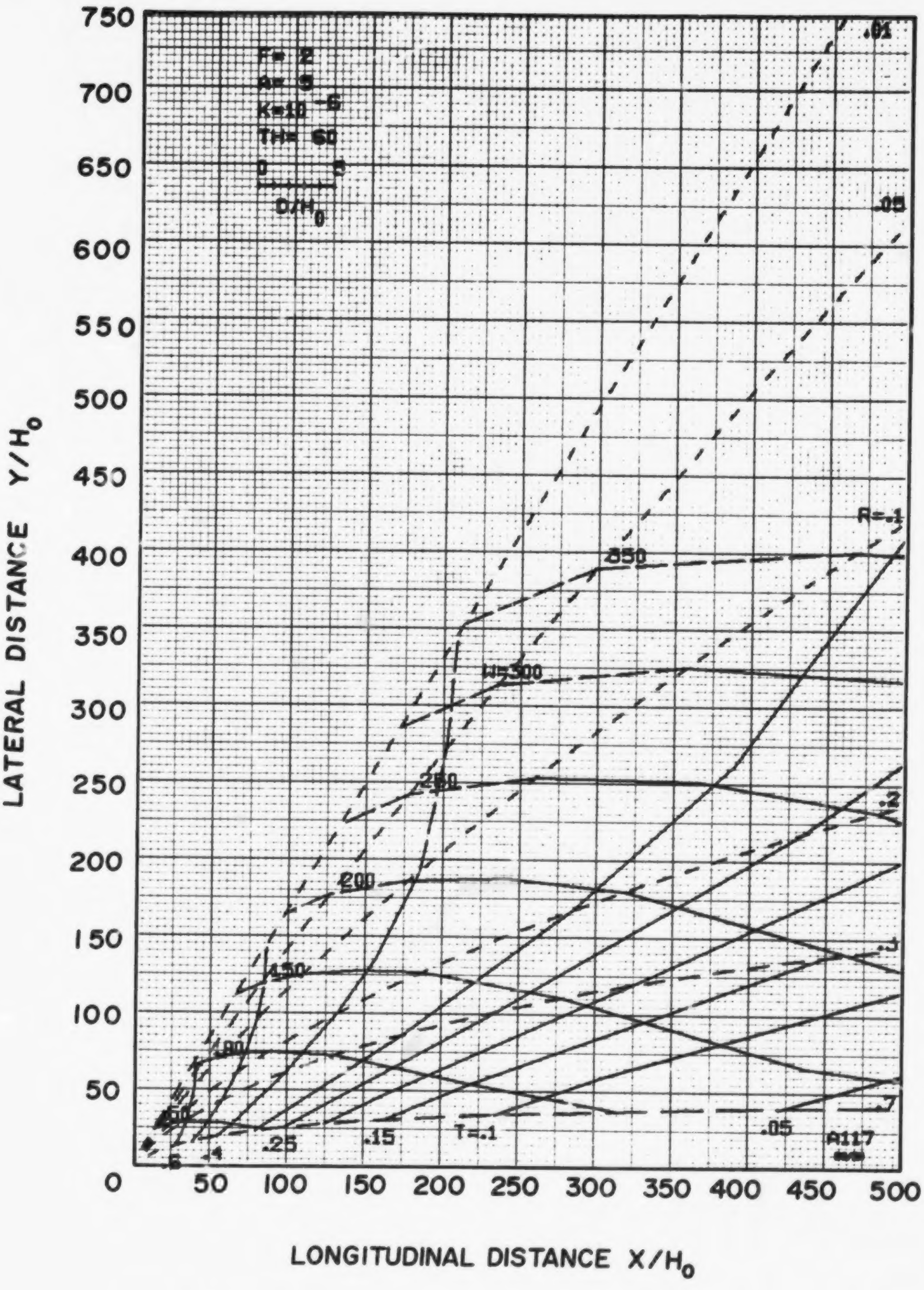

FIG (A117) TEMPERATURE, TRAJECTORY, WIDTH, AND DEPTH (TTWD)-PLOTS FOR SURFACE JET DISCHARGE

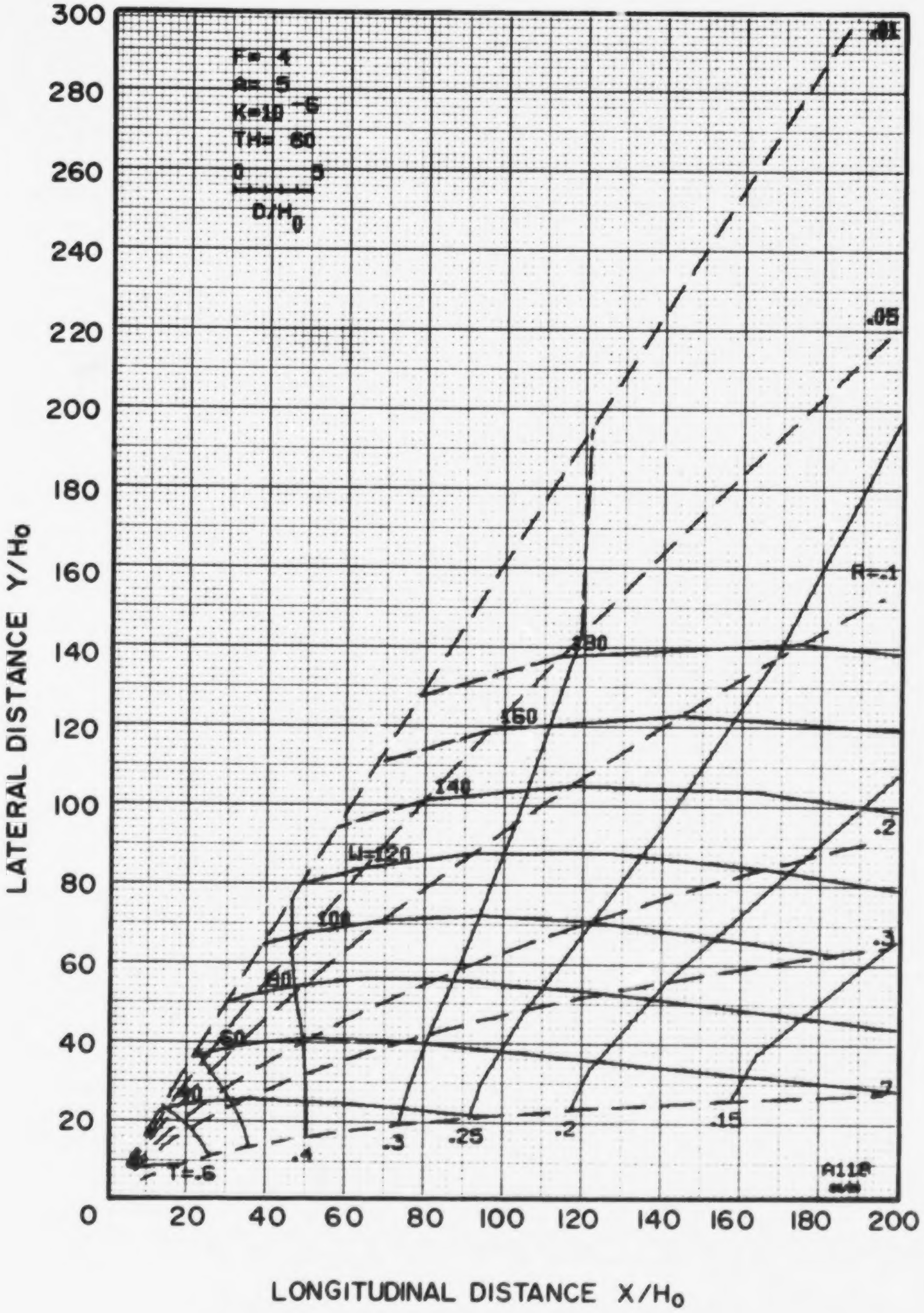

FIG (A118) TEMPERATURE, TRAJECTORY, WIDTH, AND DEPTH (TTWD)-PLOTS FOR SURFACE JET DISCHARGE

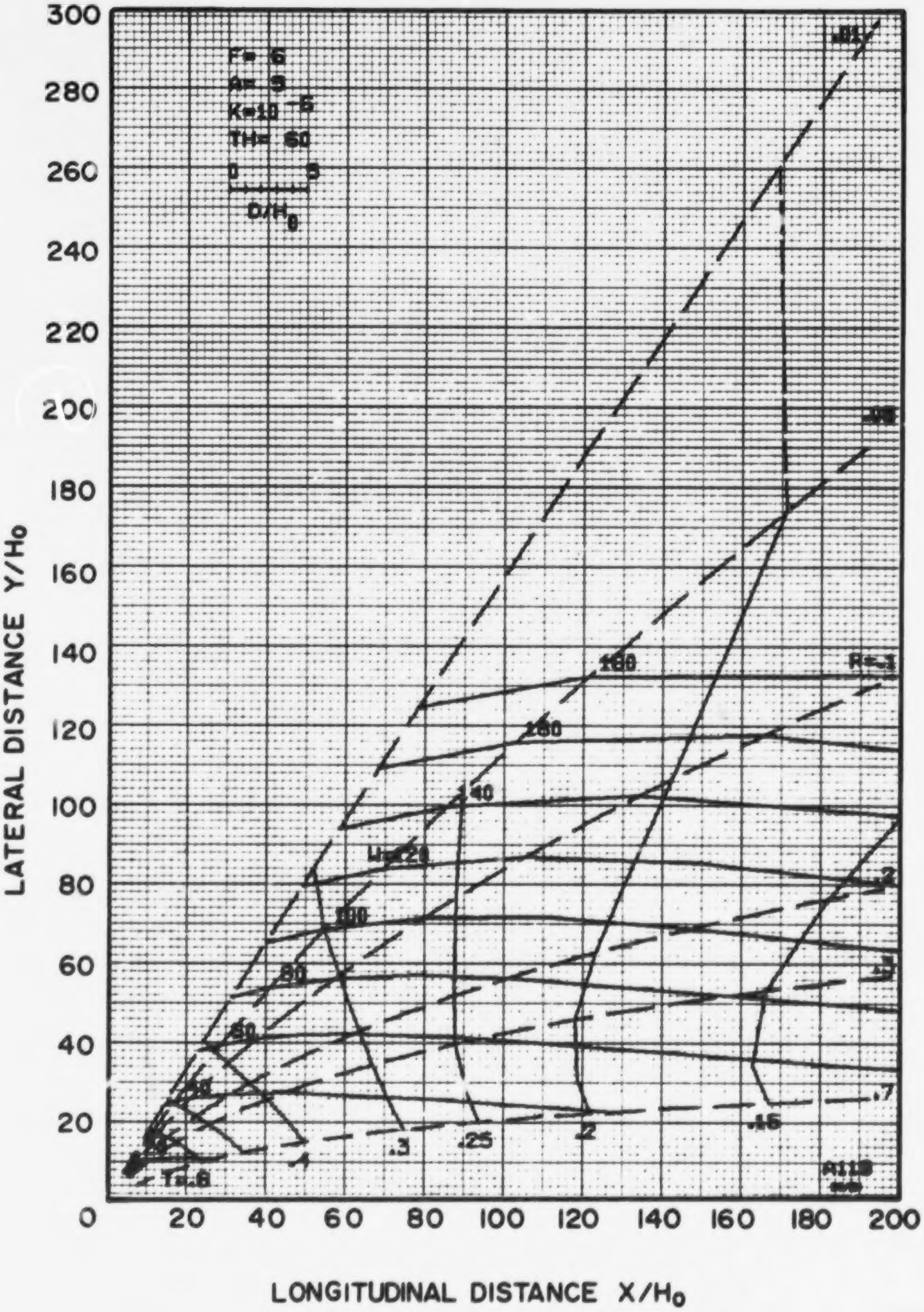

FIG (A119) TEMPERATURE, TRAJECTORY, WIDTH, AND DEPTH (TTWD)-PLOTS FOR SURFACE JET DISCHARGE

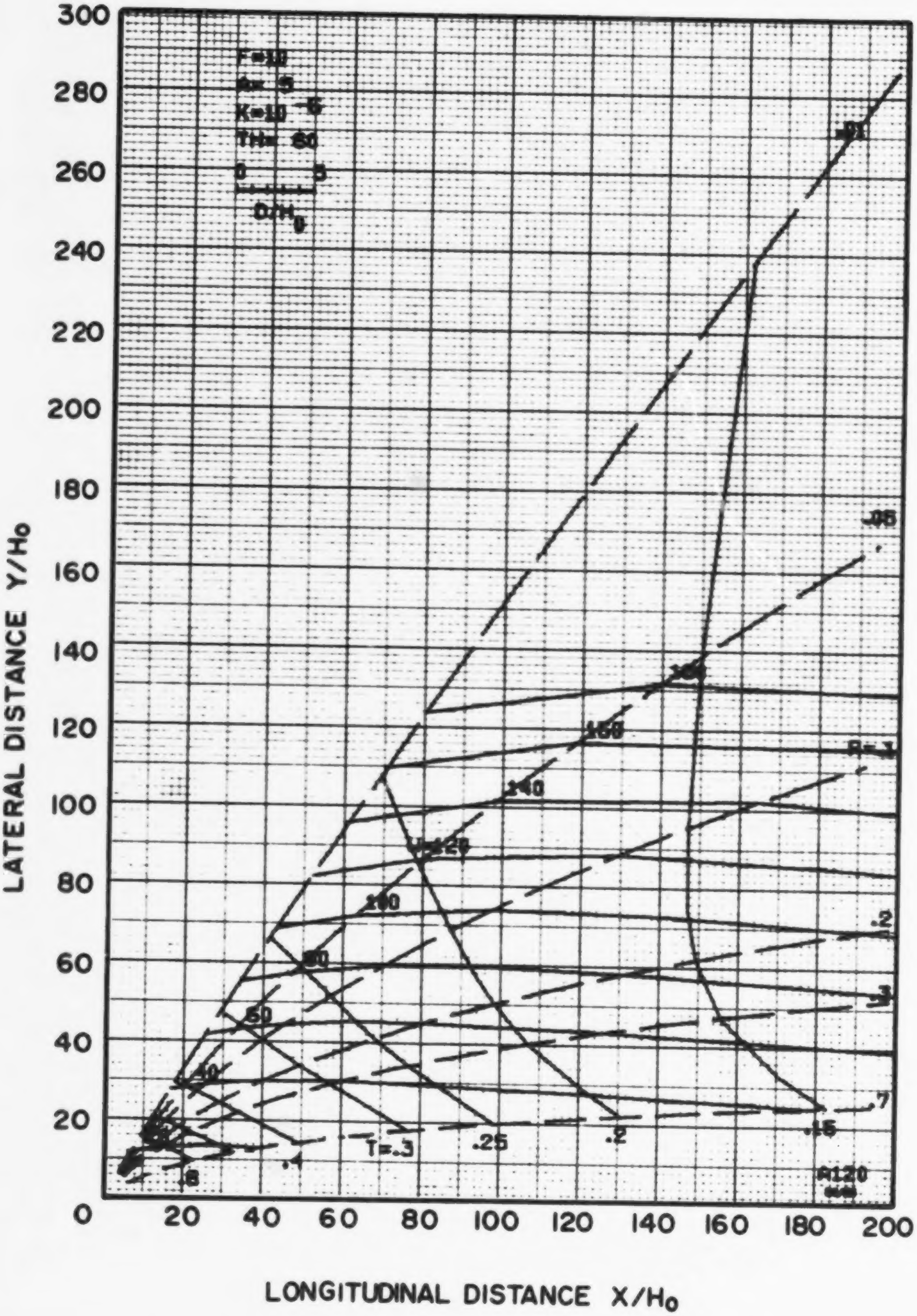

FIG (A120) TEMPERATURE, TRAJECTORY, WIDTH, AND DEPTH (TTWD)-PLOTS FOR SURFACE JET DISCHARGE

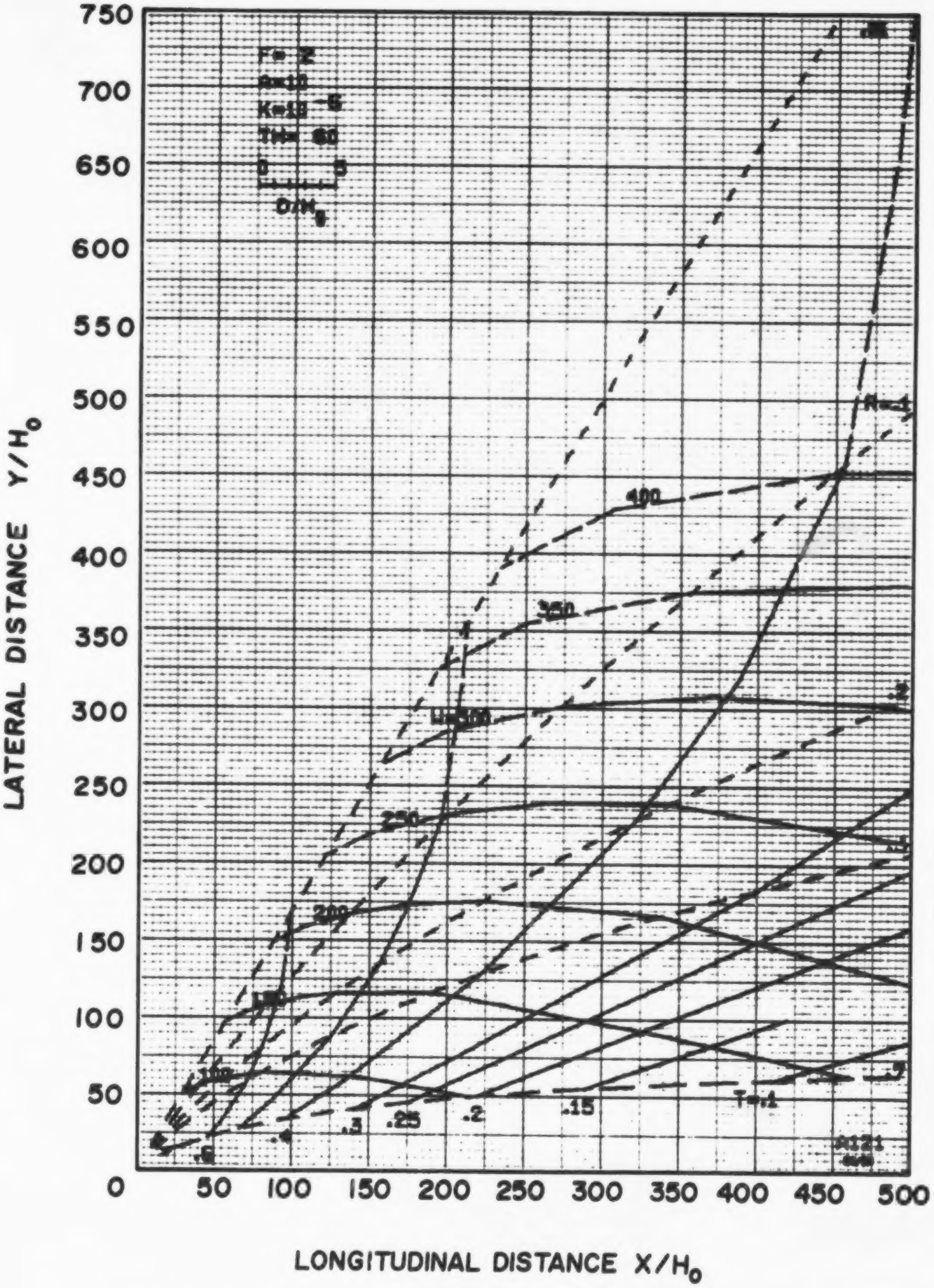

FIG (A121) TEMPERATURE, TRAJECTORY, WIDTH, AND DEPTH (TTWD)-PLOTS FOR SURFACE JET DISCHARGE

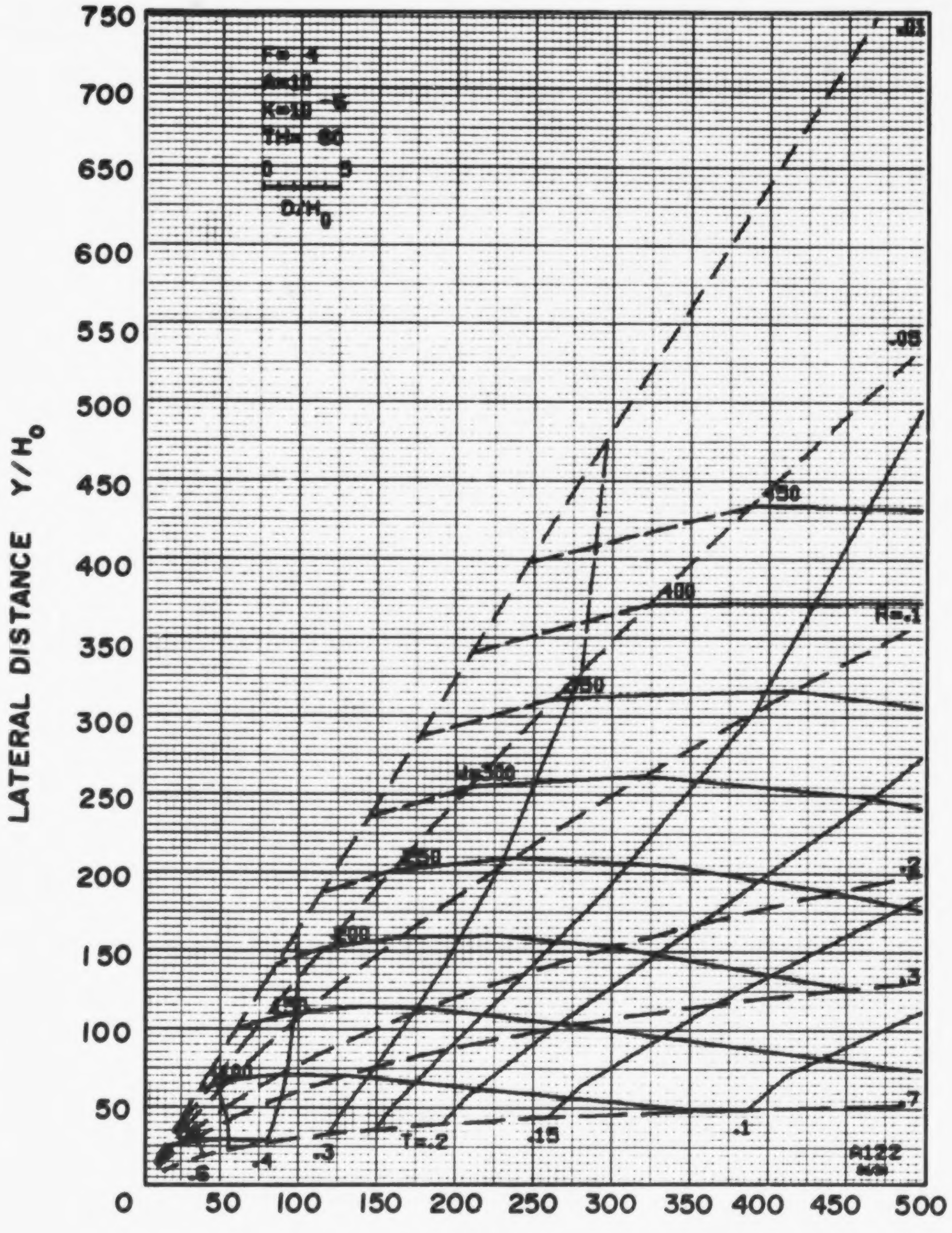

FIG (A122) TEMPERATURE, TRAJECTORY, WIDTH, AND DEPTH (TTWD)-PLOTS FOR SURFACE JET DISCHARGE

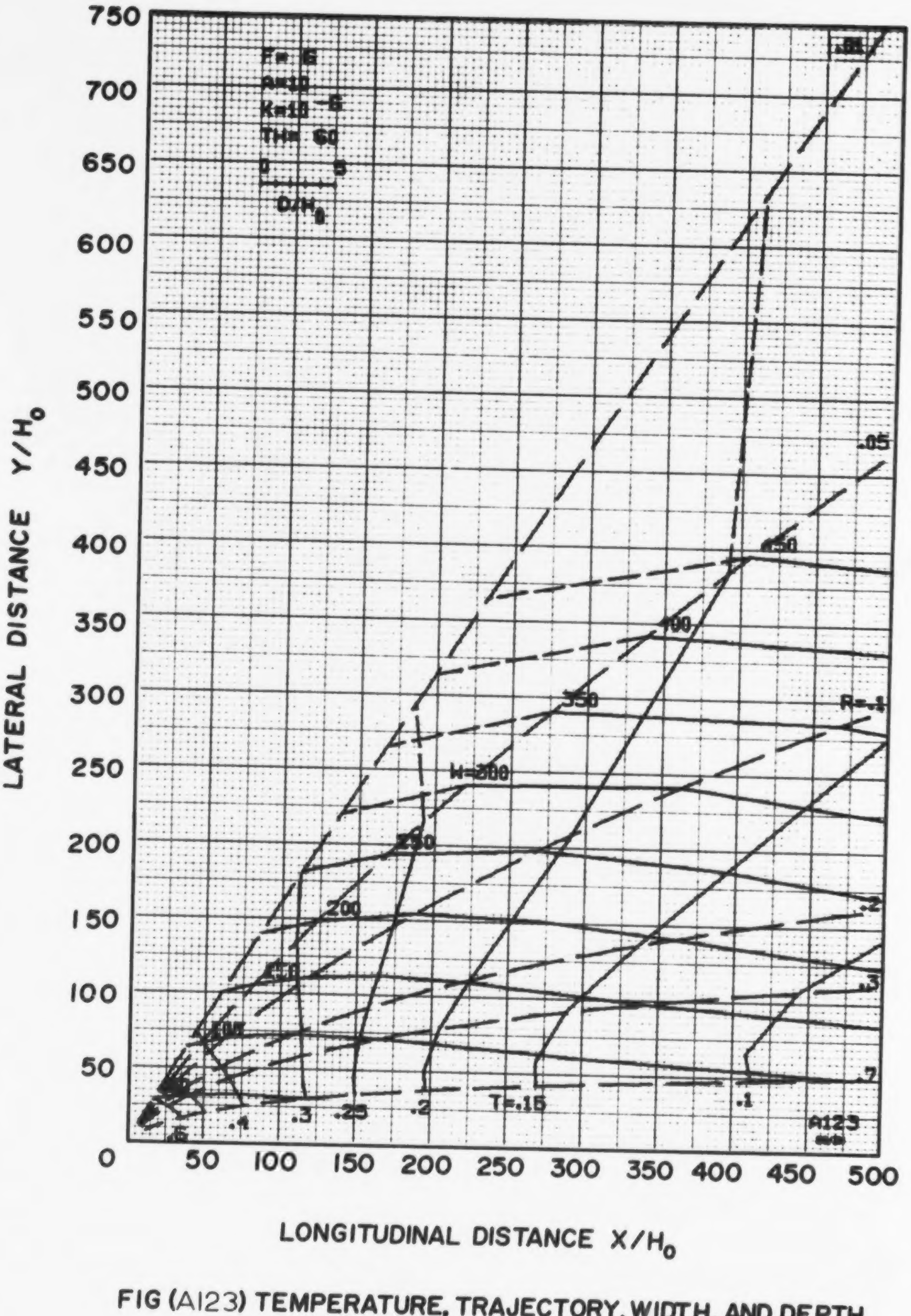

FIG (A123) TEMPERATURE, TRAJECTORY, WIDTH, AND DEPTH (TTWD)-PLOTS FOR SURFACE JET DISCHARGE

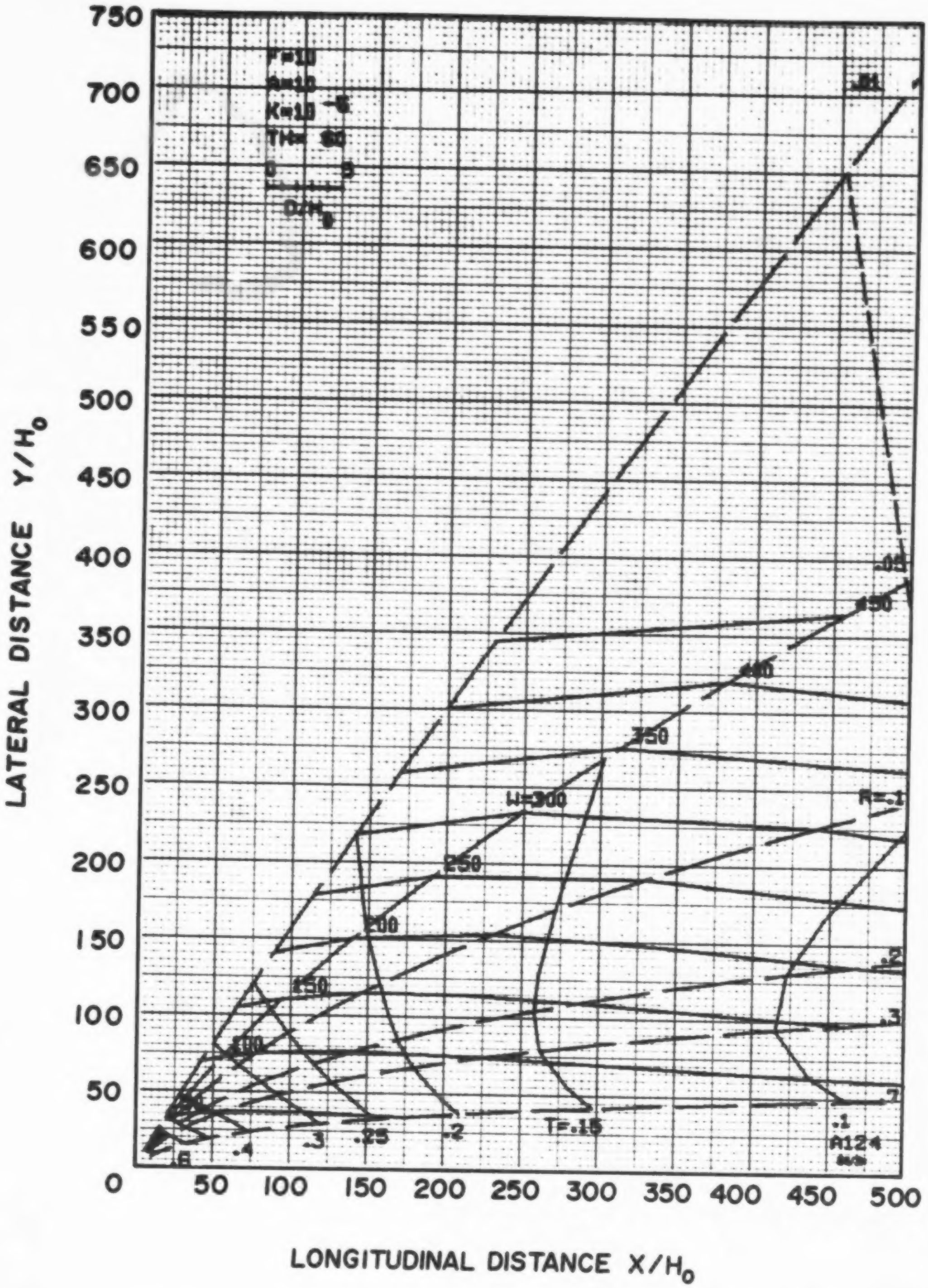

FIG (A124) TEMPERATURE, TRAJECTORY, WIDTH, AND DEPTH (TTWD)-PLOTS FOR SURFACE JET DISCHARGE

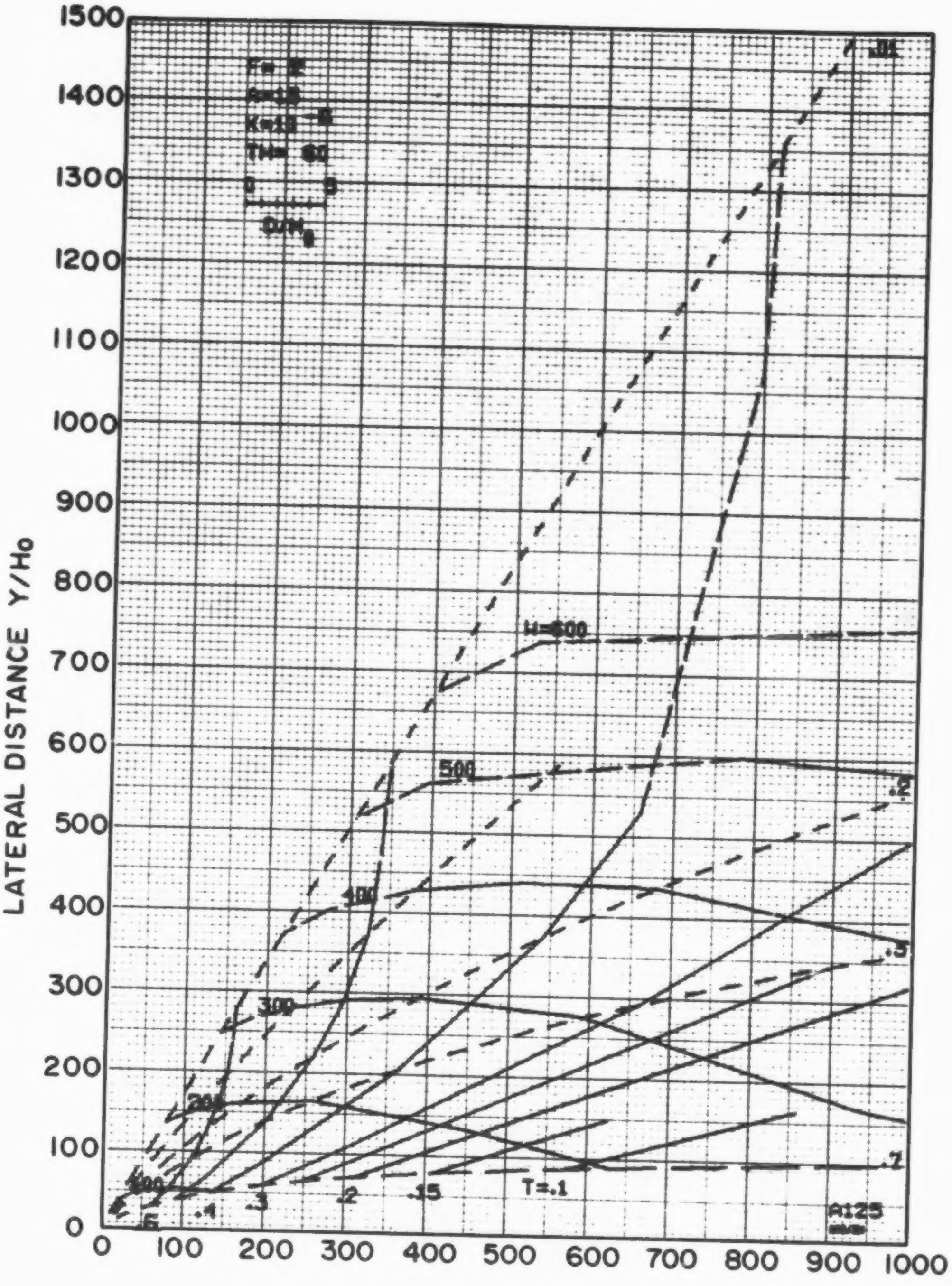

FIG (A125) TEMPERATURE, TRAJECTORY, WIDTH, AND DEPTH (TTWD)-PLOTS FOR SURFACE JET DISCHARGE

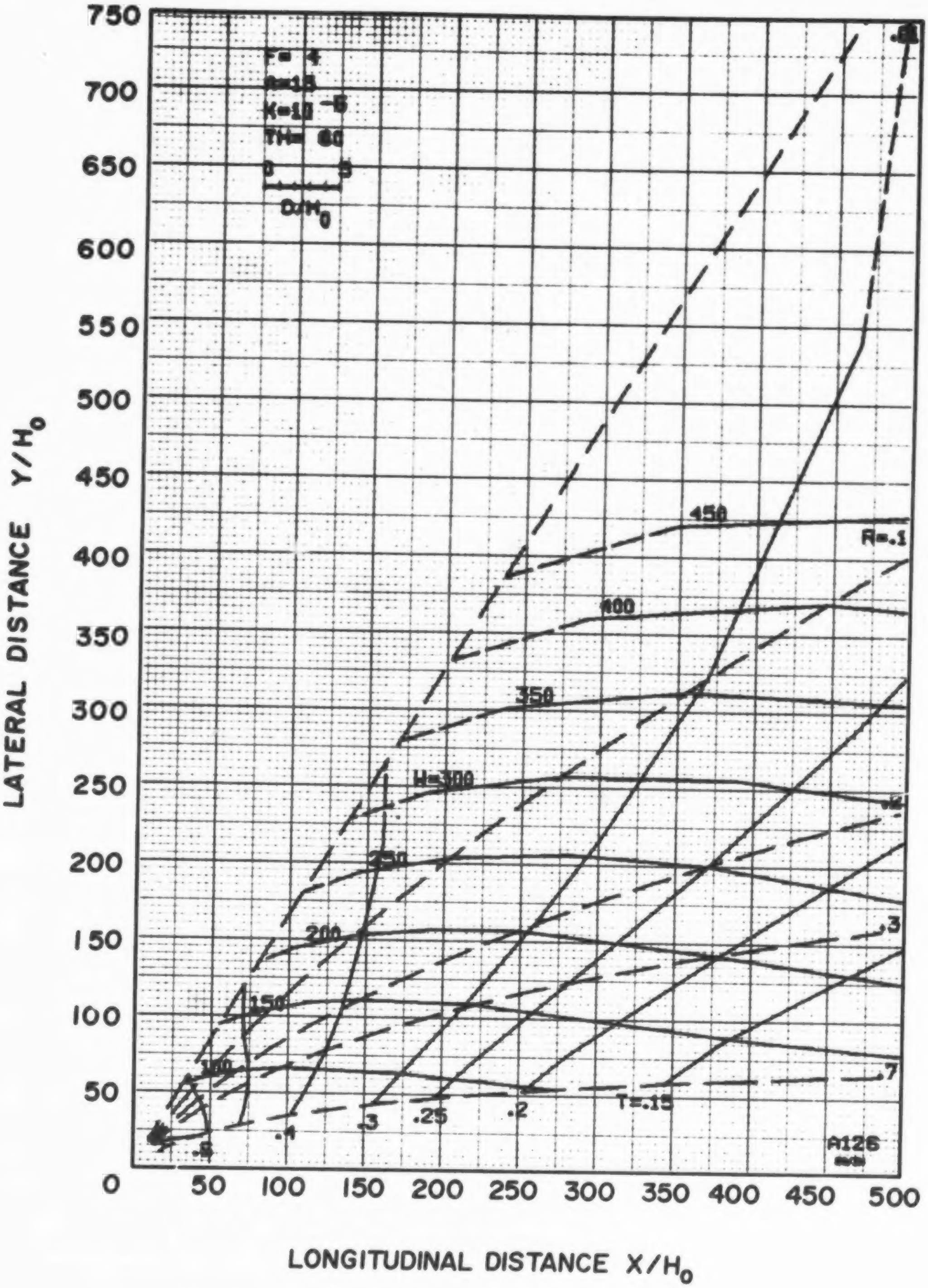

FIG (A126) TEMPERATURE, TRAJECTORY, WIDTH, AND DEPTH (TTWD)-PLOTS FOR SURFACE JET DISCHARGE

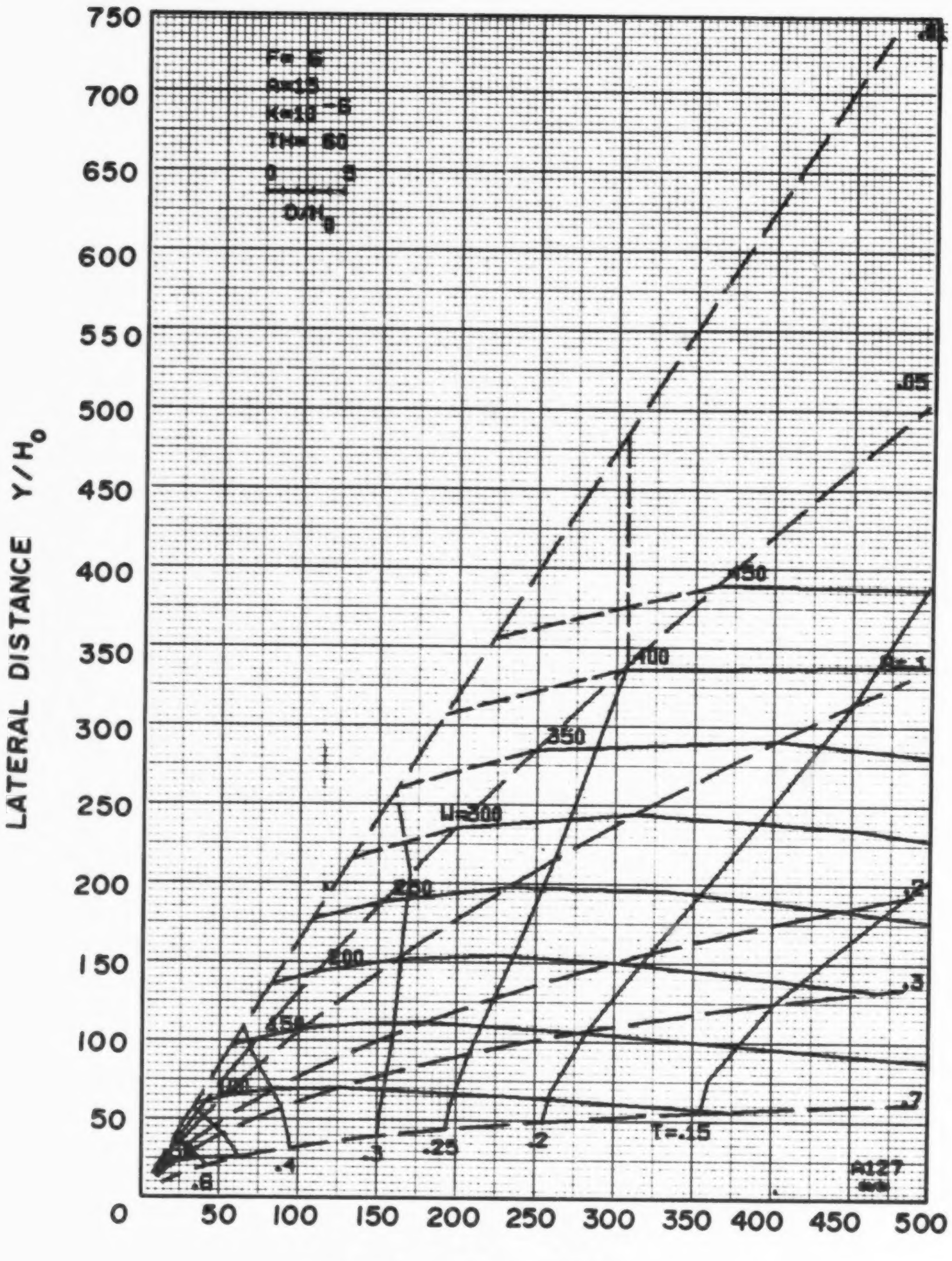

FIG (A127) TEMPERATURE, TRAJECTORY, WIDTH, AND DEPTH (TTWD)-PLOTS FOR SURFACE JET DISCHARGE

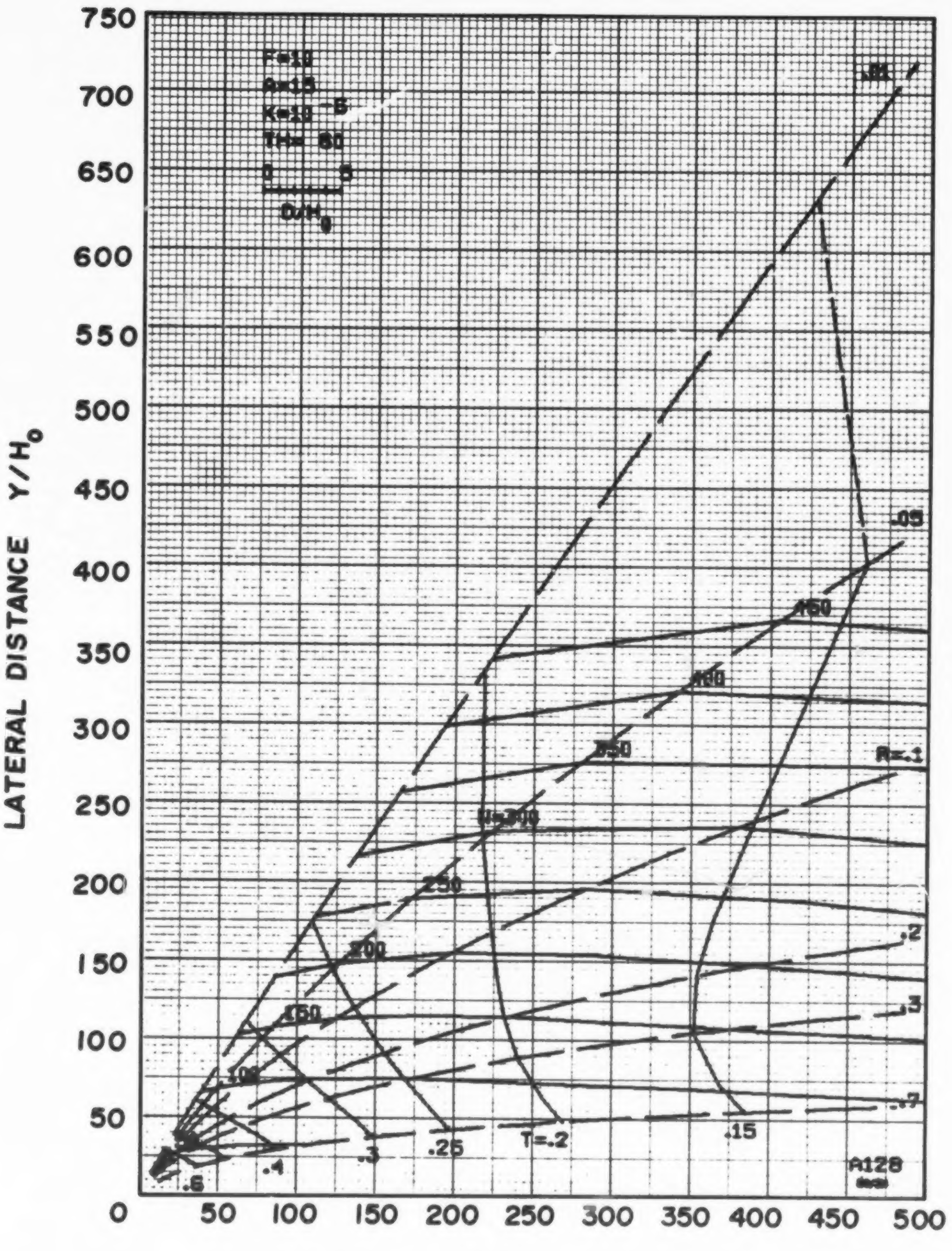

FIG (A128) TEMPERATURE, TRAJECTORY, WIDTH, AND DEPTH (TTWD)-PLOTS FOR SURFACE JET DISCHARGE

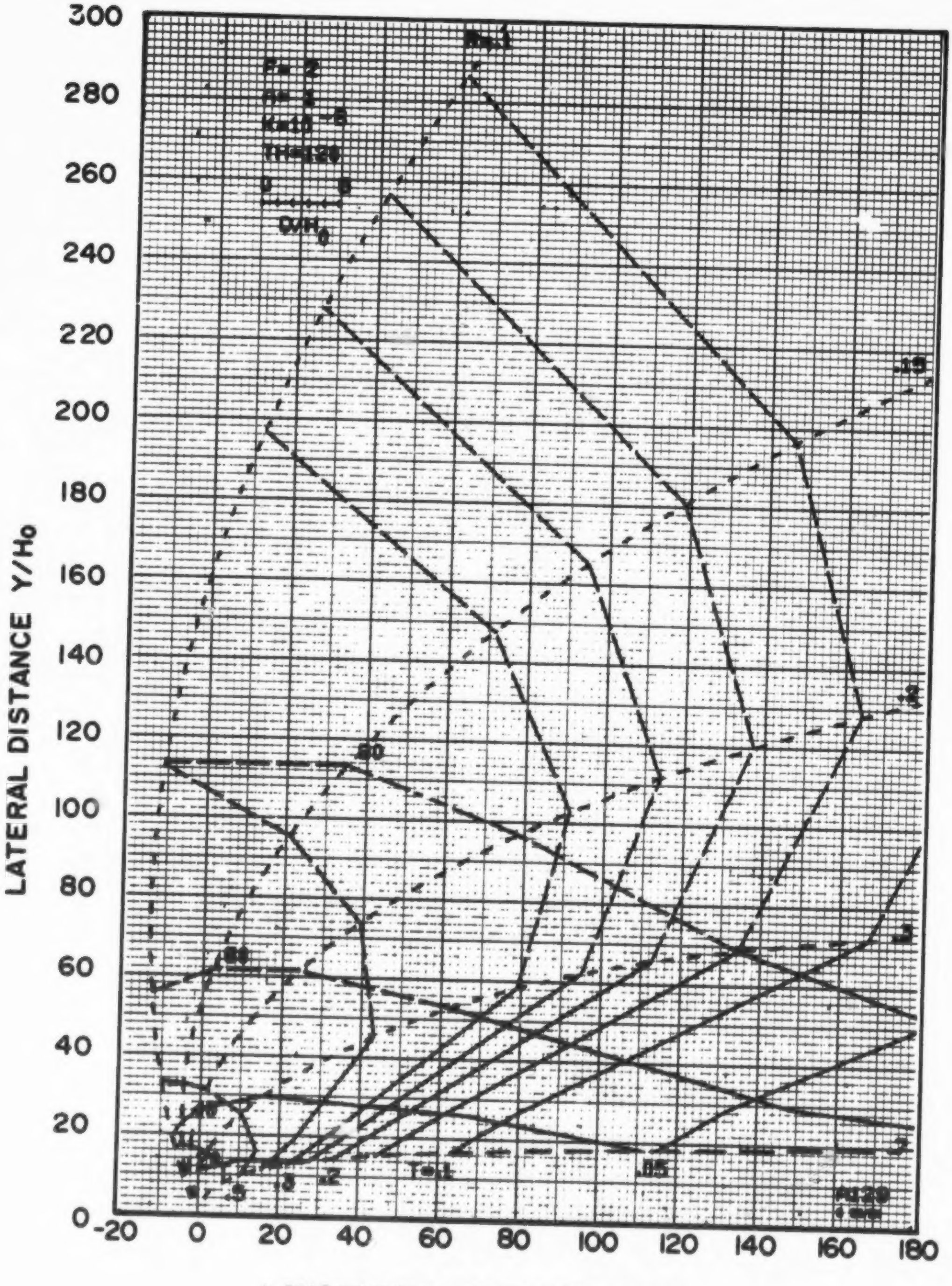

FIG (A129) TEMPERATURE, TRAJECTORY, WIDTH, AND DEPTH (TTWD)-PLOTS FOR SURFACE JET DISCHARGE

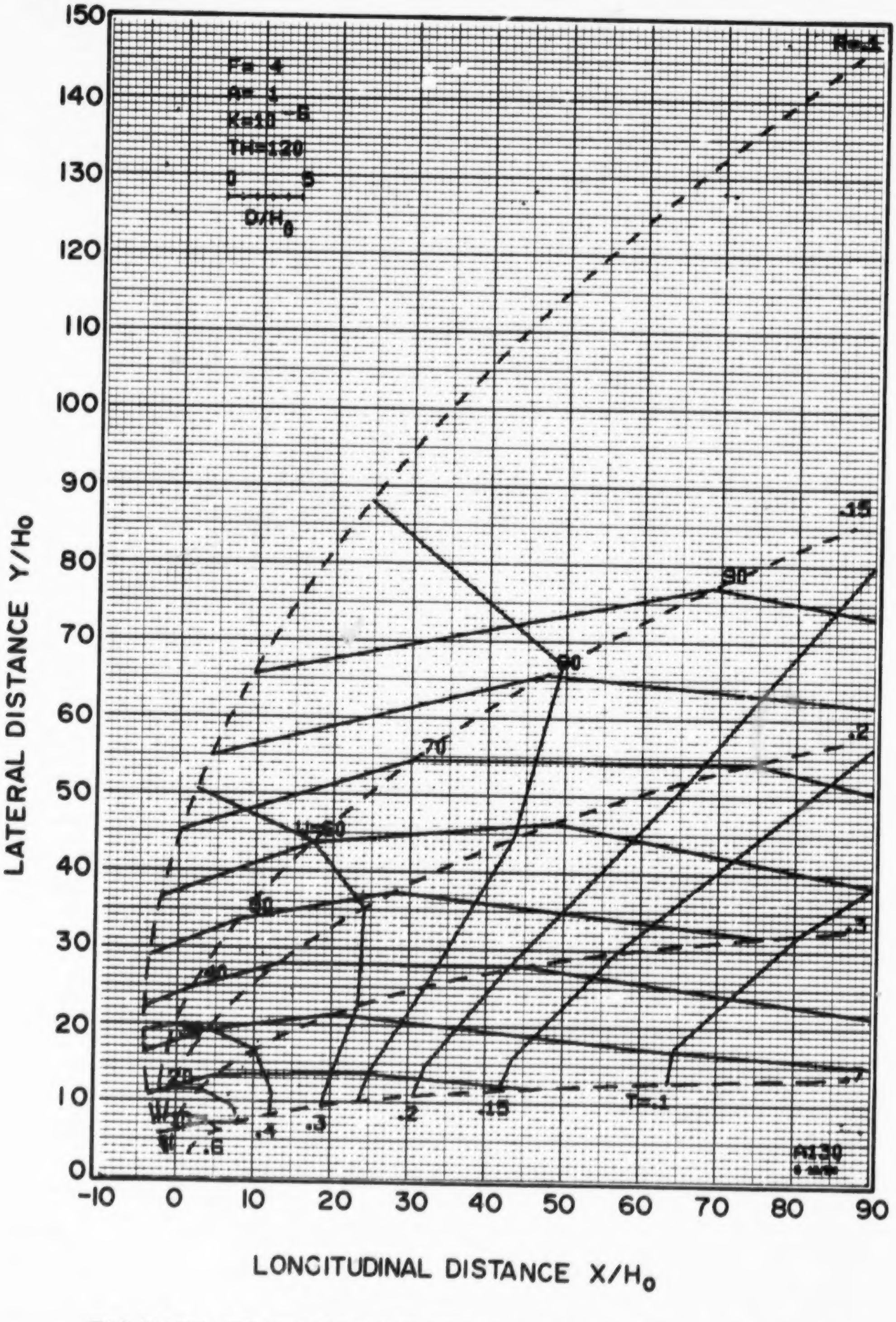

FIG (A130) TEMPERATURE, TRAJECTORY, WIDTH, AND DEPTH (TTWD)-PLOTS FOR SURFACE JET DISCHARGE

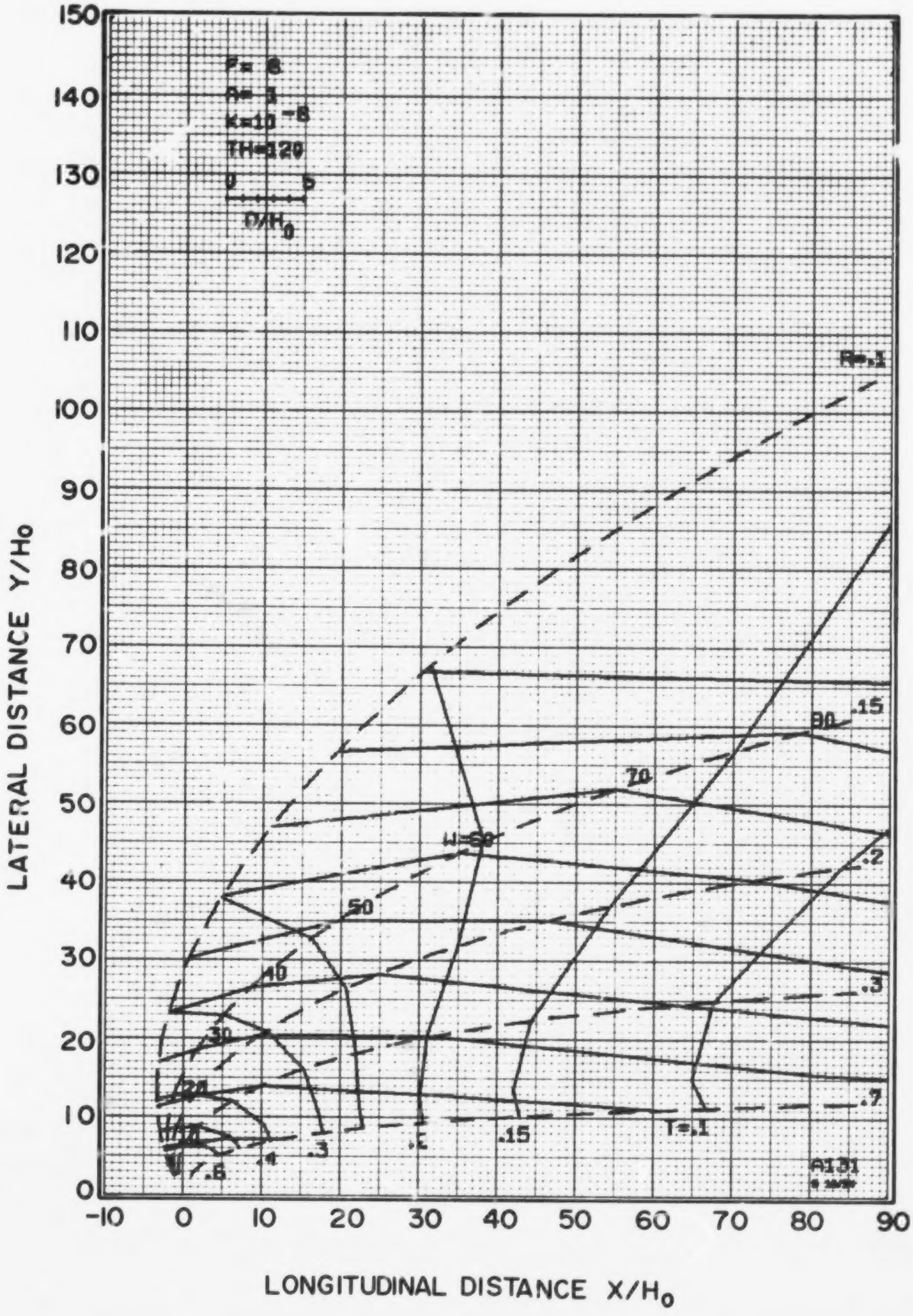

FIG (A131) TEMPERATURE, TRAJECTORY, WIDTH, AND DEPTH (TTWD)-PLOTS FOR SURFACE JET DISCHARGE

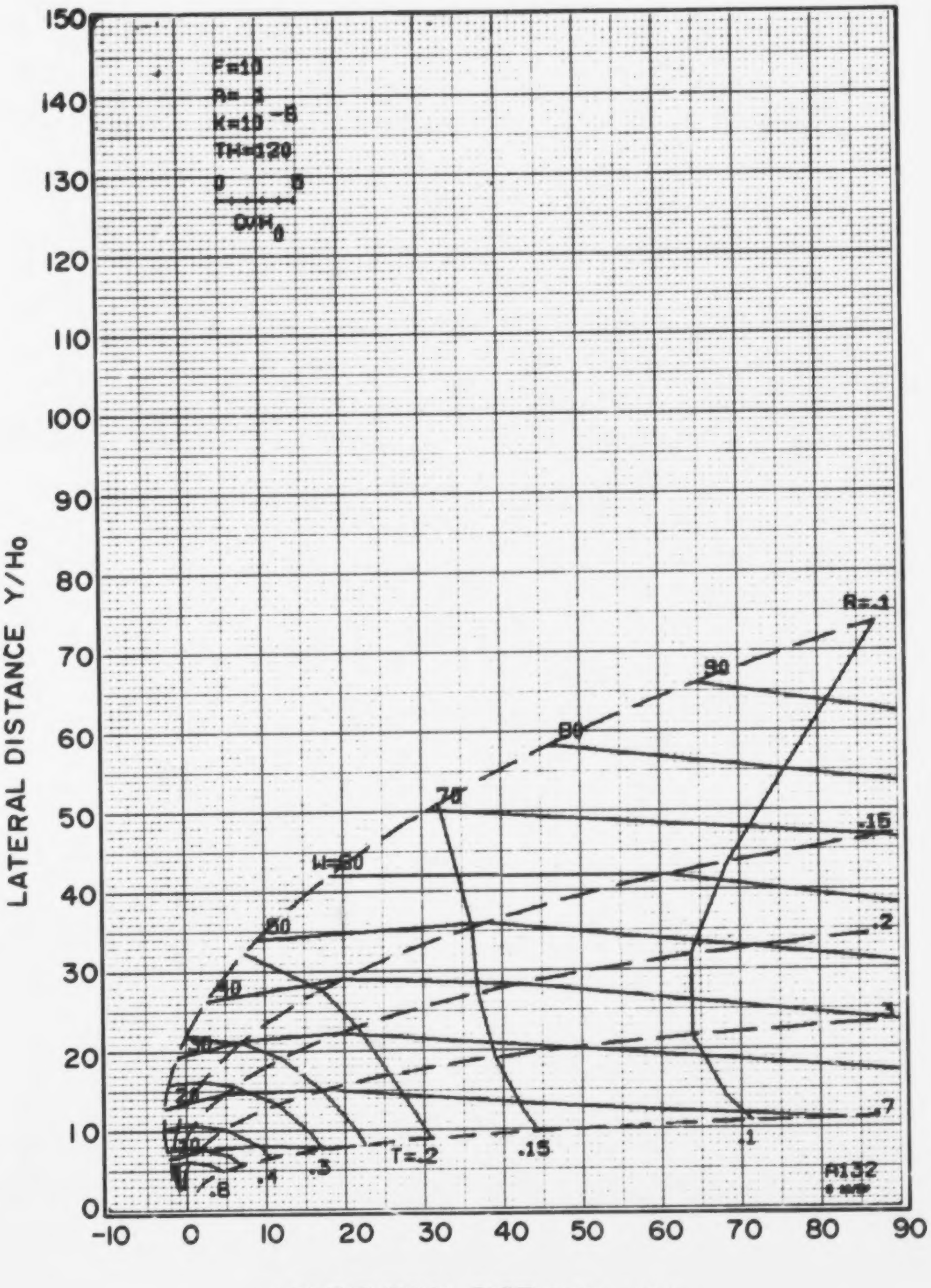

FIG (A132) TEMPERATURE, TRAJECTORY, WIDTH, AND DEPTH (TTWD)-PLOTS FOR SURFACE JET DISCHARGE

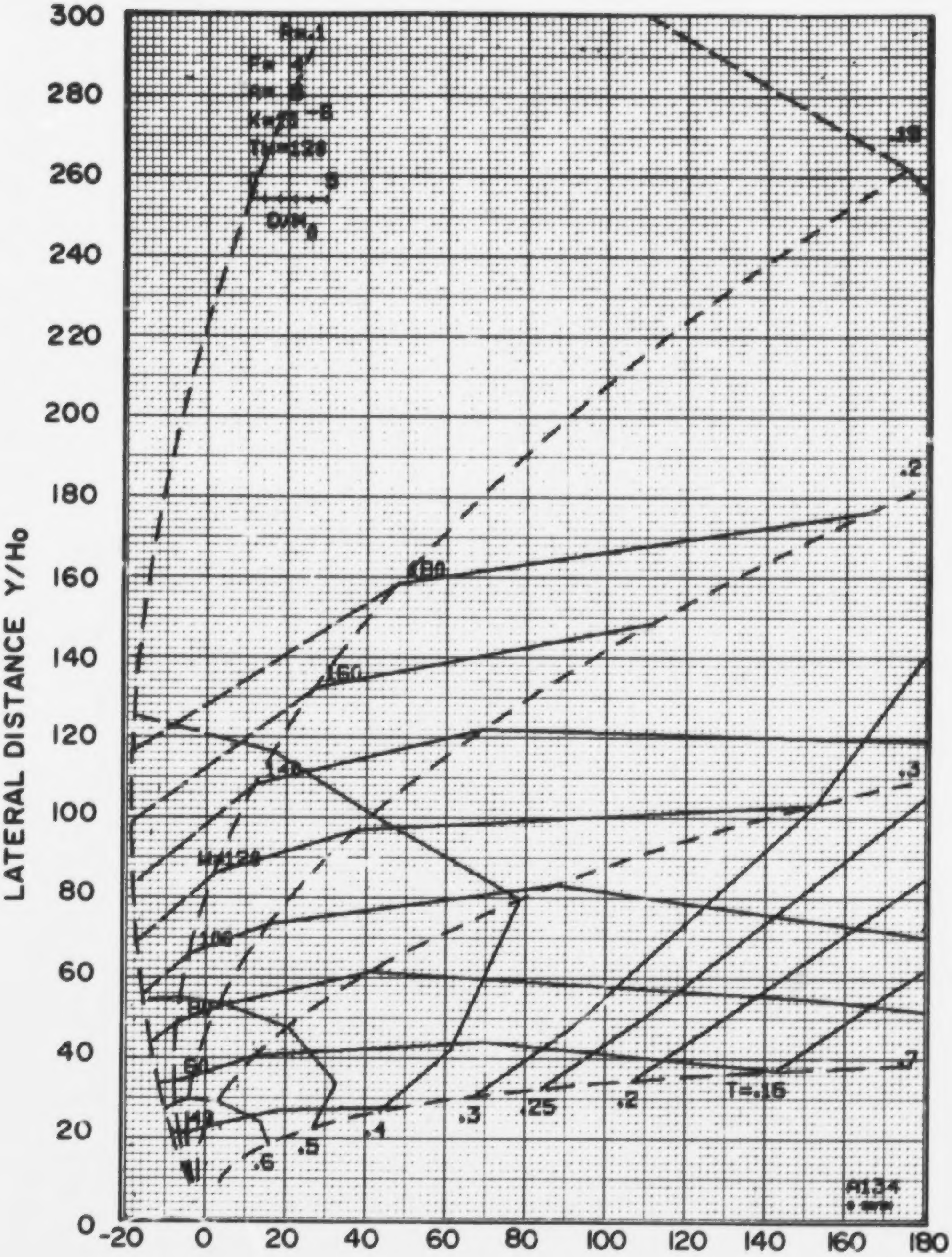

FIG (A134) TEMPERATURE, TRAJECTORY, WIDTH, AND DEPTH (TTWD)-PLOTS FOR SURFACE JET DISCHARGE

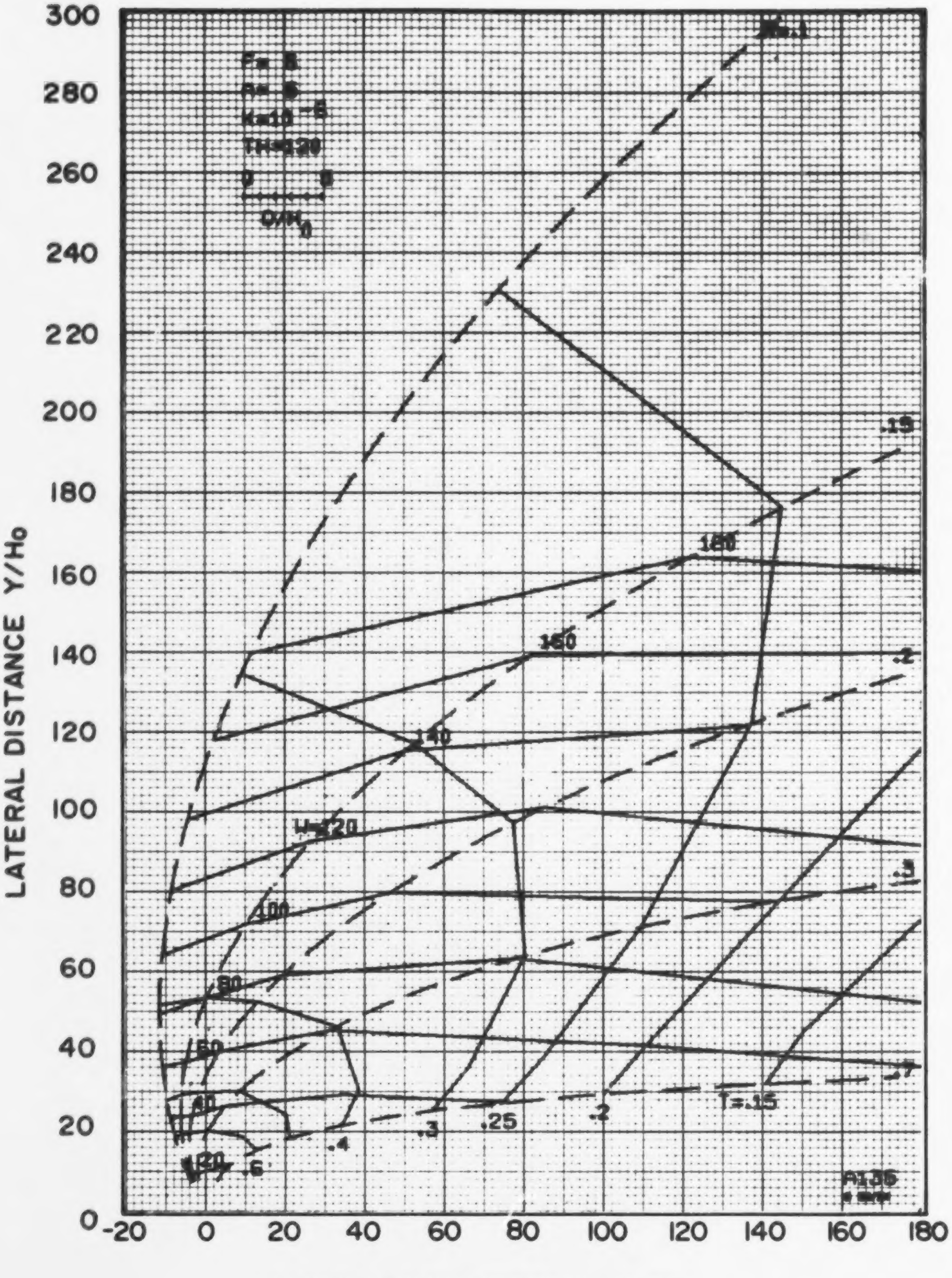

FIG (A135) TEMPERATURE, TRAJECTORY, WIDTH, AND DEPTH (TTWD)-PLOTS FOR SURFACE JET DISCHARGE

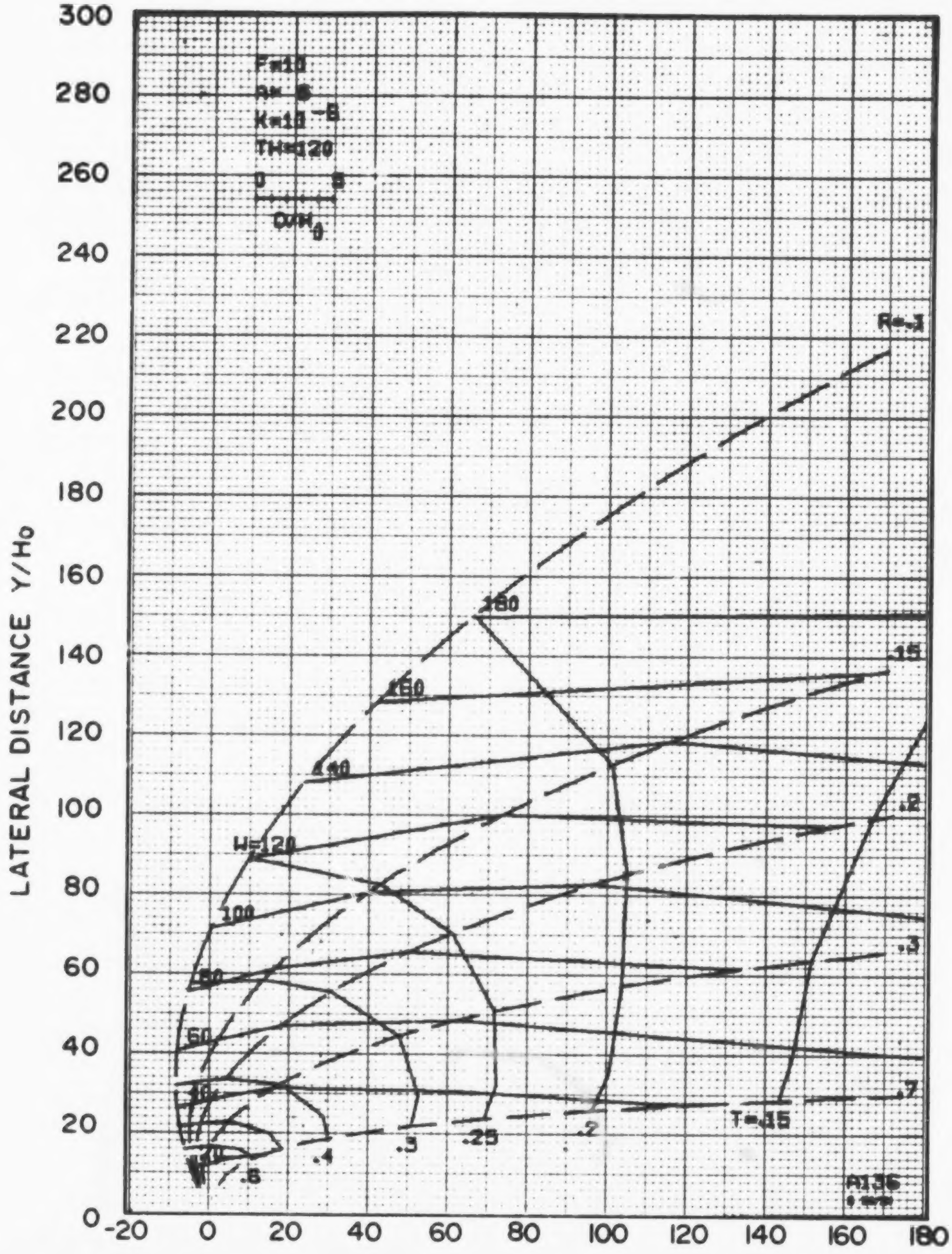

FIG (A136) TEMPERATURE, TRAJECTORY, WIDTH, AND DEPTH (TTWD)-PLOTS FOR SURFACE JET DISCHARGE

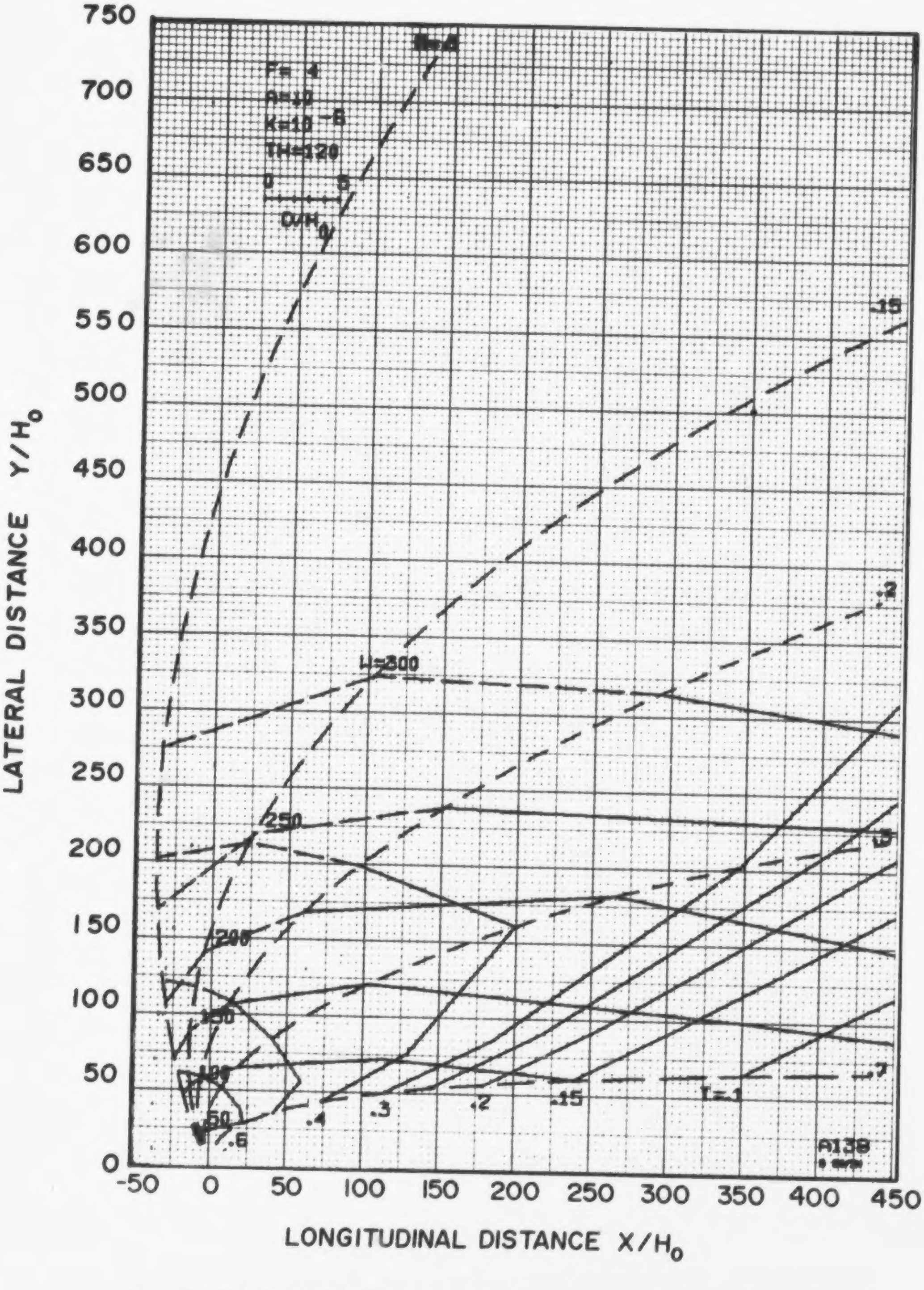

FIG (A138) TEMPERATURE, TRAJECTORY, WIDTH, AND DEPTH (TTWD)-PLOTS FOR SURFACE JET DISCHARGE

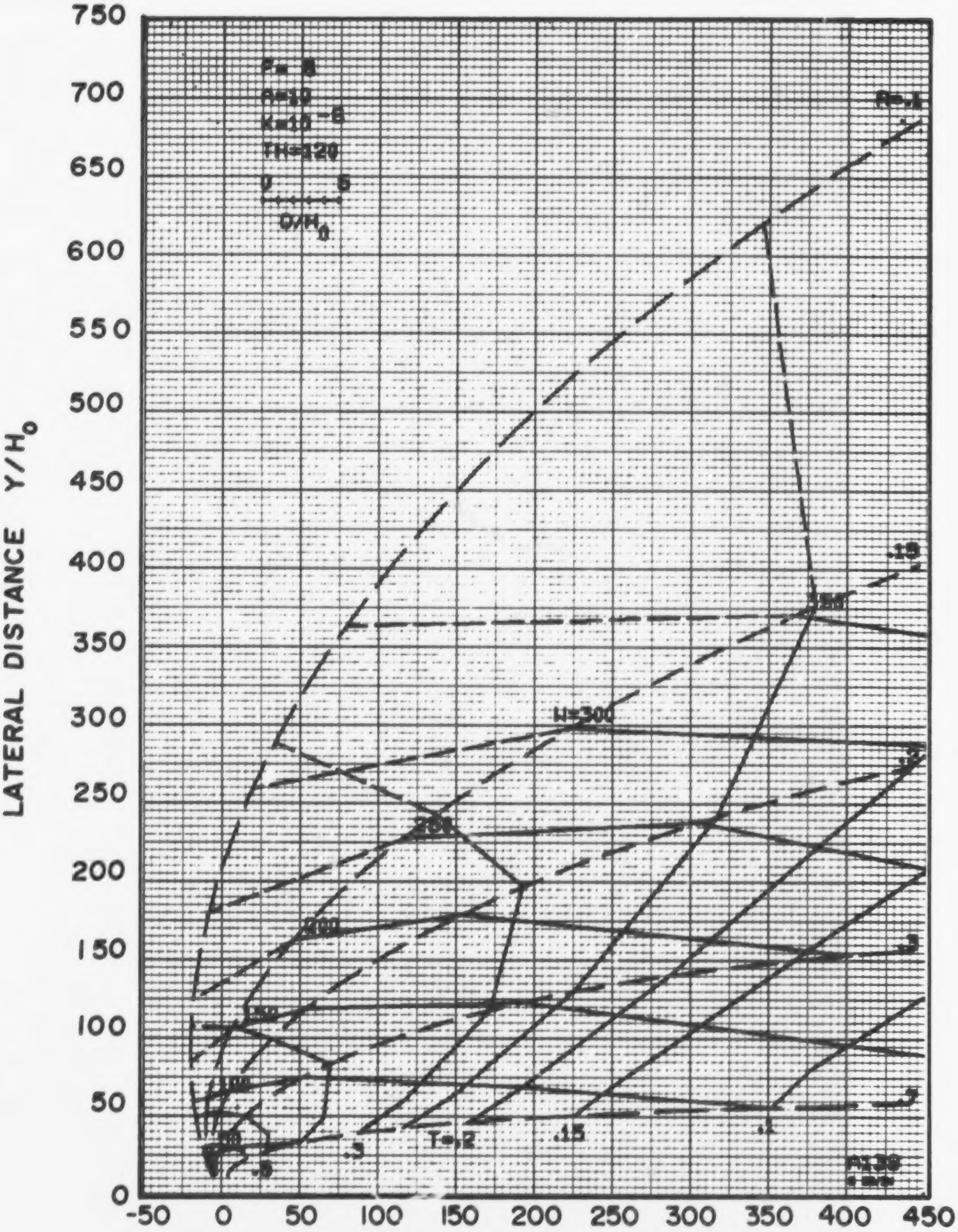

FIG (A139) TEMPERATURE, TRAJECTORY, WIDTH, AND DEPTH (TTWD)-PLOTS FOR SURFACE JET DISCHARGE

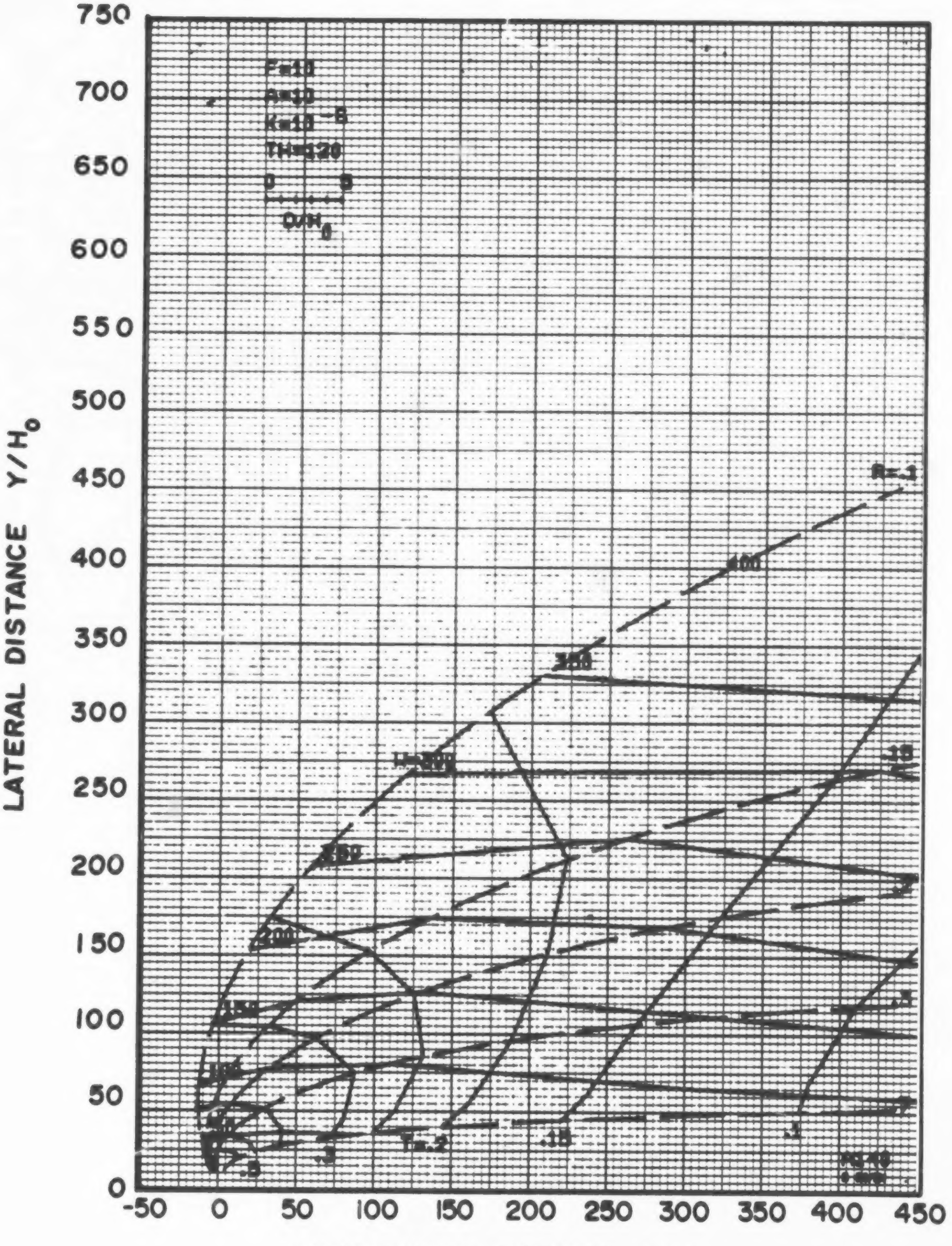

FIG (A140) TEMPERATURE, TRAJECTORY, WIDTH, AND DEPTH (TTWD)-PLOTS FOR SURFACE JET DISCHARGE

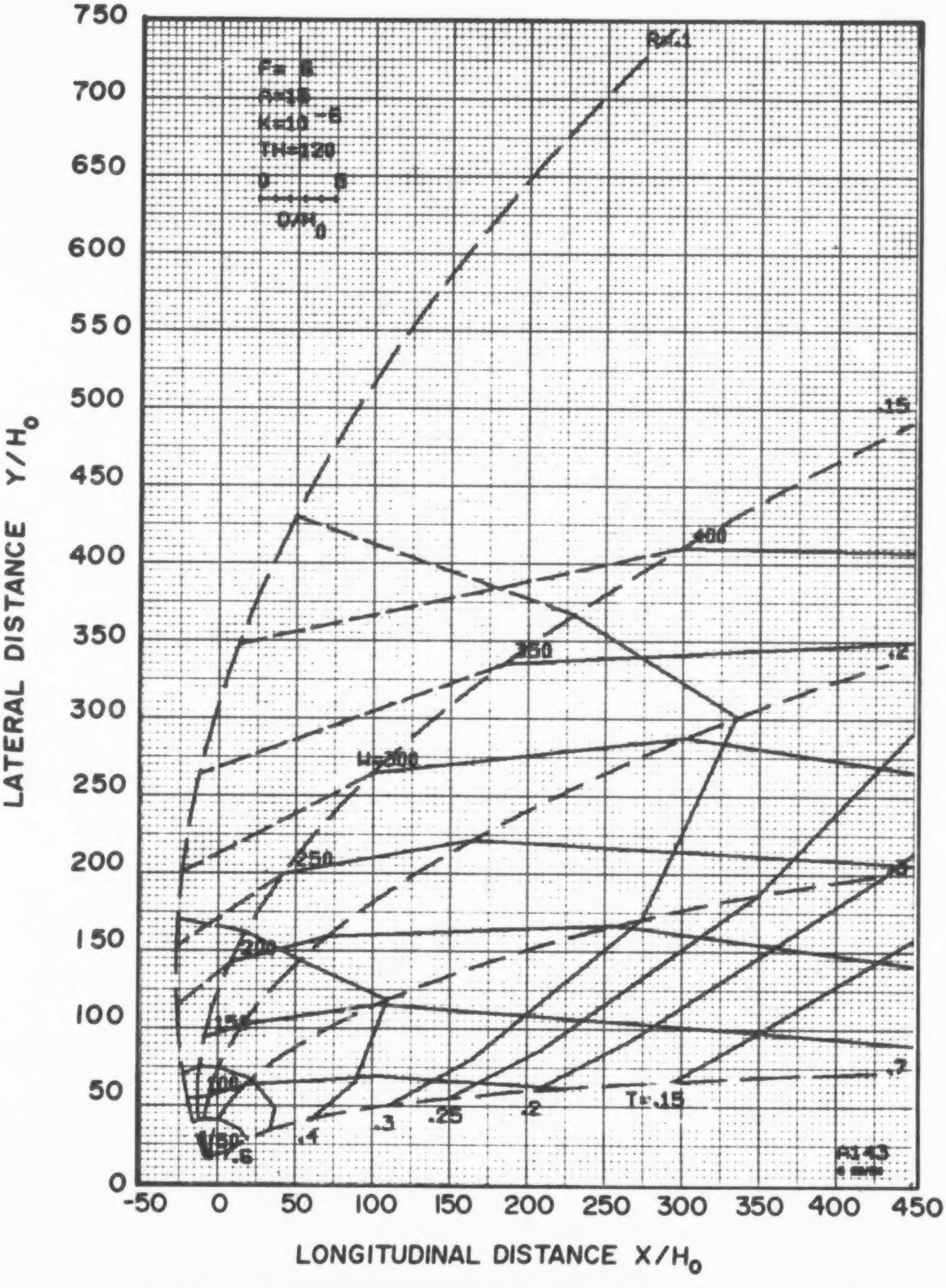

FIG (A143) TEMPERATURE, TRAJECTORY, WIDTH, AND DEPTH (TTWD)-PLOTS FOR SURFACE JET DISCHARGE

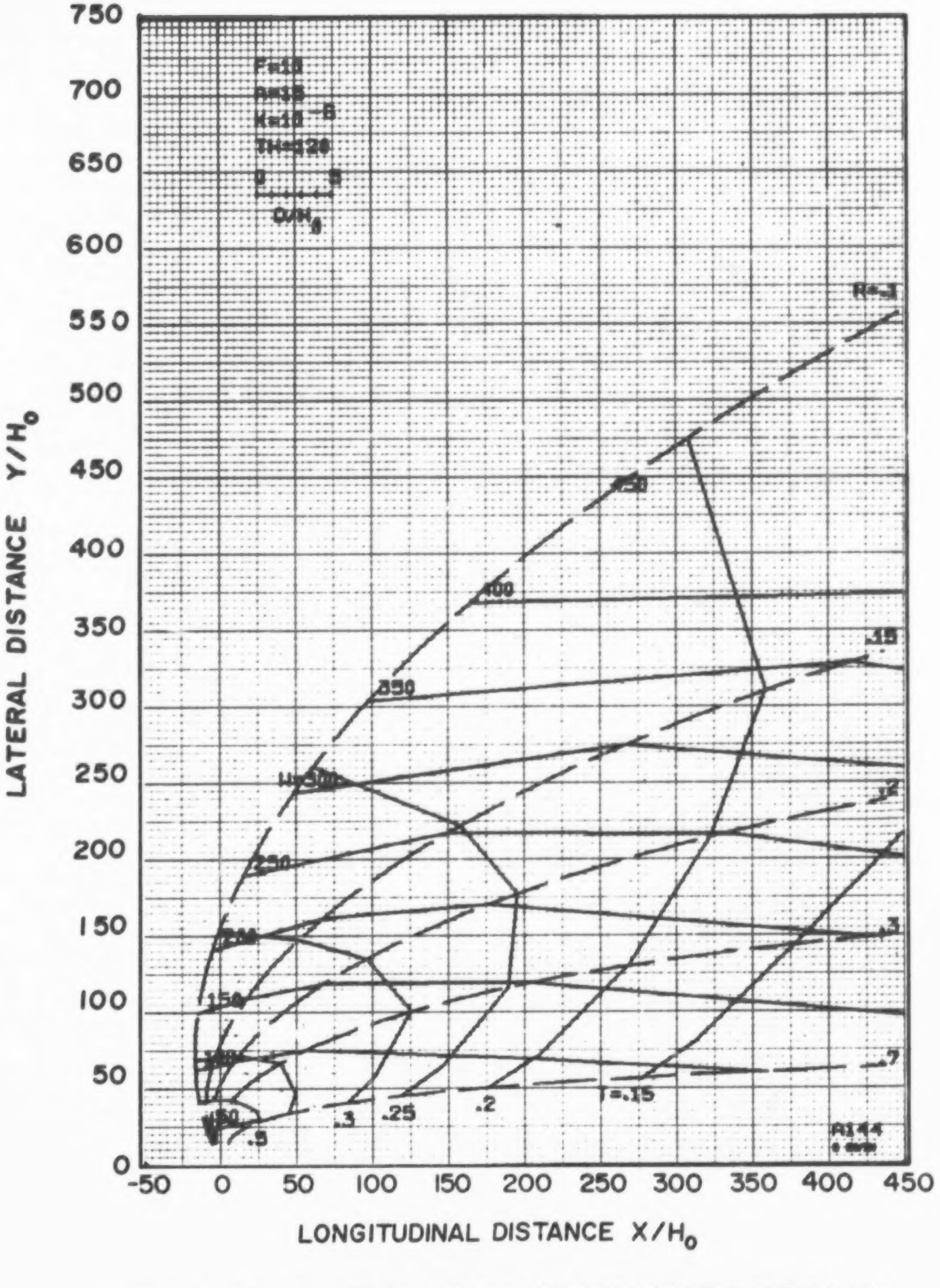

FIG (A144) TEMPERATURE, TRAJECTORY, WIDTH, AND DEPTH (TTWD)-PLOTS FOR SURFACE JET DISCHARGE

APPENDIX B
(TA) WORKING NOMOGRAMS

TABLE 3
Figure Numbers for (TA) Working Nomograms of Appendix B, $\theta_o = 90°$, $K = 10^{-5}$

F→ ↓A	2	4	6	10
1	B1	B1	B2	B2
5	B3	B3	B4	B4
10	B5	B5	B6	B6
15	B7	B7	B8	B8

TABLE 4
Summary of Figure Numbers for (TA) Working Nomograms of Appendix B

θ_o→ ↓K	90°	60°	120°
10^{-5}	B1-B8	B9-B16	B17-B24
10^{-4}	B25-B32	B33-B40	B41-B48
10^{-6}	B49-B56	B57-64	B65-B72

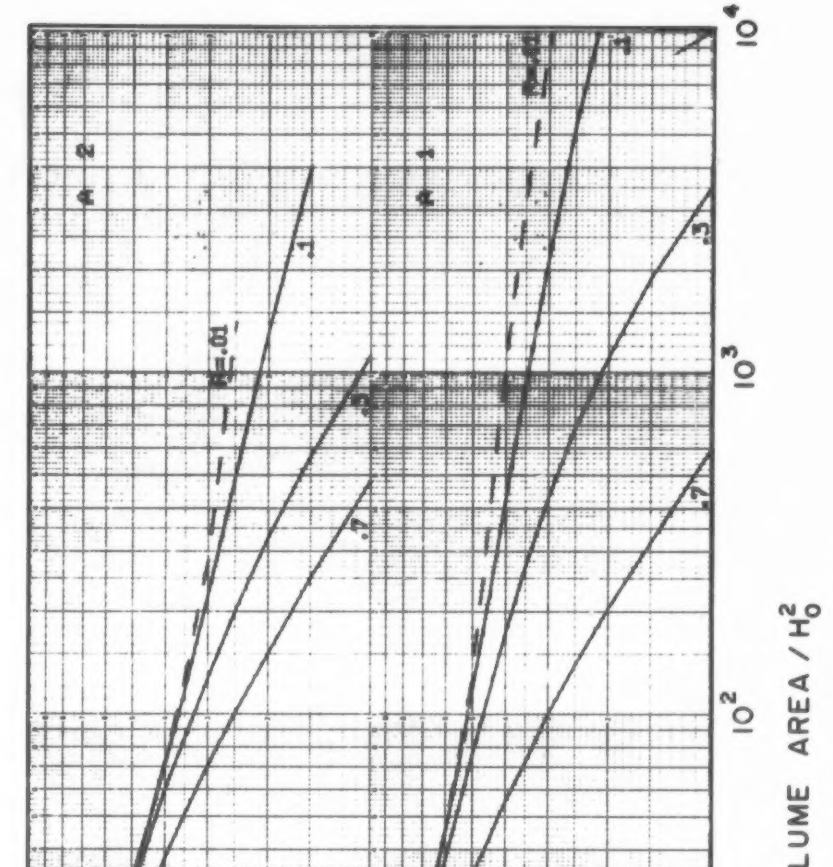

FIG(B1) TEMPERATURE, AREA (TA)-PLOT FOR SURFACE JET DISCHARGE

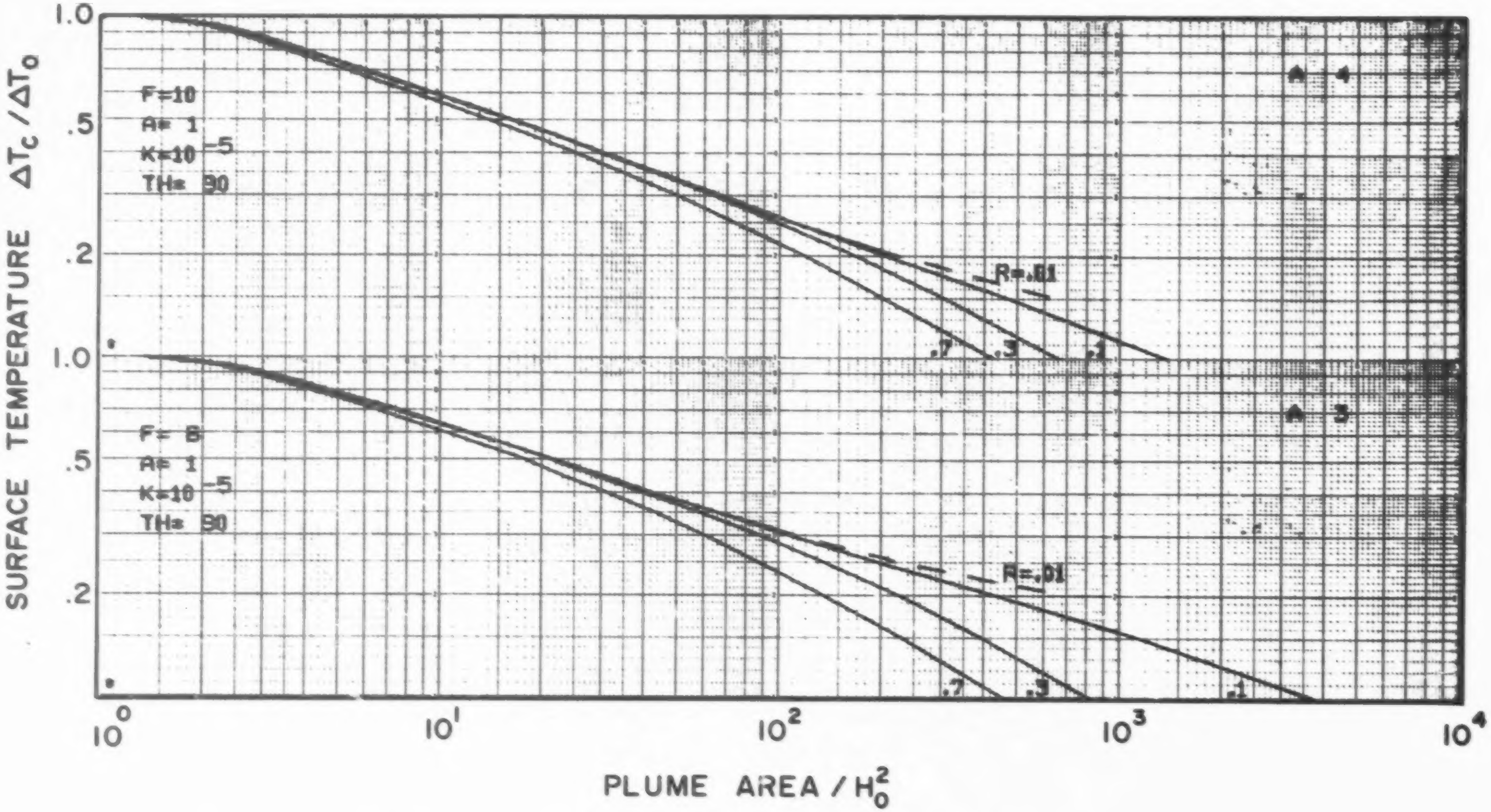

FIG(B2) TEMPERATURE, AREA (TA)-PLOT
FOR SURFACE JET DISCHARGE

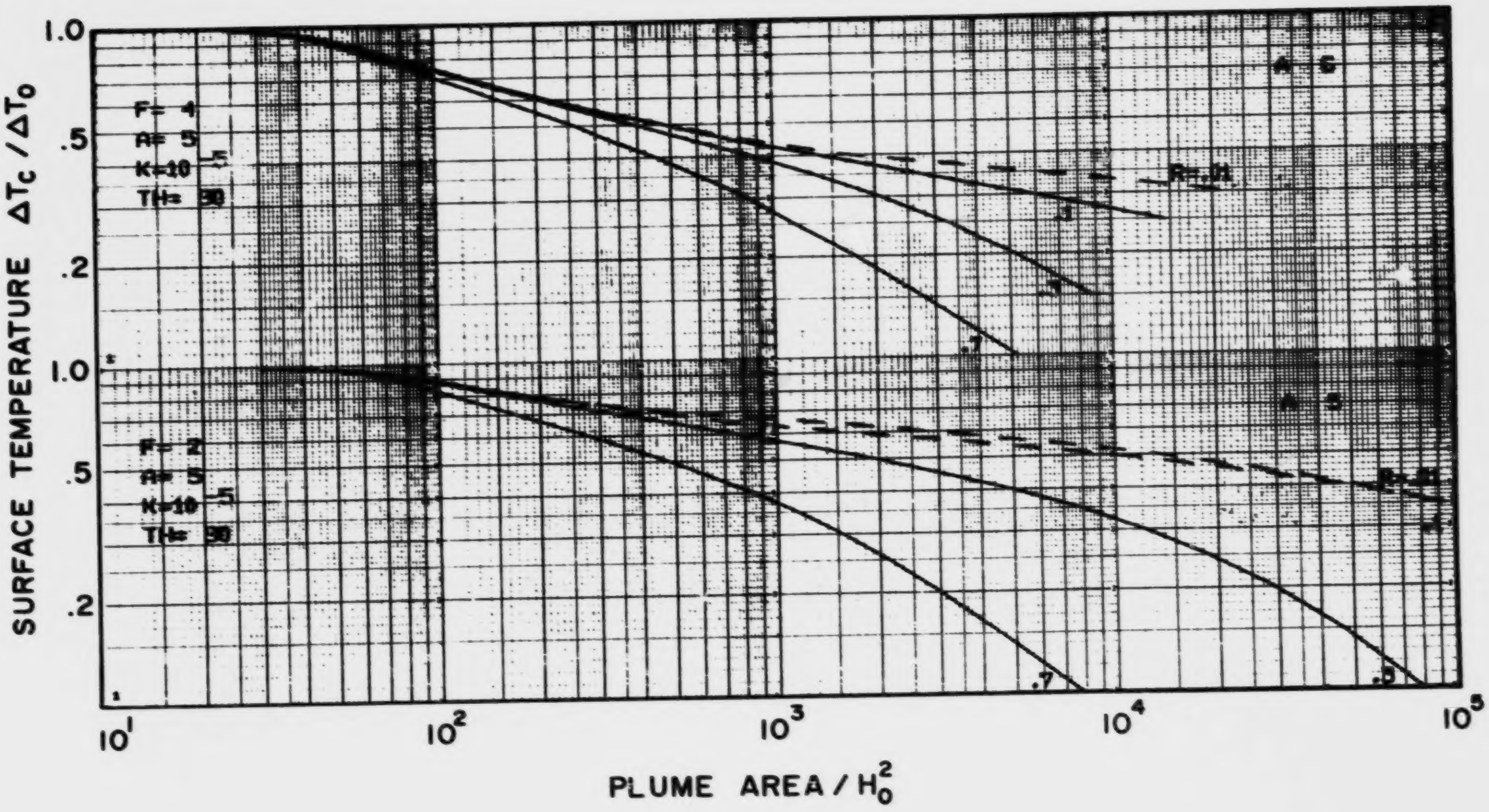

FIG (B 3) TEMPERATURE, AREA (TA)-PLOTS
FOR SURFACE JET DISCHARGE

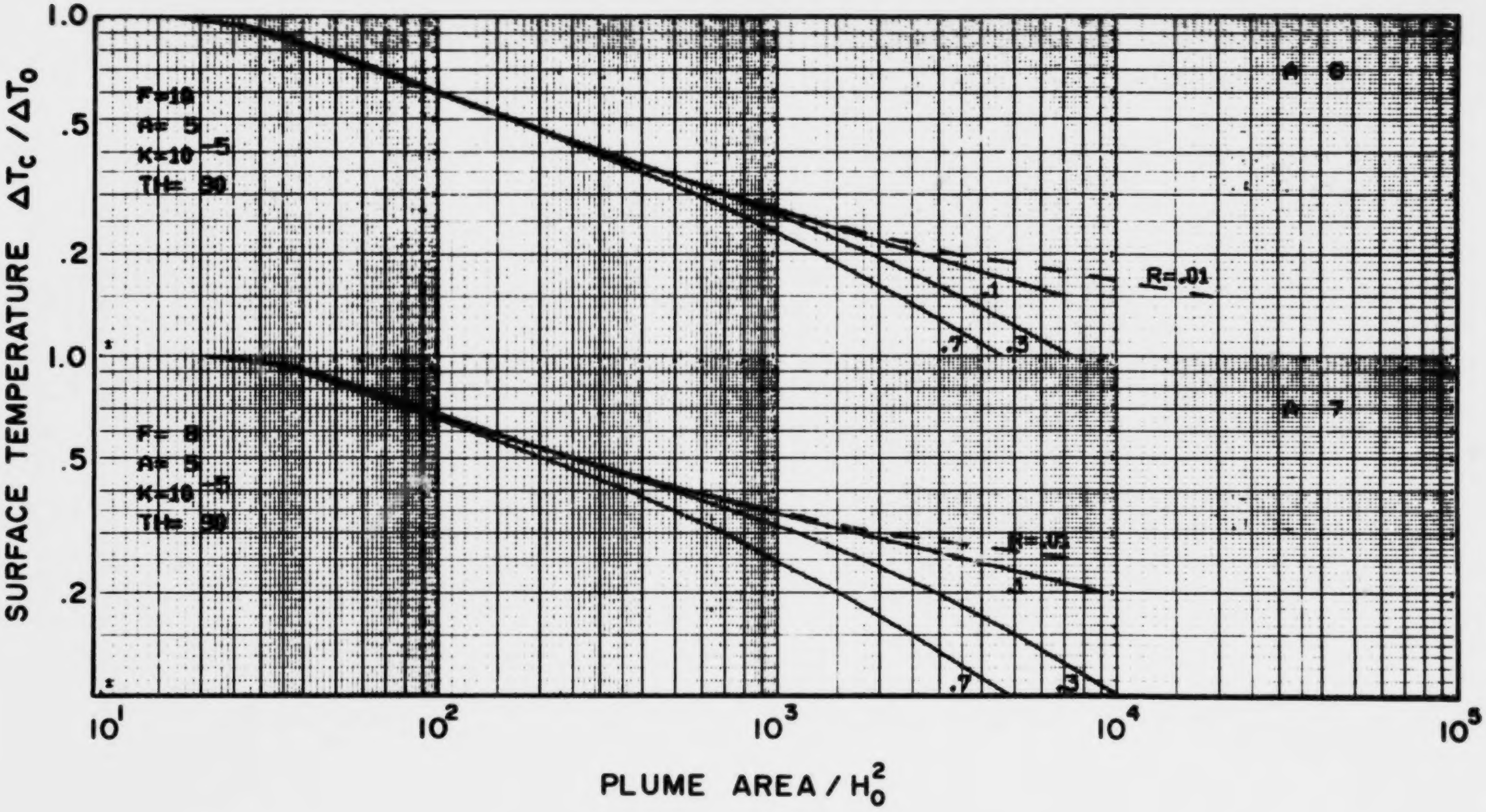

FIG (B4) TEMPERATURE, AREA (TA)-PLOTS FOR SURFACE JET DISCHARGE

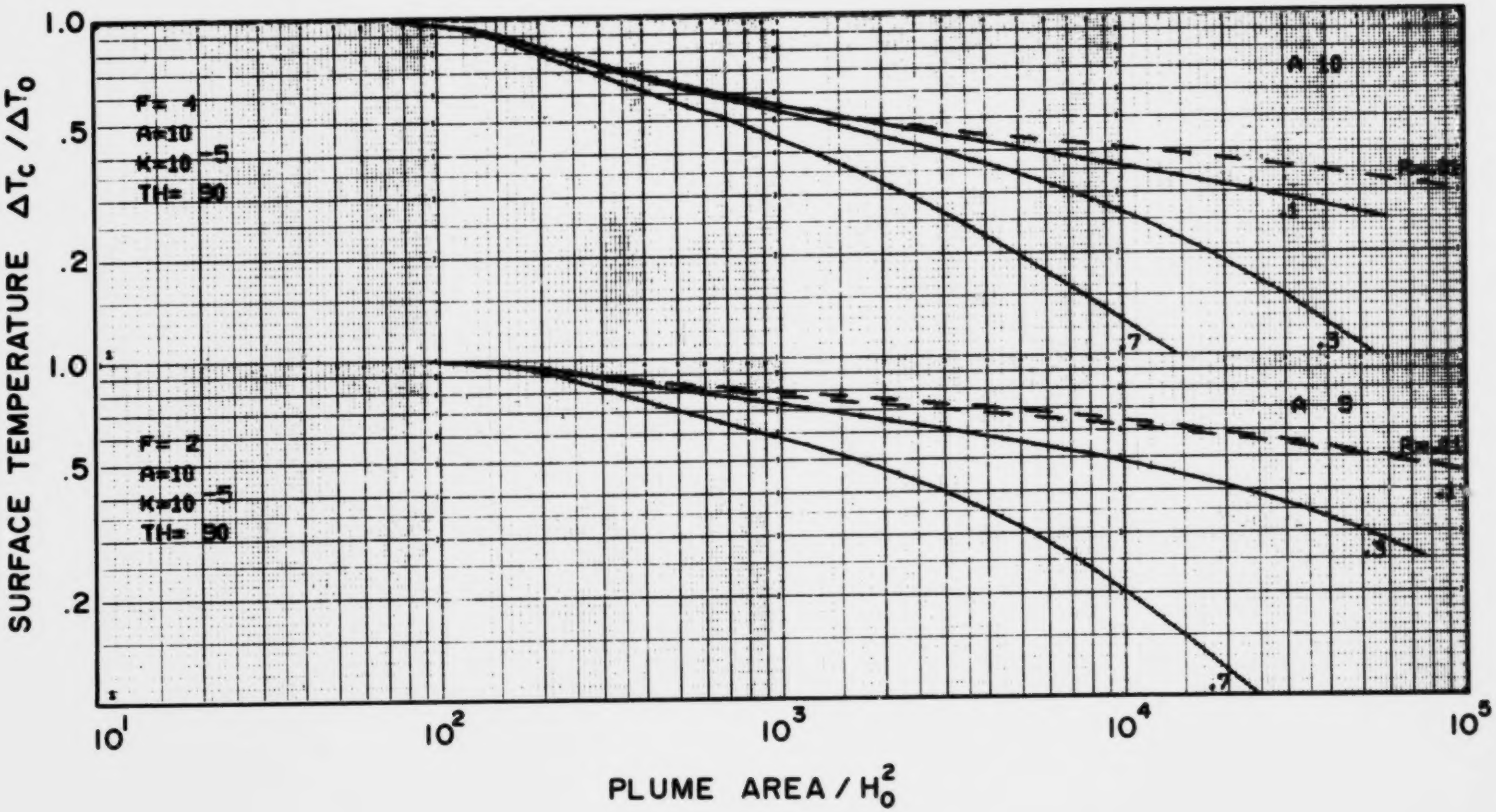

FIG (B5) TEMPERATURE, AREA (TA)-PLOTS FOR SURFACE JET DISCHARGE

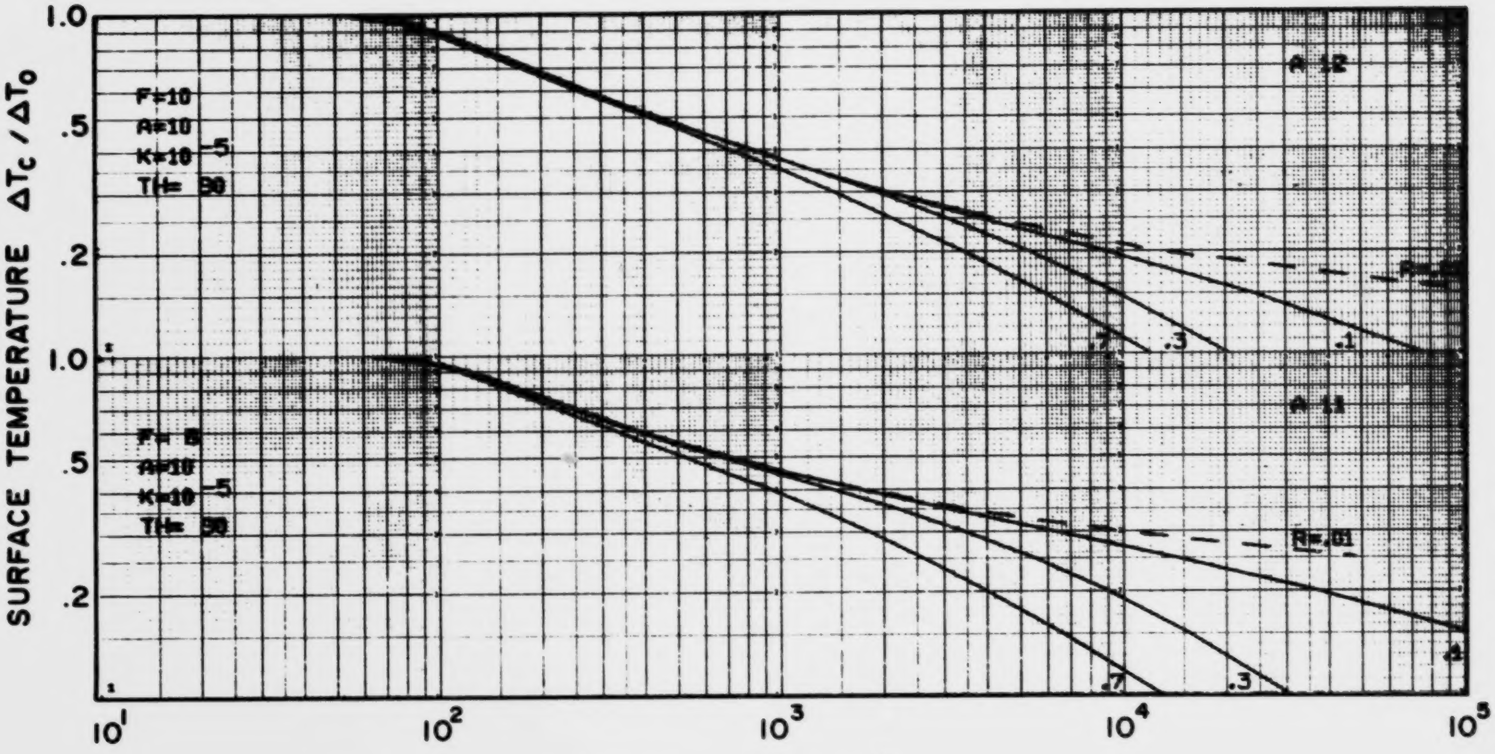

FIG (B6) TEMPERATURE, AREA (TA)-PLOTS FOR SURFACE JET DISCHARGE

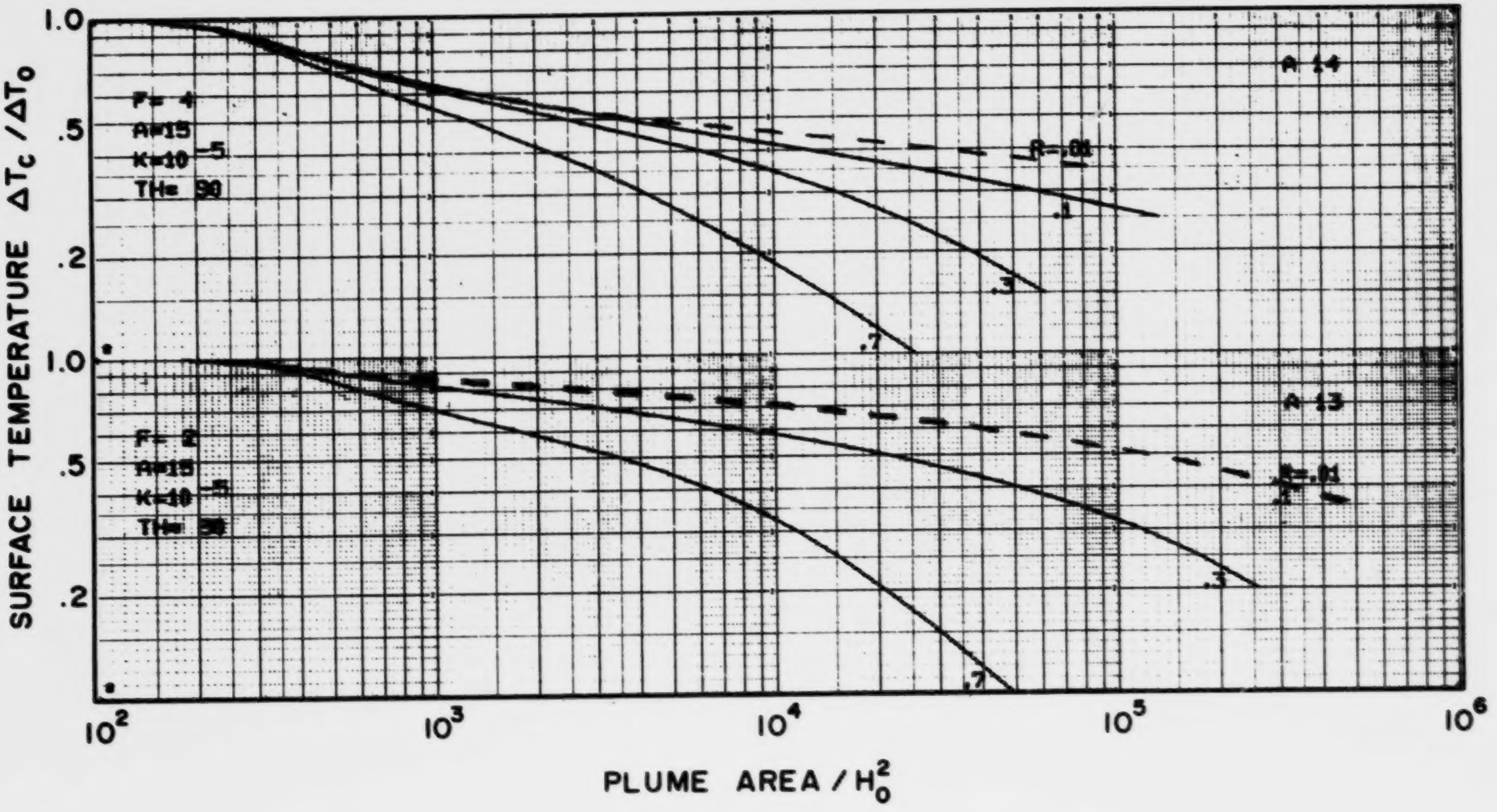

FIG (B7) TEMPERATURE, AREA (TA)-PLOTS FOR SURFACE JET DISCHARGE

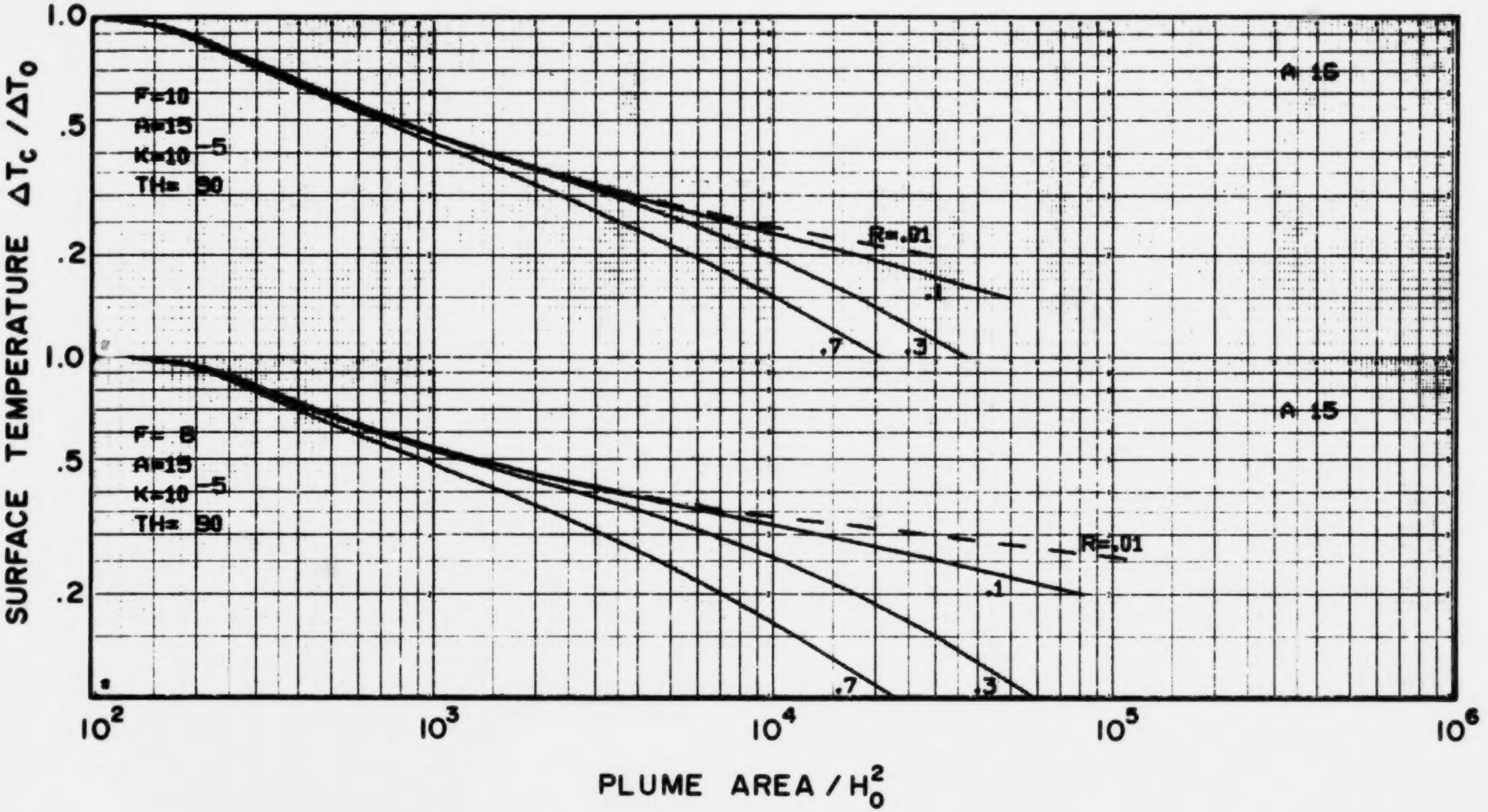

FIG (B8) TEMPERATURE, AREA (TA)-PLOTS FOR SURFACE JET DISCHARGE

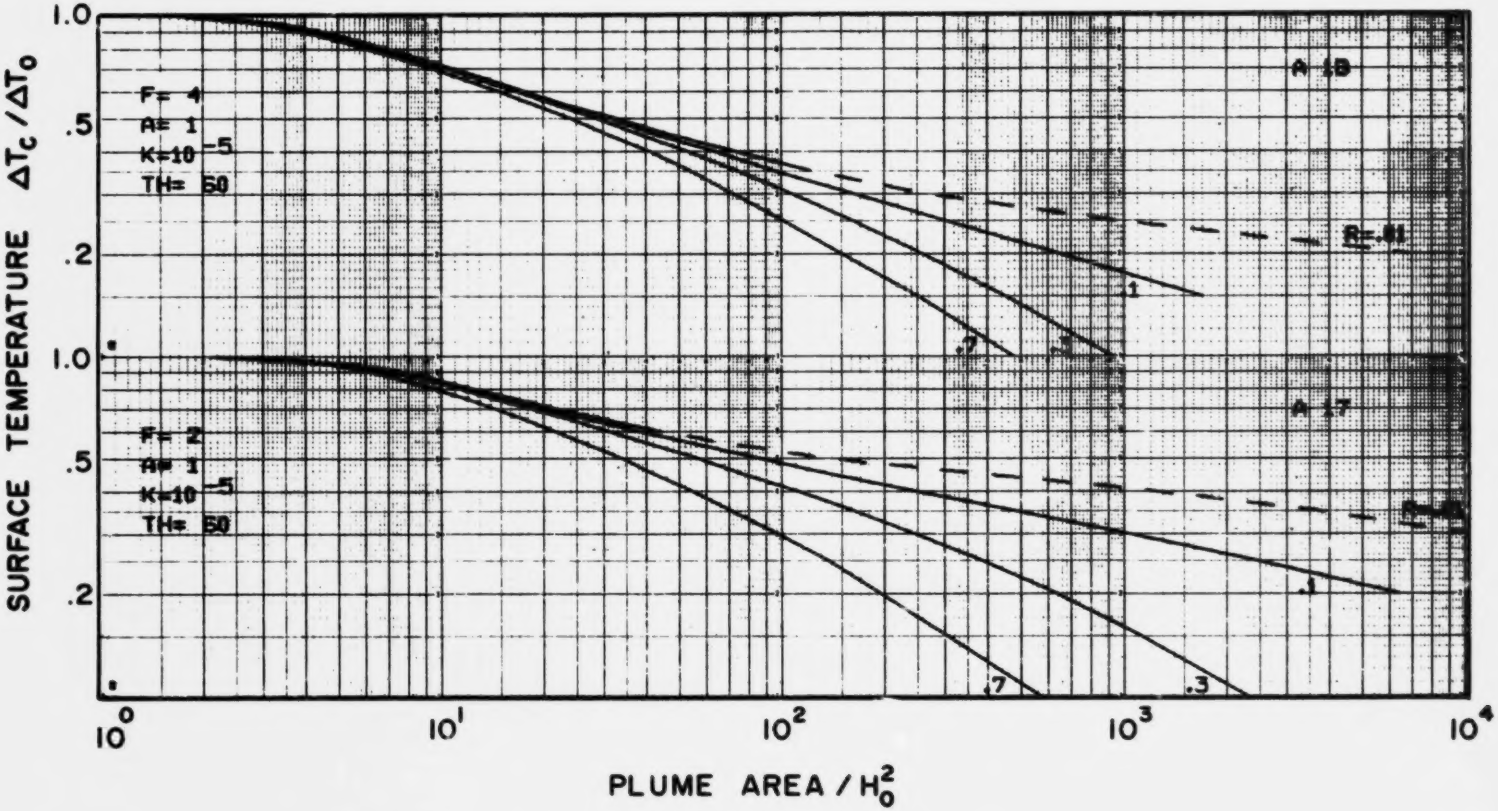

FIG(B9) TEMPERATURE, AREA (TA)-PLOT
FOR SURFACE JET DISCHARGE

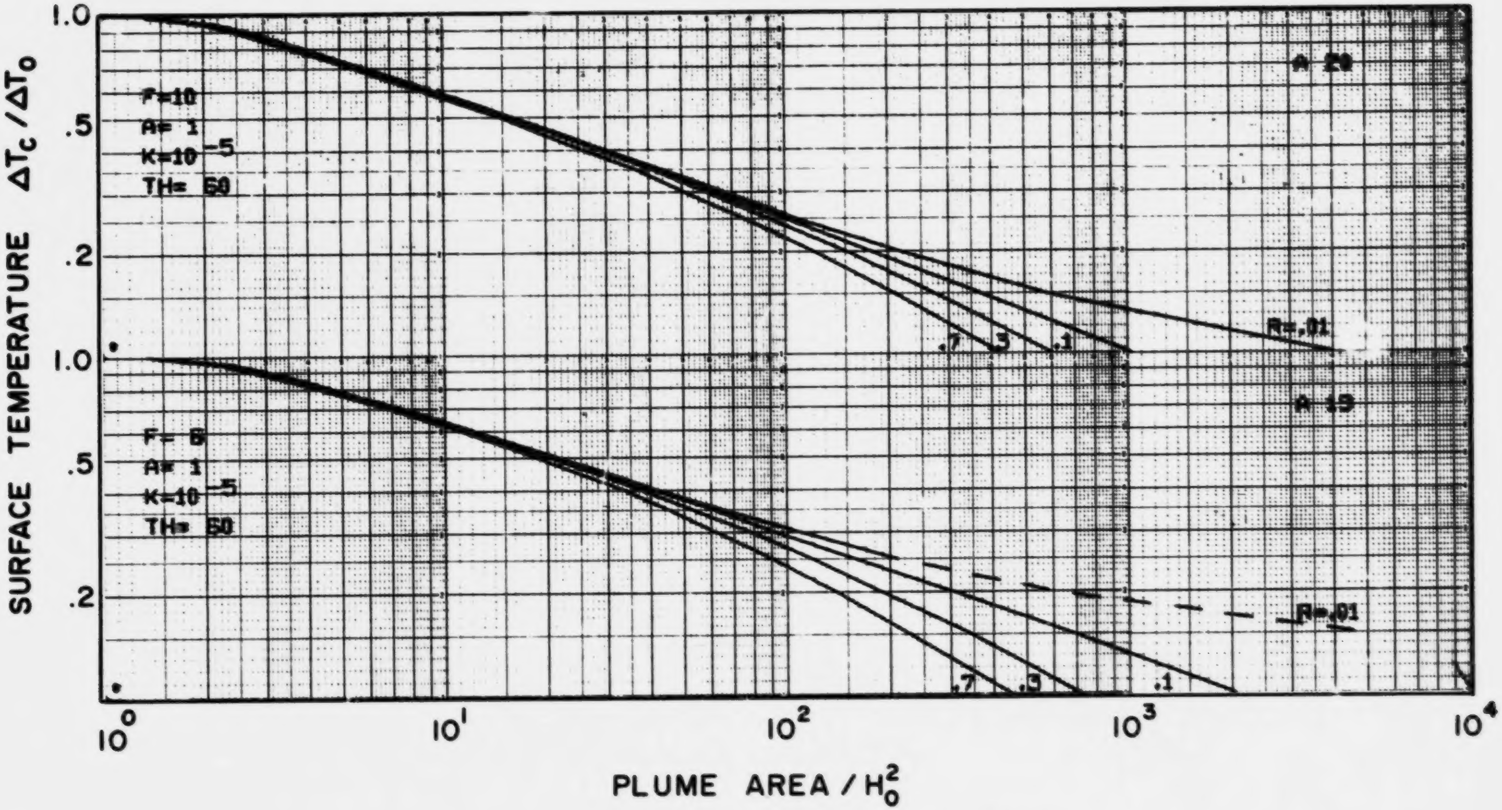

FIG(B10) TEMPERATURE, AREA (TA)-PLOT
FOR SURFACE JET DISCHARGE

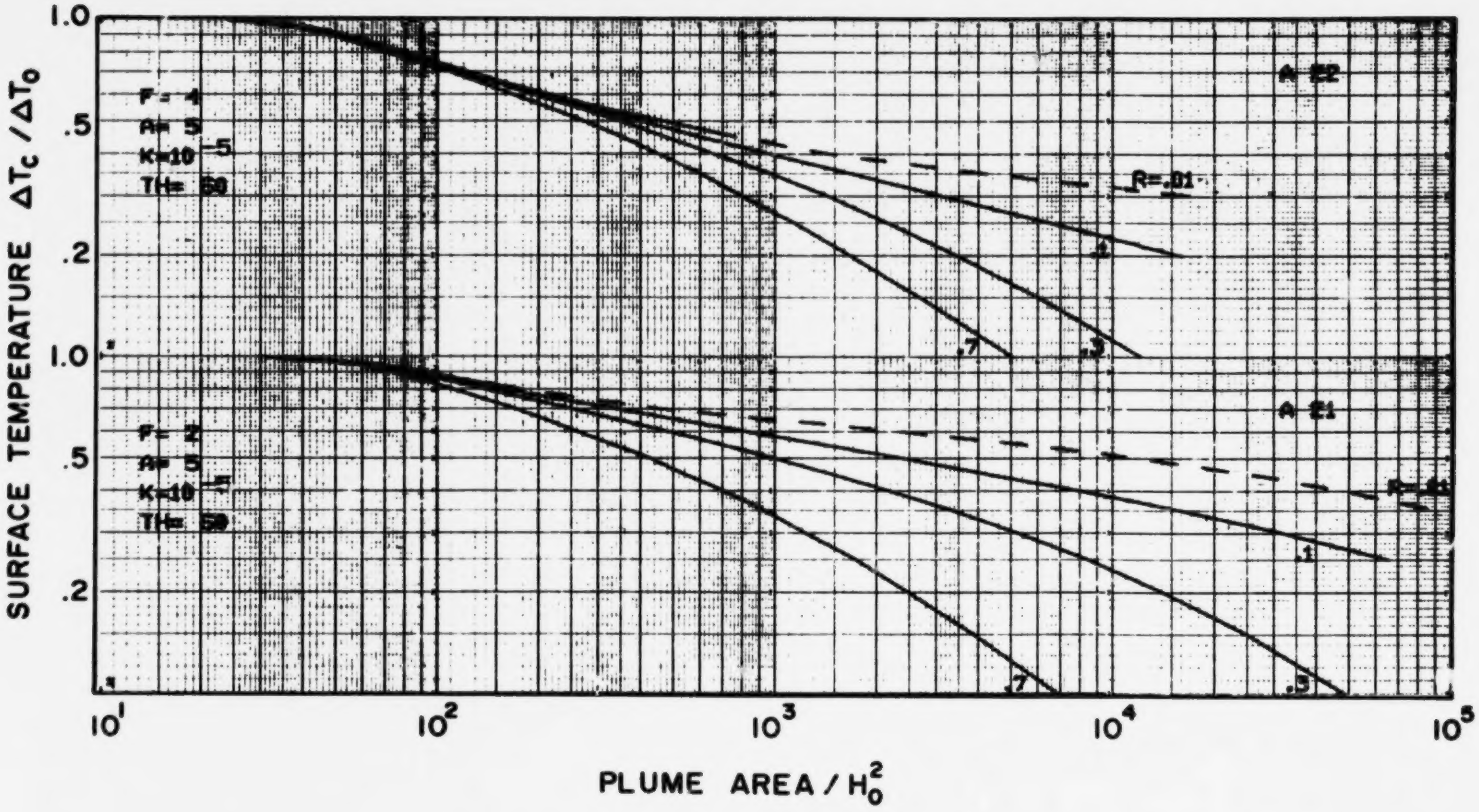

FIG (B11) TEMPERATURE, AREA (TA)-PLOTS FOR SURFACE JET DISCHARGE

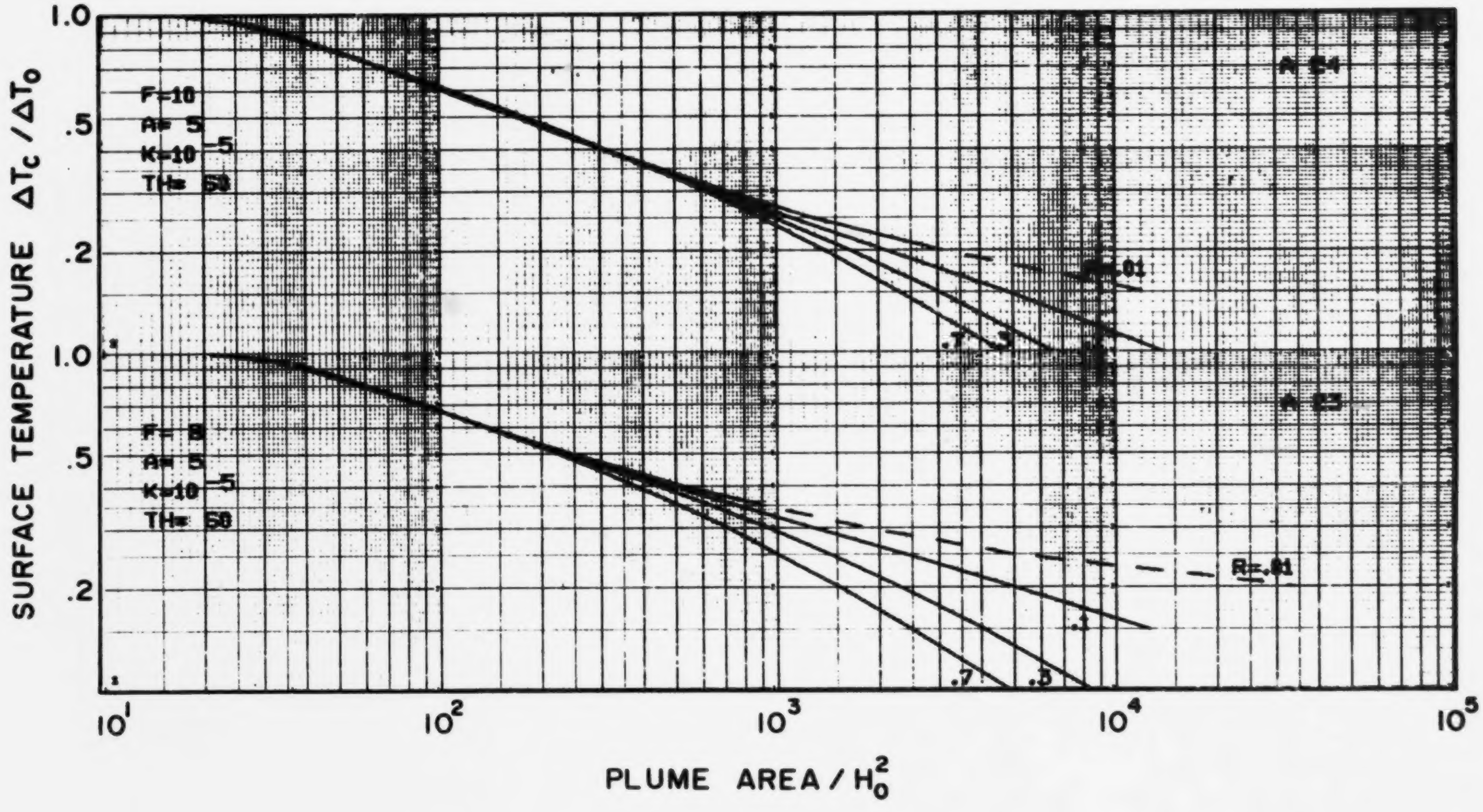

FIG (B12) TEMPERATURE, AREA (TA)-PLOTS FOR SURFACE JET DISCHARGE

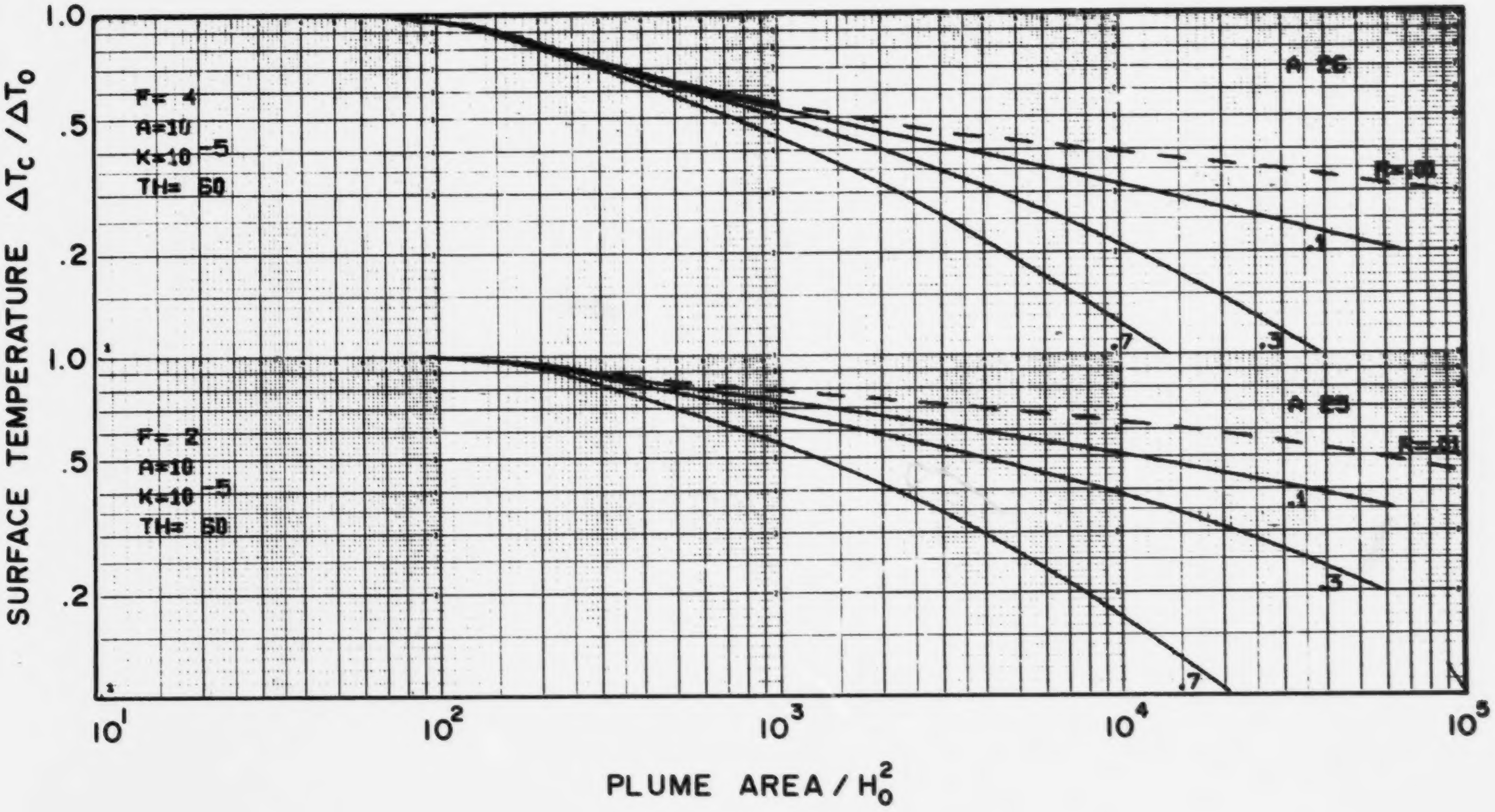

FIG (B13) TEMPERATURE, AREA (TA)-PLOTS FOR SURFACE JET DISCHARGE

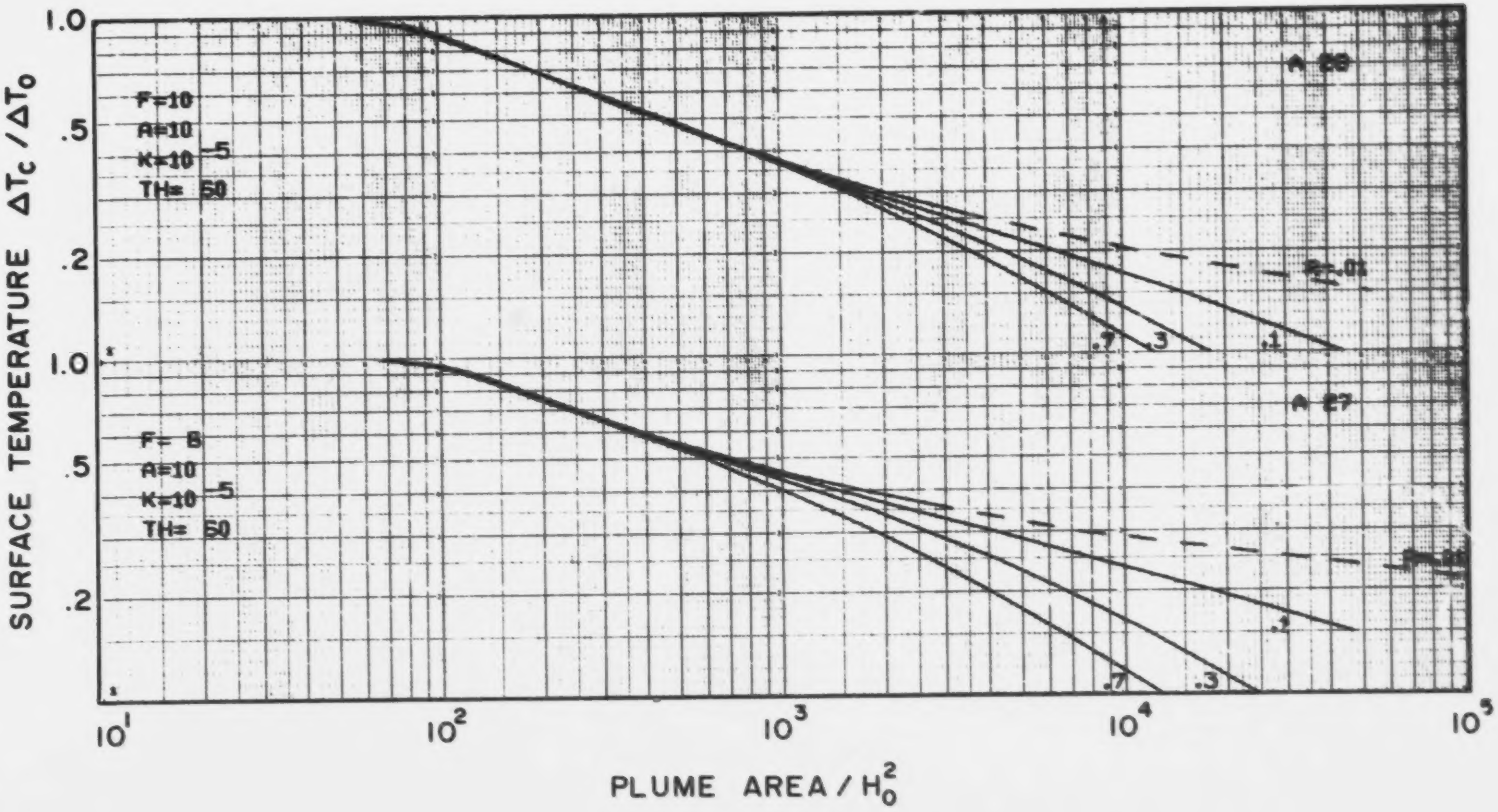

FIG (B14) TEMPERATURE, AREA (TA)-PLOTS
FOR SURFACE JET DISCHARGE

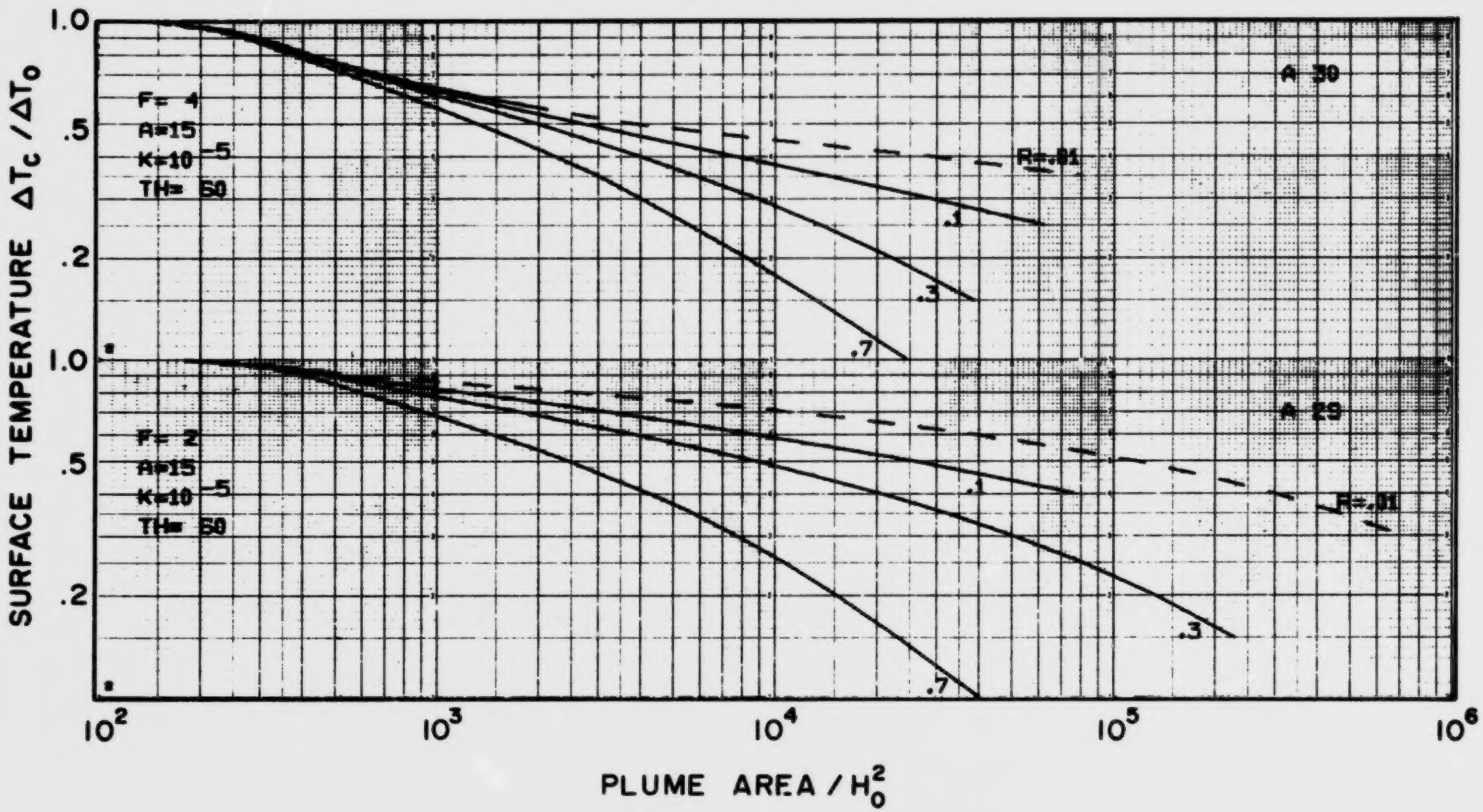

FIG (B15) TEMPERATURE, AREA (TA)-PLOTS FOR SURFACE JET DISCHARGE

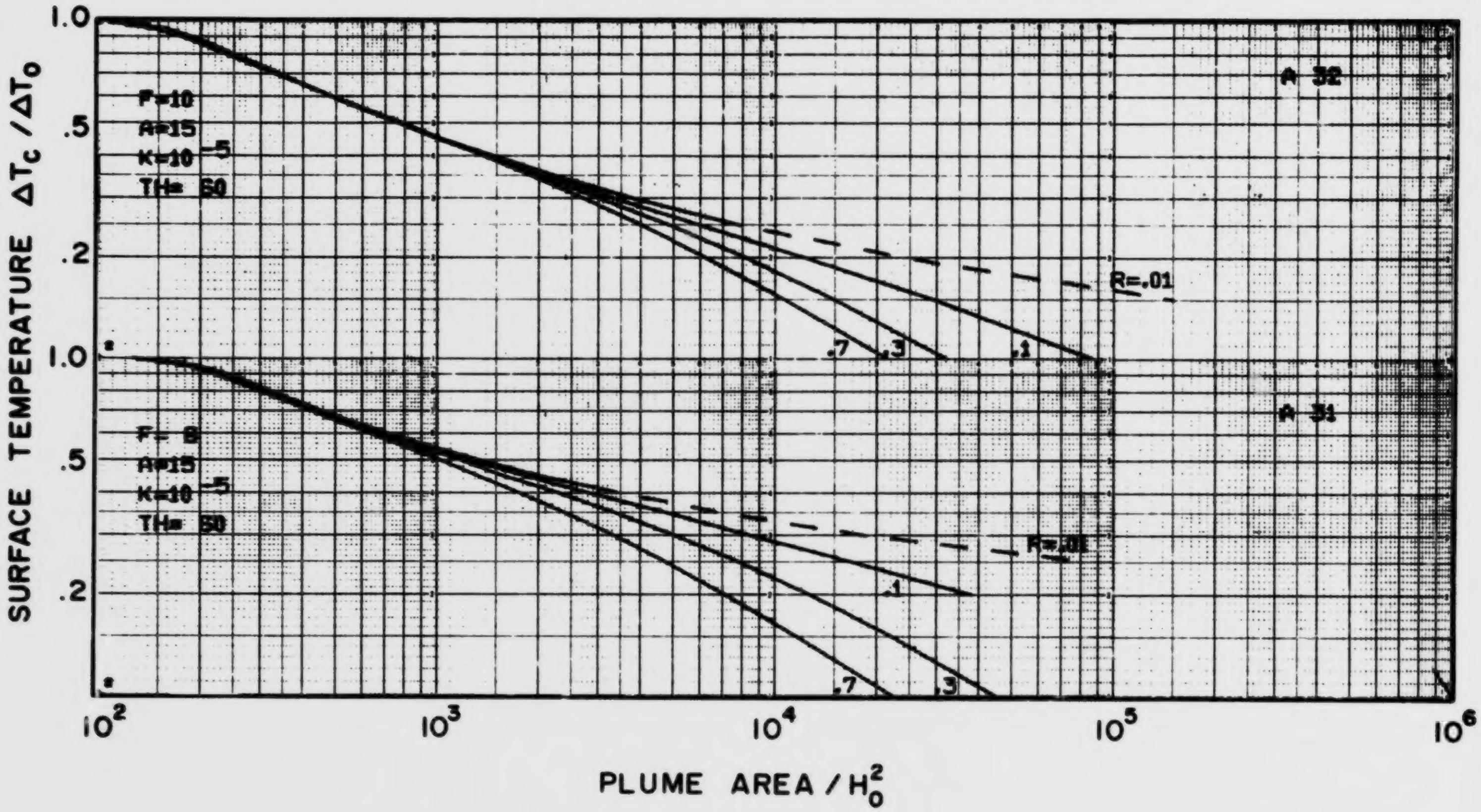

FIG (B16) TEMPERATURE, AREA (TA)-PLOTS
FOR SURFACE JET DISCHARGE

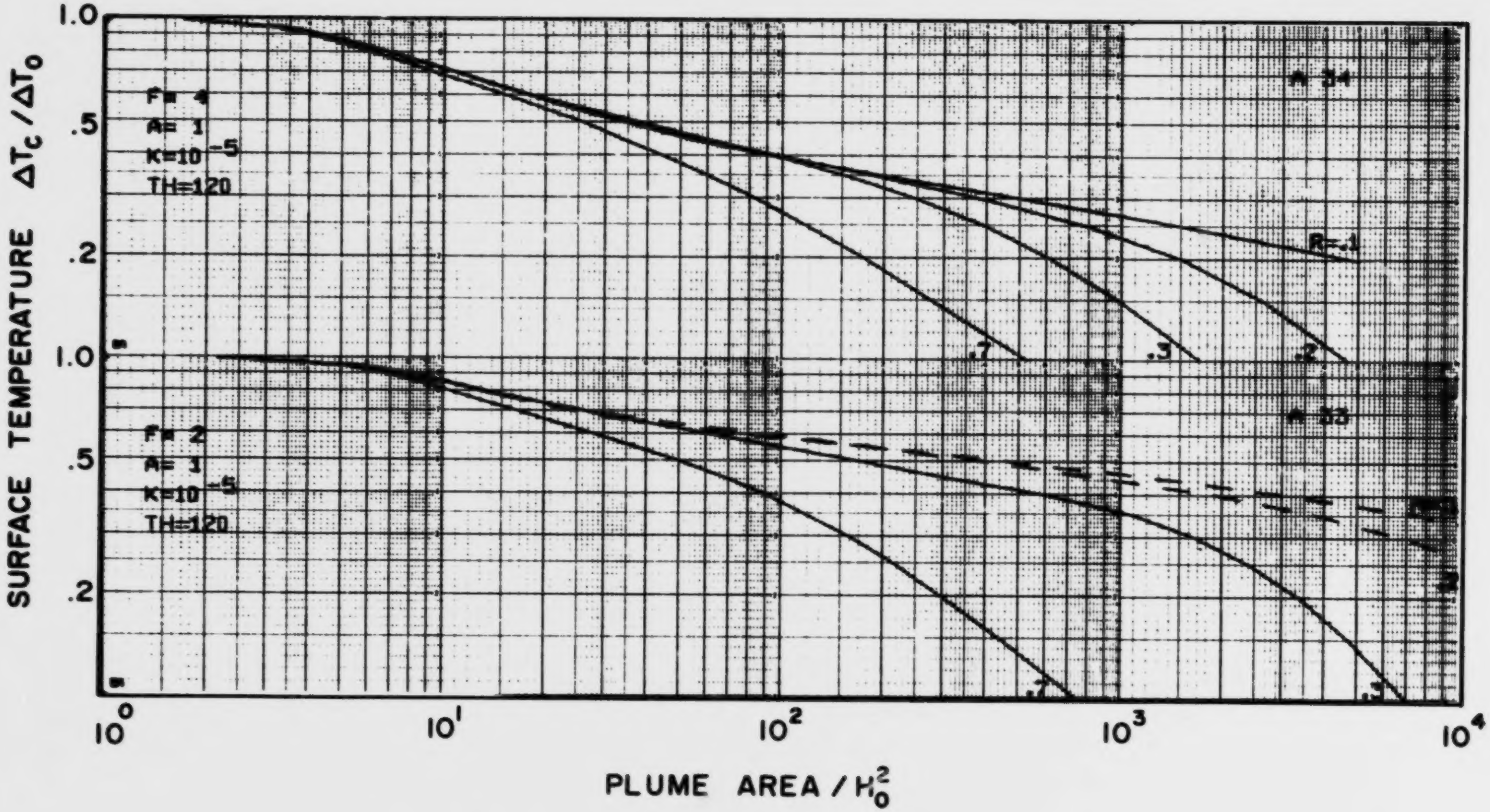

FIG(B17) TEMPERATURE, AREA (TA)-PLOT
FOR SURFACE JET DISCHARGE

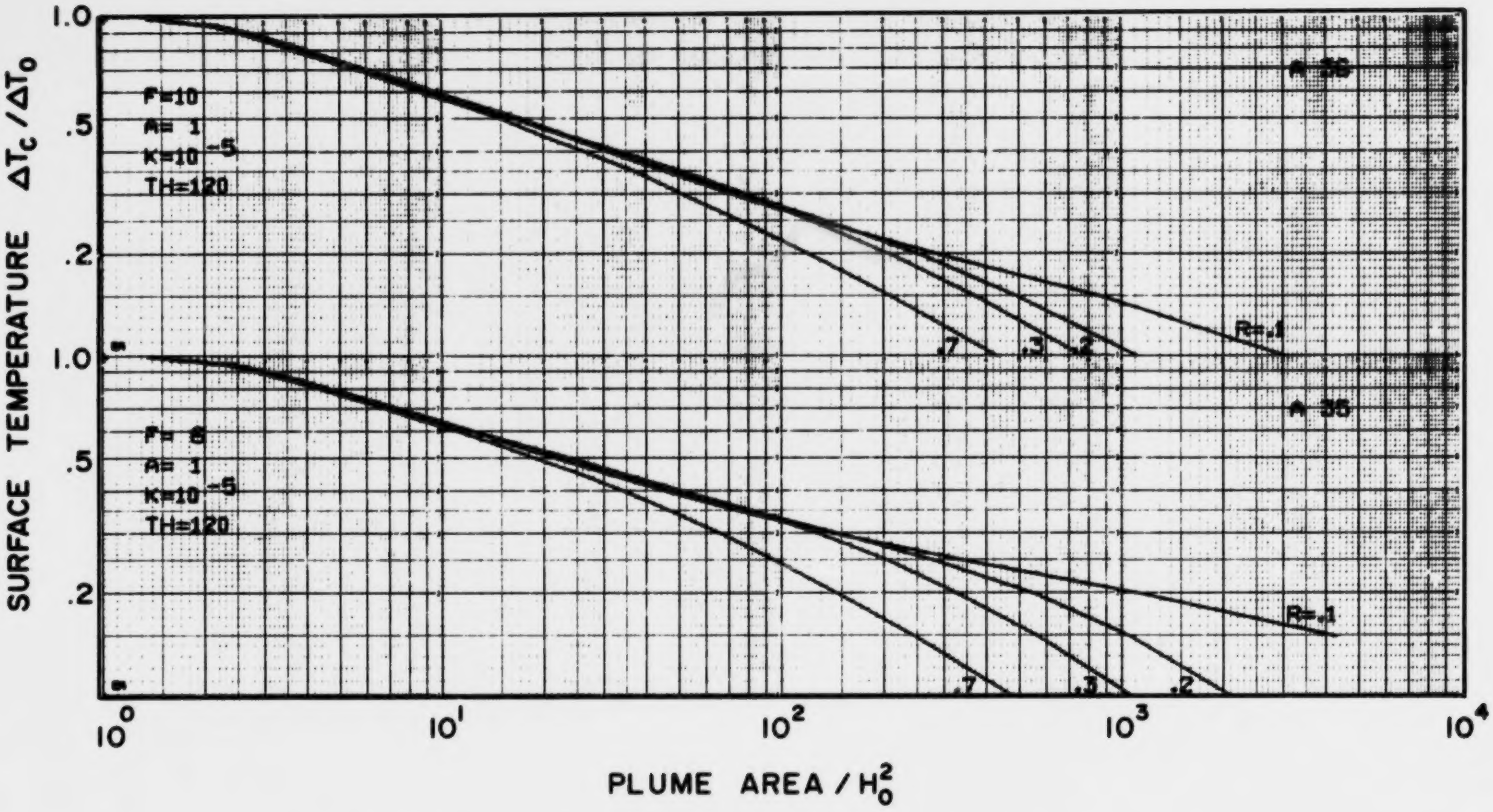

FIG(B18) TEMPERATURE, AREA (TA)-PLOT
FOR SURFACE JET DISCHARGE

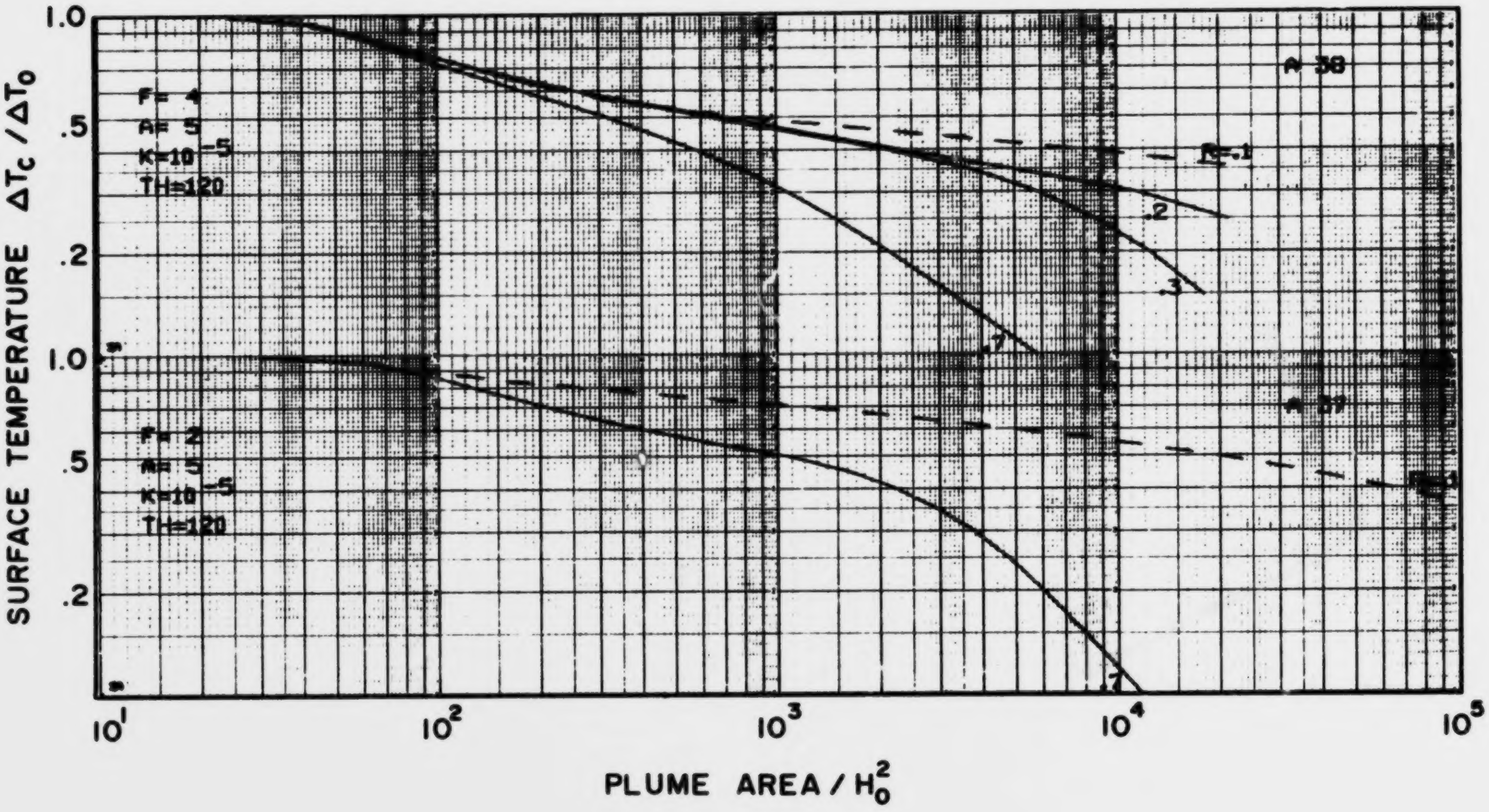

FIG (B 19) TEMPERATURE, AREA (TA)-PLOTS FOR SURFACE JET DISCHARGE

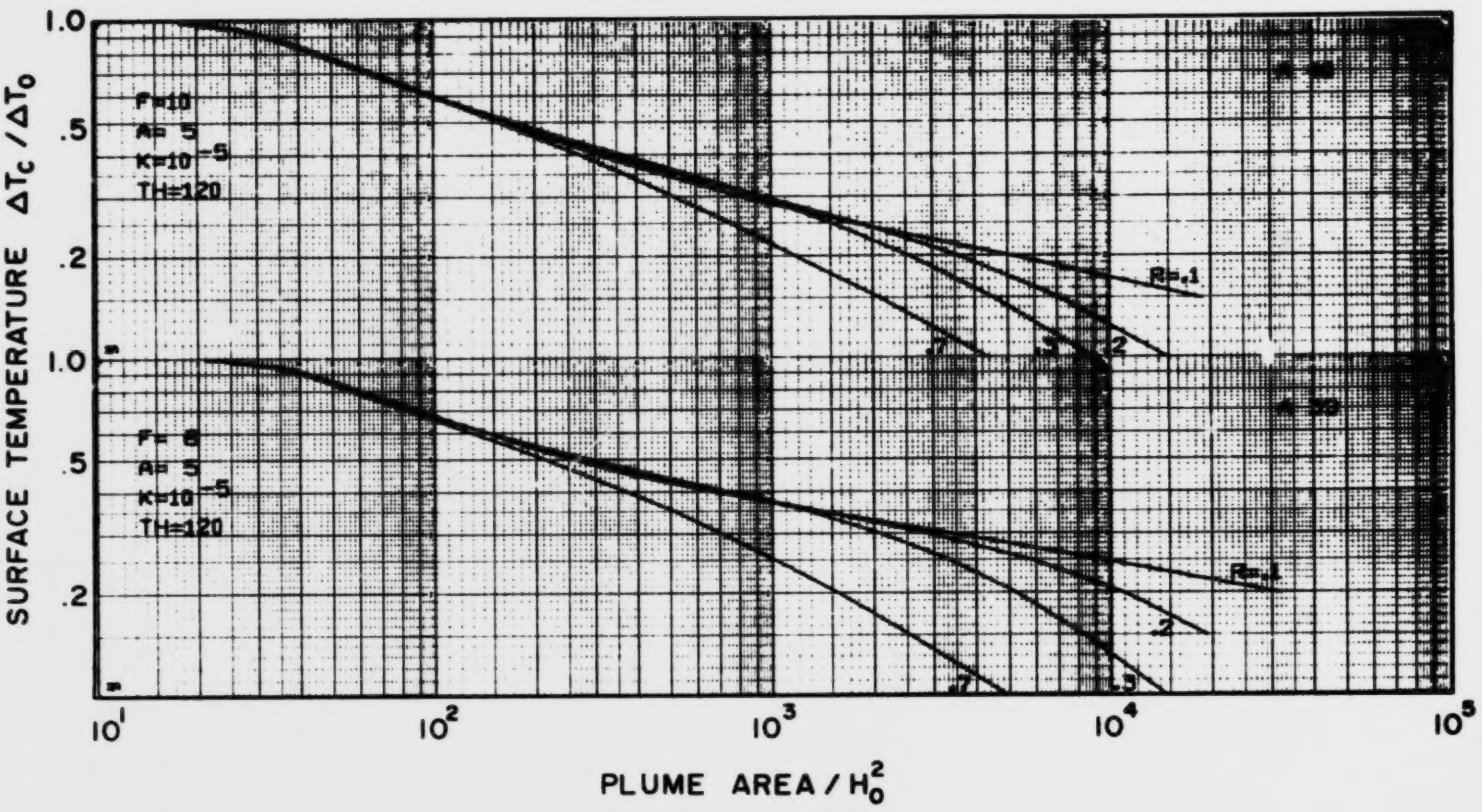

FIG (B20) TEMPERATURE, AREA (TA)-PLOTS FOR SURFACE JET DISCHARGE

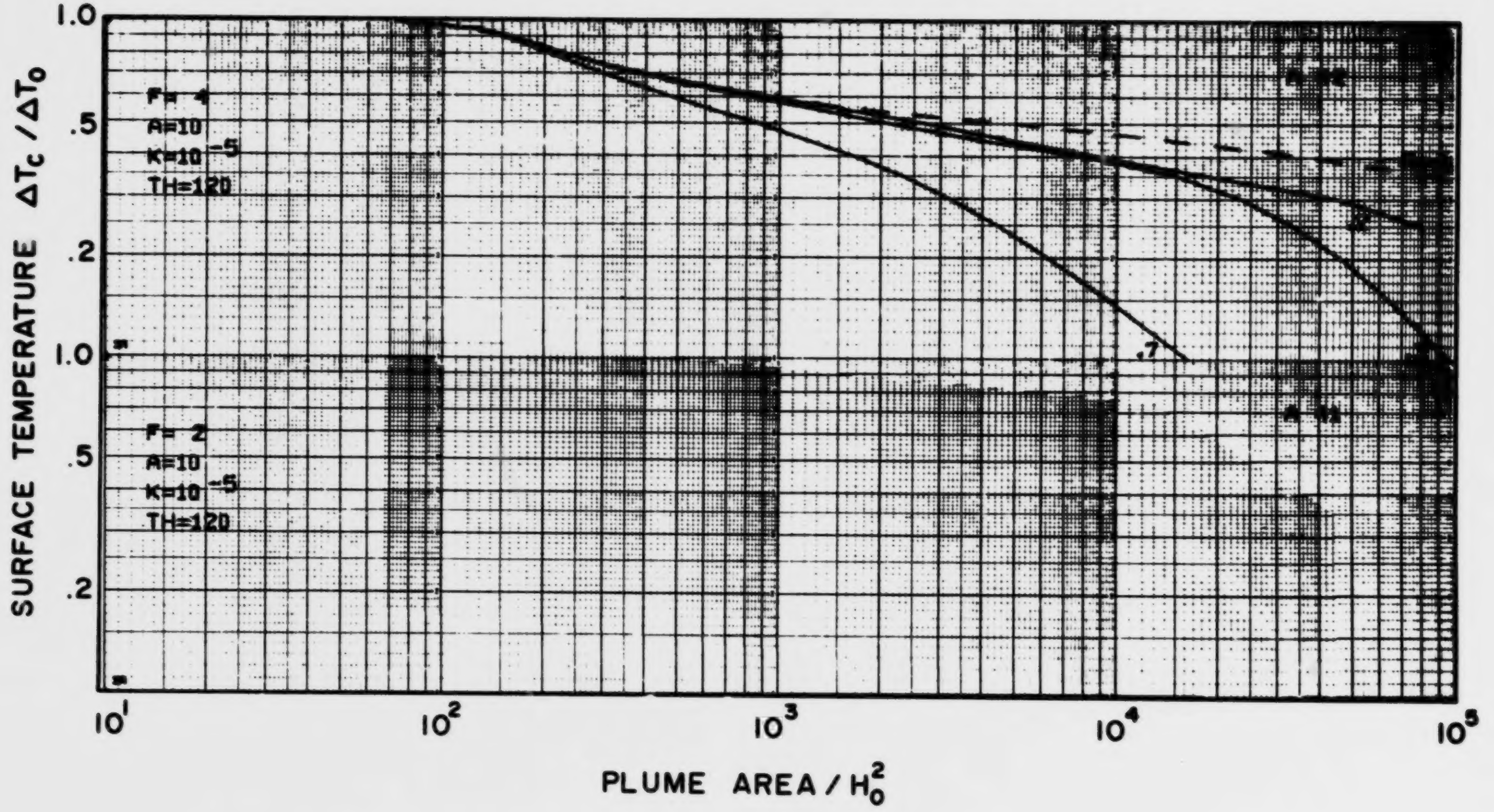

FIG (B 21) TEMPERATURE, AREA (TA)-PLOTS FOR SURFACE JET DISCHARGE

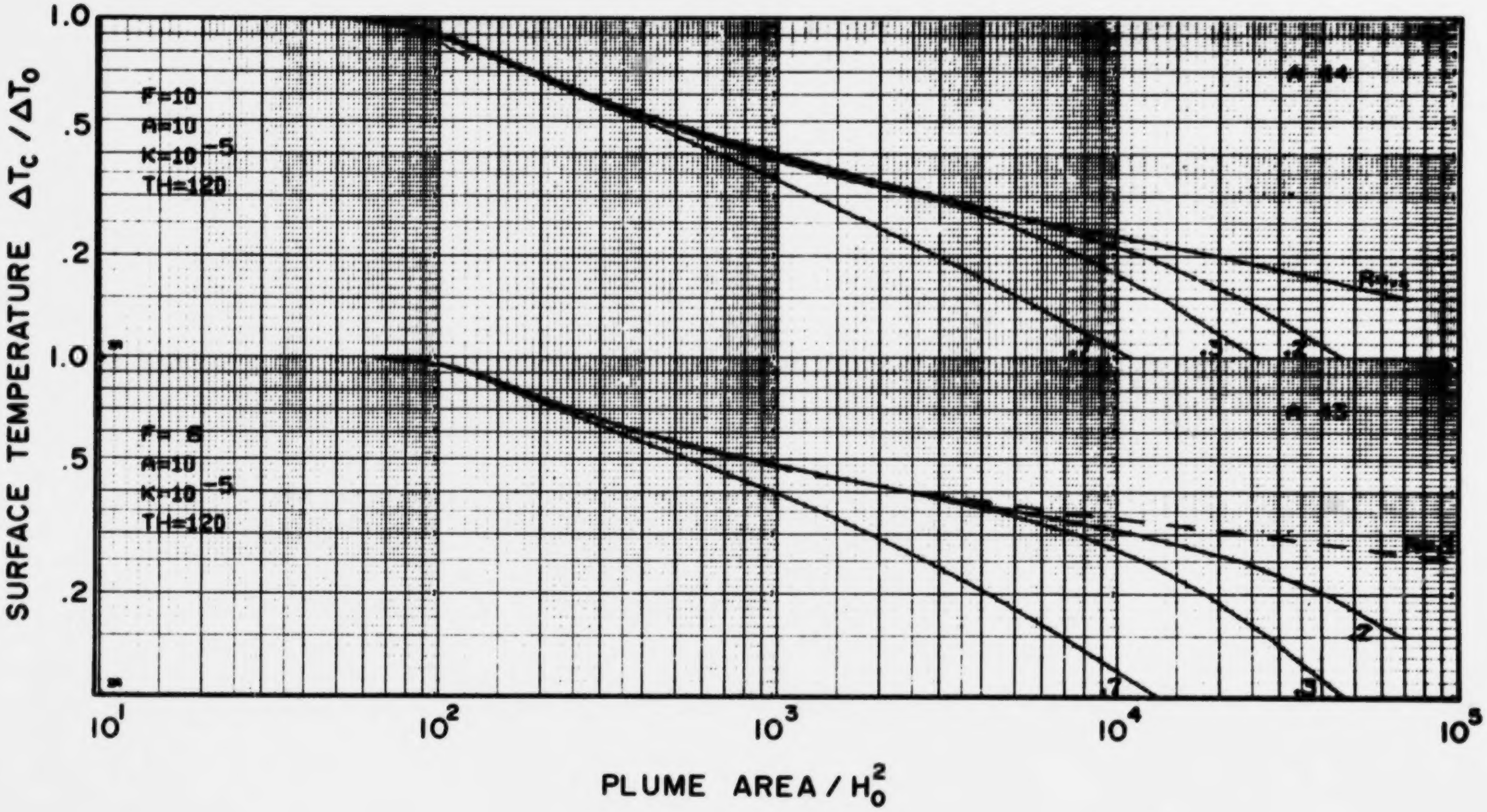

FIG (B 22) TEMPERATURE, AREA (TA)-PLOTS
FOR SURFACE JET DISCHARGE

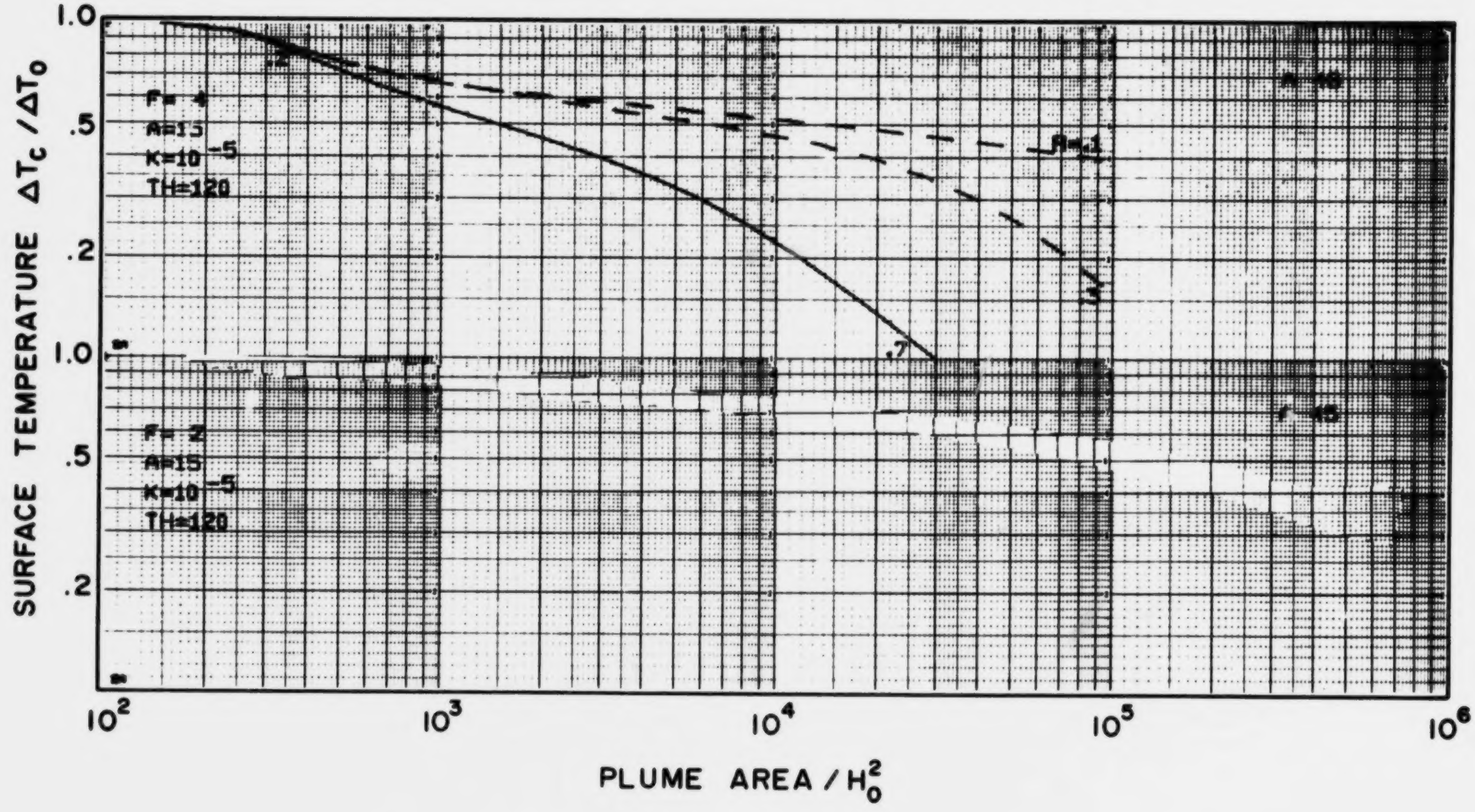

FIG (B 23) TEMPERATURE, AREA (TA)-PLOTS FOR SURFACE JET DISCHARGE

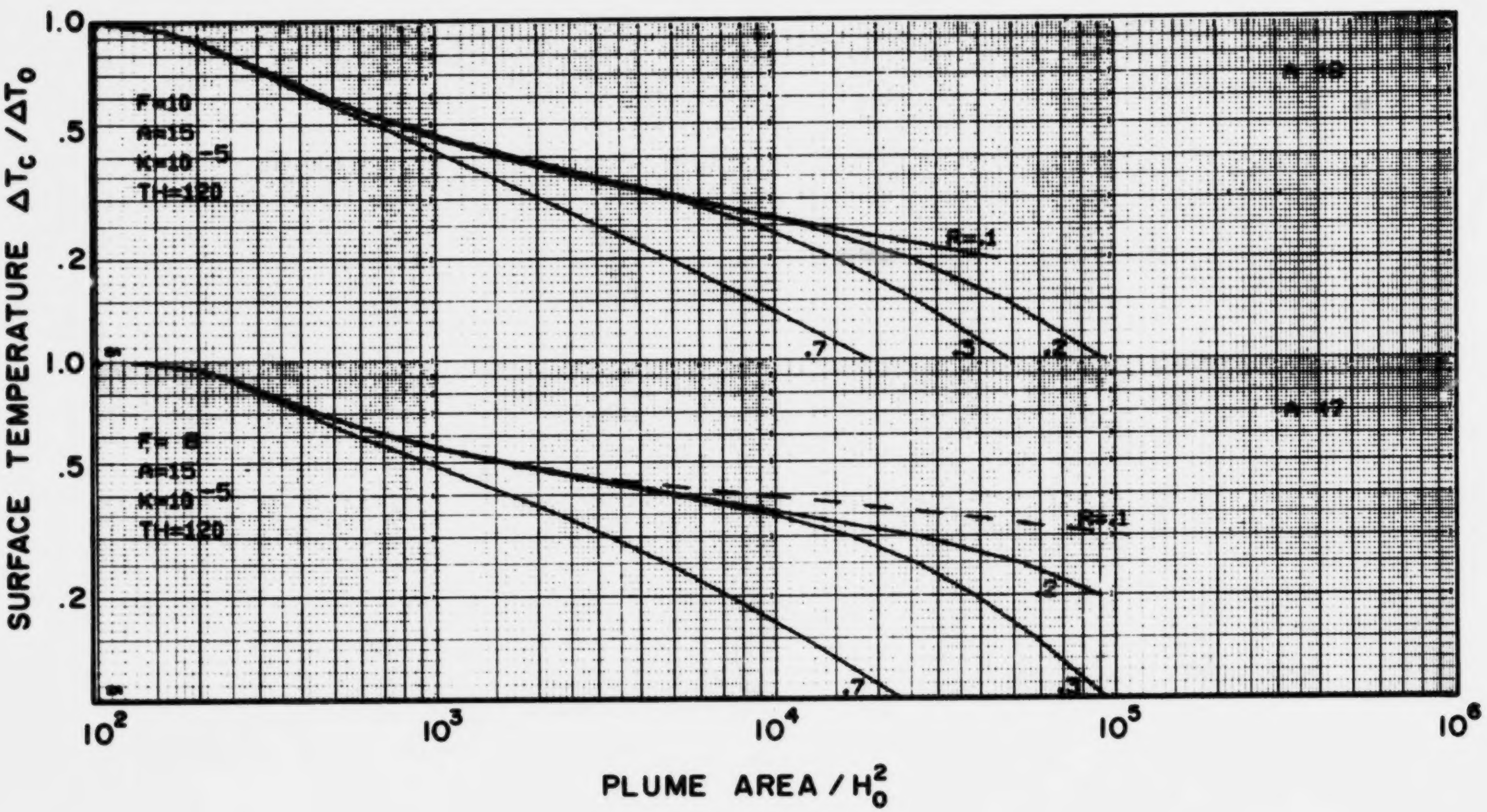

FIG (B24) TEMPERATURE, AREA (TA)-PLOTS
FOR SURFACE JET DISCHARGE

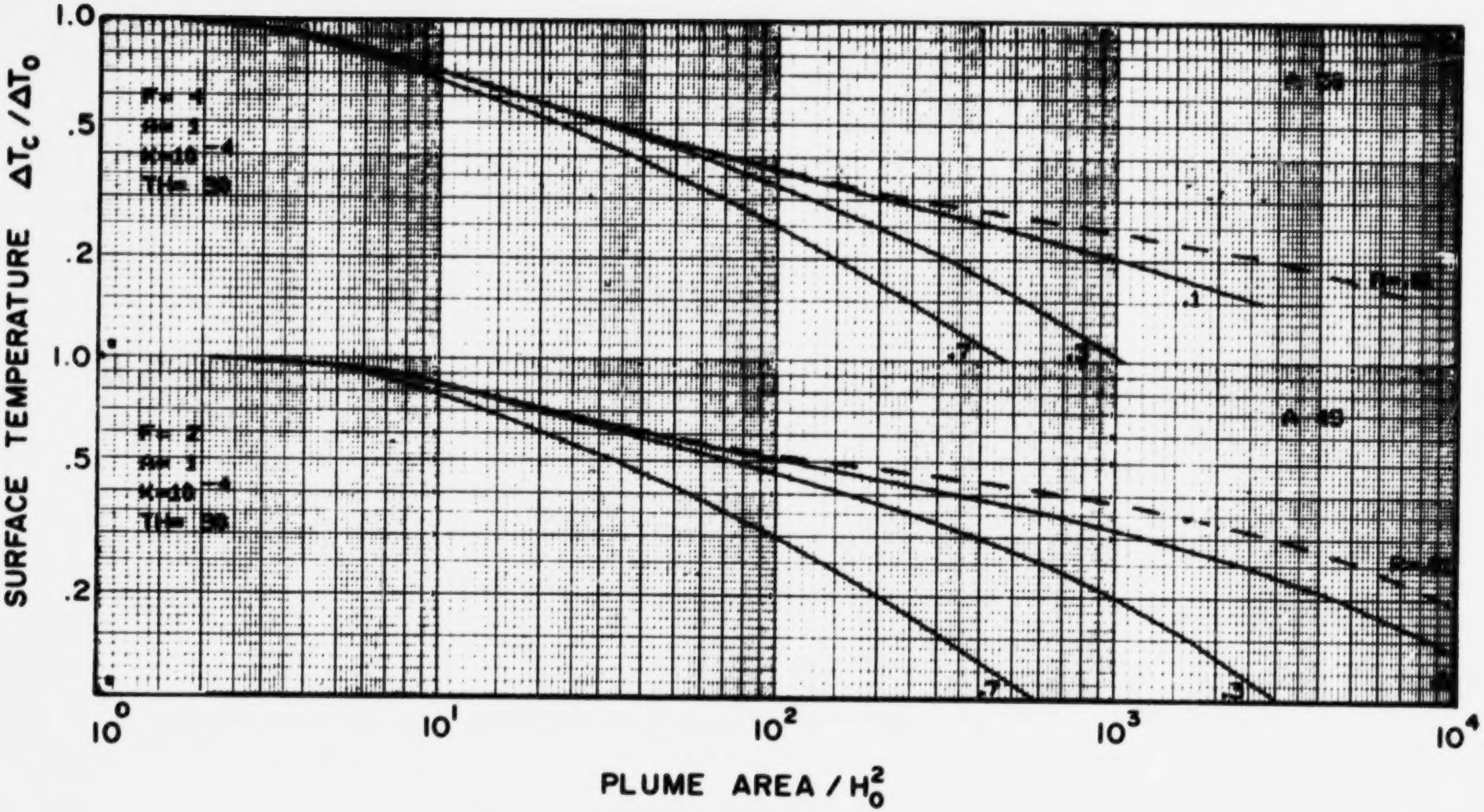

FIG (B 25) TEMPERATURE, AREA (TA)-PLOT
FOR SURFACE JET DISCHARGE

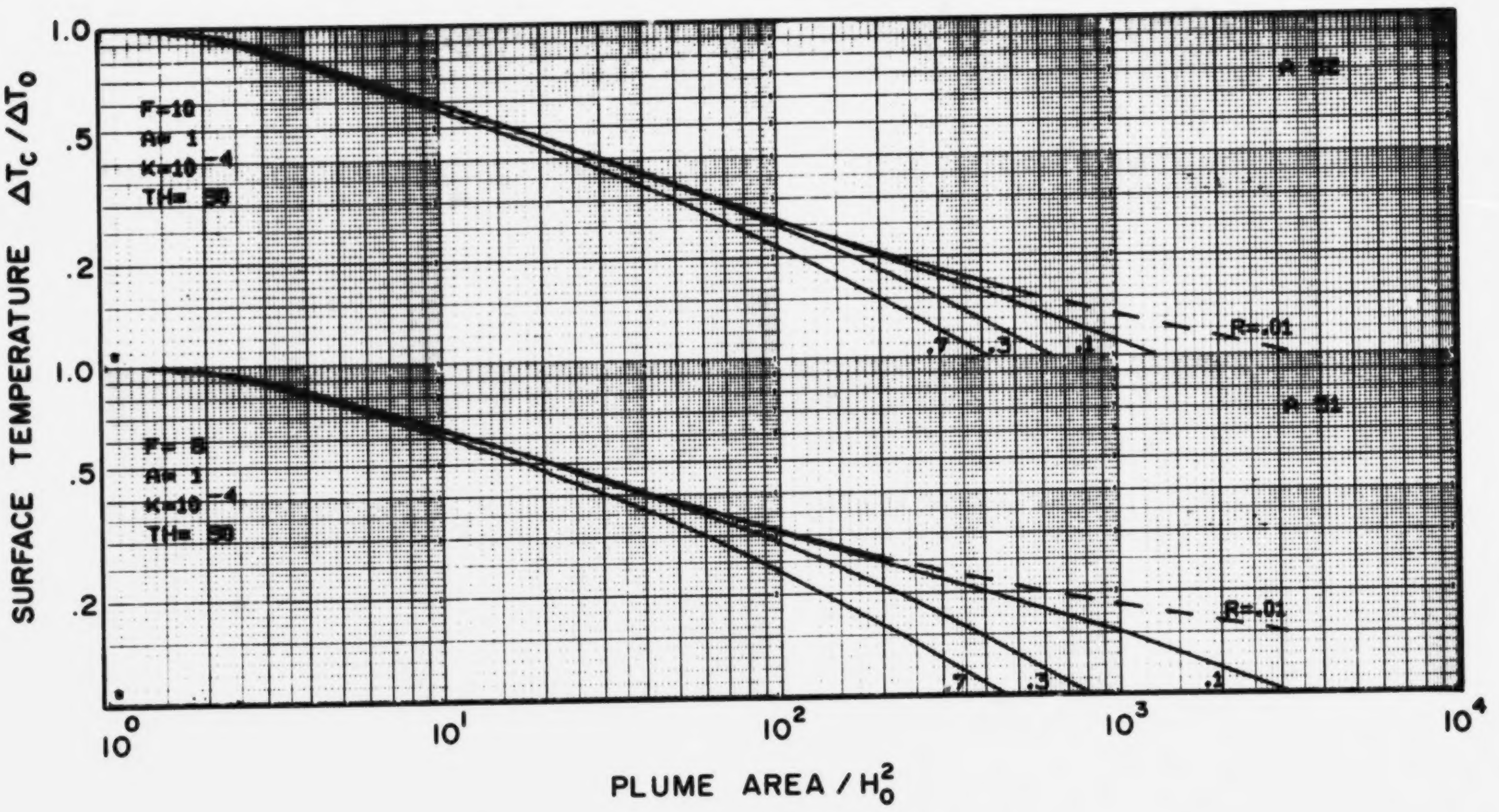

FIG(B26) TEMPERATURE, AREA (TA)-PLOT
FOR SURFACE JET DISCHARGE

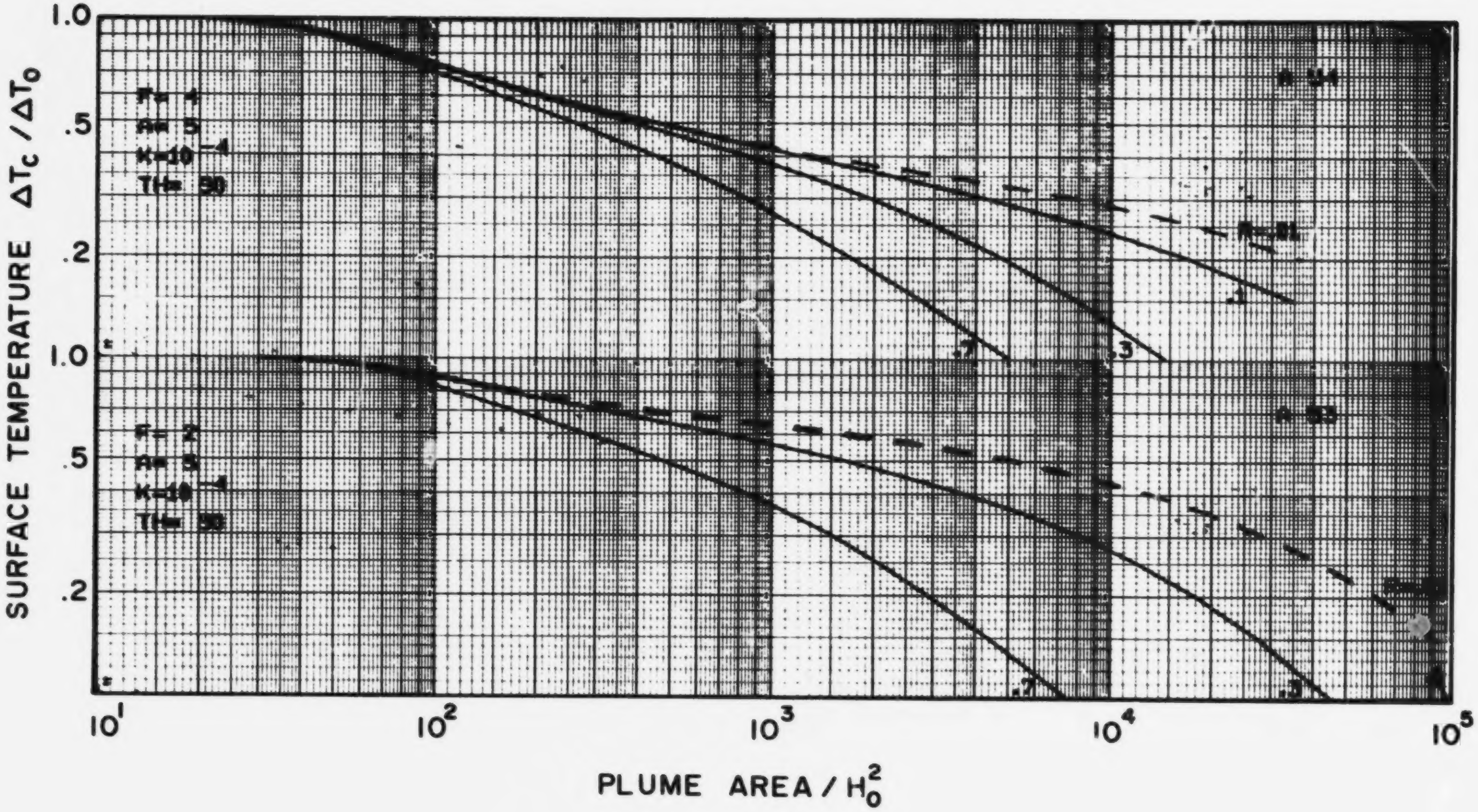

FIG (B 27) TEMPERATURE, AREA (TA)-PLOTS FOR SURFACE JET DISCHARGE

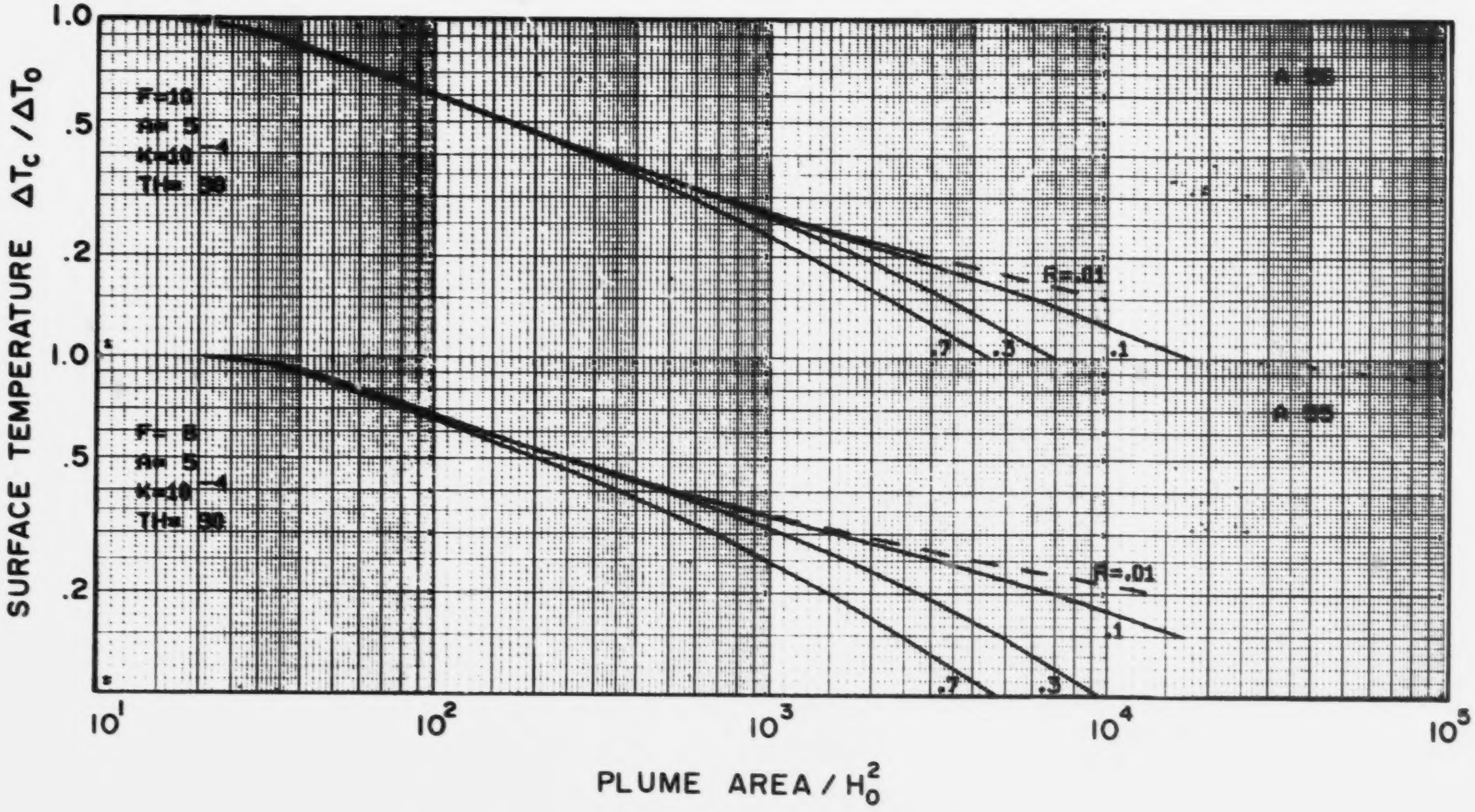

FIG (B 28) TEMPERATURE, AREA (TA)-PLOTS FOR SURFACE JET DISCHARGE

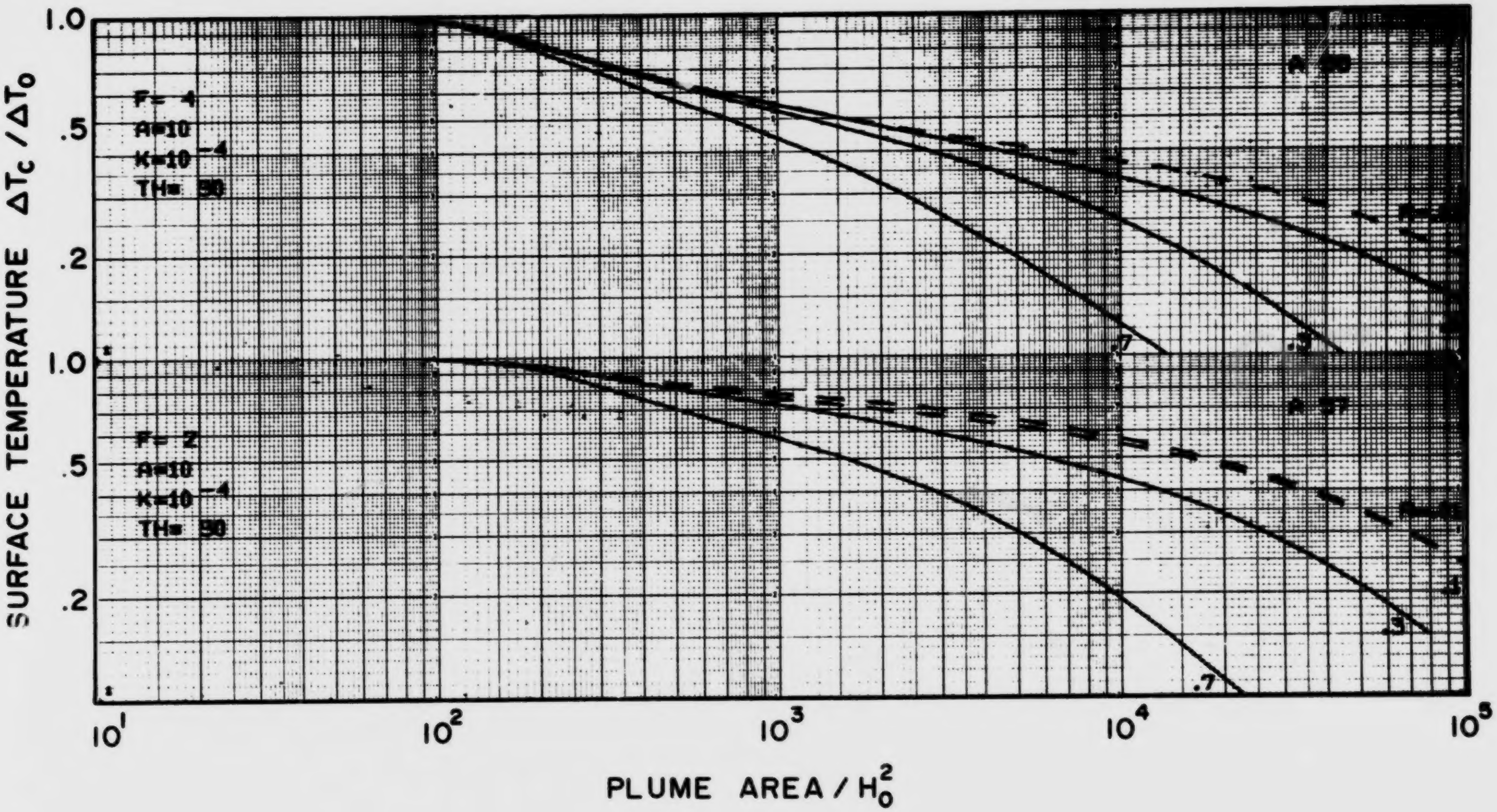

FIG (B 29) TEMPERATURE, AREA (TA)-PLOTS FOR SURFACE JET DISCHARGE

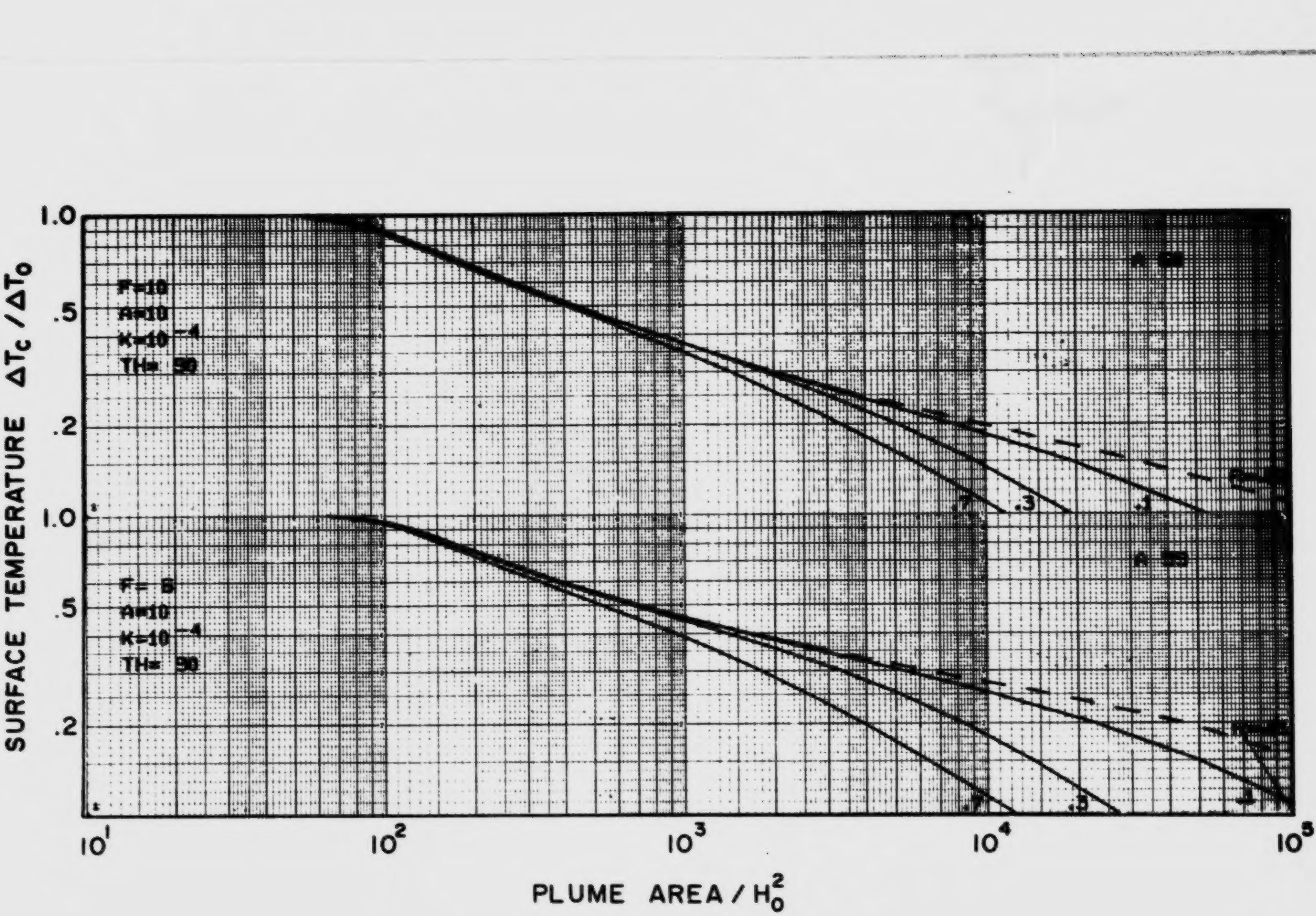

FIG (B30) TEMPERATURE, AREA (TA)-PLOTS FOR SURFACE JET DISCHARGE

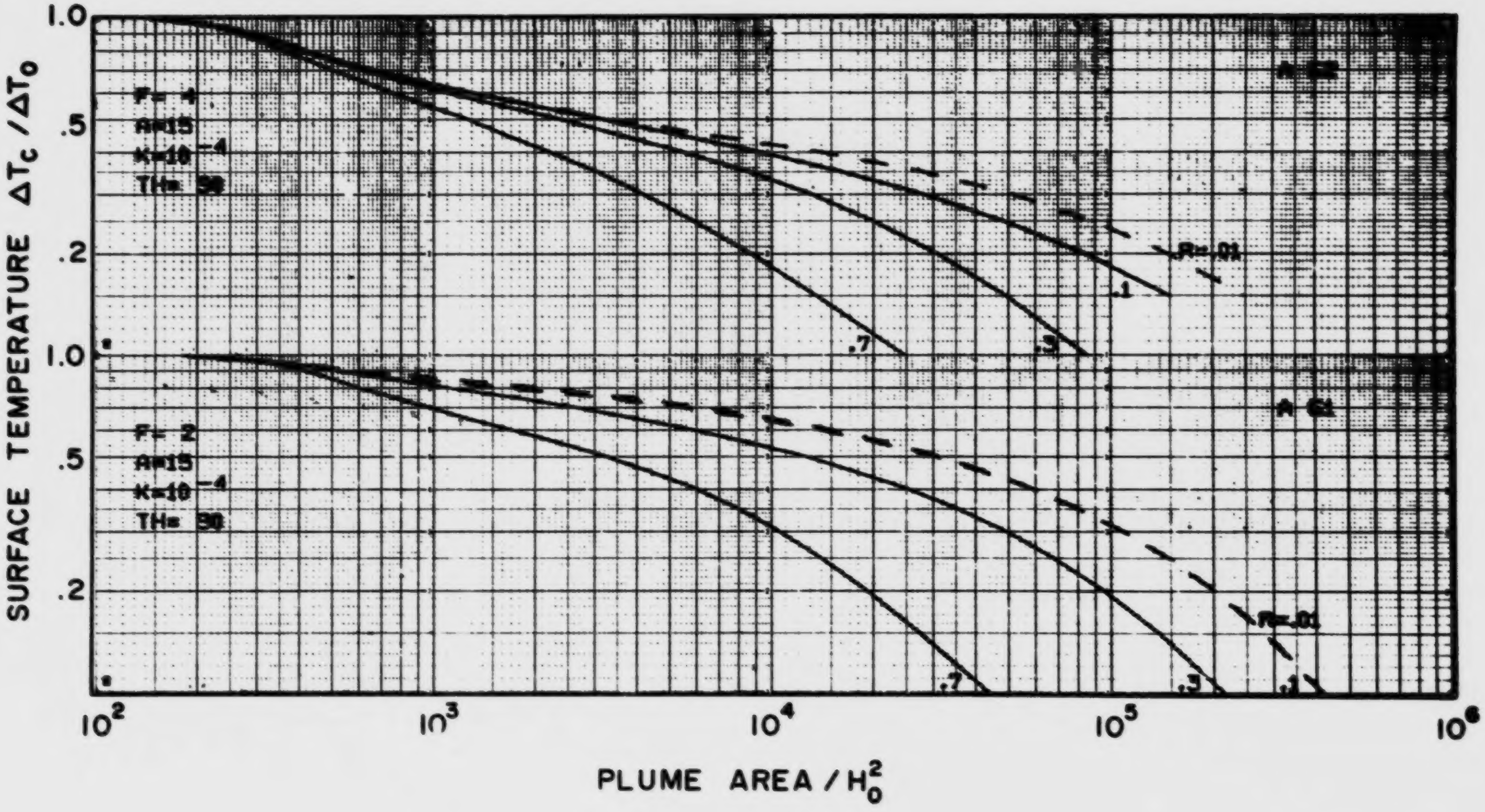

FIG (B31) TEMPERATURE, AREA (TA)-PLOTS
FOR SURFACE JET DISCHARGE

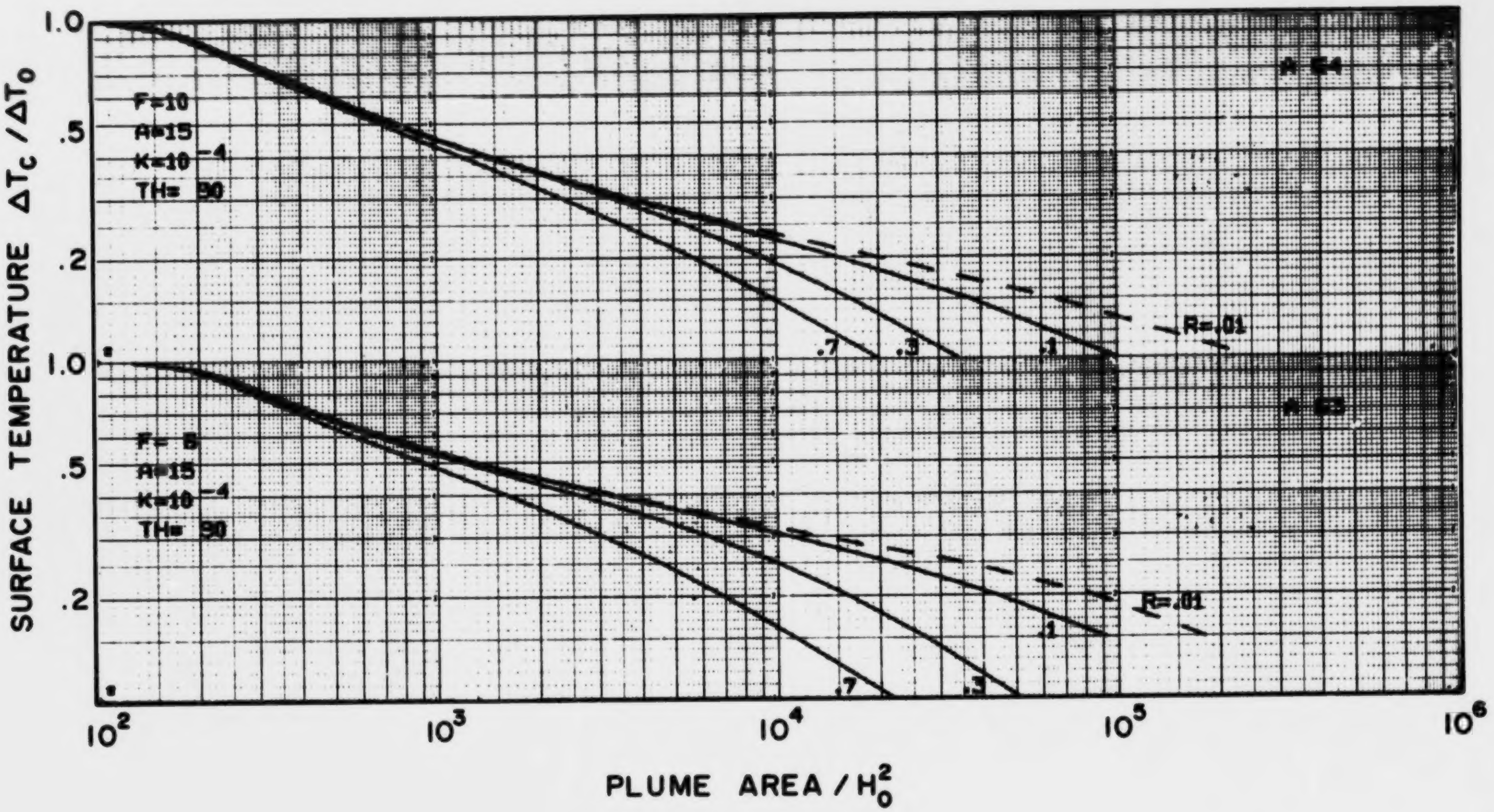

FIG (B32) TEMPERATURE, AREA (TA)-PLOTS
FOR SURFACE JET DISCHARGE

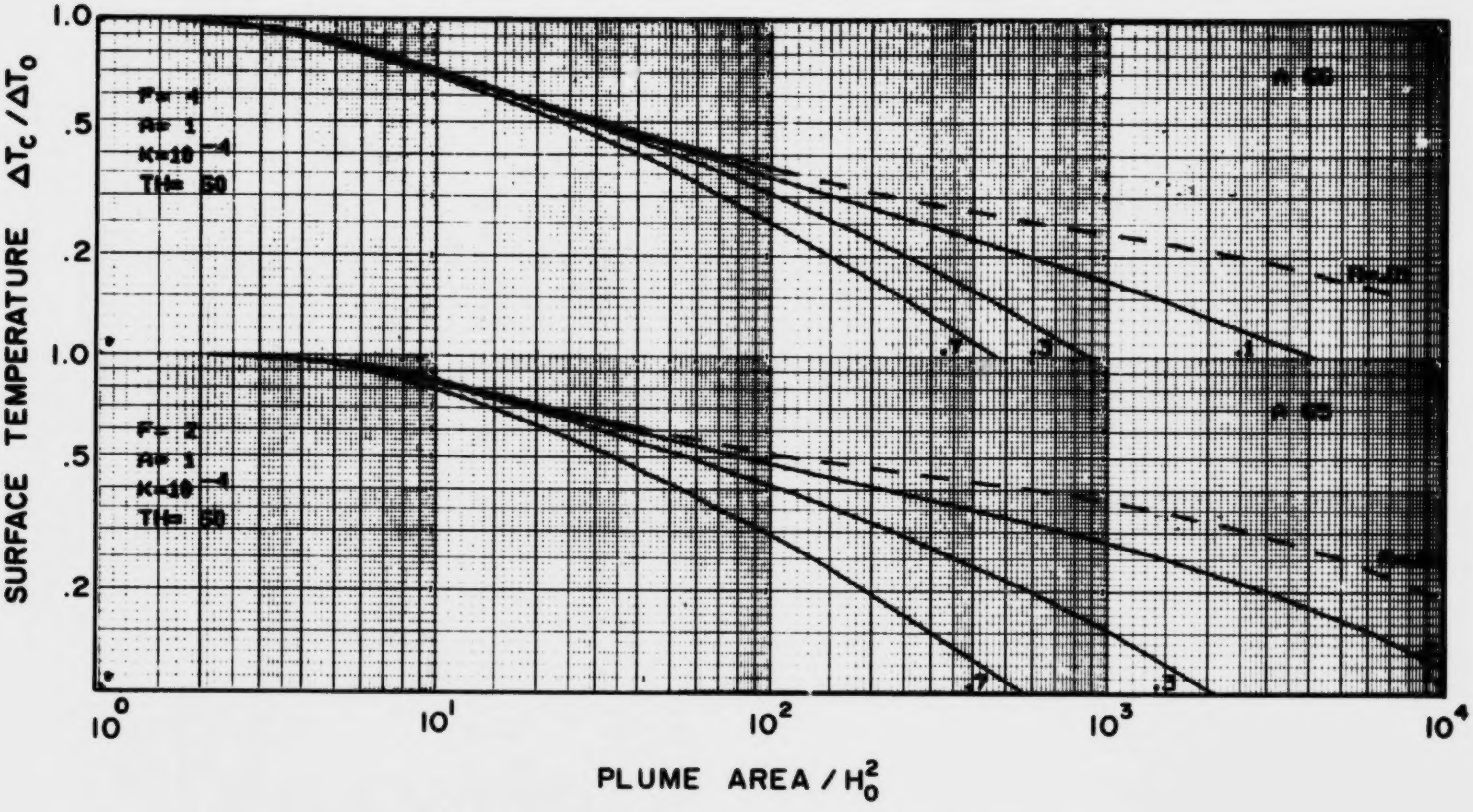

FIG (B 33) TEMPERATURE, AREA (TA)-PLOT FOR SURFACE JET DISCHARGE

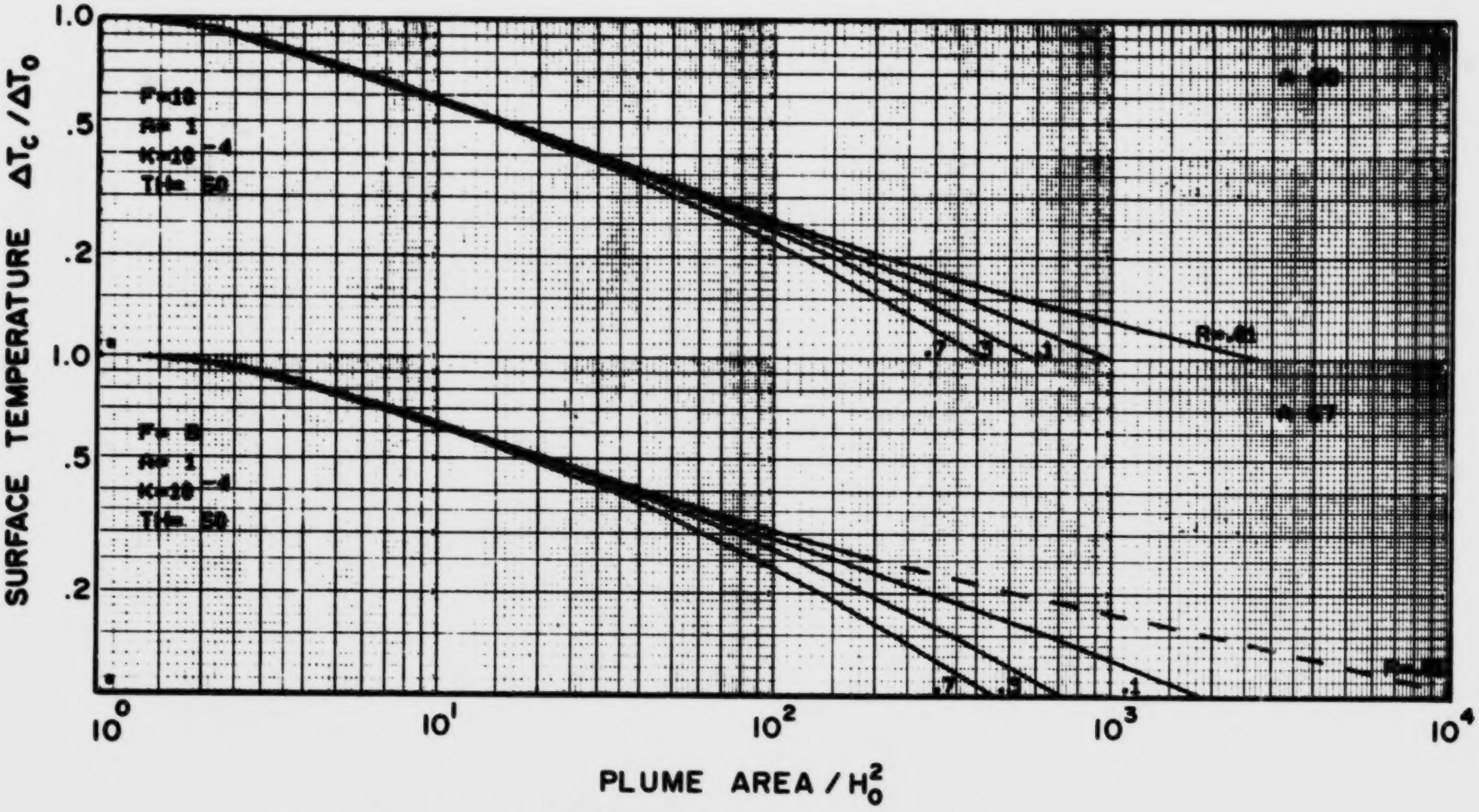

FIG (B 34) TEMPERATURE, AREA (TA)-PLOT FOR SURFACE JET DISCHARGE

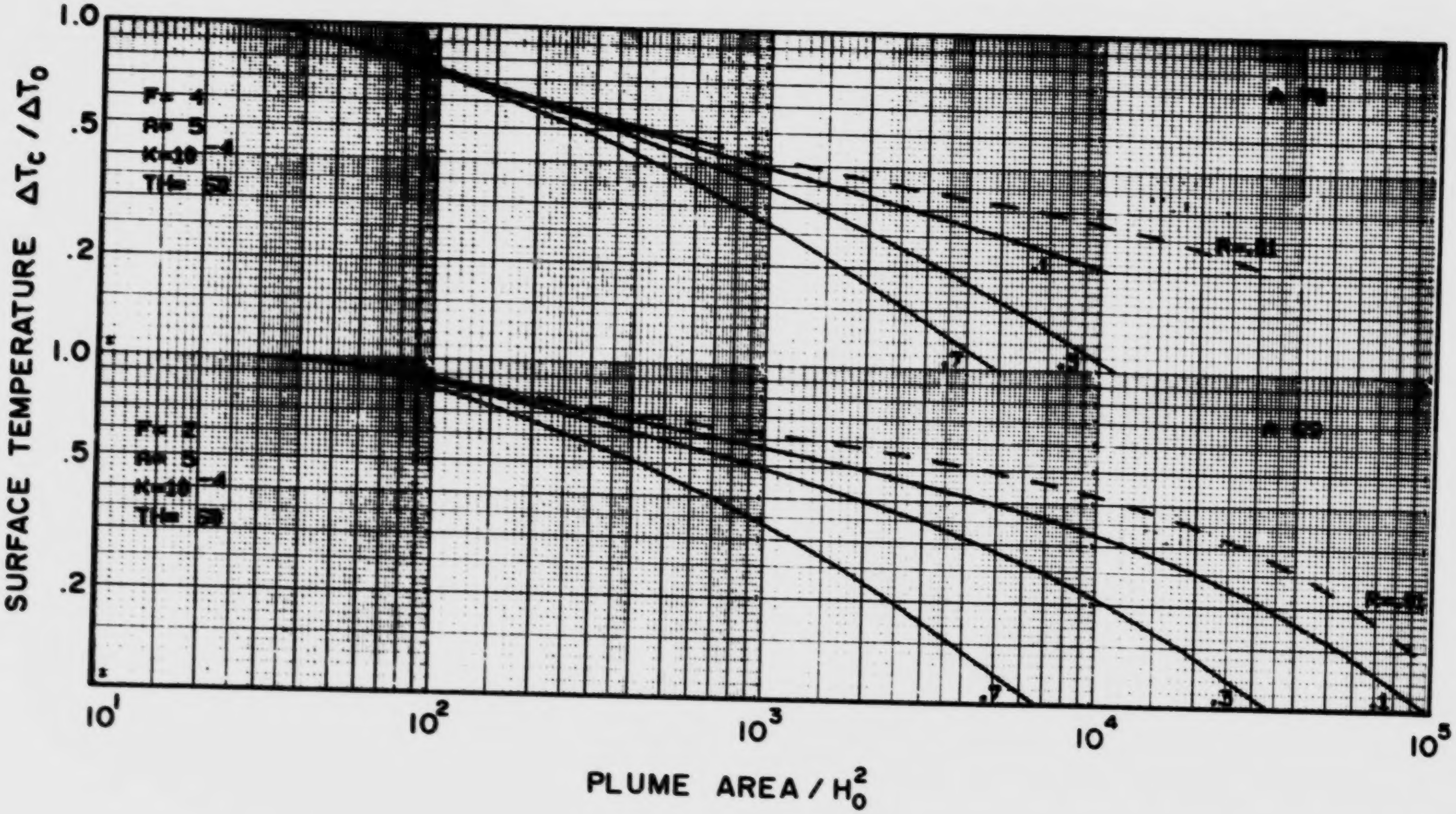

FIG (B 35) TEMPERATURE, AREA (TA)-PLOTS FOR SURFACE JET DISCHARGE

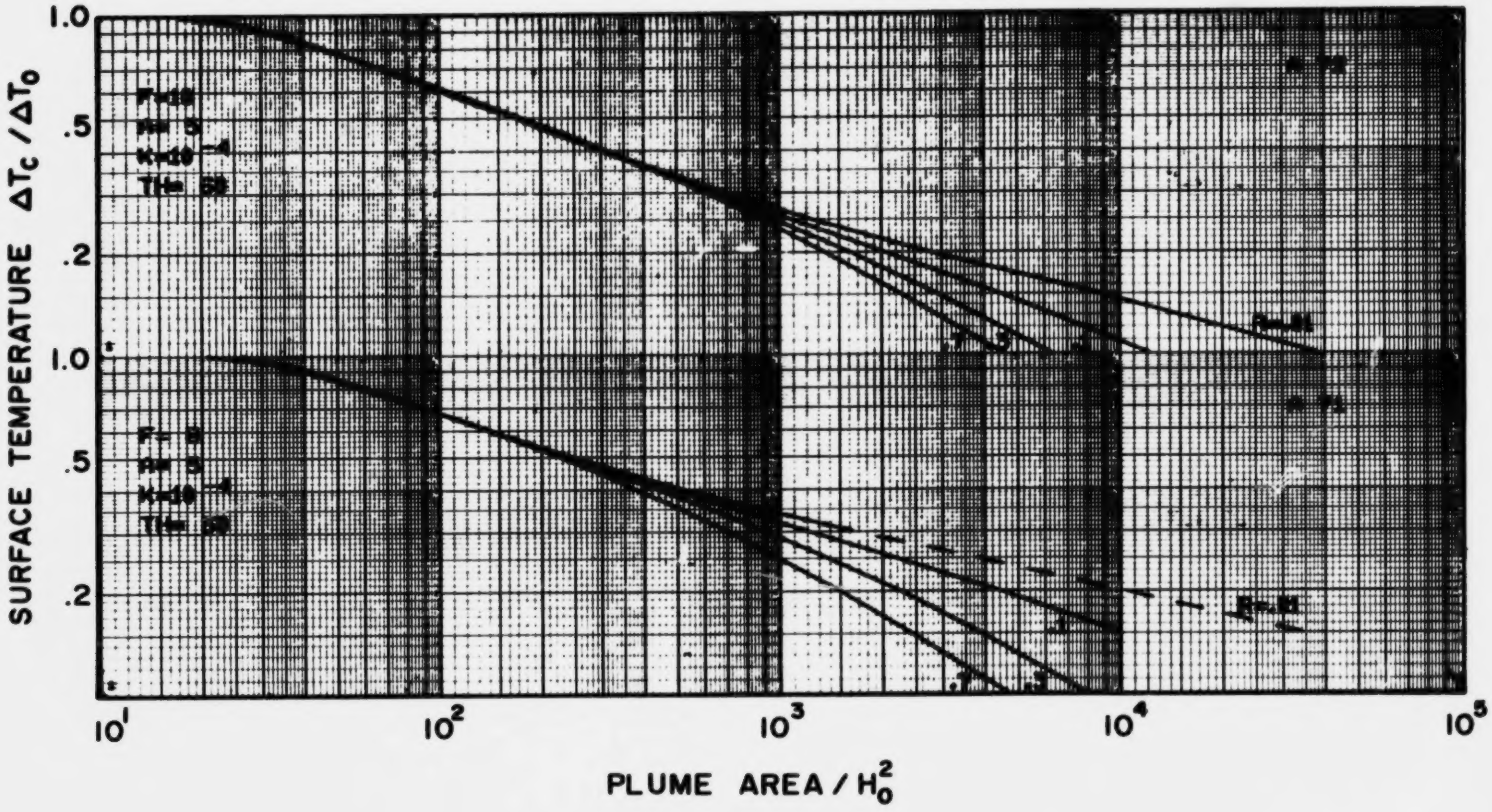

FIG (B36) TEMPERATURE, AREA (TA)-PLOTS
FOR SURFACE JET DISCHARGE

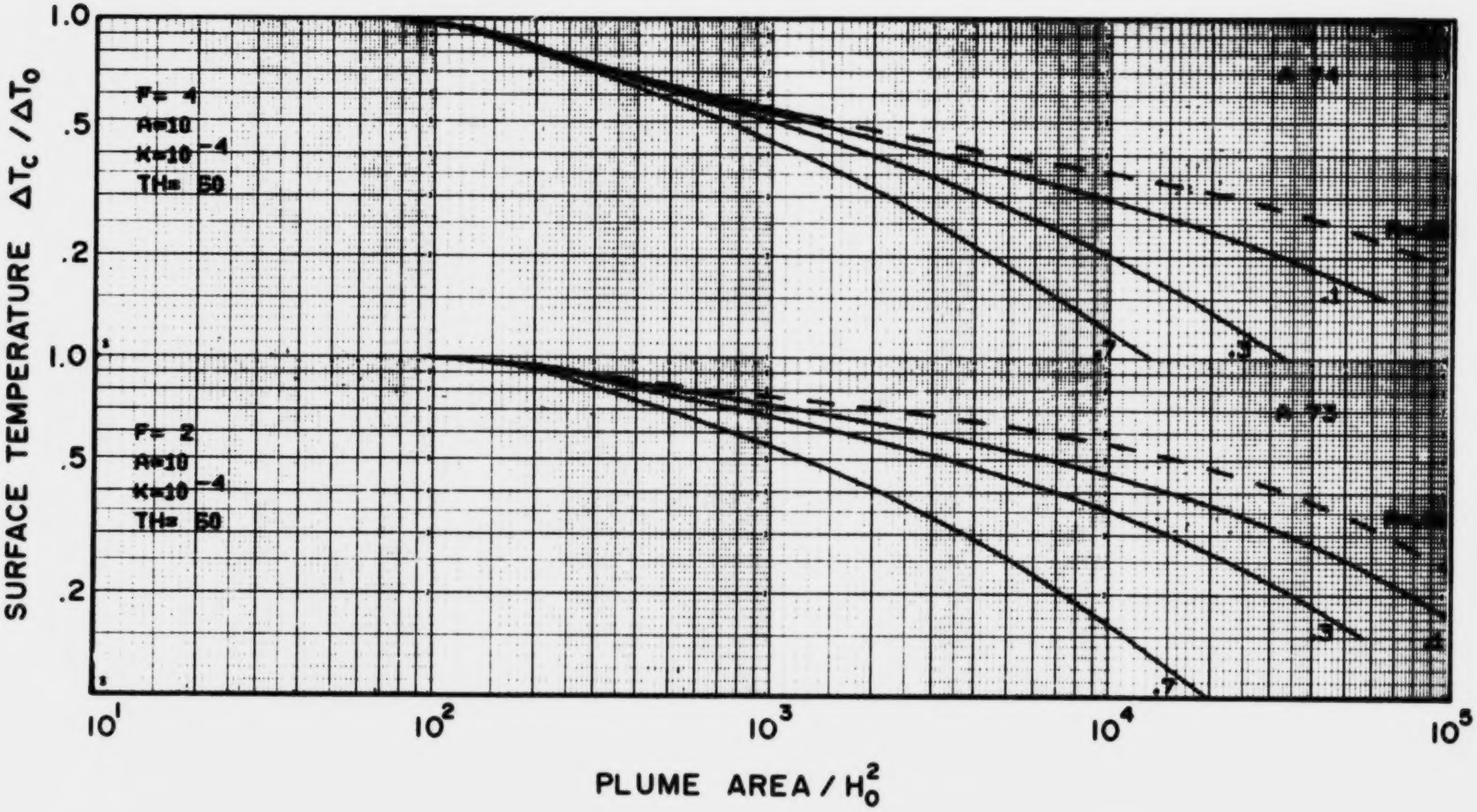

FIG (B 37) TEMPERATURE, AREA (TA)-PLOTS FOR SURFACE JET DISCHARGE

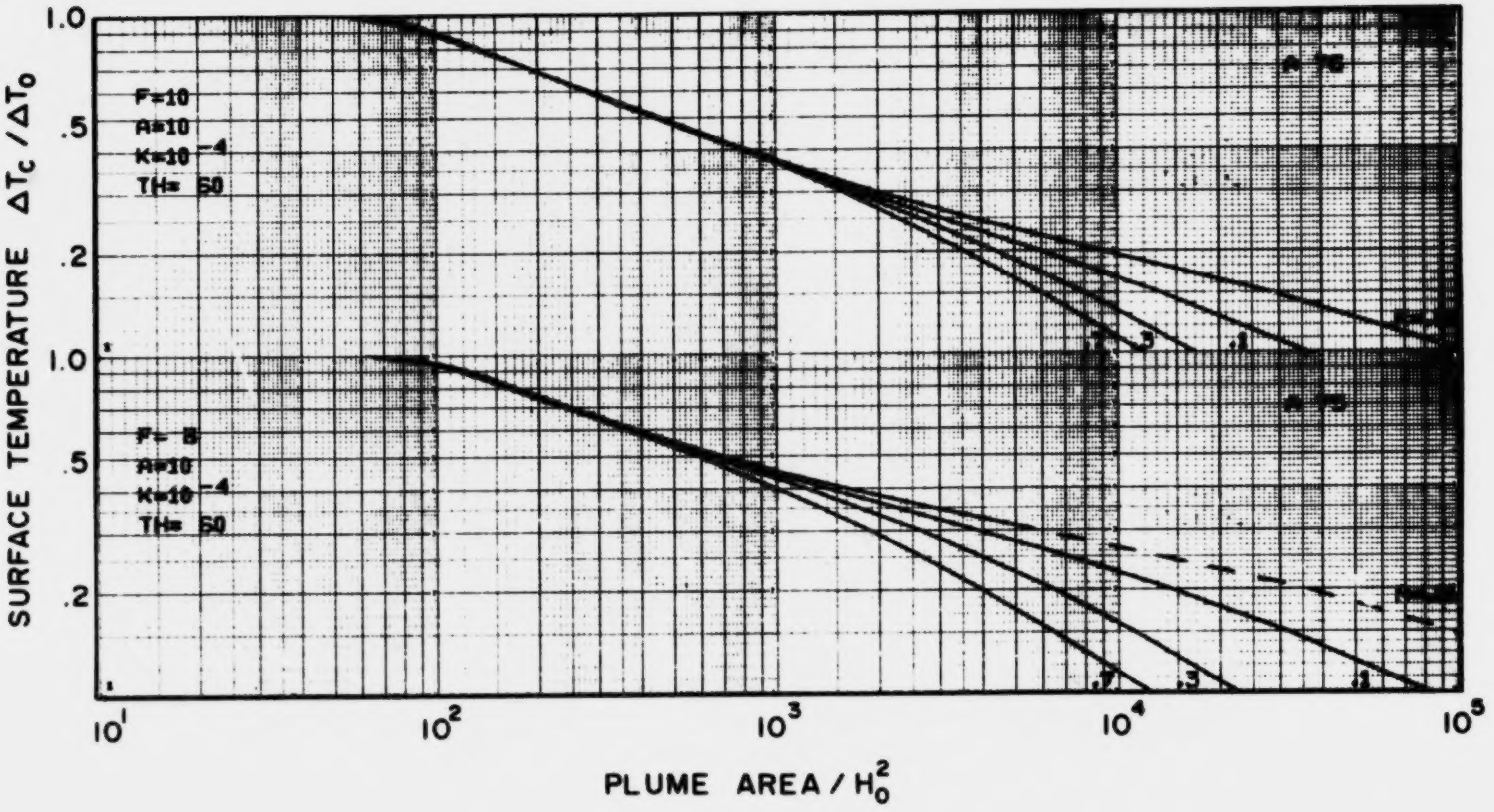

FIG (B 38) TEMPERATURE, AREA (TA)-PLOTS FOR SURFACE JET DISCHARGE

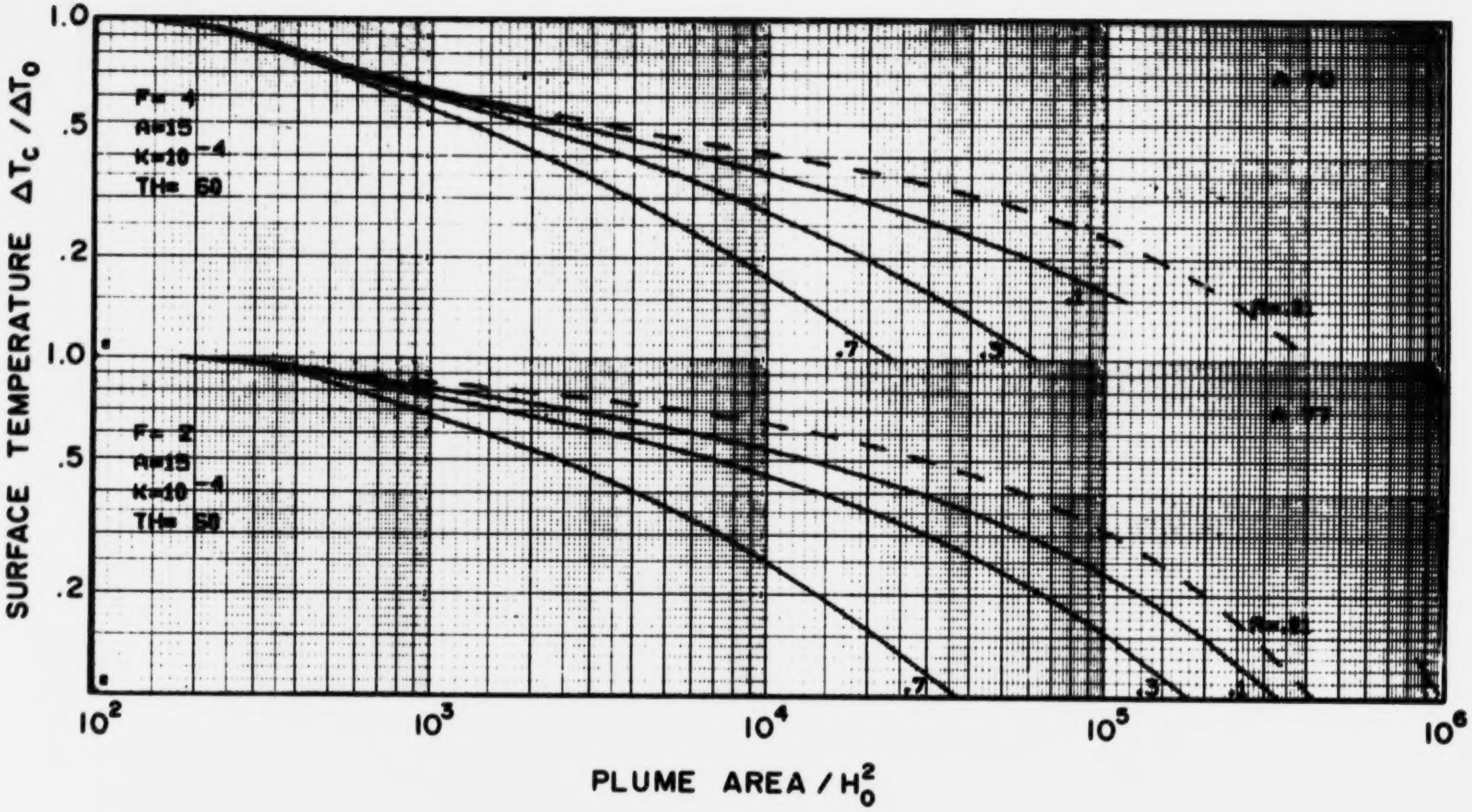

FIG (B 39) TEMPERATURE, AREA (TA)-PLOTS FOR SURFACE JET DISCHARGE

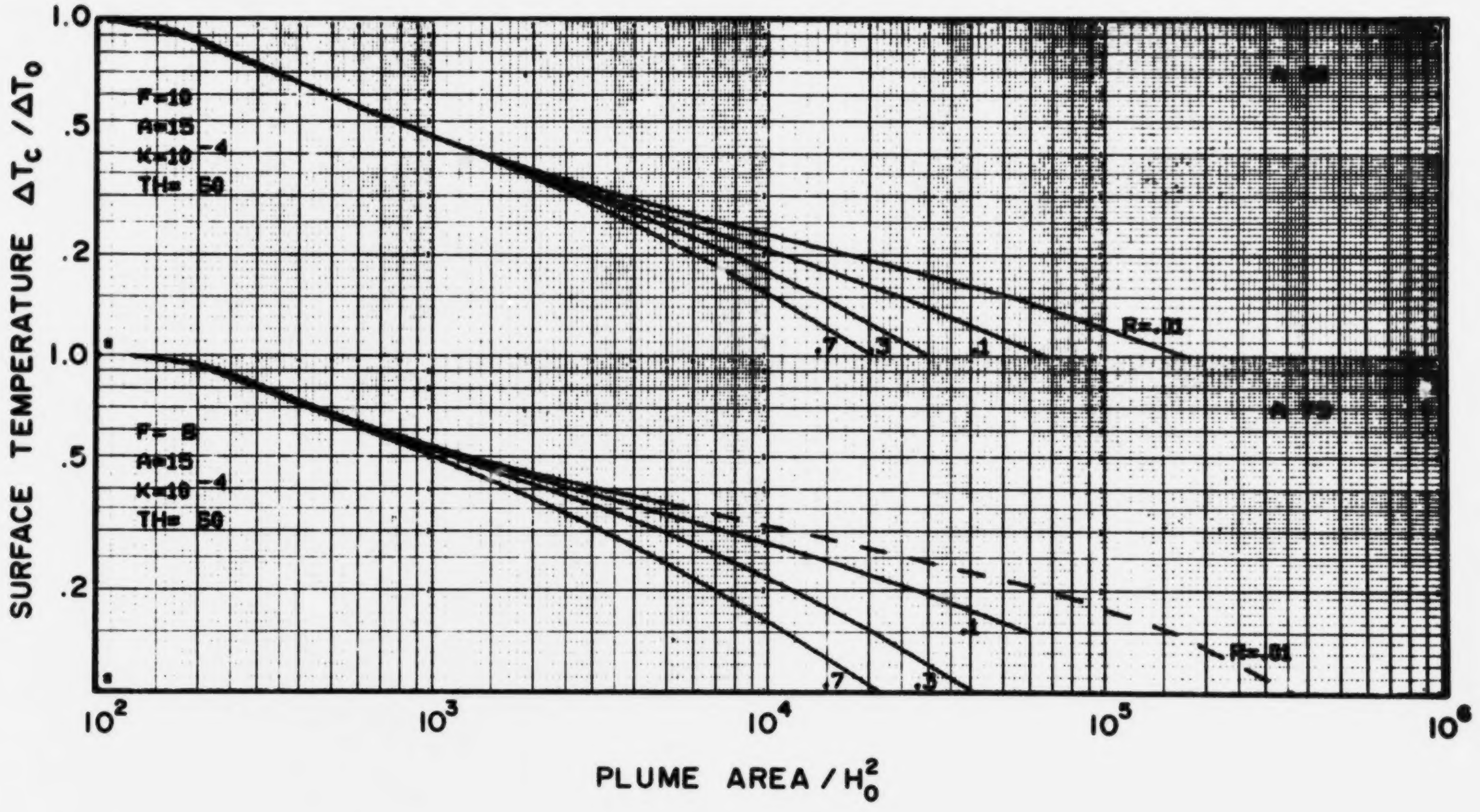

FIG (B40) TEMPERATURE, AREA (TA)-PLOTS
FOR SURFACE JET DISCHARGE

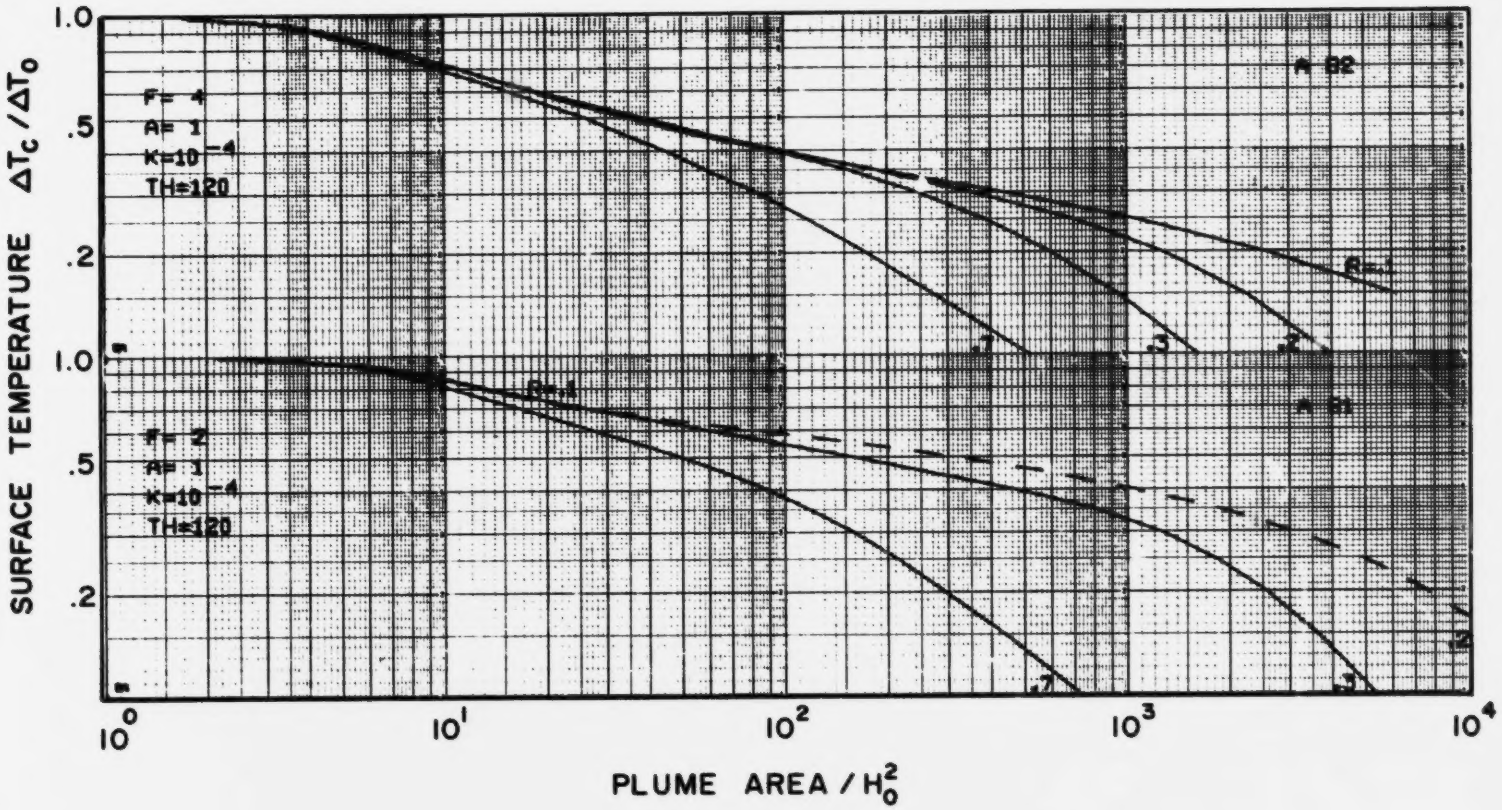

FIG(B41) TEMPERATURE, AREA (TA)-PLOT
FOR SURFACE JET DISCHARGE

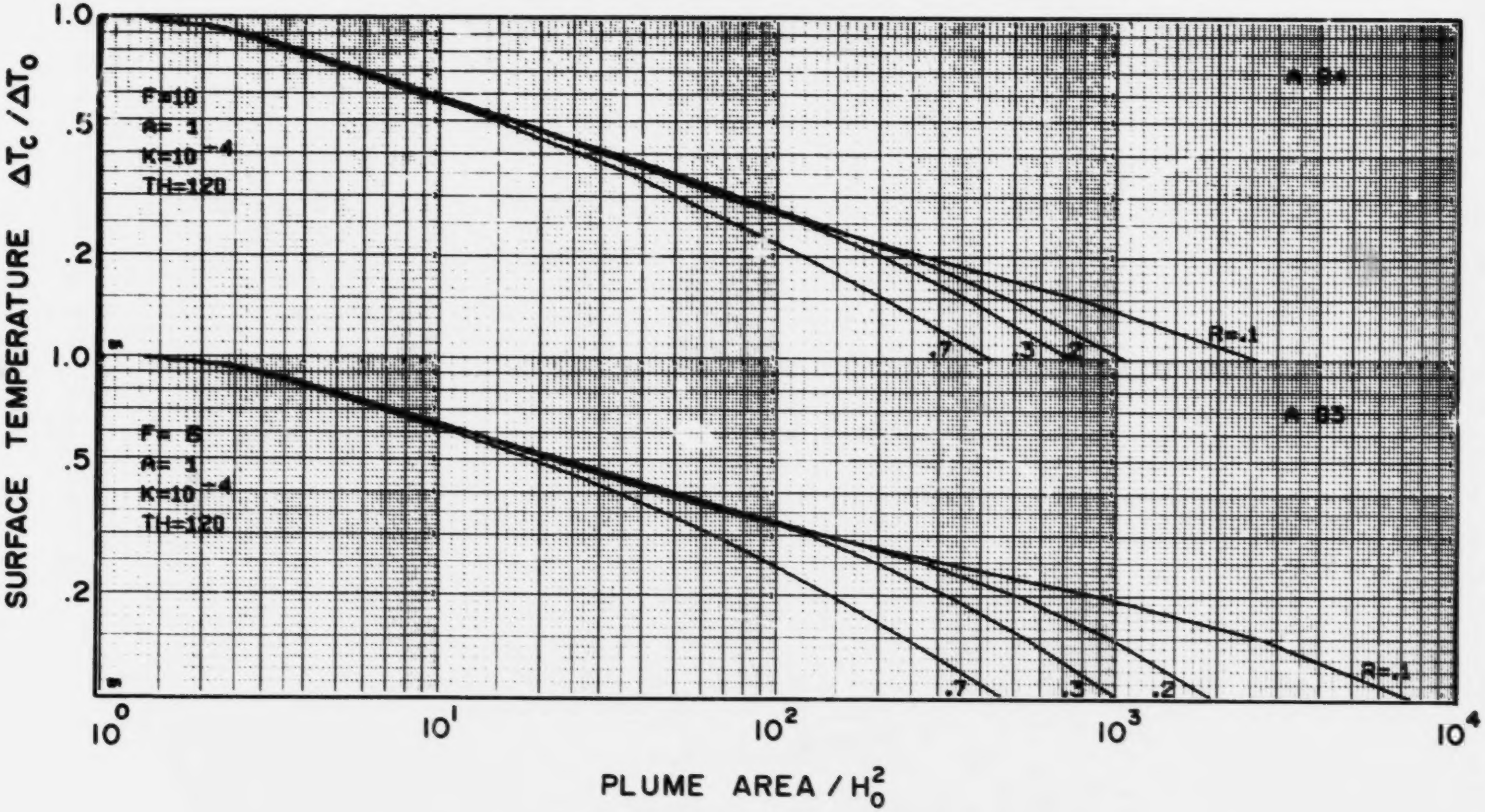

FIG(B42) TEMPERATURE, AREA (TA)-PLOT
FOR SURFACE JET DISCHARGE

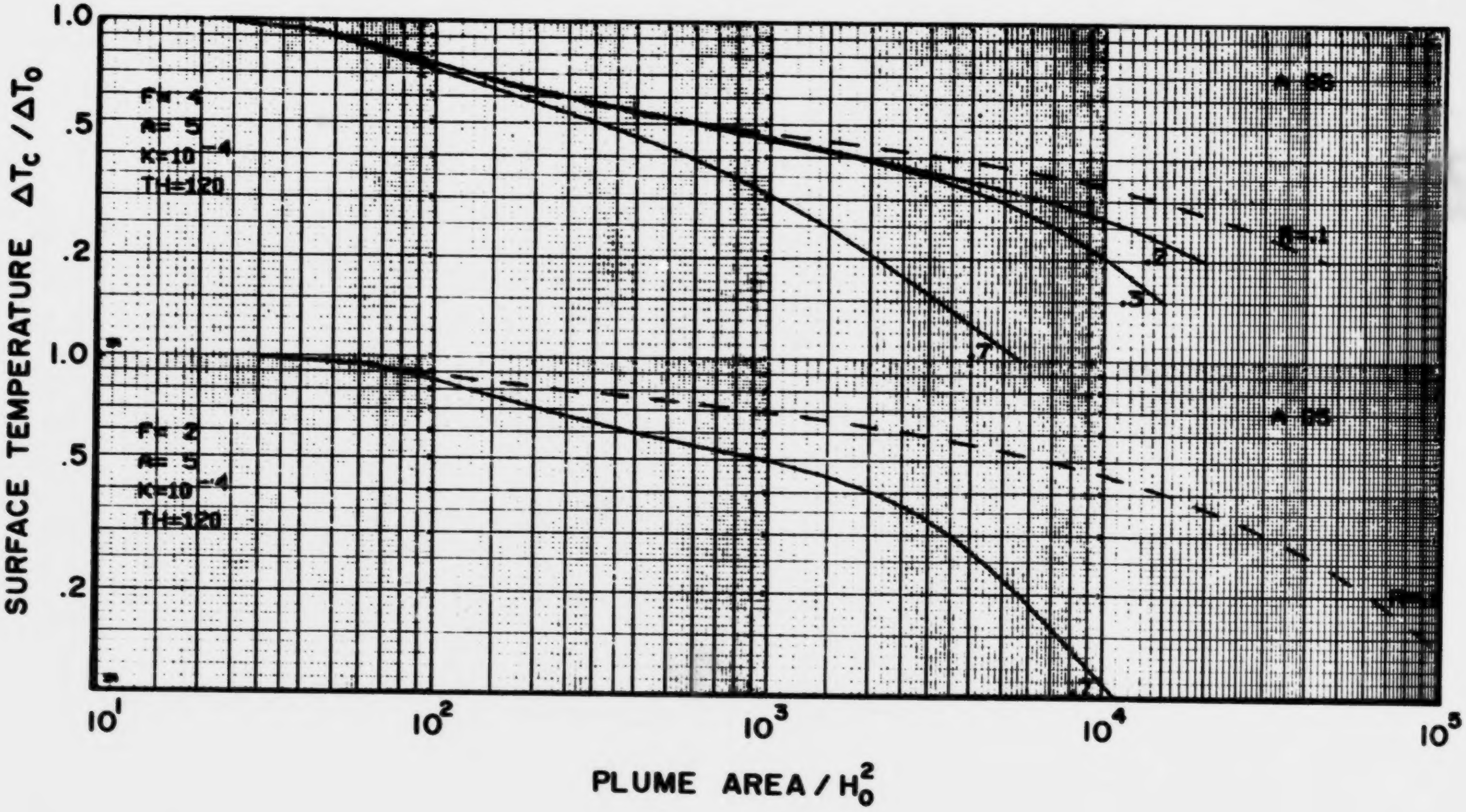

FIG (B43) TEMPERATURE, AREA (TA)-PLOTS FOR SURFACE JET DISCHARGE

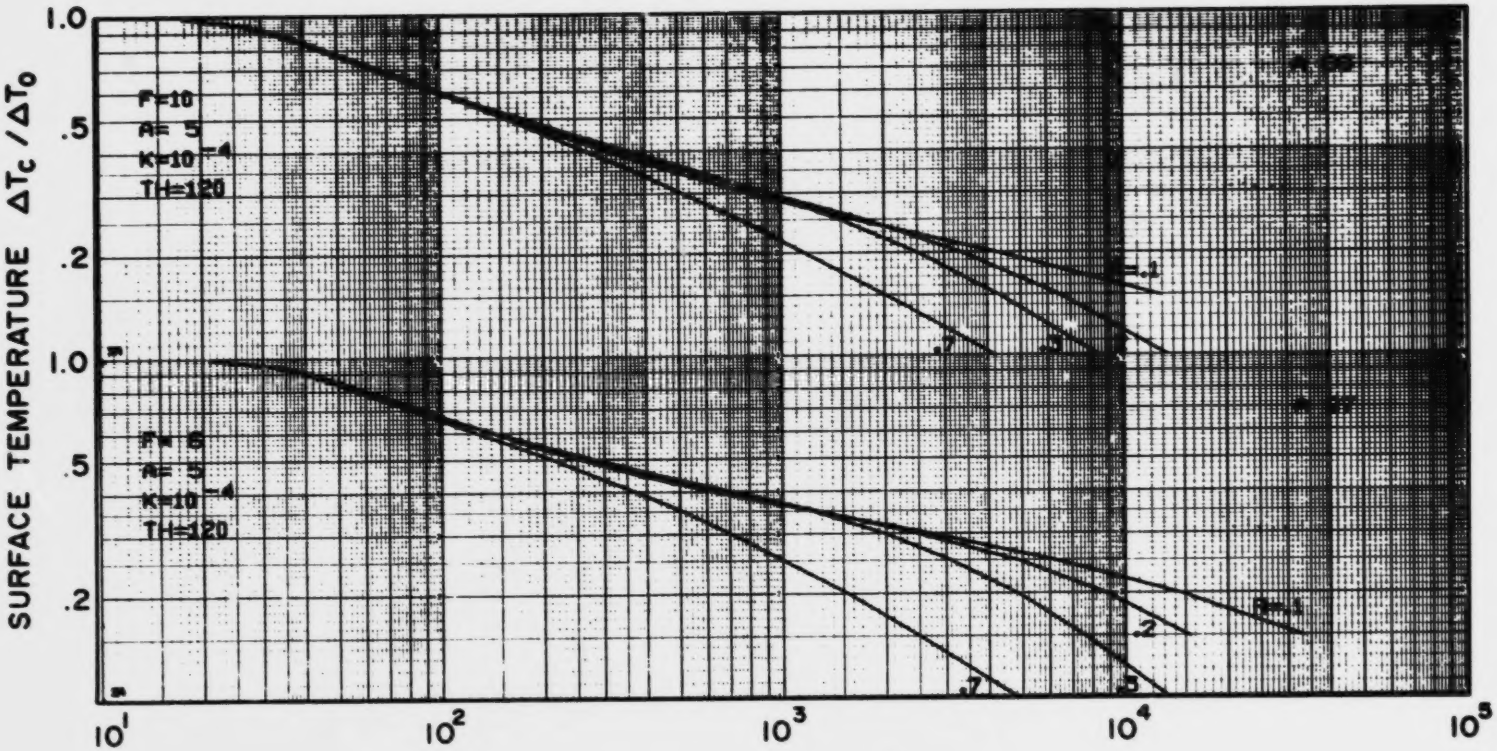

FIG (B44) TEMPERATURE, AREA (TA)-PLOTS
FOR SURFACE JET DISCHARGE

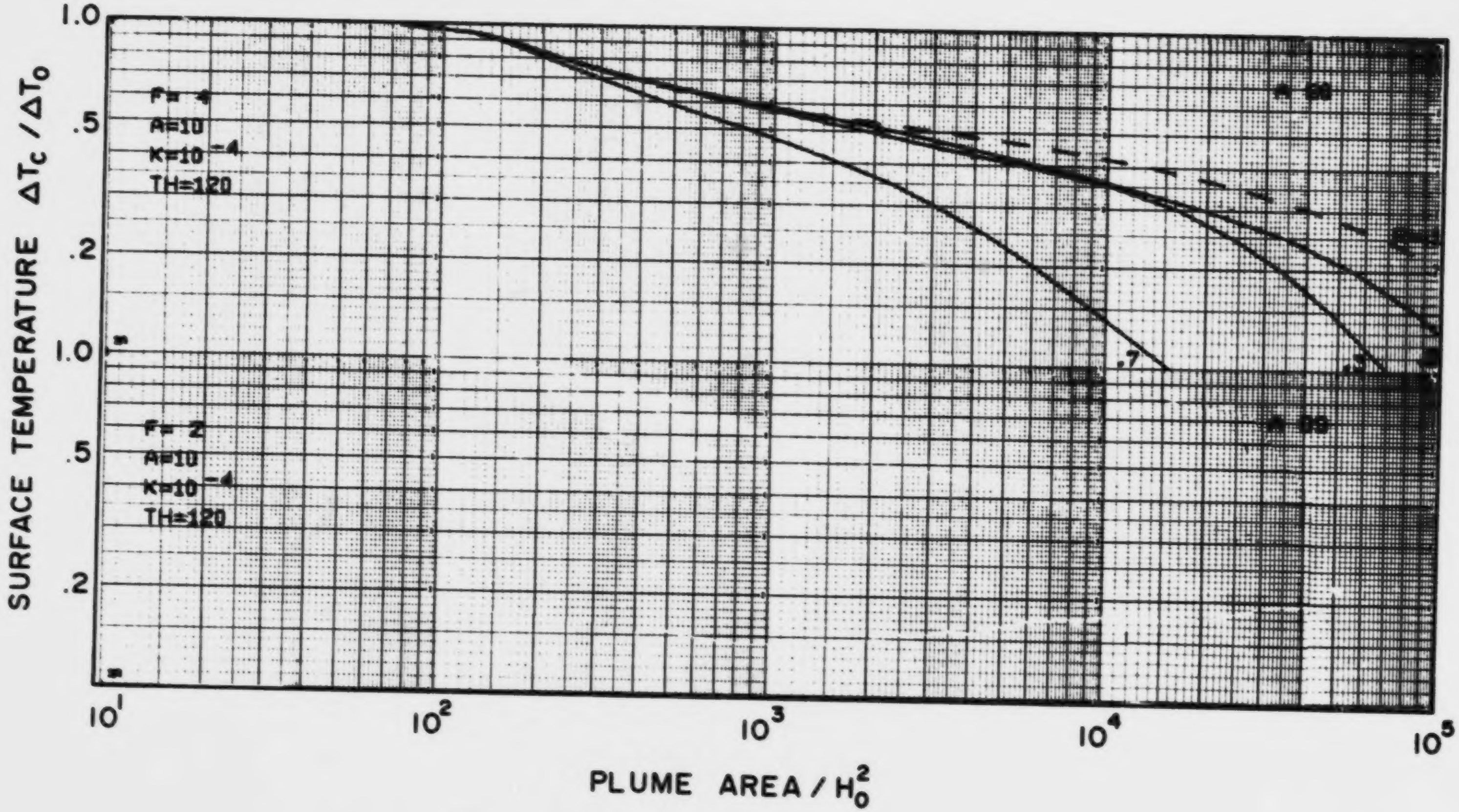

FIG (B45) TEMPERATURE, AREA (TA)-PLOTS FOR SURFACE JET DISCHARGE

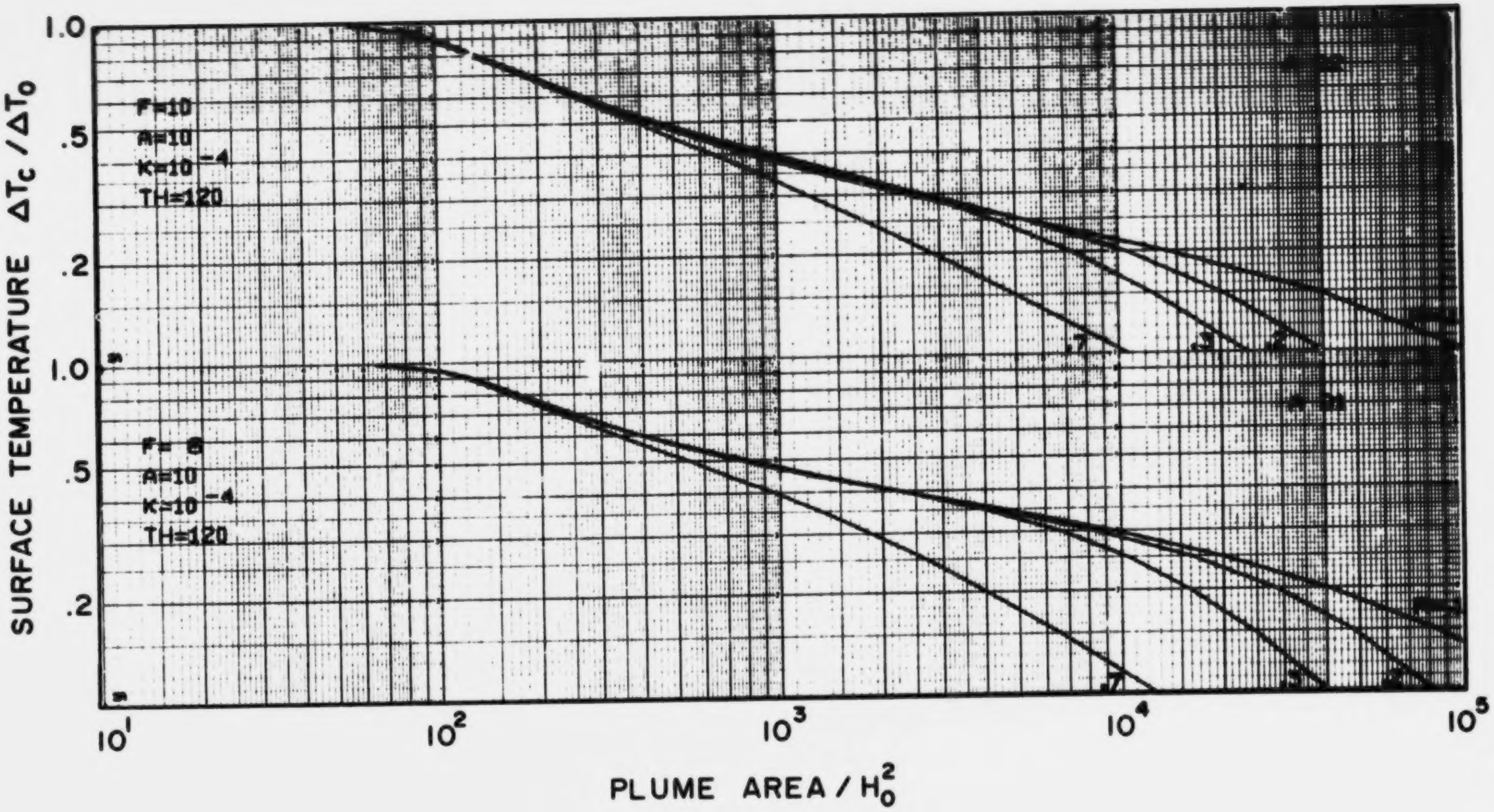

FIG (B46) TEMPERATURE, AREA (TA)-PLOTS FOR SURFACE JET DISCHARGE

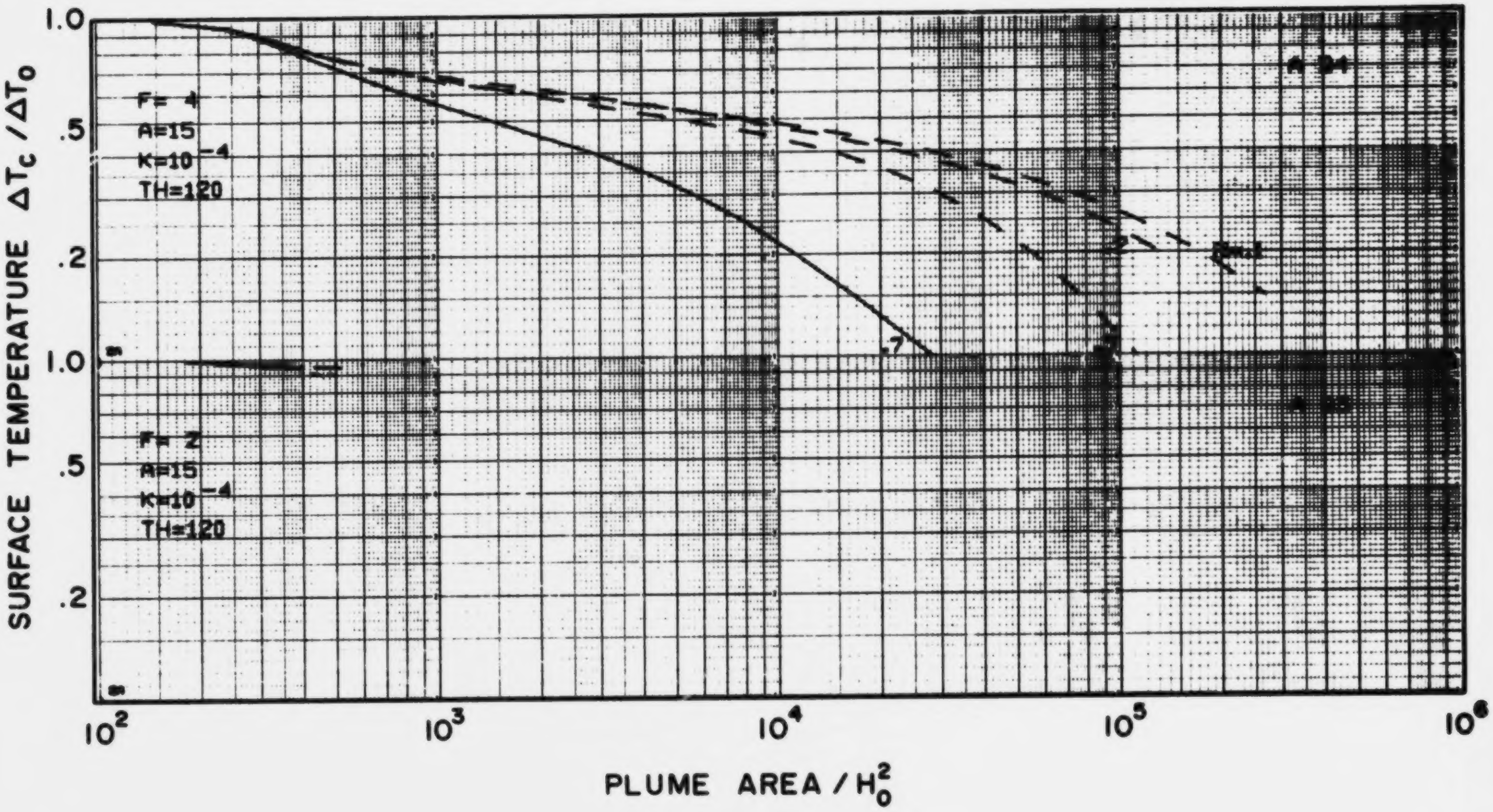

FIG (B47) TEMPERATURE, AREA (TA)-PLOTS FOR SURFACE JET DISCHARGE

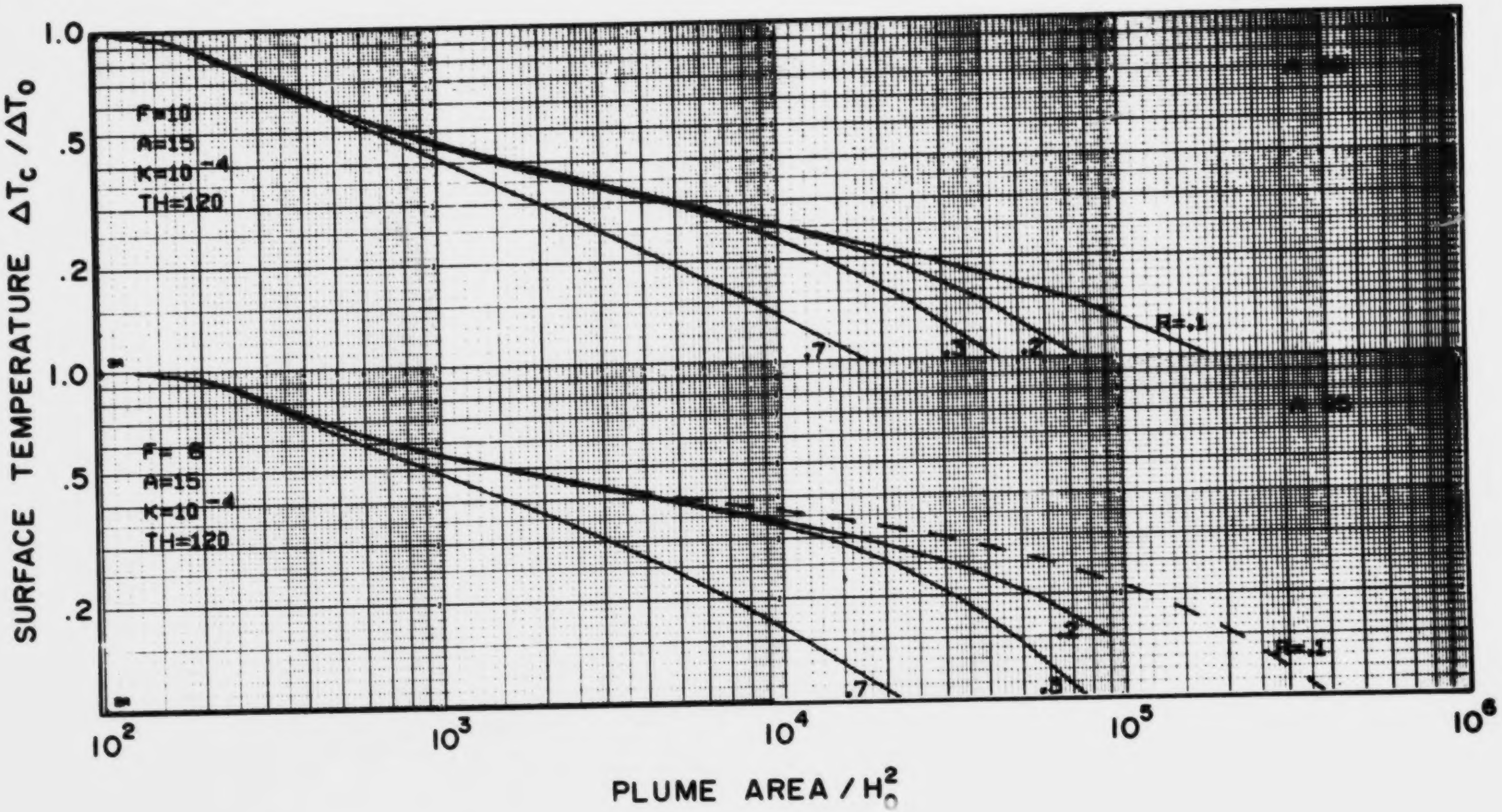

FIG (B48) TEMPERATURE, AREA (TA)-PLOTS FOR SURFACE JET DISCHARGE

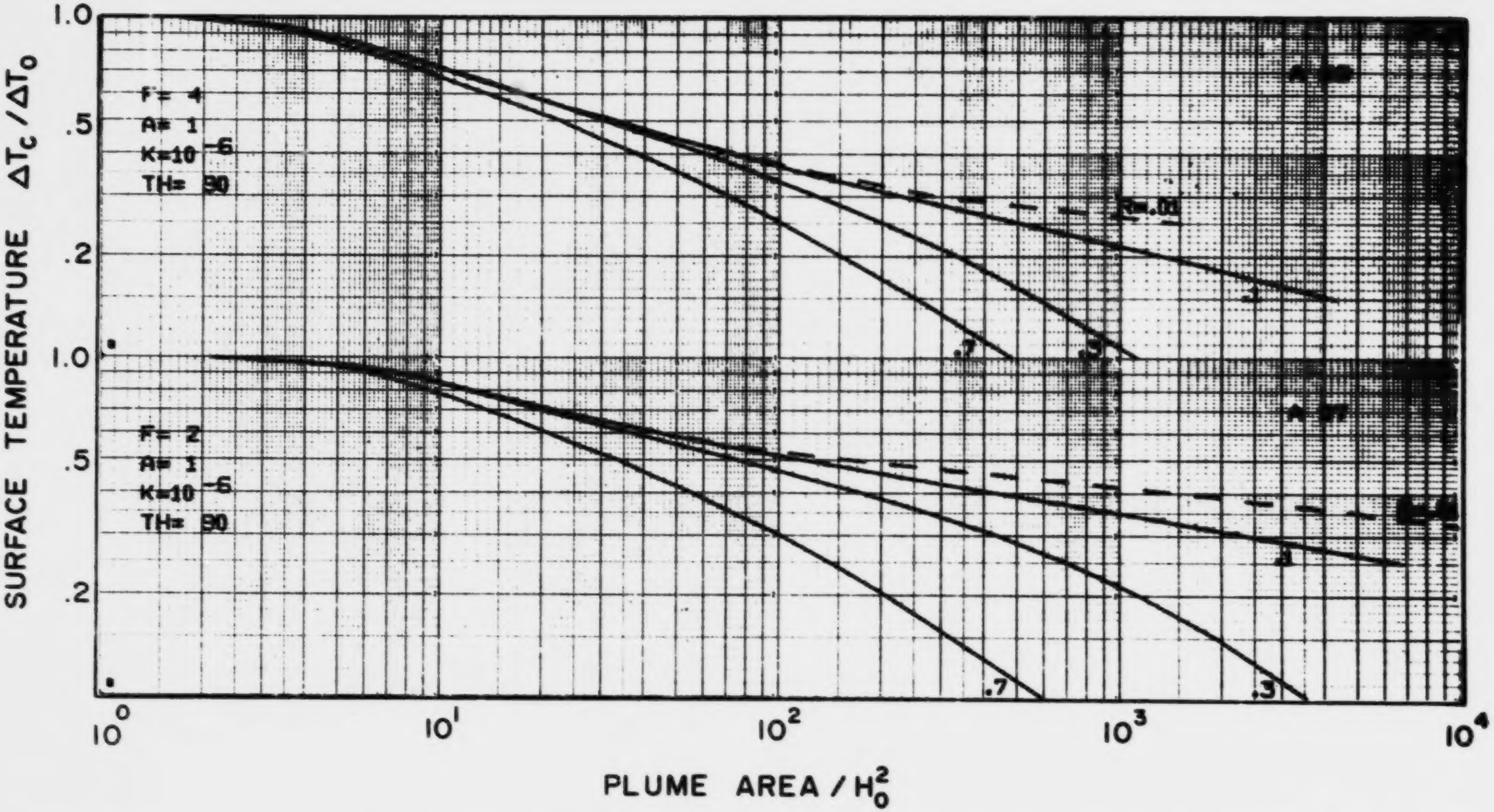

FIG(B 49) TEMPERATURE, AREA (TA)-PLOT
FOR SURFACE JET DISCHARGE

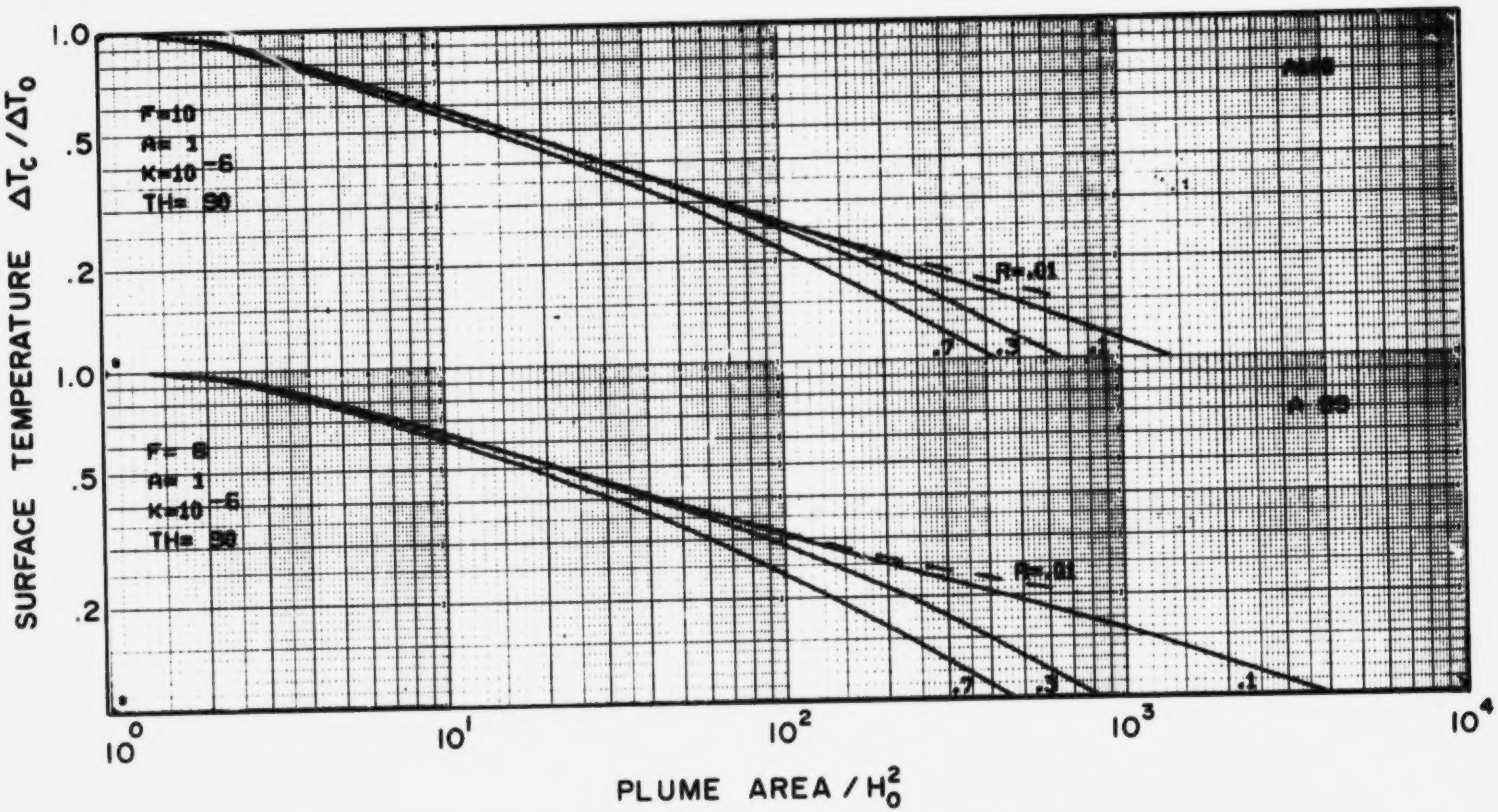

FIG(B50) TEMPERATURE, AREA (TA)-PLOT
FOR SURFACE JET DISCHARGE

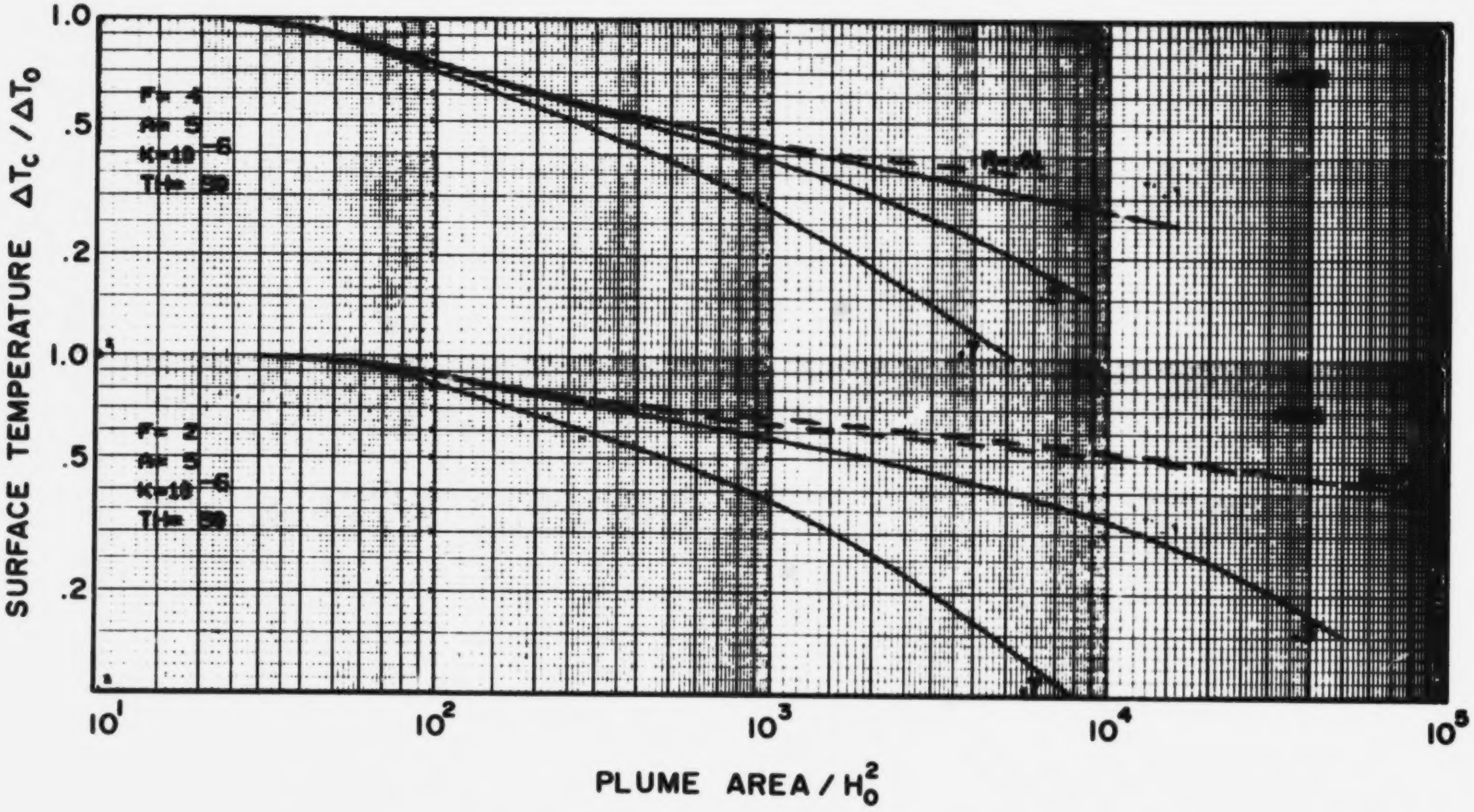

FIG (B 51) TEMPERATURE, AREA (TA)-PLOTS FOR SURFACE JET DISCHARGE

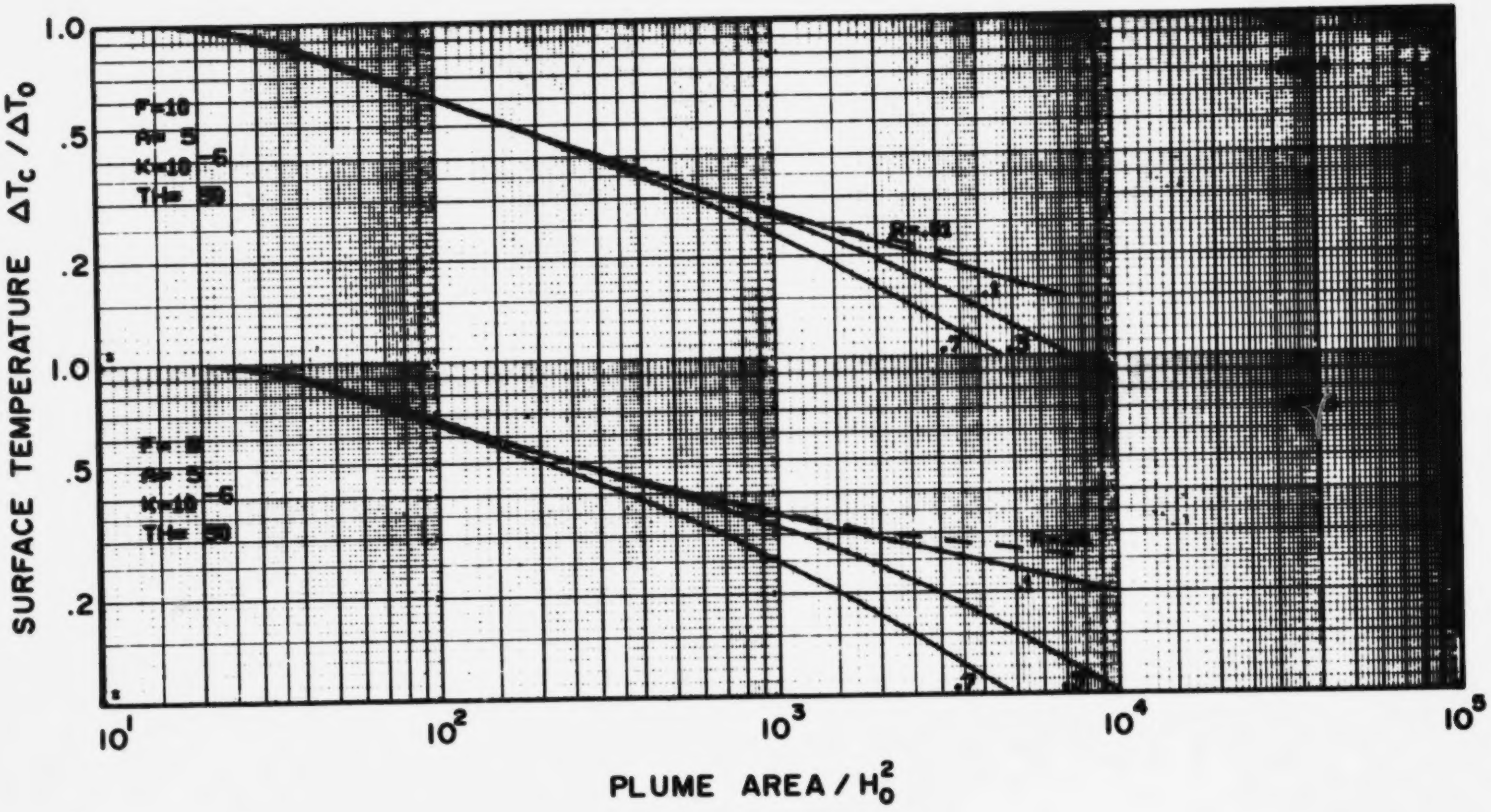

FIG (B52) TEMPERATURE, AREA (TA)-PLOTS FOR SURFACE JET DISCHARGE

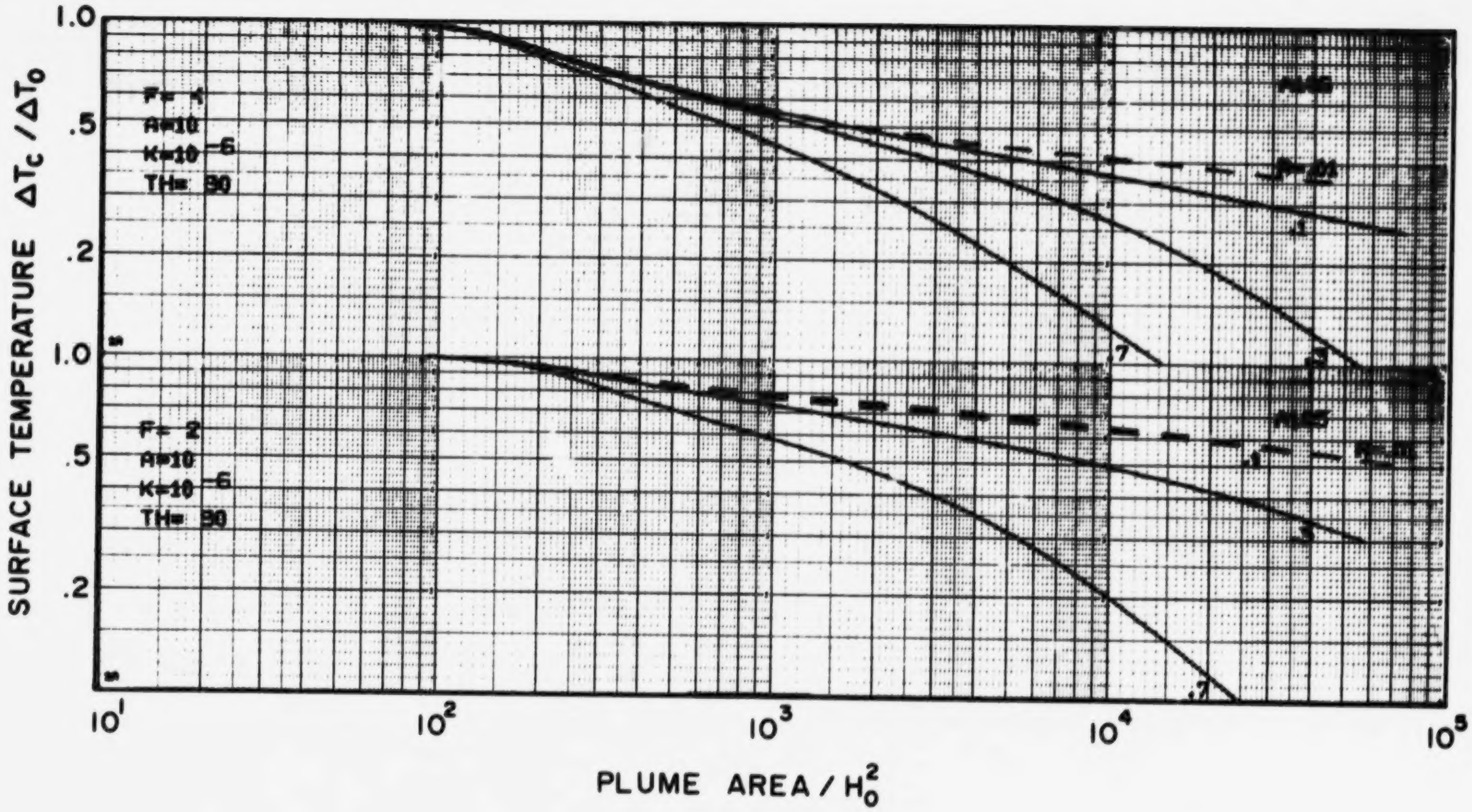

FIG (B 53) TEMPERATURE, AREA (TA)-PLOTS FOR SURFACE JET DISCHARGE

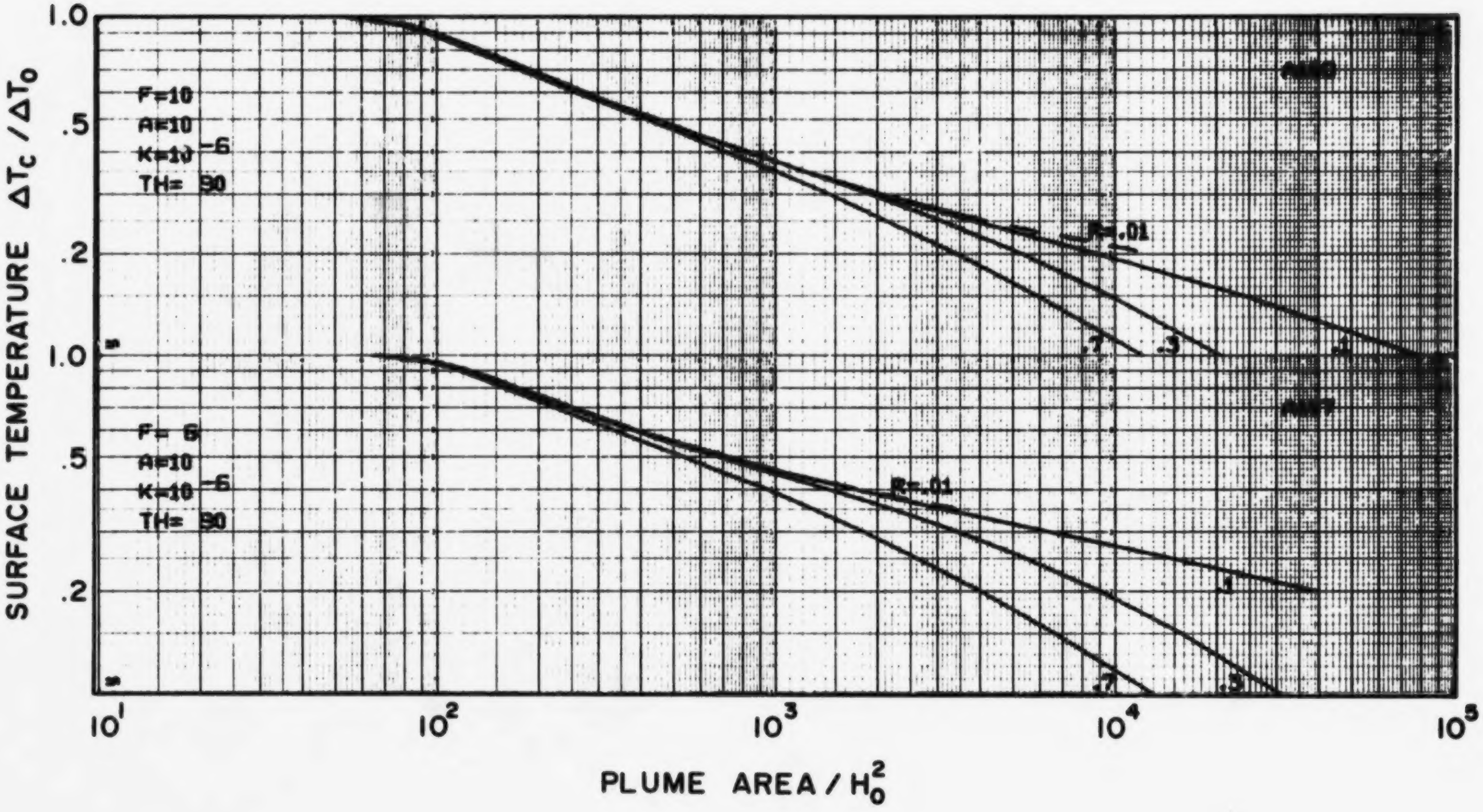

FIG (B54) TEMPERATURE, AREA (TA)-PLOTS
FOR SURFACE JET DISCHARGE

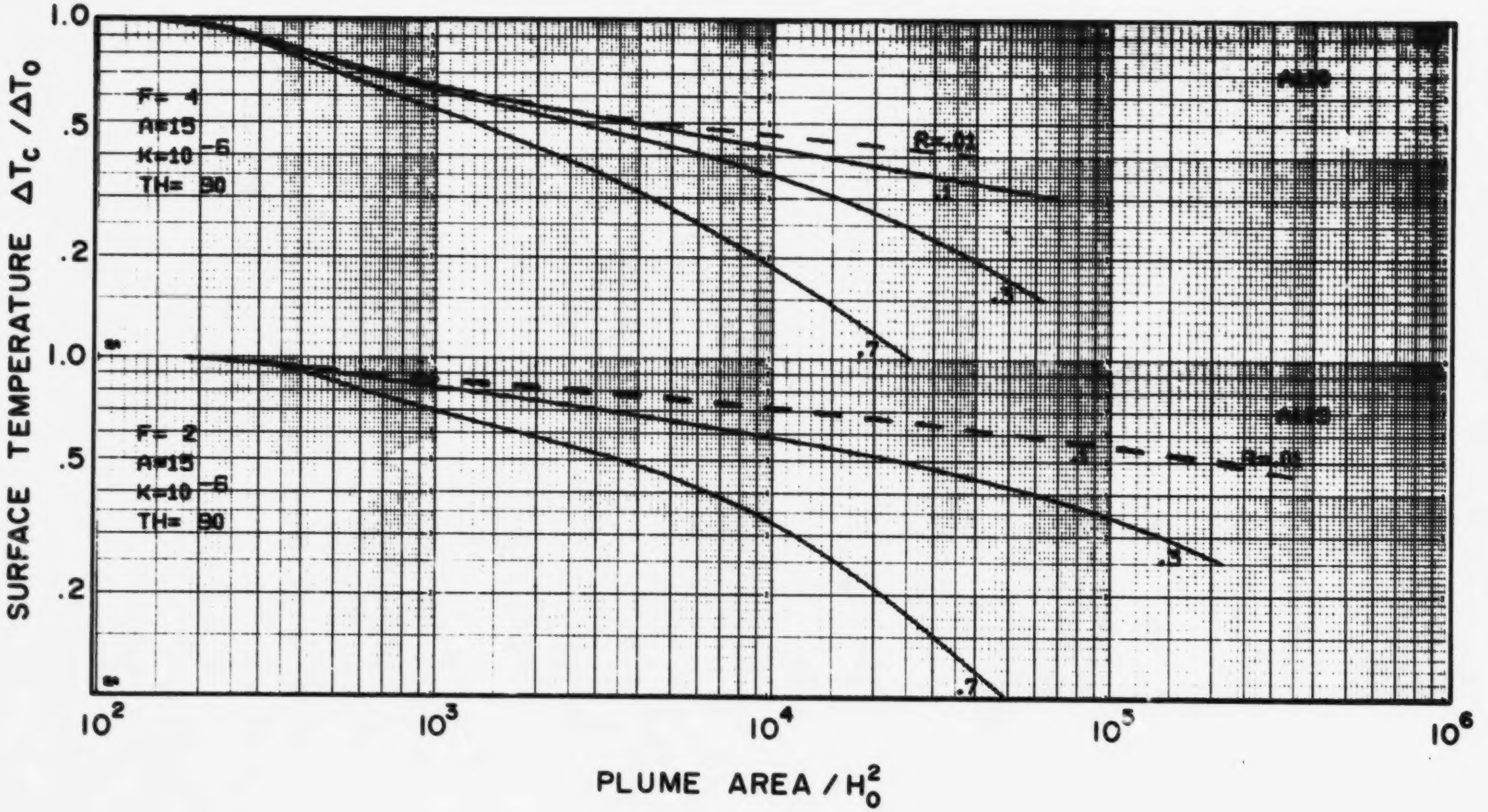

FIG (B55) TEMPERATURE, AREA (TA)-PLOTS FOR SURFACE JET DISCHARGE

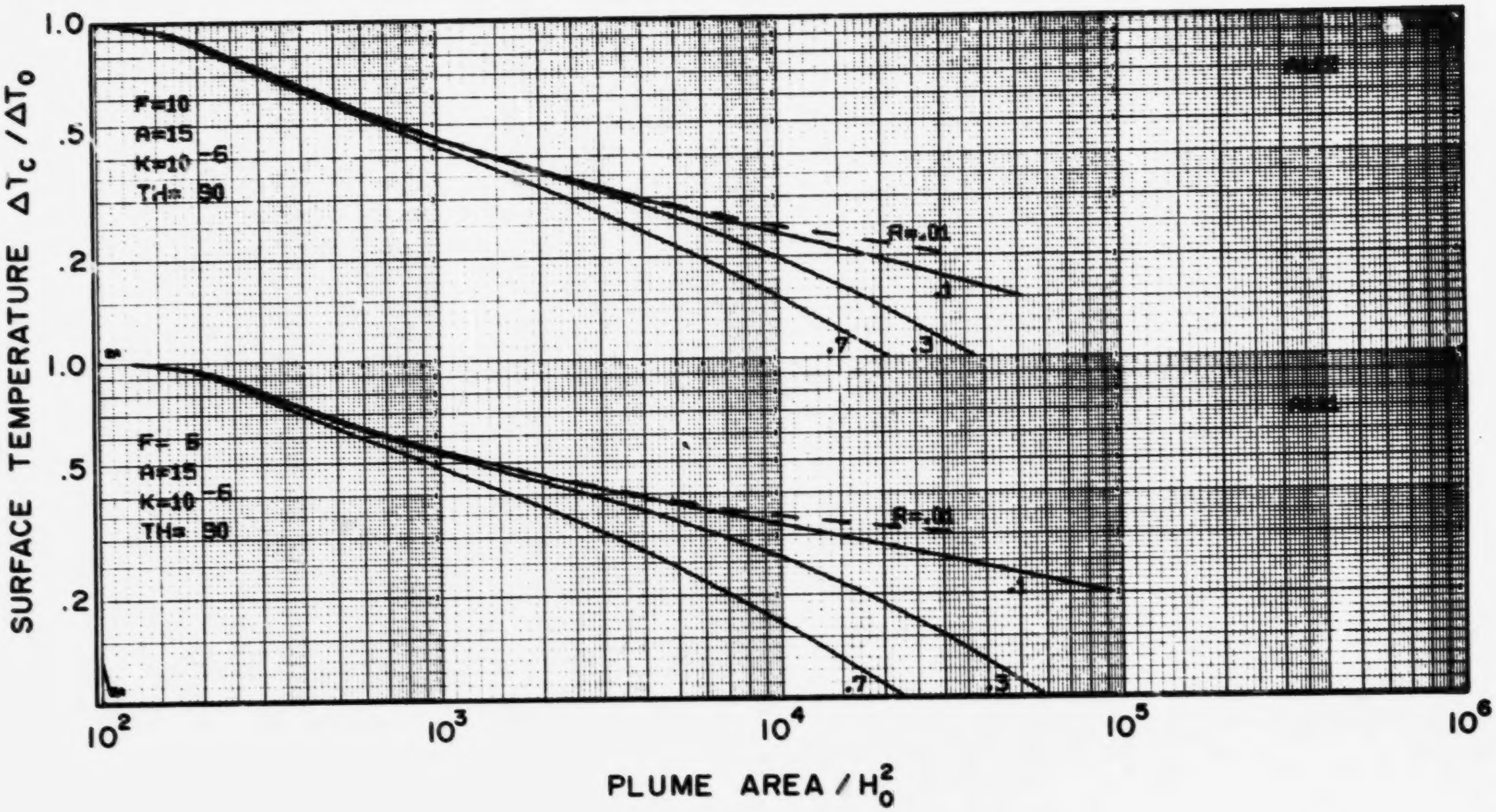

FIG (B 56) TEMPERATURE, AREA (TA)-PLOTS FOR SURFACE JET DISCHARGE

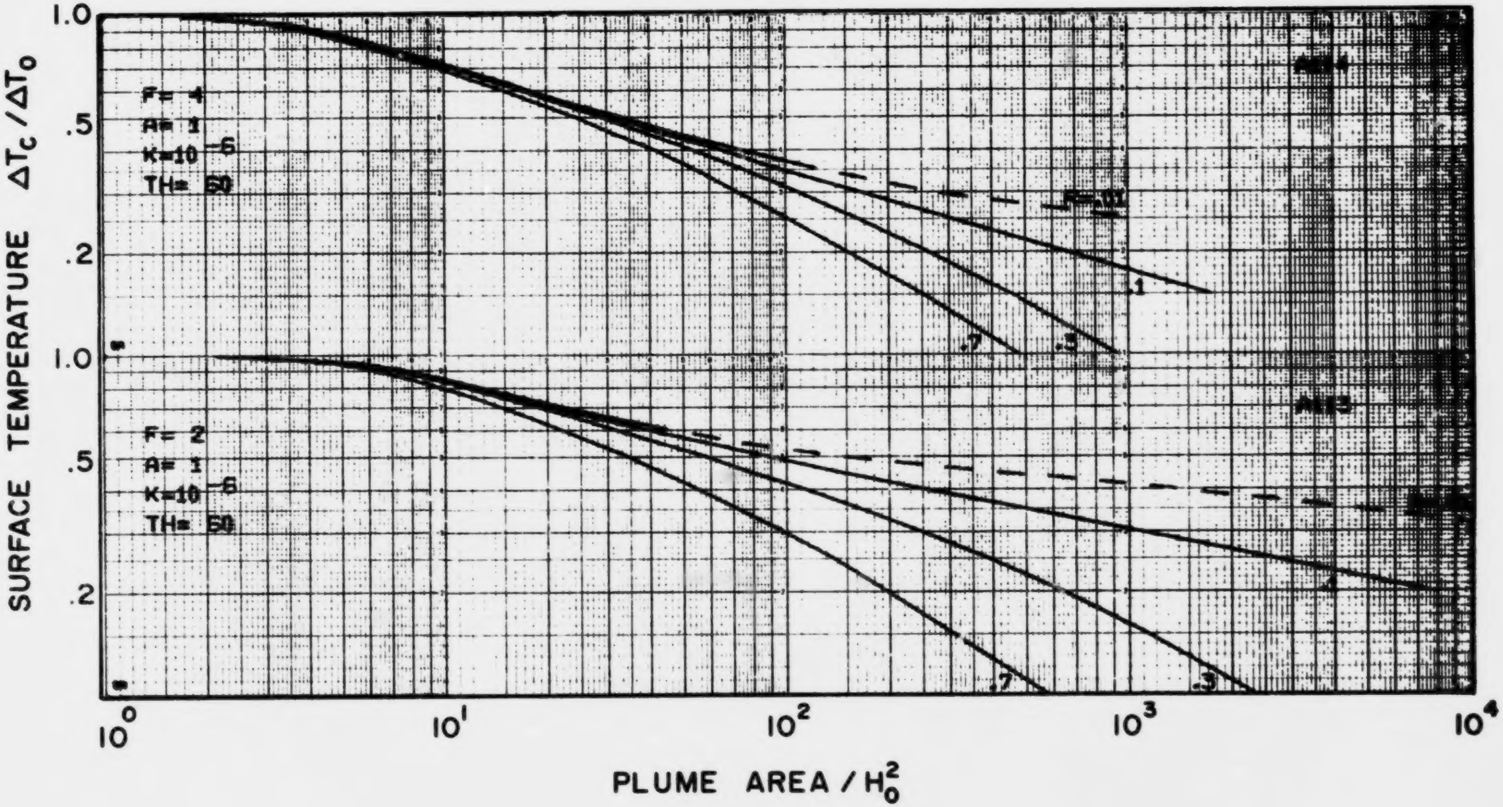

FIG(B57) TEMPERATURE, AREA (TA)-PLOT FOR SURFACE JET DISCHARGE

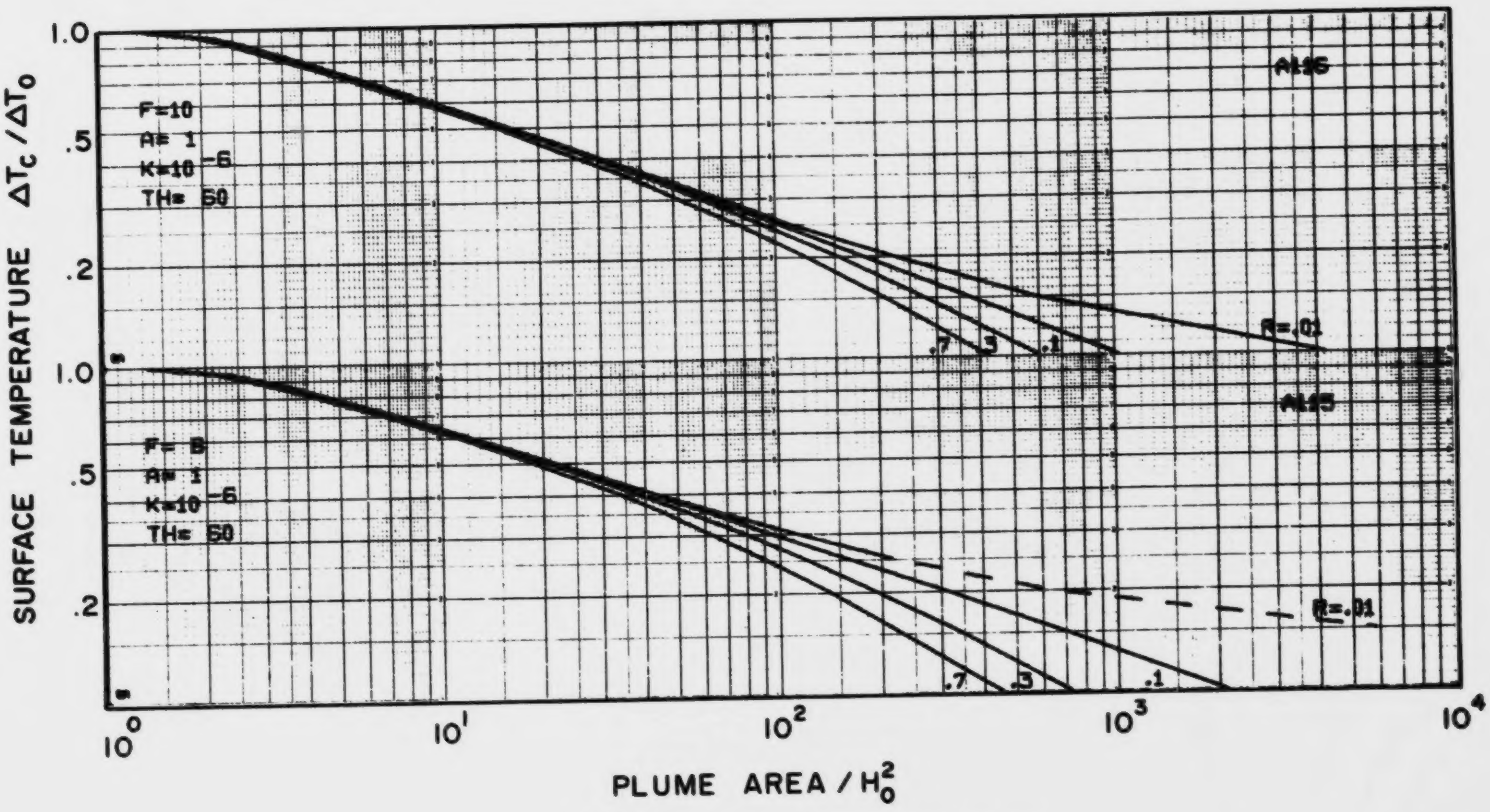

FIG(B 58) TEMPERATURE, AREA (TA)-PLOT
FOR SURFACE JET DISCHARGE

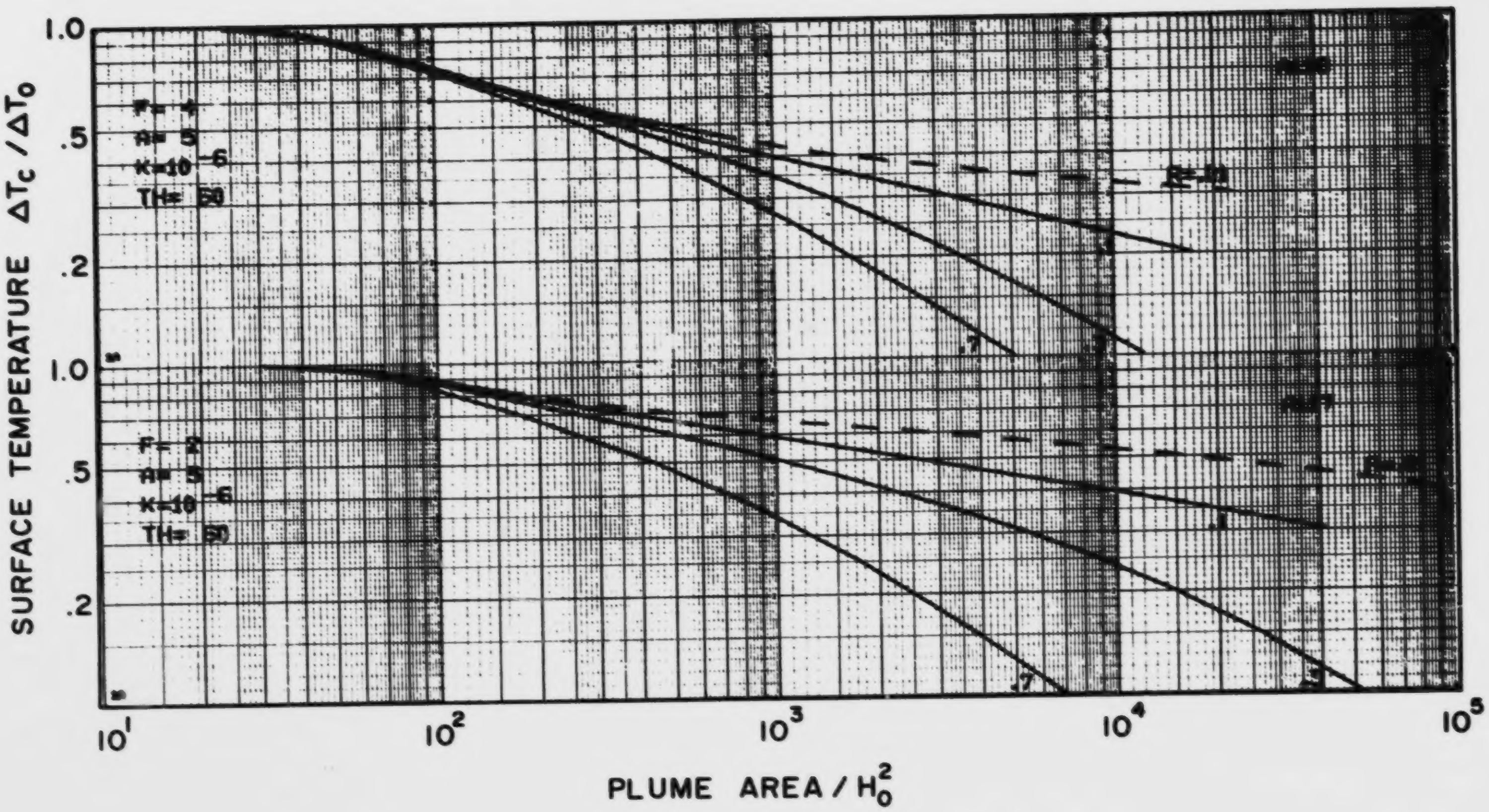

FIG (B 59) TEMPERATURE, AREA (TA)-PLOTS FOR SURFACE JET DISCHARGE

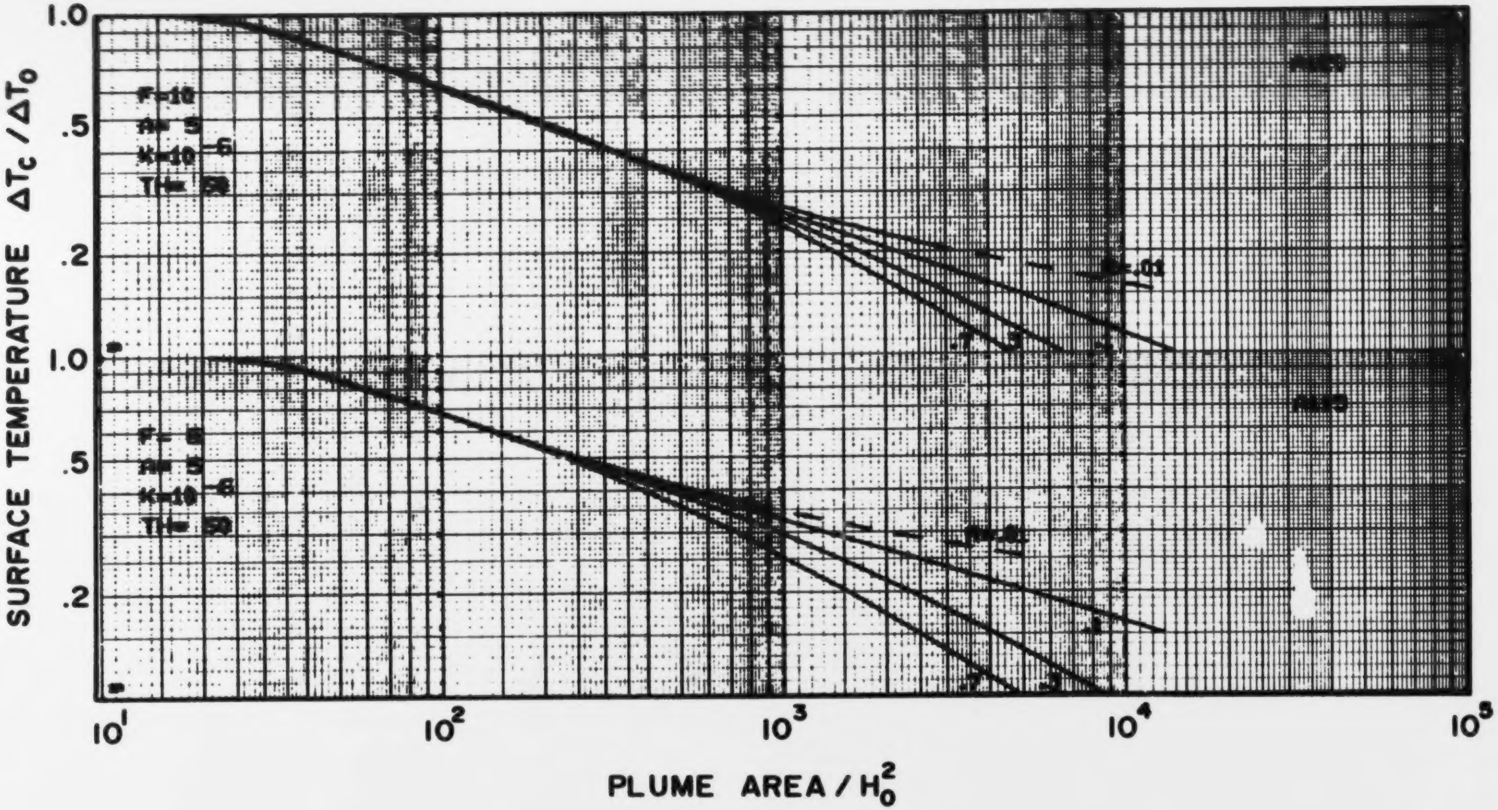

FIG (B60) TEMPERATURE, AREA (TA)-PLOTS FOR SURFACE JET DISCHARGE

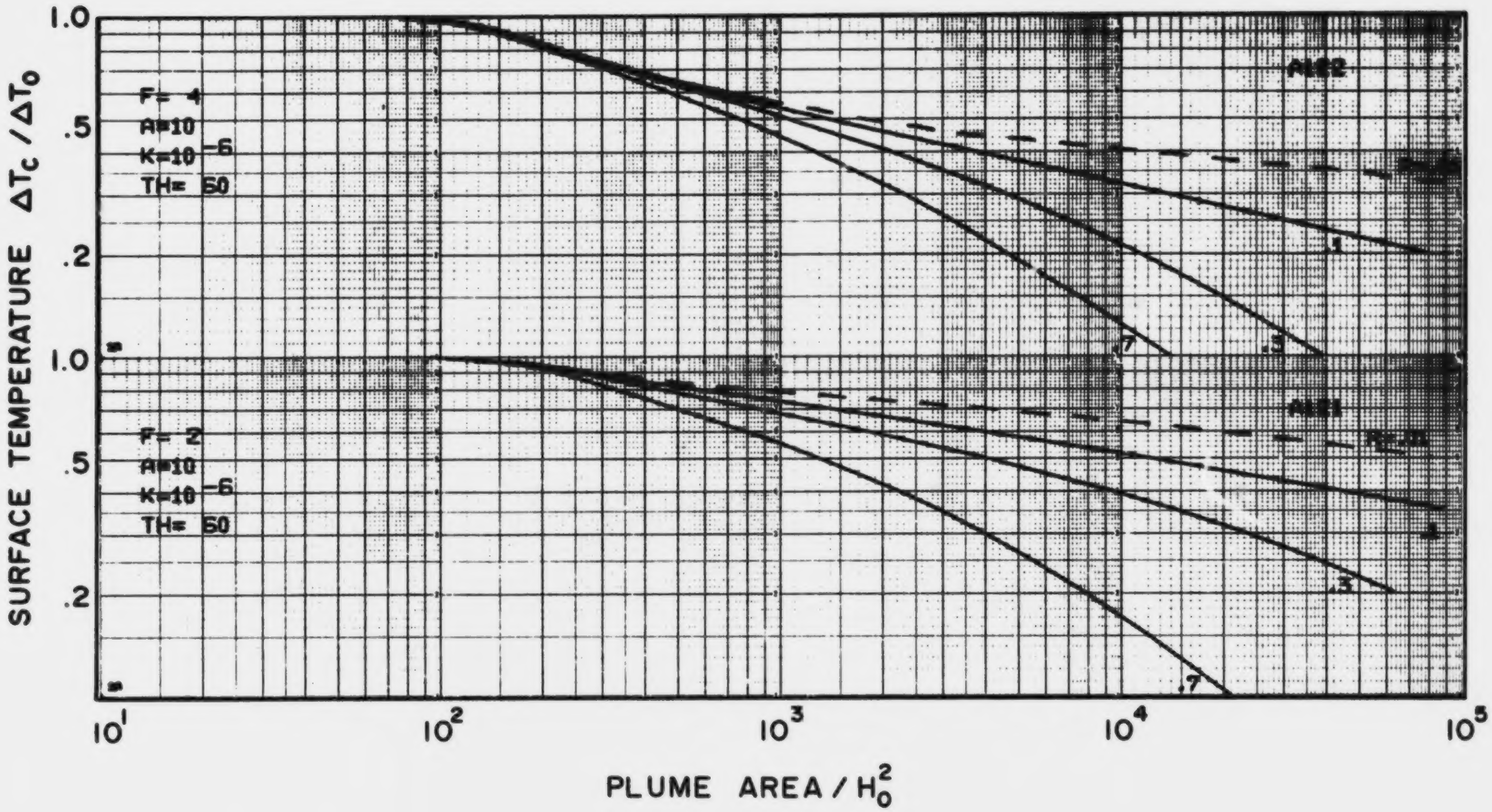

FIG (B 61) TEMPERATURE, AREA (TA)-PLOTS
FOR SURFACE JET DISCHARGE

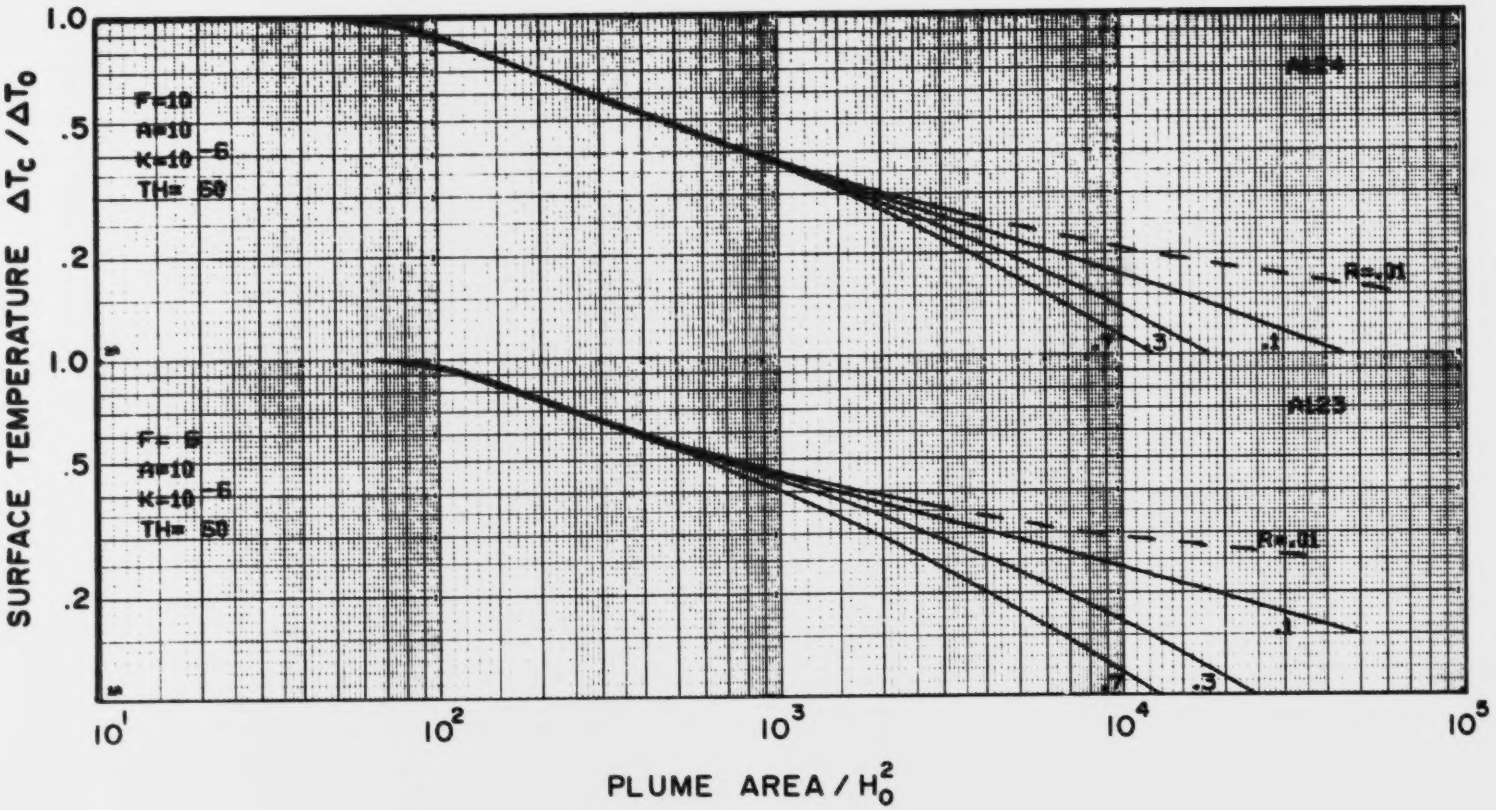

FIG (B62) TEMPERATURE, AREA (TA)-PLOTS
FOR SURFACE JET DISCHARGE

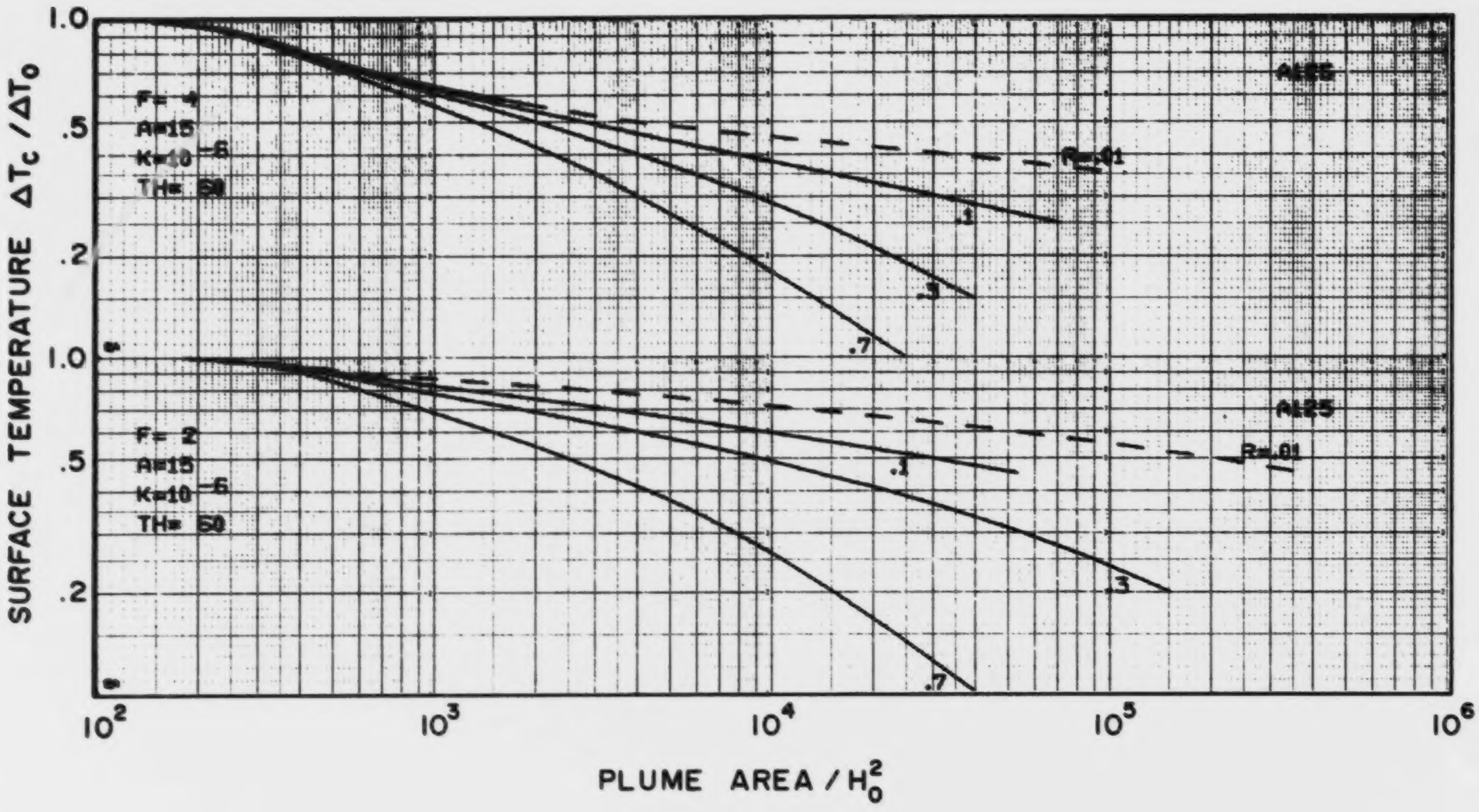

FIG (B63) TEMPERATURE, AREA (TA)-PLOTS
FOR SURFACE JET DISCHARGE

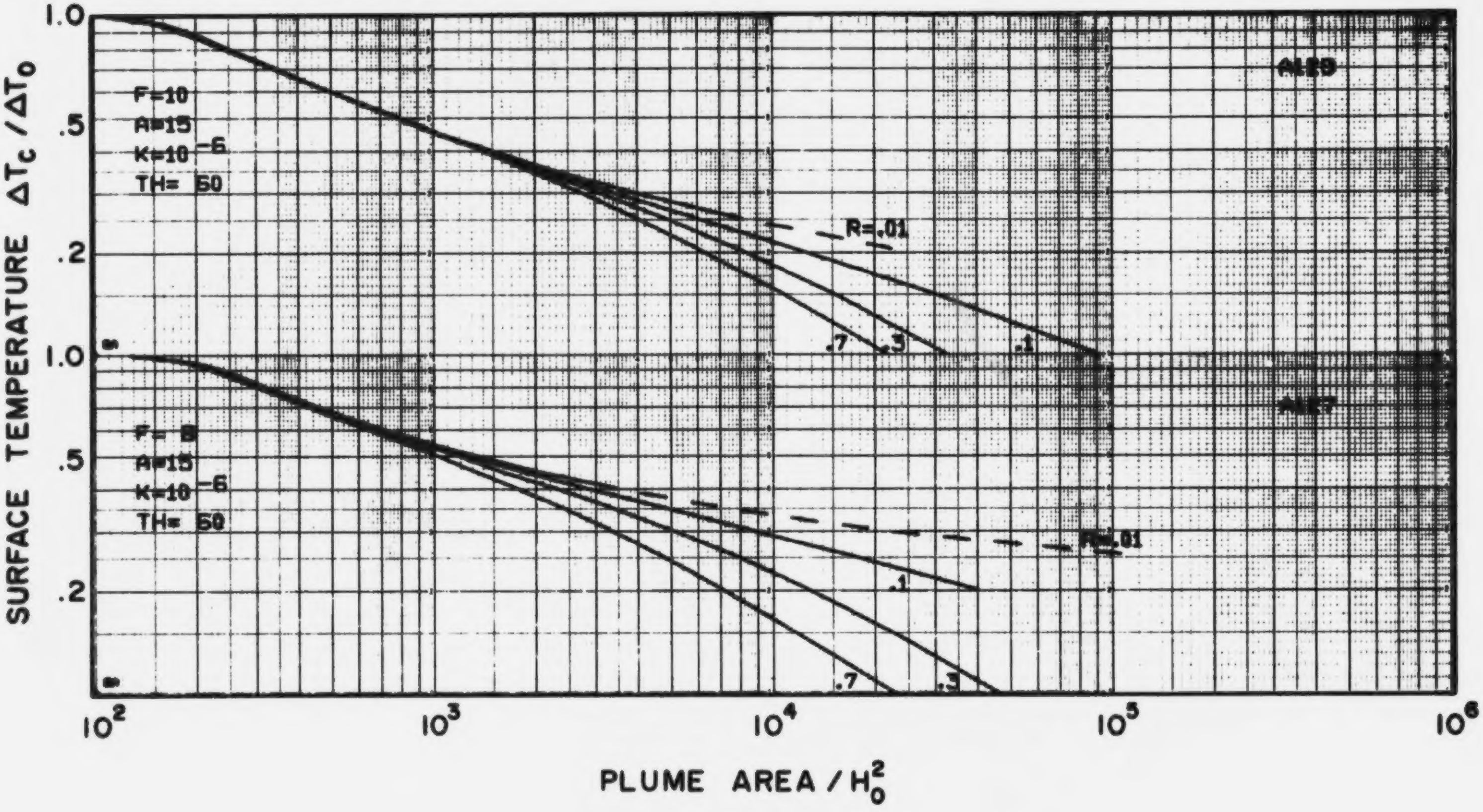

FIG (B64) TEMPERATURE, AREA (TA)-PLOTS FOR SURFACE JET DISCHARGE

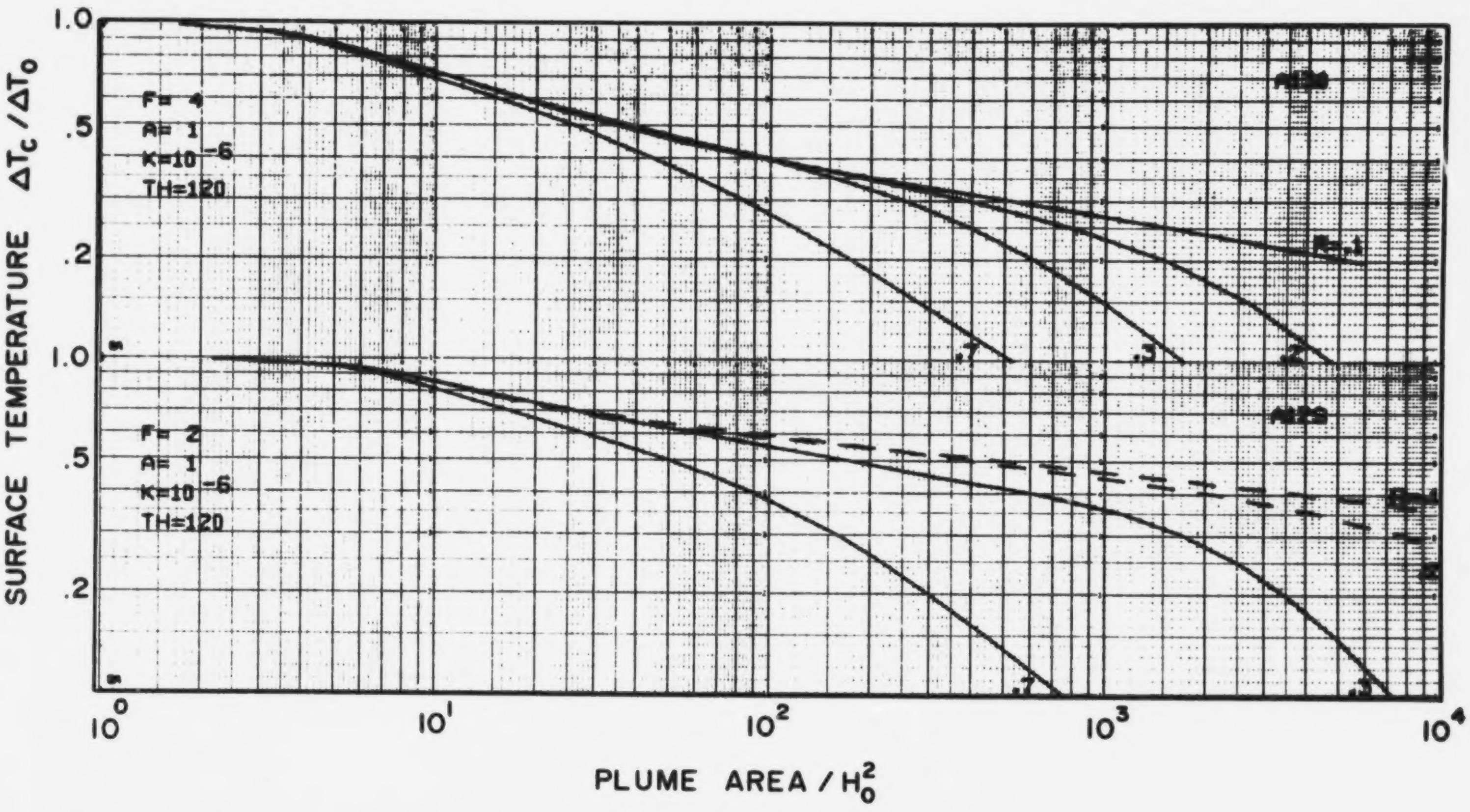

FIG(B65) TEMPERATURE, AREA (TA)-PLOT FOR SURFACE JET DISCHARGE

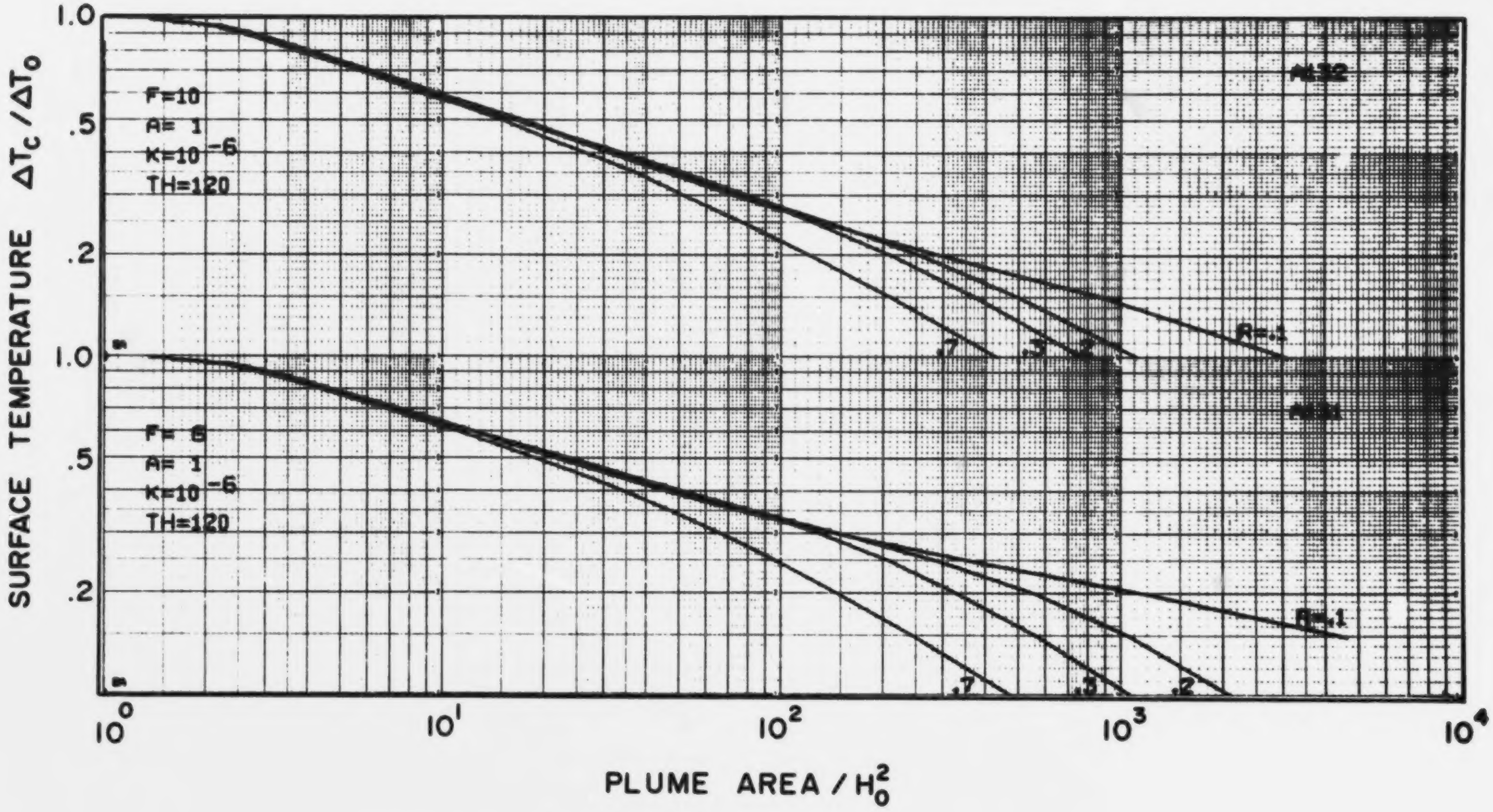

FIG(B66) TEMPERATURE, AREA (TA)-PLOT
FOR SURFACE JET DISCHARGE

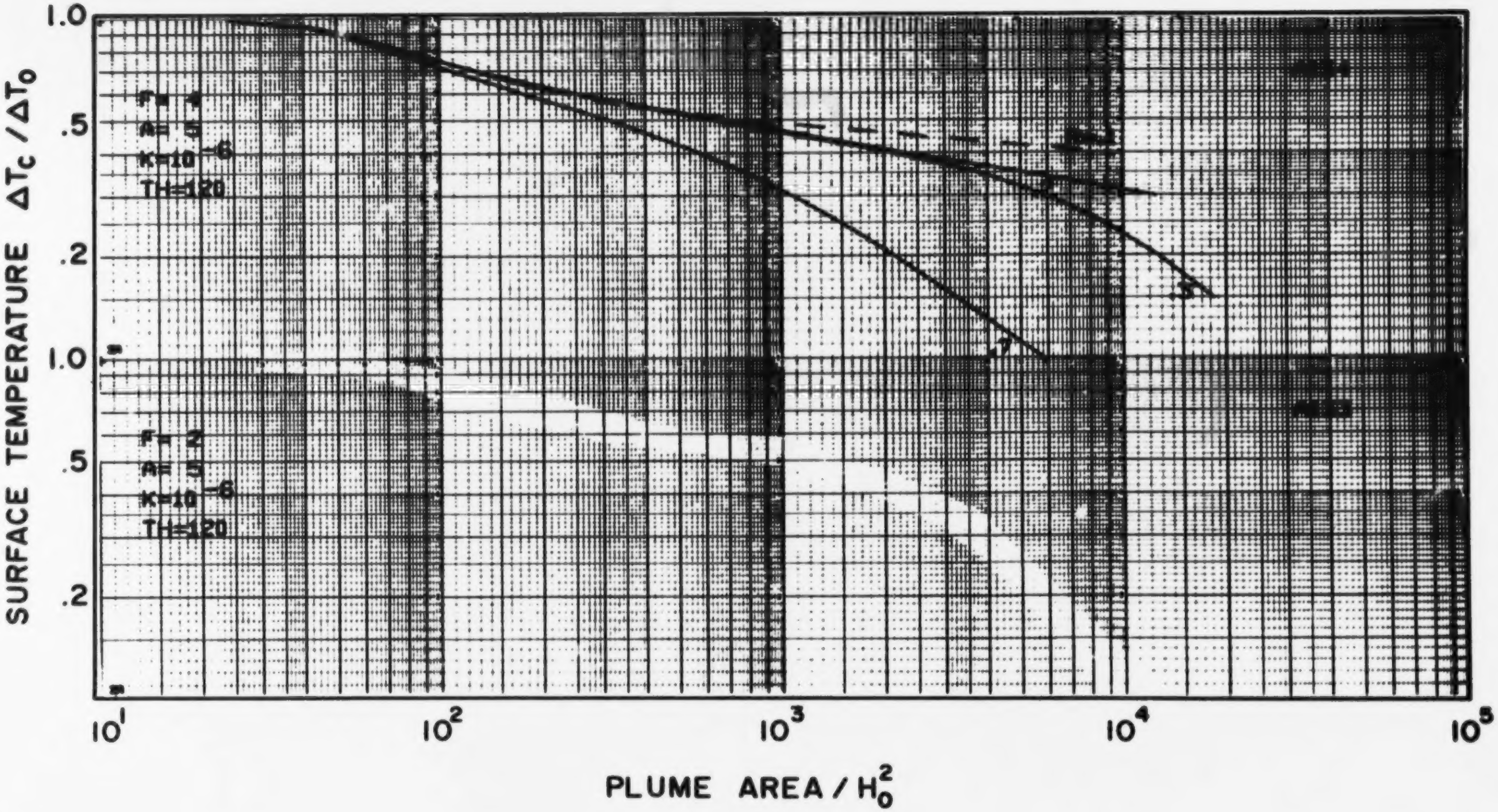

FIG (B67) TEMPERATURE, AREA (TA)-PLOTS FOR SURFACE JET DISCHARGE

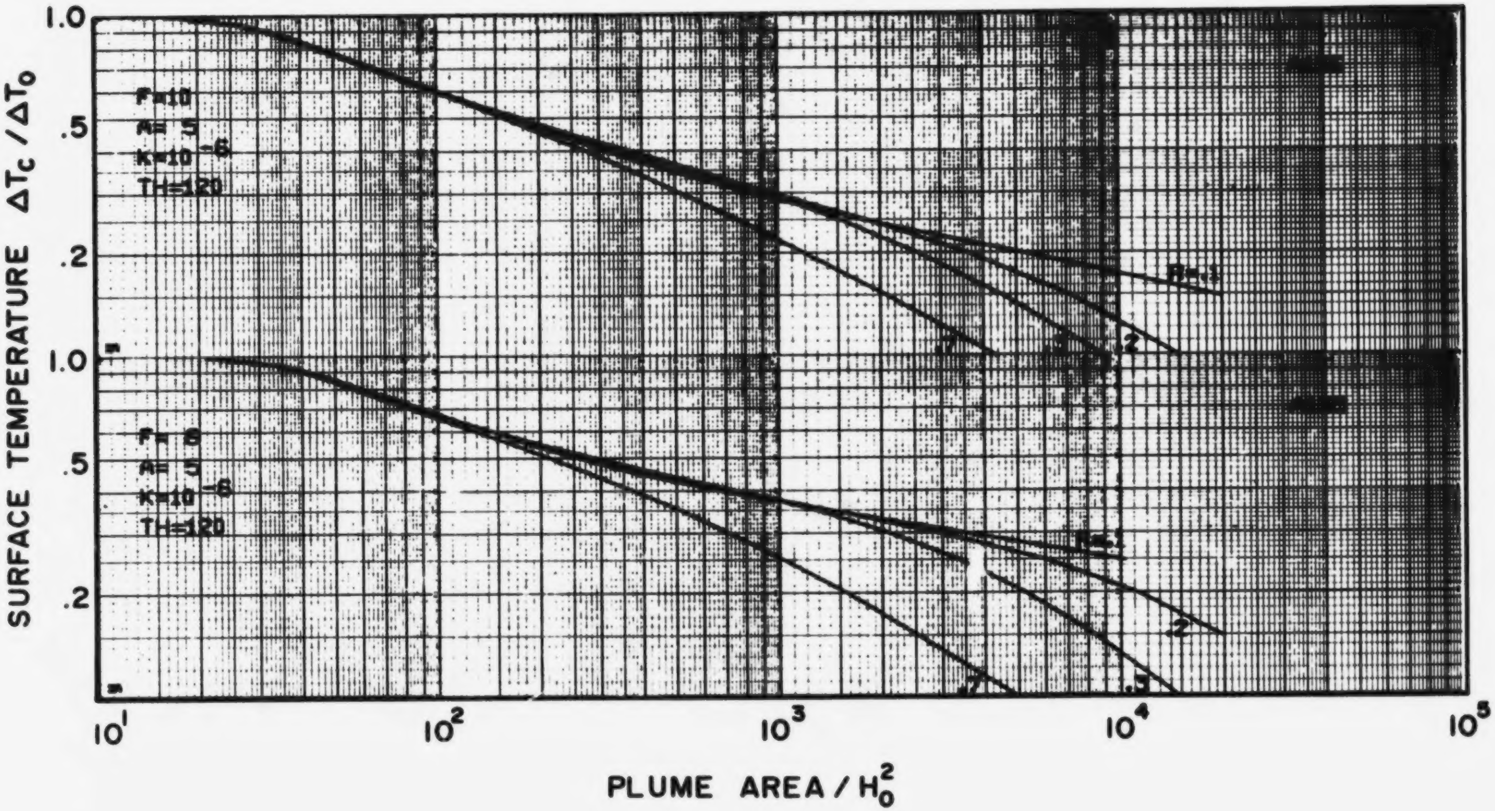

FIG (B68) TEMPERATURE, AREA (TA)-PLOTS FOR SURFACE JET DISCHARGE

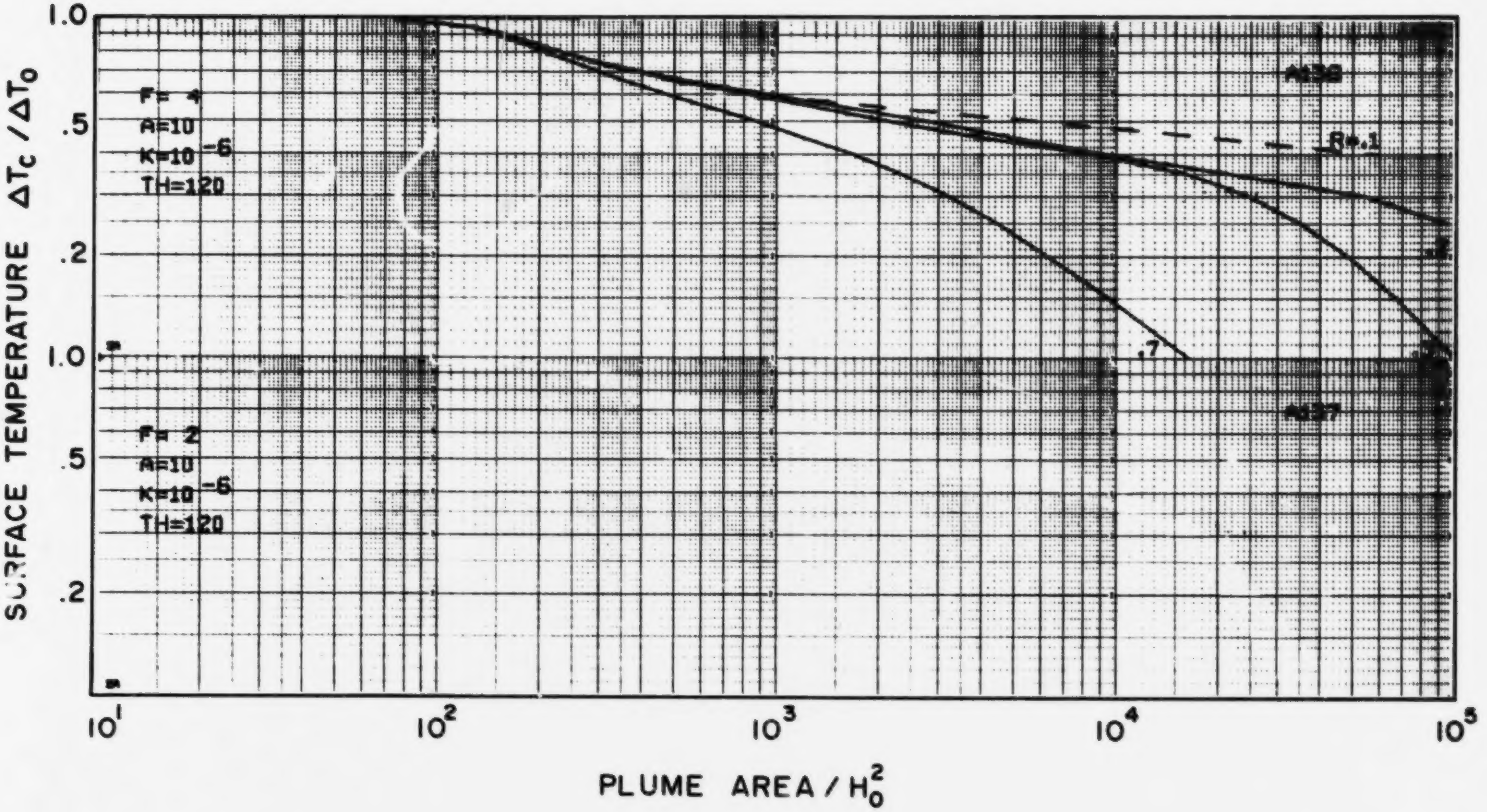

FIG (B69) TEMPERATURE, AREA (TA)-PLOTS FOR SURFACE JET DISCHARGE

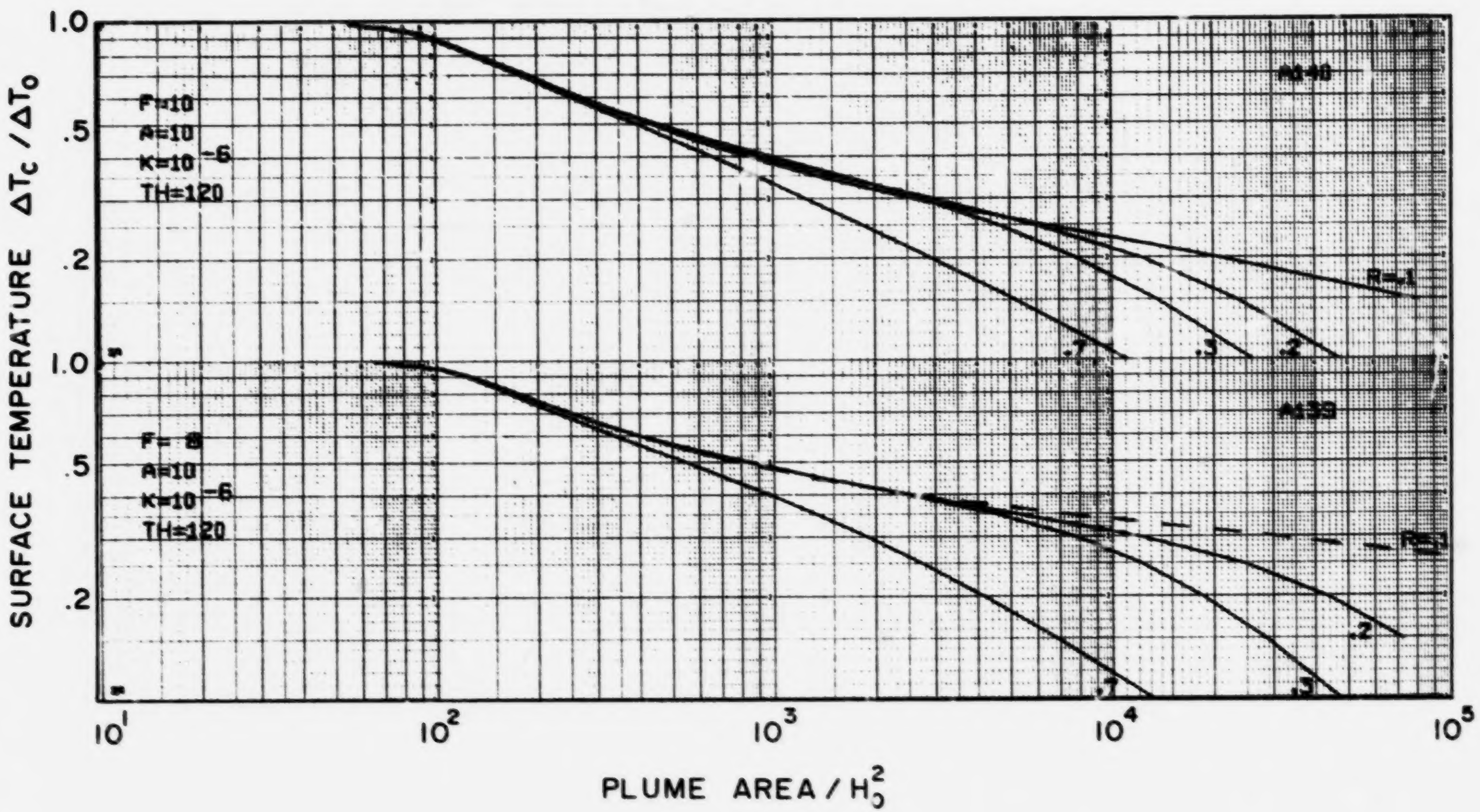

FIG (B 70) TEMPERATURE, AREA (TA)-PLOTS FOR SURFACE JET DISCHARGE

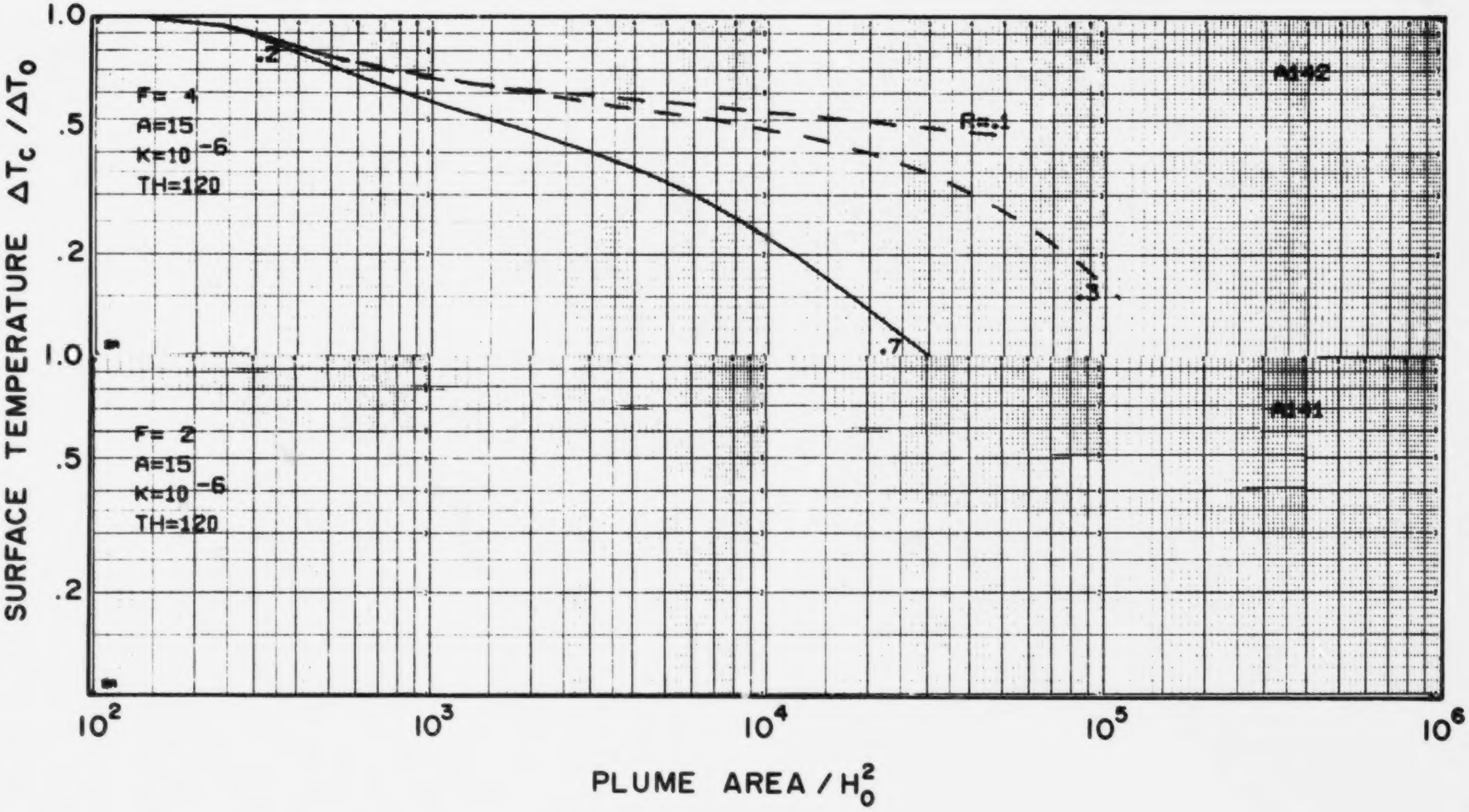

FIG (B71) TEMPERATURE, AREA (TA)-PLOTS FOR SURFACE JET DISCHARGE

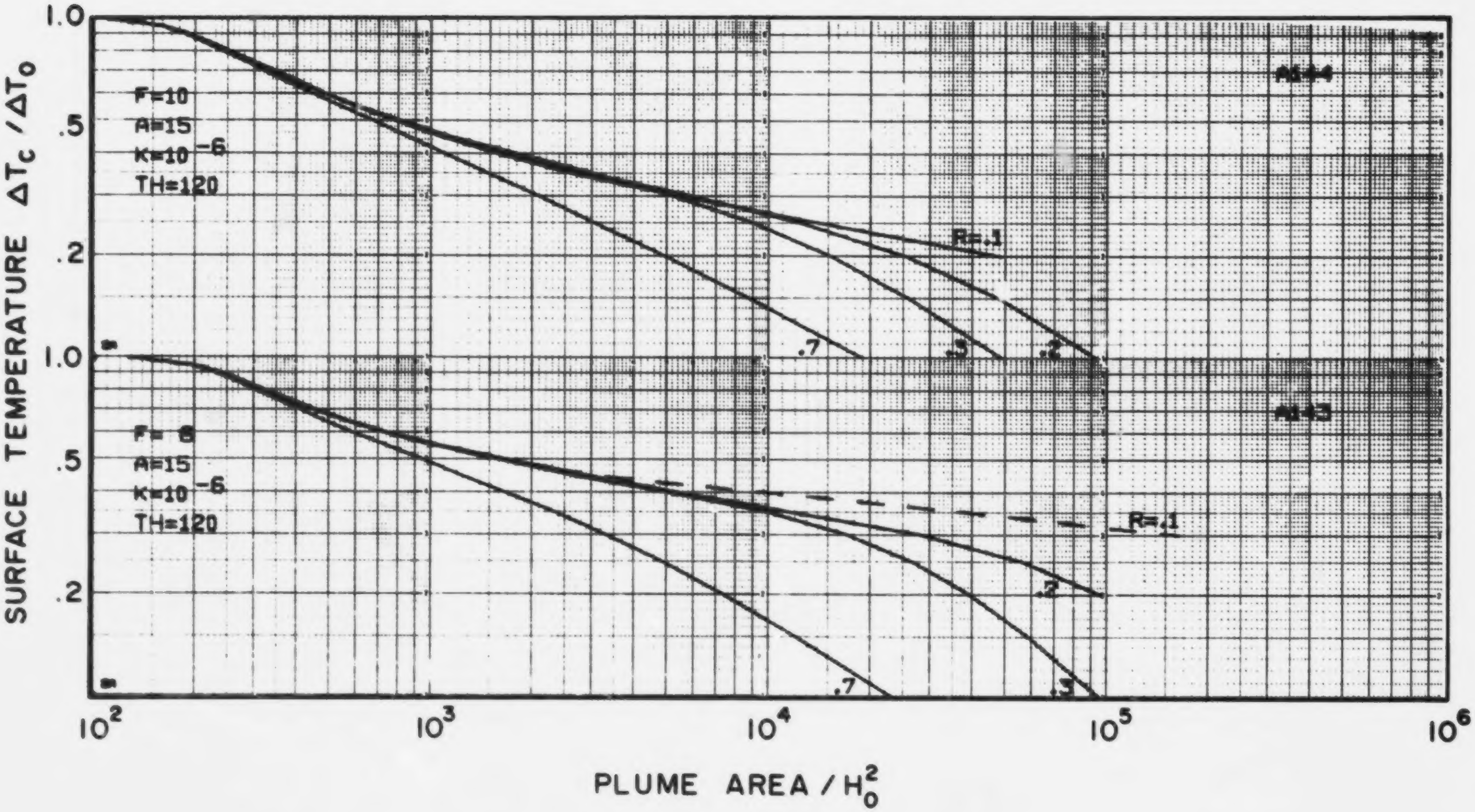

FIG (B 72) TEMPERATURE, AREA (TA)-PLOTS
FOR SURFACE JET DISCHARGE

APPENDIX C
(Tt) WORKING NOMOGRAMS

TABLE 5

Figure Numbers for (Tt) Working Nomograms of Appendix C, $\Theta_o = 90°$, $K = 10^{-5}$

F→ ↓A	2	4	6	10
1	C1	C1	C2	C2
5	C3	C3	C4	C4
10	C5	C5	C6	C6
15	C7	C7	C8	C8

TABLE 6

Summary of Figure Numbers for (Tt) Working Nomograms of Appendix C

Θ_o → ↓K	90°	60°	120°
10^{-5}	C1- 8	C9-C16	C17-C24
10^{-4}	C25-C32	C33-C40	C41-C48
10^{-6}	C49-C56	C57-C64	C65-C72

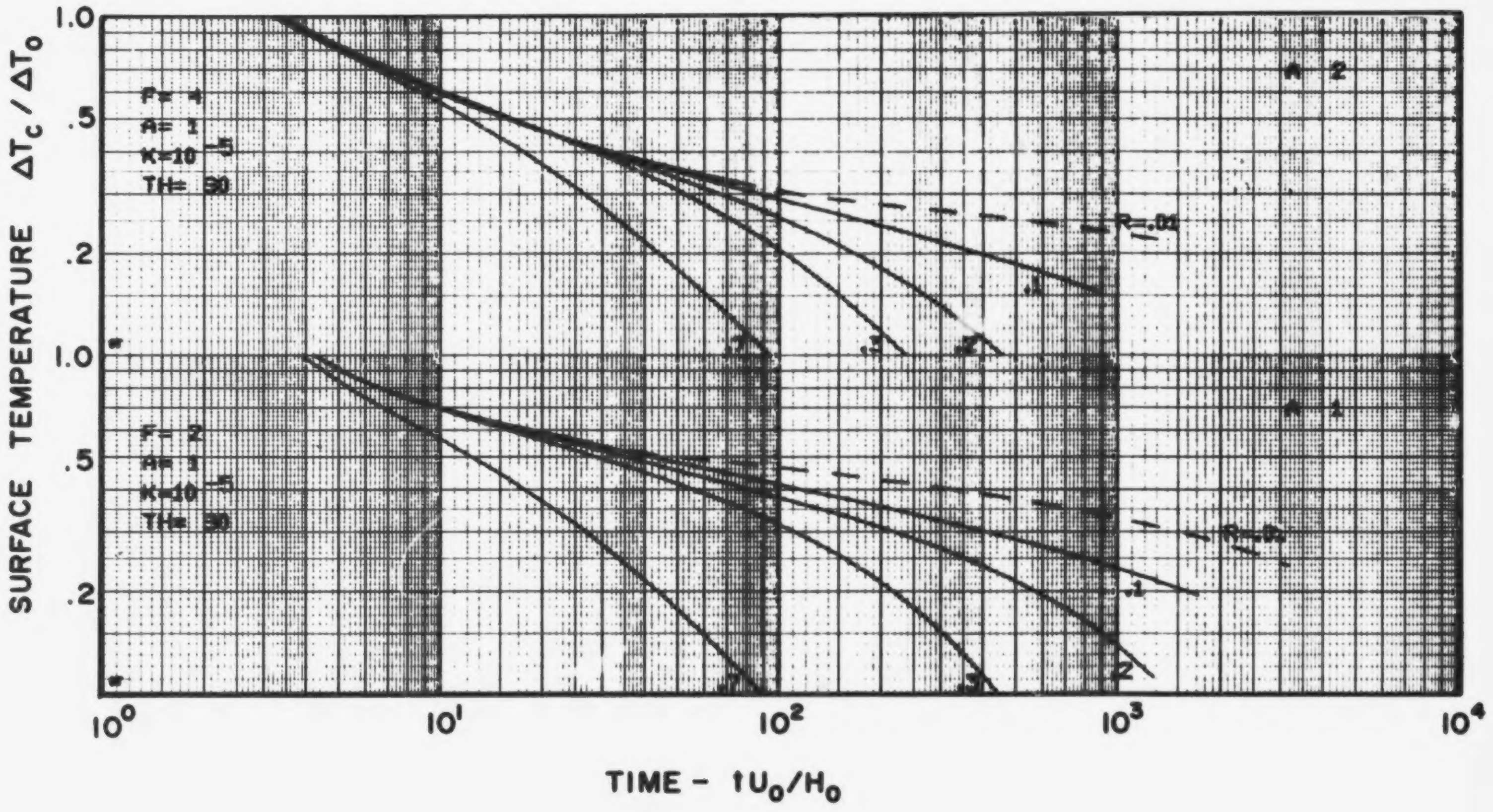

FIG (C1) TEMPERATURE, TIME ~~(Tt)~~-PLOTS
FOR SURFACE JET DISCHARGE

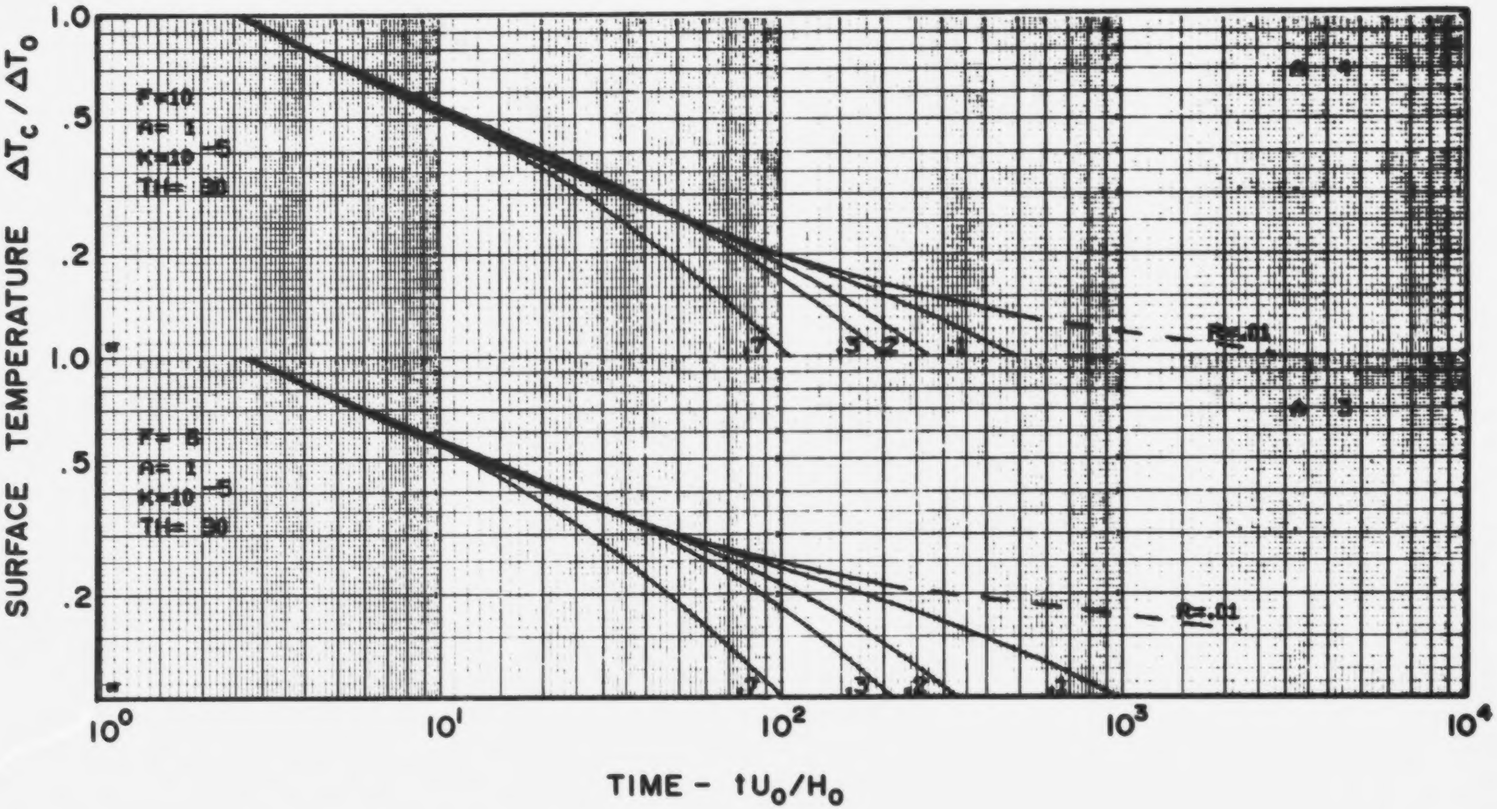

FIG (C2) TEMPERATURE, TIME (Tt)-PLOTS
FOR SURFACE JET DISCHARGE

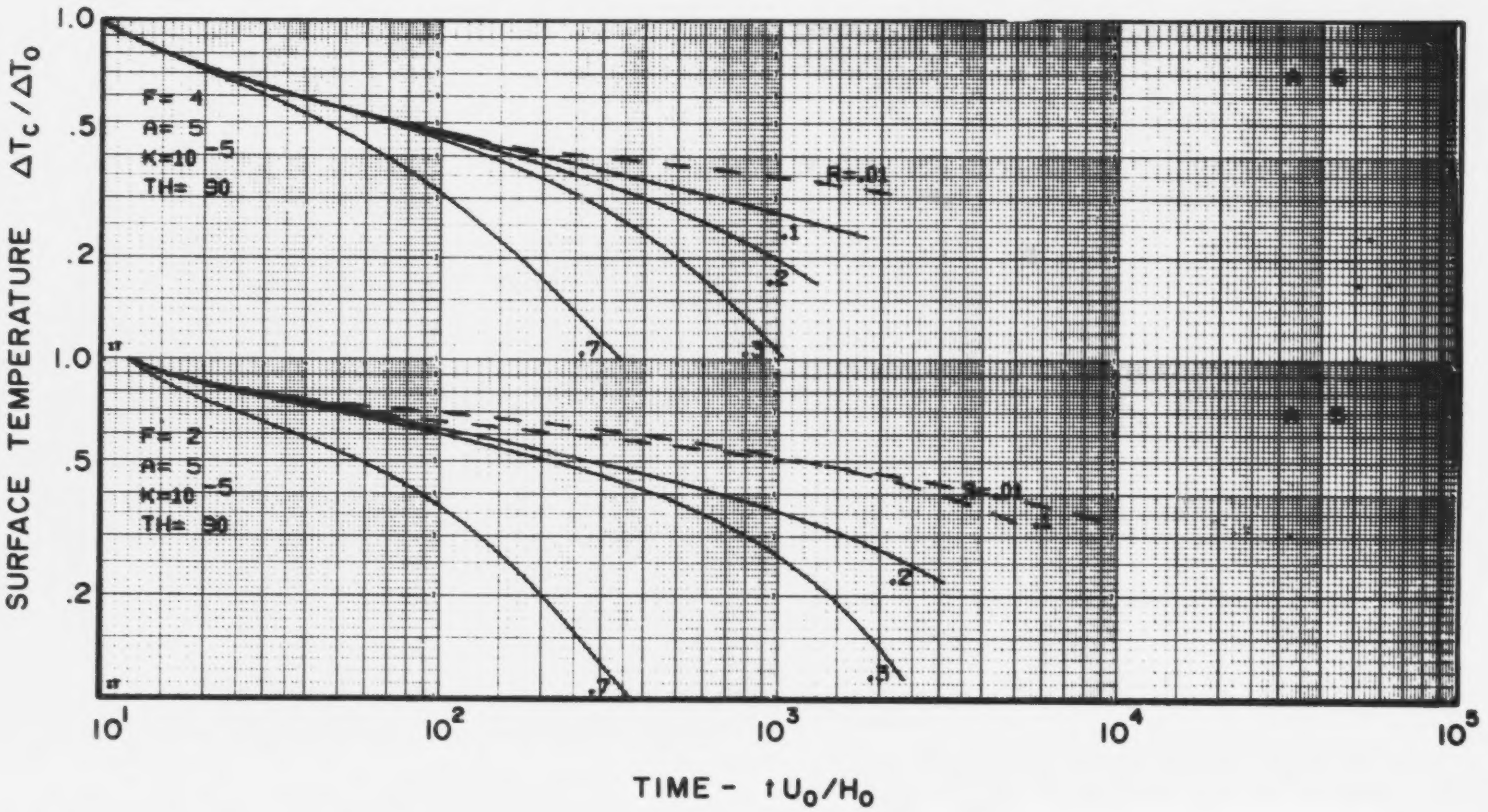

FIG (C3) TEMPERATURE, TIME (Tt)-PLOTS
FOR SURFACE JET DISCHARGE

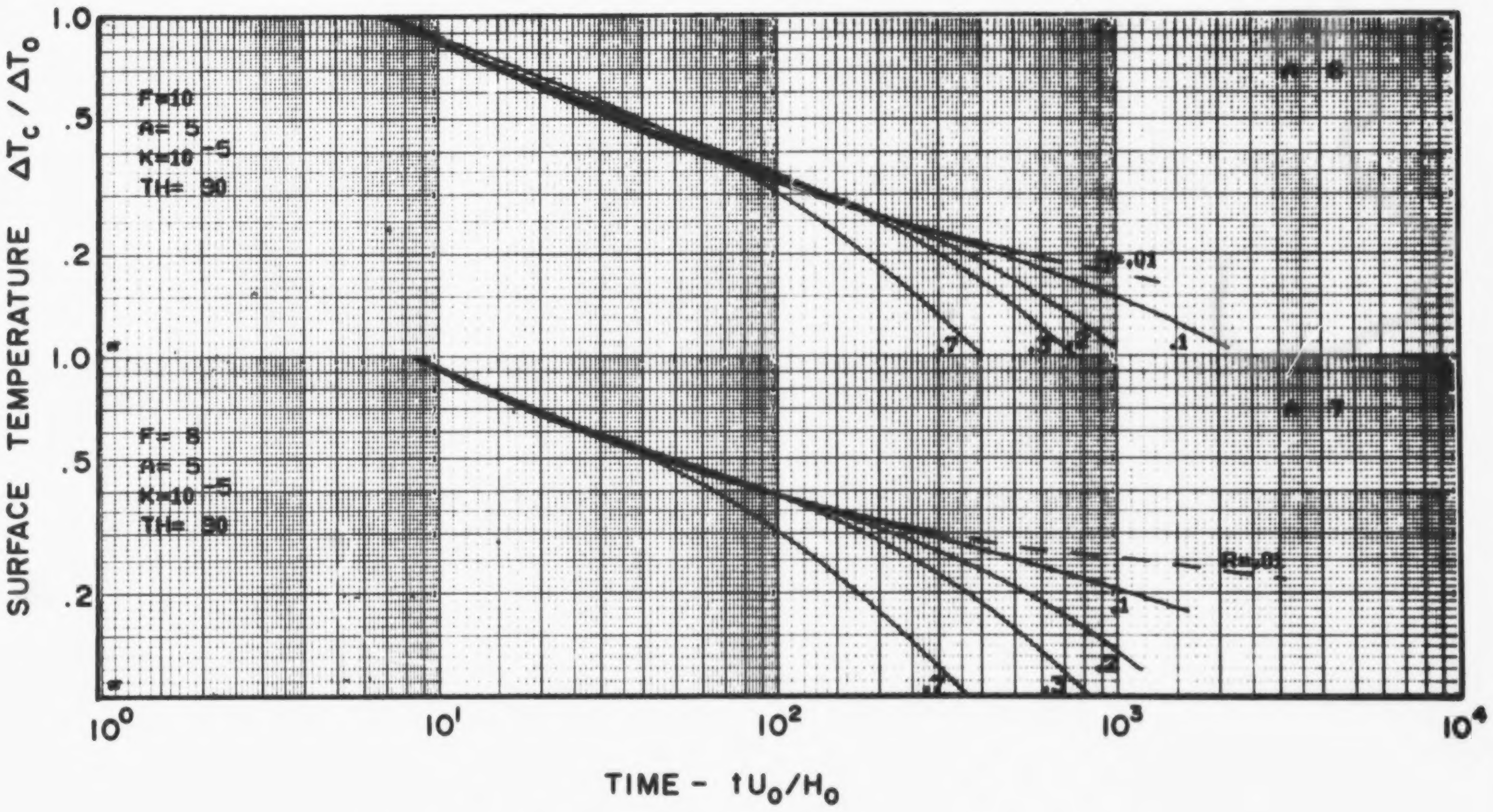

FIG (C4) TEMPERATURE, TIME (Tt)-PLOTS FOR SURFACE JET DISCHARGE

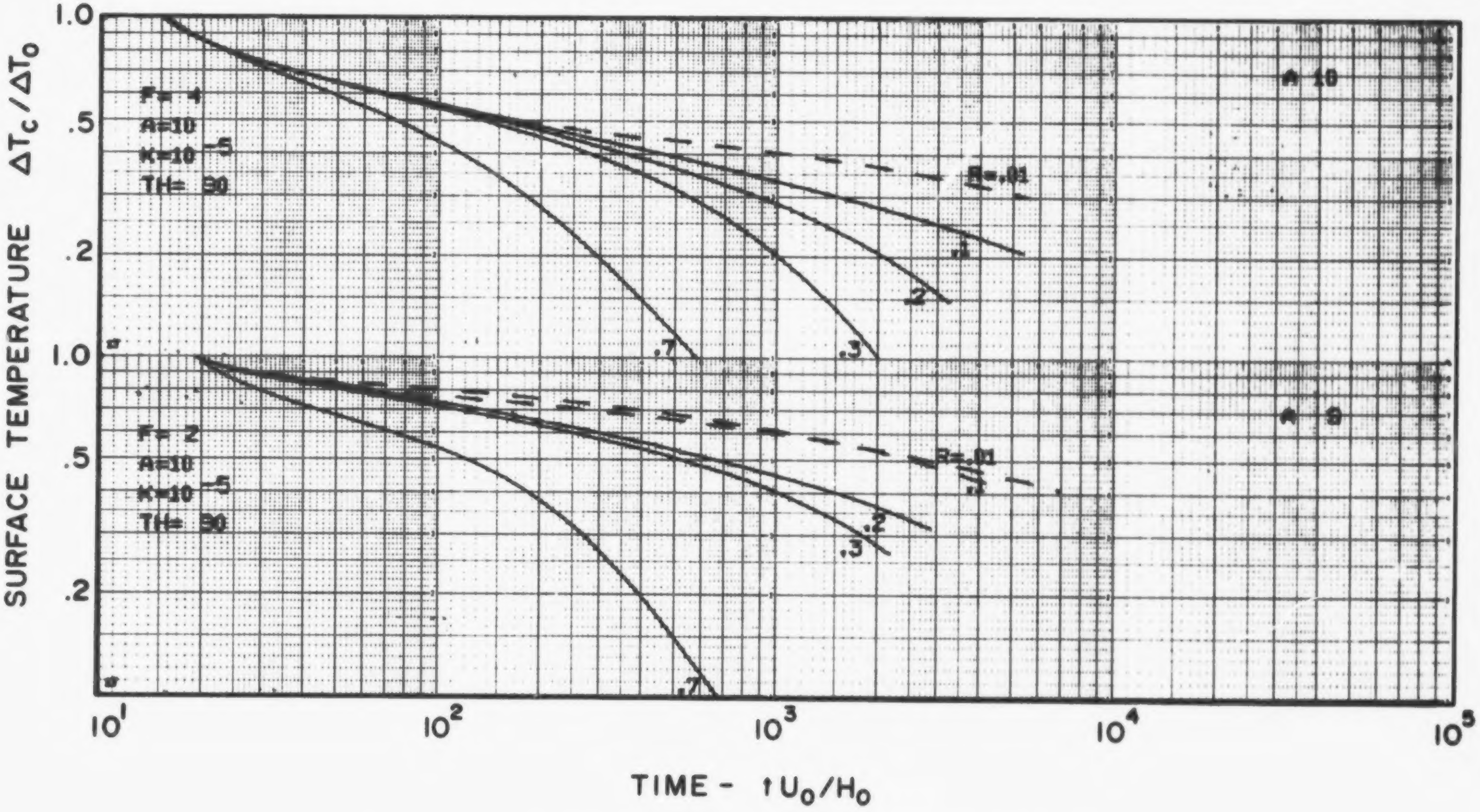

FIG (C5) TEMPERATURE, TIME (Tt)-PLOTS FOR SURFACE JET DISCHARGE

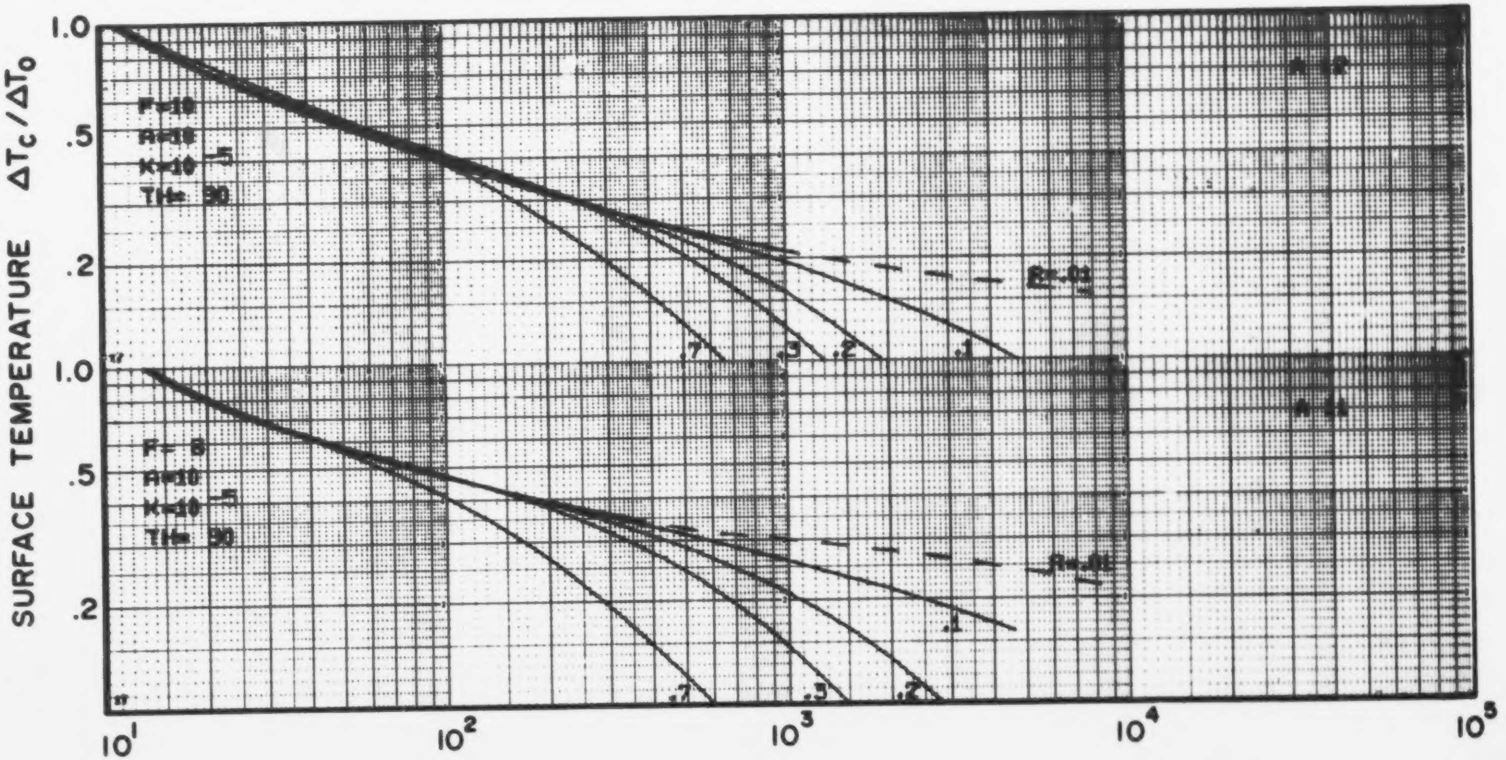

FIG (C6) TEMPERATURE, TIME (Tt)-PLOTS
FOR SURFACE JET DISCHARGE

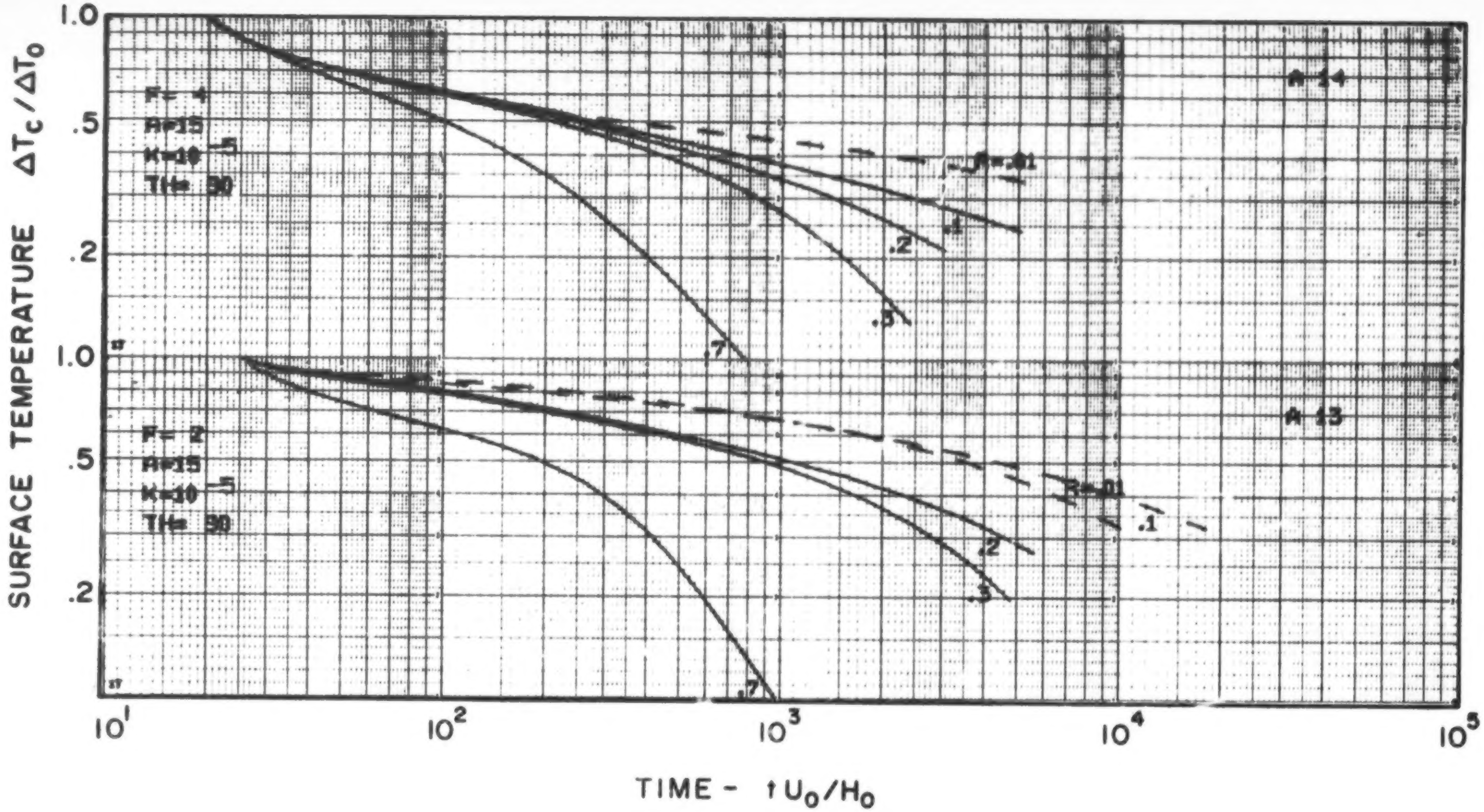

FIG (C7) TEMPERATURE, TIME (Tt)-PLOTS FOR SURFACE JET DISCHARGE

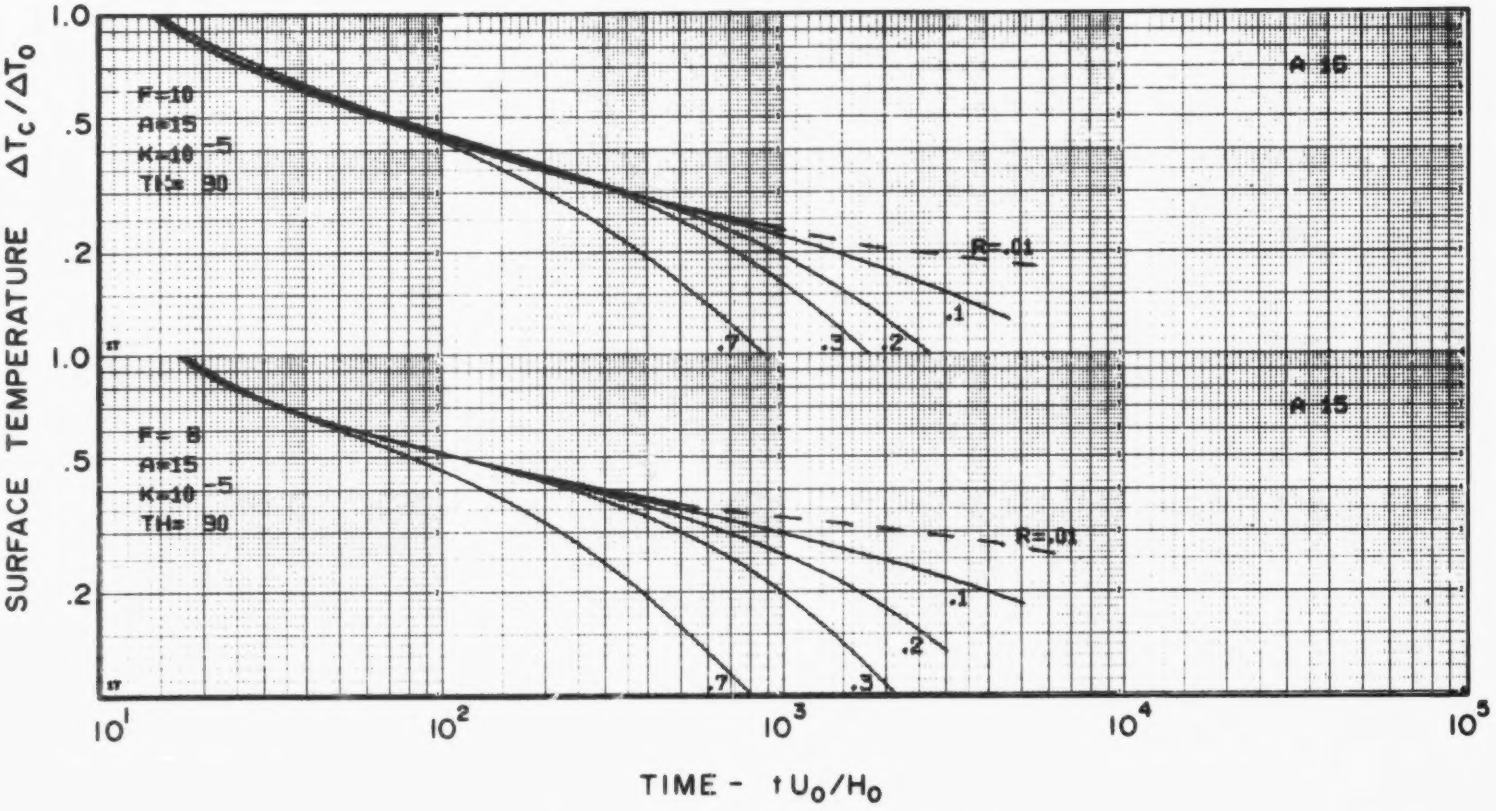

FIG (C8) TEMPERATURE, TIME (Tt)-PLOTS
FOR SURFACE JET DISCHARGE

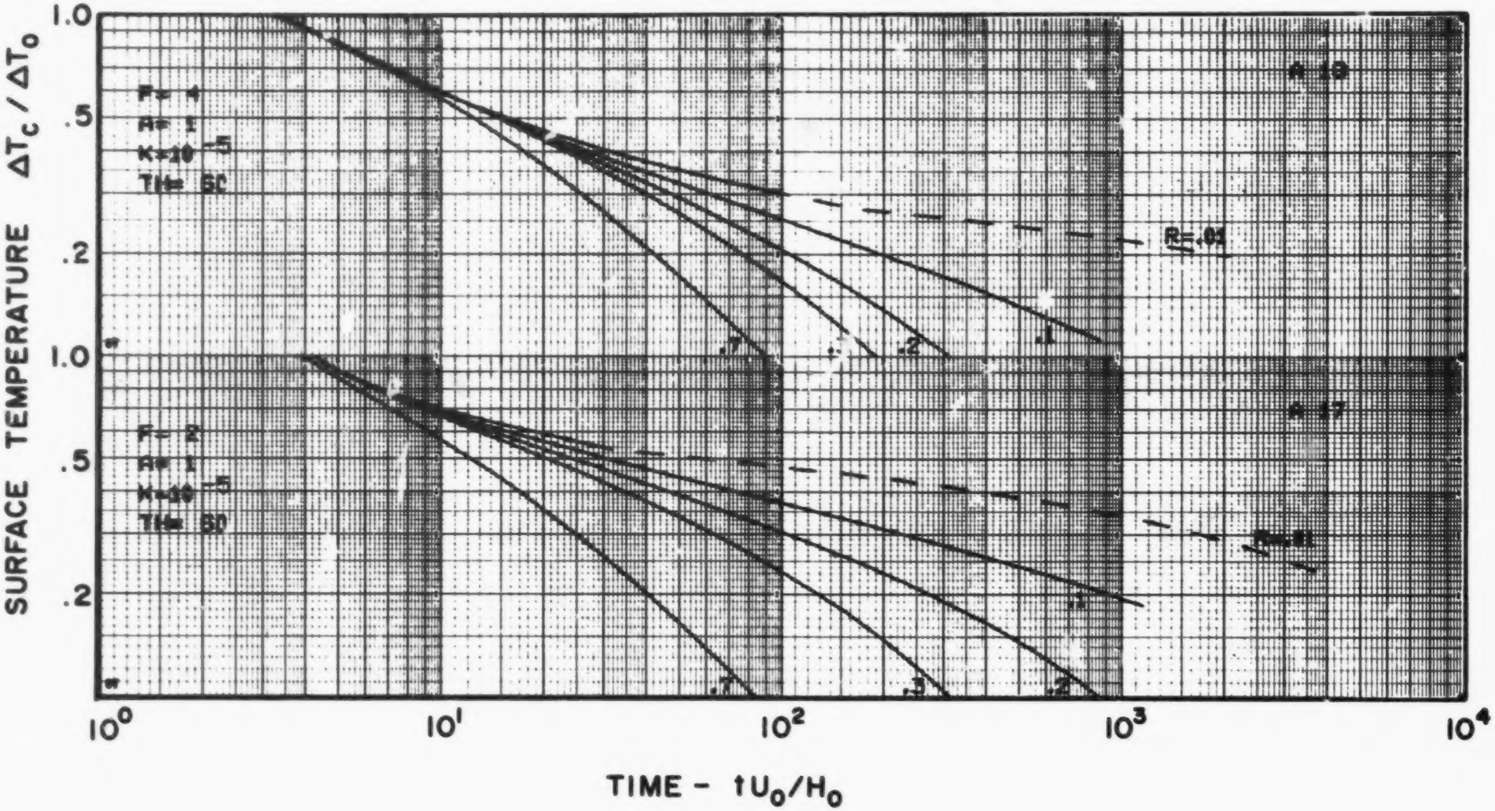

FIG (C9) TEMPERATURE, TIME (Tt)-PLOTS
FOR SURFACE JET DISCHARGE

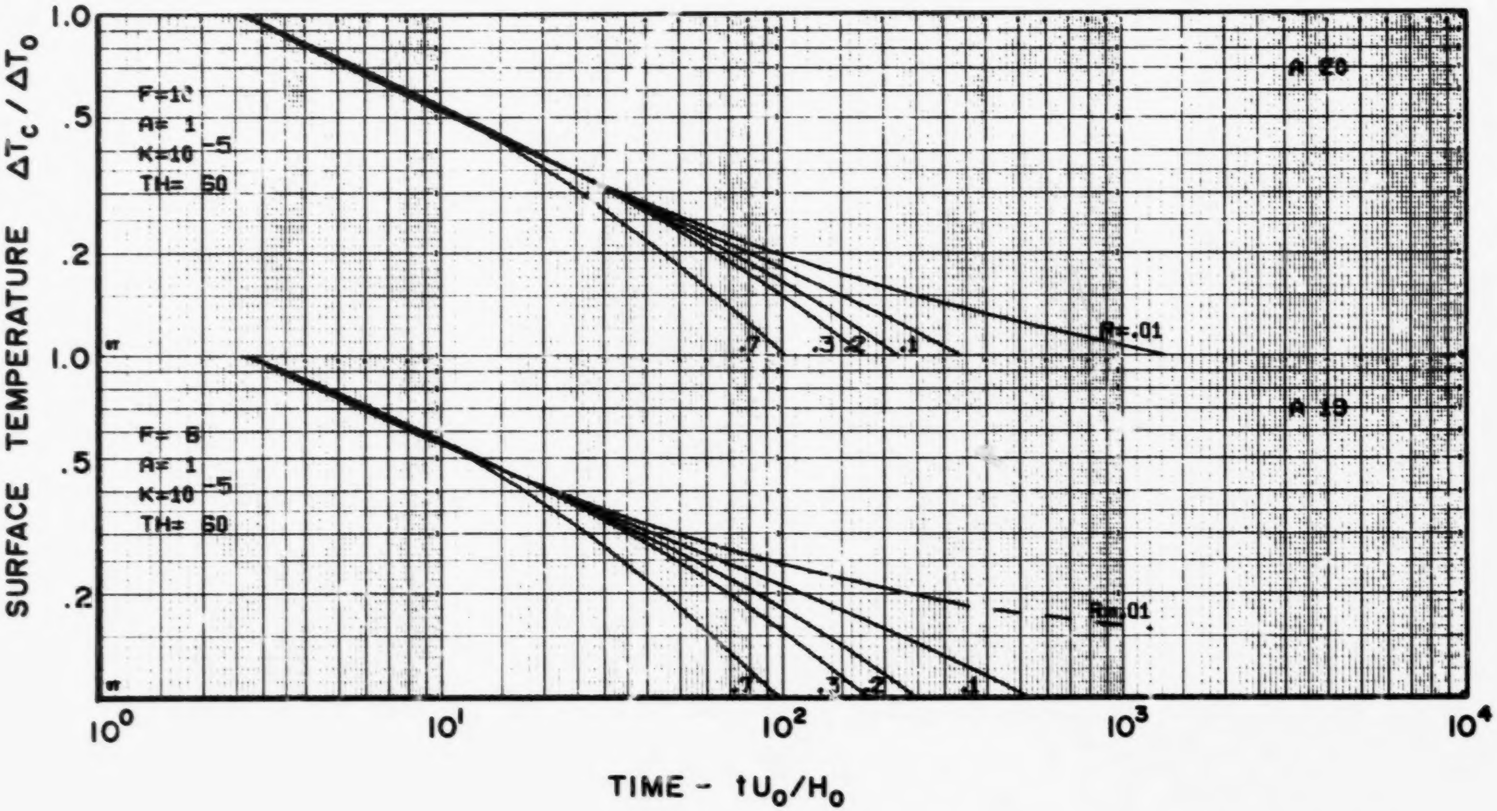

FIG (C 10) TEMPERATURE, TIME (Tt)-PLOTS FOR SURFACE JET DISCHARGE

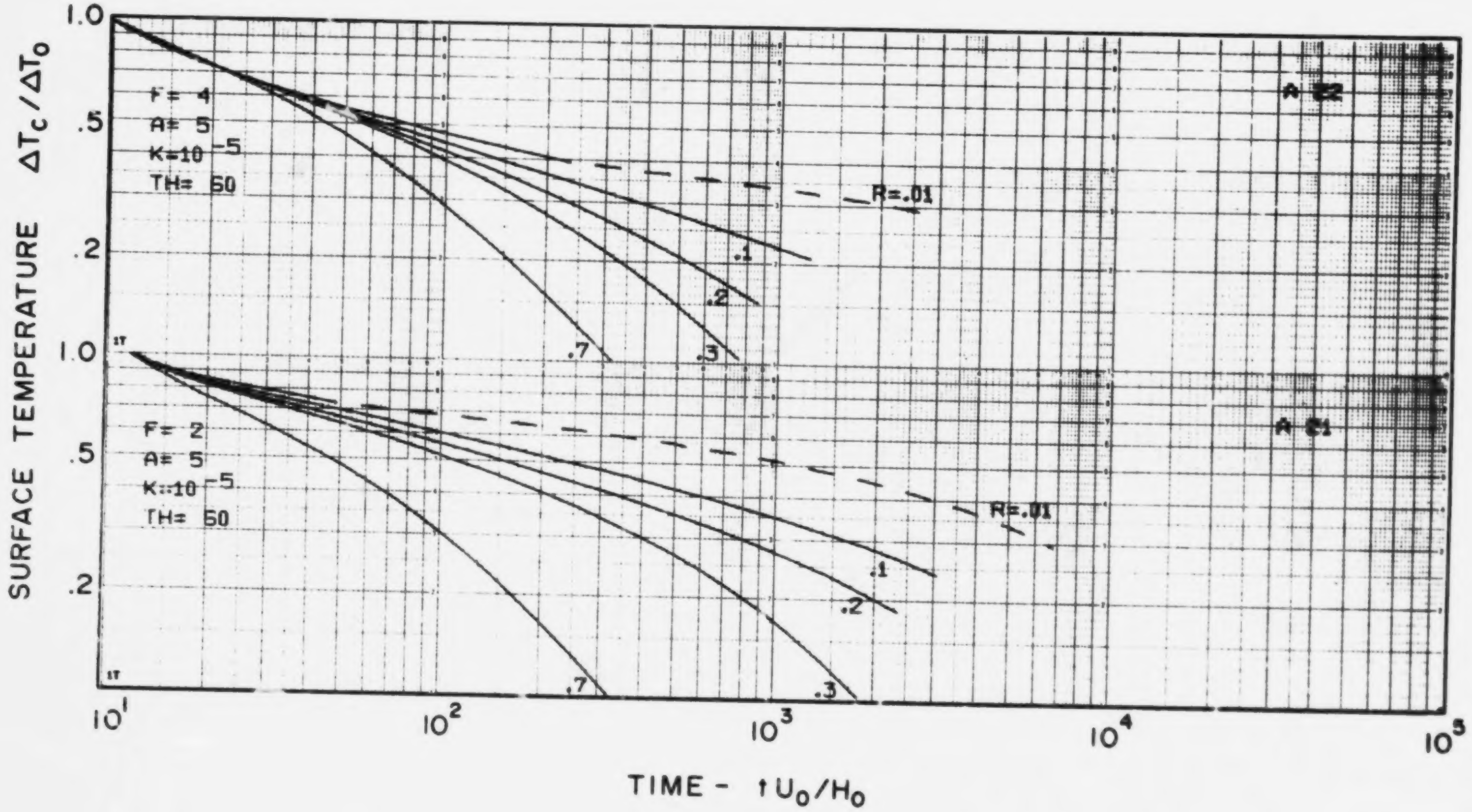

FIG (C11) TEMPERATURE, TIME (Tt)-PLOTS
FOR SURFACE JET DISCHARGE

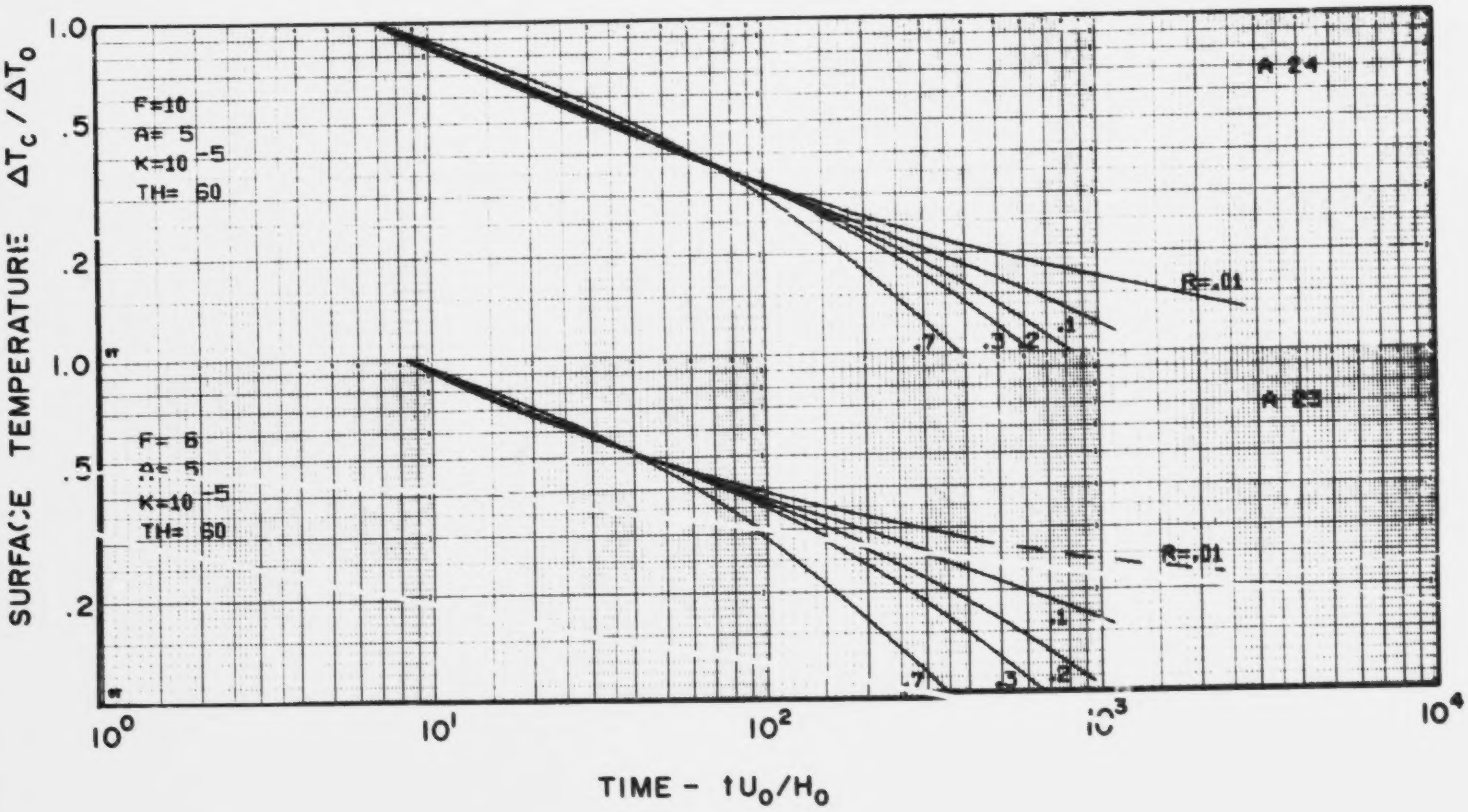

FIG (C12) TEMPERATURE, TIME (Tt)-PLOTS FOR SURFACE JET DISCHARGE

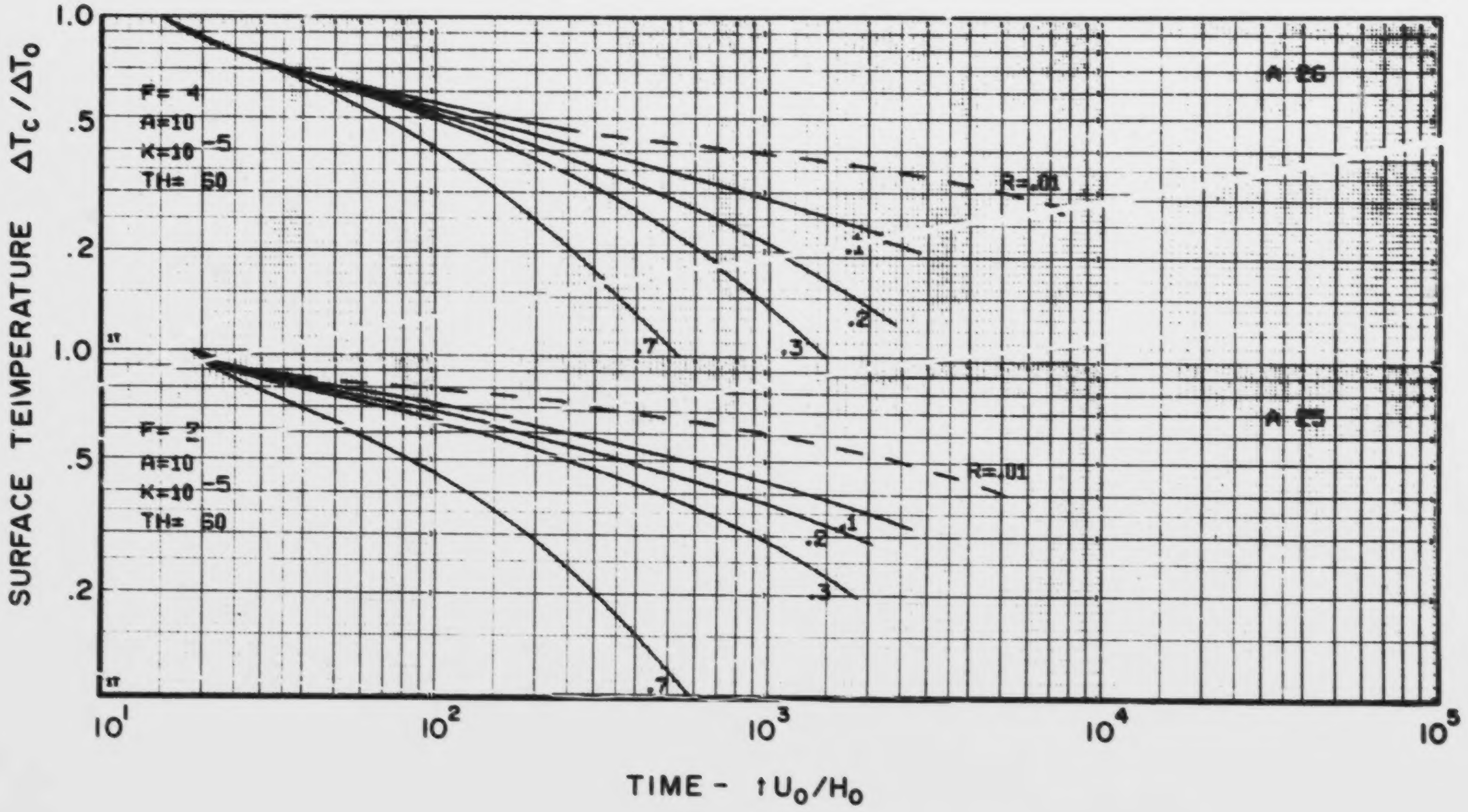

FIG (C13) TEMPERATURE, TIME (Tt)-PLOTS FOR SURFACE JET DISCHARGE

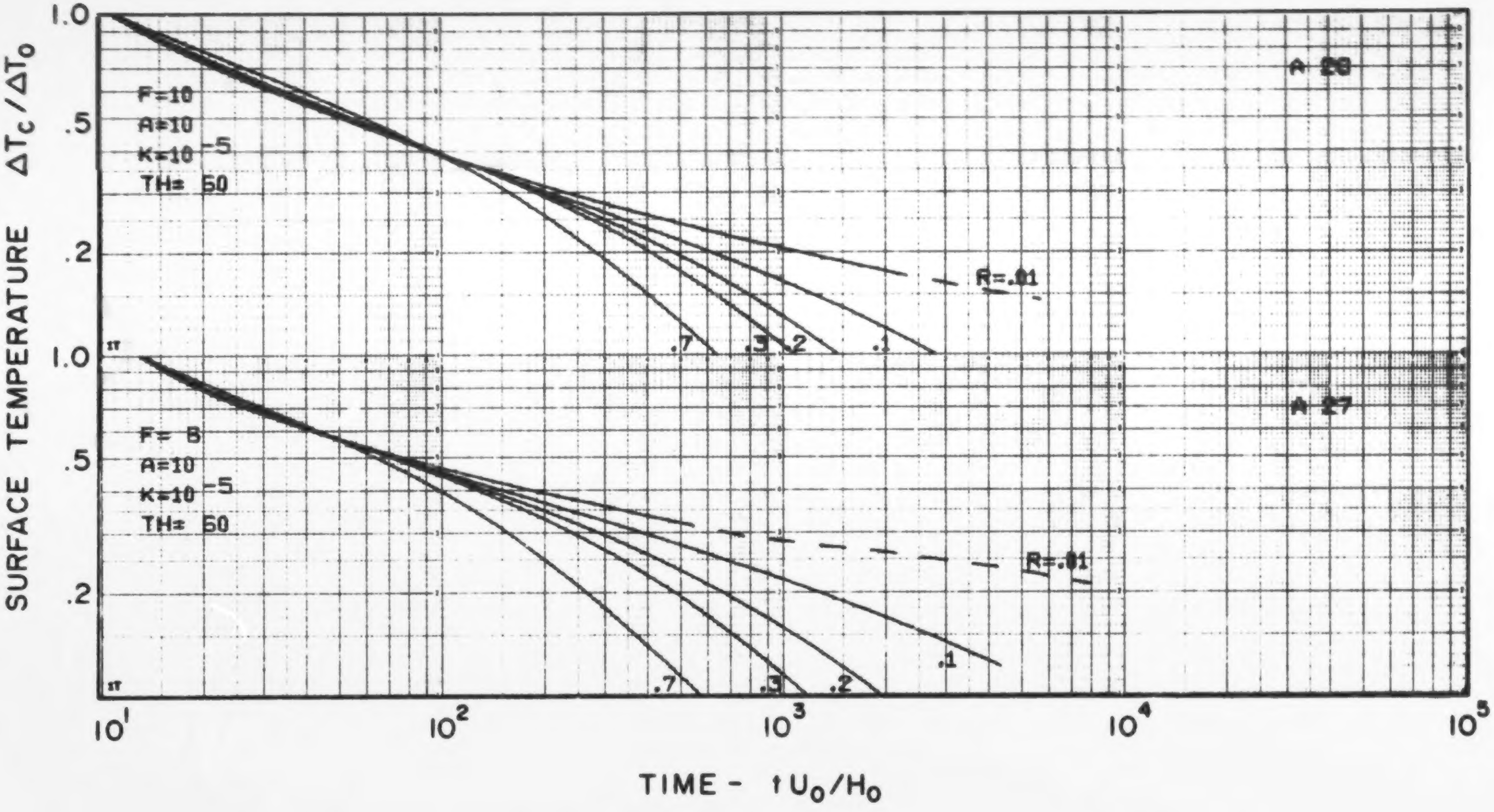

FIG (C14) TEMPERATURE, TIME (Tt)-PLOTS
FOR SURFACE JET DISCHARGE

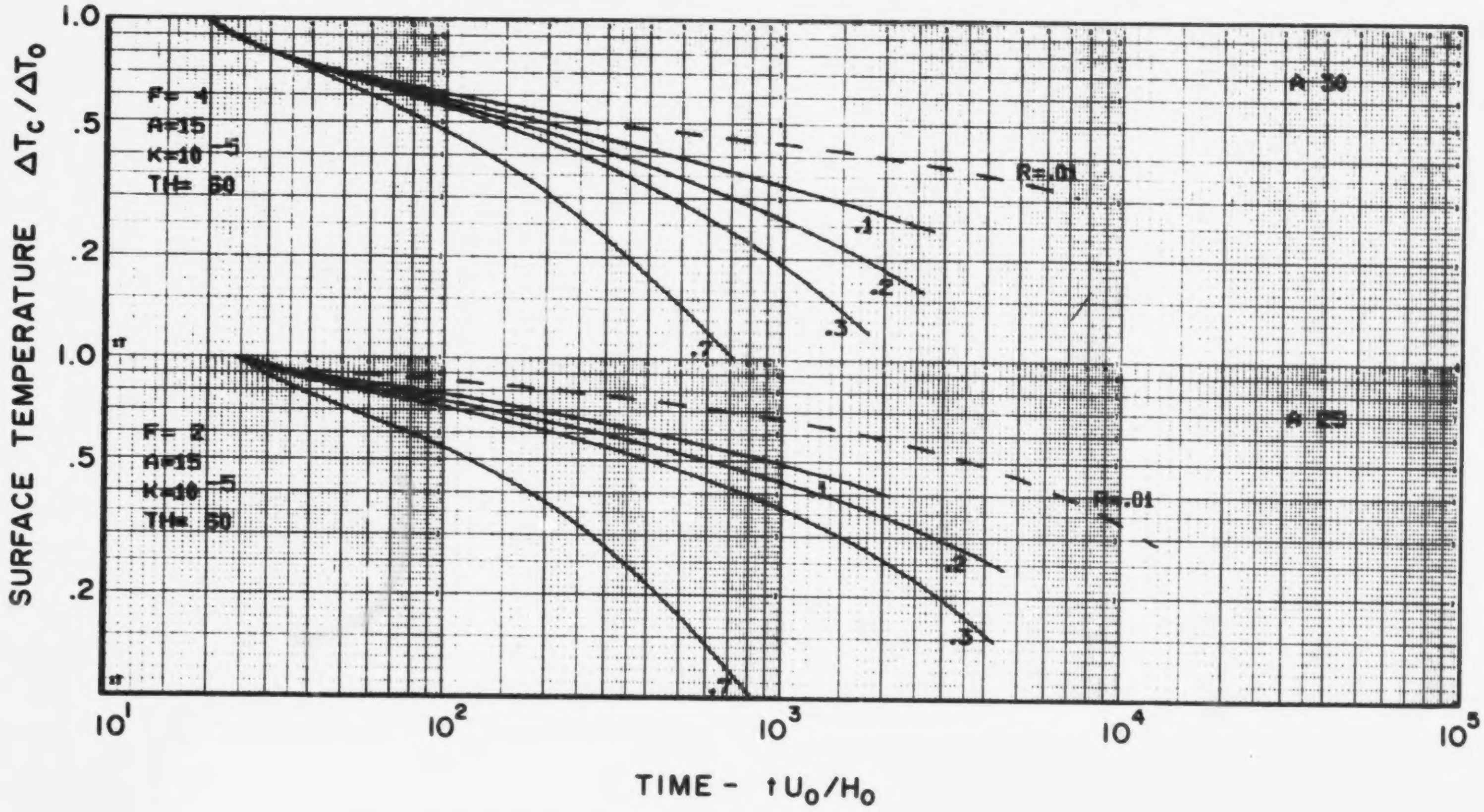

FIG (C15) TEMPERATURE, TIME (Tt)-PLOTS
FOR SURFACE JET DISCHARGE

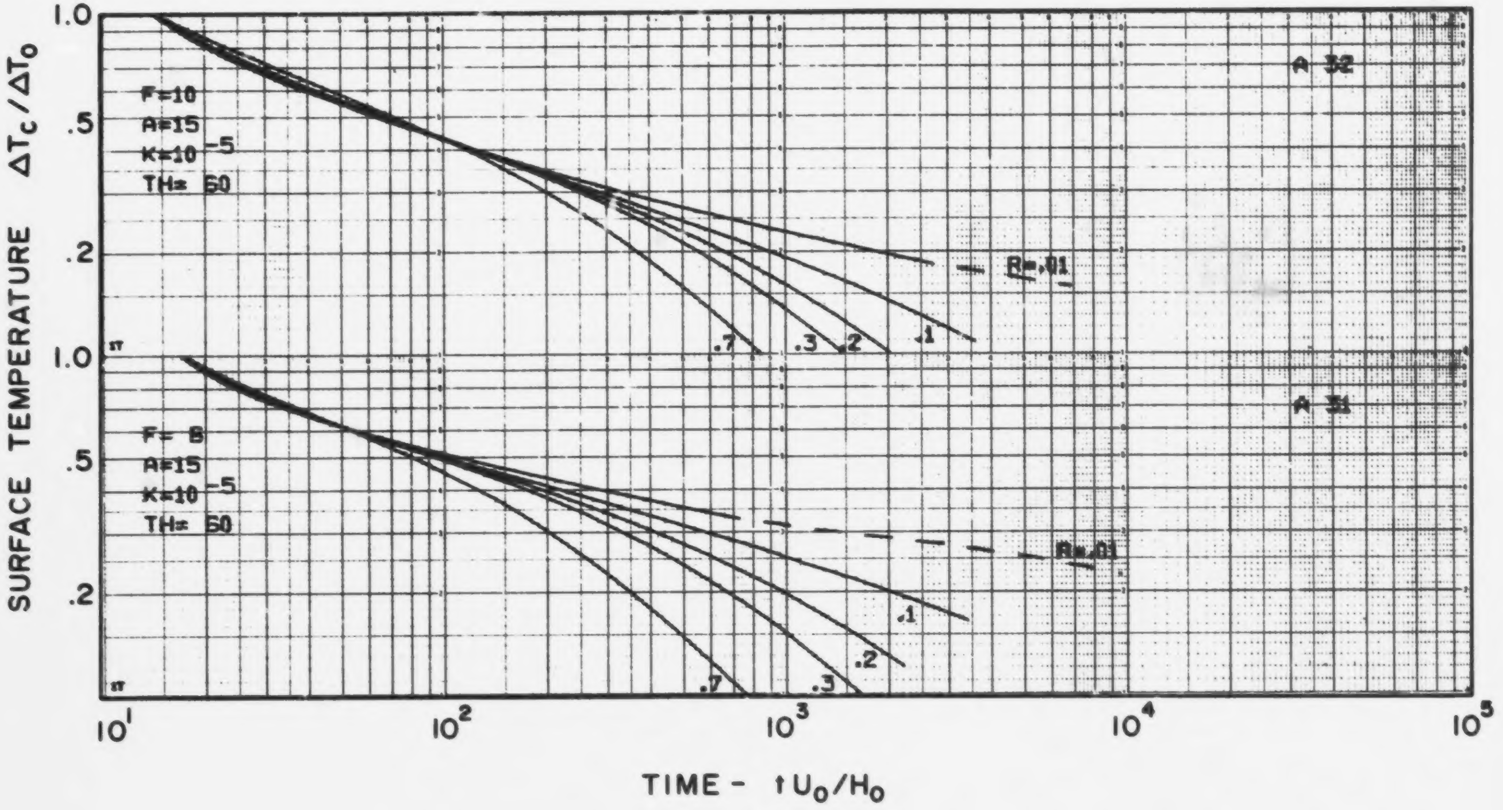

FIG (C16) TEMPERATURE, TIME (Tt)-PLOTS
FOR SURFACE JET DISCHARGE

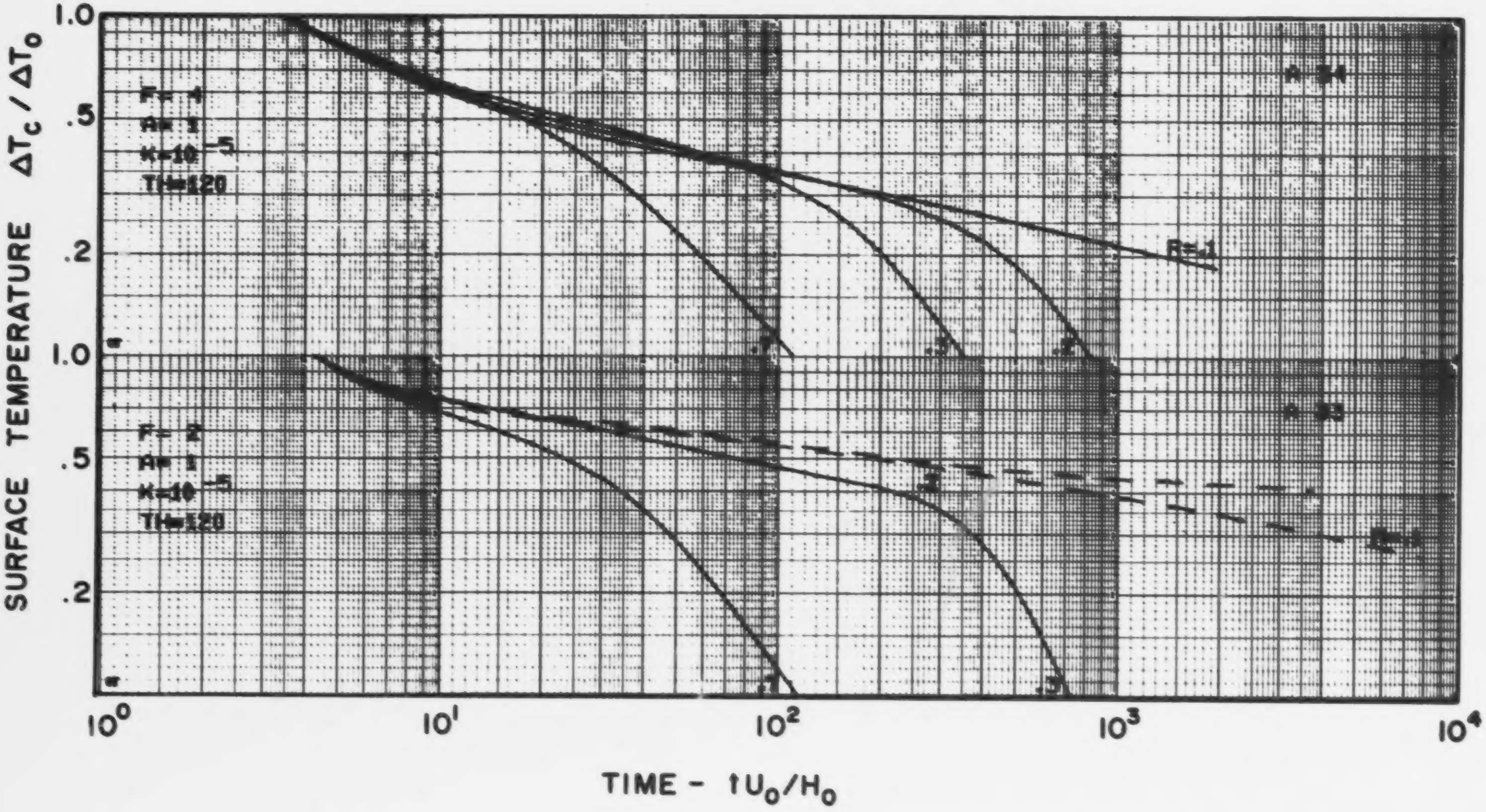

FIG (C17) TEMPERATURE, TIME (Tt)-PLOTS FOR SURFACE JET DISCHARGE

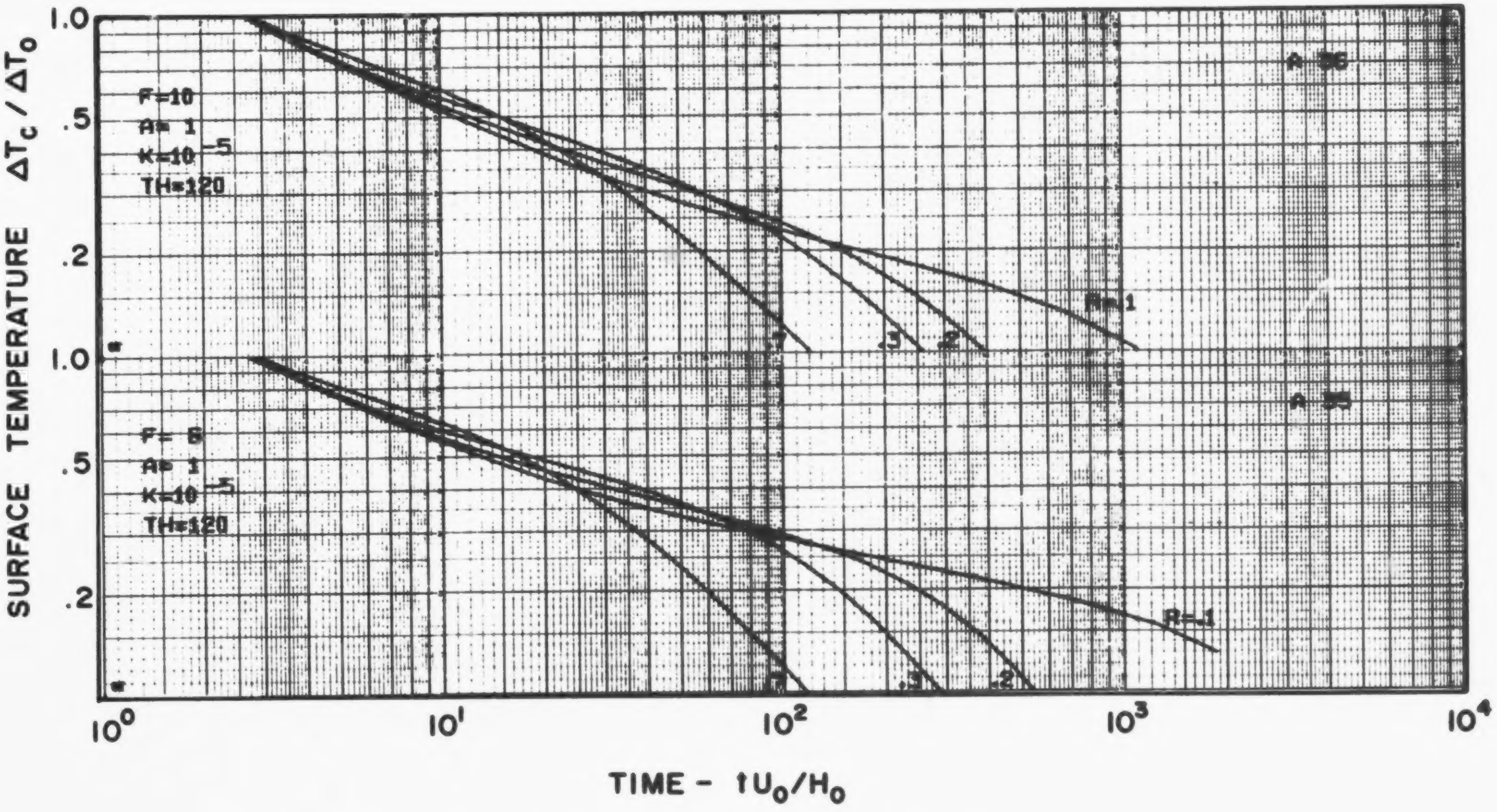

FIG (C18) TEMPERATURE, TIME (Tt)-PLOTS FOR SURFACE JET DISCHARGE

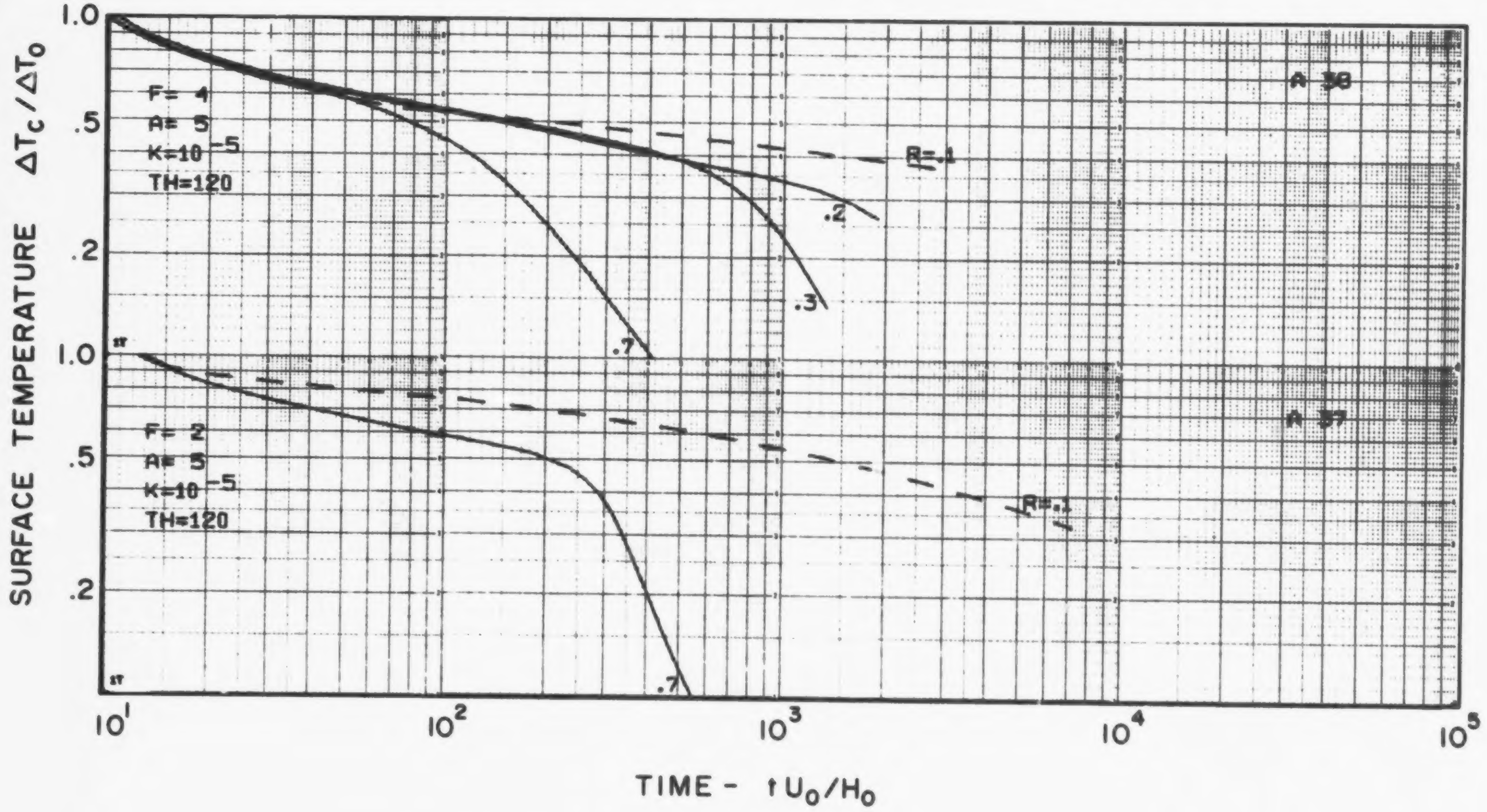

FIG (C19) TEMPERATURE, TIME (Tt)-PLOTS
FOR SURFACE JET DISCHARGE

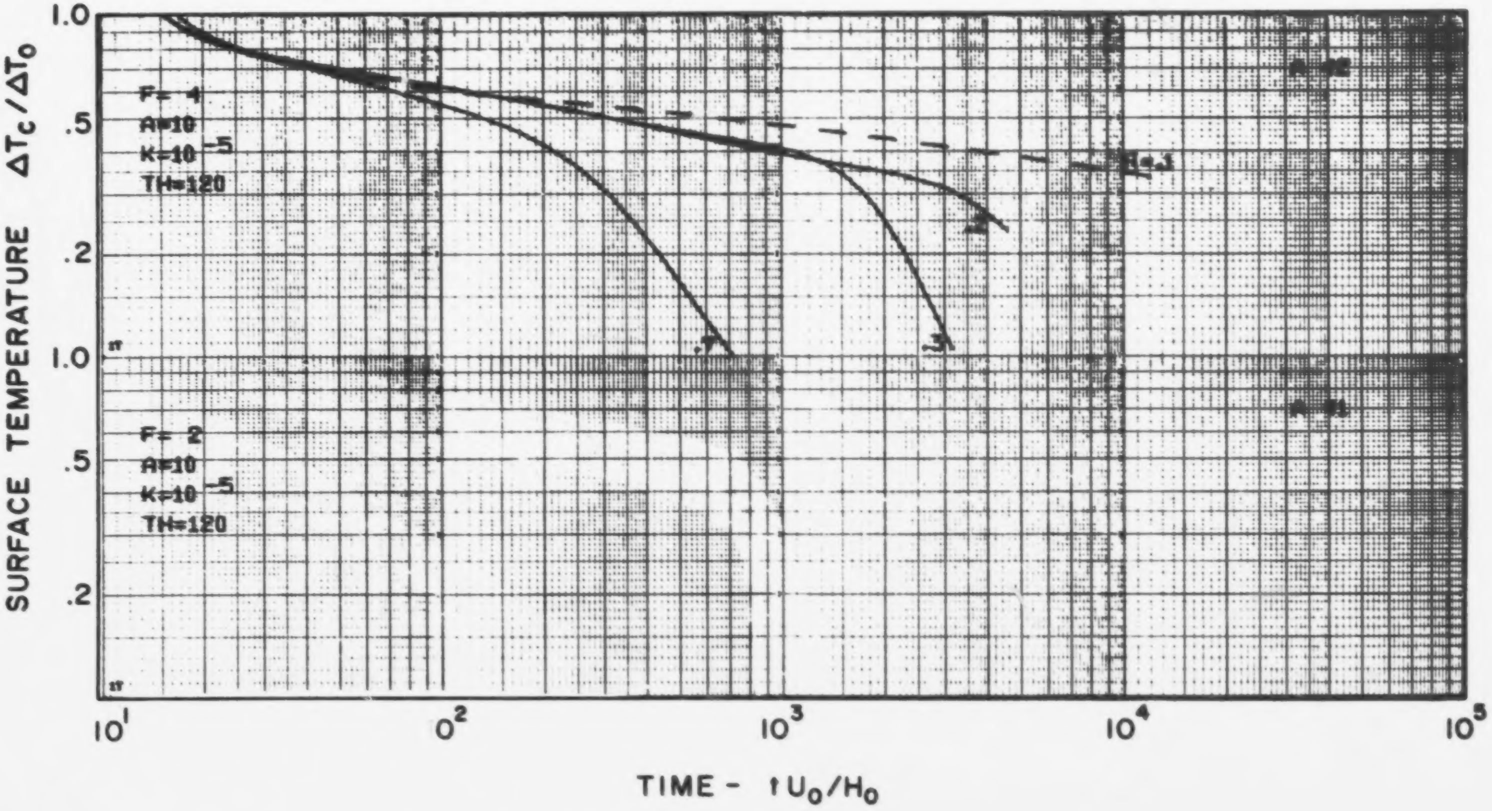

FIG (C21) TEMPERATURE, TIME (Tt)-PLOTS FOR SURFACE JET DISCHARGE

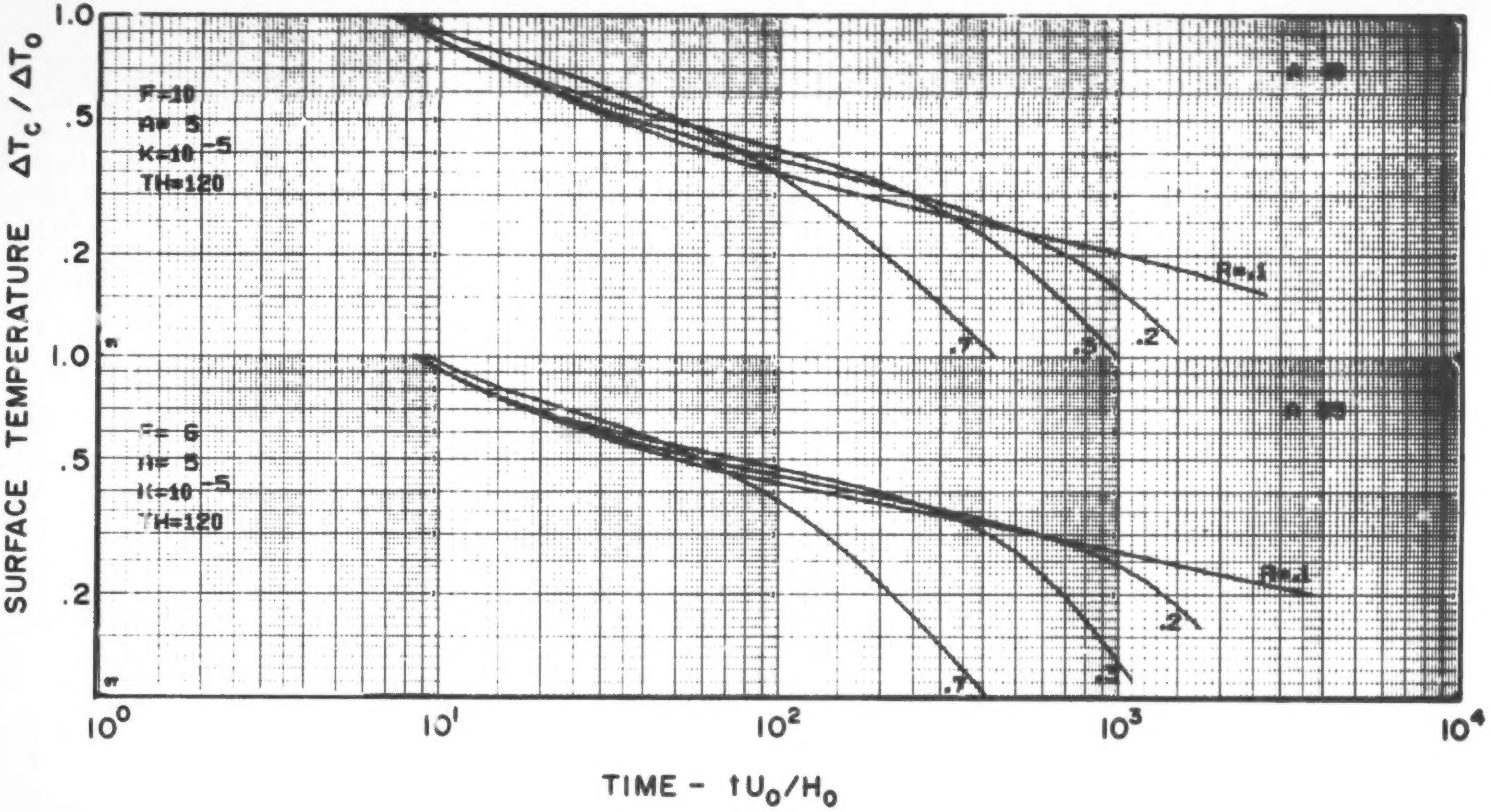

FIG (C20) TEMPERATURE, TIME (Tt)-PLOTS
FOR SURFACE JET DISCHARGE

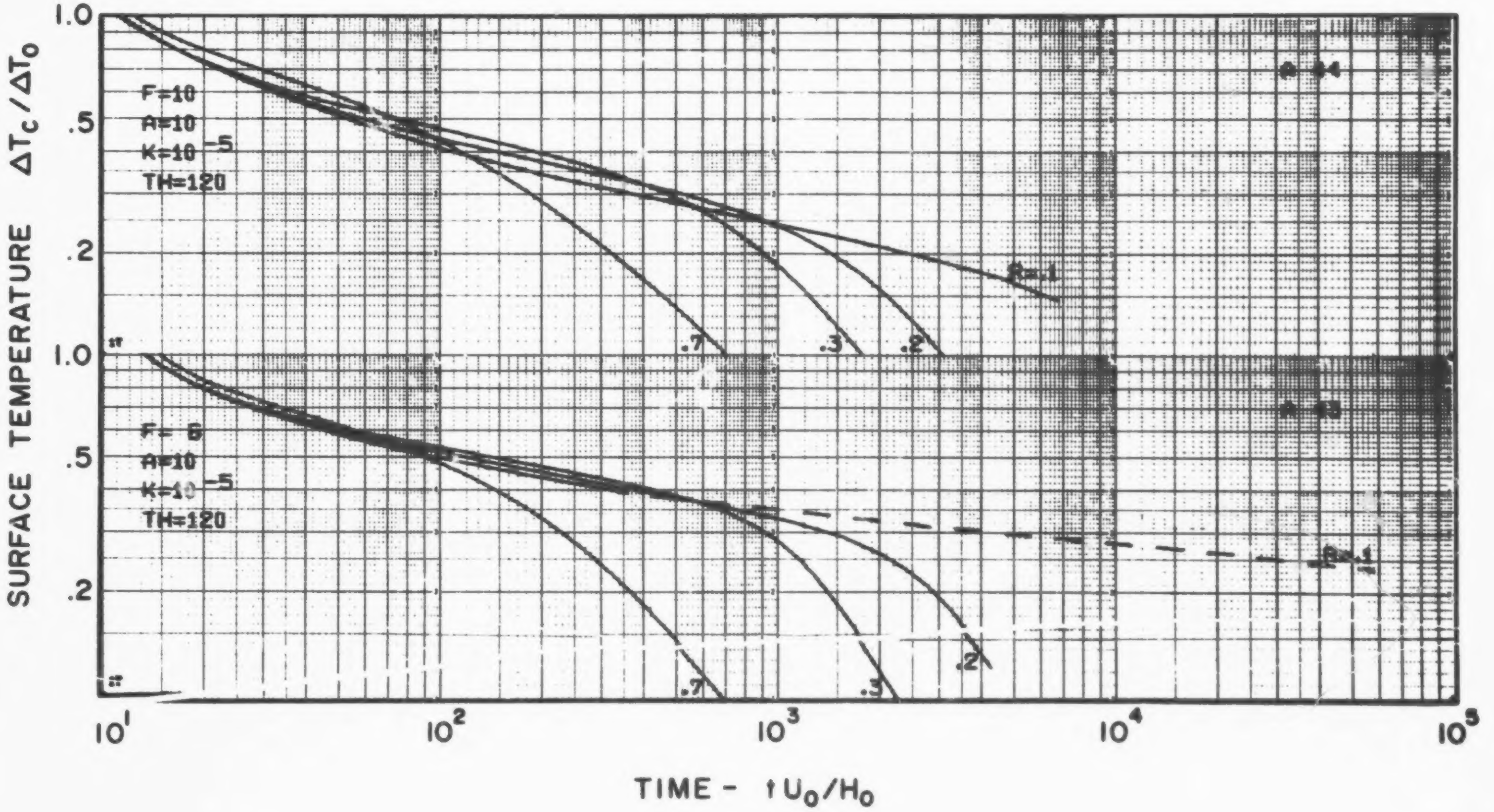

FIG (C22) TEMPERATURE, TIME (Tt)-PLOTS FOR SURFACE JET DISCHARGE

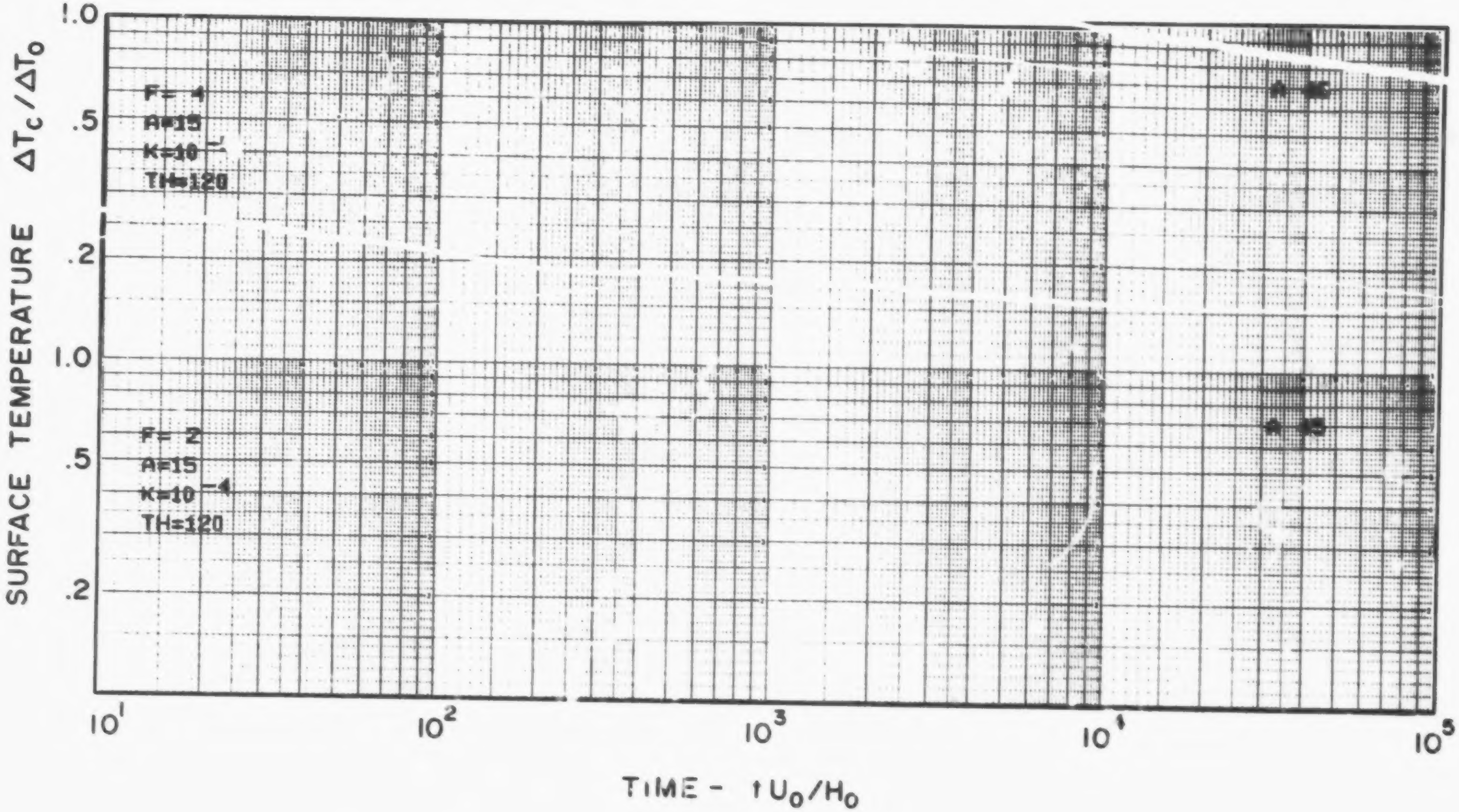

FIG (C23) TEMPERATURE, TIME (Tt)-PLOTS FOR SURFACE JET DISCHARGE

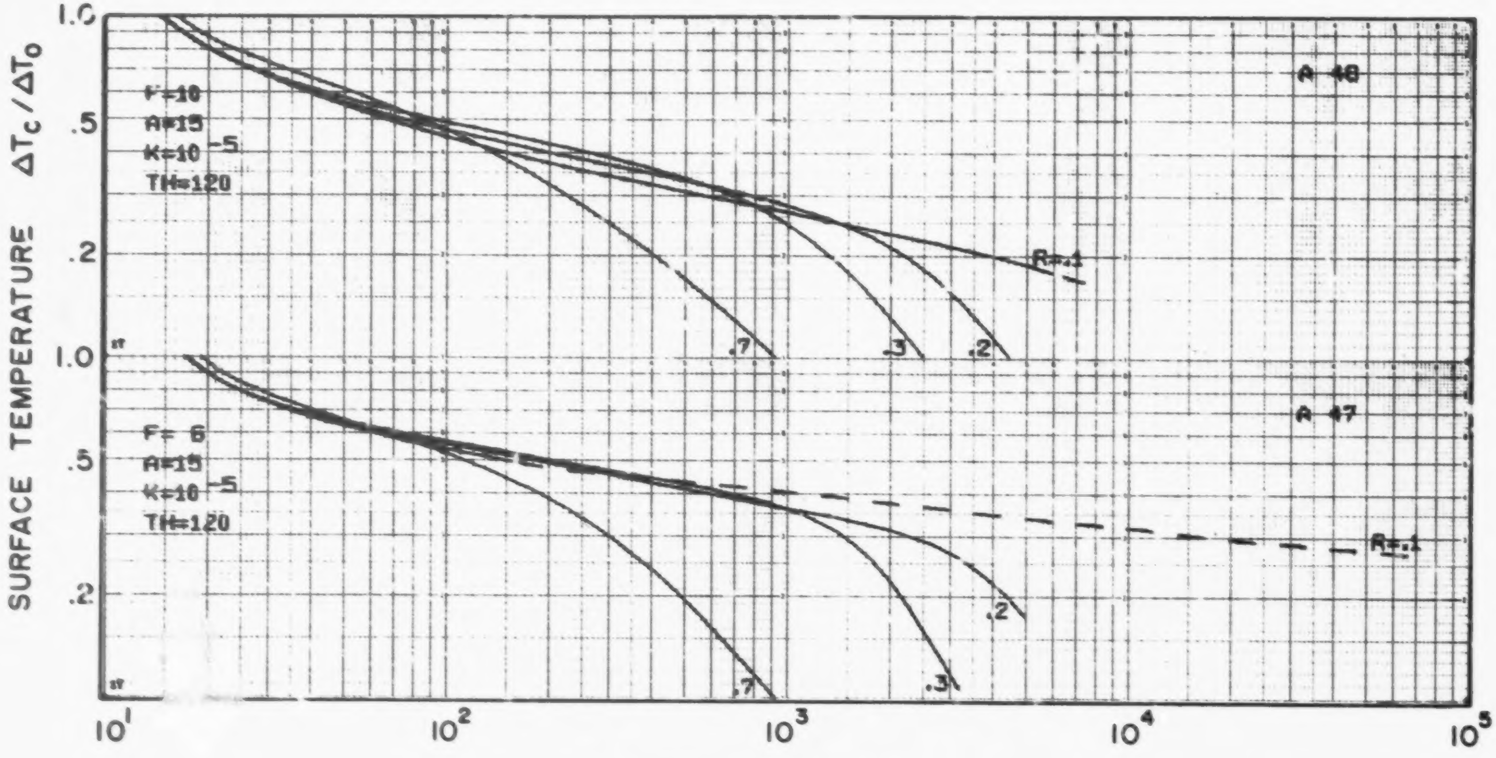

FIG (C24) TEMPERATURE, TIME (Tt)-PLOTS FOR SURFACE JET DISCHARGE

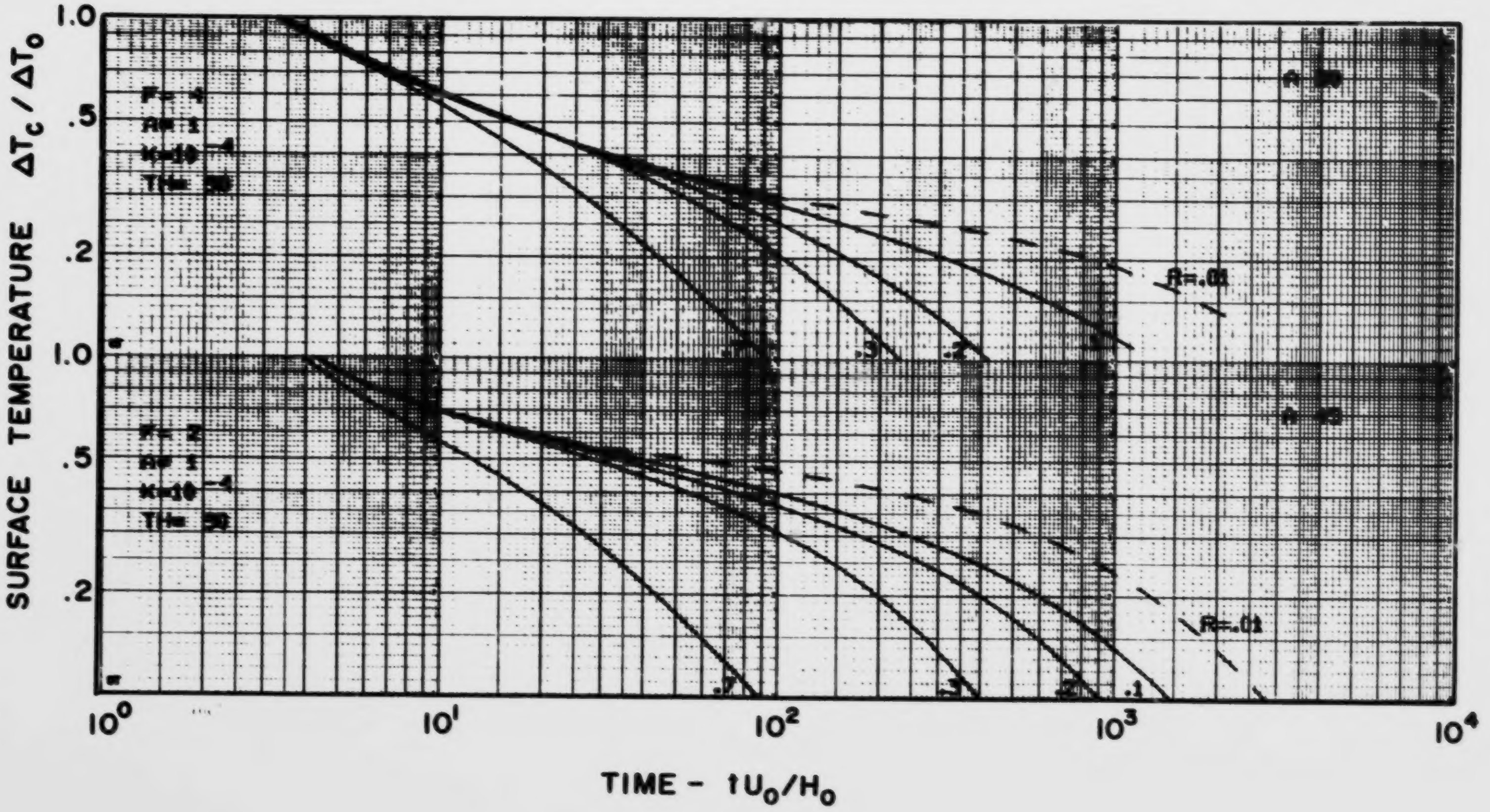

FIG (C25) TEMPERATURE, TIME (Tt)-PLOTS FOR SURFACE JET DISCHARGE

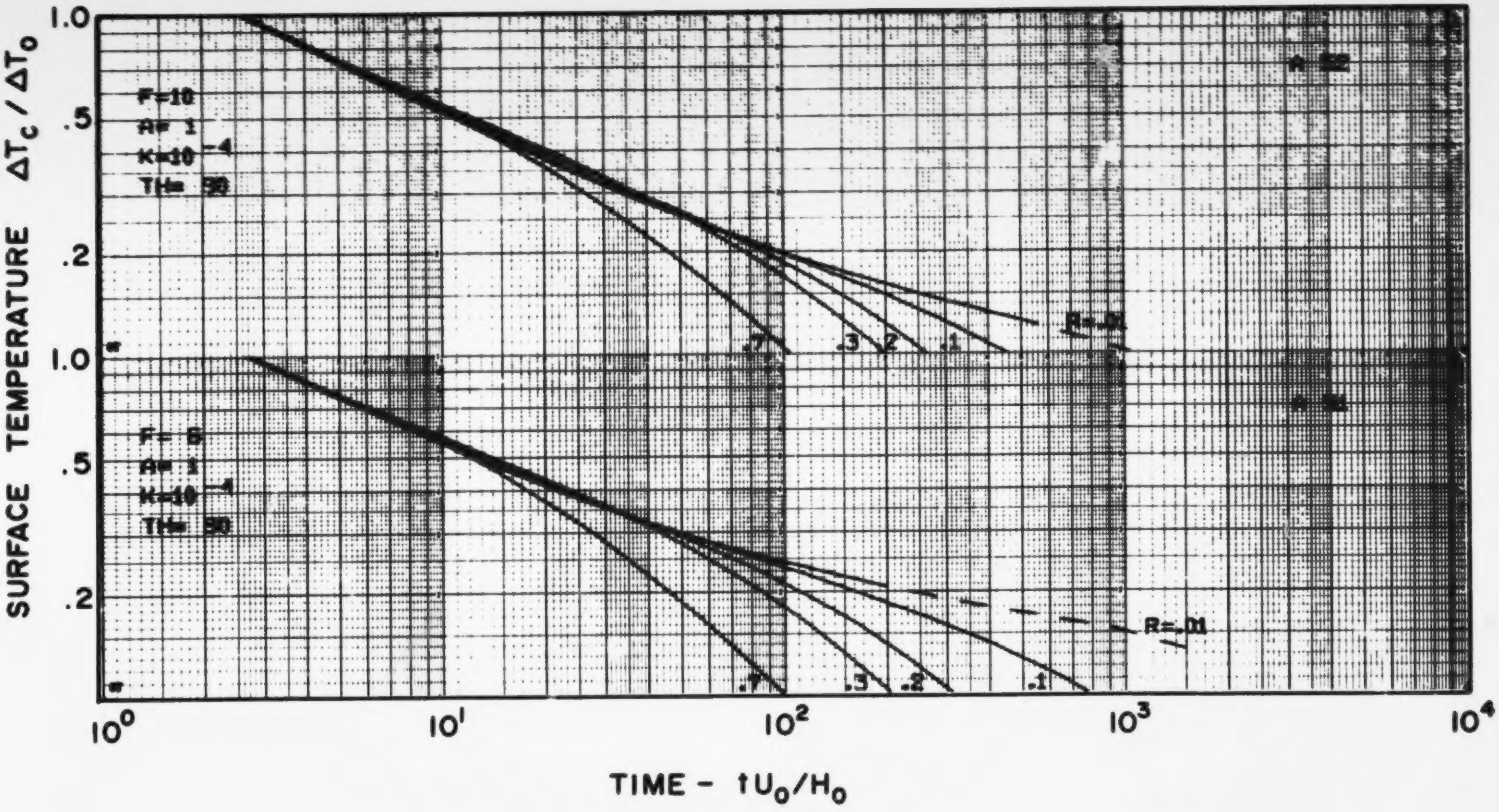

FIG (C26) TEMPERATURE, TIME (Tt)-PLOTS FOR SURFACE JET DISCHARGE

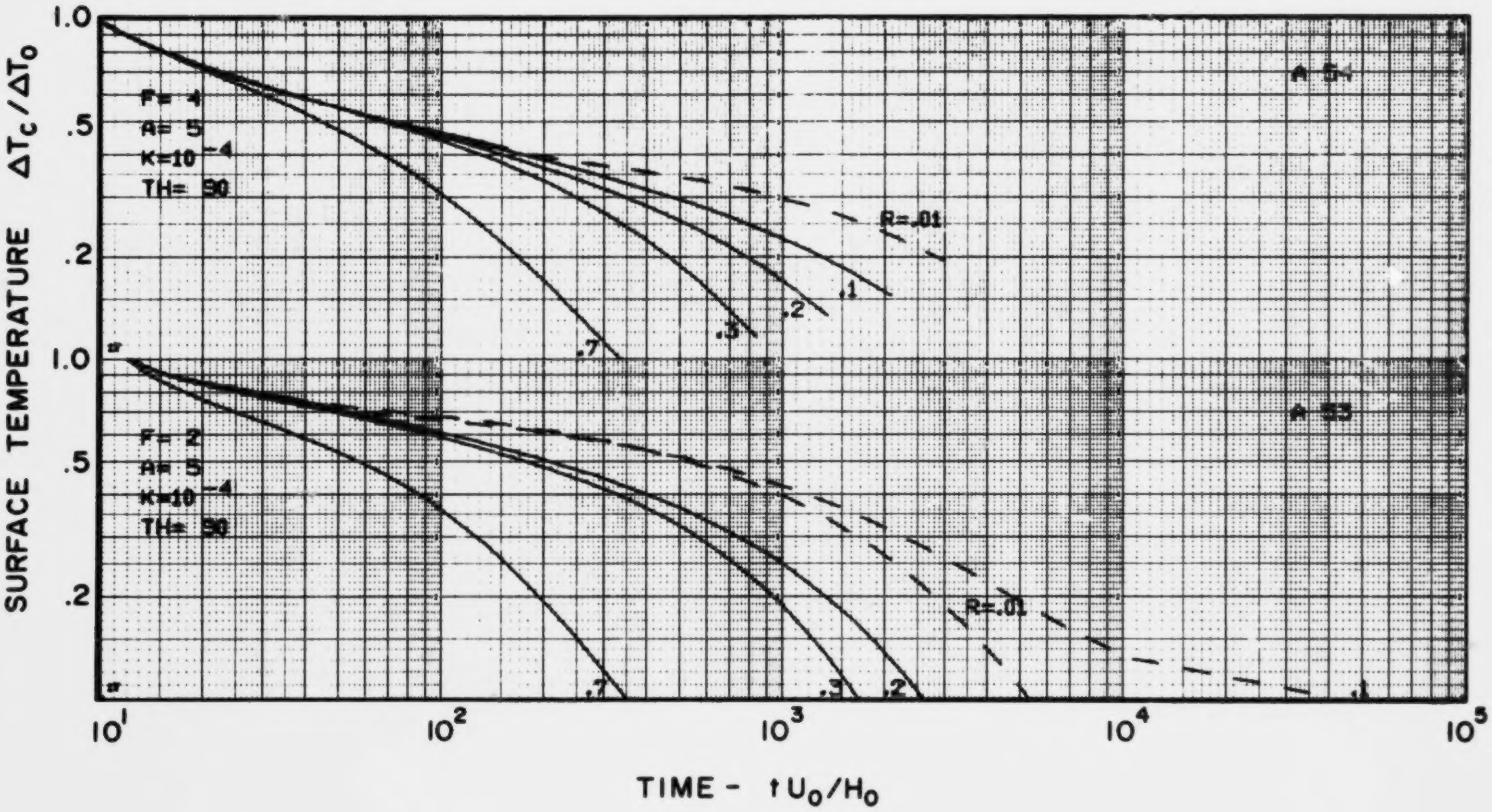

FIG (C27) TEMPERATURE, TIME (Tt)-PLOTS FOR SURFACE JET DISCHARGE

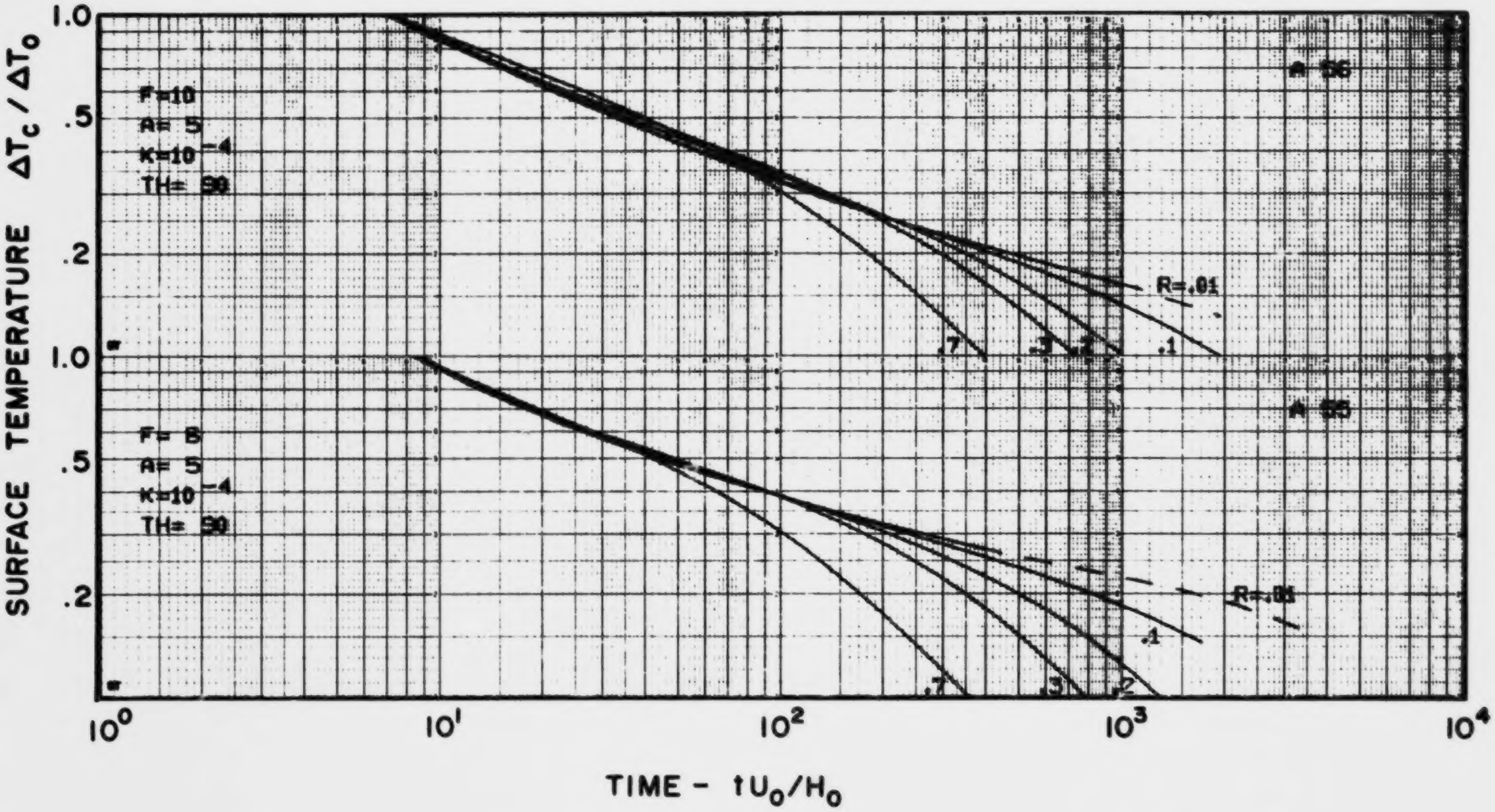

FIG (C28) TEMPERATURE, TIME (Tt)-PLOTS
FOR SURFACE JET DISCHARGE

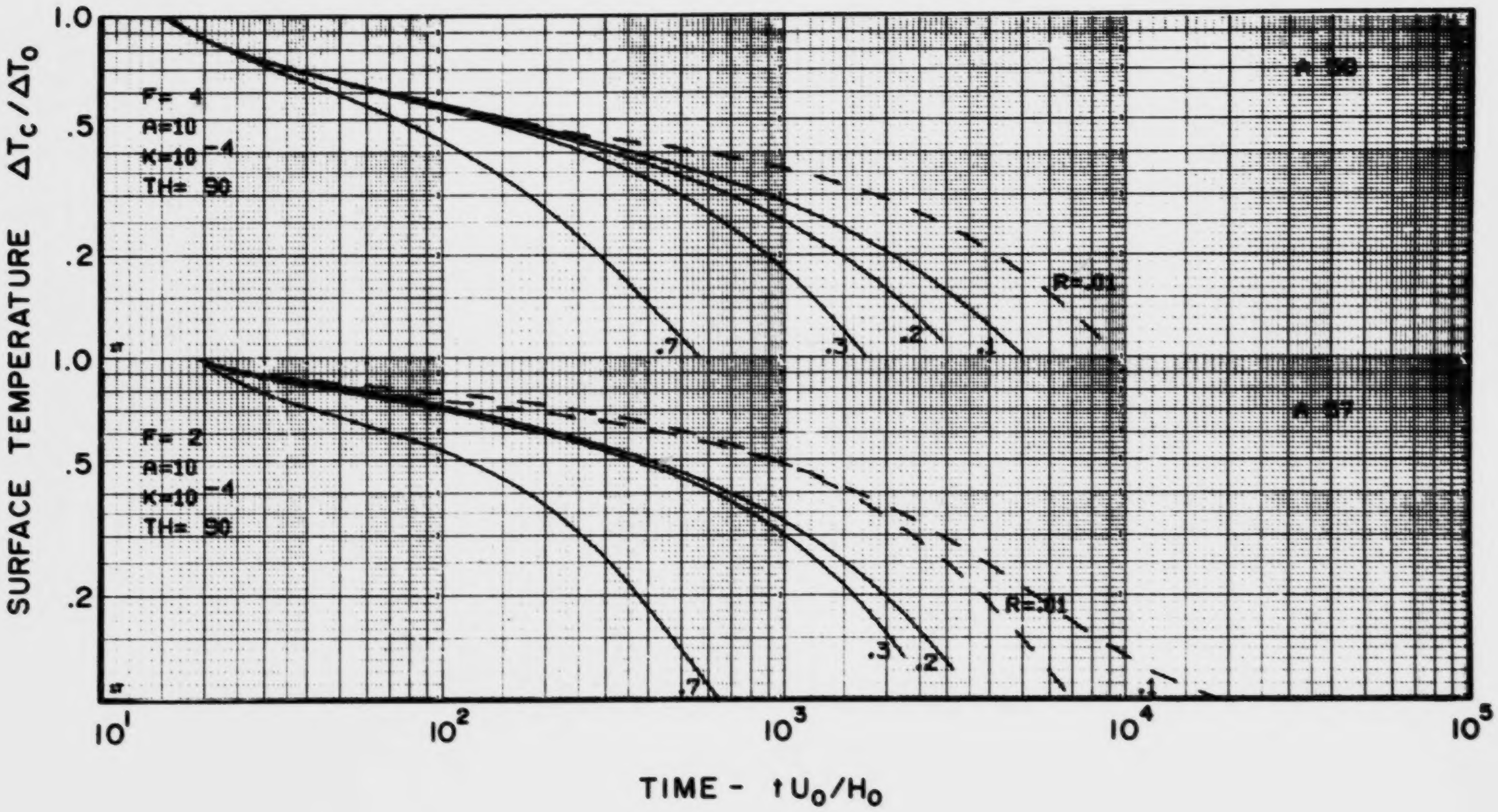

FIG (C29) TEMPERATURE, TIME (Tt)-PLOTS FOR SURFACE JET DISCHARGE

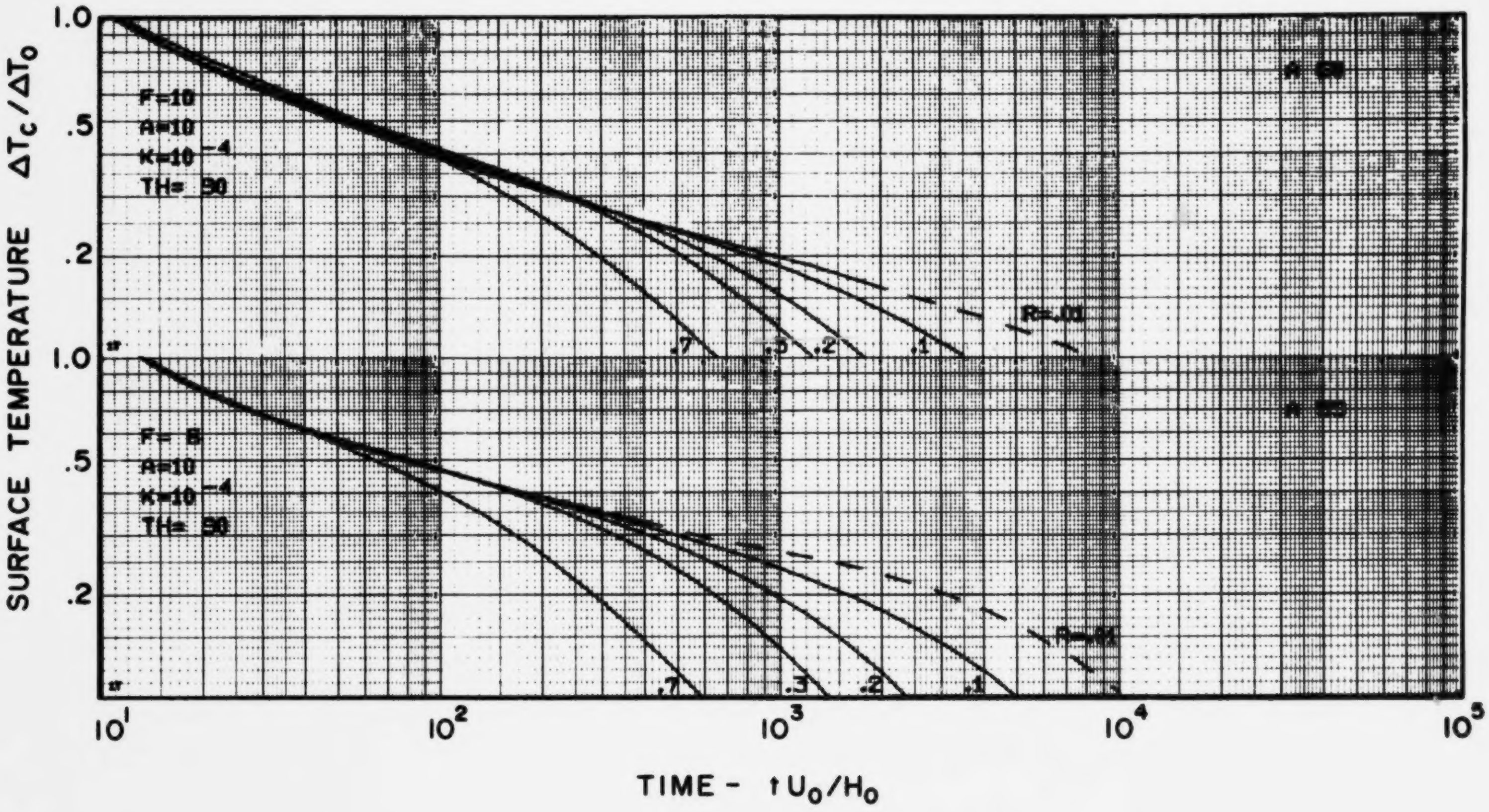

FIG (C30) TEMPERATURE, TIME (Tt)-PLOTS
FOR SURFACE JET DISCHARGE

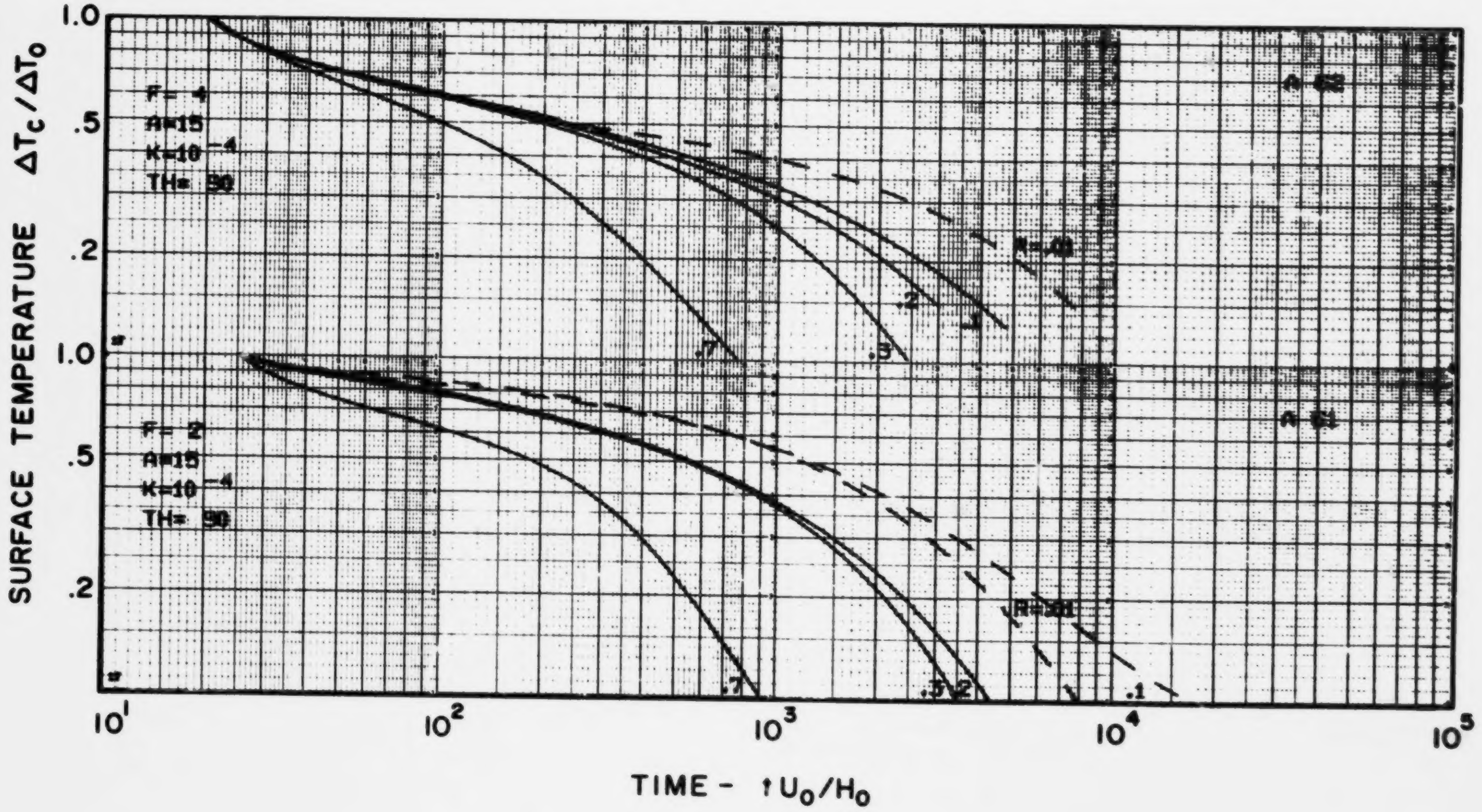

FIG (C31) TEMPERATURE, TIME (Tt)-PLOTS
FOR SURFACE JET DISCHARGE

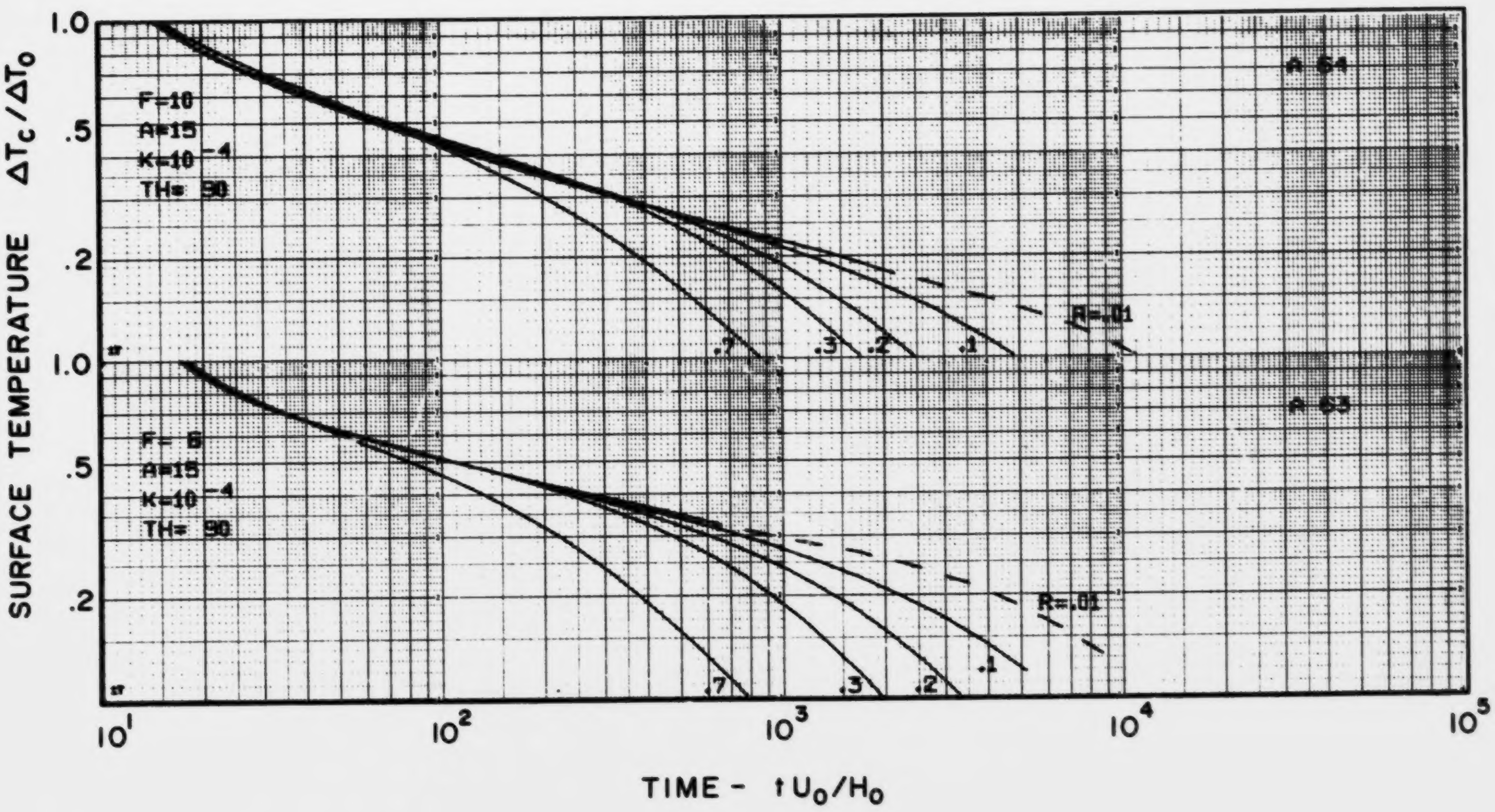

FIG (C32) TEMPERATURE, TIME (Tt)-PLOTS FOR SURFACE JET DISCHARGE

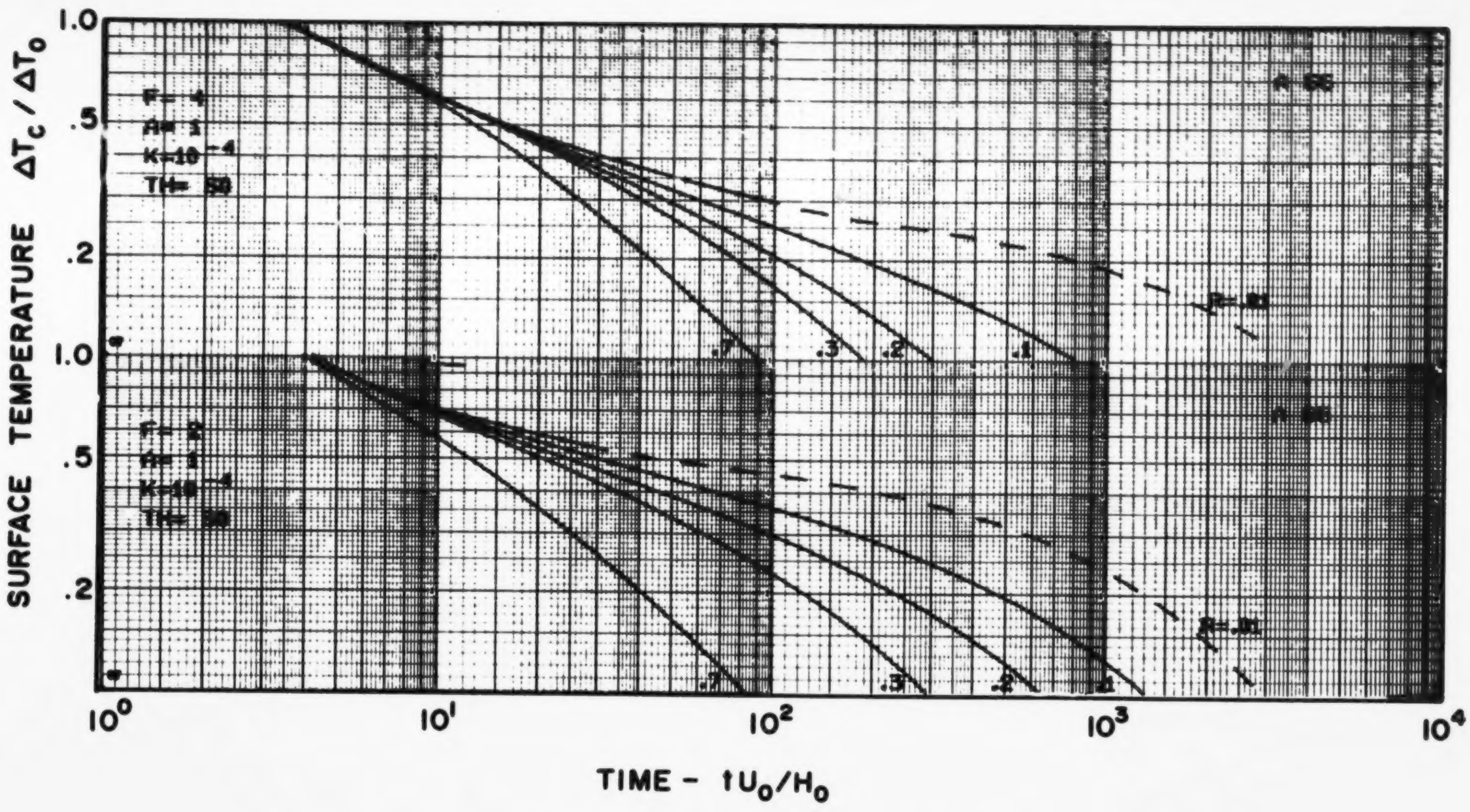

FIG (C33) TEMPERATURE, TIME (Tt)-PLOTS FOR SURFACE JET DISCHARGE

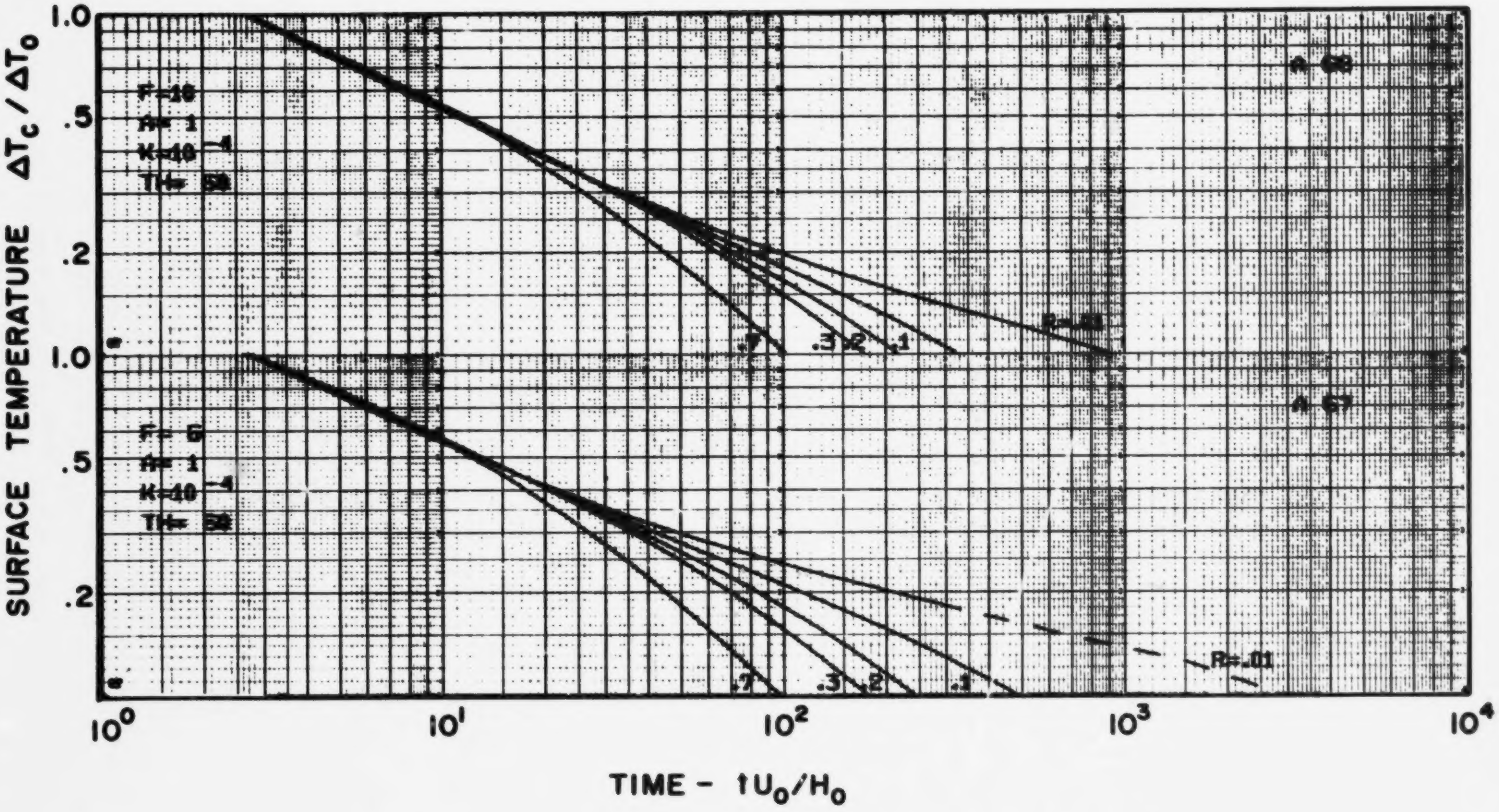

FIG (C34) TEMPERATURE, TIME (Tt)-PLOTS FOR SURFACE JET DISCHARGE

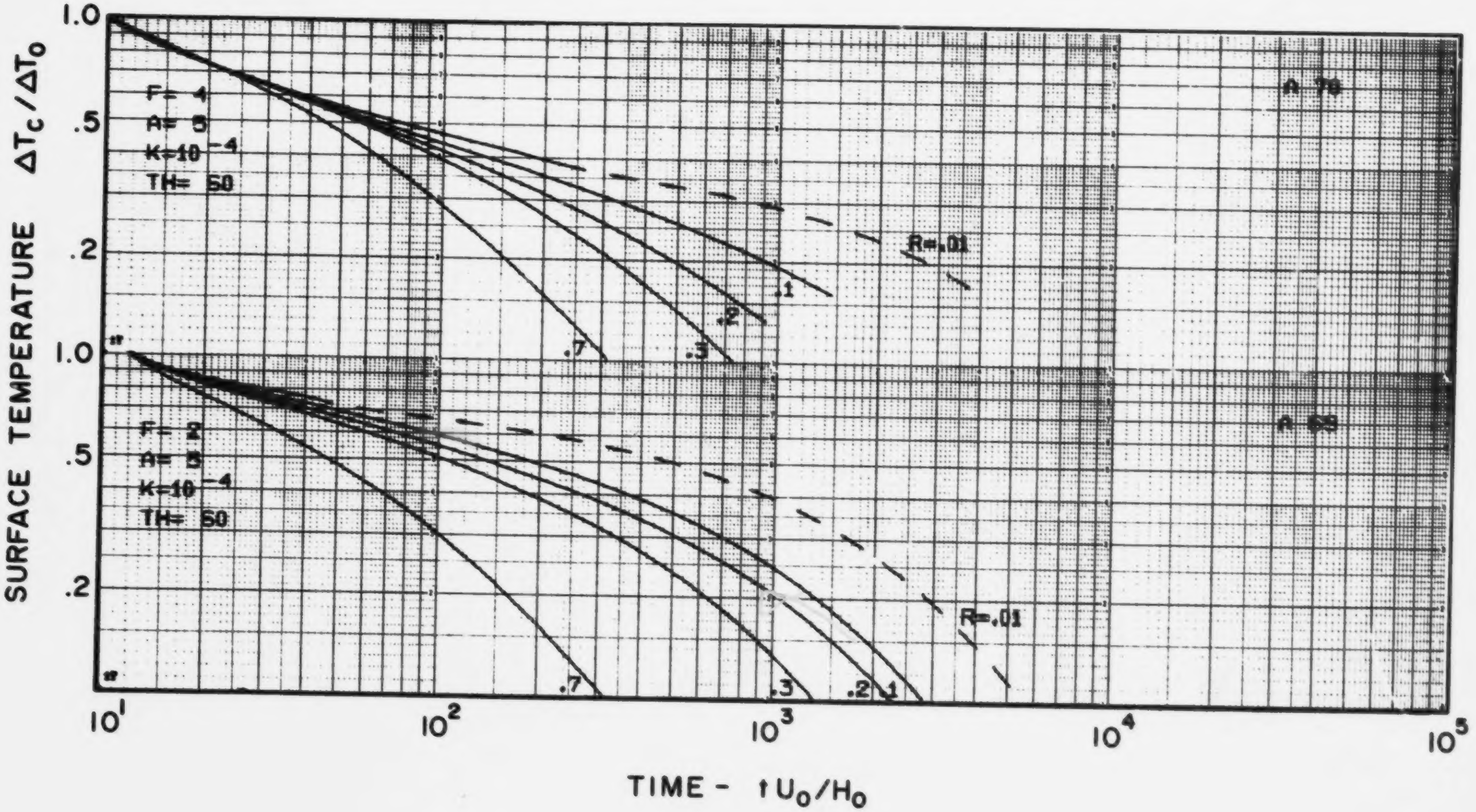

FIG (C35) TEMPERATURE, TIME (Tt)-PLOTS
FOR SURFACE JET DISCHARGE

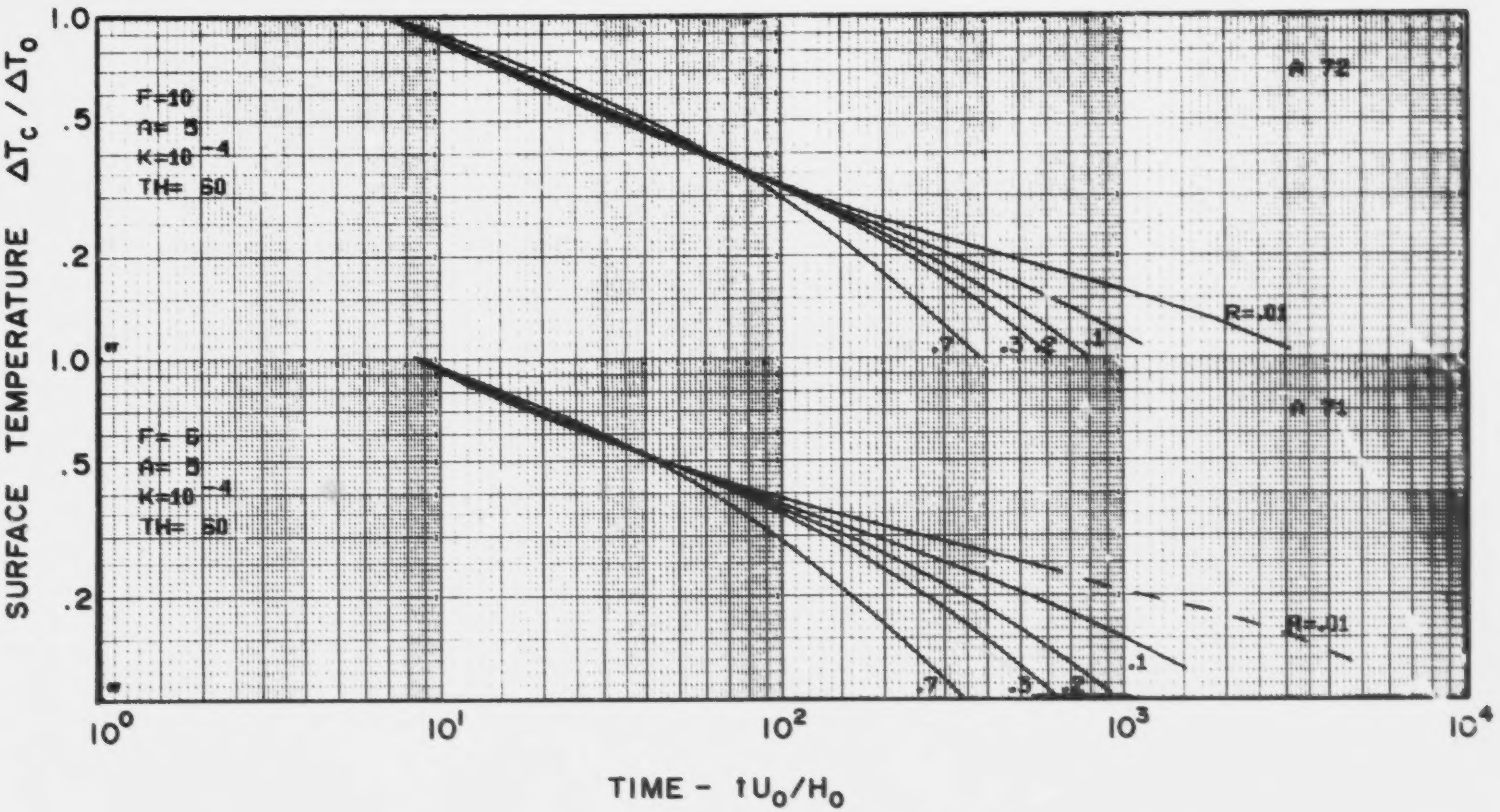

FIG (C36) TEMPERATURE, TIME (Tt)-PLOTS
FOR SURFACE JET DISCHARGE

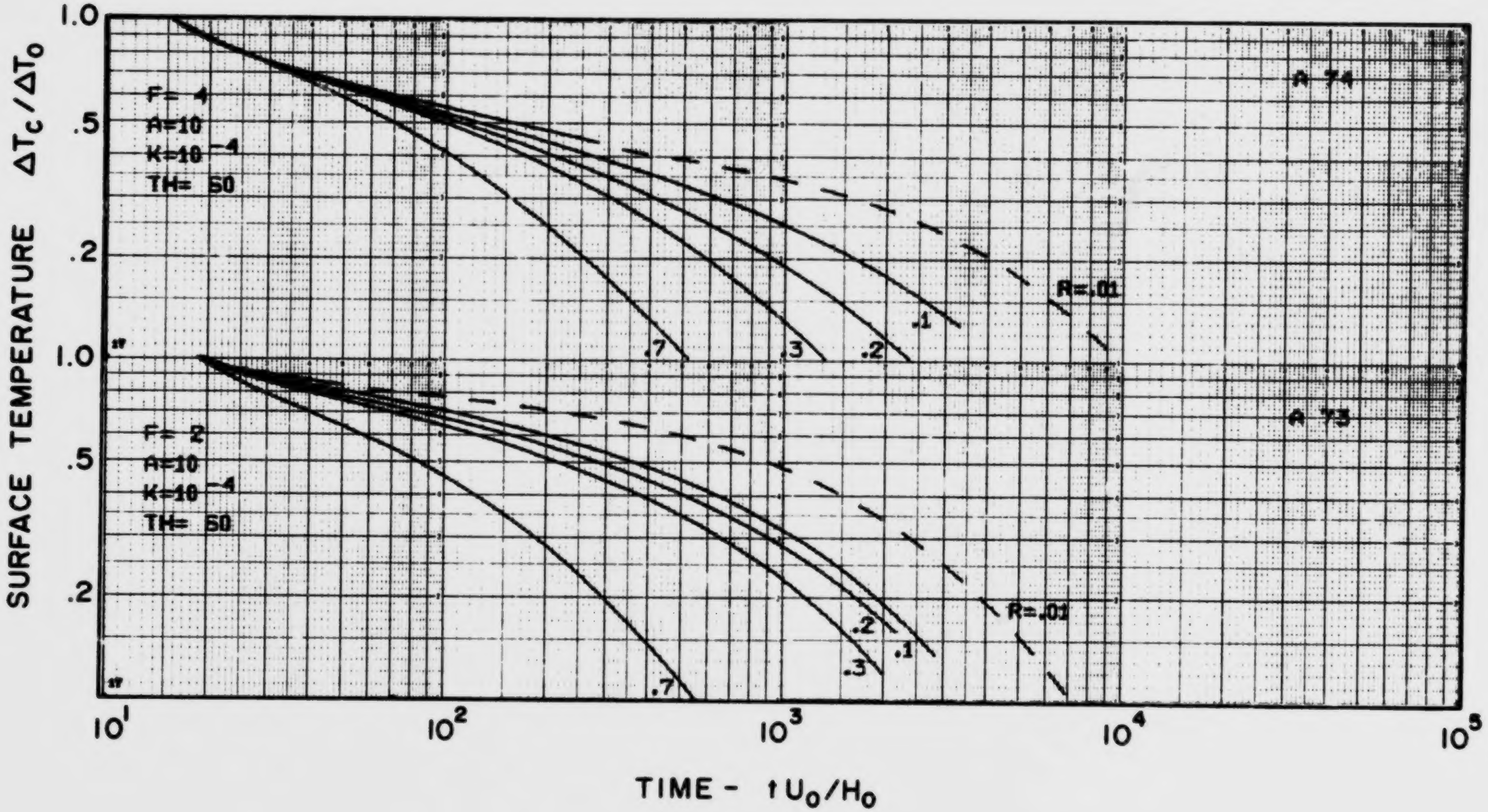

FIG (C37) TEMPERATURE, TIME (Tt)-PLOTS
FOR SURFACE JET DISCHARGE

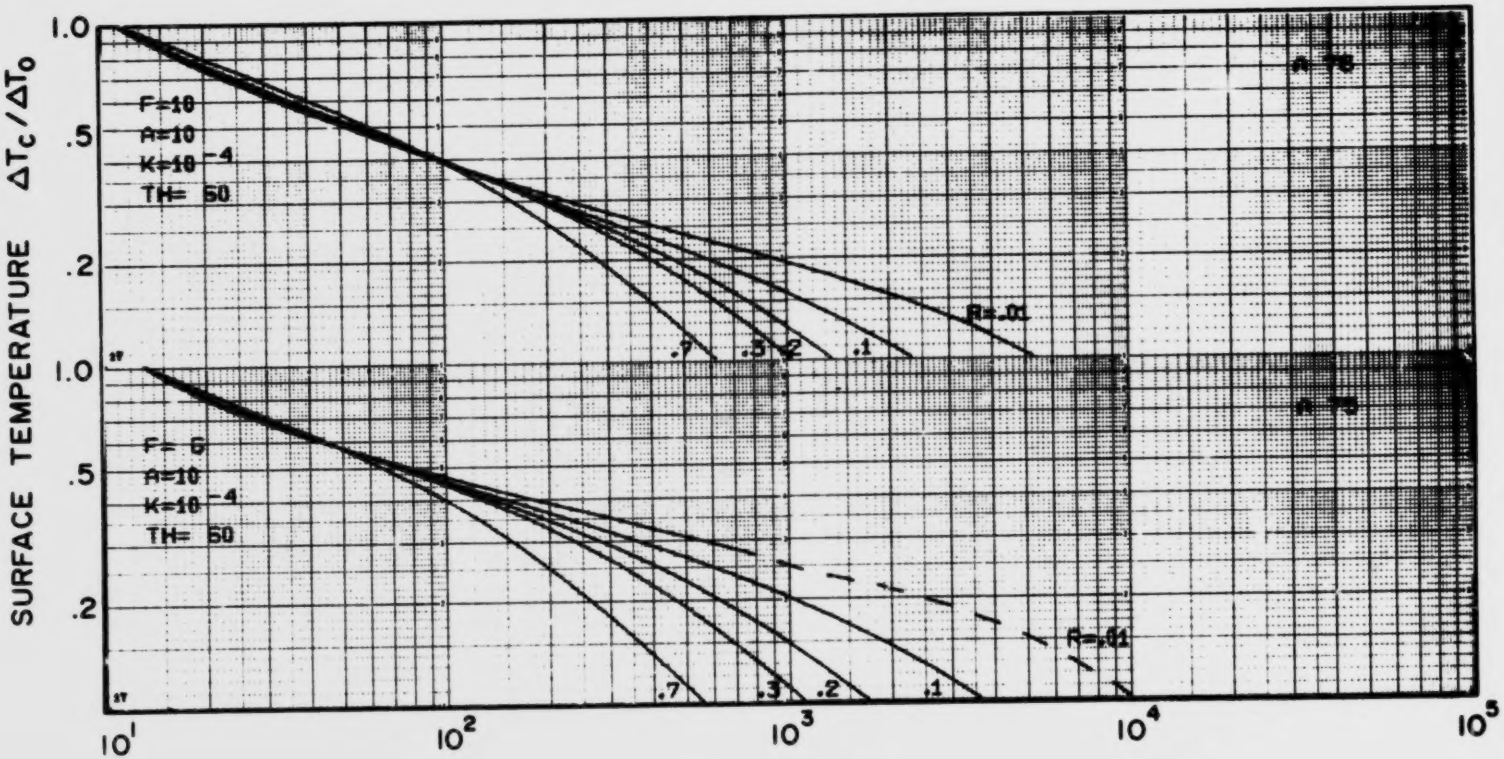

FIG (C38) TEMPERATURE, TIME (Tt)-PLOTS FOR SURFACE JET DISCHARGE

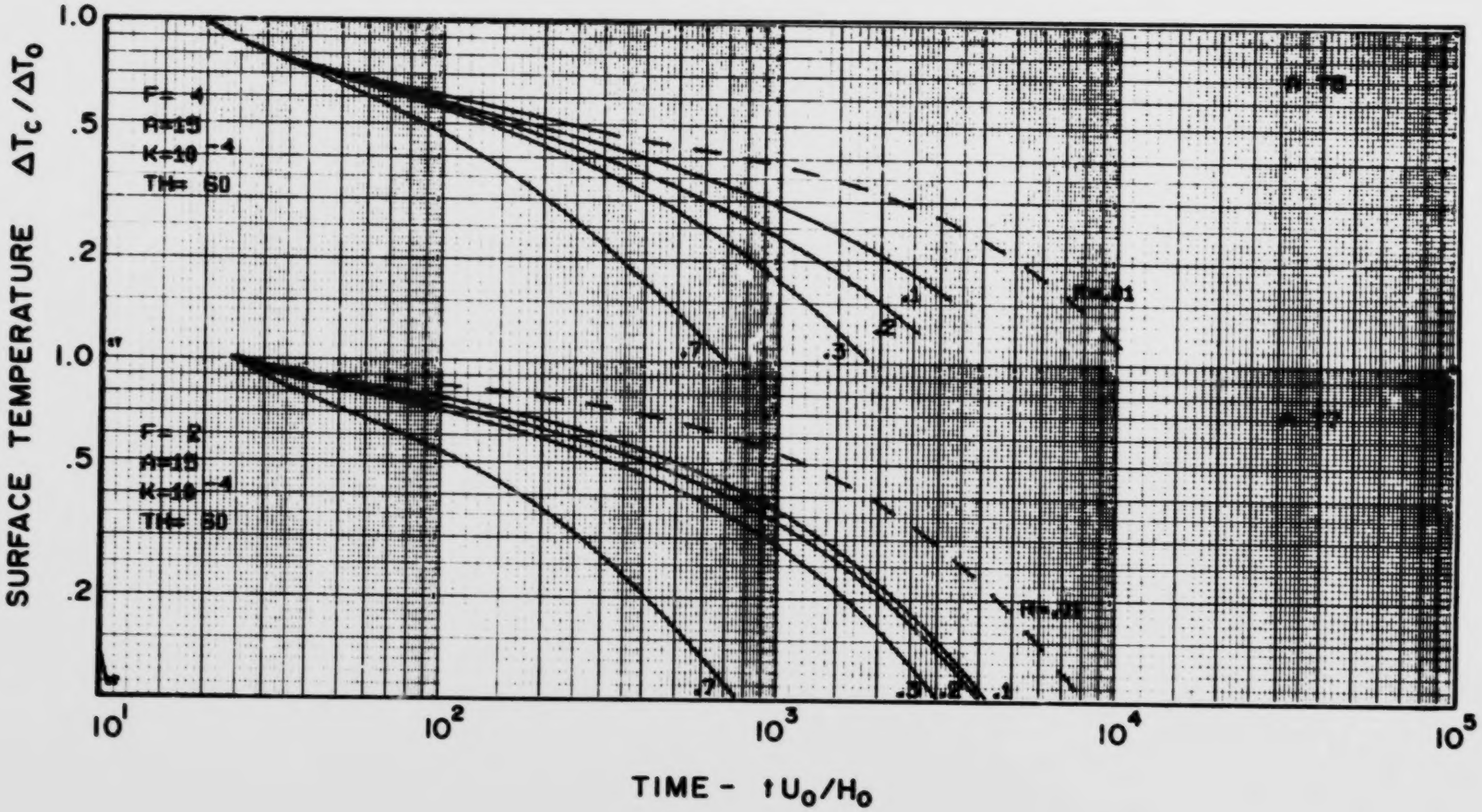

FIG (C39) TEMPERATURE, TIME (Tt)-PLOTS FOR SURFACE JET DISCHARGE

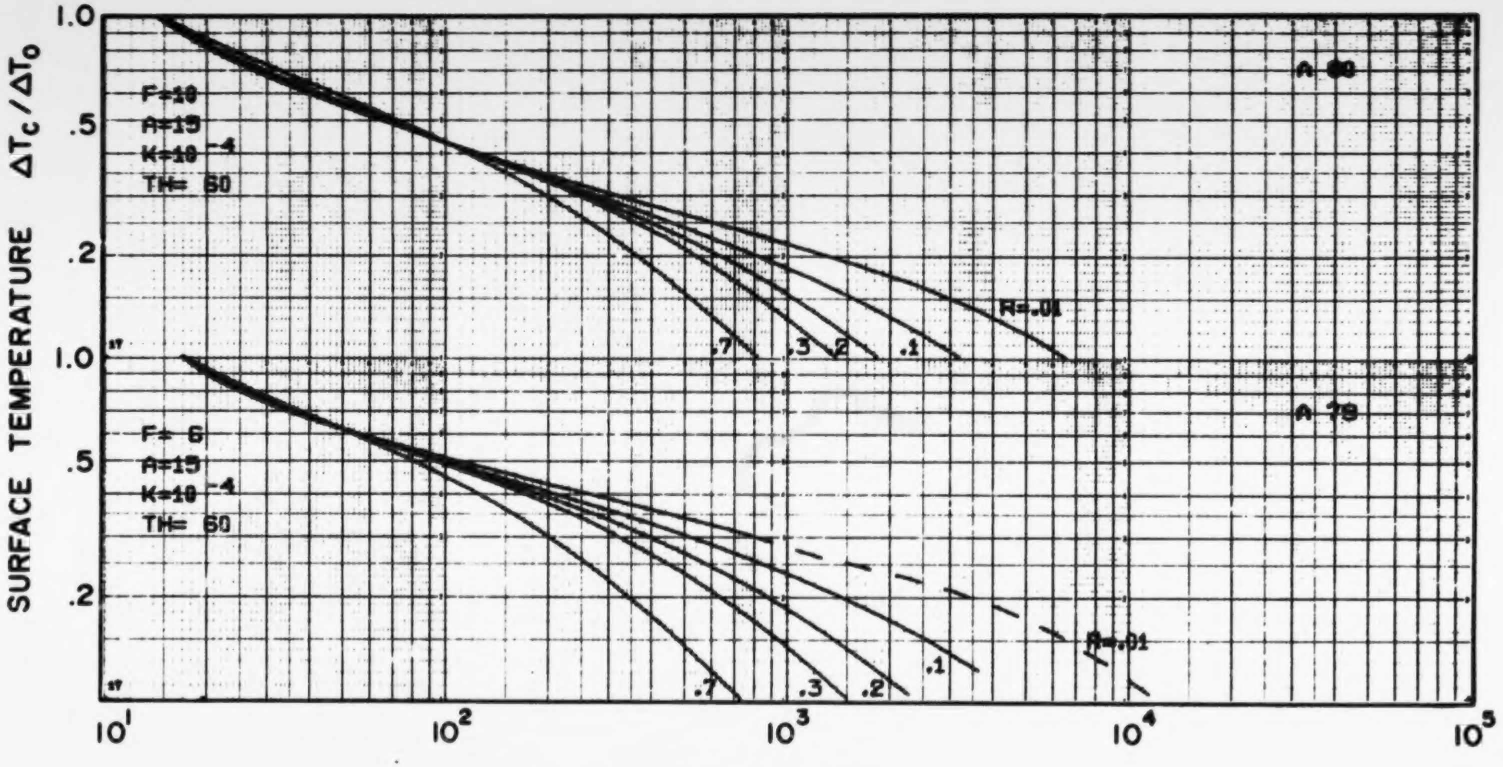

FIG (C40) TEMPERATURE, TIME (Tt)-PLOTS FOR SURFACE JET DISCHARGE

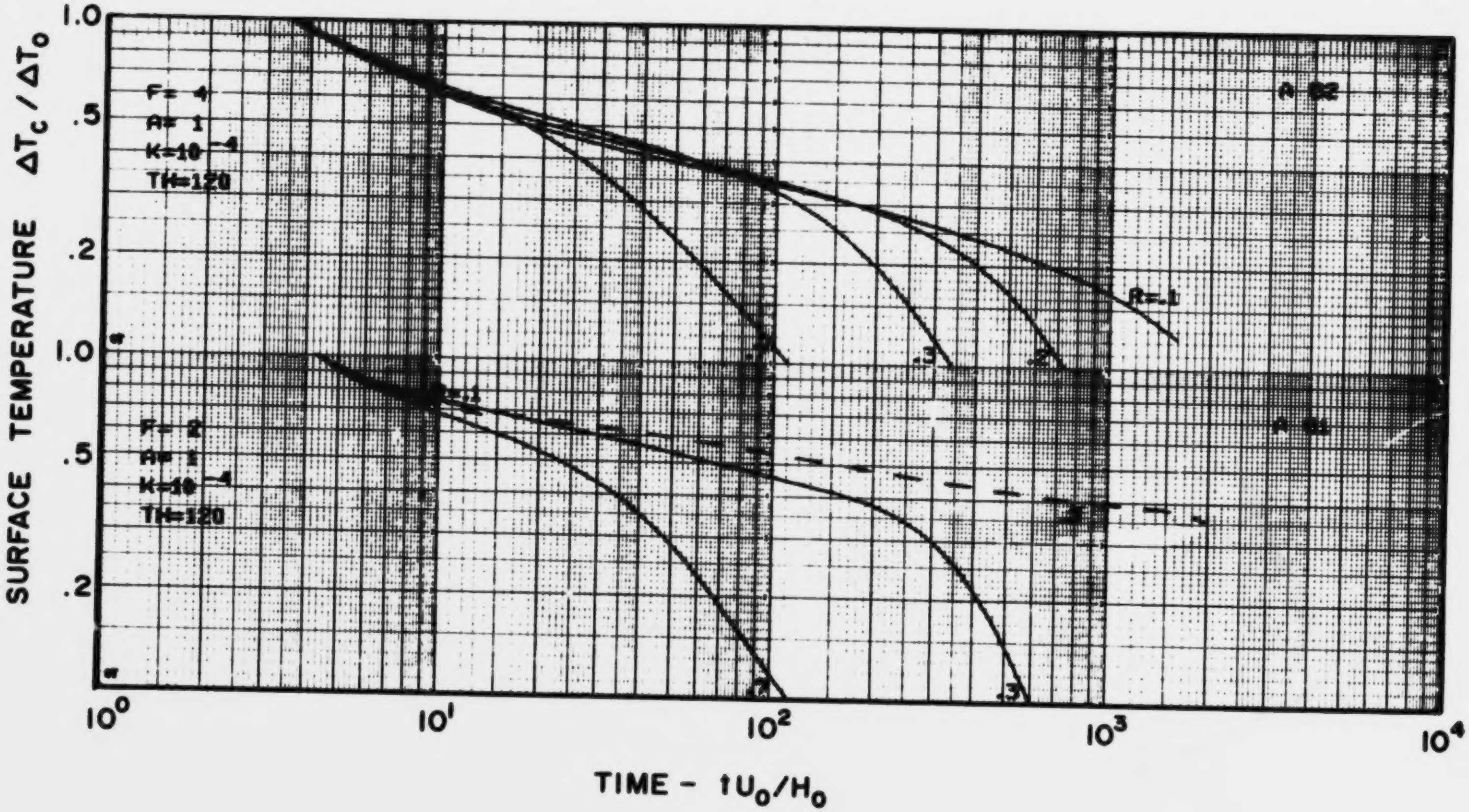

FIG (C41) TEMPERATURE, TIME (Tt)-PLOTS FOR SURFACE JET DISCHARGE

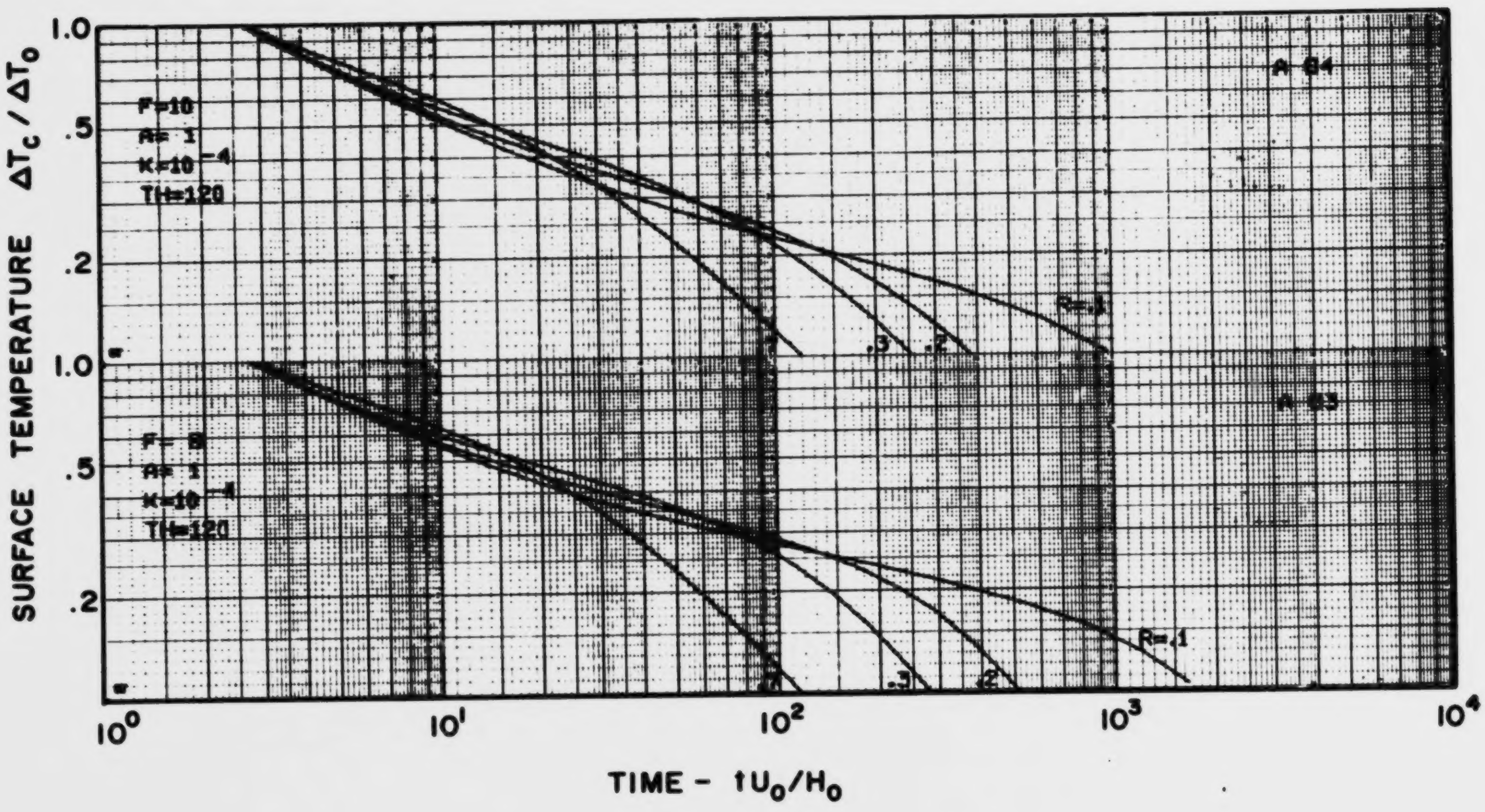

FIG (C42) TEMPERATURE, TIME (Tt)-PLOTS FOR SURFACE JET DISCHARGE

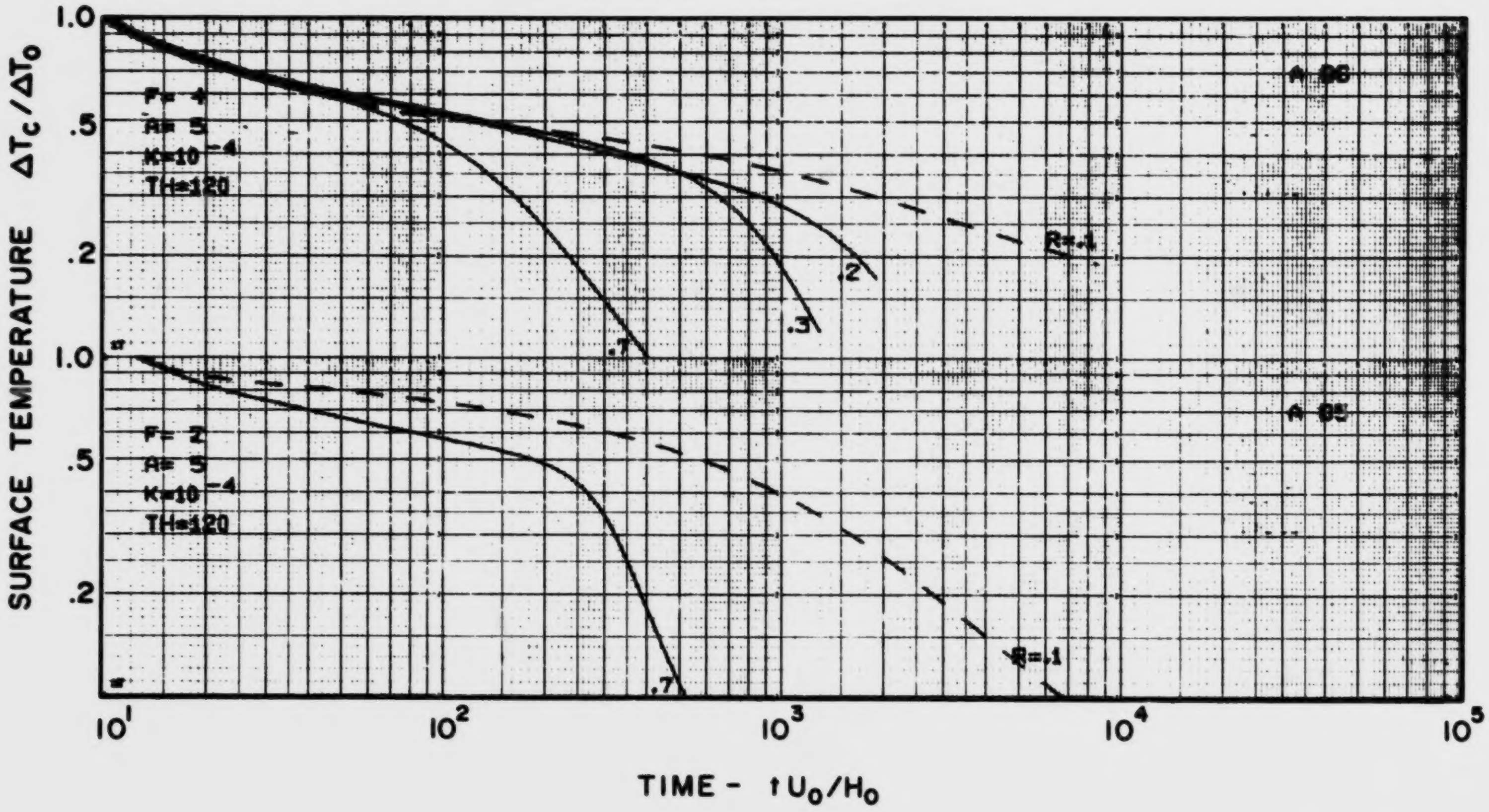

FIG (C43) TEMPERATURE, TIME (Tt)-PLOTS FOR SURFACE JET DISCHARGE

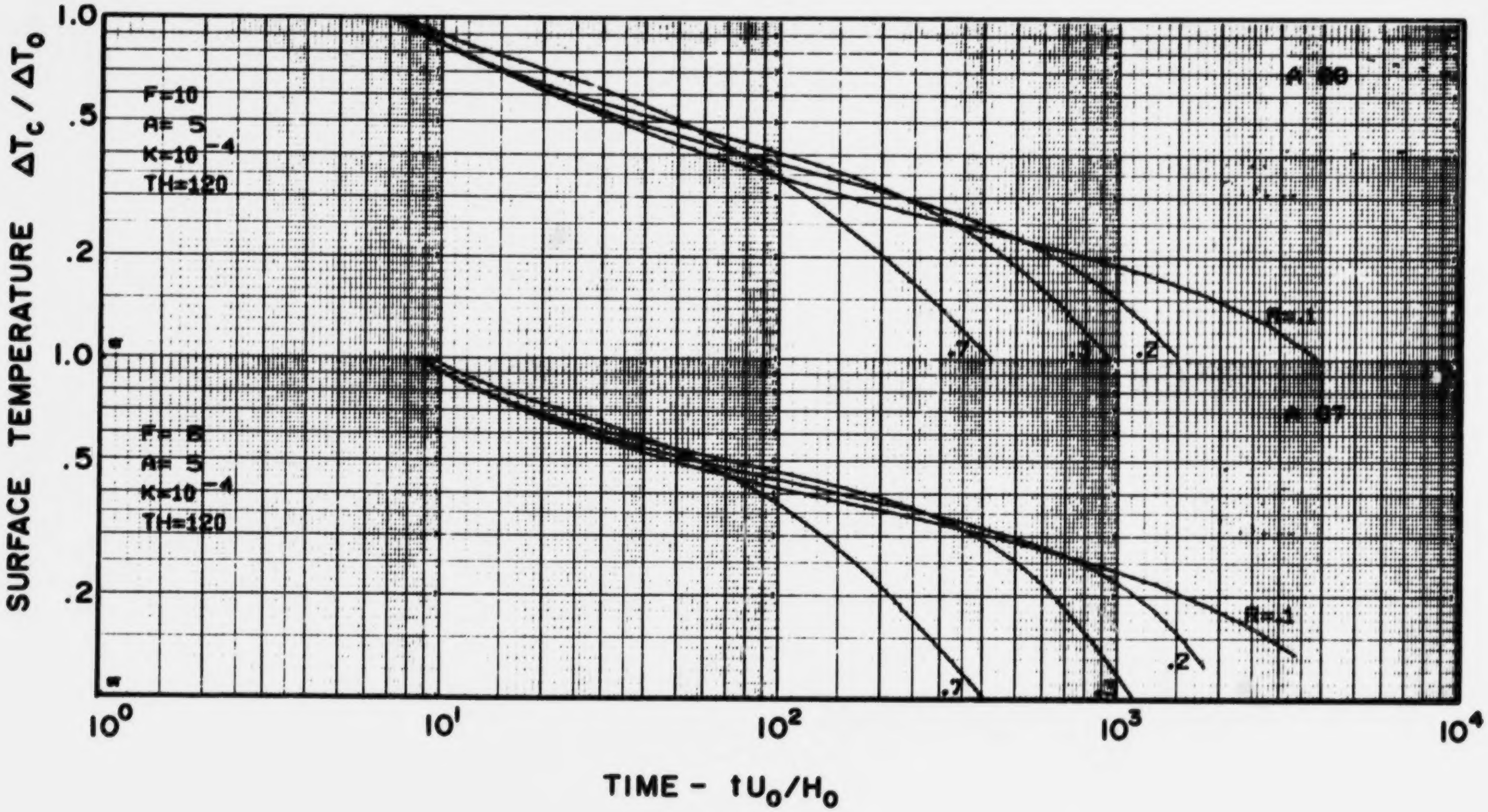

FIG (C44) TEMPERATURE, TIME (Tt)-PLOTS
FOR SURFACE JET DISCHARGE

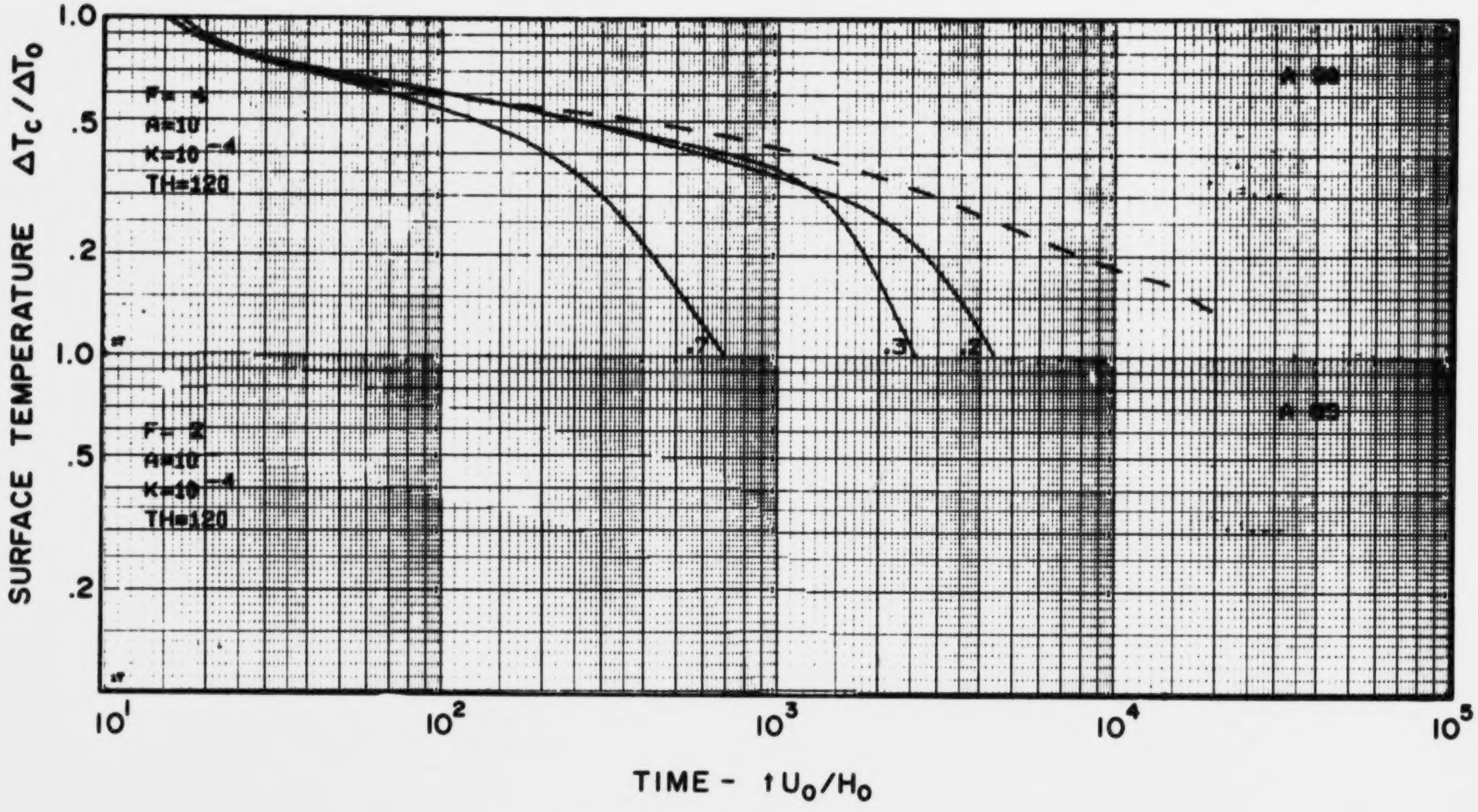

FIG (C45) TEMPERATURE, TIME (Tt)-PLOTS
FOR SURFACE JET DISCHARGE

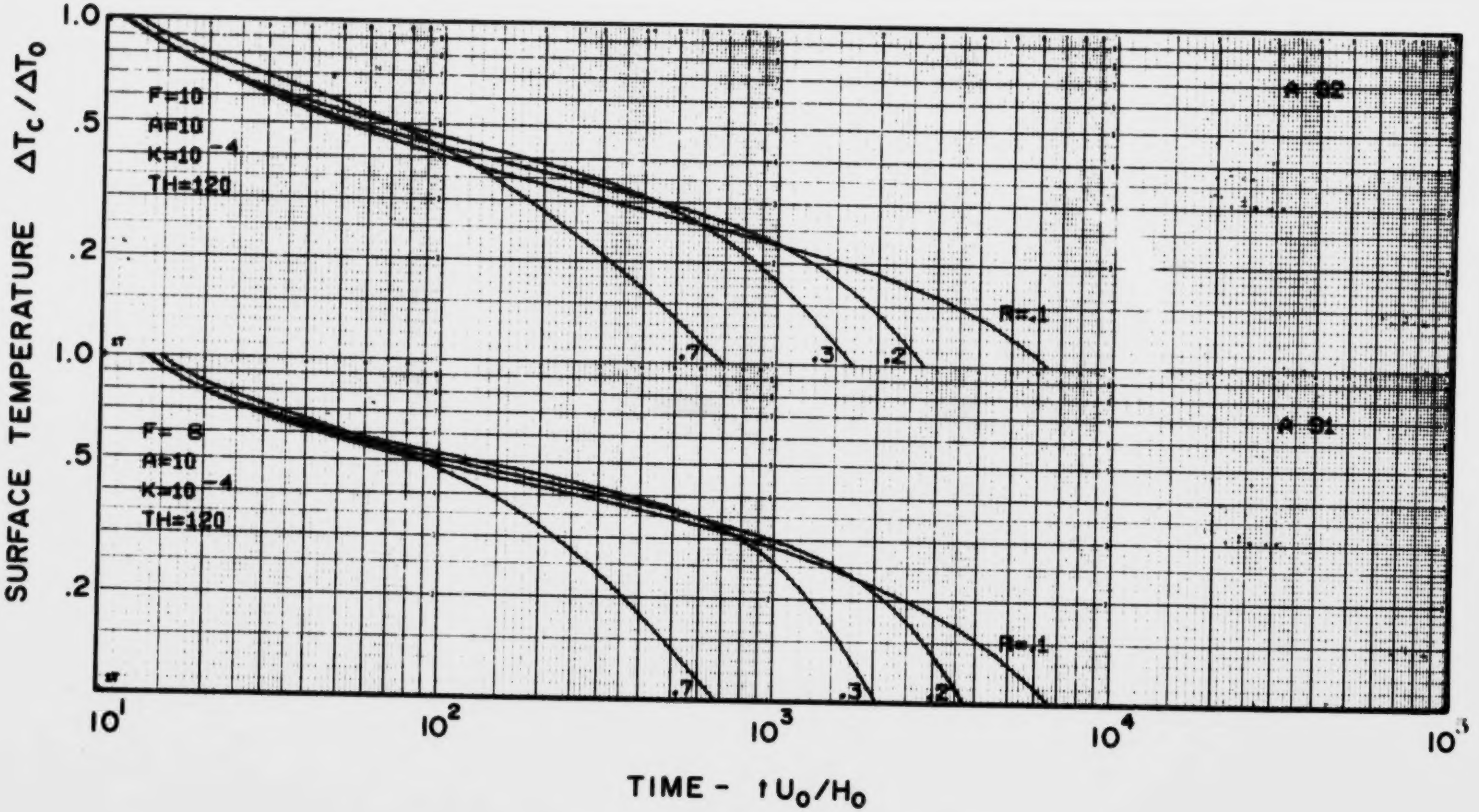

FIG (C46) TEMPERATURE, TIME (Tt)-PLOTS FOR SURFACE JET DISCHARGE

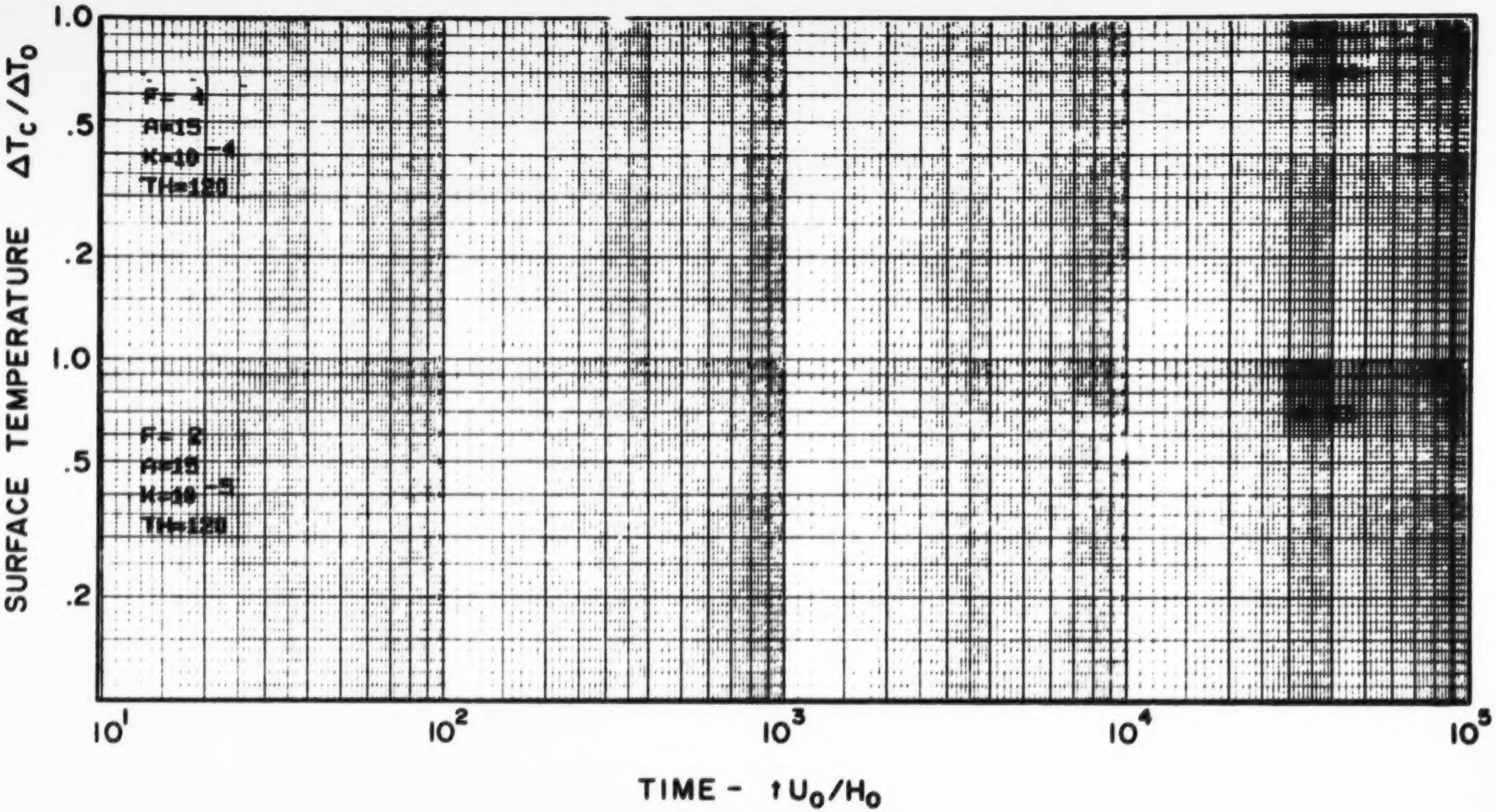

FIG (C47) TEMPERATURE, TIME (Tt)-PLOTS FOR SURFACE JET DISCHARGE

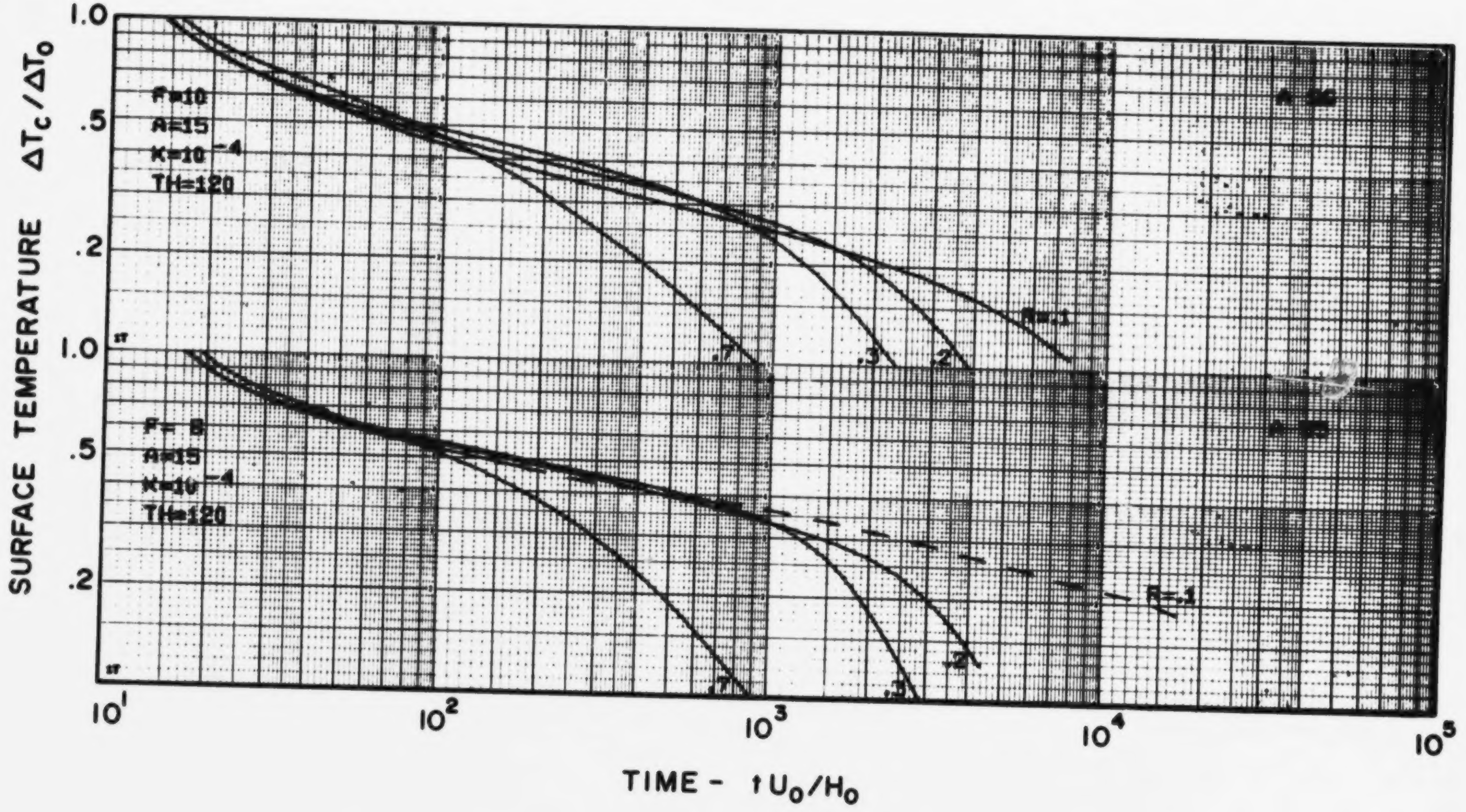

FIG (C48) TEMPERATURE, TIME (Tt)-PLOTS FOR SURFACE JET DISCHARGE

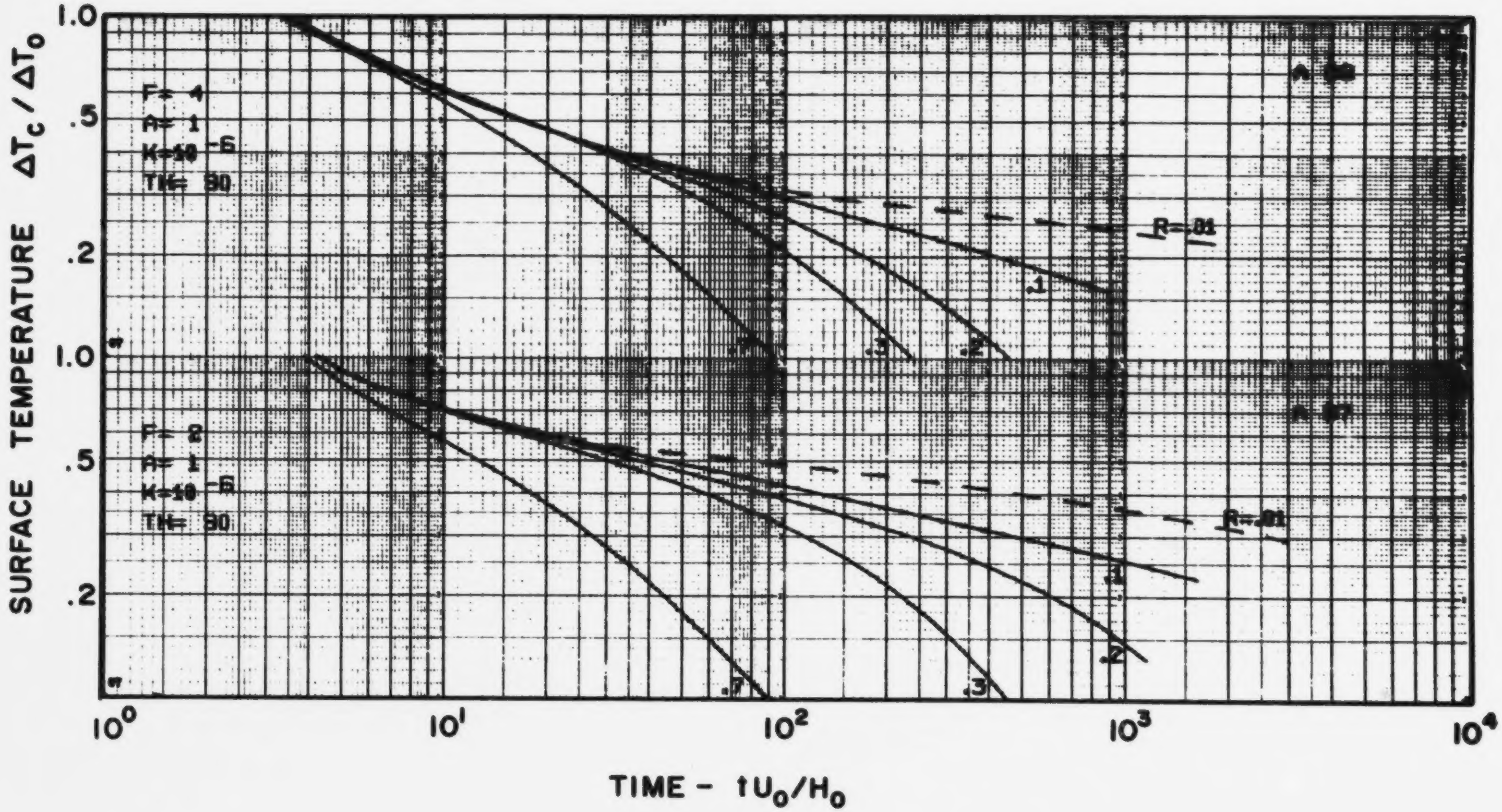

FIG (C49) TEMPERATURE, TIME (Tt)-PLOTS
FOR SURFACE JET DISCHARGE

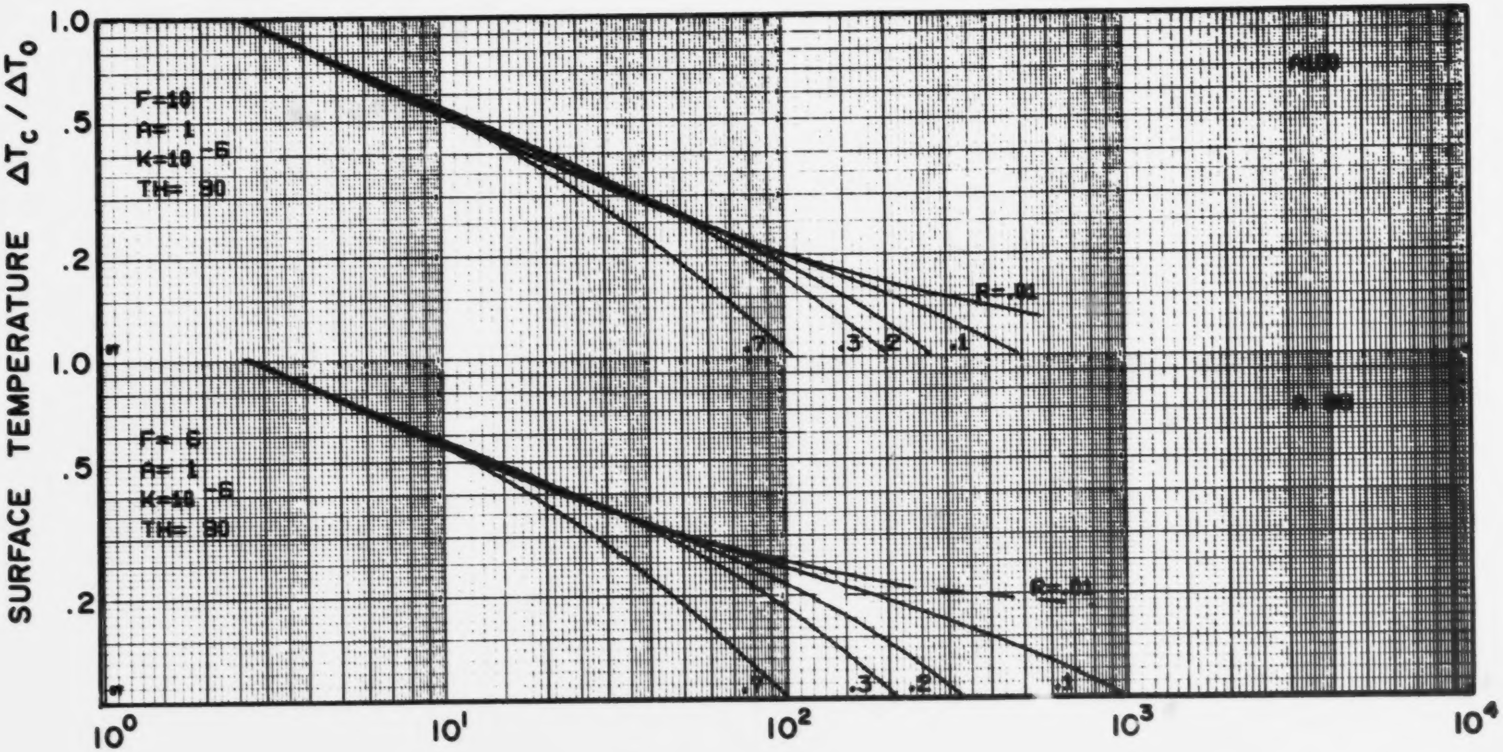

FIG (C50) TEMPERATURE, TIME (Tt)-PLOTS FOR SURFACE JET DISCHARGE

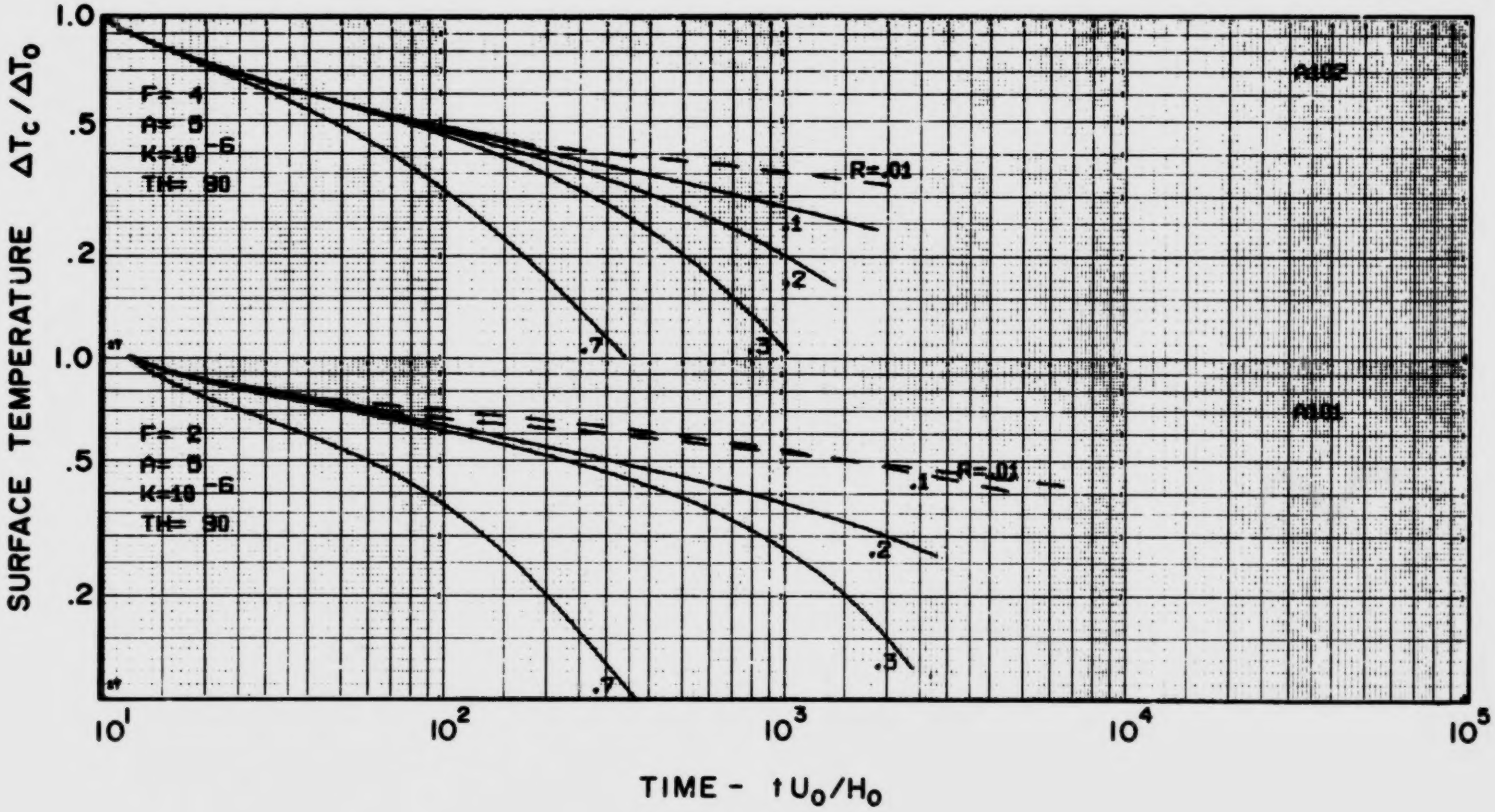

FIG (C51) TEMPERATURE, TIME (Tt)-PLOTS FOR SURFACE JET DISCHARGE

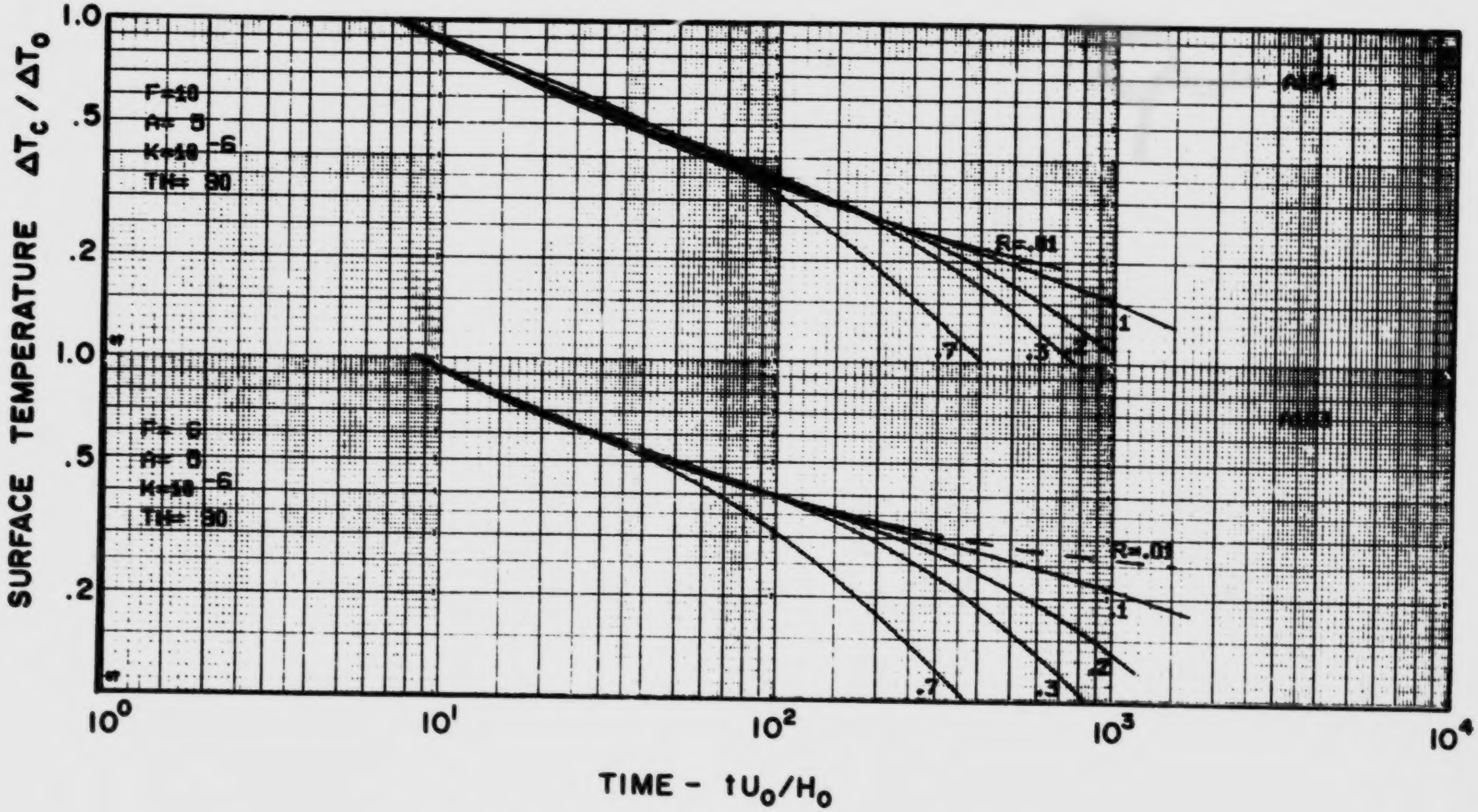

FIG (C52) TEMPERATURE, TIME (Tt)-PLOTS
FOR SURFACE JET DISCHARGE

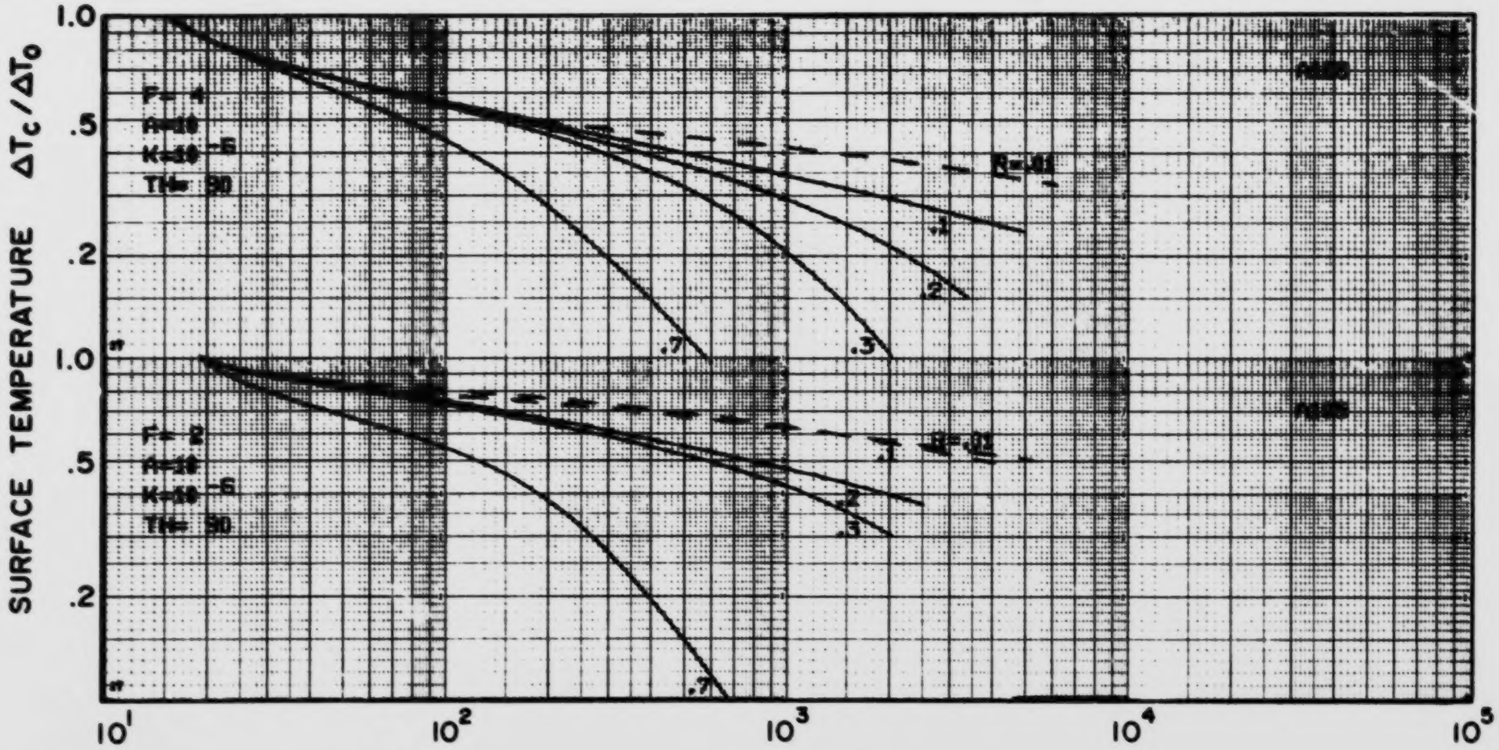

FIG (C53) TEMPERATURE, TIME (Tt)-PLOTS
FOR SURFACE JET DISCHARGE

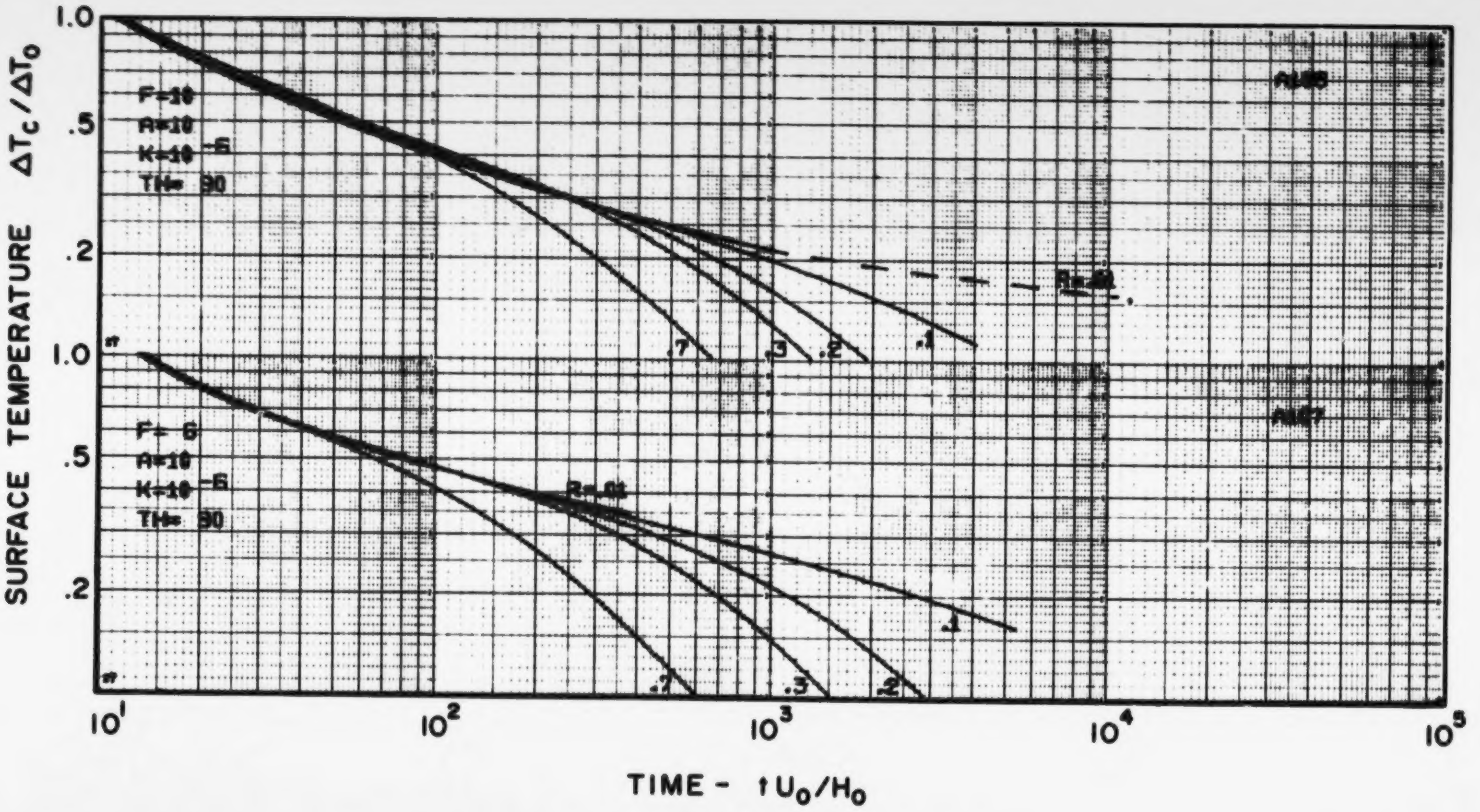

FIG (C54) TEMPERATURE, TIME (Tt)-PLOTS FOR SURFACE JET DISCHARGE

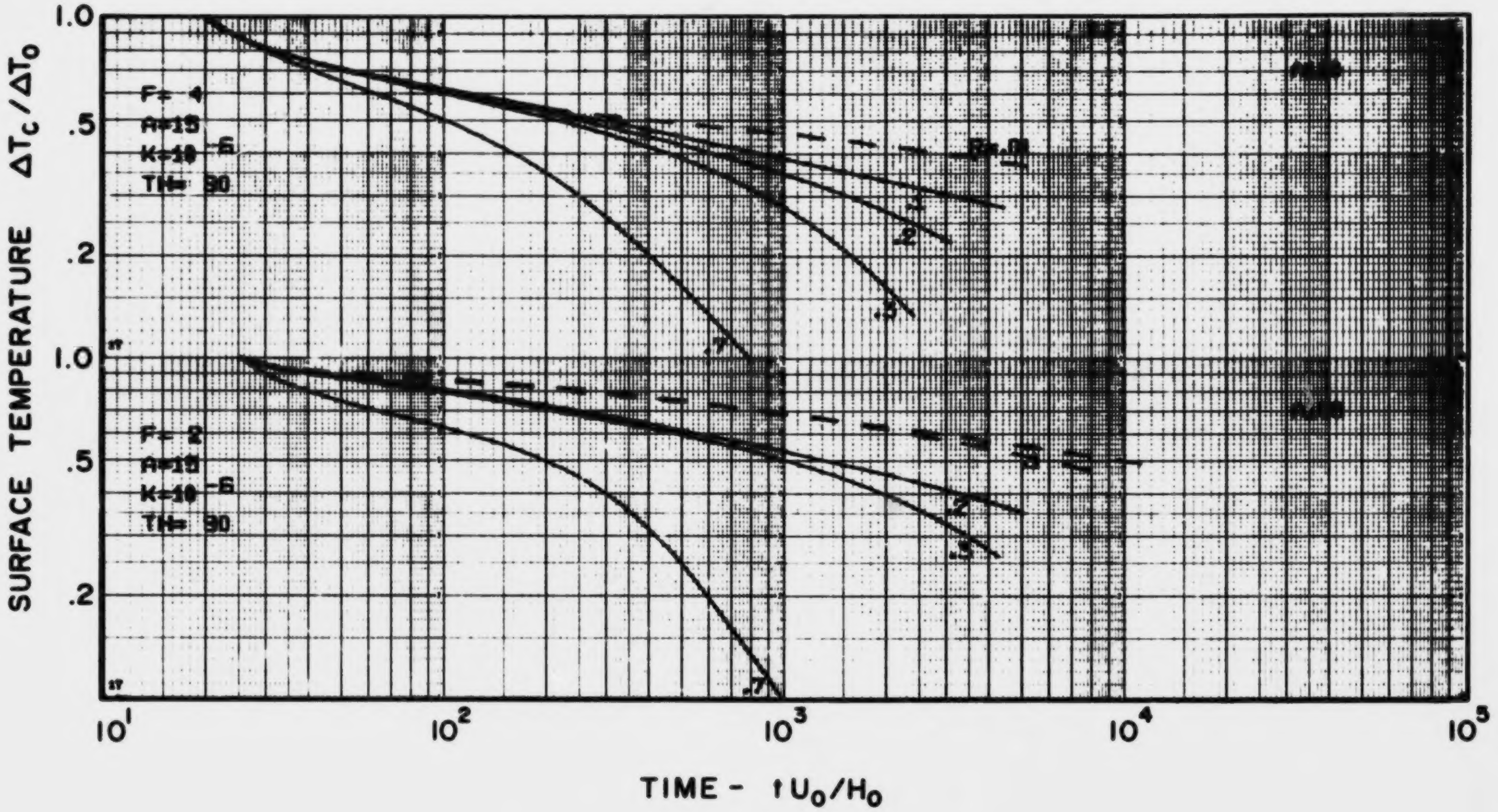

FIG (C 55) TEMPERATURE, TIME (Tt)-PLOTS
FOR SURFACE JET DISCHARGE

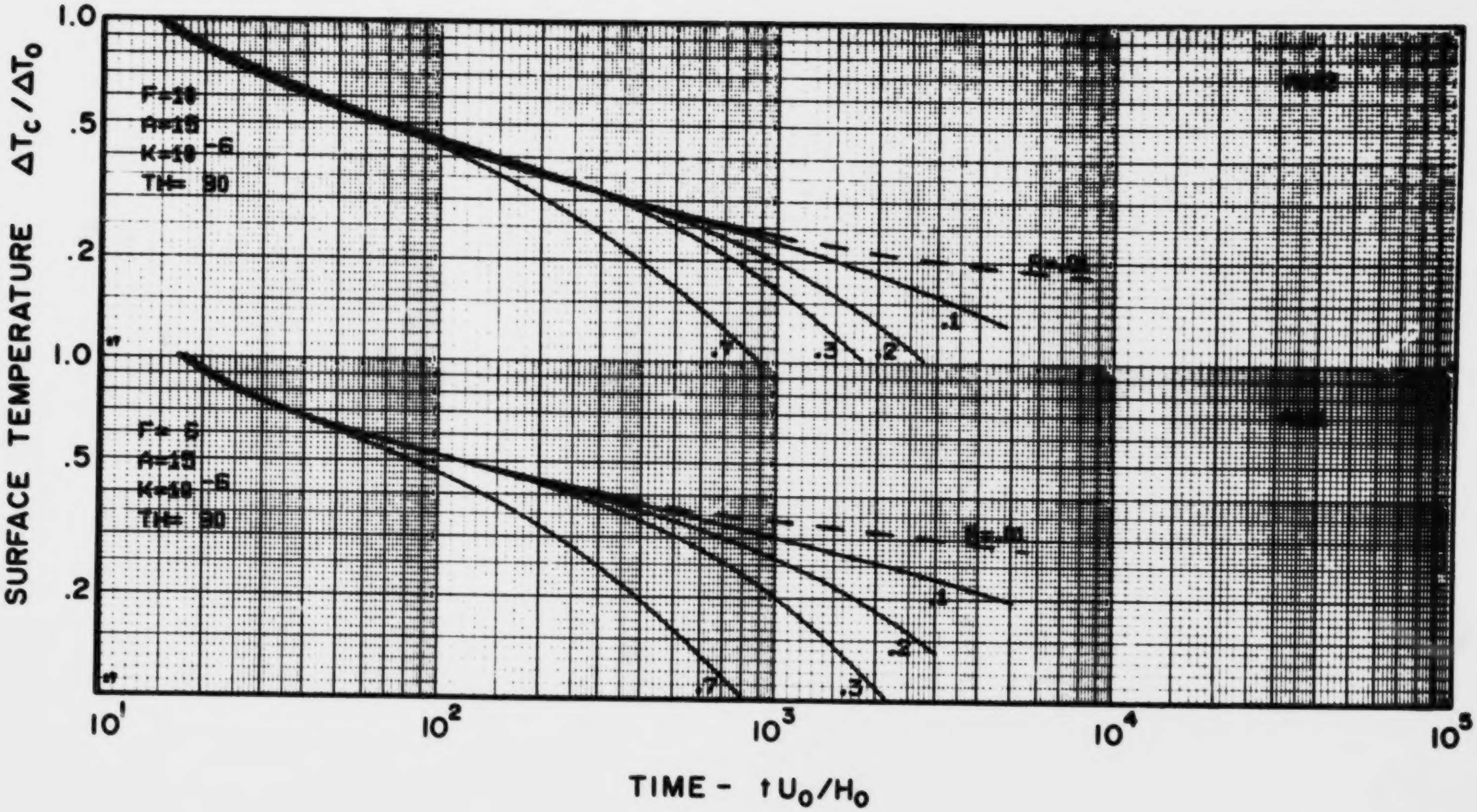

FIG (C56) TEMPERATURE, TIME (Tt)-PLOTS FOR SURFACE JET DISCHARGE

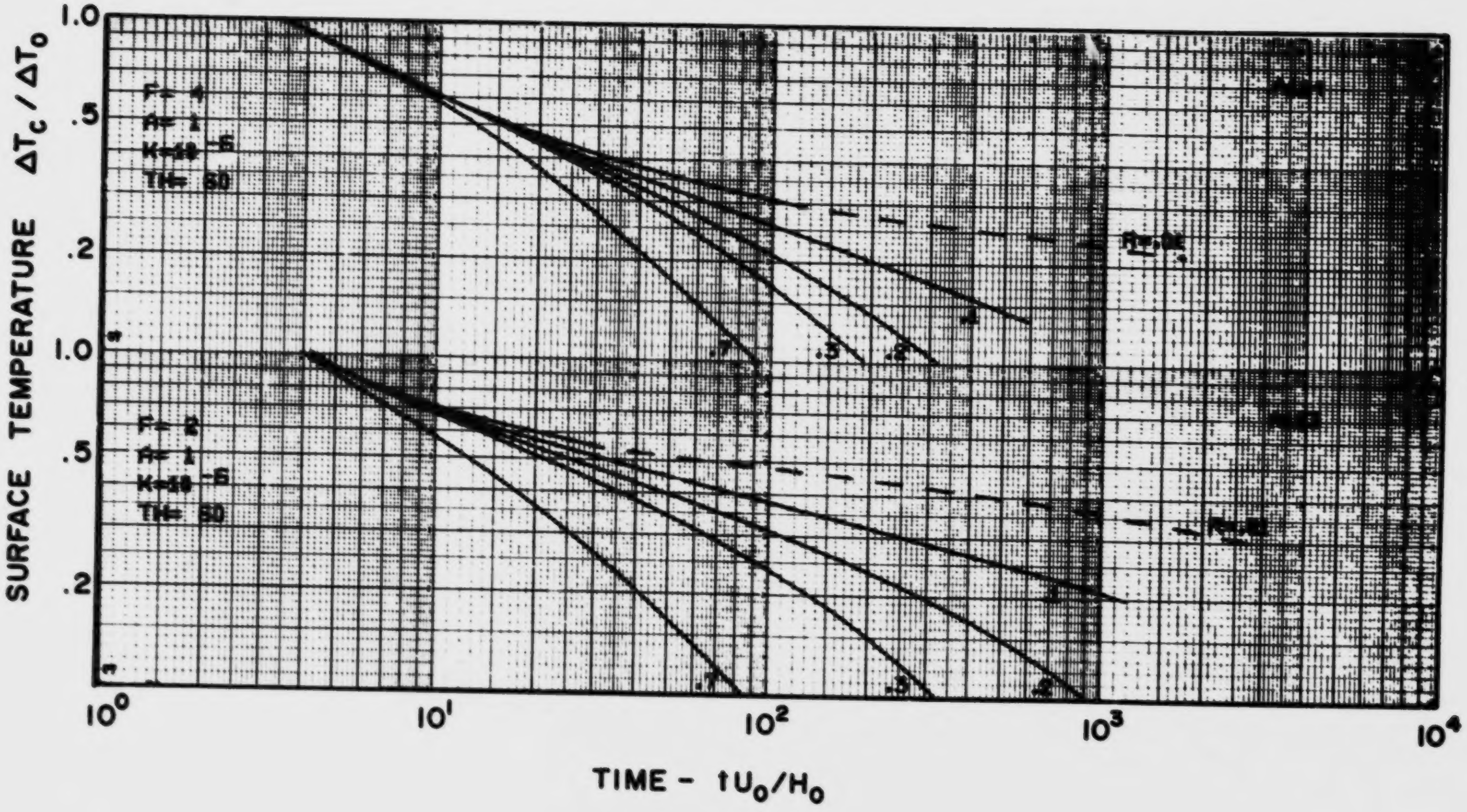

FIG (C57) TEMPERATURE, TIME (Tt)-PLOTS
FOR SURFACE JET DISCHARGE

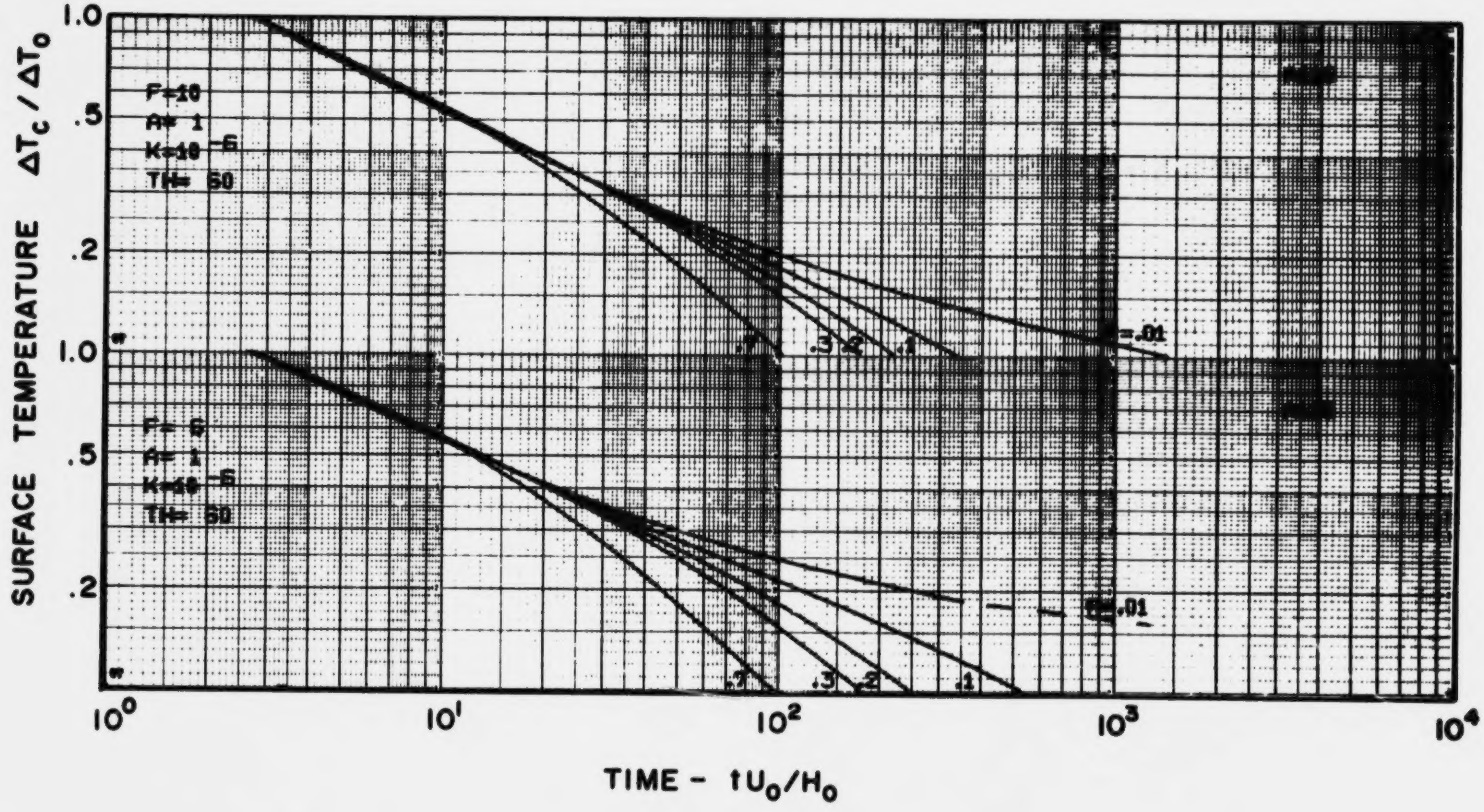

FIG (C58) TEMPERATURE, TIME (Tt)-PLOTS FOR SURFACE JET DISCHARGE

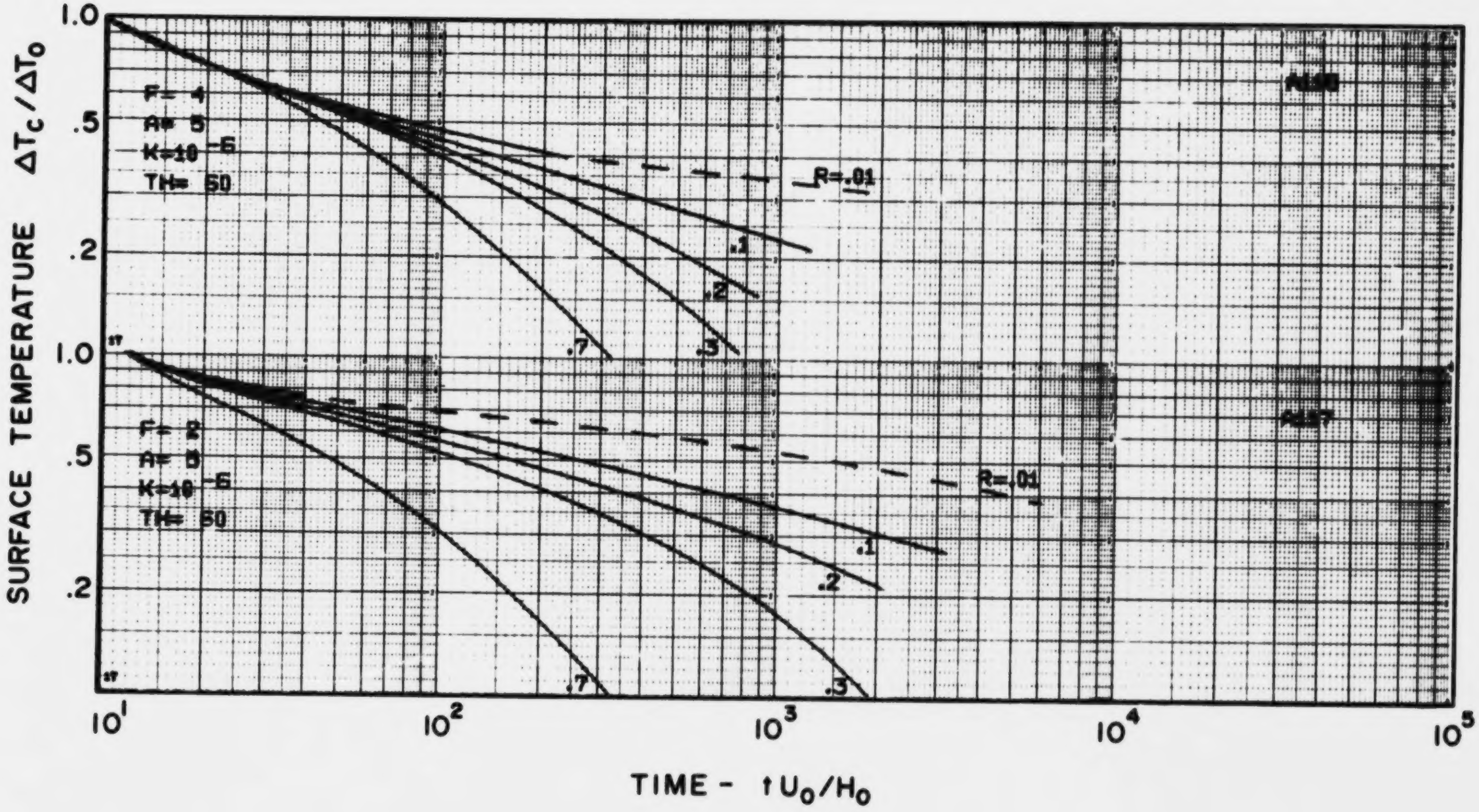

FIG (C59) TEMPERATURE, TIME (Tt)-PLOTS FOR SURFACE JET DISCHARGE

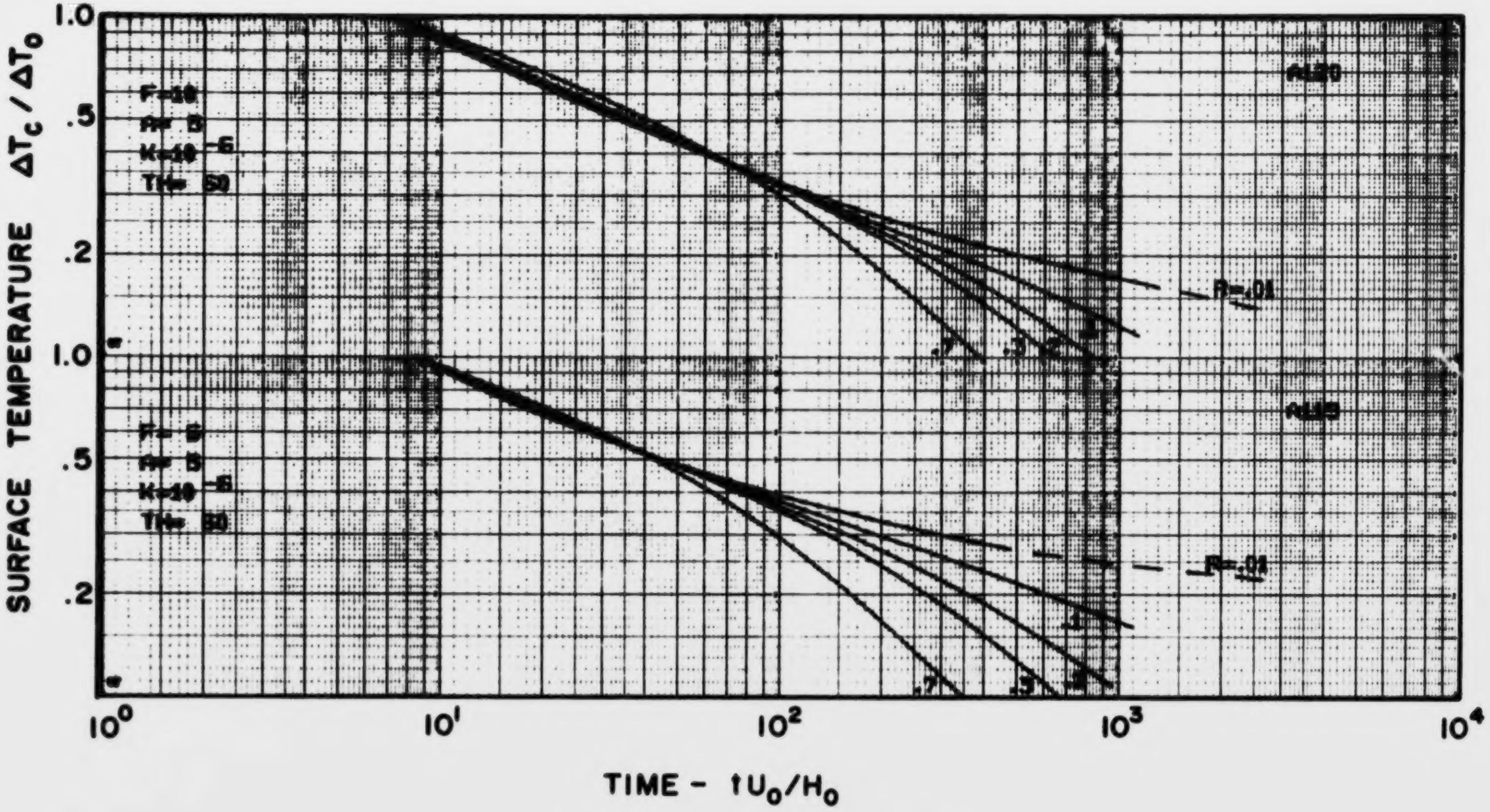

FIG (C60) TEMPERATURE, TIME (Tt)-PLOTS FOR SURFACE JET DISCHARGE

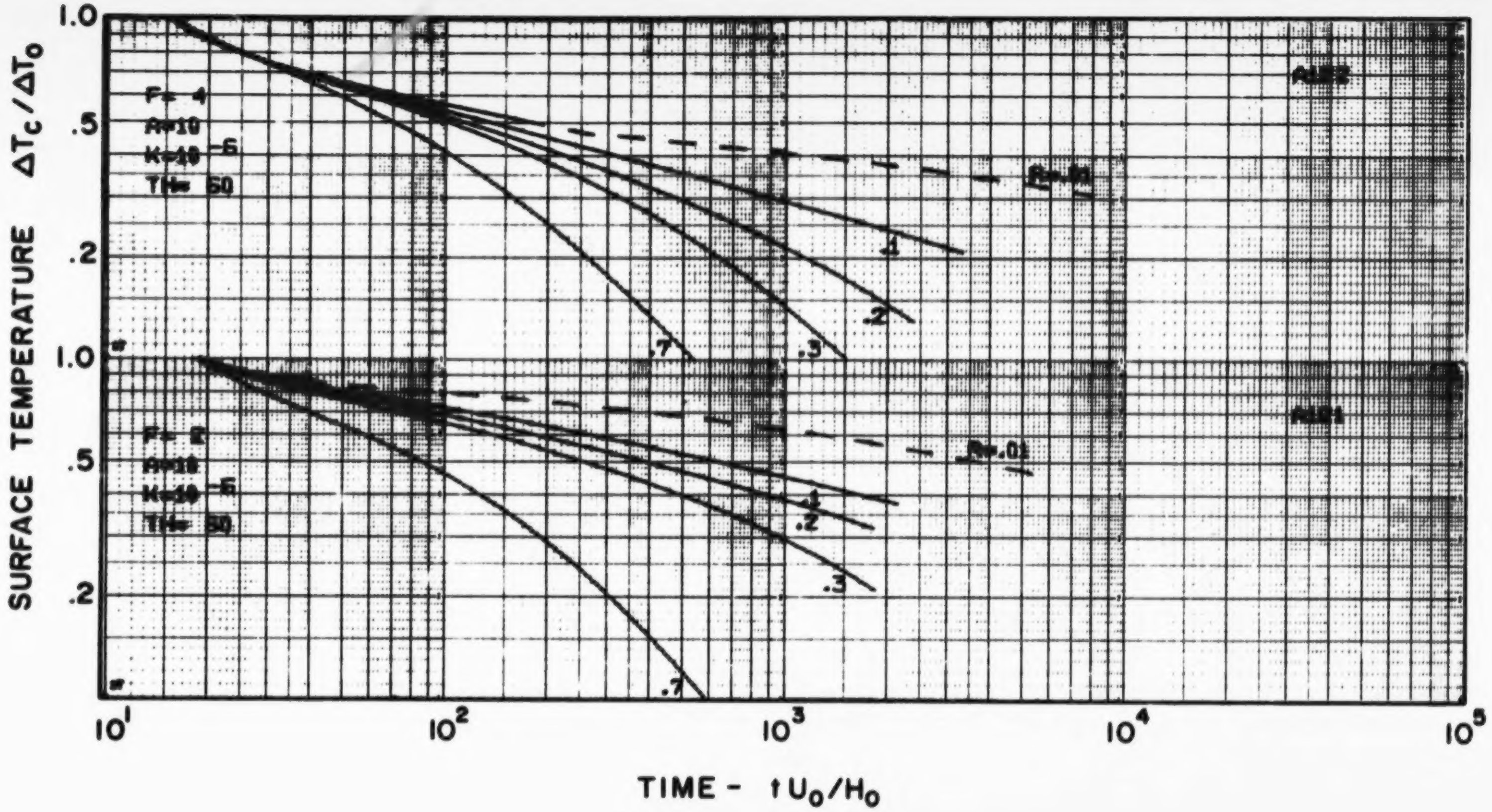

FIG (C61) TEMPERATURE, TIME (Tt)-PLOTS FOR SURFACE JET DISCHARGE

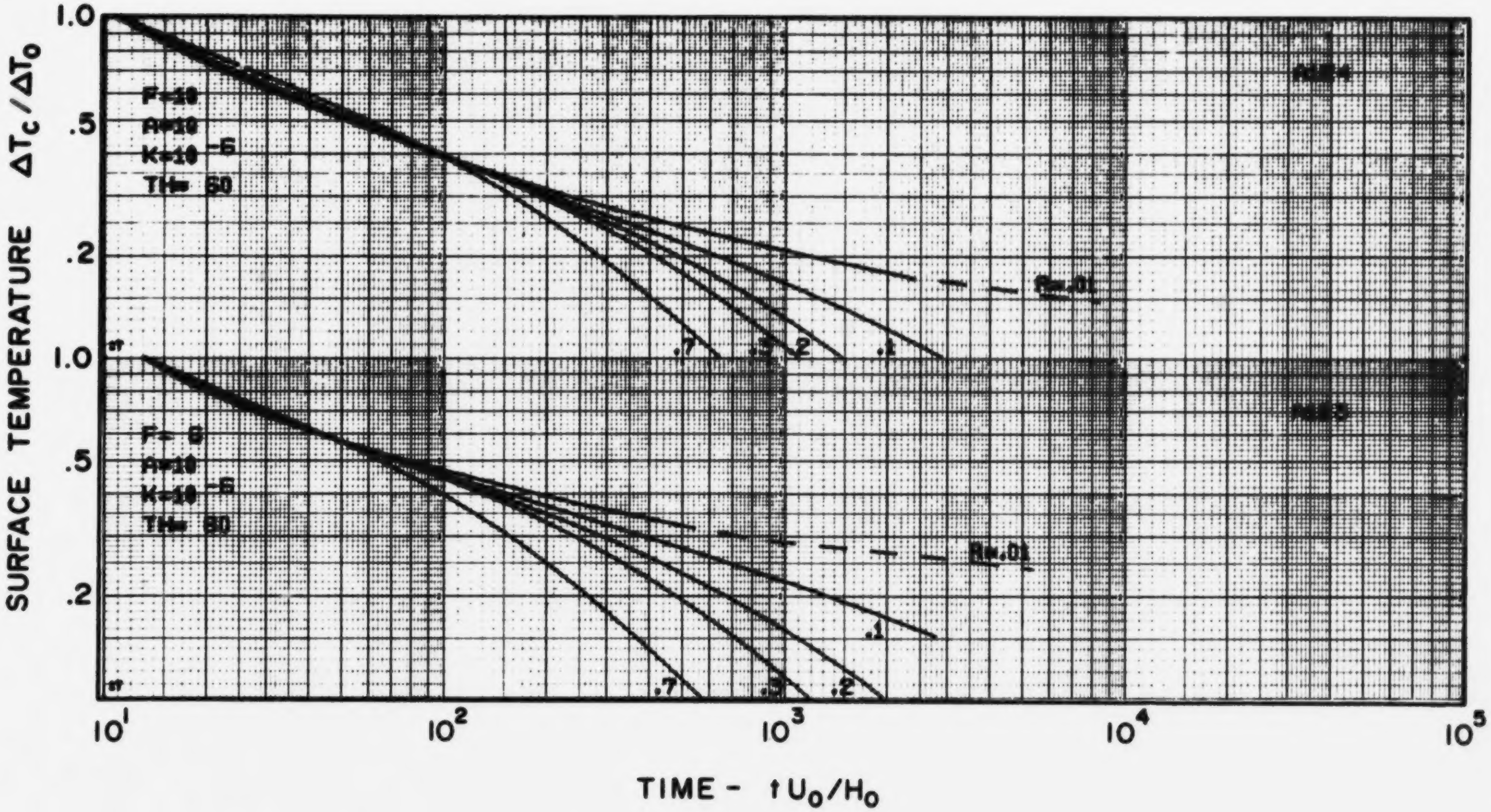

FIG (C62) TEMPERATURE, TIME (Tt)-PLOTS FOR SURFACE JET DISCHARGE

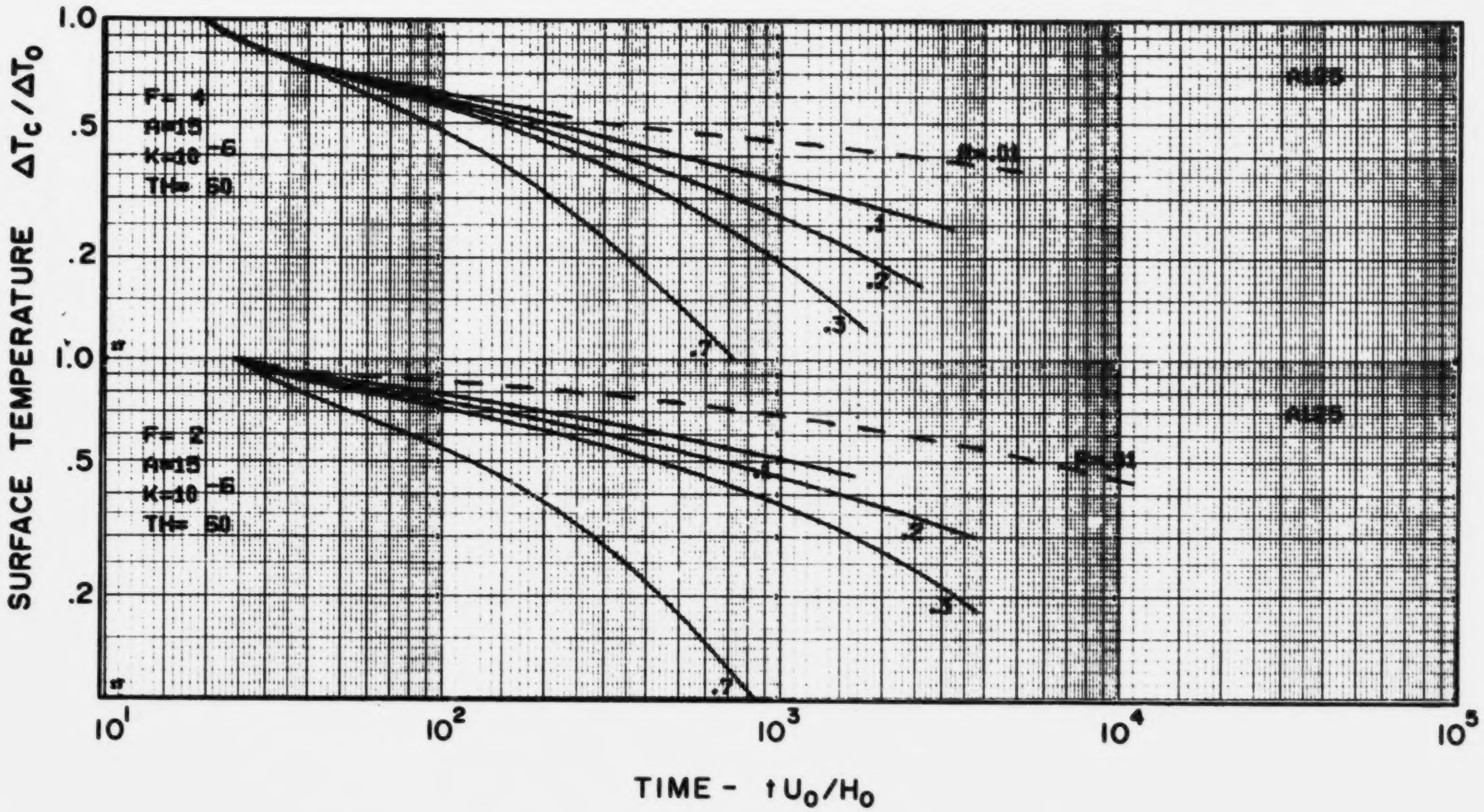

FIG (C63) TEMPERATURE, TIME (Tt)-PLOTS
FOR SURFACE JET DISCHARGE

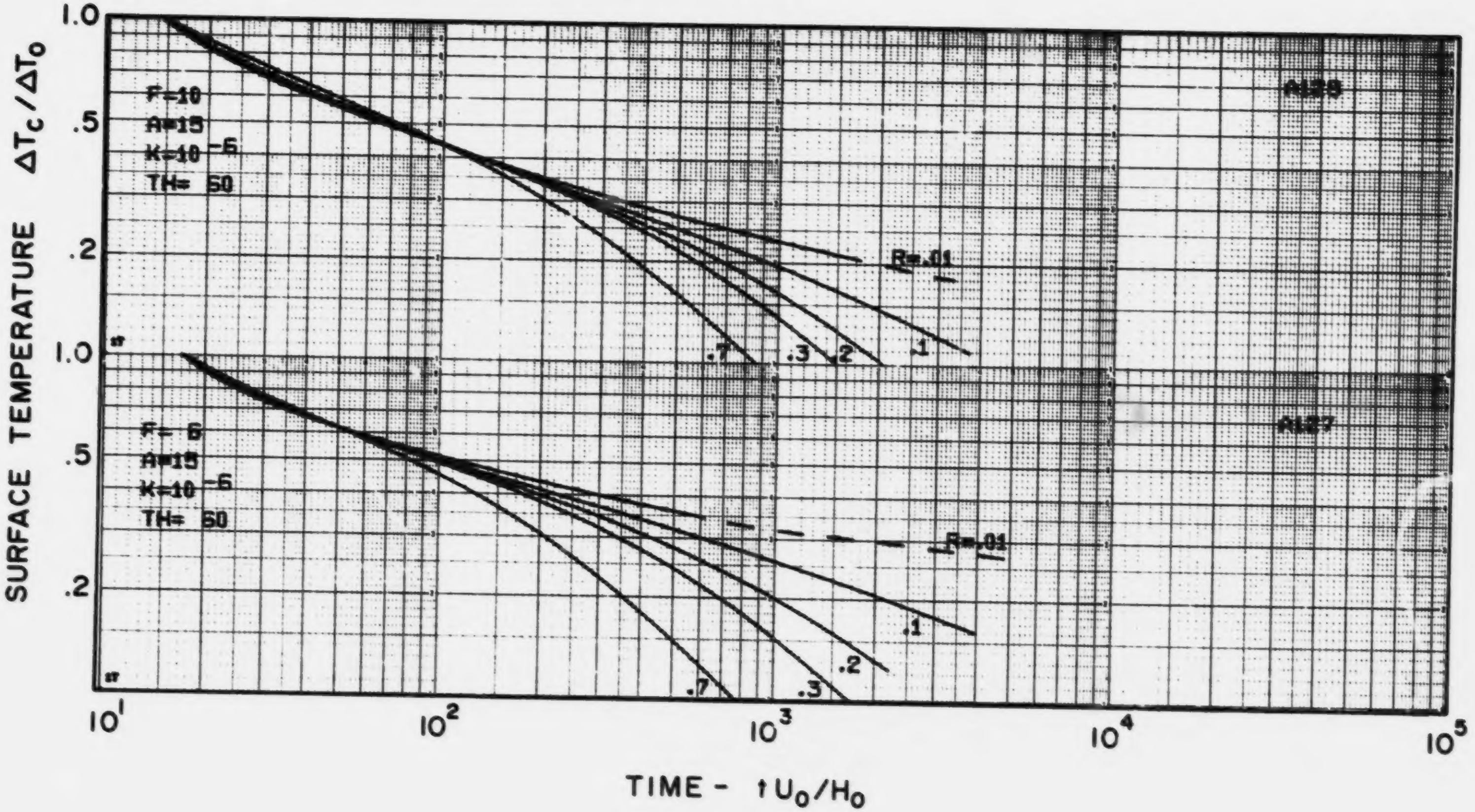

FIG (C64) TEMPERATURE, TIME (Tt)-PLOTS
FOR SURFACE JET DISCHARGE

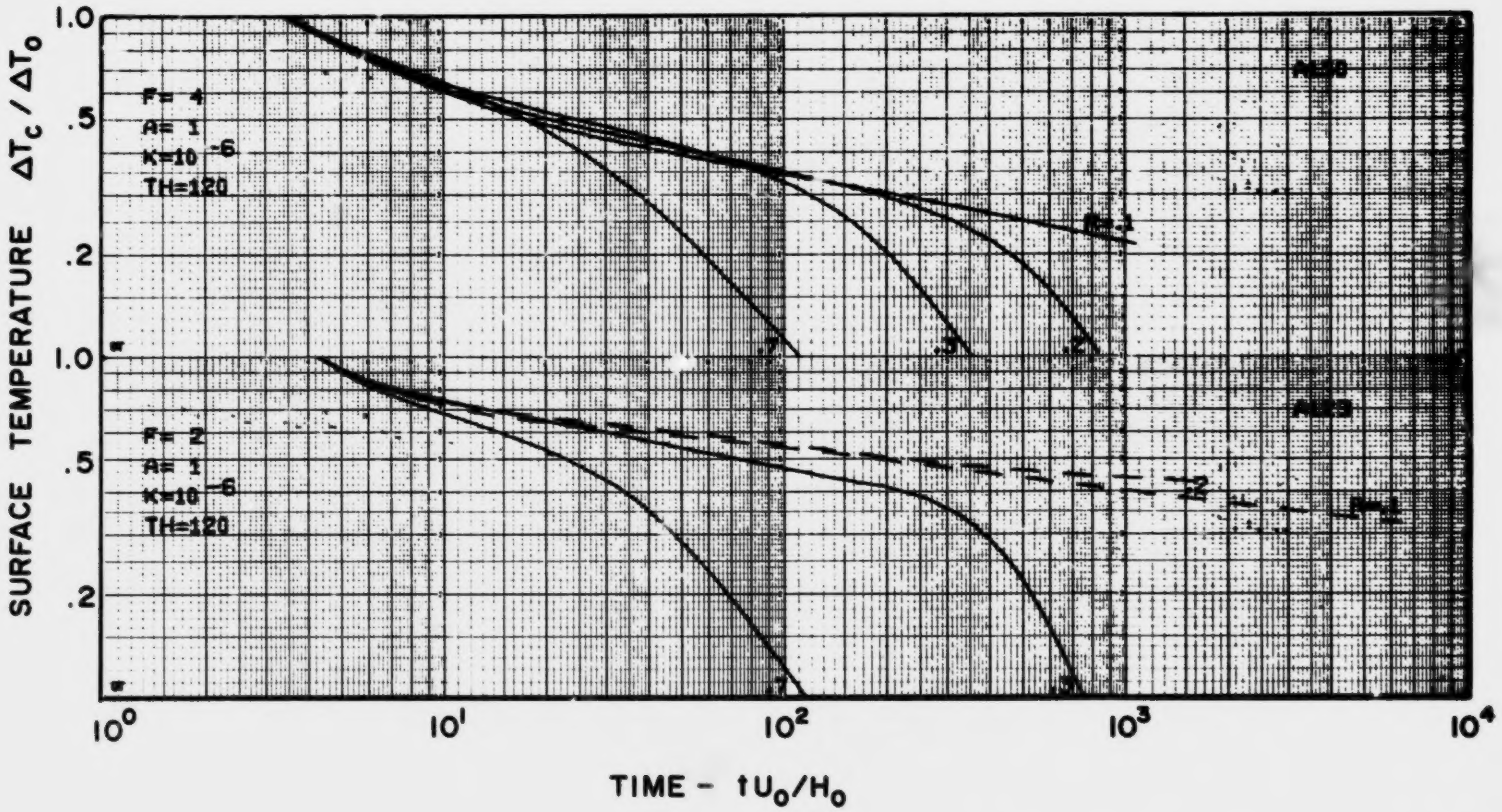

FIG (C65) TEMPERATURE, TIME (Tt)-PLOTS FOR SURFACE JET DISCHARGE

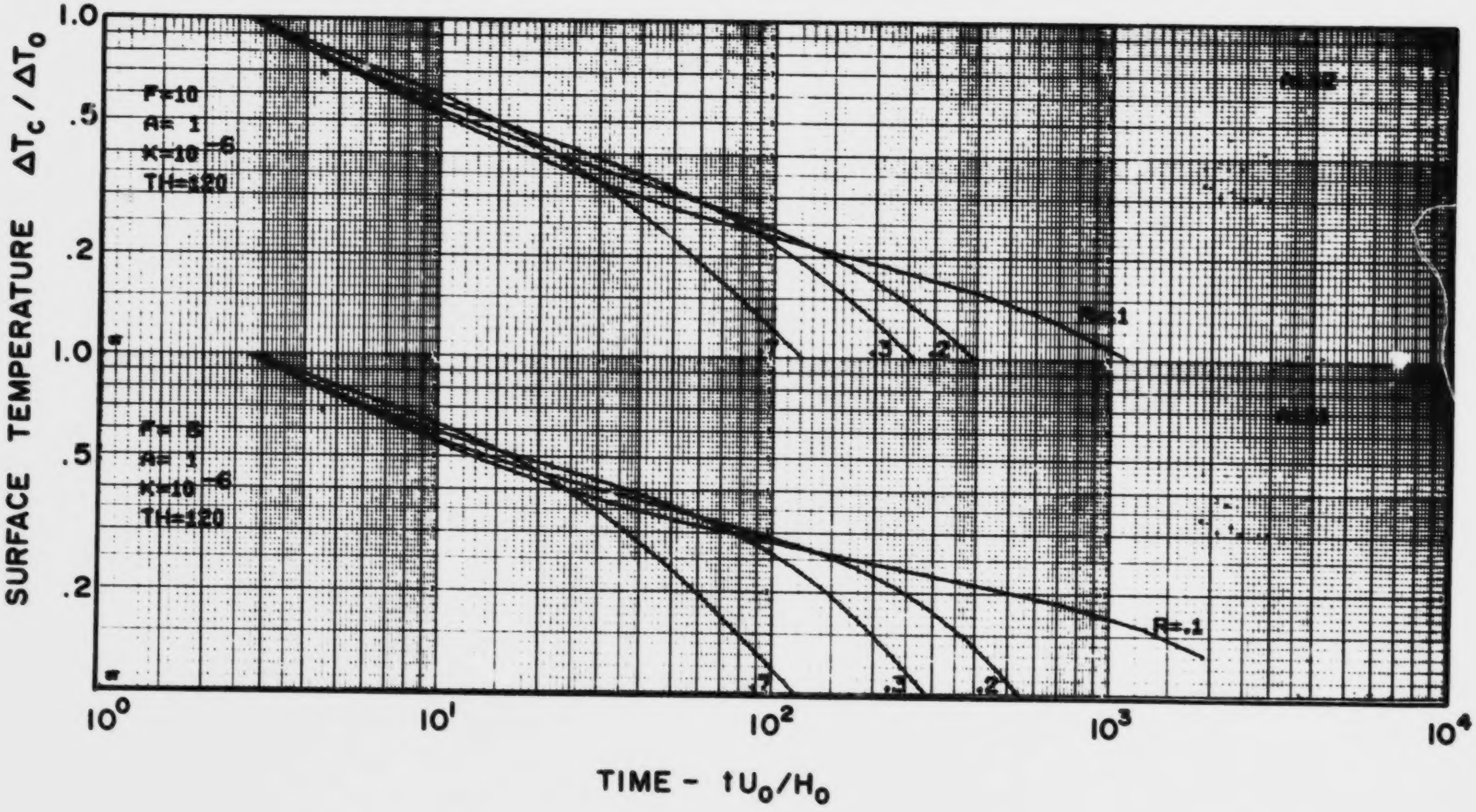

FIG (C66) TEMPERATURE, TIME (Tt)-PLOTS FOR SURFACE JET DISCHARGE

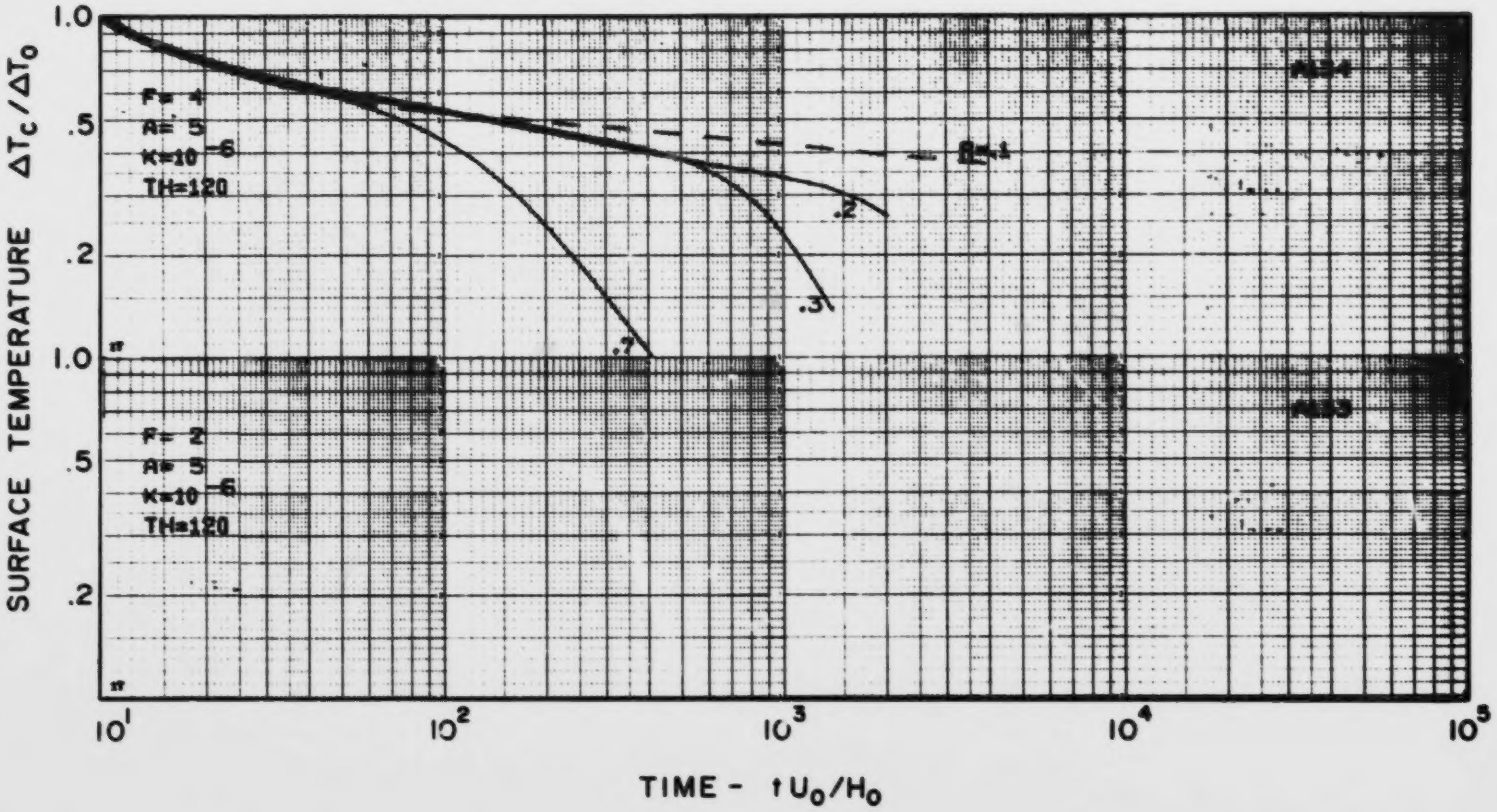

FIG (C67) TEMPERATURE, TIME (Tt)-PLOTS
FOR SURFACE JET DISCHARGE

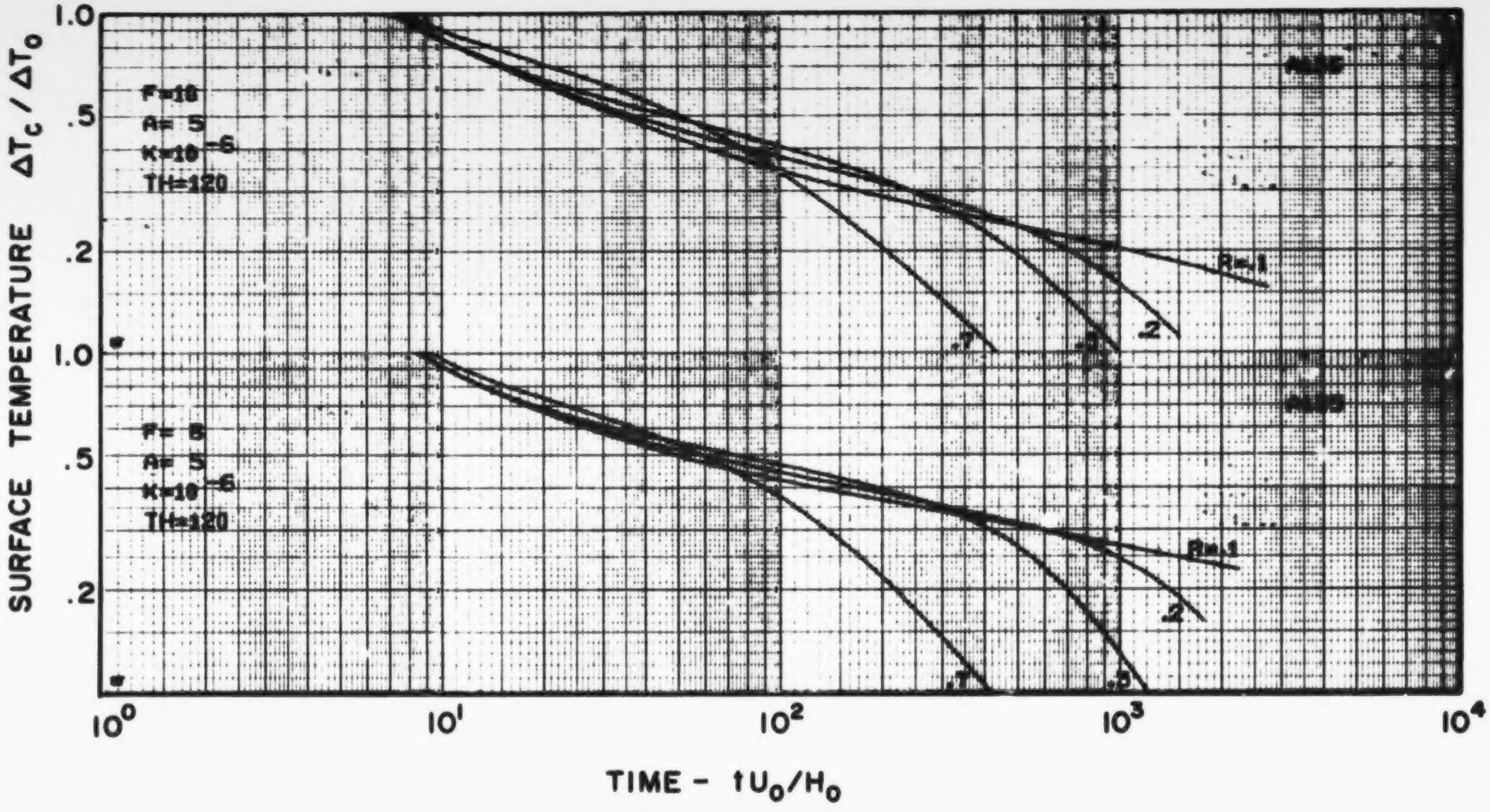

FIG (C68) TEMPERATURE, TIME (Tt)-PLOTS FOR SURFACE JET DISCHARGE

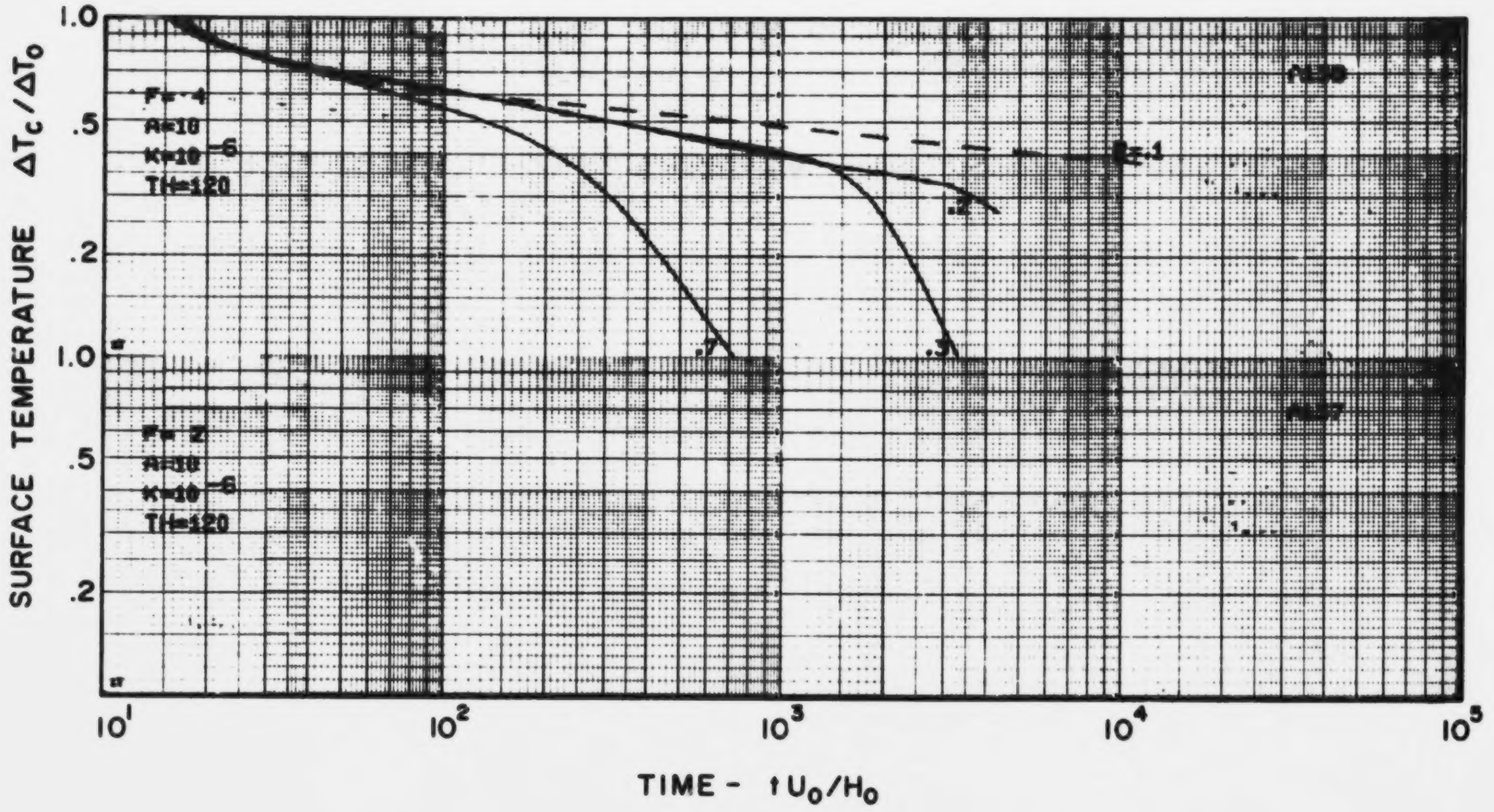

FIG (C69) TEMPERATURE, TIME (Tt)-PLOTS FOR SURFACE JET DISCHARGE

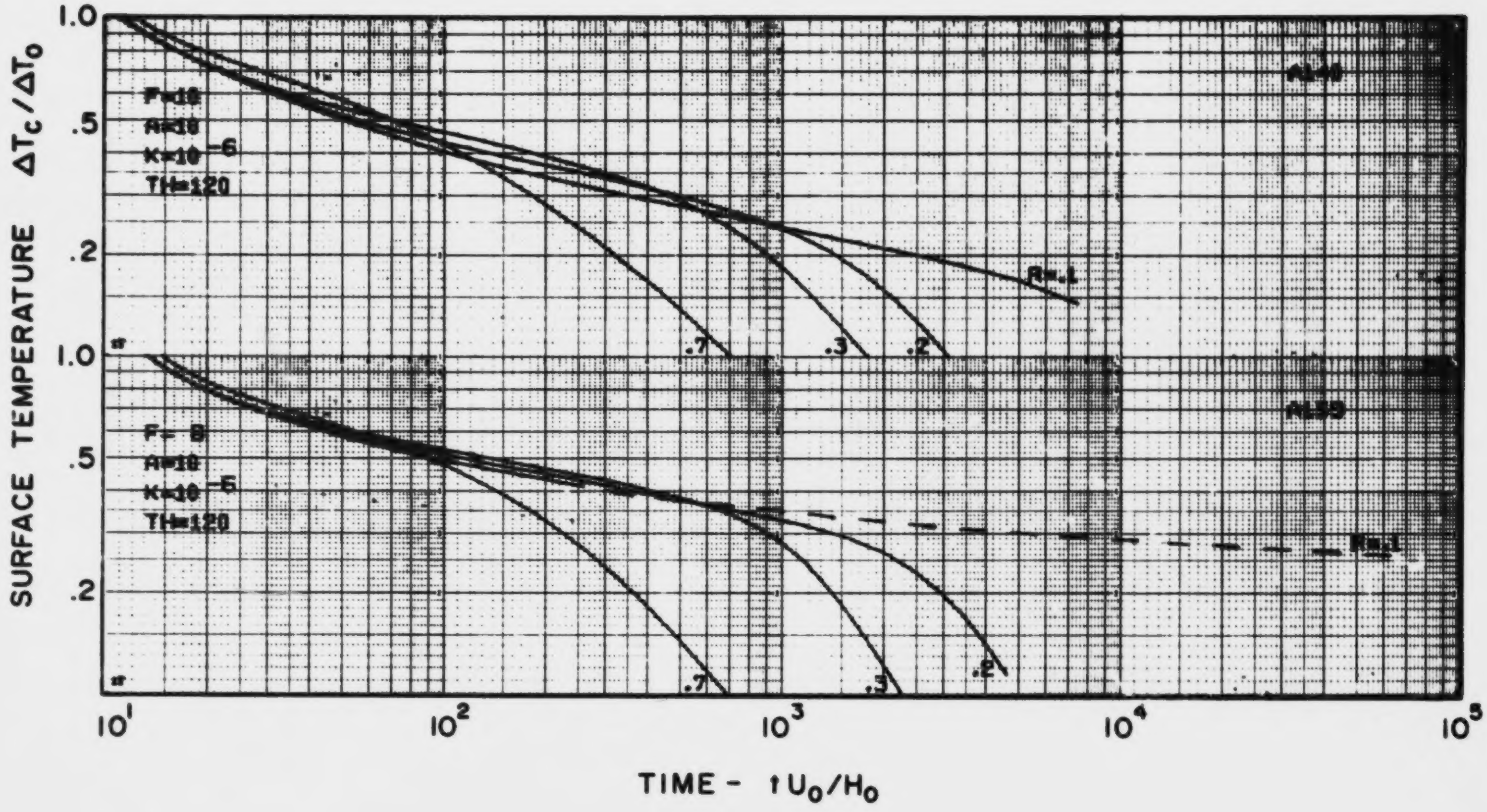

FIG (C70) TEMPERATURE, TIME (Tt)-PLOTS FOR SURFACE JET DISCHARGE

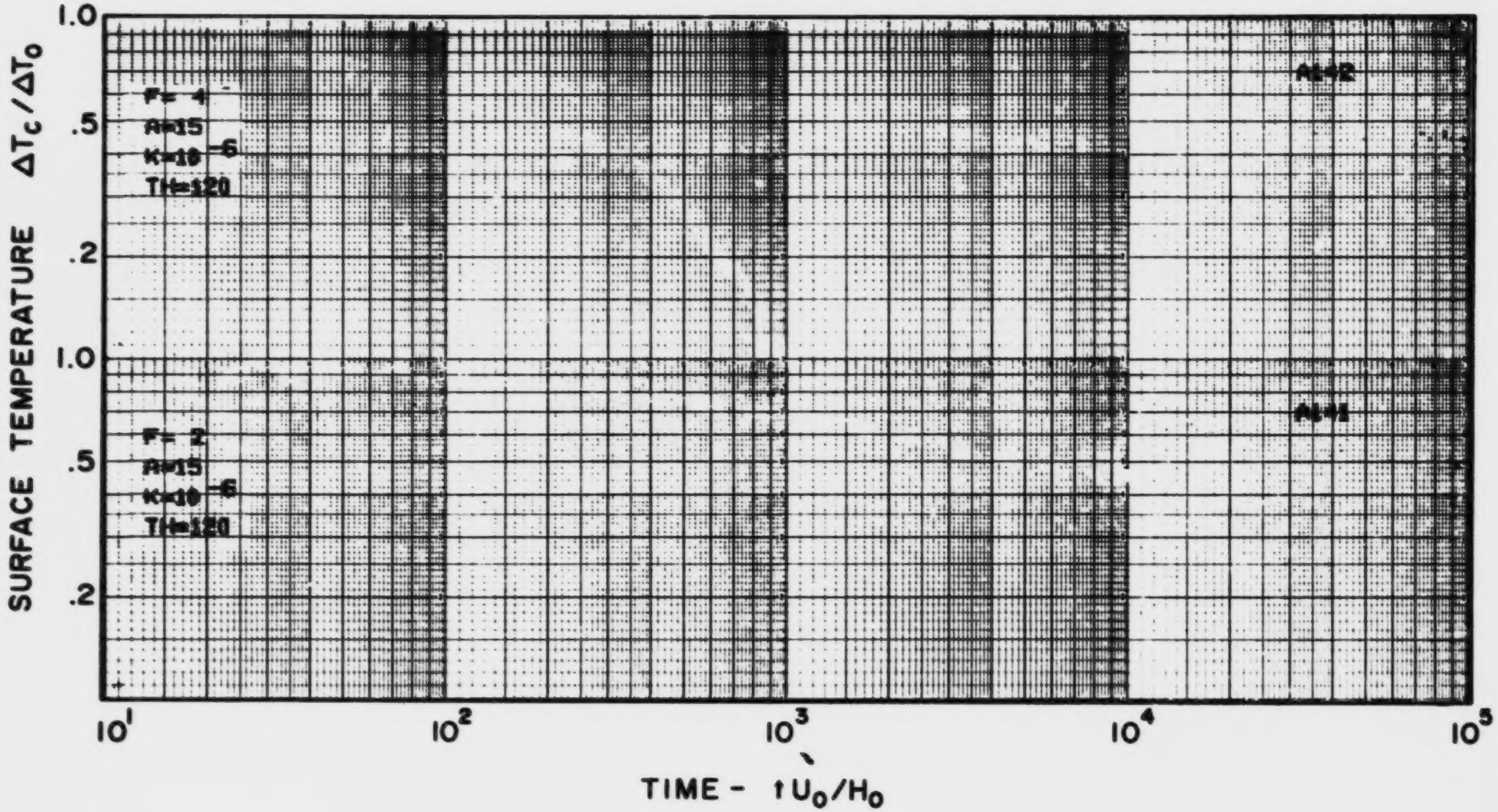

FIG (C71) TEMPERATURE, TIME (Tt)-PLOTS FOR SURFACE JET DISCHARGE

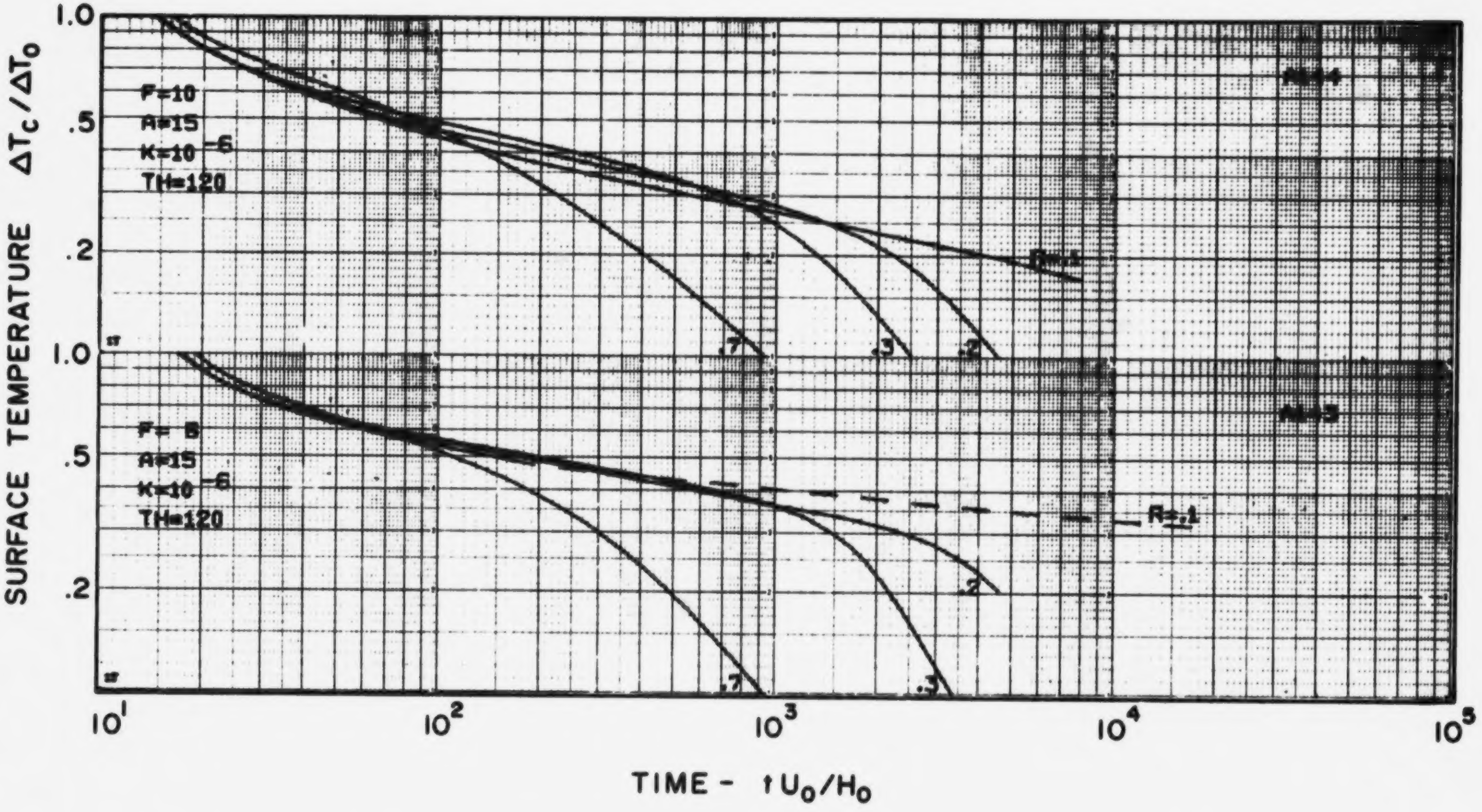

FIG (C72) TEMPERATURE, TIME (Tt)-PLOTS FOR SURFACE JET DISCHARGE

APPENDIX D
(TTWD) SUPPLEMENTARY NOMOGRAMS

TABLE 7
Figure Numbers for (TTWD) Supplementary Nomograms of Appendix D, $\Theta_b = 90°$, $K = 10^{-5}$, $F = 4$, $A = .5$

$E_h \rightarrow$ $\downarrow E_v/E_h$	.005	.02	.1
.001	D1	D2	D3
.01	D4	D5	D6
.2	D7	D8	D9

TABLE 8
Summary of Figure Numbers for (TTWD) Supplementary Nomograms of Appendix D

E_o	.01	D1-D9
	.05	D10-18
	.15	D19-D27

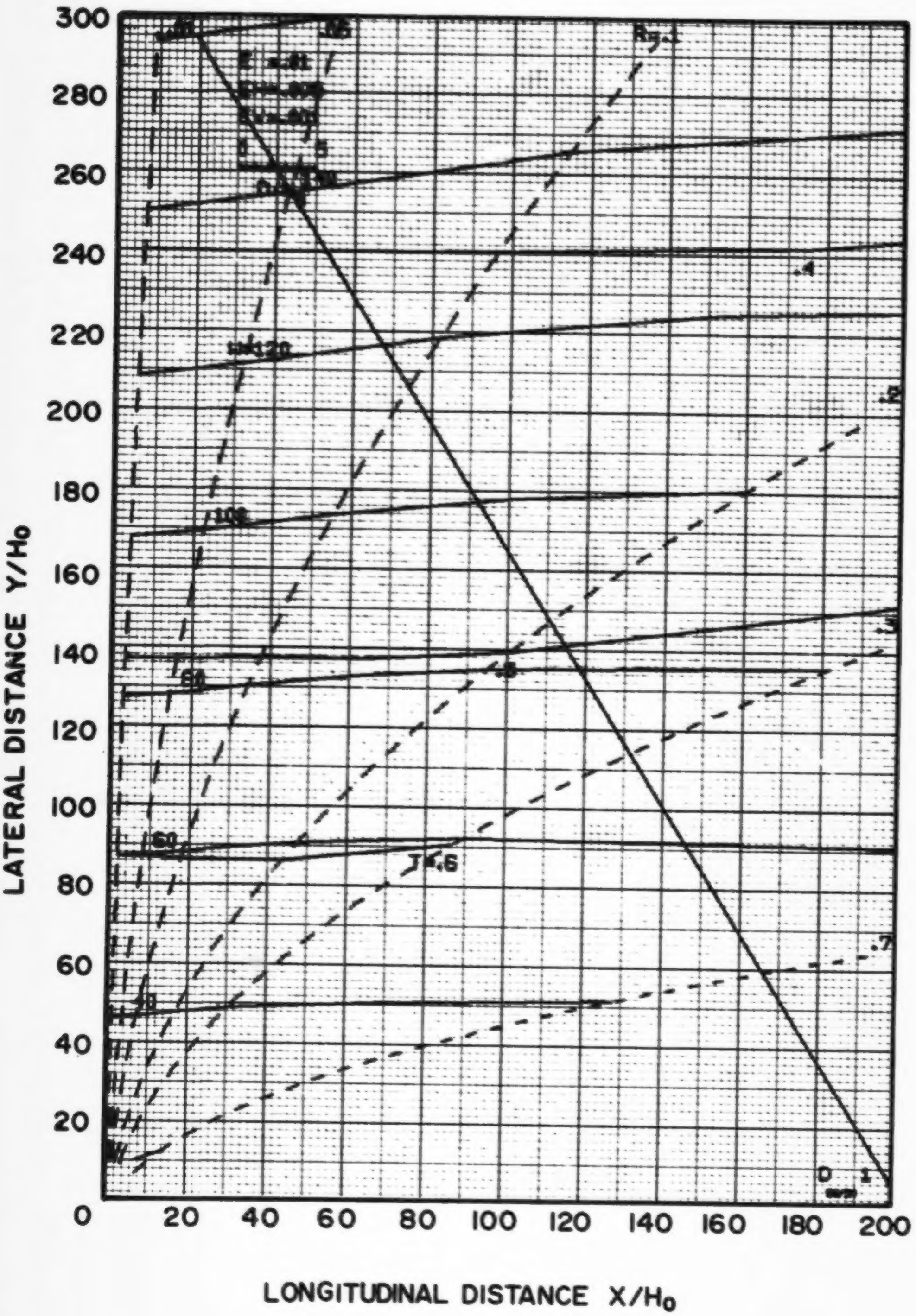

FIG(D1) TEMPERATURE, TRAJECTORY, WIDTH, AND DEPTH (TTWD)-PLOTS FOR SURFACE JET DISCHARGE

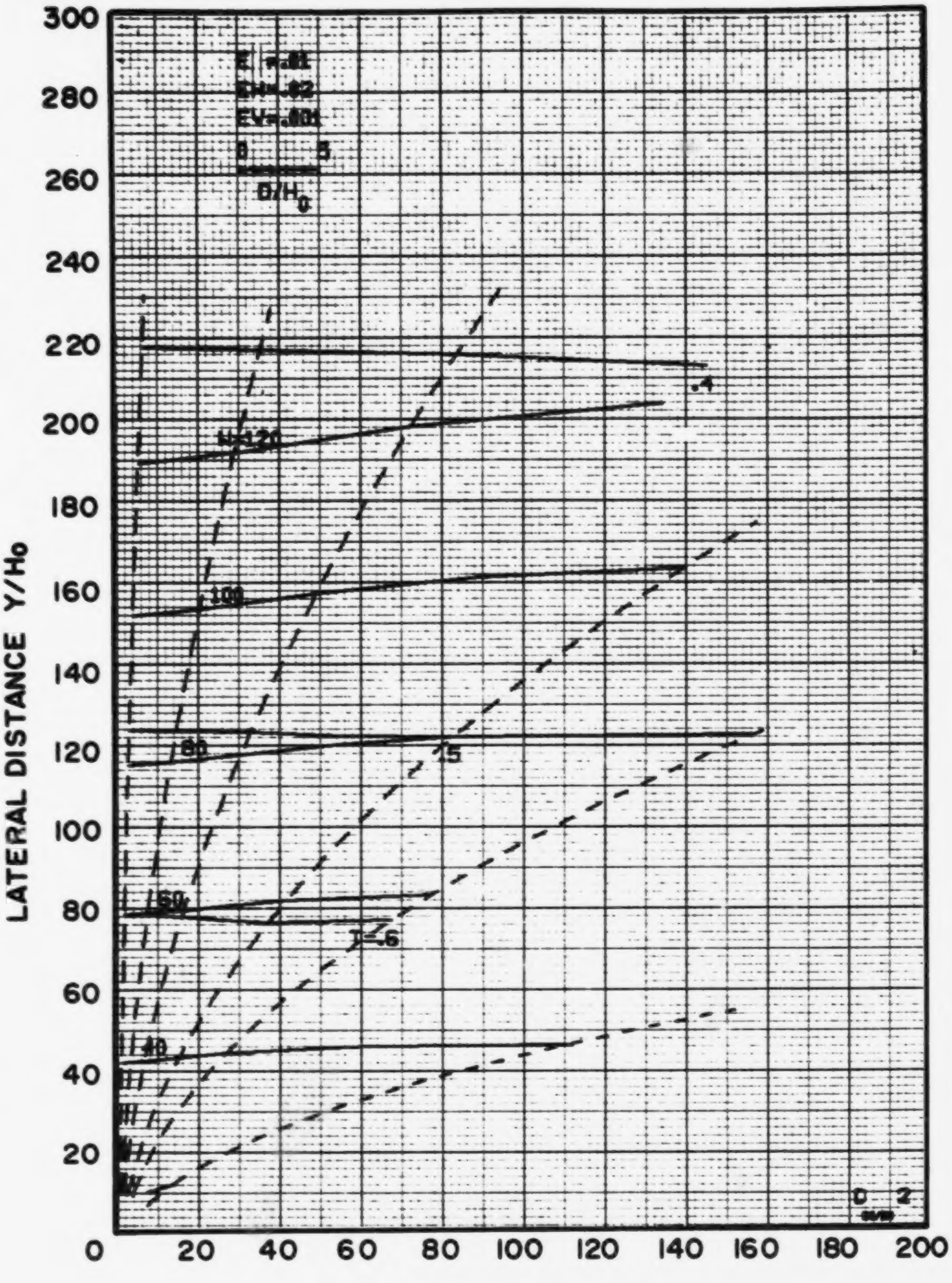

FIG (D2) TEMPERATURE, TRAJECTORY, WIDTH, AND DEPTH (TTWD)-PLOTS FOR SURFACE JET DISCHARGE

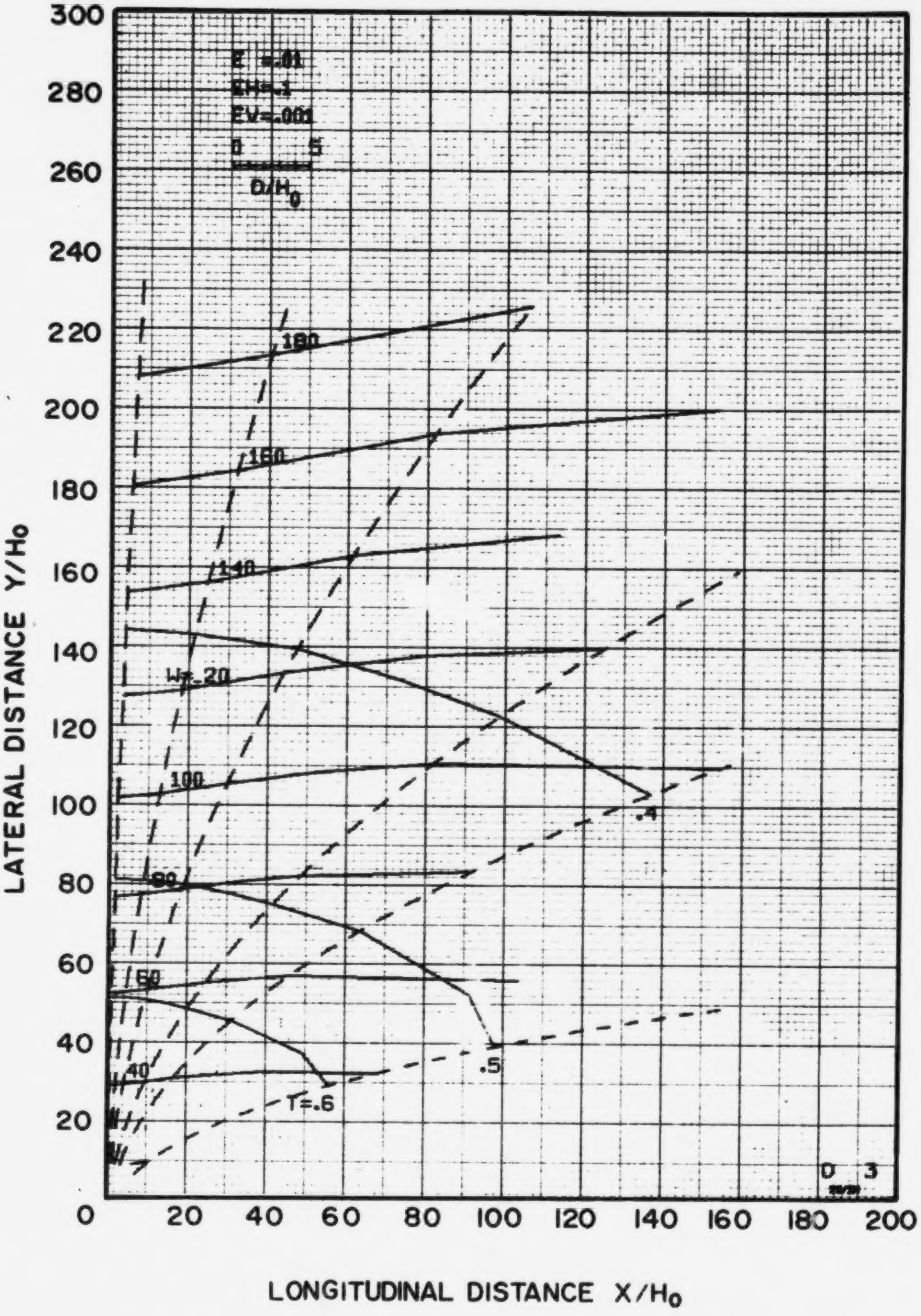

FIG (D 3) TEMPERATURE, TRAJECTORY, WIDTH, AND DEPTH (TTWD)-PLOTS FOR SURFACE JET DISCHARGE

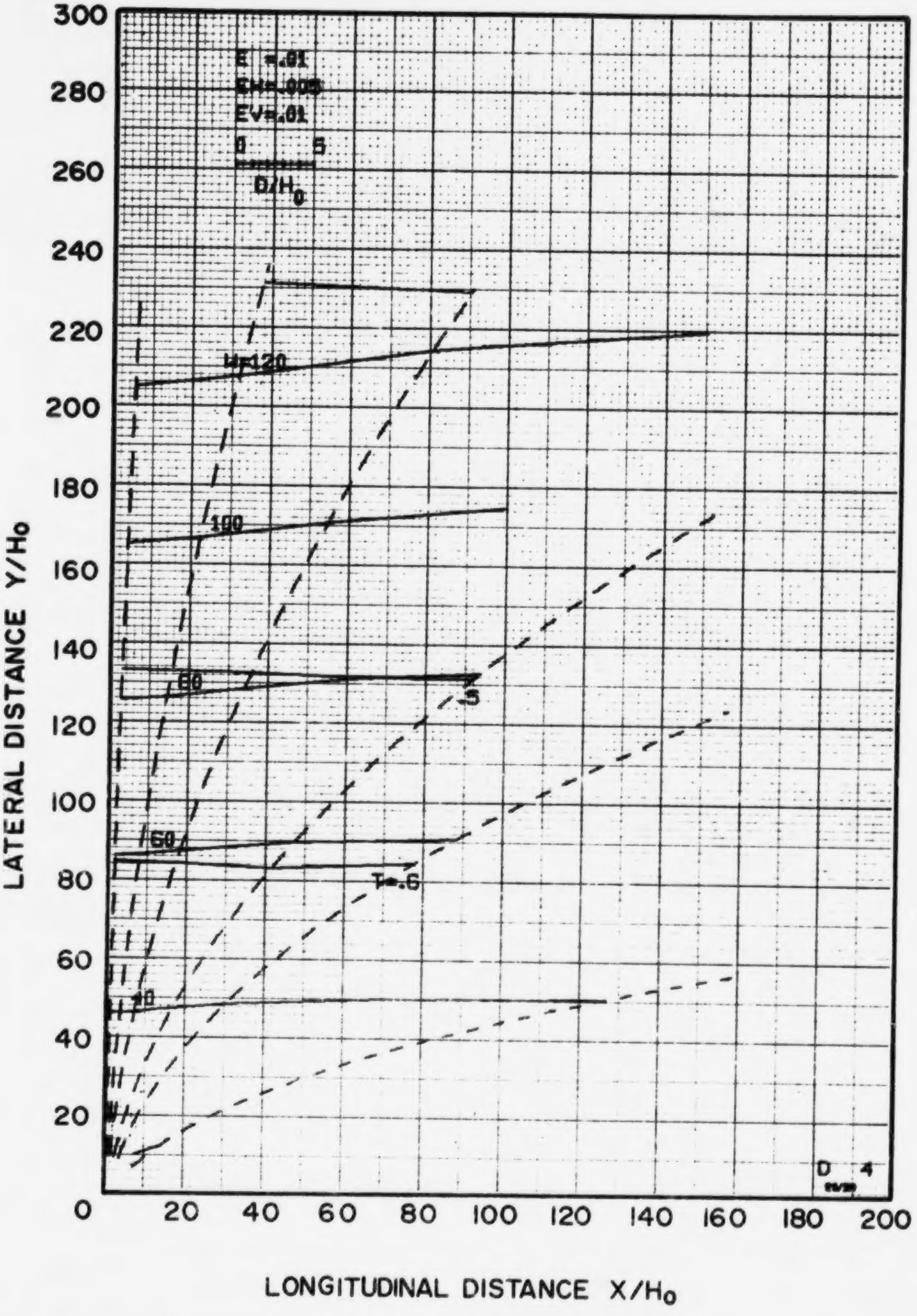

FIG (D4) TEMPERATURE, TRAJECTORY, WIDTH, AND DEPTH (TTWD)-PLOTS FOR SURFACE JET DISCHARGE

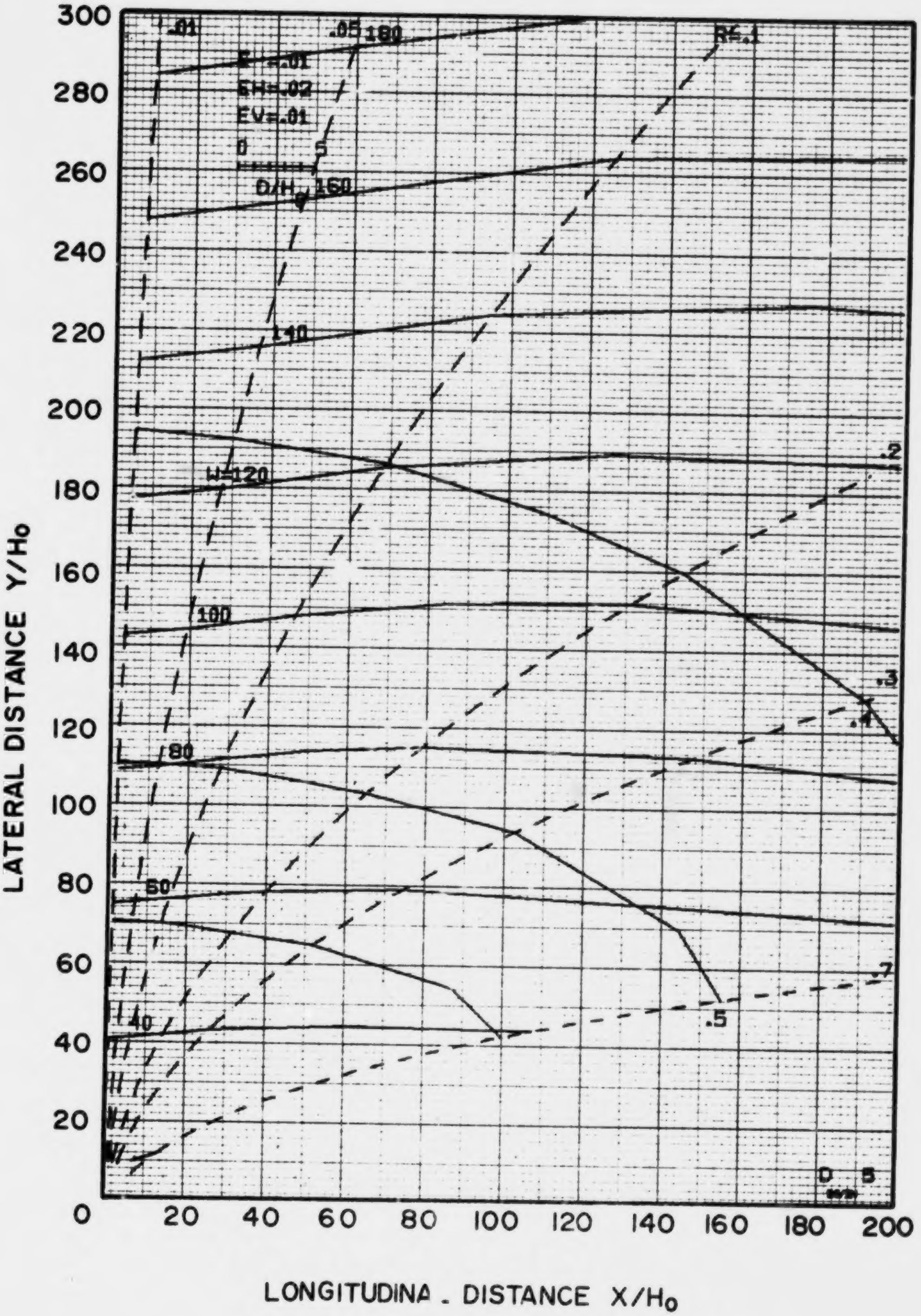

FIG(D5) TEMPERATURE, TRAJECTORY, WIDTH, AND DEPTH (TTWD)-PLOTS FOR SURFACE JET DISCHARGE

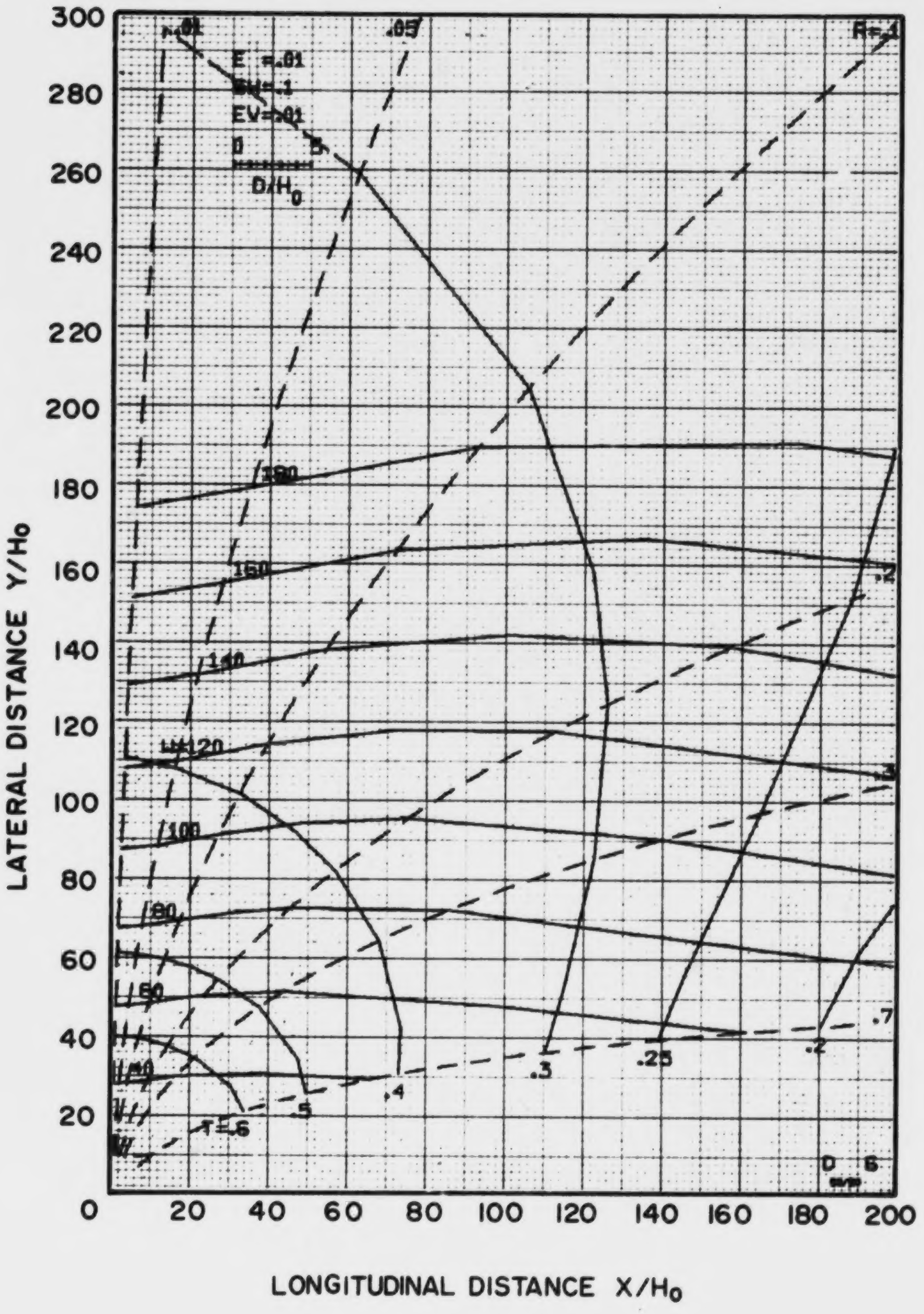

FIG(D6) TEMPERATURE, TRAJECTORY, WIDTH, AND DEPTH (TTWD)-PLOTS FOR SURFACE JET DISCHARGE

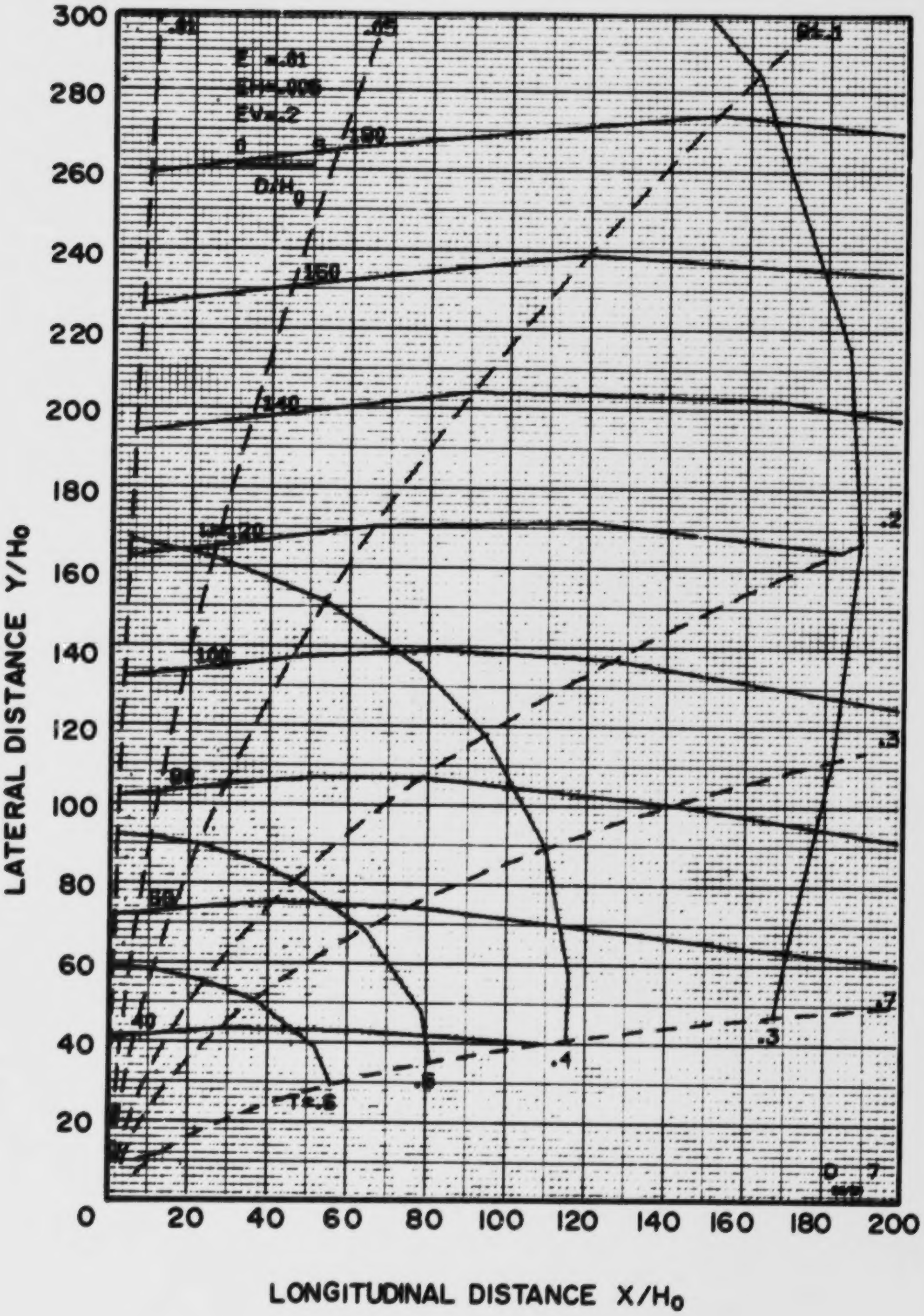

FIG (D 7) TEMPERATURE, TRAJECTORY, WIDTH, AND DEPTH (TTWD)-PLOTS FOR SURFACE JET DISCHARGE

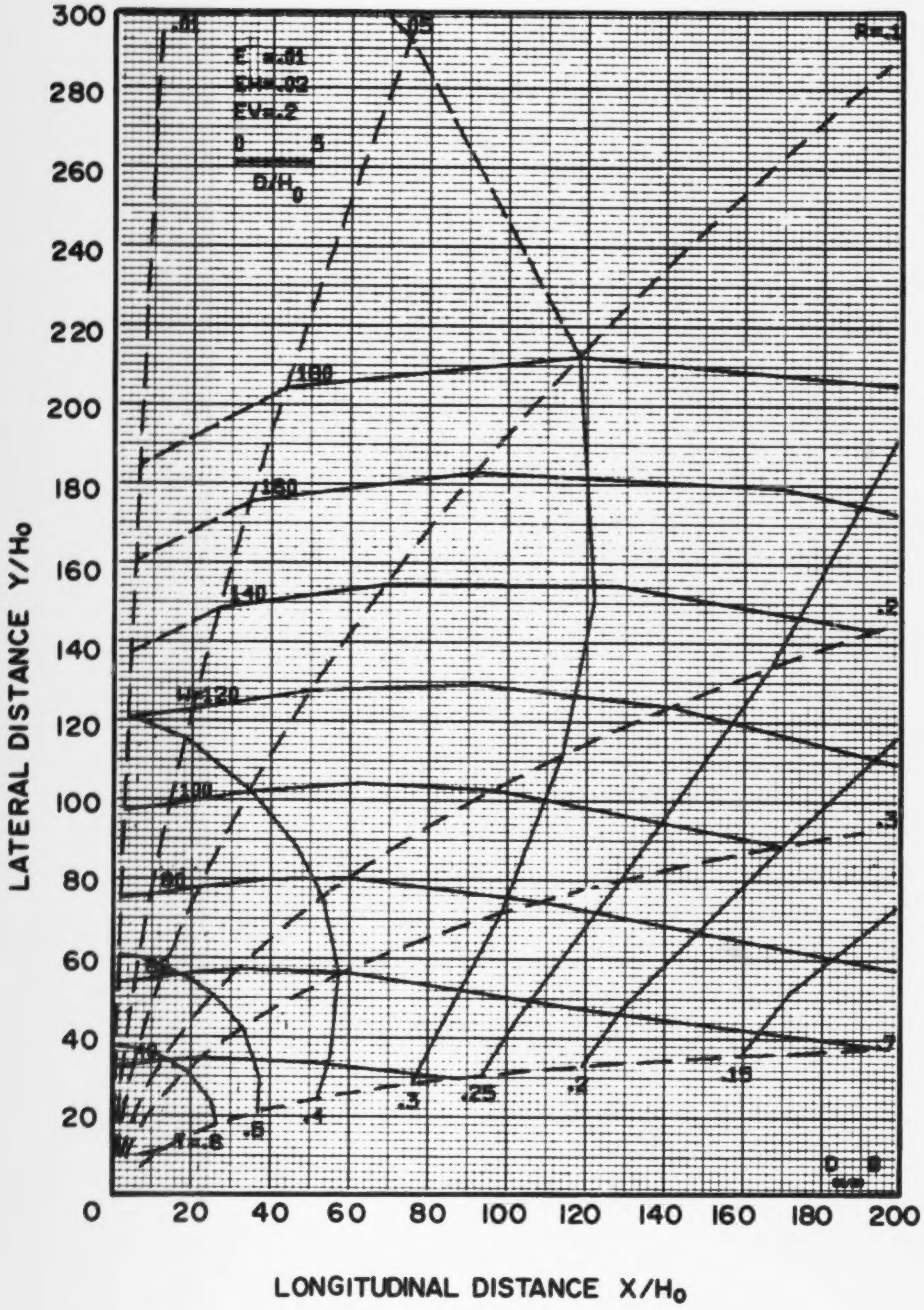

FIG (D8) TEMPERATURE, TRAJECTORY, WIDTH, AND DEPTH (TTWD)-PLOTS FOR SURFACE JET DISCHARGE

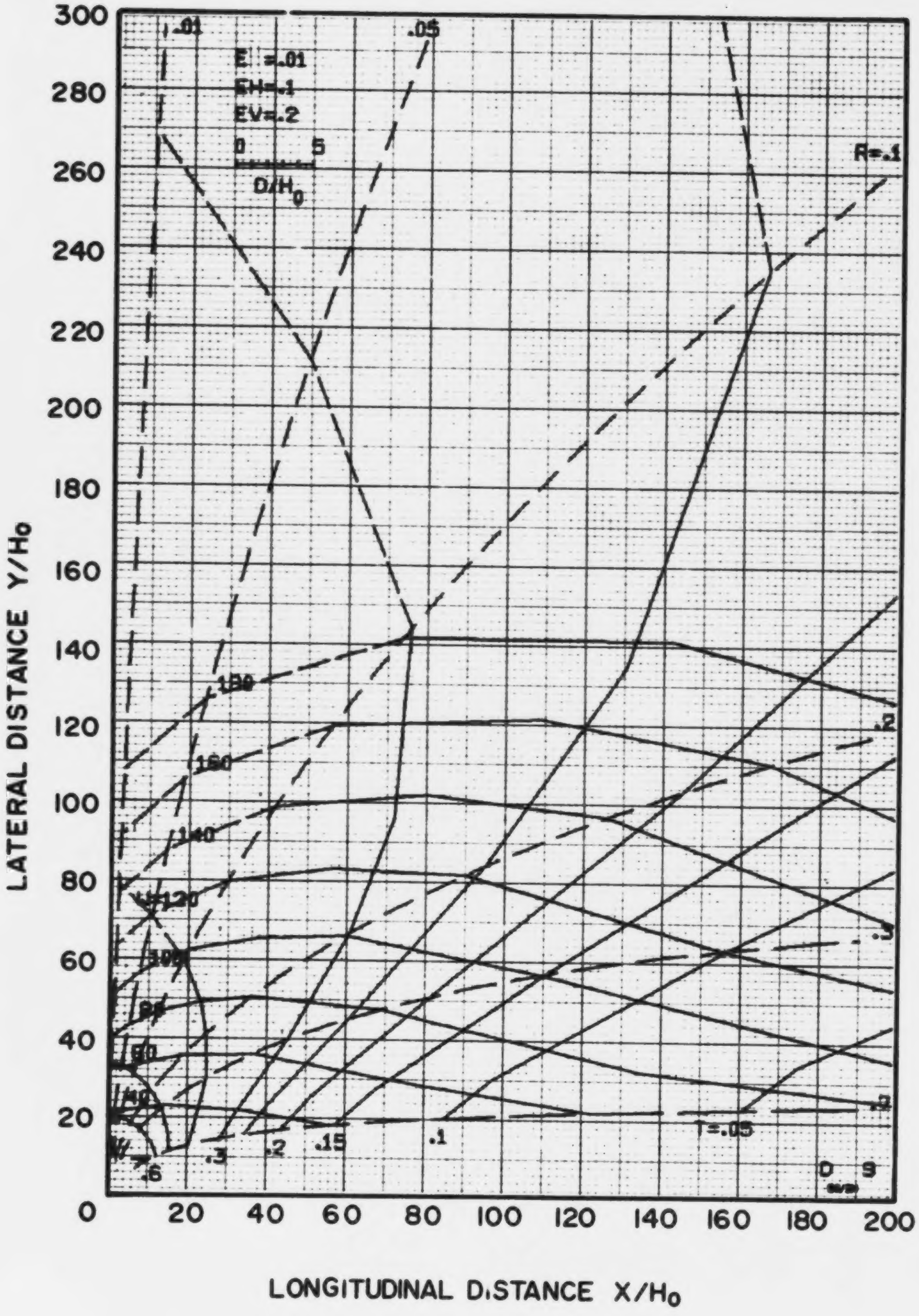

FIG(D9) TEMPERATURE, TRAJECTORY, WIDTH, AND DEPTH (TTWD)-PLOTS FOR SURFACE JET DISCHARGE

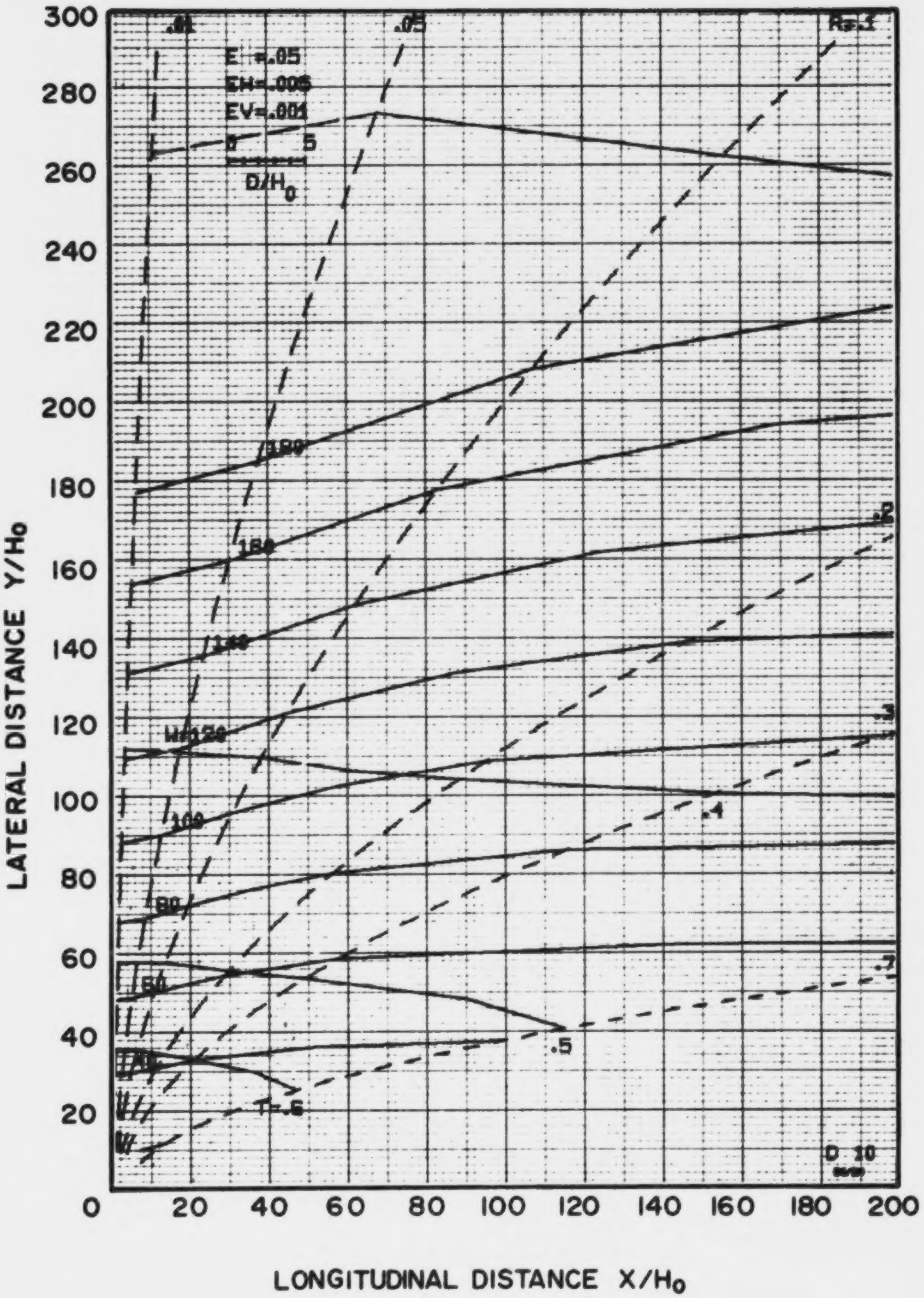

FIG (D10) TEMPERATURE, TRAJECTORY, WIDTH, AND DEPTH (TTWD)-PLOTS FOR SURFACE JET DISCHARGE

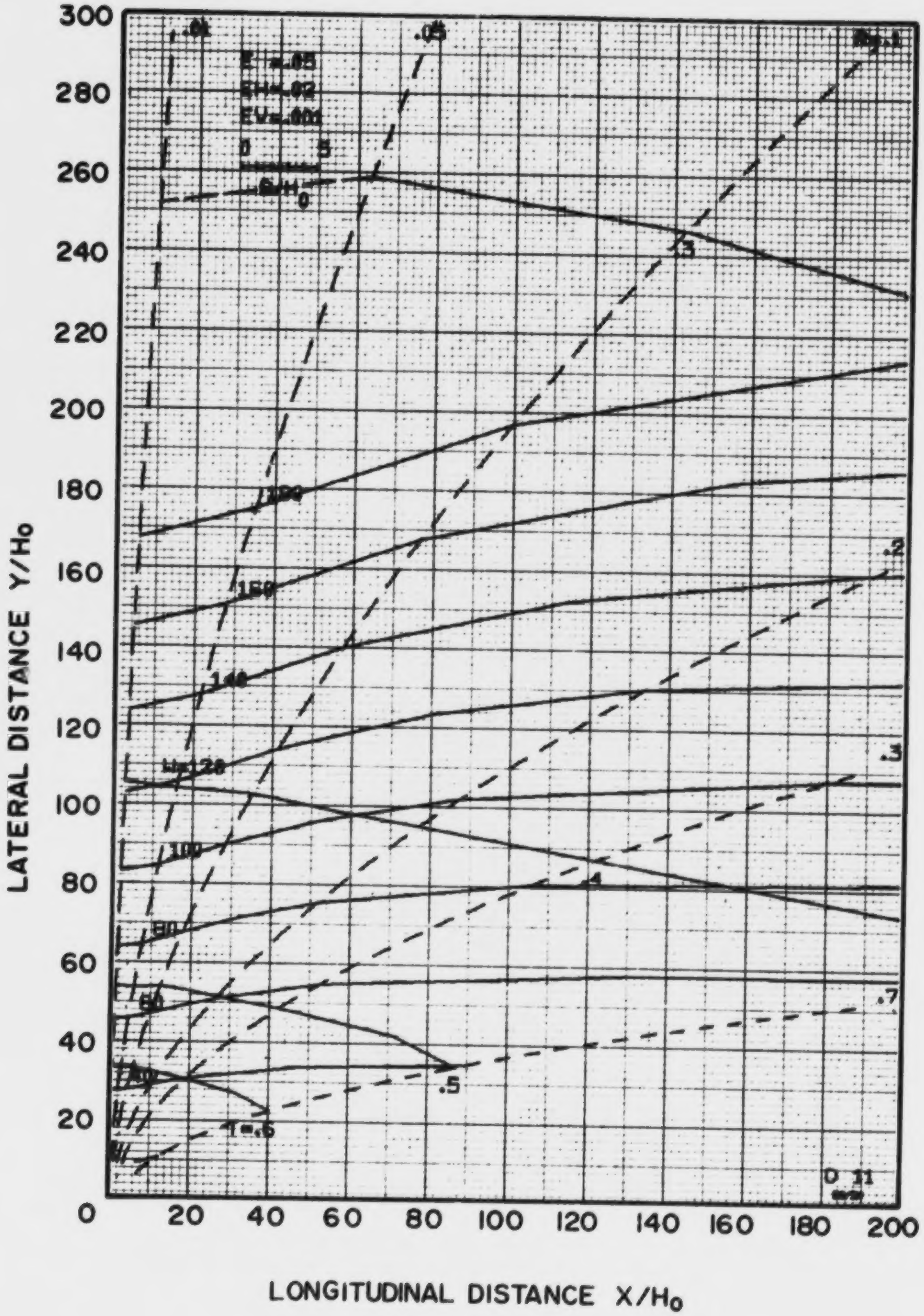

FIG (D11) TEMPERATURE, TRAJECTORY, WIDTH, AND DEPTH (T T WD)-PLOTS FOR SURFACE JET DISCHARGE

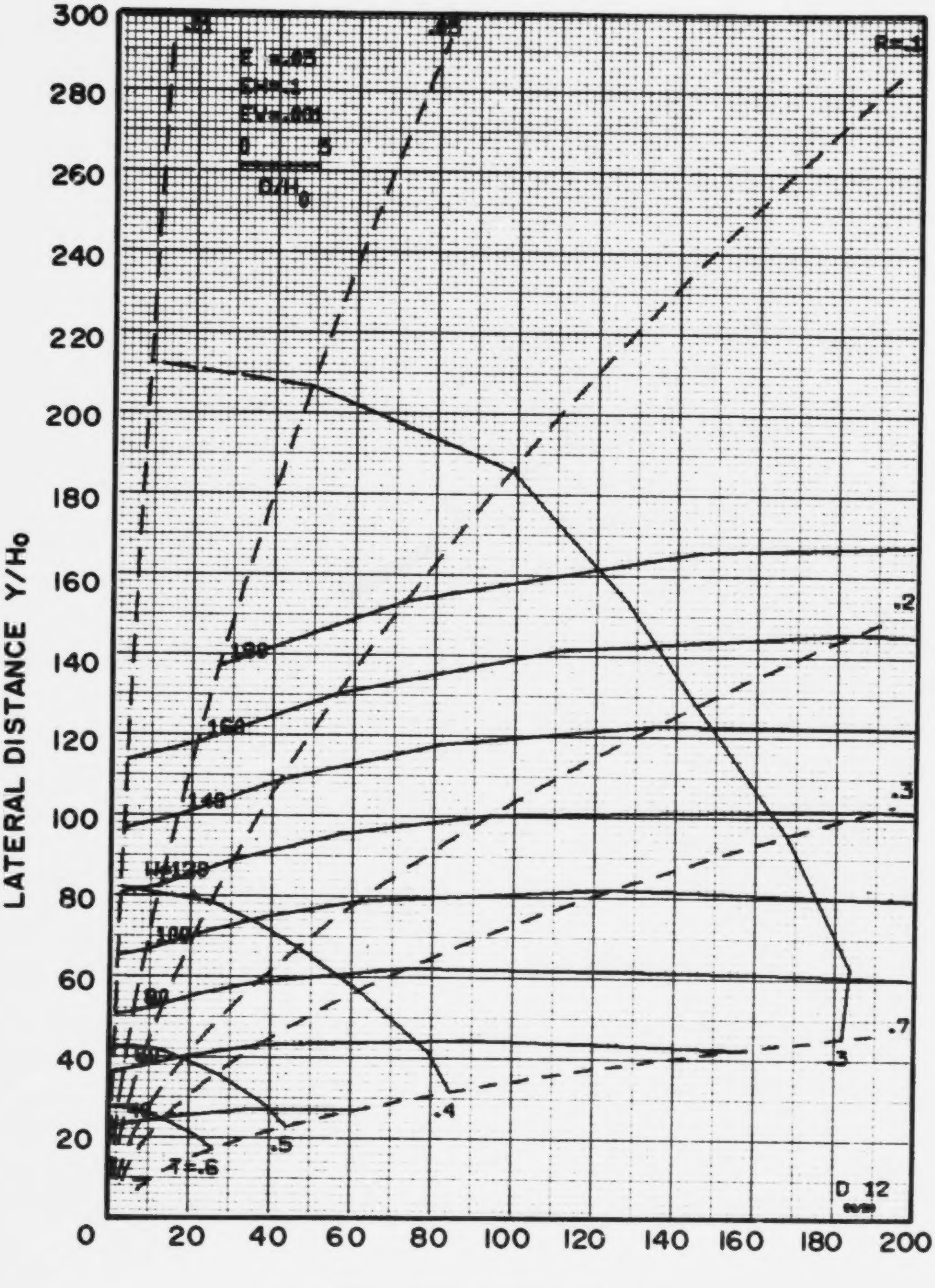

FIG (D 12) TEMPERATURE, TRAJECTORY, WIDTH, AND DEPTH (TTWD)-PLOTS FOR SURFACE JET DISCHARGE

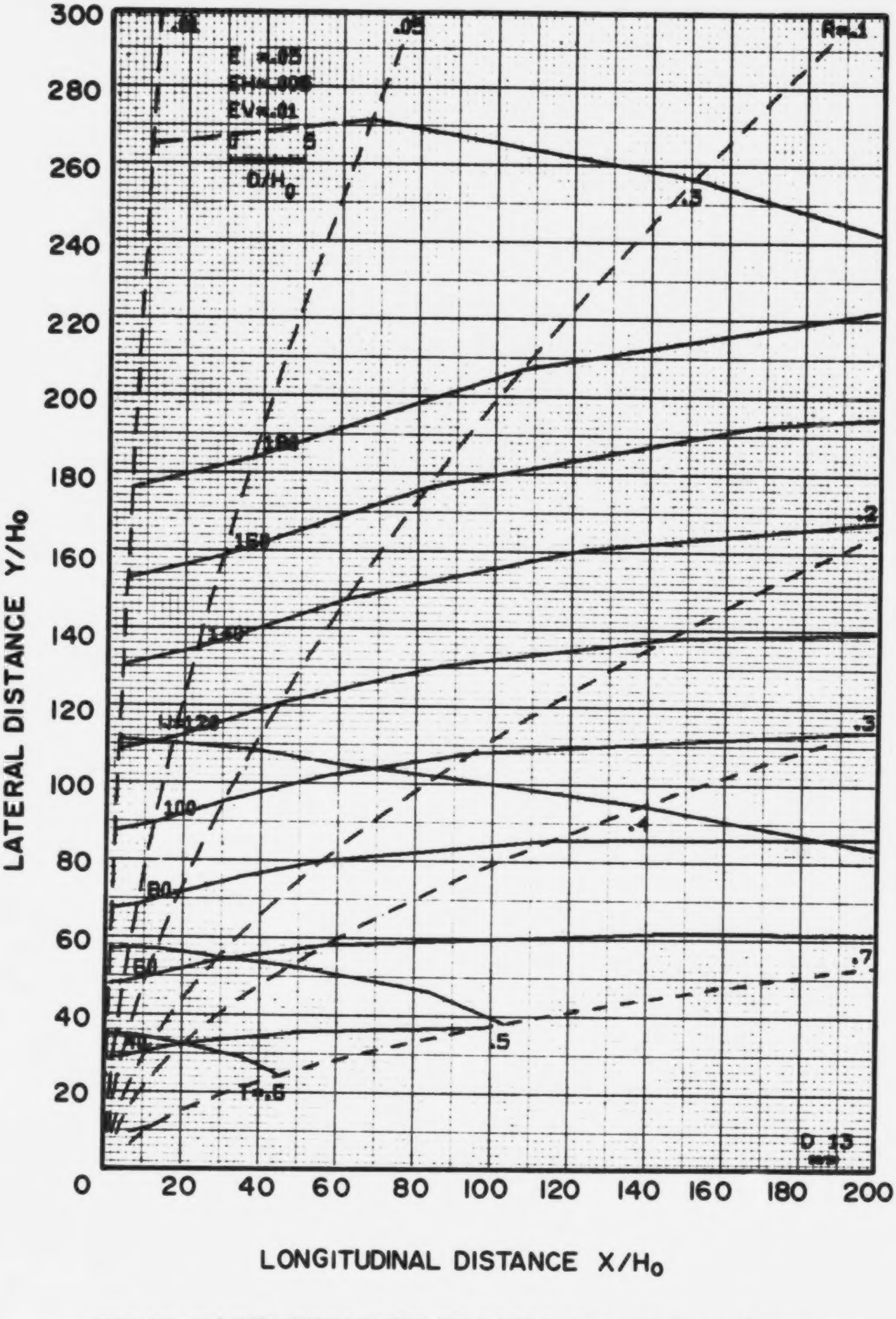

FIG (D13) TEMPERATURE, TRAJECTORY, WIDTH, AND DEPTH (TTWD)-PLOTS FOR SURFACE JET DISCHARGE

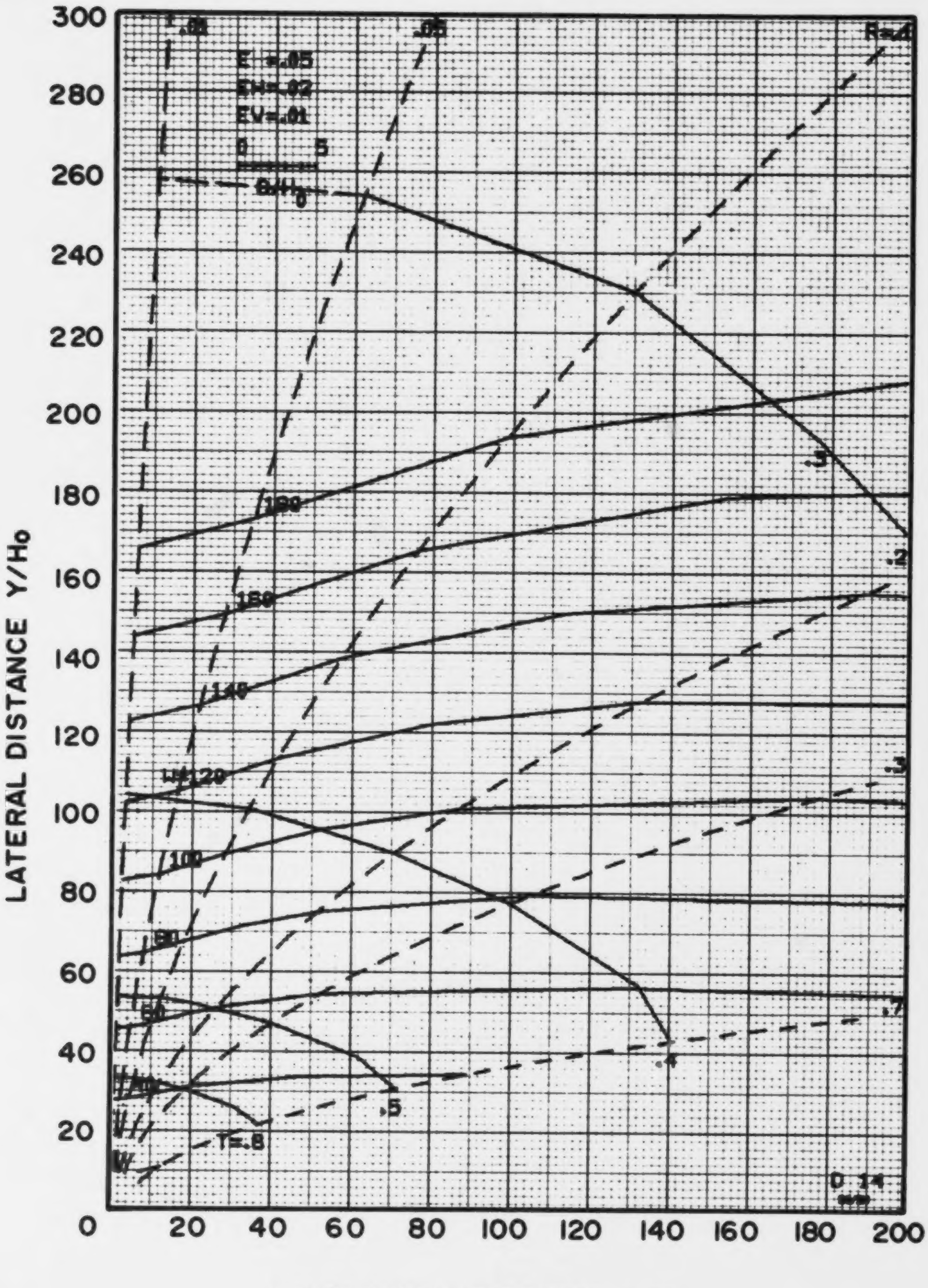

FIG (D14) TEMPERATURE, TRAJECTORY, WIDTH, AND DEPTH (TTWD)-PLOTS FOR SURFACE JET DISCHARGE

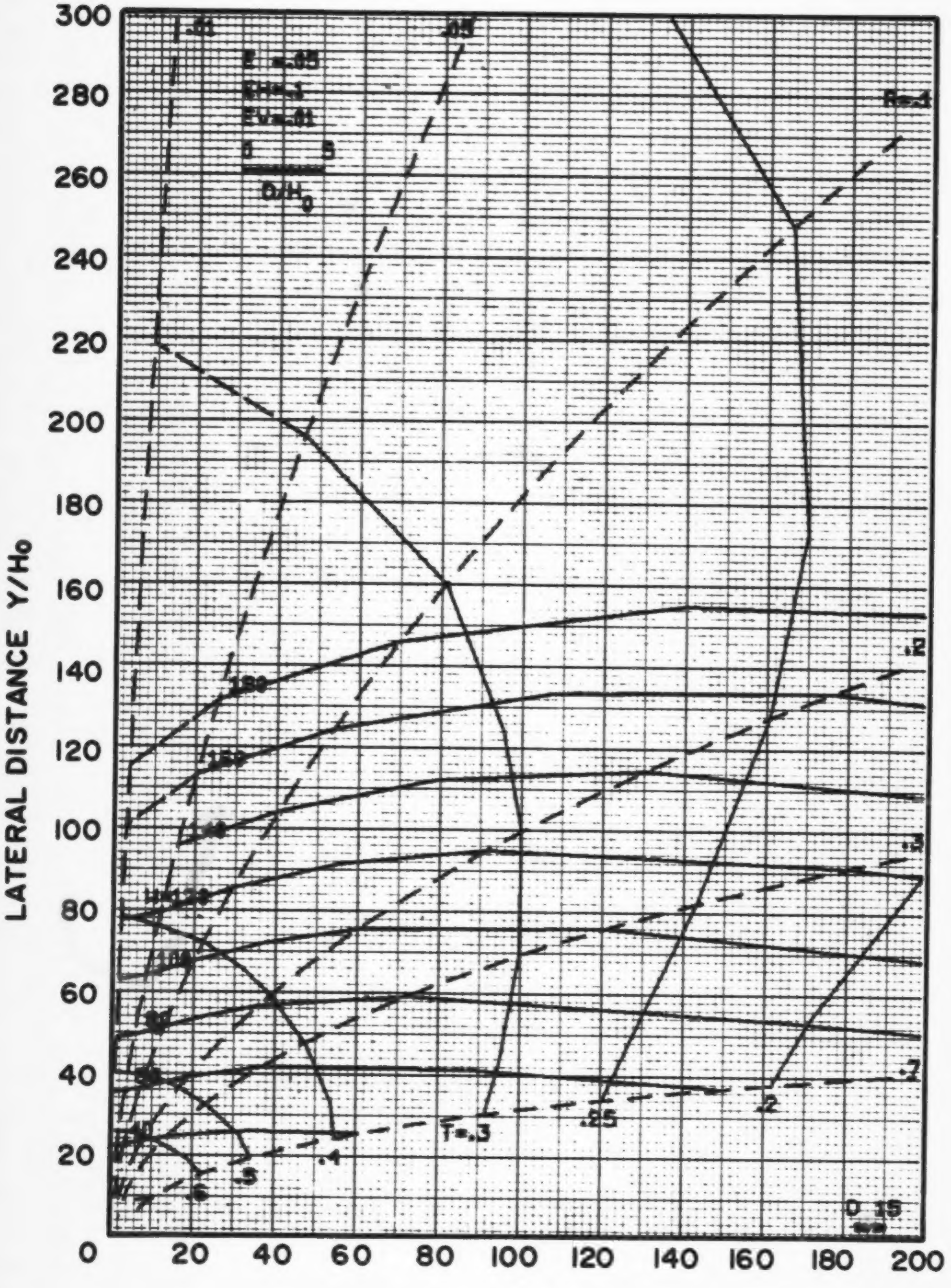

FIG(D15) TEMPERATURE, TRAJECTORY, WIDTH, AND DEPTH (TTWD)-PLOTS FOR SURFACE JET DISCHARGE

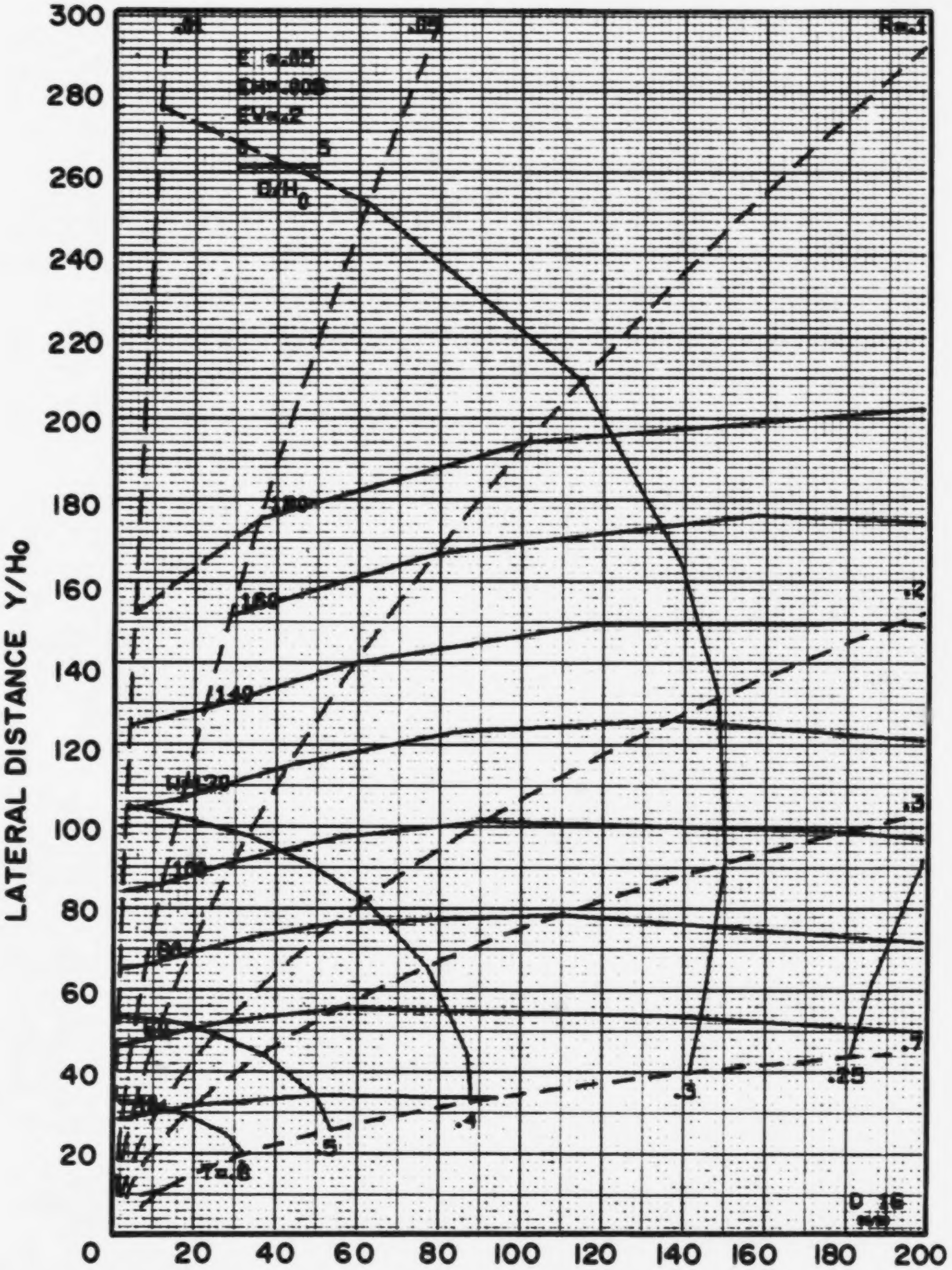

FIG (D 16) TEMPERATURE, TRAJECTORY, WIDTH, AND DEPTH (TTWD)-PLOTS FOR SURFACE JET DISCHARGE

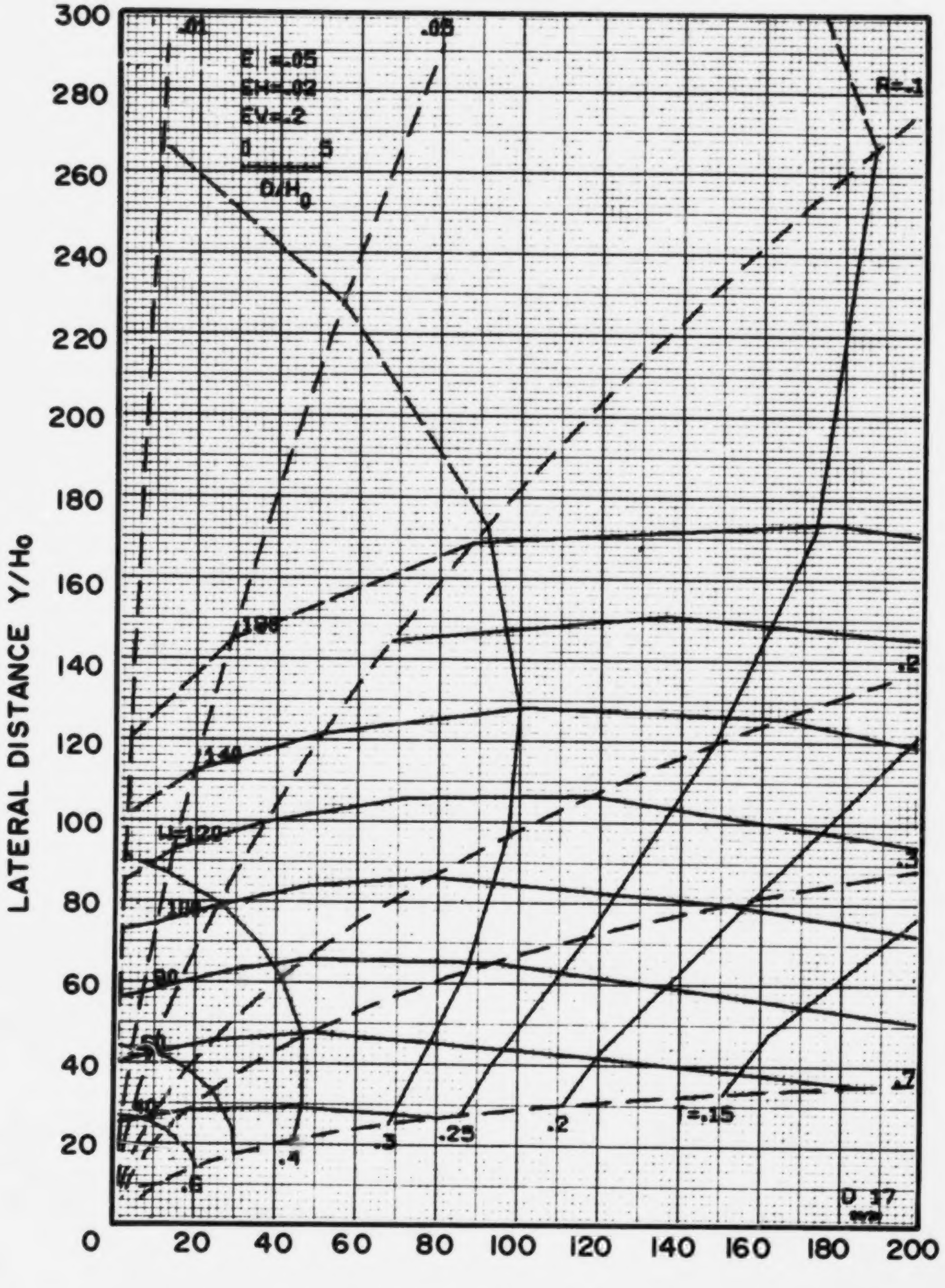

FIG (D17) TEMPERATURE, TRAJECTORY, WIDTH, AND DEPTH (TTWD)-PLOTS FOR SURFACE JET DISCHARGE

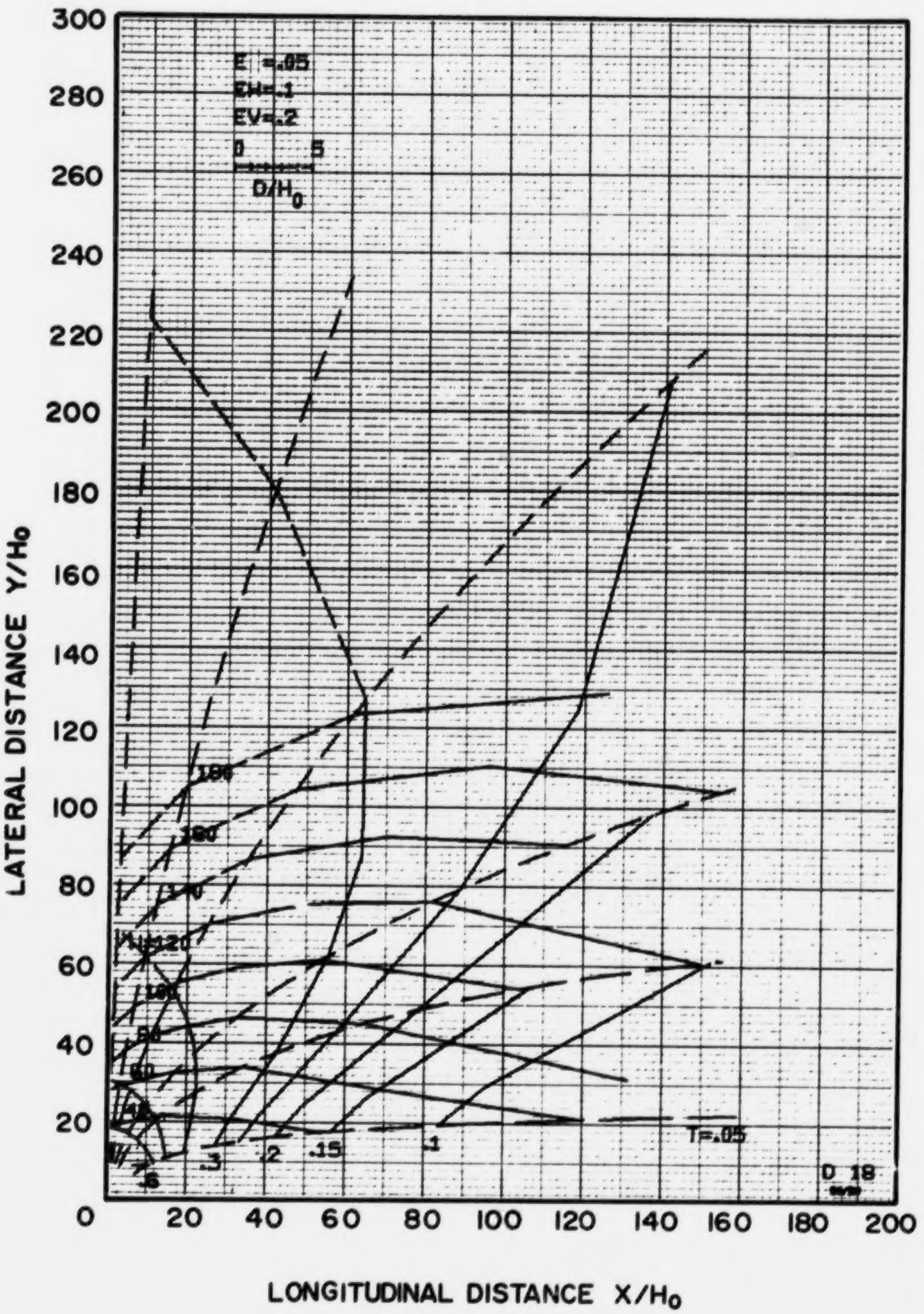

FIG (D18) TEMPERATURE, TRAJECTORY, WIDTH, AND DEPTH (TTWD)-PLOTS FOR SURFACE JET DISCHARGE

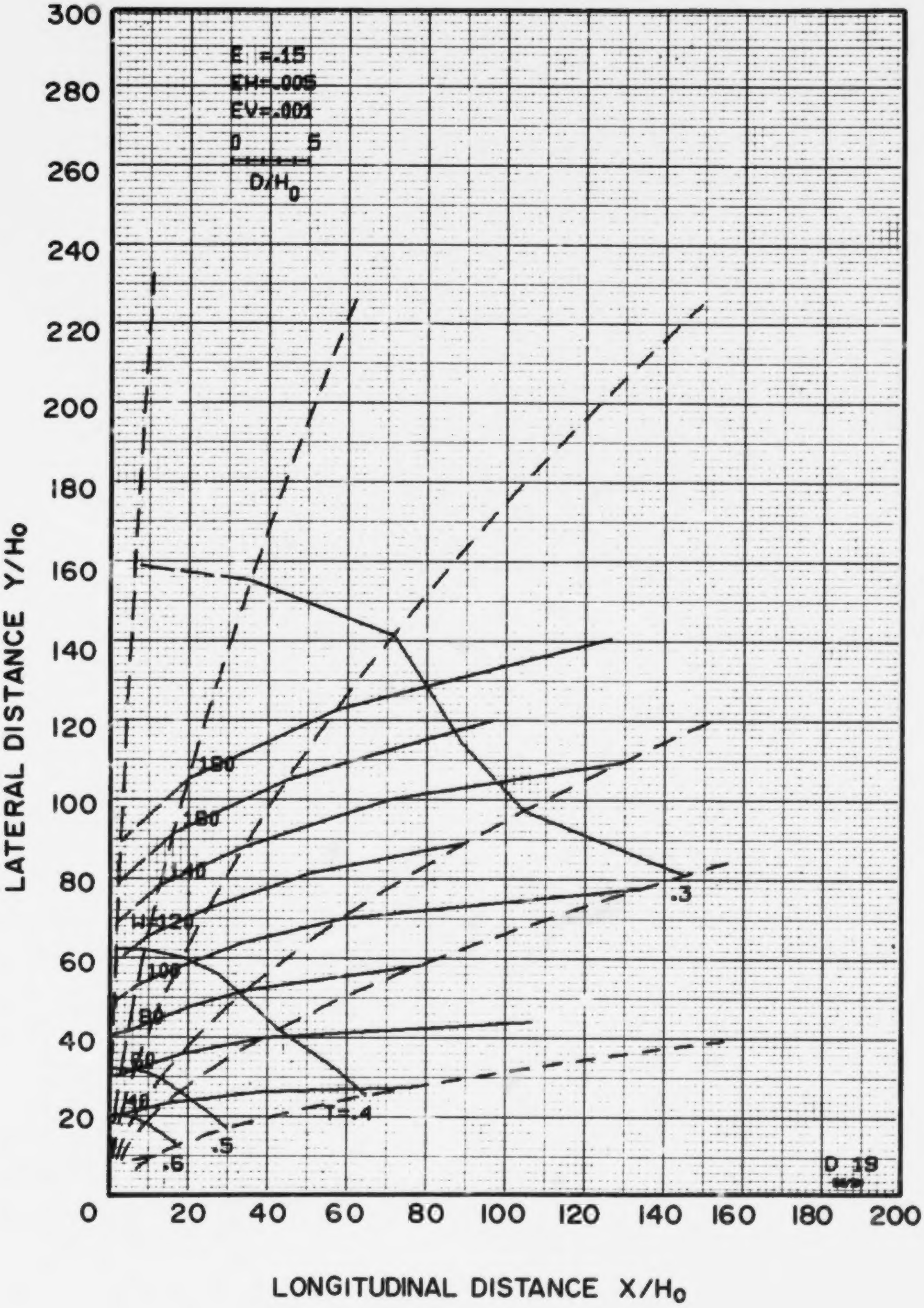

FIG(D19) TEMPERATURE, TRAJECTORY, WIDTH, AND DEPTH (TTWD)-PLOTS FOR SURFACE JET DISCHARGE

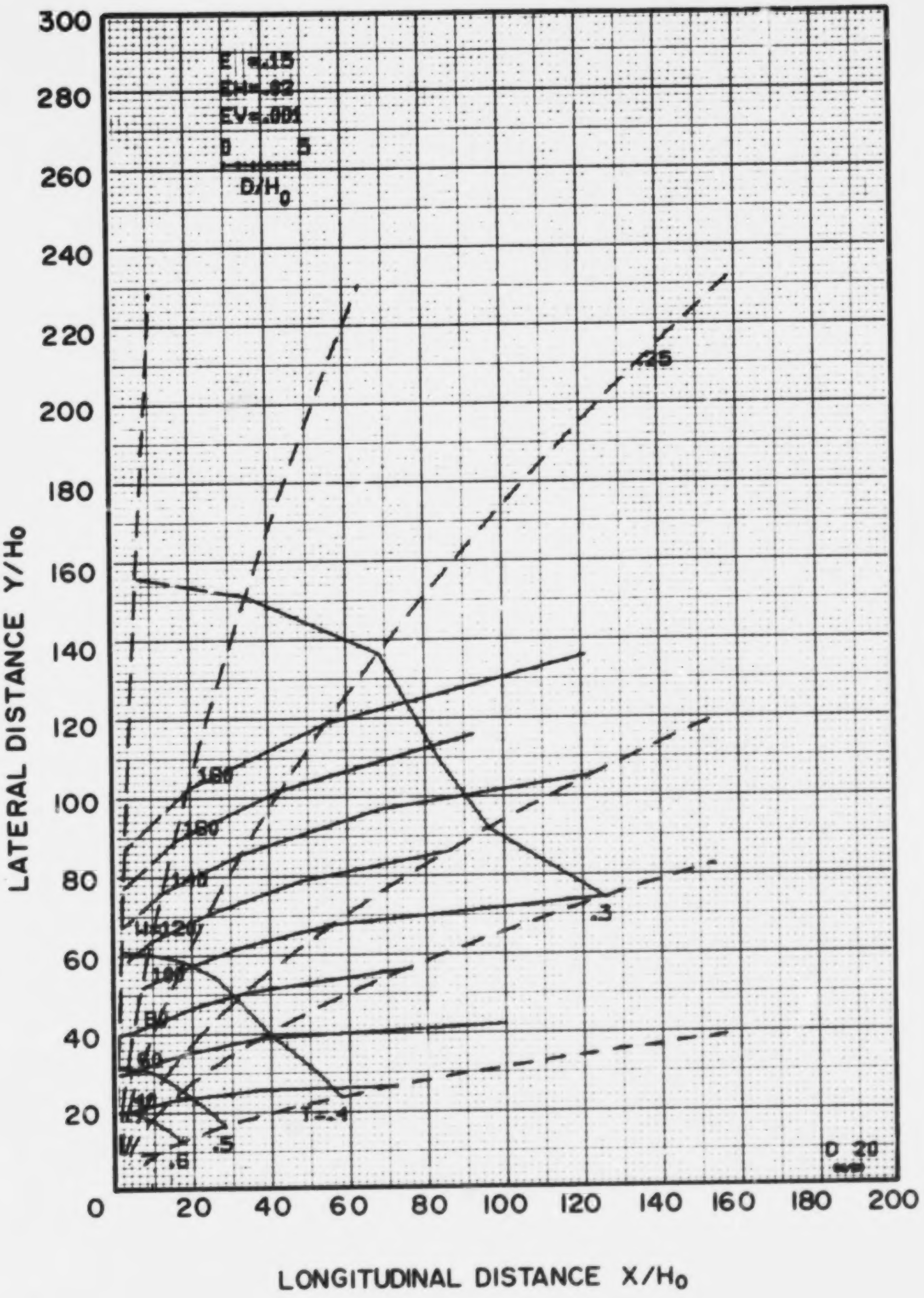

FIG (D 20) TEMPERATURE, TRAJECTORY, WIDTH, AND DEPTH (TTWD)-PLOTS FOR SURFACE JET DISCHARGE

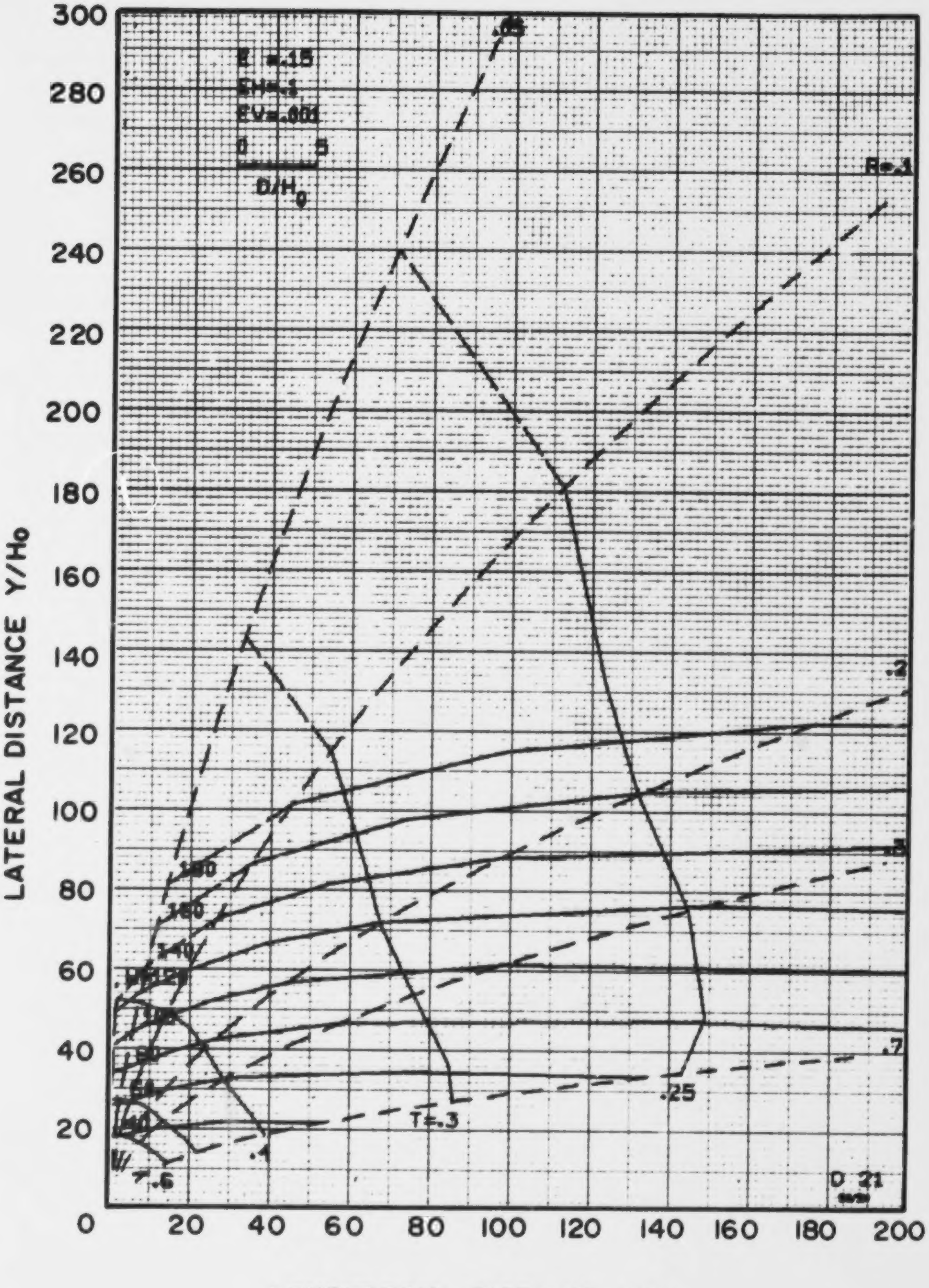

FIG(D21) TEMPERATURE, TRAJECTORY, WIDTH, AND DEPTH (TTWD)-PLOTS FOR SURFACE JET DISCHARGE

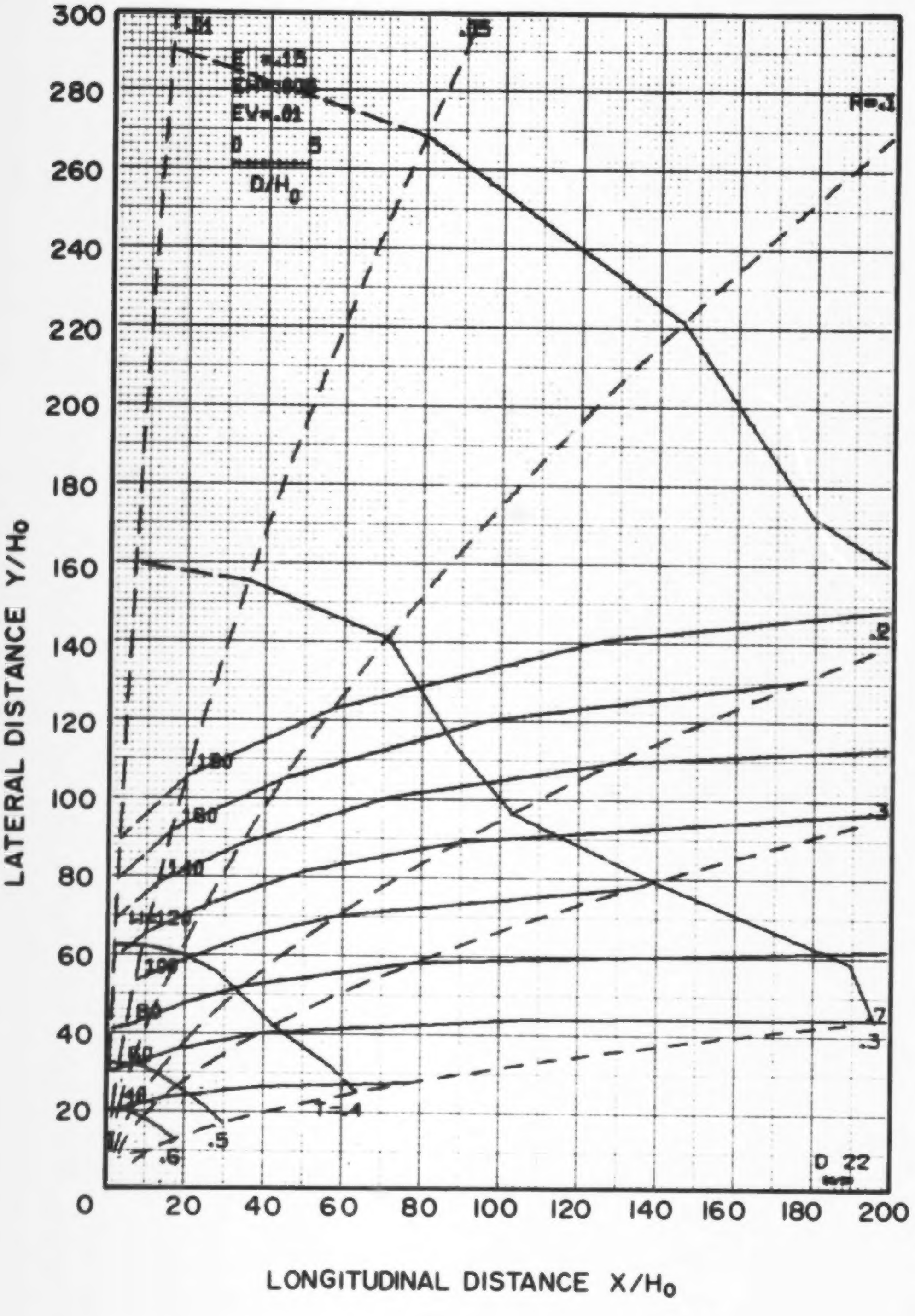

FIG (D 22) TEMPERATURE, TRAJECTORY, WIDTH, AND DEPTH (TTWD)-PLOTS FOR SURFACE JET DISCHARGE

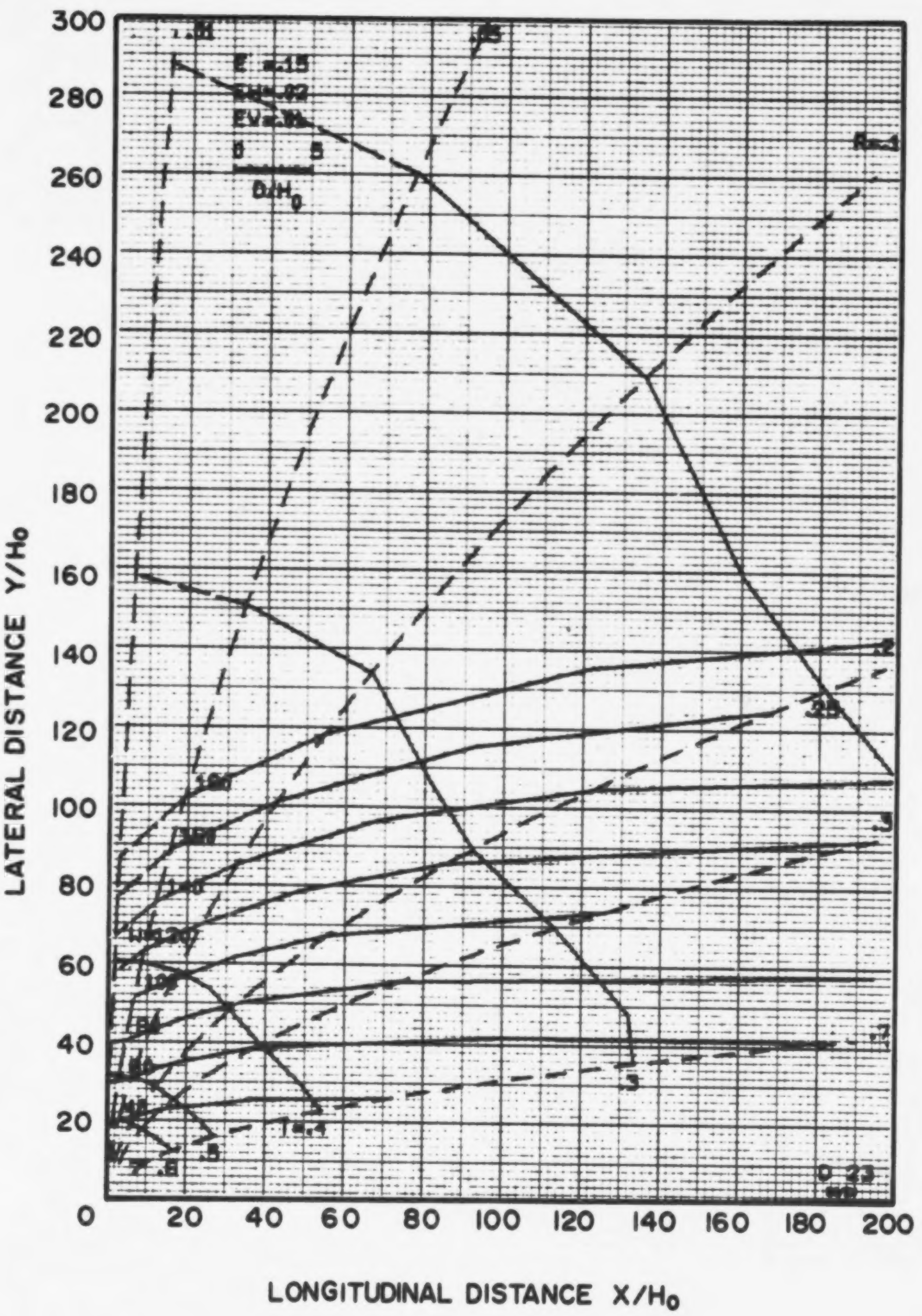

FIG (D23) TEMPERATURE, TRAJECTORY, WIDTH, AND DEPTH (TTWD)-PLOTS FOR SURFACE JET DISCHARGE

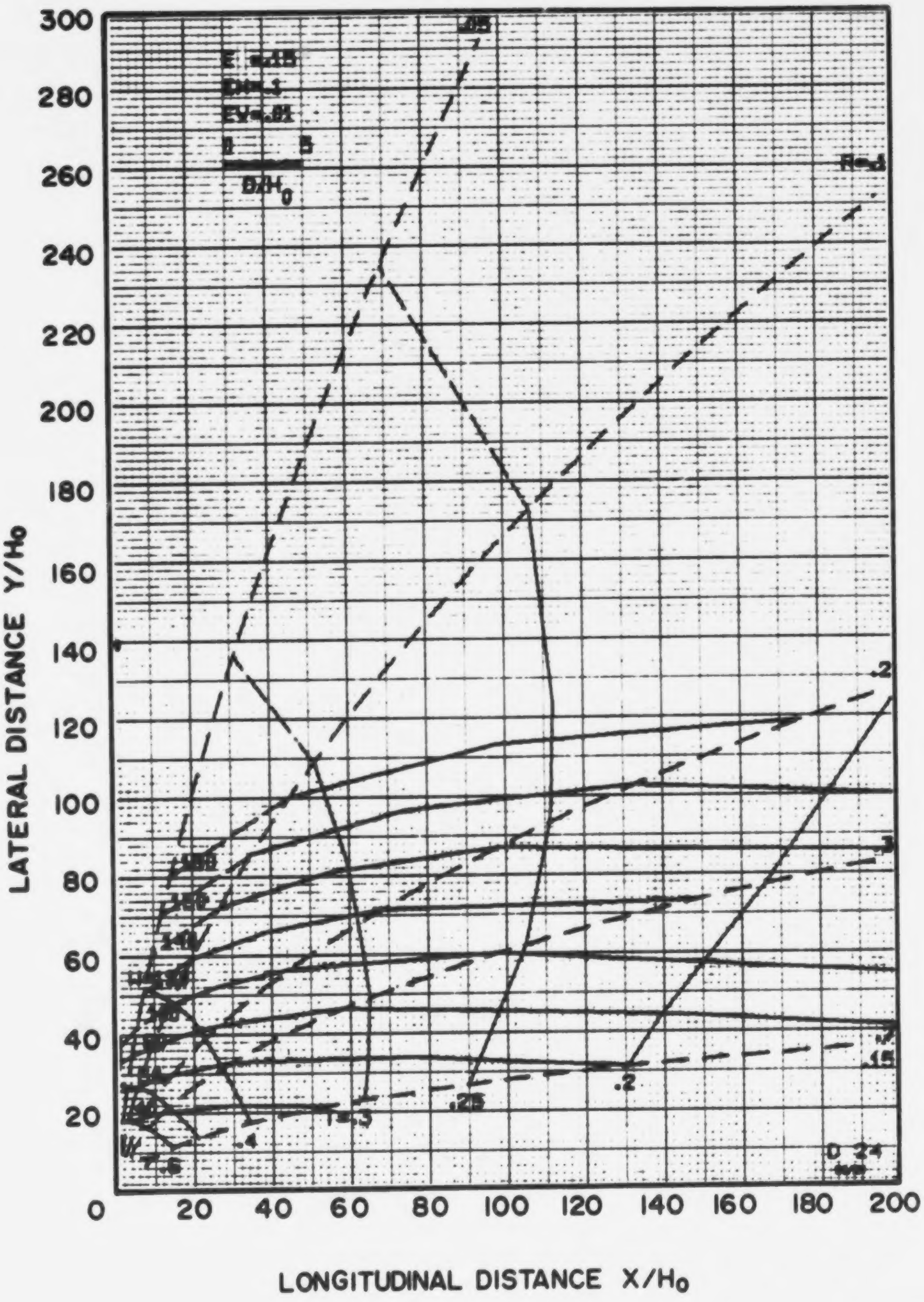

FIG (D24) TEMPERATURE, TRAJECTORY, WIDTH, AND DEPTH (TTWD)-PLOTS FOR SURFACE JET DISCHARGE

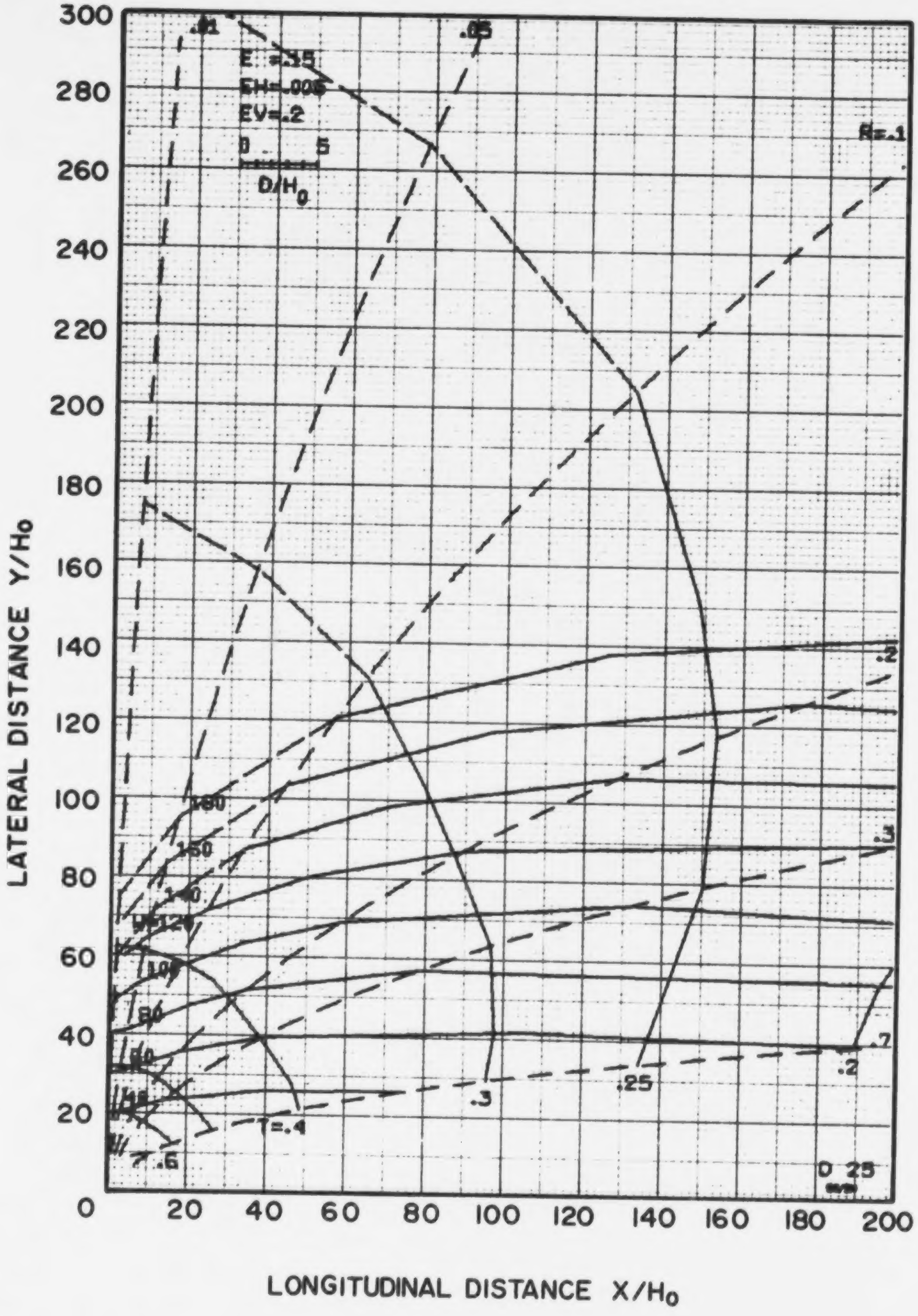

FIG (D25) TEMPERATURE, TRAJECTORY, WIDTH, AND DEPTH (TTWD)-PLOTS FOR SURFACE JET DISCHARGE

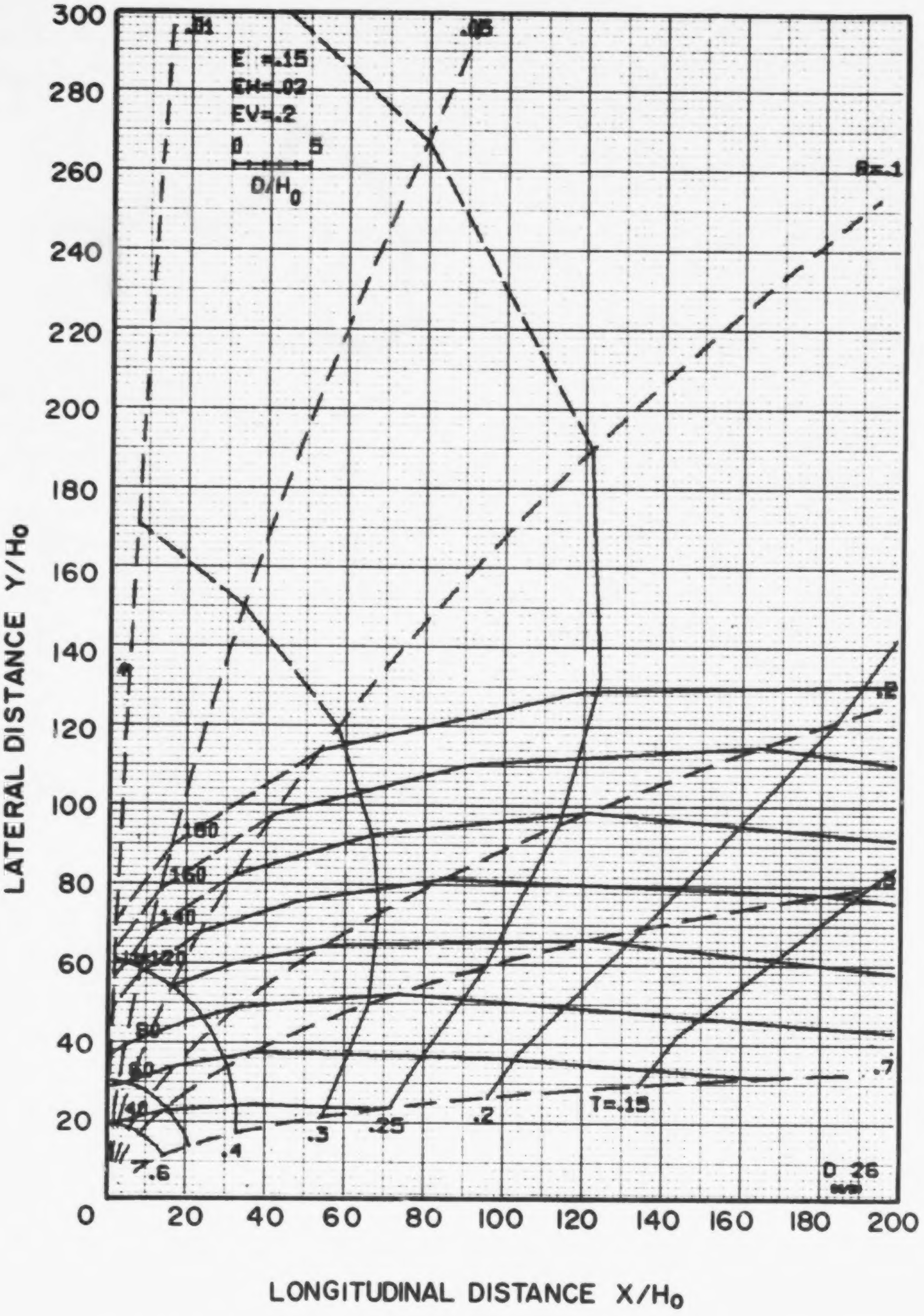

FIG (D26) TEMPERATURE, TRAJECTORY, WIDTH, AND DEPTH (TTWD)-PLOTS FOR SURFACE JET DISCHARGE

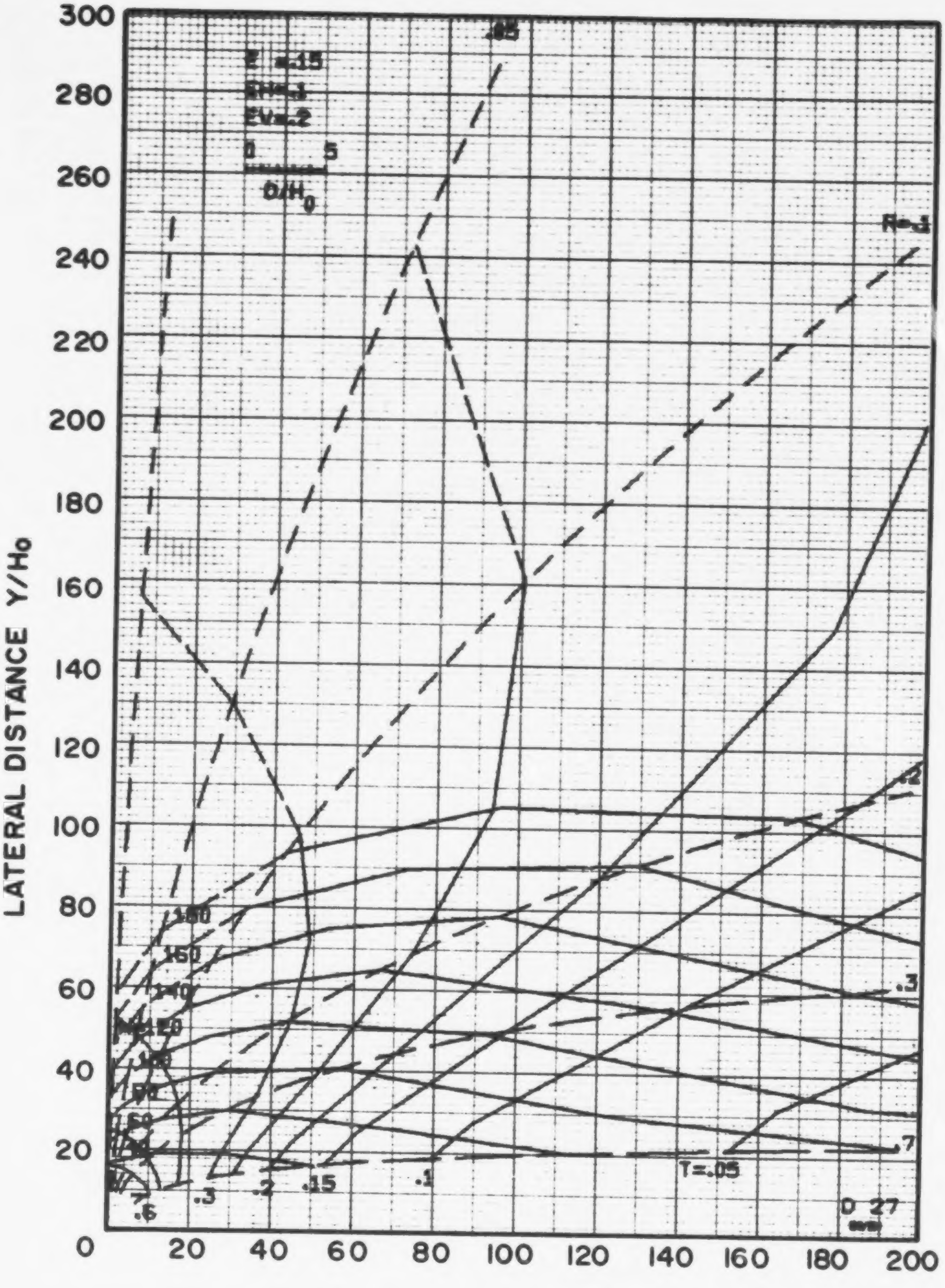

FIG(D27) TEMPERATURE, TRAJECTORY, WIDTH, AND DEPTH (TTWD)-PLOTS FOR SURFACE JET DISCHARGE

APPENDIX E

TEMPERATURE DENSITY NOMOGRAMS AND COMPUTATIONAL AIDS

FIGURES

No.		Page
E1	Temperature-density Relations for Fresh and Salt Water.	358
E2	Temperature-density Relations for Salt Water.	359
E3	Temperature-density Relations for Froude Number Calculations.	360
E4	Temperature-density Relations for Froude Number Calculations.	361
E5	Gaussian Distribution Curve Used for Calculating Off-Centerline Temperatures.	362

COMPUTATIONAL AIDS

In order to aid in the calculation of discharge Froude numbers, the following figures have been prepared. Figures E1 and E2 are curves of $\Delta\rho/\rho$ as a function of the temperature difference, ambient temperature, and salinity. The figures are for salinities of $S=0$ (fresh water), 10, 30, and 40 ppt. The ambient temperature differences and temperatures have been given in both °C and °F for convenience.

Figures E1 and E2 were used to determine values for the curves plotted on Figures E3 and E4. The latter two figures present values of $G = (g\ \Delta\rho/\rho)^{-1/2}$ (such that the Froude number $F = GU_0/\sqrt{H_0}$) for selected values of S and T_a as a function of ΔT. Figure E3 is for the metric system of units where U_0 is in cm/sec, H_0 in cm, and temperature in °C. Figure E4 is for the British engineering system of units with U_0 in ft/sec, H_0 in ft, and temperature in °F.

The distribution of temperature and velocity within the fully developed region of the plume are assumed to be Gaussian both in the lateral and vertical directions. Figure E5 is a Gaussian distribution curve with $\eta = 0$ at the plume centerline or water surface. The variable η can be thought of as either $4n/W$ or $2\ Z/D$ depending on whether the lateral or vertical direction is considered. Also indicated on the curve is the part where the local excess temperature is 1/2 the centerline excess temperature, $T_r-T_a/T_0-T_a = 0.5$. The value of η at this point is 1.1775. This point is of interest since many investigators use $\eta_{0.5}$ as a measure of plume size. The relationship between $\eta_{0.5}$ and $W/2$ or D is $W/2 = 1.7\ \eta_{0.5}$ or $D = 1.7\ \eta_{0.5}$.

Table E1 in this appendix is a comprehensive list of conversion factors useful in solving practical problems.

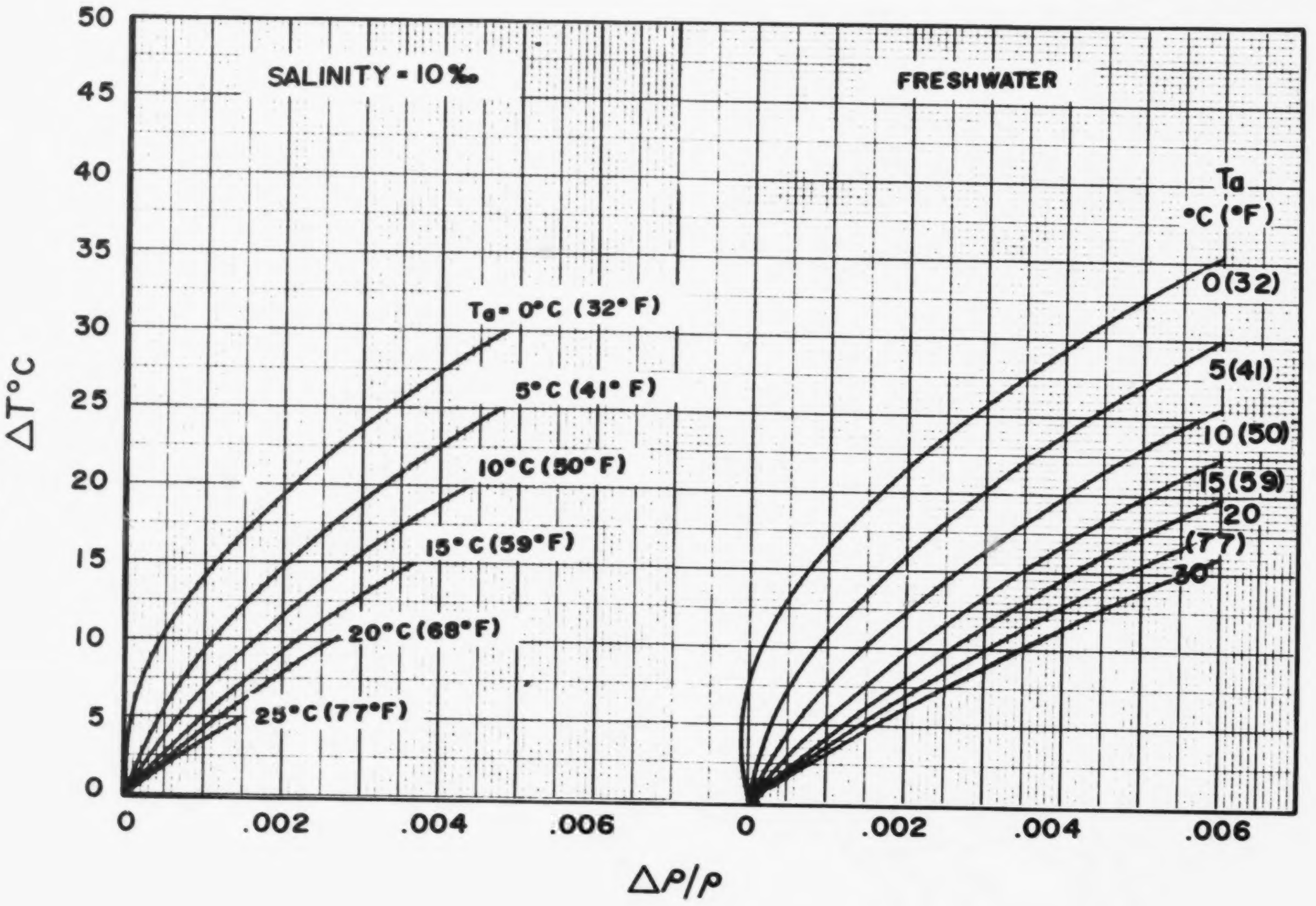

Figure E1 Temperature-density Relations for Fresh and Salt Water.

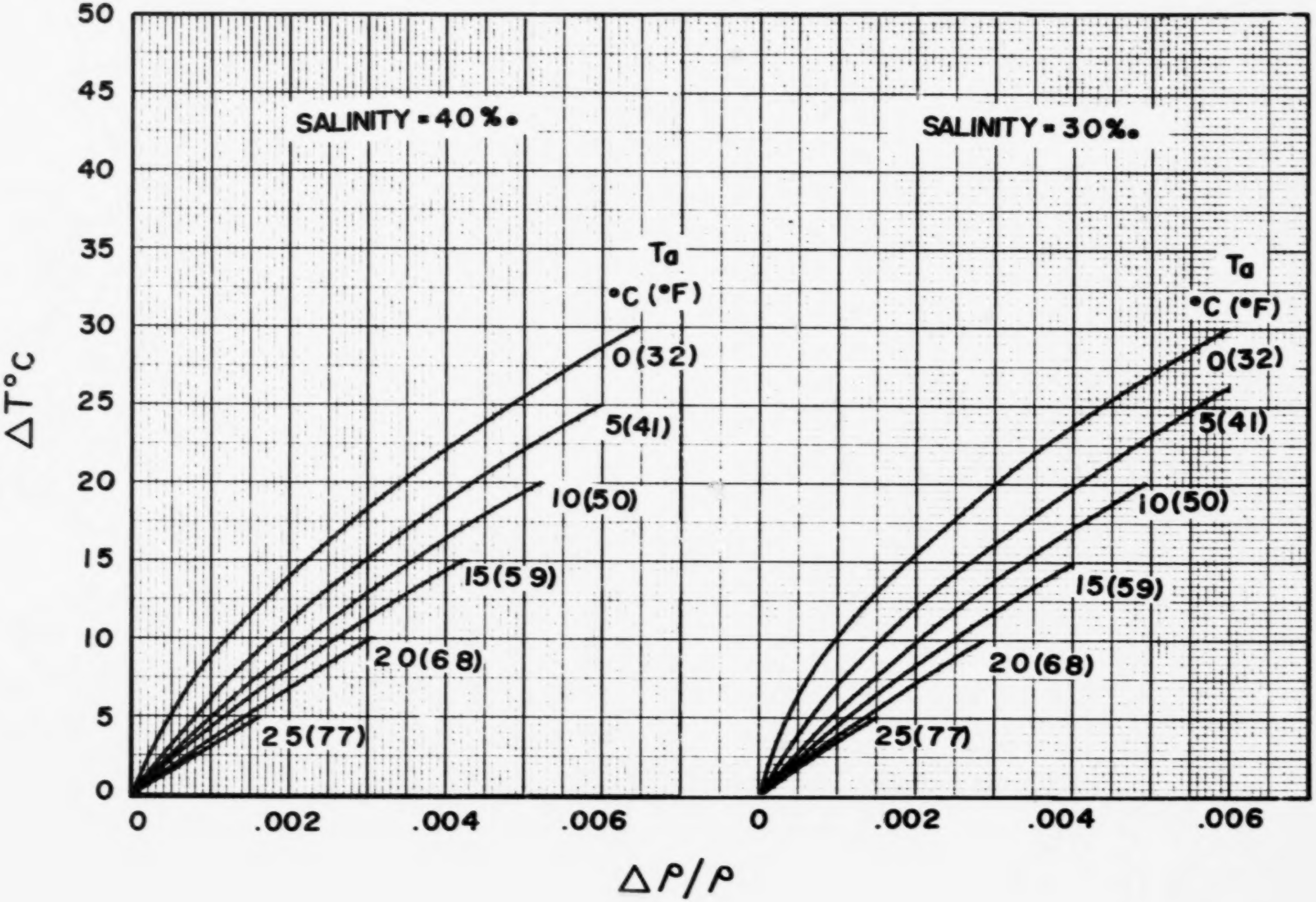

Figure E2 Temperature-density Relations for Salt Water.

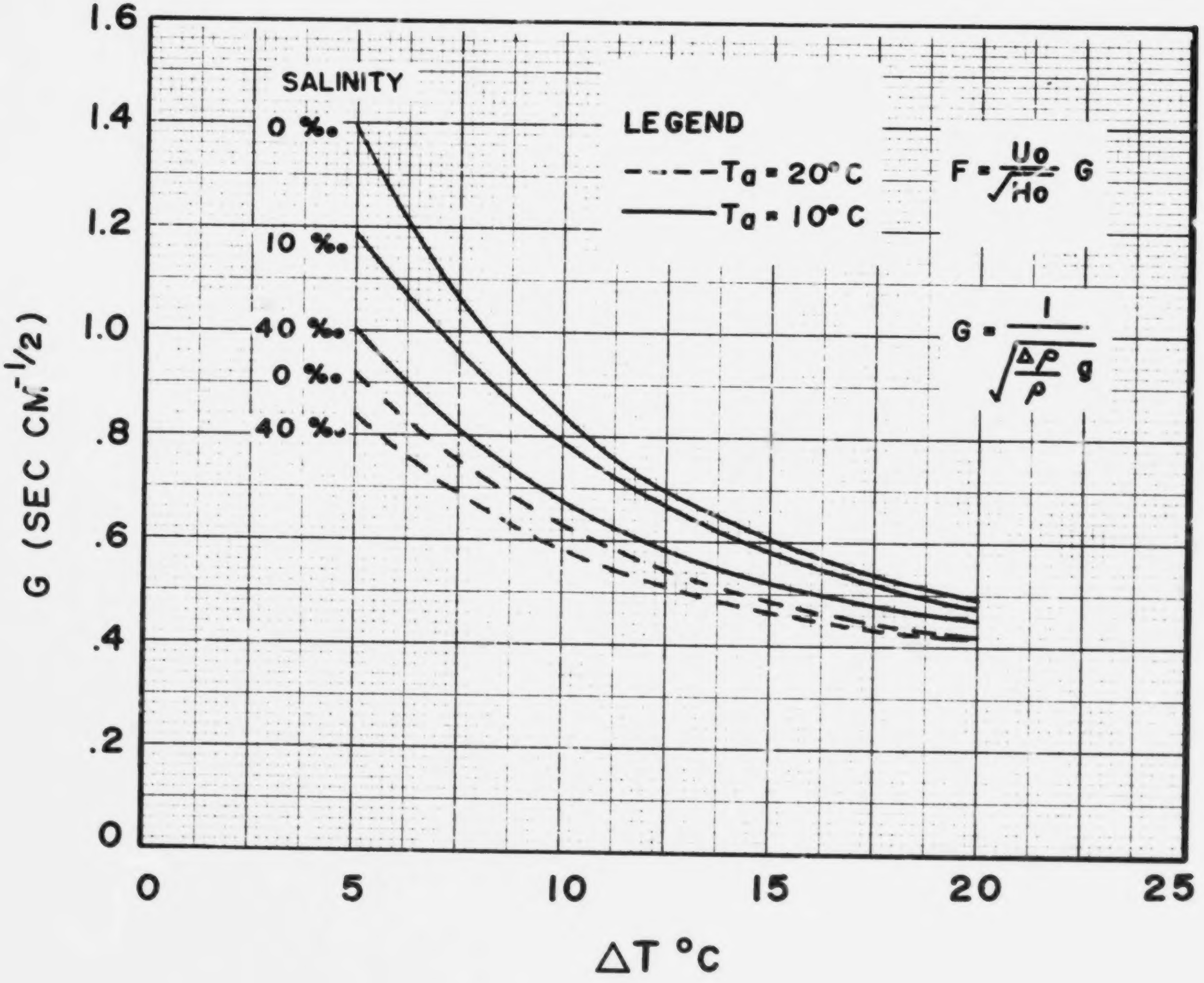

Figure E3 Temperature-density Relations for Froude Number Calculations.

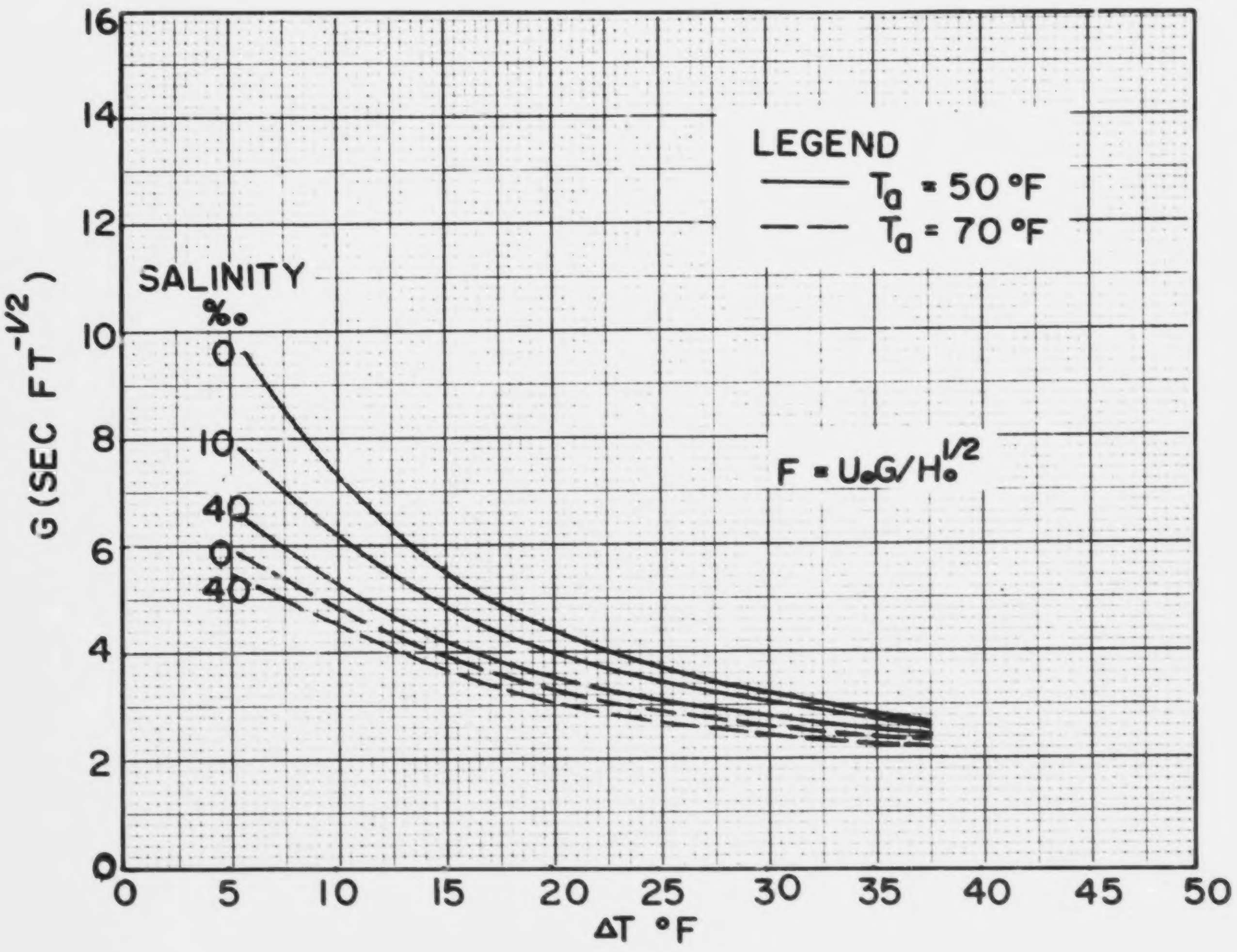

Figure E4 Temperature-density Relations for Froude Number Calculations.

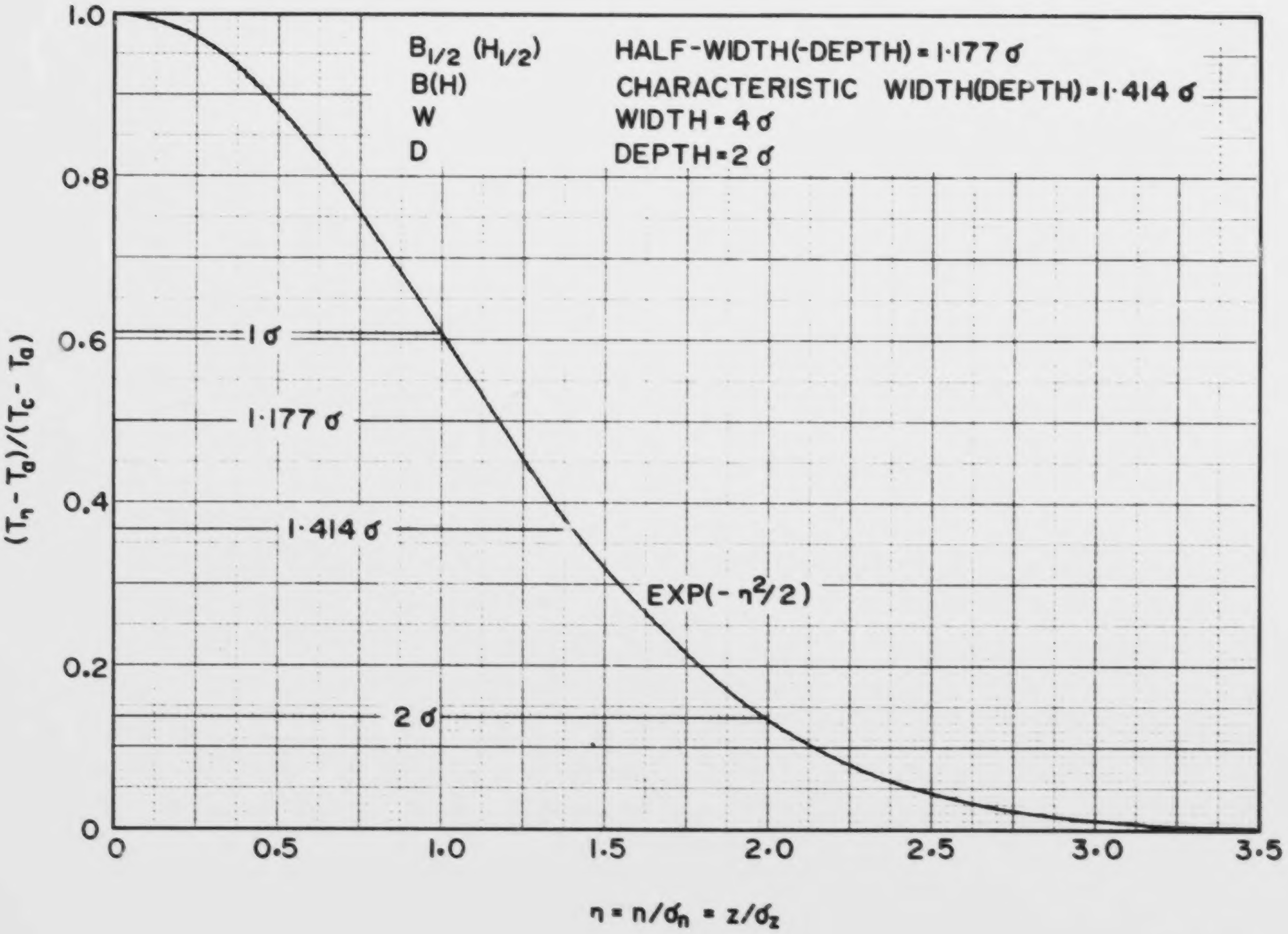

Figure E5 Gaussian Distribution Curve Used for Calculating Off-Centerline Temperatures.

Table E1 (Continued):

Multiply	By	To Obtain
Centimeter/sec^2	.03281	Feet/sec^2
Feet/sec^2	30.48	Centimeters/sec^2

g_o = 980.7 Cm/sec
= 32.17 Ft/sec
= 35.30 Km/hr
= 9.807 Meters/sec^2
= 21.94 Meters/hr

Feet /sec	30.48	Centimeters/sec
Feet/sec	1.097	Kilometers /hour
Feet/sec	.0183	Kilometers/minute
Feet/sec	.592	Knots (nautical miles/hr)
Feet/sec	.3048	Meters/sec
Feet/sec	.6818	Miles/hr
Centimeters/sec	1.969	Feet/minute
Centimeters/sec	.0328	Feet/sec
Centimeters/sec	.036	Kilometer/hr
Centimeters/sec	.0194	Knots
Centimeters/sec	.0224	Miles/hr
Meters/sec	3.281	Feet/sec
Meter/sec	1.943	Knots
Meters/sec	2.237	Miles/hr
Knots	51.48	Centimeters/sec
Knots	1.689	Feet/sec
Knots	1.853	Kilometers/hr
Knots	.5148	Meters/sec
Knots	1.152	Miles/hr
Pounds	453.6	Grams
Pounds	.4536	Kilograms
Kilogram	2.205	Pounds
British Thermal Unit (Btu)	1.076×10^7	Centimeter-grams
Btu	778.3	Foot-pounds
Btu	3.929×10^{-4}	Horsepower-hours
Btu	1054.8	Joules (Watt-seconds)
Btu	.2520	Kilogram-calories
Btu	2.93×10^{-4}	Kilowatt-hours
Btu	.2930	Watt-hours
Horsepower-hours	2545	Btu
Horsepower-hours	1.98×10^6	Foot-Pounds
Horsepower-hours	2.684×10^6	Joules (Watt-sec)
Hoursepower-hours	.7457	Kilowatt-hours
Joules (watt-sec)	9.48×10^{-4}	Btu
Kilowatt-hours	3413	Btu

TABLE E1
CONVERSION FACTORS

Multiply	By	to Obtain
Centimeters	0.3937	Inches
Centimeters	0.0328	Feet
Inches	2.540	Centimeters
Feet	30.48	Centimeters
Feet	.3048	Meters
Meters	3.281	Feet
Acres	43,560	Square feet
Acres	4,047	Square Meters
Acres	.001562	Square Miles
Acres	.004047	Square Kilometers
Acres	.4047	Hectares
Square Miles	640	Acres
Square Kilometers	247.1	Acres
Hectares	2.471	Acres
Cubic Feet	.02832	Cubic Meters
Cubic Feet	7.481	Gallons
Cubic Feet	28.32	Liters
Cubic Meters	35.31	Cubic Feet
Cubic Meters	264.2	Gallons
Gallons	.1337	Cubic Feet
Gallons	.003785	Cubic Meters
Gallons	3.785	Liters
Liters	.2642	Gallons
Acre Feet	1233	Cubic Meters
Cubic Feet/sec	448.86	Gallons per minute
Cubic Feet/sec	.0283	Cubic Meters per second
Cubic Feet/sec	.6464	Million Gallons per day
Cubic Meters/sec	15850	Gallons per minute
Cubic Meters/sec	35.31	Cubic Feet per second
Cubic Meters/sec	22.82	Million Gallons/day
Acre Feet/year	.62	Gallons/minute
Gallons per minute	.00223	Cubic Feet per second
Cubic Meters per second	.0283	Cubic Feet per second
Million Gallons/day	1.547	Cubic Feet per second
Million Gallons/day	54.63	Cubic Meters per second

Table E1 (Continued):

Multiply	By	To Obtain
Kilogram-Calories	3.969	Btu
Kilogram-Calories	3089	Foot-pounds
Kilogram-Calories	1.559×10^{-3}	Horsepower-hours
Kilogram-Calories	1.163×10^{-3}	Kilowatt-hours
Joules(Watt-seconds)	9.48×10^{-4}	Btu
Joules(Watt-seconds)	.7376	Foot-pounds
Joules(Watt-seconds)	3.722×10^{-7}	Horsepower-hours
Btu per square Foot	.2713	Gram Calories per square Cm
Gram Calories per square Centimeter	3.687	Btu per square Foot
Degrees Kelvin	1.8	Degrees Rankine

$$°C = \frac{5}{9}(°F - 32)$$

$$°F = 32 + 1.8°C$$

APPENDIX F
FURTHER ANALYTICAL CONSIDERATIONS
AND
COMPUTER PROGRAM

CONTENTS
APPENDIX F

	Page
List of Symbols	368-370
List of Figures	371-372

Sections

I. Modifications Leading to PDS Model
- A. Introduction 373-374
- B. Buoyant Spreading 374-376
- C. Development Length 377-378
- D. Temperature-Time Exposure 378-379
- E. Temperature-Area Calculations 379
- F. Extrapolating the Model 379-381
- G. Dimensionless PDS Program 382

II. Fitting PDS with Data 383
- A. Turbulent Exchange Coefficients E_h, E_v 384-385
- B. Entrainment Coefficient E_o 385-389
- C. Drag Coefficient C_D 389-396
- D. Conclusions 396-399

III. Theoretical Analysis 400-409

IV Computer Program 410-428

V. References 429-430

LIST OF SYMBOLS

B	Local characteristic width of jet = $\sqrt{2}\,\sigma_n$
B_o	Half width of outlet
$B_{1/2}$	Plume half width = $1.177\,\sigma_h$
C_D	Form drag coefficient
C_F	Interfacial shear drag coefficient
c	Celerity of a density front
D	Local plume depth = $2\sigma_z$
E_h	Dimensionless horizontal eddy diffusion coefficient ε_h/U_oH_o
E_o	Entrainment coeffient
EV	Ratio of vertical to horizontal eddy diffusion coefficients E_v/E_h
F	Gross densimetric Froude number, $\frac{\pi^{1/4}(U'/2 + V' \cos \Theta)F_o}{\sqrt{H'}}$
F_D	Form drag per unit length of jet
F_o	Densimetric Froude number at outlet, $U_o/\sqrt{g'H_o}$
g	Acceleration due to gravity
g'	Reduced gravitational acceleration, $g\,\Delta\rho/\rho_a$
H	Local characteristic thickness of jet
H_o	Depth of outlet
K_E	Atmospheric heat transfer coefficient
M	Local s-momentum flux in jet
n	Horizontal coordinate perpendicular to s
PDS	Prych model modified by Davis and Shirazi
P	Pressure force on jet cross section
Q	Local volume flux in jet
Ri	Richardson number
S_F	Shear forces in X- and Y- directions per unit length of jet
s	Curvilinear coordinate along jet centerline
S_i	Distance from outlet to end of initial zone
$\Delta\bar{T}_c$	Local excess water surface temperature on jet centerline
ΔT_o	Difference between outlet and ambient water temperatures
t	Time of travel along centerline trajectory

TH	Angle between positive S- and X- directions (Θ)
T_r	Local plume temperature $T(s, n, Z)$
U_c	Local excess jet velocity on jet centerline
U	Velocity in s-direction
U_r	Local plume velocity $U(s,n,Z)$
U_o	Discharge velocity from outlet
X	Rectilinear coordinate parallel to ambient current
Y	Rectilinear coordinate, horizontal and perpendicular to X
Z	Coordinate in vertical direction
V	Ambient current velocity
α	Angle used in data analysis of Ref. (2) $\alpha = \pi - \Theta_o$
$\Delta\rho$	Difference between outlet and ambient water densities
$\varepsilon_h, \varepsilon_v$	Ambient turbulent diffusion coefficient for horizontal and vertical directions
Θ	Angle between positive s- and χ- directions (TH)
Θ_o	Angle between χ-axis and outlet velocity direction
ν_o	Kinematic viscosity
ρ	Fluid density
τ_o	Shear stress

SUBSCRIPTS

a	Ambient conditions
c	Centerline value at surface
i	Refers to variables at end of development zone
o	Discharge conditions
r	Indicates variable is a function of s, n, Z directions

DIMENSIONLESS VARIABLS

$U' = U_c/U_o$

$B' = B/H_o$

$H' = H/H_o$

$T' = \Delta T_c/\Delta T_o$

$K' = K_E/\rho C_p U_o$

$S' = S/H_o$

$X' = X/H_o$

$Y' = Y/H_o$

$V' = V/U_o$

$P' = P/U_o^2 H_o^2$

$M' = M/U_o^2 H_o^2$

$S_F' = S_F/U_o^2 H_o^2$

$F_D' = F_D/U_o^2 H_o^2$

$Q' = Q/U_o H_o^2$

$A = 2B_o/H_o$

$R = V/U_o$

$R_e = U_o H_o/\nu$

List of figures
Appendix F

Figure No. Page

F1 Comparison of Original Model Predictions of References 1 and 3 for Plume Width with a Typical Measured Plume Width from Reference 3. 375

F2 Correlation of Measured Surface Plume Temperature Data from a Jet Initially Discharged in a Turbulent Coflowing Channel with Zero Relative Velocity, R=1. 386

F3 Comparison of Calculated Temperatures with Mean Measured Centerline Plume Temperature Data of Figure F2. 387

F4 Comparison of Calculated Widths with Mean Measured Width for a Jet Initially Discharged at the Surface in a Turbulent Coflowing Channel with Zero Relative Velocity, R=1. 388

F5 Correlation of Selected Field and Laboratory Surface Plume Temperature for Typical Froude Number and Aspect Ratio at Zero or Negligibly Small Ambient Current. 390

F6 Comparison of Calculated Temperatures with Mean Measured Surface Plume Temperature Data Shown in Fig. F5 391

F7 Correlation of Selected Field and Laboratory Surface Plume Width Data for Typical Jet Froude Number and Aspect Ratio at Zero or Negligibly Small Ambient Current. 392

F8 Comparison of Calculated Widths with Mean Measured Surface Plume Width Data of Fig. F7. 393

F9 Correlation of Selected Field and Laboratory Surface Plume Trajectory Data for Typical Jet Froude Number, Aspect Ratio and Ambient Cross Current. 394

F10 Comparison of Calculation with Mean Measured Surface Plume Trajectory Data of Fig. F9. 395

F11 Comparison of Calculated Widths with Selected Field and Laboratory Surface Plume Width Data Correlated for Typical Jet Froude Number, Aspect Ratio and Ambient Cross Current. 397

Figure No. Page

F12 Comparison of Calculated Temperatures with Selected Field and Laboratory Surface Plume Temperature Data, Correlated for Typical Jet Froude Number, Aspect Ratio and Ambient Cross Current. 398

F13 Schematics of a Surface Plume Showing the Coordinate System. 399

I. MODIFICATIONS LEADING TO PDS MODEL

A. INTRODUCTION

Various mathematical models of heated surface jets are available for the prediction of two and three dimensional plume configurations. Two widely accepted methods are used for solving the equations in these models, namely one based on the integral analysis approach and the other based on the differential numerical analysis methods. The latter approach, while capable of greater generality, is considerably more costly and due to limited funds and resources was excluded from further consideration for this work. However, a certain degree of generality of results is retained by considering only three dimensional plume models for generating the nomograms in this workbook.

A comprehensive review of thermal plume models is presented in Reference 4. Among the three dimensional surface jet models seriously considered for generating the nomograms in this workbook is one by Stolzenbach and Harleman (MIT Model), another by Prych and the third model by Stefan, et al. These are discussed in References 1, 3, 5, and 10. It is outside the scope of this Workbook to discuss in detail results of all experiments performed on the three models during our attempt to provide a working program. The MIT model, despite its many fine features, has considerable computational difficulties. Prych's model is the result of reasonably successful attempt to remove from MIT's model some of these difficulties. Stefan's model was written for the developed zone alone and thus can't be compared with others directly. Even though it includes wind effects absent in the other two, it ignores the hydrostatic pressure in the longitudinal direction.

In general, the MIT and Prych models yield comparable predictions[1]. The greatest deviation between the predictions of both models and data is in plume width. Figure F1 shows the predictions of width from both models for a particular Froude number and aspect ratio as compared with the mean of experimental data of Fig. F8 and the experimental data from Run 3 of Ref. 3. Both models overestimate the plume width.

An effort is made here to introduce modifications in Prych's model to make it better agree with existing data. These modifications for improving the model, as well as certain other additions, are discussed below. The result of these changes is a modified model henceforth referred to as PDS.

B. BUOYANT SPREADING

Stolzenbach and Harleman[3] present an order of magnitude analysis of the momentum equations as applied to the jet. They show that the lateral acceleration of fluid particles within the plume is negligible only when the jet is nonbuoyant. Otherwise, the fluid particles accelerate (spread) due to the influence of two interacting forces, namely, the inertia and buoyant forces. Since the full nonlinear equations of motion describing a buoyant plume are too difficult to solve, the lateral spreading due to buoyant forces in the MIT, and Prych models are calculated independently of spreading due to nonbuoyant forces. The two spreading rates are assumed to make additive contributions, thereby ignoring the nonlinear interaction between the two forces. As a consequence of the assumptions in this linearization their analyses overestimate the plume width when the inertia and buoyant forces are the same order of magnitude (i.e., when the densimetric Froude number is not too large). When the plume inertia forces are dominant such as with strong ambient current or large densimetric Froude numbers, reasonable width predictions can be obtained.

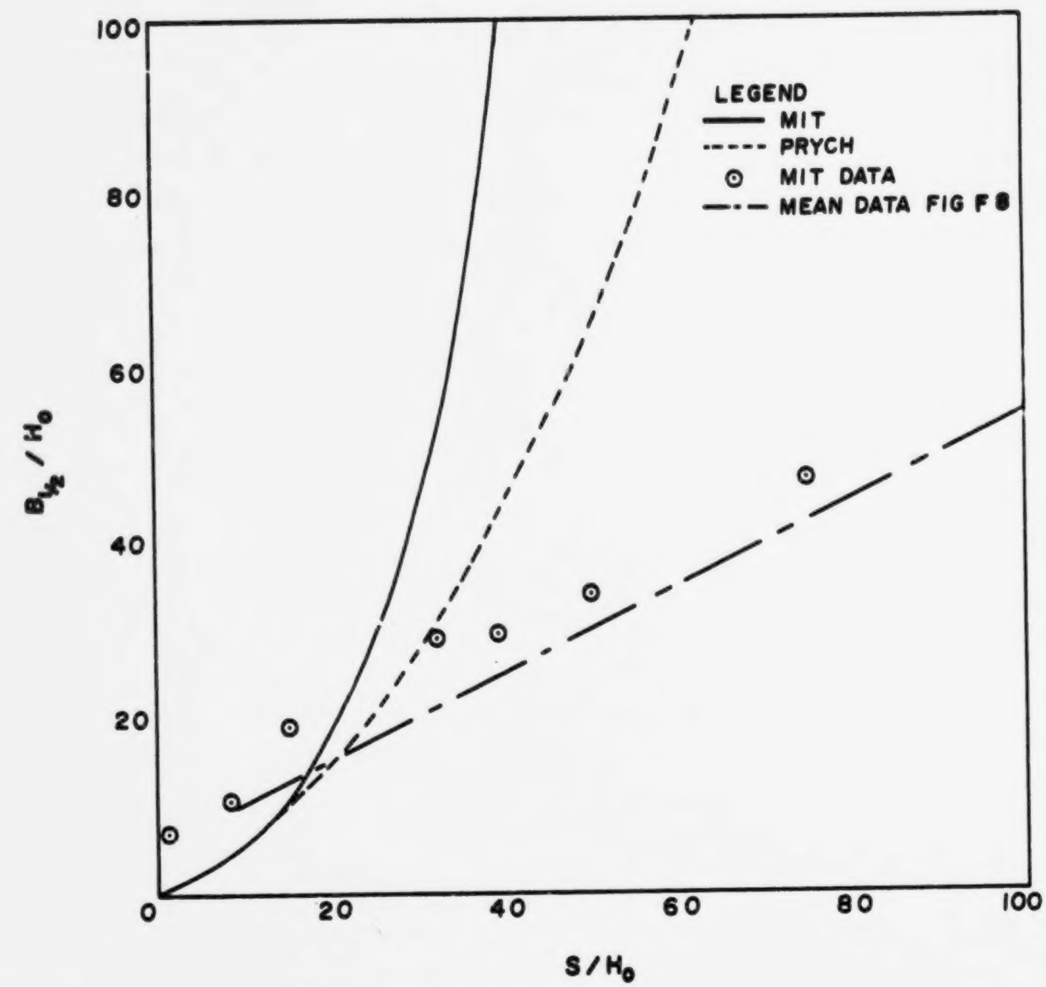

Figure F1 Comparison of Original Model Predictions of References 1 and 3 for Plume Width With a Typical Measured Plume Width from Reference 3.

The buoyant spreading function used by Prych is based on the analysis of an immiscible film, such as oil spreading over water that ignores the shear interaction between the fluid systems. In this analysis, the fluid particles are assumed to move with a velocity equal to the velocity caused by density waves alone.

In a separate analysis of a buoyant spreading of a pool of warm water, Koh and Fan[6] accounted for the interfacial shear interaction but ignored the actual entrainment of the cool water. They found that near the source the spreading velocity is in agreement with Prych's analysis and the spreading velocity and the fluid velocity are the same, i.e.,

$$V_n^2 = c^2 \sim g'H$$

Where H is the local depth of the buoyant pool. However, far away from the source where the shear forces become very important, the fluid front velocity is

$$V_n \sim \frac{g'H}{(\varepsilon/H\rho)} (H/B)$$

Where g'H is proportional to c^2, $(\varepsilon/H\rho)$ is proportional to the shear velocity and H/B is the ratio of the local pool depth to its width. If interpreted in terms of plume spread, this finding implies that spreading velocity is inversely proportional to the local aspect ratio of the plume.

The appearance of the local aspect ratio in the expression for the plume velocity offers an intuitively appealing ground for assuming,

$$V_n^2 \sim (g'H)(H/B)$$

This slight modification to Prych's analysis was introduced in the model. As a result, a satisfactory fit with data became possible.

C. DEVELOPMENT LENGTH

Analysis of the jet development zone is complicated because of the need to examine simultaneously the characteristics of a core region as well as a turbulent outer jet region. Stolzenbach and Harleman developed a three dimensional program for this region, but in his modification of the program, Prych adopted a one dimensional approach in which he employed celerity relations for the spreading of the buoyant unmixed core region. He then used the appropriate conservation equations to relate the fluid properties at four jet diameters away from the outlet to the fluid properties at the outlet. The fixed development length of four diameters is based on the assumption of a semicircle with an area 2 B_oH_o. Prych's development length S_i can be written as

$$\frac{S_i}{H_o} = 6.38A^{\frac{1}{2}}$$

where A is the channel aspect ratio.

Note that the above development length does not change with the initial densimetric Froude number. However, calculations with the MIT model show that the development length does change with initial densimetric Froude number as well as the jet aspect ratio.

Since a better agreement of model predictions with the data is expected if this aspect of the model is also appropriately adjusted, resort was made to laboratory experiments to obtain this information. Experiments were conducted in a still water tank with a heated jet at the EPA Pacific Northwest Environmental Research Laboratory. Several jet aspect ratios and jet densimetric Froude numbers were tested. A hot film anemometer probe was used to traverse the jet development zone laterally at several stations downstream from the outlet. The presence of the core was detected from subdued turbulent temperature fluctuations as well as the temperature level. The coincidence of the increased turbulence fluctuations, the beginning of the temperature drop, and the disappearance of a uniform core at a point downstream of the outlet signaled the end of development zone. The data for this length was correlated to give

$$\frac{S_i}{H_o} \simeq 5.4 \left(\frac{A^2}{F_o}\right)^{1/3}$$

This tentative result is subject to refinement (particularly with respect to the effect of the ambient current) when better experimental investigations currently underway[7] become available. Meanwhile, the use of this correlation was found very helpful to fit the model with available plume data.

It should be noted that generally the excess temperature ratio at the end of the development zone is different from unity. It is hoped that future experiments will shed light on this aspect of the problem as well. In anticipation of the latter point, we have introduced a slight modification to Prych's program to allow the use of excess temperature ratios other than unity

D. TEMPERATURE-TIME EXPOSURE

The total exposure time of organisms to a given excess temperature within the plume can be calculated if we assume that (a) such organisms are uniformly distributed within the natural water environment that supply the initial jet discharge with dilution water, and (b) that the motion of these organisms is totally governed by the motion of the entrained fluid. That is, the organisms are not self propelled and they are small enough so that they faithfully follow the motion of the entrained fluid.

Naturally, the organisms can be entrained at any point s, along the trajectory from s_1 to a second point s_2. Thus, the travel time t can be estimated from the calculated centerline plume velocity as

$$t = \int_{s_1}^{s_2} ds/U_c$$

Where U_c is the local centerline velocity, itself a function of s and calculated stepwise by the program. For each plume, unique temperatures T_1 and T_2 are calculated that correspond, respectively with s_1 and s_2.

The above calculation performed for the travel along the centerline yields a minimum time of travel between s_1 and s_2 associated with an exposure to a maximum elevated temperature existing in the plume between T_1 and T_2. Off-center, the temperatures are lower, and particles do not travel as fast as along the plume centerline.

E. TEMPERATURE-AREA CALCULATIONS

The surface area within an isotherm is calculated in Prych's program for each integration step DS by using the trapezoidal rule of integration. The areas are calculated for excess temperature ratio increments of .05 starting at 1.0. Near the source the excess temperature ratio may drop more than .05 within one integration step. As a result, the area calculations are in error. To avoid this problem in the PDS model the integration step is adjusted so that the maximum allowable drop in excess temperature per time step is .05.

F. EXTRAPOLATING THE MODEL

Prych suggests that at a local densimetric Froude number of unity, calculations with the plume model be discontinued because of mathematical singularities. In the PDS model, there are two singularities which do not occur at the same point along the trajectory.

Even though calculations can be made to continue beyond the first singularity, adequate justification is missing to support the use of information so obtained. The problem is that the first singularity can be bypassed almost all the time by a judicious selection of the step size and error terms, thereby passing from regions where the gross densimetric Froude number is slightly greater than unity to a region where it is below unity. Calculations continue normally until the second singularity is reached, there the program is terminated.

The effect of passing over a Froude number of unity while allowing calculations to continue is that the gradient of the plume depth changes sign which initiates a small damped oscillation. Conservation equations are satisfied and all plume characteristics seem to change very smoothly. The trajectory of the plume is calculated without apparent discontinuity,from the equations. The trajectory curves also agree very well with the available data. Motivated by these observations, we have decided to retain at least the trajectory calculations when the solution is allowed to continue beyond a Froude number of unity.

It is important to resolve whether the singularity at a local Froude number of unity is only a mathematical obstacle or that a discontinuity actually exists in nature at this point. The question arises because (a) examination of the available three dimensional plume data does not reveal the presence of such a discontinuity in plume characteristics for a low discharge Froude number and a small ambient current, (b) the existence of a discontinity for two dimensional plumes has been confirmed in laboratory experiments only and in analyses, of References 6 and 10 and these occur at local Froude numbers greater than unity,

(c) the uncoupling of the hydrostatic pressure forces in the longitudinal direction from the same forces in the lateral direction retains essentially the nature of a two dimensional plume in the model with respect to those factors that influence an internal hydraulic jump the most, and (d) it is difficult to insist that a singularity in the calculations occurs at a point in the plume where the internal hydraulic jump takes place based solely on the simplified analysis of the plume without confirmation with data.

The PDS model is fitted with data in a systematic way as will be discussed. Based on the model, (TTWD) plots are made that show the effect of ambient current. For nearly all cases examined, the model produces continuous data near the source as the calculations proceed from high ambient current to low and zero ambient current. However, at low densimetric Froude numbers and far away from the source, the local Froude number becomes unity and the calculations are stopped. A smooth extrapolation based on calculated data at higher ambient current (usually $R > 0.05$) to lower currents ($R < 0.01$) can be made only if there is assurance that the plume does not go through an internal hydraulic jump. Since the available data do not support the existence of discontinuity in a three dimensional model, we find it useful to present the said extrapolation. In order to avoid misunderstanding, the extrapolated curves are presented as broken lines. The reader is cautioned not to confuse the dashed extrapolation lines with the trajectory lines which are also dashed. The trajectories are completely dashed and originate at X and Y = 0.

The extrapolation of the temperature lines was obtained according to $S = a\,(1-R)^b$ where a and b are constants determined from two consecutive neighboring points just before the occurrance of singularity The width lines were extrapolated in the same manner.

G. DIMENSIONLESS PDS PROGRAM

In order to make the results of the mathematical model more general and independent of any particular system of units used, the governing equations and all calculated plume characteristics are made dimensionless by dividing all length characterisitics by H_o, velocities by U_o, momentum, pressure, shear and drag forces by $U_o^2 H_o^2$, flow rate by $U_oH_o^2$, diffusivity by U_oH_o, excess temperature by (T_o-T_a) and the kinematic heat transfer coefficient by U_o. These quantities are "primed" and listed under a separate heading in the list of symbols. The choice of H_o for nondimensionalizing the length scale is made for the convenience it offers over $\sqrt{H_oB_o}$, etc.

When the dimensionless terms are introduced in the governing equations and the primes dropped, the equations for the developed region of the jet become identical with those given by Prych if only one interprets:

$$\frac{1}{F_o^2} \text{ as } g', \; \frac{1}{R_e} \text{ as } \nu, \; K_E/U_o \text{ as } K \text{ and } \frac{\varepsilon}{U_oH_o} \text{ as } \varepsilon$$

II. FITTING PDS WITH DATA

Reference 2 provides a comprehensive set of data that is a good representation of available experiments both in the field and laboratory. The data provide a wide range of plume conditions with which one can test and accordingly adjust numerous analytical functions of the plume model. The plume model contains a number of free variables such as entrainment coefficient E_0, turbulent exchange coefficients E_h, E_v, drag coefficient C_D and shear coefficient C_F. The magnitudes of these coefficients must be prespecified so that the model produces the best fit with the measured plume characteristics.

In order to accomplish this task, the following procedure is adopted: (a) Data for plume characteristics are subgrouped with a narrow range of certain experimental parameters such as the current ratio, R, the densimetric Froude number, F_0, the jet aspect ratio, A, or the angle of discharge, Θ_0. Each subgroup consists of several experiments and several sources, thus providing considerable degree of realism with respect to possible experimental scatter and variations in experimental parameter scales. The choice of a narrow range in certain experimental parameters was dictated by the desire to obtain as strong a correlation of the data within a given subgroup as possible. (b) For each subgroup, the range and the mean of all experimental parameters are determined. (c) The data are correlated using dimensional analysis and multiple regression methods separately for each subgroup following the procedure outlined in Reference 2. (d) The measured plume characteristics are plotted against dimensionless axial distance using the correlation results. (e) A representative smooth curve is drawn through the mean data and local standard deviations are displayed on both sides of the mean curve to show the scatter. This mean curve is a fair representation of the subgroup, and is represented by the mean parameters obtained in item b above. (f) Finally, the PDS program is used to calculate the plume characteristics in each subgroup for the mean of the experimental parameters R, F, A, and Θ_o. Agreement between the calculated characteristics and the data mean is sought by adjusting one or more of the model coefficients E_o, E_h, E_v, D_D and C_F. This process is repeated for several subgroups, adjusting in each trial one or more coefficients until best fits are obtained to plume characteristics for all subgroups.

It should be pointed out that correlations of each data subgroup are useful mainly for the mean data in that subgroup. They are not universal correlations and cannot be used outside the data range they represent.

A. TURBULENT EXCHANGE COEFFICIENTS, E_h, E_v

The data set most suitable for determining the effects of ambient turbulence on plume behavior is provided by Weil[2,8]. In his experiments, Weil injected heated water at the surface in a turbulent channel from a semi-circular jet at a relatively large densimetric jet Froude number. The discharge was in the direction of the channel current ($\Theta_o = 0$). The jet velocity in all his experiments was held equal to the local channel flow velocity.* Since the relative velocity between the plume and ambient water is zero and since buoyancy effects are small due to a high Froude number, dilution is largely due to turbulence effects.

For the conditions of this experiment, the following simplifications can be introduced in the mathematical model: (a) The entrainment coefficient, E_o, can be set equal to zero because there is no relative velocity between the jet and the ambient water. (b) For the same reason, the shear coefficient, C_F, is also zero. (c) The drag coefficient C_D, is zero because the jet is parallel to the ambient current and the pressure distributions on the left and right hand sides of the plume are identical. (d) For the dimensionless surface heat exchange coefficient, one can choose a typical value of $K = 10^{-5}$ without affecting the calculated plume characteristics greatly one way or another, because we are dealing with small areas and small temperature differences. (e) Since the jet densimetric Froude number is high, the influence of the buoyant forces on the plume spread is not substantial. The plume width grows predominantly due to turbulent entrainment of the ambient water, a mechanism which the model accounts for through E_h and E_v.

---

*When retrieving Weil's data from Reference 2 the following adjustments should be made only on that data: multiply F by 1.189, S by 1.414 and W by 0.707 to account for an error in presentation.

Figure F2 is the plot of correlated temperature data showing the local mean and standard deviations. Figure F3 is a replot of the mean temperature data together with several computer calculations based on the PDS model for F = 16 , A= 2, $\Theta_o = 0$, and $K = 10^{-5}$. Calculations are made for several values of E_h and E_v/E_h as well as the free factor of the spreading function, XK1. The plots for the calculated and measured plume width data are shown in Fig. F4. The measured width data were closely spaced with excellent correlation. For this reason individual data points were not plotted. Instead, a narrow band showing the spread of all experimental data are presented.

A visual inspection of Weil's data of Figures F3 and F4 shows that the best fit is obtained with

$$E_h = .02, \; E_v/E_h = .2 \text{ and } XK1 = 1.4$$

B. ENTRAINMENT COEFFICIENT E_o

The next group of data consists of information from several sets of laboratory and some field experiments for a surface discharge

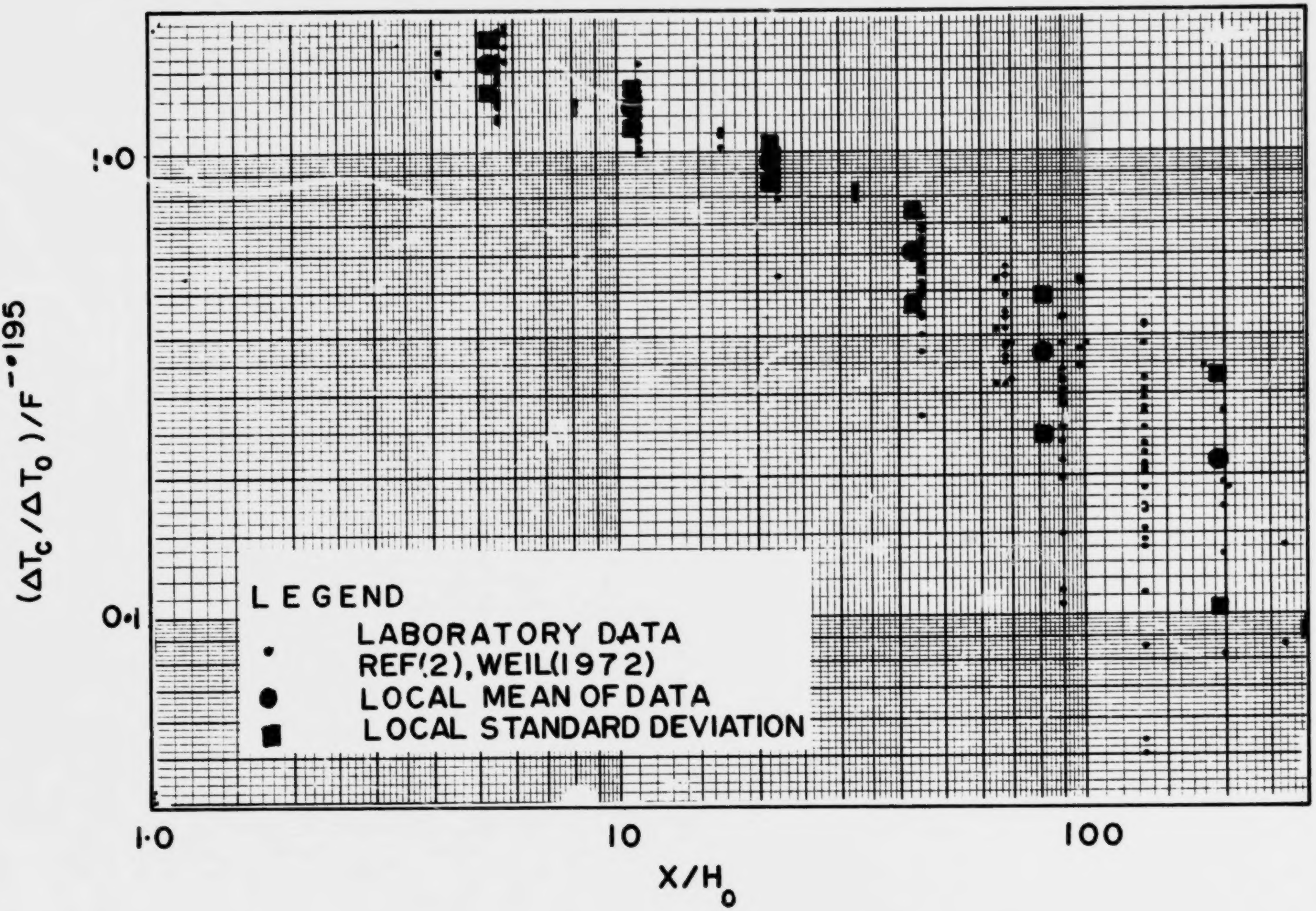

Figure F2 Correlation of Measured Surface Plume Temperature Data from a Jet Initially Discharged in a Turbulent Coflowing Channel with Zero Relative Velocity, R=1.

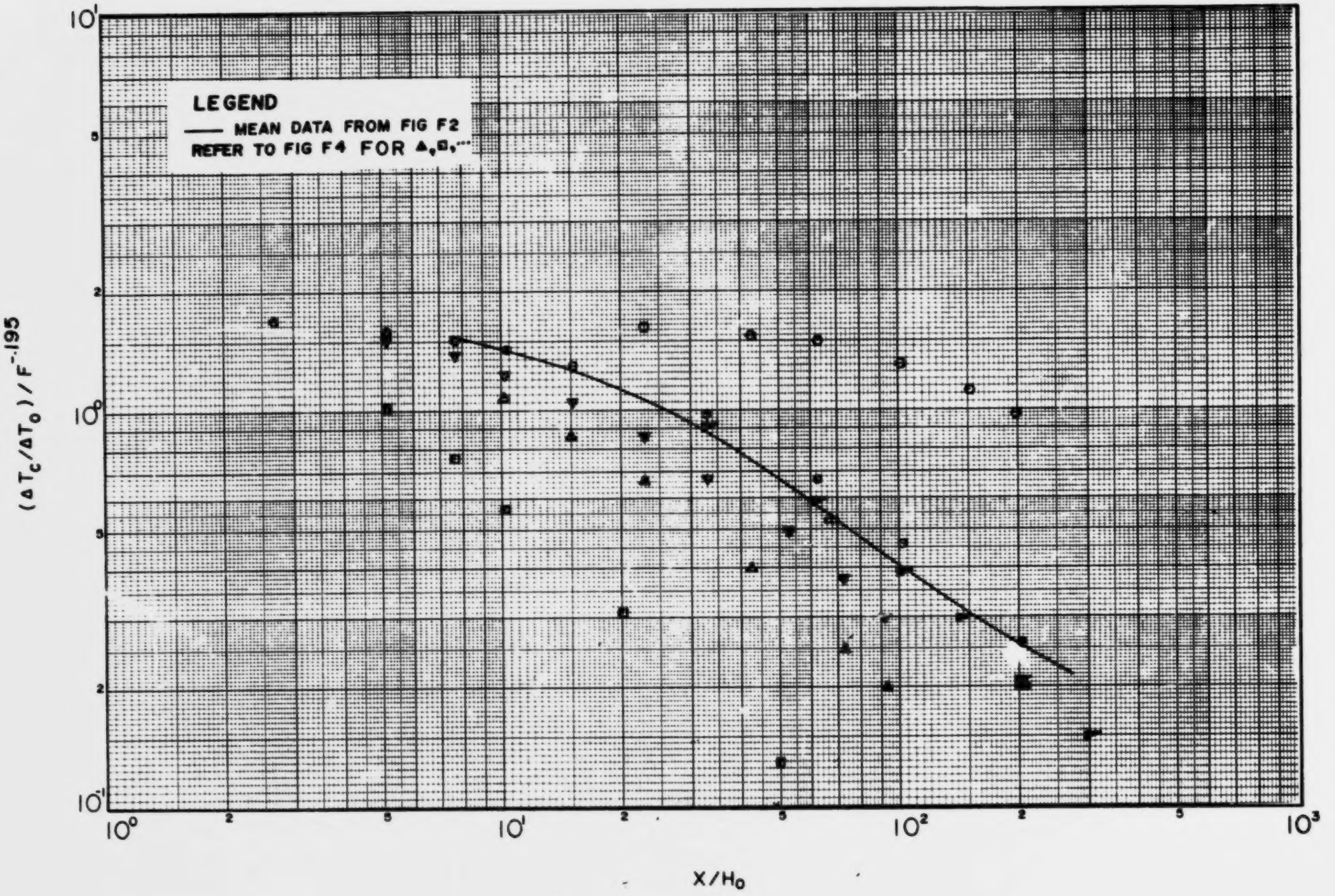

Figure F3 Comparison of Calculated Temperatures with Mean Measured Centerline Plume Temperature Data of Figure F2.

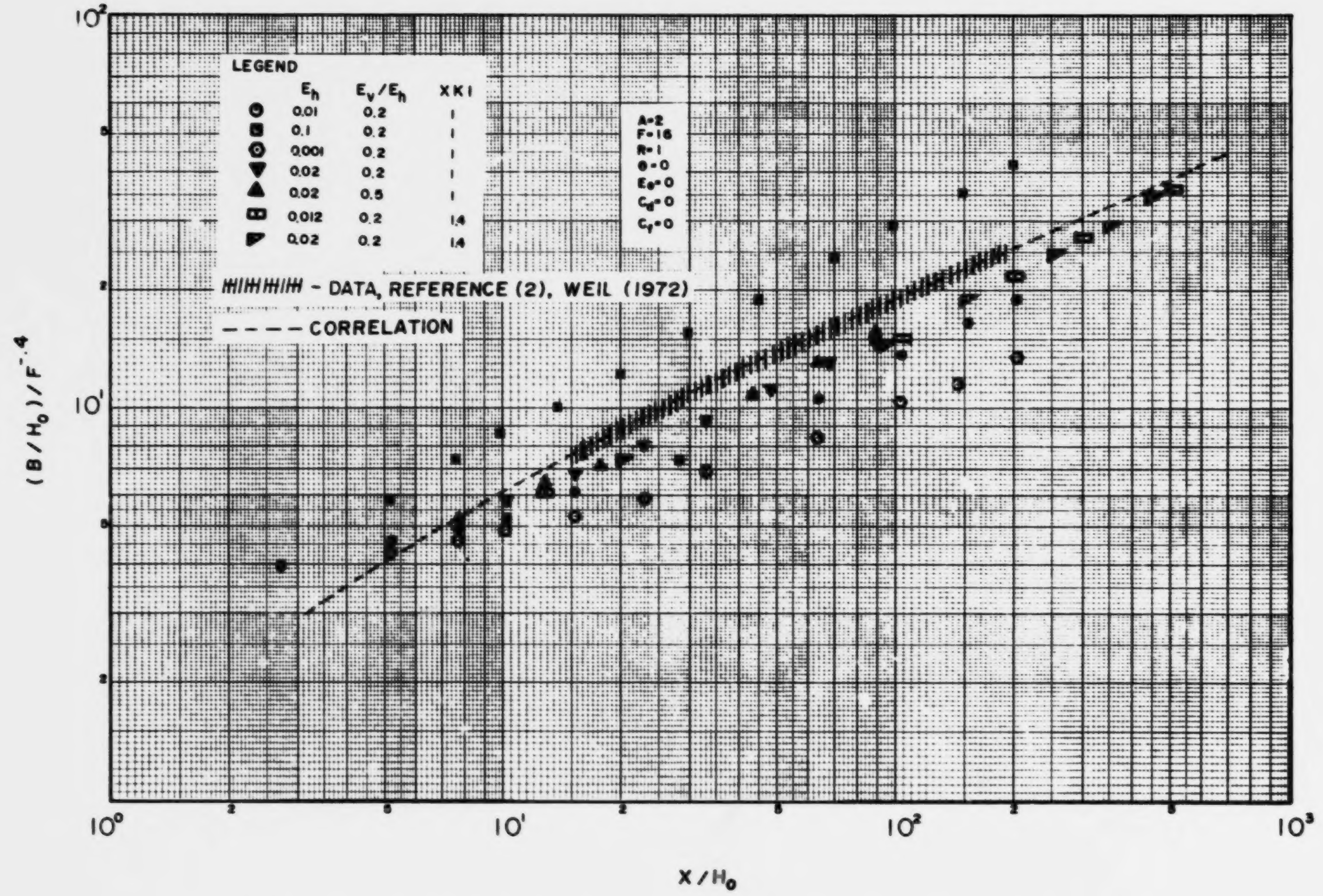

Figure F4 Comparison of Calculated Widths with Mean Measured Width for a Jet Initially Discharged at the Surface in a Turbulent Coflowing Channel with Zero Relative Velocity, R=1.

in zero or negligibly small cross current. The correlation of temperature data are plotted in Fig. F5 and the width data in Fig. F7.

For the conditions of this group, one can assume that the drag coefficient is zero. As a first approximation we also assume that the contribution of the ambient turbulence is accounted for by the previously assigned values of E_h and E_v. As we continue to adjust other coefficients in the model, we may have to reevaluate E_h and E_v.

Figures F6 and F8 show the replots of the mean data and several computer calculations of the PDS model with preassigned values of entrainment and shear coefficients. The best fit of the computer model with the data is obtained with $E_0 = 0.05$. Since the shear coefficient has negligible effect on the result, it will be set equal to zero.

C. DRAG COEFFICIENT, C_D

For given values of discharge angle, Froude number, aspect ratio, and ambient current, the plume trajectory is mainly influenced by the entrainment of ambient fluid with a minor influence due to pressure drag. Since the entrainment coefficient is prespecified from the above, only the drag coefficient can be used to further adjust the trajectory. Consequently, we need to regroup the trajectory data for a reasonably wide range of all plume parameters mentioned above. Such data are plotted in Fig. F9 showing the data sources, the local mean, and standard deviations. Figure F10 is a replot of the mean trajectory showing the comparison with computed values. Originally, considerable deviation of computed vs. mean data was found near the source. This deviation was corrected by assuming in PDS that

$$X(o) = S_1 \cos \Theta(o)$$
$$Y(o) = S_1 \sin \Theta(o)$$

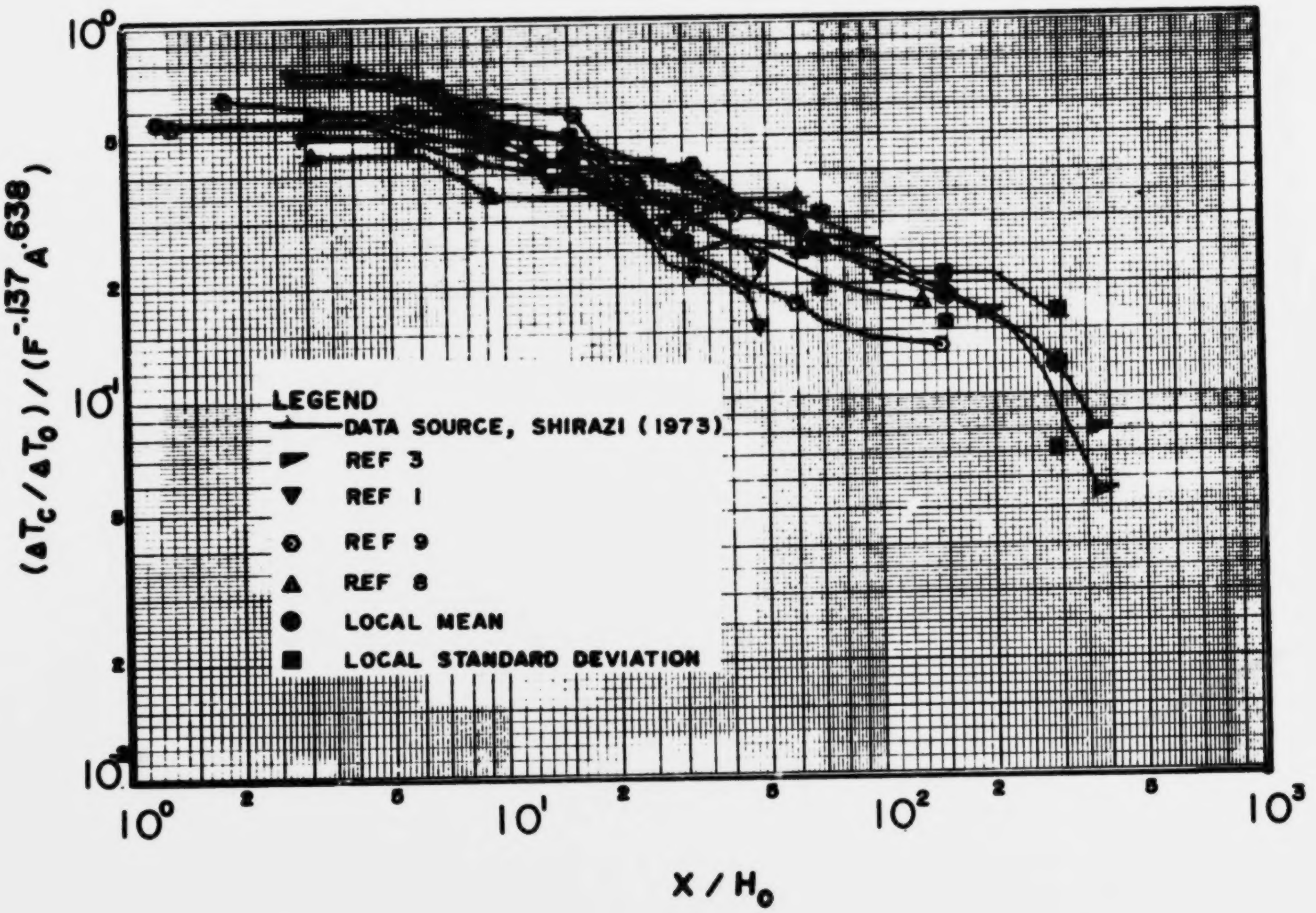

Figure F5 Correlation of Selected Field and Laboratory Surface Plume Temperature for Typical Froude Number and Aspect Ratio at Zero or Negligibly Small Ambient Current.

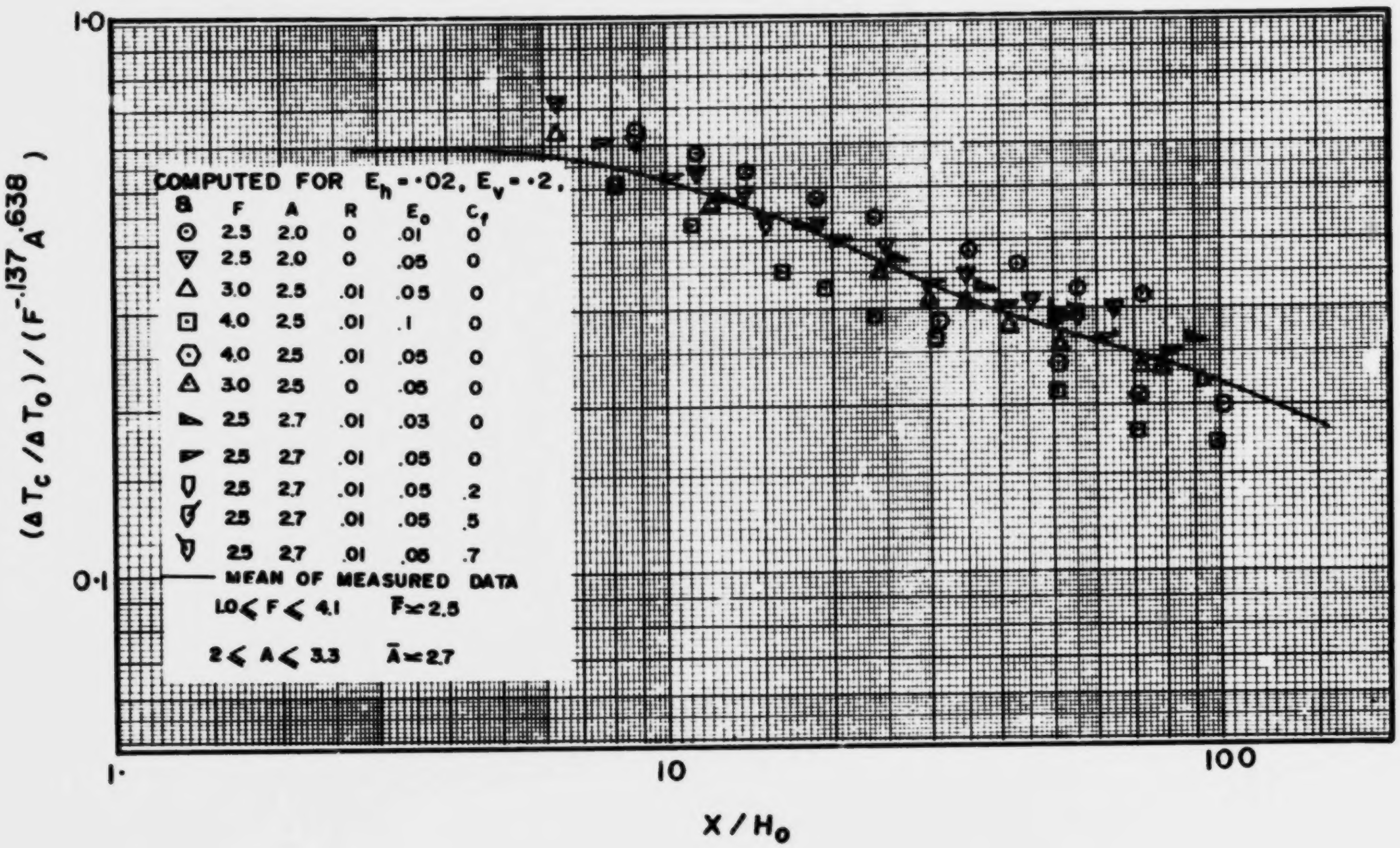

Figure F6 Comparison of Calculated Temperatures with Mean Measured Surface Plume Temperature Data Shown in Fig. F5

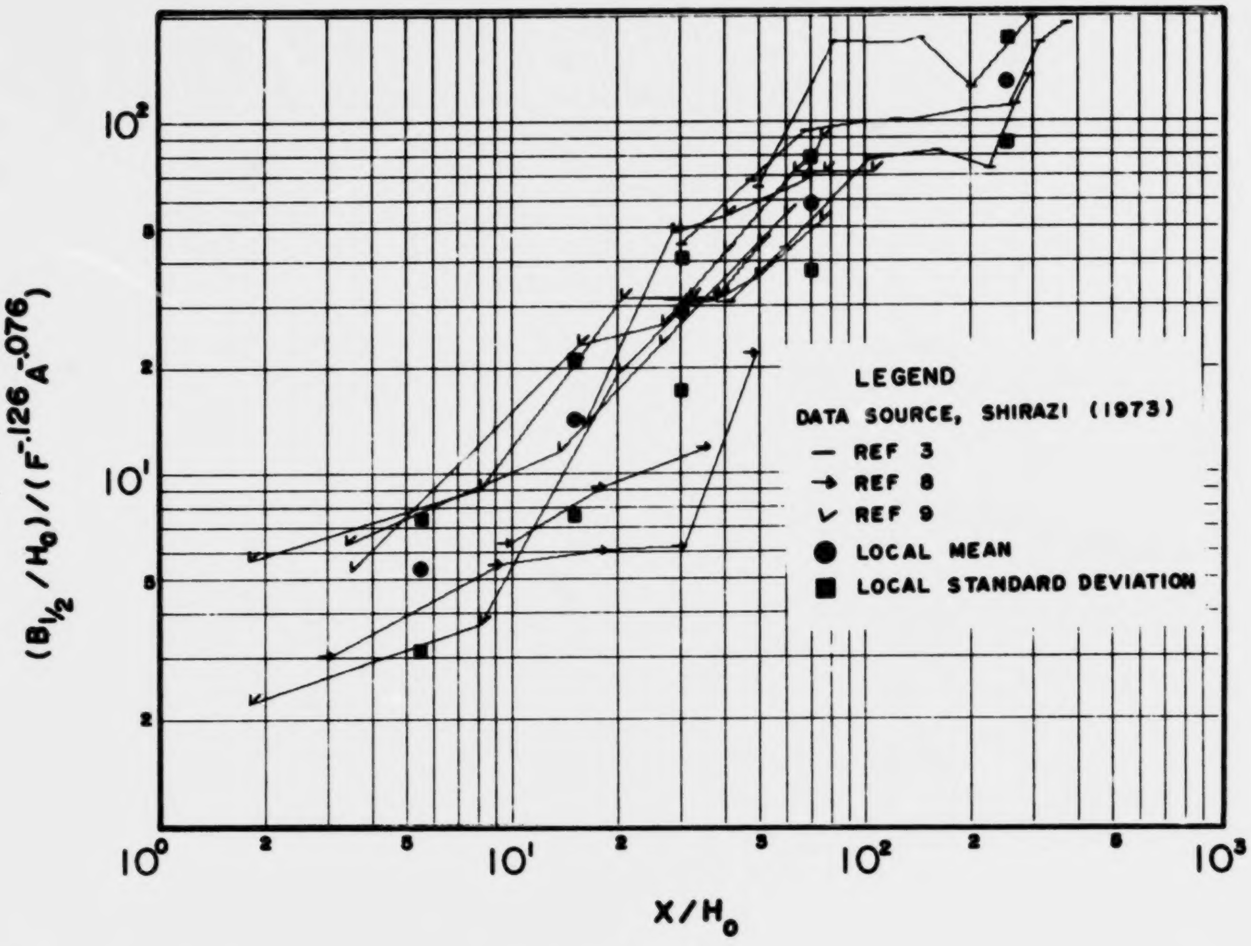

Figure F7 Correlation of Selected Field and Laboratory Surface Plume Width Data for Typical Jet Froude Number and Aspect Ratio at Zero or Negligibly Small Ambient Current.

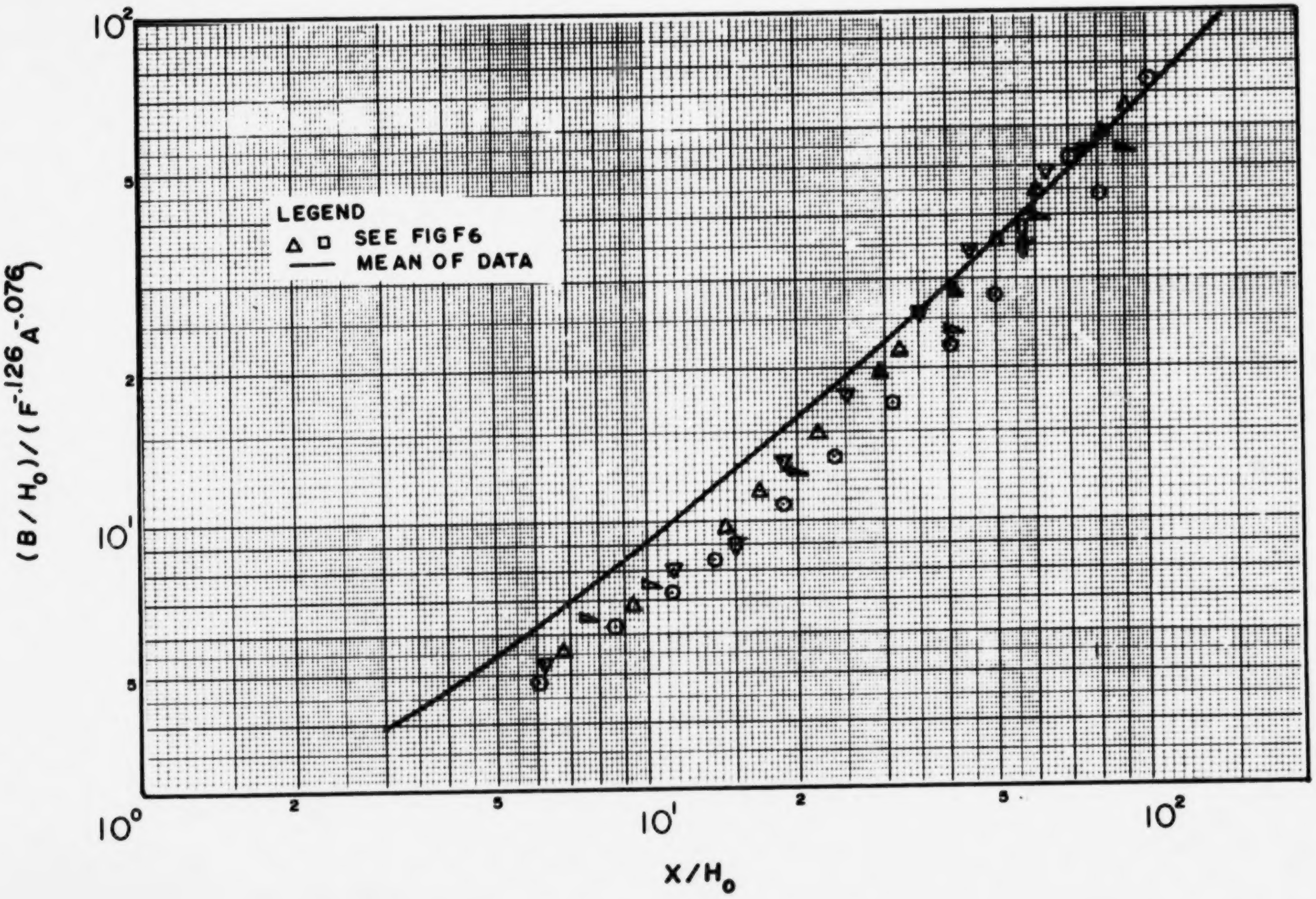

Figure F8 Comparison of Calculated Widths with Mean Measured Surface Plume Width Data of Fig. F7.

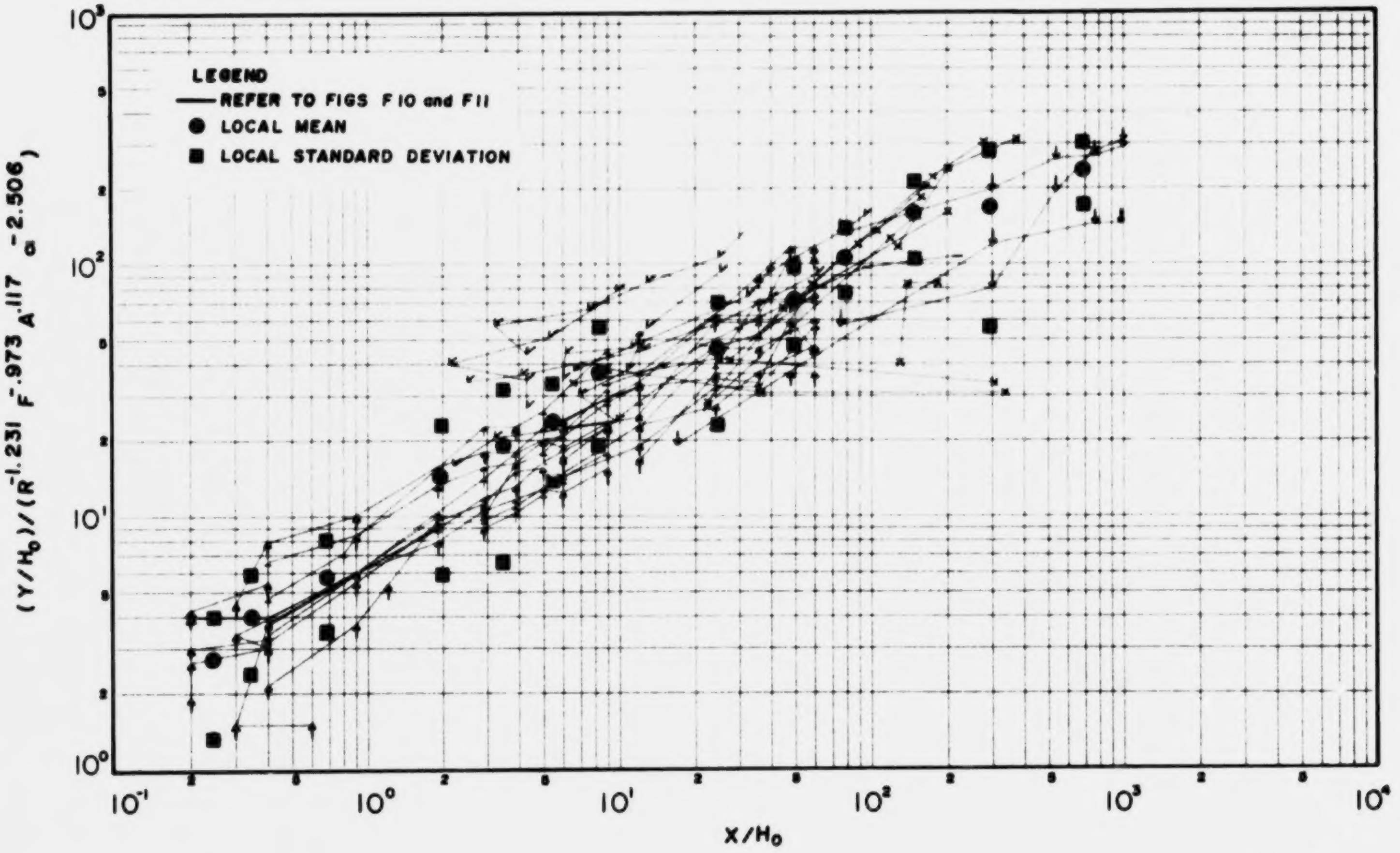

Figure F9 Correlation of Selected Field and Laboratory Surface Plume Trajectory Data for Typical Jet Froude Number, Aspect Ratio and Ambient Cross Current.

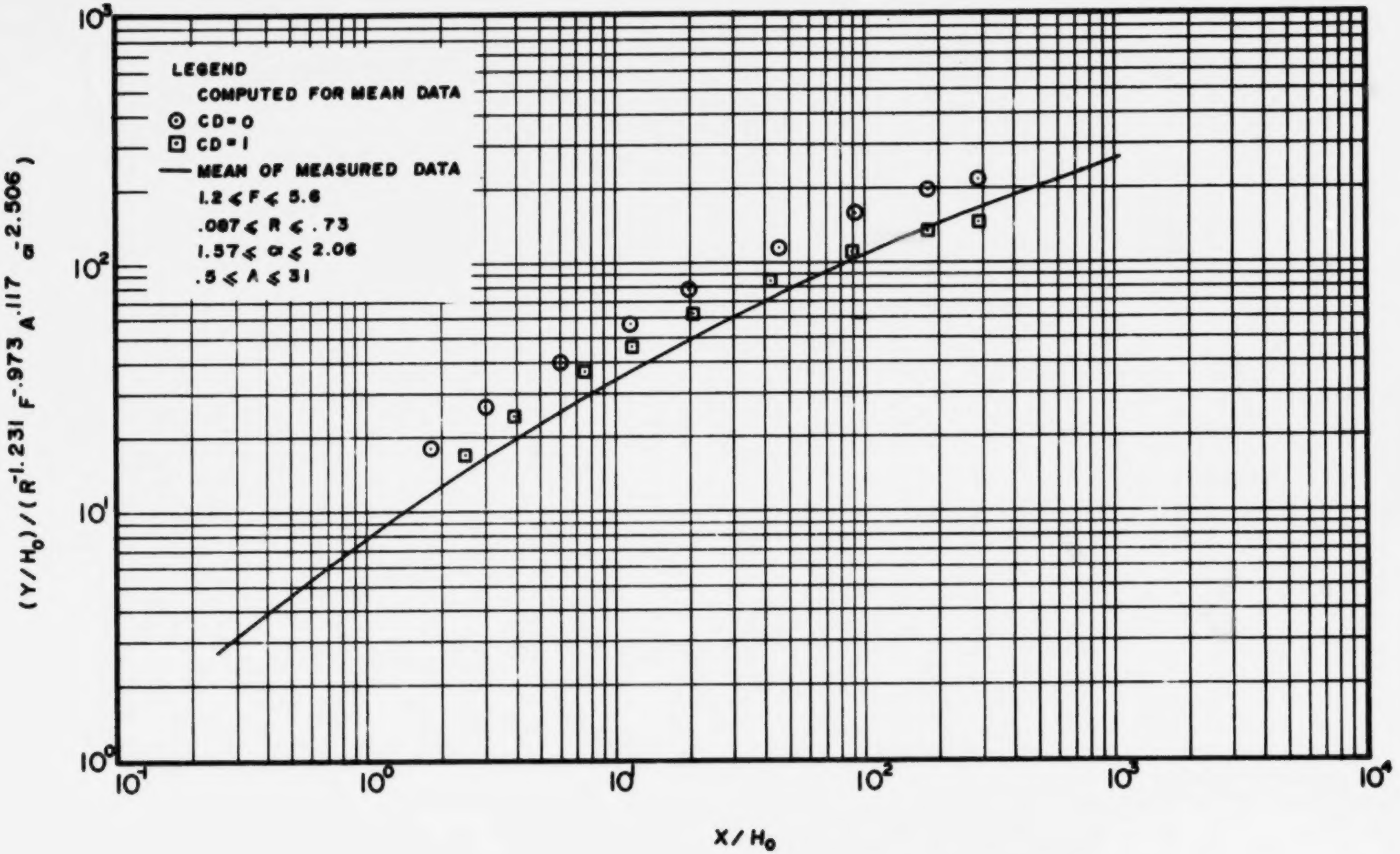

Figure F10 Comparison of Calculation with Mean Measured Surface Plume Trajectory Data of Fig. F9.

which replaces Prych's assumptions,

$$X(o) = S_1 \cos \frac{\theta_o + \theta(o)}{2}$$

$$Y(o) = S_1 \sin \frac{\theta_o + \theta(o)}{2}$$

Figure F10 shows that further improvement can be obtained by setting $C_d = 1.0$.

In order to complete the adjustment of the PDS model to fit the data, we need to check the model against measured plume width and temperature for a wide range of parameters. If agreement is obtained with such data without the need to readjust the previously specified coefficients E_o, E_h, E_v, C_F and C_D, then the fitting of PDS with data is considered complete.

The raw data and calculated values based on the previously determine coefficients are compared in Fig. F11 for plume width and Fig. F12 for plume temperature. The agreement obtained from the comparison of calculated and measured plume width is excellent and the agreement for plume temperature is reasonably good.

D. CONCLUSIONS

The PDS model is best fitted to a wide range of field and laboratory experimental data if we set $E_o = .05$, $E_h = .02$, $E_v/E_h = 0.2$, $C_D = 1.0$ and $C_F = 0$. It is felt that PDS can be used to predict typical situations for surface discharge consistent with the major assumptions made in the model. Calculations based on extreme, but perhaps possible, values of these coefficients are also presented in the supplementary nomograms of Appendix D.

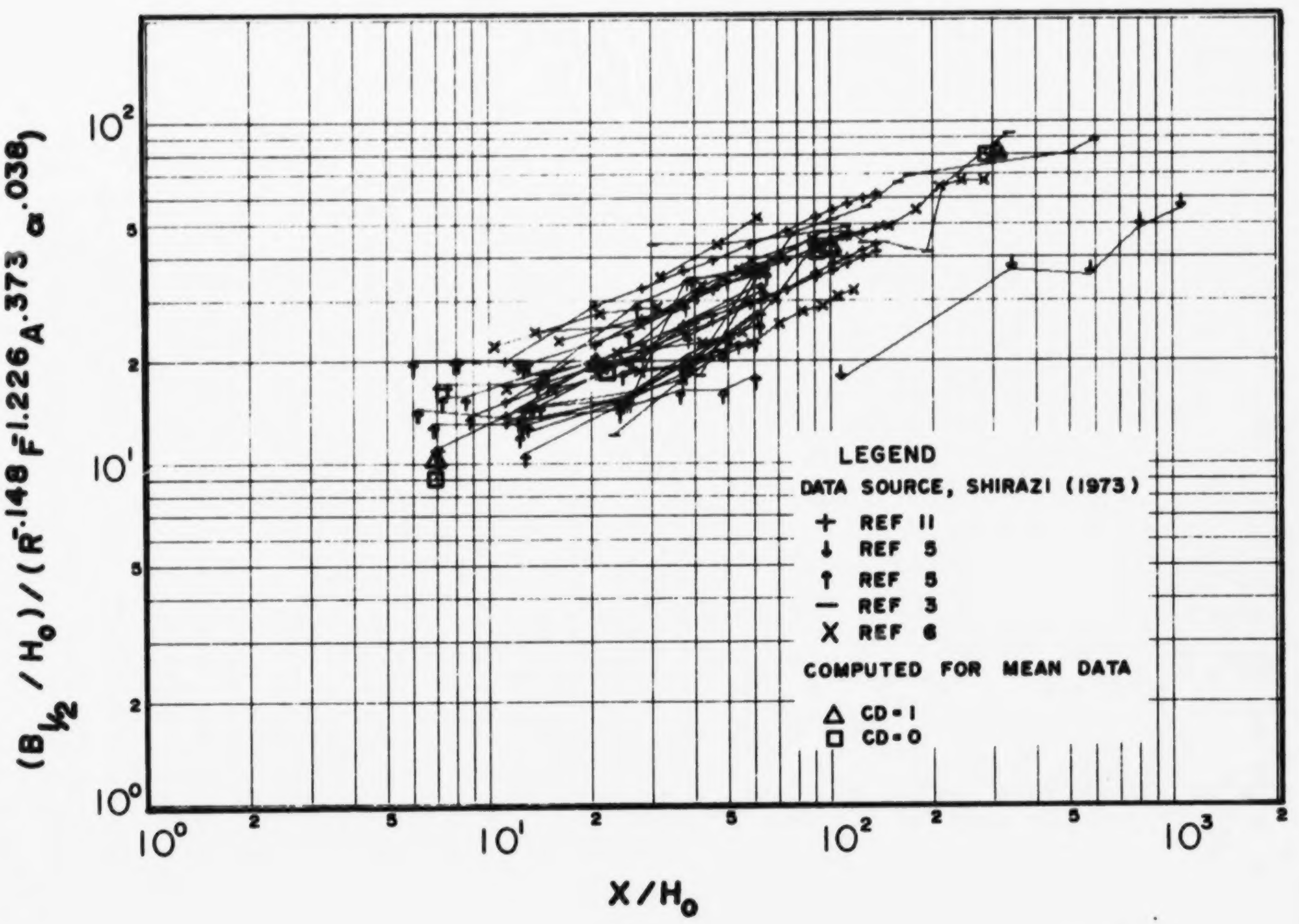

Figure F11 Comparison of Calculated Widths with Selected Field and Laboratory Surface Plume Width Data Correlated for Typical Jet Froude Number, Aspect Ratio and Ambient Cross Current.

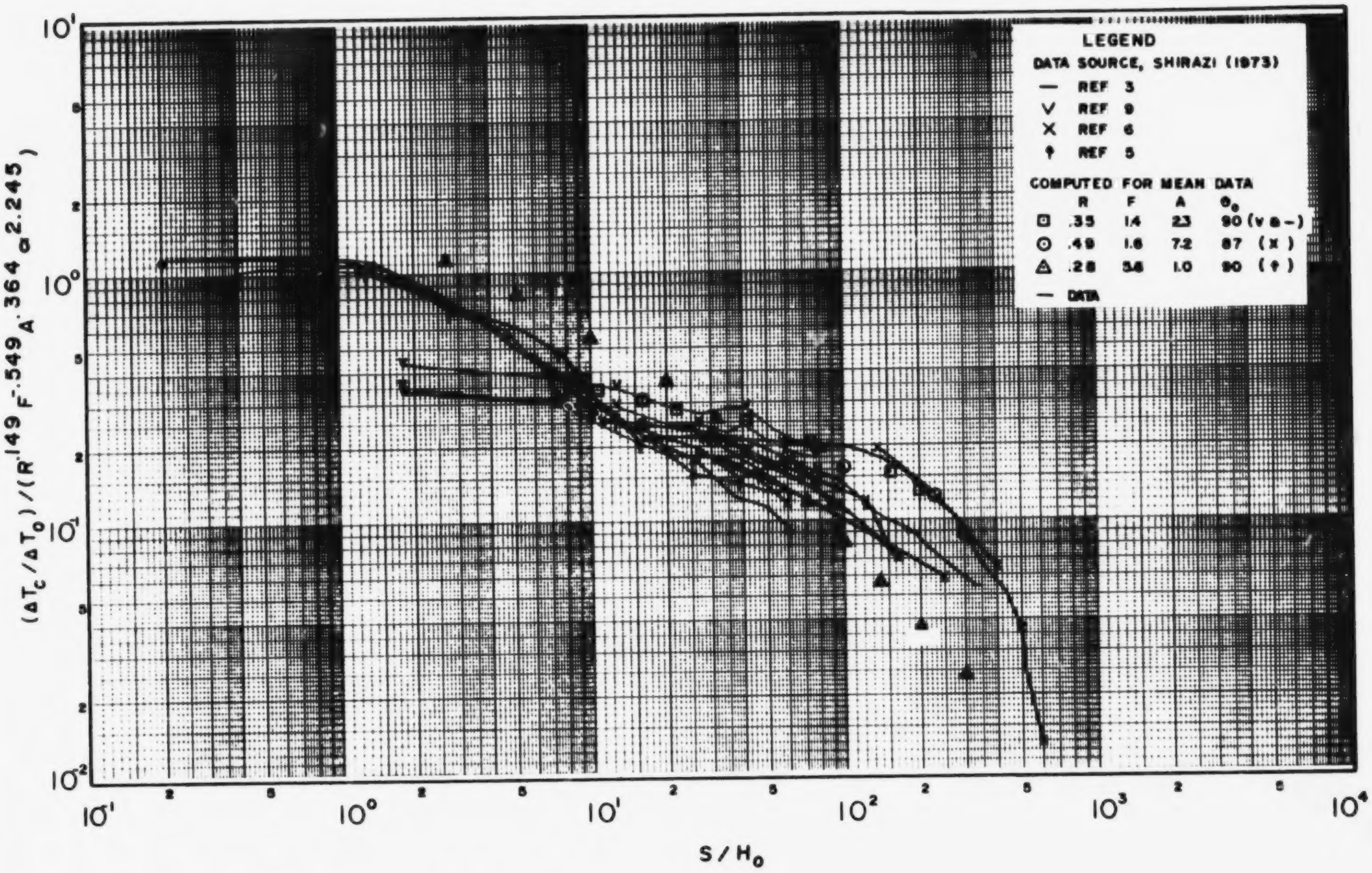

Figure F12 Comparison of Calculated Temperatures with Selected Field and Laboratory Surface Plume Temperature Data, Correlated for Typical Jet Froude Number, Aspect Ratio and Ambient Cross Current.

III. THEORETICAL ANALYSIS

The theoretical analysis used to develop the three-dimensional surface plume program (PDS) is based on Prych's model which has been non-dimensionalized and modified according to previous sections. The analysis is given here in an abbreviated form for completeness. The terms have all been non-dimensionalized as mentioned above and primes have been omitted for convenience.

The method of analysis is an integral approach which assumes similarity of temperature and velocity profiles and the principle of entrainment. The profiles assumed are Gaussian such that

$$T_r = T \exp(-n^2/B^2) \cdot \exp(-Z^2/H^2) \qquad (1)$$

$$U_r = U \exp(-n^2/B^2) \cdot \exp(-Z^2/H^2) + V \cos \Theta \qquad (2)$$

Where n and Z are distances perpendicular to the plume centerline in the lateral and vertical directions, respectively. T and U are the centerline temperature and velocity, respectively. See Figure F13.

With the temperature and velocity profile assumed, the energy, volume, and momentum fluxes can be integrated across the plume at any cross section leaving them in terms of centerline values and plume characteristic width, B, and depth, H. Accordingly, the volume flux

$$Q = \iint_A (U_r + V \cos \Theta)\, dndZ = \pi BH(\frac{U}{2} + V \cos \Theta) \qquad (3)$$

where the limits of integration for V cos Θ are taken as the bottom half of the region.

$$(\frac{n}{\sqrt{2}\ B})^2 + (\frac{Z}{\sqrt{2}\ H})^2 \leq 1 \qquad (4)$$

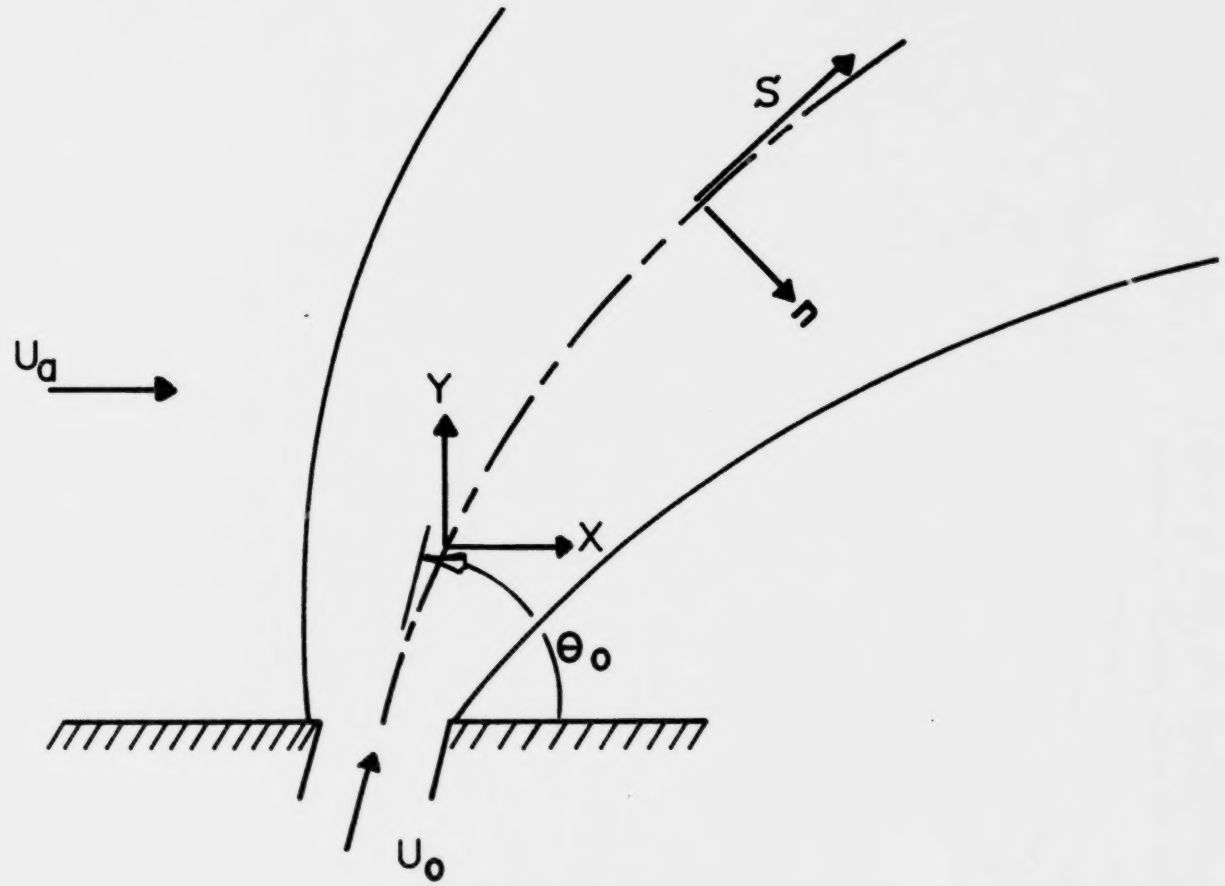
S
n
U_a
Y
X
Θ_o
U_o

Figure F13 Schematics of a Surface Plume Showing the Coordinate System.

solving (3) for U, yields

$$U = 2\left(\frac{Q}{\pi BH} - V\cos\Theta\right) \qquad (5)$$

The heat flux, J, is

$$J = \iint_A U_r T_r \, dndZ = \frac{\pi}{2} TBH \left(\frac{U}{2} + \cos\Theta\right) = \frac{QT}{2} \qquad (6)$$

The momentum flux, M, is

$$M = \iint_A U_r^{\,2} \, dndZ = \pi BH \left(\frac{U}{2} + V\cos\Theta\right)^2 \qquad (7)$$

$$M = \frac{Q^2}{\pi BH} \qquad (8)$$

The quantities dQ/ds, dT/ds, and dM/ds are calculated from the conservation equations. dQ/ds is assumed to be due to contributions of jet entrainment and ambient turbulent mixing, thus

$$\frac{dQ}{ds} = \frac{dQ}{ds}\Big|_j + \frac{dQ}{ds}\Big|_a \qquad (9)$$

The jet and ambient contributions are both divided into vertical and horizontal components. The horizontal jet entrained fluid is

$$\frac{dQ}{ds}\Big|_{j,h} = 2E_o \int_{-\sqrt{2}H}^{0} \Delta U dZ \qquad (10)$$

where

$$\Delta U = (U^2 + V^2 \sin^2 \Theta)^{1/2} \ \exp(-Z^2/H^2) \tag{11}$$

and E_o is an entrainment coefficient. By inserting (11) into (10), we obtain

$$\frac{dQ}{ds}\Big|_{j,h} = \sqrt{\pi}\, HE_o(U^2 + V^2 \sin^2 \Theta)^{1/2} \tag{12}$$

The vertical jet entrained fluid is

$$\frac{dQ}{ds}\Big|_{j,v} = 2 \int_o^{\sqrt{2}\,B} E \, \Delta U_v \, dZ \tag{13}$$

where

$$E = E_o \, f(R_i) \tag{14}$$

R_i is the local Richardson number given by

$$R_i = \frac{\sqrt{2}}{F_o^{\,2}} \ \frac{HT(s,n,o)}{\Delta U_v^2}$$

The function f (R_i) is a curve fit to the experimental data of Ellison and Turner which gives

$$f = [\exp(-5R_i) - .0183]/.982 \tag{15}$$

The velocity difference ΔU_v is given by

$$\Delta U_v = [U^2 \exp(-2n^2/B^2) + V^2 \sin^2 \Theta]^{1/2}$$

The term T is the surface excess temperature at the distance n from the plume centerline. The value of the integral (13) is determined numerically in the program.

The effective entrainment due to ambient turbulent mixing is due to an analysis used by Prych[1] which is

$$\frac{dQ}{ds}\Big|_{a,h} = 11.0\,\frac{H}{B}\,\frac{\varepsilon_h}{U_o H_o} \qquad (16)$$

$$\frac{dQ}{ds}\Big|_{a,v} = 11.0\,\frac{B}{H}\,\frac{\varepsilon_v}{U_o H_o}\,f(R_i') \qquad (17)$$

where

$$R_i' = \sqrt{2}\,HT/[F_o^2(U + V\cos\Theta)^2]$$

and ε_n and ε_v are the horizontal and vertical turbulent diffusion coefficients, respectively.

The change in heat flux along the plume due to heat exchange with the atmosphere is expressed as

$$\frac{dJ}{ds} = -2\int_o^{\sqrt{2}\,B} K\ T_r dn = \sqrt{\pi}\,KTB \qquad (18)$$

Where K is the dimensionless heat exchange coefficient.

Substituting (18) into (11) yields

$$\frac{dT}{ds} = \frac{-T}{Q}\left(2\sqrt{\pi}\,KB + \frac{dQ}{ds}\right) \qquad (19)$$

The conservation of momentum is applied in the s-direction and then divided into X and Y components. The net forces on the plume are balanced by the change in momentum flux. The forces considered important are (a) internal pressure forces due to buoyancy, (b) form drag due to ambient current and (c) interfacial shear forces.

The pressure forces are found by determining the excess pressure due to buoyancy as a function of depth and then integrating the pressure over the vertical cross section of the plume. Thus, the normalized pressure force is

$$P = \frac{1}{F_o^2} \iint_A \{ \int_{-\infty}^{Z} T_r dZ \} dA = \sqrt{\pi}\, TH^2 B/2F_o^2 \qquad (20)$$

The form drag acting normal to the plume centerline is assumed similar to the drag on a solid body such that

$$F_D = \frac{1}{2} C_D \sqrt{2}\, HV\, |V| \sin^2 \Theta \qquad (21)$$

where C_D is a drag coefficient

The interfacial shear forces are assumed to be similar to turbulent flow over a flat surface with a boundary layer thickness of $\sqrt{2}$ H and a velocity equal to the vector velocity difference between the plume and ambient current. Accordingly, the X and Y components of this shear force reduce to

$$SF_X = C_F\left(\frac{1}{R_e H}\right)^{1/4} \int_0^{\sqrt{2}B} \Delta U_v^{3/4} [V \sin^2 \Theta - U \cos \Theta \exp(-n^2/B^2)] dn \qquad (22)$$

$$SF_Y = -C_F\left(\frac{1}{R_e H}\right)^{1/4} \int_0^{\sqrt{2}B} \Delta U_v^{3/4} [V \cos \Theta + U \exp(-n^2/B^2)] dn \qquad (23)$$

where C_F is a friction coefficient and R_e is the jet discharge Reynolds number. The value of C_F includes constants carried throughout Prych's program.

The change in momentum flux includes the effects of the momentum of the entrained ambient fluid, $V \frac{dQ}{ds}$, which acts in the X-direction. Equating the forces to the change in momentum flux in the X and Y directions yields

$$\frac{d}{ds}\,(M+P)\cos\Theta = SF_X + F_D\sin\Theta + V\,\frac{dQ}{ds} \qquad (24)$$

$$\frac{d}{ds}\,(M+P)\sin\Theta = SF_Y - F_D\cos\Theta \qquad (25)$$

Using equations (8) and (20) for M and P, multiplying (24) by - sin Θ, (25) by cos Θ and combining yields an expression for the change in flow direction

$$\frac{dQ}{ds} = \frac{SF_Y\cos\Theta - SF_X\sin\Theta - F_D - V\sin\Theta\,(dQ/ds)}{\frac{Q^2}{\pi BH} + \frac{\sqrt{\pi}}{2F_o^2}\,TH^2B} \qquad (26)$$

Differentiating M and P, multiplying (24) by cos Θ and (25) by sin Θ and combining yields

$$\begin{aligned}\frac{dH}{ds} = {} & [SF_y\sin\Theta + SF_X\cos\Theta + (V\cos\Theta - 2Q/\pi BH)(dQ/ds)\\ & -(\sqrt{\pi}\,BH^2/2F_o^2)(dT/ds) + (Q^2/\pi B^2H - \sqrt{\pi}H^2T/2F_o^2)(dB/ds)]\\ & [\sqrt{\pi}THB/2F_o^2 - Q^2/\pi BH^2]^{-1} \qquad (27)\end{aligned}$$

It is noted that this expression for change in depth is undefined when the denominator is zero. Hence, results beyond this singularity are questionable.

Momentum in the lateral direction is included only indirectly through lateral spreading. It is assumed that the contributions to spreading by nonbuoyant horizontal jet mixing and buoyancy are independent of one another such that

$$\frac{dB}{ds} = \left(\frac{dB}{ds}\right)_{nb} + \left(\frac{dB}{ds}\right)_b$$

where the subscripts b and nb denote buoyant and nonbuoyant terms.

The nonbuoyant spreading is found by writing equation (27) without the buoyancy terms (any term containing F_o) and assuming that

$$\left(\frac{dB/ds}{dH/ds}\right)_{nb} = (B/H)(dQ/ds)_h/(dQ/ds)_v$$

where $(dQ/ds)_h$ and $(dQ/ds)_v$ are the horizontal and vertical entrainment rates. This yields

$$\left(\frac{dB}{ds}\right)_{nb} = \frac{SF_Y \sin \Theta + SF_X \cos \Theta + \left(V \cos \Theta - \frac{2Q}{\pi BH}\right) \frac{dQ}{ds}}{-(Q^2/\pi BH)[(dQ/ds)_v/(dQ/ds)_h + 1]} \qquad (28)$$

This equation differs from one given by Prych in that all terms containing the local densimetric Froude number are deleted.

As discussed earlier in this appendix, the spreading due to buoyancy is assumed to be a function of the local excess density ratio, plume depth and aspect ratio such that

$$\left(\frac{dB}{ds}\right)_b = \frac{XK1}{\left(\frac{B}{H} F^2 - 1\right)^{1/2}} \qquad (29)$$

where XK1 is a constant and F is the local Froude number. It is noted that this also has a singularity. But due to the fact that B/H is usually large, the singularity is not encountered.

The preceeding equations are sufficient to perform a step-wise integration along the plume. From the local conditions of the plume, dQ/ds is calculated. When this is known dT/ds, dΘ/ds and dB/ds are calculated. With these known, dH/ds can be calculated. These derivatives are integrated step--wise along the plume trajectory to give local values of X, Y, T, H, B, Θ, and Q.

In order to start the integration within the developed zone where the above analysis is valid, starting conditions must be calculated. These are determined by a simplified analysis of the development zone.

As was mentioned earlier in this appendix, the length of the development zone is assumed to be

$$S_i = 5.4 \left(\frac{A^2}{F_o} \right)^{1/3} \qquad (30)$$

The values of B and H at the end of the development zone are calculated from a method that superimposes entrained fluid, and fully developed temperature and velocity profiles at the end of development onto an analysis which ignores entrainment. For the no-entrainment case, the plume remains rectangular with $2bhU_o = Q_o$ such that $b_i h_i = B_o H_o$. However, it is assumed that b spreads due to buoyancy such that

$$\frac{db}{ds} = [g'h/(U_o^2 - g'h)]^{1/2} \qquad (31)$$

Since bh is assumed constant (31) can be integrated from S = 0 to $S = S_i$ to give

$$b_i = \frac{B_o}{F_o^2} \{ [\frac{3}{2} \ \frac{S_i}{B_o} F_o^2 + (F_o^2 - 1)^{3/2}]^{2/3} + 1 \} \qquad (32)$$

Thus

$$h_i = H_o B_o / b_i \qquad (33)$$

It is now assumed that the actual plume including entrainment has an aspect ratio equal to b_i/h_i such that

$$\frac{B_i}{H_i} = \frac{b_i}{h_i} \qquad (34)$$

The actual flow rate at the end of the development zone is calculated assuming fully developed profiles and ignoring surface heat losses such that J is constant. Using equation (6) yields

$$Q_1 = \frac{2Q_o}{T} \tag{35}$$

Where T is the excess temperature at the end of development and Q_o is the discharge flow rate.

The X and Y component to the momentum equations are written as in the previous section over the length of the development zone.

$$(M_o + P_o) \cos \Theta_o + V\, Q_o \left(\frac{2}{T} - 1\right) + F_{D1} \sin \Theta_o + SF_{1x} = (M_1 + P_1) \cos \Theta_1 \tag{36}$$

$$(M_o + P_o) \sin \Theta_o + F_{Di} \cos \Theta_o + SF_{1Y} = (M_1 + P_1) \sin \Theta_1 \tag{37}$$

Where the drag and shear forces are approximated by

$$F_{Di} = \frac{C_D}{2} S_i \left(\frac{1 + h_1}{2}\right) V\, |V| \sin^2 \Theta_o \tag{38}$$

$$SF_{1x} = C_F S_1\, (B_o + b_1)\, |\bar{V} - \bar{U}_o| \left(\frac{2}{R_e(1 + h_1)|\bar{V} - \bar{U}_o|}\right)^{1/4} (V - \cos \Theta_o) \tag{39}$$

$$SF_{1Y} = SF_{1X} \frac{\sin \Theta_o}{V - \cos \Theta_o} \tag{40}$$

and $\bar{U}_o$ is a unit vector in the direction of Θ_o and $\bar{V}$ is the vector velocity of the ambient current.

Multiplying (36) by $\sin \Theta_1$ and (37) by $\cos \Theta_1$ and subtracting yields

$$\Theta = \text{arc tan } \{[(M_o + P_o) \sin \Theta_o - F_{D1} \cos \Theta_o + SF_{1y}]/[(M_o + P_o) \cos \Theta_o + Q_o V(2/T - 1) + F_{D1} \sin \Theta_o + SF_{1x}]\} \tag{41}$$

Multiplying (36) by cos Θ_1 and (37) by sin Θ_1 and combining yields

$$(M_o + P_o) \cos (\Theta_1 - \Theta_o) + VQ_o \cos \Theta_1 \left(\frac{2}{T} - 1\right) + (SF_{1X} + F_{D1} \cos \Theta_o) \cos \Theta_1$$

$$+ (SF_{1Y} - F_{D1} \sin \Theta_o) \sin \Theta_1 = M_1 + P_1 \qquad (42)$$

Using equations (8), (20), (32) and $2B_o/H_o = A$, equation (42) after some manipulation becomes

$$\mathrm{LHS} = \frac{8.0\ A}{T^2 \pi} \left(\frac{b_1}{B_1}\right)^2 + \frac{\sqrt{\pi}}{8} \left(\frac{B_1}{b_1}\right)^3 \frac{TA^2}{F_o^2 b_1} \qquad (43)$$

Where LHS is the left hand side of (42). This equation is solved numerically in the program for B_1. Equation (33) is used to find H_1. The value of T at the end of the development zone is retained as a variable depending on the expression for S_1. Equation 30 is used for development length when $T = 1.0$.

IV. COMPUTER PROGRAM

The computer program used to generate the nomograms for this workbook is presented in this section. The program is written in FORTRAN 4 and consists of a main program entitled PDS and five subroutines KHPCG, AREA, FCT, RED, and OUTP.

The main program PDS reads the input variables, initializes constants, and calls subroutine KHPCG which performs the actual calculation. Subroutine KHPCG is a standard IBM scientific subroutine which performs the stepwise integration of differential equations by the Hamming Predictor-Corrector Method. It has been modified slightly for compatability of common statements. This method was found to be faster than the fourth order Range-Kutta solution used by Prych.

Subroutine AREA is a step-wise integration of the area enclosed by surface isotherms. Subroutine FCT calculates the derivatives of the program variables which are used in KHPCG. Subroutine RED calculates the reduction in the vertical entrainment coefficient as a function of local Richardson's number.

Subroutine OUTP prints out the input parameters followed by desired dimensionless variables at each integration step along the trajectory of the plume. The variables printed out are S', X', Y', TH, T', U', t', Q/Q_0, HT, H', B', F, RI, and IHLF. See the list of symbols in this appendix for definition of these terms.

Input to the PDS program consists of one card giving the number of cases to be calculated followed by a set of three cards for each case. The variables on each card and the required format are as follows:

Card 1

Format (I3)

Number of cases to be calculated

Card 2

Format (20A4)

Any information the user wishes to have printed out relating to this case. This information is printed out at the top of each output page.

Card 3

Format (7F10.5)

F_o = Discharge densimetric Froude number
A = Aspect ratio
V' = Ambient current, V/U_o
RE = Reynolds number (only used when $CF \neq 0$)
Θ_o = Discharge angle (degrees) $\Theta_o = 0$ is in the direction of the ambient current
CD = Drag coefficient (1.0 is suggested)
CF = Interfacial shear (friction) coefficient (0.0 is suggested)

Card 4

Format (7F10.5)

E_o = Entrainment coefficient (0.05 suggested)
K = Surface heat exchange coefficient $K_E/\rho C_p U_o$
SLIM = Value of S' at which integration is to stop
DS = Largest integration step to be used ($DS = 5\sqrt{A}$ is reasonable)

EV = The ratio of vertical to horizontal ambient turbulence diffusion coefficients(0.2 is suggested).

EH = Dimensionless horizontal ambient turbulent diffusion coefficient (0.02 is suggested)

XK1 = Spreading coefficient (1.4 is suggested)

Cards 2-4 are repeated for each case to be run.

Following are (a) listings of sample input, (b) sample output and (c) complete program listing.

SAMPLE INPUT DATA

```
 1
SAMPLE RUN OF PDS PROGRAM
4.          5.         .1                      90.        1.
.05         .00001     500.       5.           .2         .02        1.4
```

OUTPUT

```
FLOATING WARM WATER JETS --  SAMPLE RUN OF PDS PROGRAM

FRO =   4.0     2B0/HO =  5.0     V/UO =    .100     ANGLE = 90.0     SURFACE H = 1.000E-05

E =  .0500   CD = 1.0000   CF =      0   RE =      0E 00   EV = 2.000E-01   EH = 2.000E-02

      S         X         Y       TH       T       U      TIME     Q        HT       H       B        F        RI     IHLF

     9.6       1.0       9.5     84.1   1.000    .951   9.8E 00  2.000    1.000     .88     7.4    2.751     .086     0
     9.9       1.0       9.8     83.8    .980    .928   1.0E 01  2.041    1.000     .91     7.5    2.675     .091     4
    10.2       1.1      10.1     83.6    .962    .906   1.0E 01  2.080    1.000     .94     7.6    2.606     .096     4
    10.5       1.1      10.5     83.3    .944    .886   1.1E 01  2.118    1.000     .96     7.7    2.542     .101     4
    10.8       1.1      10.8     83.1    .928    .867   1.1E 01  2.155    1.000     .98     7.8    2.483     .106     4
    11.1       1.2      11.1     82.9    .913    .849   1.1E 01  2.190    1.000    1.00     7.9    2.429     .111     4
    11.4       1.2      11.4     82.7    .899    .832   1.2E 01  2.225    1.000    1.03     8.1    2.379     .116     4
    12.1       1.3      12.0     82.3    .873    .801   1.3E 01  2.291    1.000    1.06     8.3    2.289     .126     3
    12.7       1.4      12.6     81.9    .849    .773   1.3E 01  2.354    1.000    1.10     8.5    2.210     .136     3
    13.3       1.5      13.2     81.5    .829    .748   1.4E 01  2.414    1.000    1.13     8.8    2.141     .145     3
    13.9       1.6      13.9     81.1    .809    .725   1.5E 01  2.472    1.000    1.16     9.0    2.080     .155     3
    15.2       1.8      15.1     80.4    .775    .684   1.7E 01  2.579    1.000    1.21     9.5    1.976     .173     2
    16.4       2.0      16.3     79.8    .746    .649   1.9E 01  2.679    1.000    1.24    10.0    1.892     .190     2
    17.7       2.2      17.6     79.2    .721    .619   2.0E 01  2.772    1.000    1.28    10.5    1.822     .207     2
    18.9       2.4      18.8     78.6    .699    .592   2.2E 01  2.859    1.000    1.30    11.0    1.762     .224     2
    21.4       3.0      21.2     77.5    .662    .547   2.7E 01  3.019    1.000    1.34    12.1    1.667     .254     1
    23.9       3.5      23.7     76.5    .632    .511   3.1E 01  3.163    1.000    1.37    13.2    1.595     .283     1
    26.4       4.1      26.1     75.5    .607    .481   3.6E 01  3.295    1.000    1.39    14.2    1.539     .310     1
    28.9       4.8      28.5     74.6    .585    .455   4.1E 01  3.416    1.000    1.40    15.3    1.493     .335     1
    31.4       5.5      30.9     73.8    .567    .433   4.6E 01  3.529    1.000    1.41    16.3    1.456     .359     1
    33.9       6.2      33.3     73.0    .550    .413   5.2E 01  3.634    1.000    1.41    17.4    1.425     .381     1
    38.9       7.7      38.1     71.6    .522    .381   6.4E 01  3.826    1.000    1.41    19.4    1.376     .424     0
    43.9       9.3      42.8     70.2    .500    .355   7.6E 01  3.998     .999    1.41    21.4    1.341     .461     0
    48.9      11.1      47.5     69.0    .481    .334   8.9E 01  4.154     .999    1.40    23.3    1.316     .496     0
    53.9      12.9      52.1     67.8    .465    .315   1.0E 02  4.298     .999    1.39    25.2    1.295     .529     0
    58.9      14.8      56.7     66.7    .451    .300   1.2E 02  4.431     .999    1.38    27.0    1.279     .559     0
    63.9      16.9      61.3     65.7    .438    .286   1.3E 02  4.555     .999    1.37    28.8    1.267     .587     0
    68.9      19.0      65.9     64.8    .427    .274   1.5E 02  4.672     .998    1.36    30.5    1.257     .615     0
    73.9      21.1      70.4     63.8    .417    .264   1.6E 02  4.783     .998    1.34    32.2    1.250     .640     0
    78.9      23.4      74.8     63.0    .408    .254   1.8E 02  4.887     .998    1.33    33.8    1.244     .664     0
    83.9      25.7      79.3     62.1    .400    .245   2.0E 02  4.987     .998    1.32    35.4    1.239     .689     0
    88.9      28.0      83.7     61.3    .392    .237   2.1E 02  5.083     .997    1.31    37.0    1.236     .711     0
    93.9      30.5      88.0     60.6    .385    .230   2.3E 02  5.174     .997    1.30    38.5    1.234     .733     0
    98.9      32.9      92.4     59.8    .379    .223   2.5E 02  5.263     .997    1.29    40.0    1.231     .756     0
   103.9      35.5      96.7     59.1    .373    .217   2.7E 02  5.348     .997    1.28    41.5    1.230     .777     0
   108.9      38.1     101.0     58.4    .367    .211   2.9E 02  5.430     .996    1.28    42.9    1.229     .798     0
   113.9      40.7     105.2     57.8    .362    .206   3.1E 02  5.510     .996    1.27    44.3    1.228     .819     0
   118.9      43.4     109.4     57.1    .356    .200   3.3E 02  5.588     .996    1.26    45.7    1.228     .841     0
   123.9      46.1     113.6     56.5    .351    .196   3.5E 02  5.664     .995    1.25    47.0    1.227     .862     0
   128.9      48.9     117.8     55.9    .347    .191   3.7E 02  5.738     .995    1.25    48.4    1.227     .882     0
   133.9      51.8     121.9     55.3    .342    .187   3.9E 02  5.809     .995    1.24    49.7    1.228     .903     0
   138.9      54.6     126.0     54.7    .338    .182   4.1E 02  5.879     .995    1.23    51.0    1.228     .923     0
   143.9      57.5     130.1     54.2    .334    .179   4.3E 02  5.948     .994    1.23    52.2    1.229     .942     0
   148.9      60.5     134.1     53.6    .331    .175   4.5E 02  6.014     .994    1.22    53.5    1.230     .962     0
   153.9      63.5     138.1     53.1    .327    .171   4.7E 02  6.079     .994    1.21    54.7    1.231     .981     0
```

```
FLOATING WARM WATER JETS --  SAMPLE RUN OF PDS PROGRAM

FR0 =   4.0      2R0/H0 =  5.0     V/U0 =    .100     ANGLE = 90.0     SURFACE H = 1.000E-05

E =  .0500   CD = 1.0000   CF =       0   WE =      0E 00   EV = 2.000E-01   EH = 2.000E-02

    S          X          Y        TH        T        U      TIME     Q          HT        H          B         F          RI        IHLF


  158.9      66.5      142.1     52.6      .323     .168   4.9E 02  6.143      .993     1.21       55.9     1.233     1.000        0
  163.9      69.5      146.1     52.1      .320     .165   5.1E 02  6.206      .993     1.20       57.1     1.235     1.019        0
  168.9      72.6      150.0     51.6      .317     .162   5.4E 02  6.267      .993     1.20       58.3     1.236     1.037        0
  173.9      75.7      153.9     51.2      .314     .159   5.6E 02  6.327      .992     1.19       59.4     1.238     1.056        0
  178.9      78.9      157.8     50.7      .311     .156   5.8E 02  6.386      .992     1.19       60.5     1.240     1.074        0
  183.9      82.1      161.6     50.2      .308     .153   6.1E 02  6.443      .992     1.18       61.7     1.242     1.092        0
  188.9      85.3      165.5     49.8      .305     .151   6.3E 02  6.500      .991     1.18       62.8     1.244     1.109        0
  193.9      88.5      169.3     49.4      .302     .148   6.5E 02  6.556      .991     1.17       63.9     1.246     1.127        0
  198.9      91.8      173.0     48.9      .300     .146   6.8E 02  6.611      .991     1.17       64.9     1.249     1.145        0
  203.9      95.1      176.8     48.5      .297     .144   7.0E 02  6.665      .990     1.16       66.0     1.251     1.162        0
  208.9      98.4      180.5     48.1      .295     .142   7.2E 02  6.718      .990     1.16       67.1     1.253     1.180        0
  213.9     101.8      184.3     47.7      .292     .140   7.5E 02  6.770      .990     1.16       68.1     1.256     1.197        0
  218.9     105.1      187.9     47.3      .290     .137   7.7E 02  6.822      .989     1.15       69.1     1.258     1.214        0
  223.9     108.5      191.6     47.0      .288     .135   8.0E 02  6.873      .989     1.15       70.1     1.260     1.231        0
  228.9     112.0      195.3     46.6      .286     .134   8.2E 02  6.923      .989     1.14       71.1     1.263     1.248        0
  233.9     115.4      198.9     46.2      .283     .132   8.4E 02  6.973      .988     1.14       72.1     1.265     1.265        0
  238.9     118.9      202.5     45.9      .281     .130   8.7E 02  7.022      .988     1.14       73.1     1.268     1.282        0
  243.9     122.4      206.1     45.5      .279     .128   9.0E 02  7.070      .987     1.13       74.1     1.270     1.299        0
  248.9     125.9      209.6     45.2      .277     .127   9.2E 02  7.118      .987     1.13       75.0     1.273     1.315        0
  253.9     129.4      213.1     44.9      .275     .125   9.5E 02  7.165      .987     1.13       76.0     1.275     1.332        0
  258.9     133.0      216.7     44.5      .274     .123   9.7E 02  7.212      .986     1.12       76.9     1.278     1.349        0
  263.9     136.5      220.2     44.2      .272     .122   1.0E 03  7.258      .986     1.12       77.9     1.280     1.366        0
  268.9     140.1      223.6     43.9      .270     .120   1.0E 03  7.304      .986     1.12       78.8     1.283     1.382        0
  273.9     143.8      227.1     43.6      .268     .119   1.0E 03  7.349      .985     1.11       79.7     1.285     1.399        0
  278.9     147.4      230.5     43.3      .266     .117   1.1E 03  7.393      .985     1.11       80.6     1.288     1.415        0
  283.9     151.0      233.9     43.0      .265     .116   1.1E 03  7.438      .984     1.11       81.5     1.290     1.432        0
  288.9     154.7      237.3     42.7      .263     .115   1.1E 03  7.481      .984     1.10       82.4     1.293     1.449        0
  293.9     158.4      240.7     42.4      .261     .113   1.2E 03  7.525      .984     1.10       83.3     1.295     1.465        0
  298.9     162.1      244.1     42.1      .260     .112   1.2E 03  7.568      .983     1.10       84.1     1.298     1.482        0
  303.9     165.8      247.4     41.8      .258     .111   1.2E 03  7.611      .983     1.10       85.0     1.300     1.498        0
  308.9     169.6      250.7     41.5      .257     .110   1.2E 03  7.653      .982     1.09       85.8     1.302     1.515        0
  313.9     173.3      254.1     41.2      .255     .108   1.3E 03  7.695      .982     1.09       86.7     1.305     1.532        0
  318.9     177.1      257.3     41.0      .254     .107   1.3E 03  7.736      .982     1.09       87.5     1.307     1.548        0
  323.9     180.9      260.6     40.7      .252     .106   1.3E 03  7.778      .981     1.09       88.4     1.310     1.565        0
  328.9     184.7      263.9     40.4      .251     .105   1.3E 03  7.818      .981     1.09       89.2     1.312     1.581        0
  333.9     188.5      267.1     40.2      .250     .104   1.4E 03  7.859      .981     1.08       90.0     1.314     1.598        0
  338.9     192.3      270.3     39.9      .248     .103   1.4E 03  7.899      .980     1.08       90.8     1.317     1.615        0
  343.9     196.1      273.5     39.7      .247     .102   1.4E 03  7.939      .980     1.08       91.6     1.319     1.631        0
  348.9     200.0      276.7     39.4      .245     .101   1.5E 03  7.979      .979     1.08       92.4     1.322     1.648        0
  353.9     203.9      279.9     39.2      .244     .100   1.5E 03  8.019      .979     1.07       93.2     1.324     1.665        0
  358.9     207.7      283.0     39.0      .243     .099   1.5E 03  8.058      .979     1.07       94.0     1.326     1.681        0
  363.9     211.6      286.2     38.7      .242     .098   1.5E 03  8.097      .978     1.07       94.8     1.328     1.698        0
  368.9     215.5      289.3     38.5      .240     .097   1.6E 03  8.135      .978     1.07       95.6     1.331     1.715        0
  373.9     219.5      292.4     38.3      .239     .096   1.6E 03  8.174      .977     1.07       96.4     1.333     1.732        0
  378.9     223.4      295.5     38.0      .238     .095   1.6E 03  8.212      .977     1.07       97.1     1.335     1.748        0
```

```
FLOATING WARM WATER JETS --  SAMPLE RUN OF PDS PROGRAM

FRO =   4.0     290/HO =  5.0     V/UO =   .100     ANGLE = 90.0     SURFACE H = 1.000E-05

E =  .0500   CD = 1.0000   CF =       0   WE =      0E 00   EV = 2.000E-01   EH = 2.000E-02

    S        X         Y        TH       T       U     TIME     Q          HT       H        B        F        RI      IHLF

  383.9    227.3    298.5    37.8     .237    .094  1.7E 03  8.250     .976    1.06     97.9   1.337    1.765     0
  388.9    231.3    301.6    37.6     .236    .093  1.7E 03  8.288     .976    1.06     98.6   1.340    1.782     0
  393.9    235.3    304.6    37.4     .234    .092  1.7E 03  8.325     .976    1.06     99.4   1.342    1.799     0
  398.9    239.2    307.7    37.2     .233    .092  1.7E 03  8.363     .975    1.06    100.1   1.344    1.816     0
  403.9    243.2    310.7    36.9     .232    .091  1.8E 03  8.400     .975    1.06    100.9   1.346    1.833     0
  408.9    247.2    313.7    36.7     .231    .090  1.8E 03  8.437     .974    1.06    101.6   1.348    1.850     0
  413.9    251.2    316.7    36.5     .230    .089  1.8E 03  8.473     .974    1.05    102.3   1.351    1.867     0
  418.9    255.3    319.6    36.3     .229    .088  1.9E 03  8.510     .974    1.05    103.1   1.353    1.884     0
  423.9    259.3    322.6    36.1     .228    .088  1.9E 03  8.546     .973    1.05    103.8   1.355    1.901     0
  428.9    263.3    325.5    35.9     .227    .087  1.9E 03  8.583     .973    1.05    104.5   1.357    1.919     0
  433.9    267.4    328.5    35.7     .226    .086  2.0E 03  8.619     .972    1.05    105.2   1.359    1.936     0
  438.9    271.5    331.4    35.5     .225    .085  2.0E 03  8.654     .972    1.05    105.9   1.361    1.953     0
  443.9    275.5    334.3    35.3     .224    .085  2.0E 03  8.690     .971    1.05    106.6   1.363    1.970     0
  448.9    279.6    337.2    35.2     .223    .084  2.0E 03  8.726     .971    1.05    107.3   1.365    1.988     0
  453.9    283.7    340.0    35.0     .222    .083  2.1E 03  8.761     .971    1.04    108.0   1.367    2.005     0
  458.9    287.8    342.9    34.8     .221    .082  2.1E 03  8.796     .970    1.04    108.7   1.369    2.023     0
  463.9    291.9    345.7    34.6     .220    .082  2.1E 03  8.832     .970    1.04    109.4   1.371    2.040     0
  468.9    296.0    348.6    34.4     .219    .081  2.2E 03  8.867     .969    1.04    110.1   1.373    2.058     0
  473.9    300.2    351.4    34.2     .218    .080  2.2E 03  8.901     .969    1.04    110.8   1.375    2.076     0
  478.9    304.3    354.2    34.1     .217    .080  2.2E 03  8.936     .968    1.04    111.5   1.377    2.093     0
  483.9    308.5    357.0    33.9     .216    .079  2.3E 03  8.971     .968    1.04    112.1   1.379    2.111     0
  488.9    312.6    359.8    33.7     .215    .079  2.3E 03  9.005     .968    1.04    112.8   1.381    2.129     0
  493.9    316.8    362.5    33.5     .214    .078  2.3E 03  9.040     .967    1.04    113.5   1.383    2.147     0
  498.9    320.9    365.3    33.4     .213    .077  2.3E 03  9.074     .967    1.04    114.1   1.385    2.165     0
  503.9    325.1    368.0    33.2     .212    .077  2.4E 03  9.108     .966    1.03    114.8   1.387    2.183     0
  508.9    329.3    370.8    33.0     .211    .076  2.4E 03  9.142     .966    1.03    115.4   1.389    2.201     0
  513.9    333.5    373.5    32.9     .210    .076  2.4E 03  9.176     .965    1.03    116.1   1.391    2.219     0
  518.9    337.7    376.2    32.7     .210    .075  2.5E 03  9.210     .965    1.03    116.7   1.393    2.237     0
  523.9    341.9    378.9    32.6     .209    .074  2.5E 03  9.244     .965    1.03    117.4   1.394    2.255     0
  528.9    346.1    381.6    32.4     .208    .074  2.5E 03  9.277     .964    1.03    118.0   1.396    2.274     0
  533.9    350.4    384.3    32.2     .207    .073  2.6E 03  9.311     .964    1.03    118.7   1.398    2.292     0
  538.9    354.6    386.9    32.1     .206    .073  2.6E 03  9.344     .963    1.03    119.3   1.400    2.310     0
  543.9    358.8    389.6    31.9     .205    .072  2.6E 03  9.378     .963    1.03    119.9   1.402    2.329     0
  548.9    363.1    392.2    31.8     .205    .072  2.7E 03  9.411     .962    1.03    120.6   1.404    2.347     0
  553.9    367.3    394.8    31.6     .204    .071  2.7E 03  9.444     .962    1.03    121.2   1.405    2.366     0
  558.9    371.6    397.5    31.5     .203    .071  2.7E 03  9.477     .962    1.03    121.8   1.407    2.385     0
  563.9    375.9    400.1    31.3     .202    .070  2.8E 03  9.510     .961    1.03    122.4   1.409    2.404     0
  568.9    380.1    402.7    31.2     .201    .070  2.8E 03  9.543     .961    1.03    123.0   1.411    2.422     0
  573.9    384.4    405.2    31.0     .201    .069  2.8E 03  9.576     .960    1.02    123.7   1.412    2.441     0
  578.9    388.7    407.8    30.9     .200    .069  2.9E 03  9.609     .960    1.02    124.3   1.414    2.460     0
  583.9    393.0    410.4    30.8     .199    .068  2.9E 03  9.642     .959    1.02    124.9   1.416    2.479     0
  588.9    397.3    412.9    30.6     .198    .068  2.9E 03  9.674     .959    1.02    125.5   1.418    2.499     0
  593.9    401.6    415.5    30.5     .197    .067  3.0E 03  9.707     .958    1.02    126.1   1.419    2.518     0
  598.9    405.9    418.0    30.3     .197    .067  3.0E 03  9.740     .958    1.02    126.7   1.421    2.537     0
  603.9    410.2    420.5    30.2     .196    .066  3.0E 03  9.772     .958    1.02    127.3   1.423    2.556     0
```

```
A R E A S  O F  E X C E S S  T E M P E R A T U R E  F O R
 SAMPLE RUN OF PDS PROGRAM

REL. TEMP.     AREA

    .05      1.205E 05  PARTIAL AREA - CALCULATION VALID TO T = .196
    .10      9.037E 04  PARTIAL AREA - CALCULATION VALID TO T = .196
    .15      6.637E 04  PARTIAL AREA - CALCULATION VALID TO T = .196
    .20      3.044E 04
    .25      1.449E 04
    .30      5.097E 03
    .35      2.676E 03
    .40      1.336E 03
    .45      7.493E 02
    .50      4.518E 02
    .55      3.049E 02
    .60      2.182E 02
    .65      1.627E 02
    .70      1.236E 02
    .75      9.819E 01
    .80      8.039E 01
    .85      6.470E 01
    .90      5.208E 01
    .95      4.186E 01
   1.00      2.393E 01
```

PROGRAM LISTING

```
      PROGRAM PDS
      COMMON E,CD,CF,EH,EV,GP,DR,AK,V,A,DS,P,SP,S2,HE
      COMMON THO,FRO,FS,INFO(20),NLINE,NPAGE,XK1
      COMMON  Y(7), D(7), PRMT(5), AUX(20,7),AR(20),YY(8),IHLF,S
      COMMON U1,S1,TIME
      COMMON/IDASH/Y2LAST
      EQUIVALENCE (Y(1),Q), (Y(2),T), (Y(3),TH), (Y(4),B), (Y(5),H)
      EQUIVALENCE (Y(6),XP), (Y(7),YP)
      REAL M,LHS
C
      READ(5,1) KK
    1 FORMAT (5I3)
      DO 100 K=1,KK
C
C     READ ALL DATA FOR ONE JET
      READ(5,2) (INFO(I),I=1,20)
          READ(5,3)FRO,A,V,RE,TH,CD,CF
          READ(5,3)E,AK,SLIM,DS,EV,EH,XK1
      WRITE (6,6) (INFO(I),I=1,20)
    2 FORMAT (20A4)
    3 FORMAT (8F10.5)
    6 FORMAT (1H1,////,1X,20A4)
C
C     SET INITIAL CONSTANTS
      Y2LAST=1.
      P = 3.14159
      SP = SQRT(P)
      S2 = SQRT(2.0)
      S1=0.
      U1=1.
      TIME=0.
         Q=A
         FS=FRO*FRO
         U=1.
         T=1.
         B=A/2.
         H=1.
         GP=1./FS
         XP=0.
         YP=0.
      CALL AREA(0)
C
C    CALCULATE CONDITIONS AT END OF DEVELOPMENT ZONE
C
         SI=5.4*FRO**(-.33)*A**(.64)
      B1=((1.5*SI*FS/B+(FS-1.0)**1.5)**.667+1.0)*H/FS
      H1=H*B/B1
      THO = 1.5707963*TH/90.0
      M=A*(1.+.5*GP)
      STH = SIN(THO)
      CTH = COS(THO)
      N=0
      DELH=.2
      BM=1.0
31    CONTINUE
      FD = 0.5*CD*V*ABS(V)*STH*STH*SI*(1.+H1)/2.0
      RV = SQRT(U*U - 2.0*U*V*CTH + V*V)
      IF (RV.EQ.0.0) GO TO 17
      SF = RV*0.5*(1.+H1)
      SF = SQRT(SQRT(1./(RE*SF)))
      SF = 0.0206*SF*RV*RV
      SF = CF*SI*(.5*A+H1)*SF
      SFX = SF*(V-U*CTH)/RV
      SFY = -SF*U*STH/RV
      GO TO 19
   17 SFX = 0.0
      SFY = 0.0
   19 CONTINUE
C
C     CALCULATE INITIAL ANGLE
      TH = M*STH - FD*CTH + SFY
      TH = ATAN(TH/(M*CTH + Q*V*(2./T-1.) + FD*STH + SFX))
      IF (TH.LT.0.0) TH=P+TH
C
C     CALCULATE INITIAL THICKNESS AND WIDTH , H AND B
      LHS = M*COS(TH-THO) + V*Q*(2./T-1.)*COS(TH)
      LHS = LHS + (SFX + FD*SIN(THO))*COS(TH)
      LHS = LHS + (SFY - FD*COS(THO))*SIN(TH)
      RHS=8.0/T**2*A/(P*HM**2)+SP*.5*HM**3*T*GP*A*A*.25/H1
      DIF=RHS-LHS
      IF(N.GT.0)GO TO 32
      N=1
      DIF1=ABS(DIF)
      IF(ABS(DIF1/LHS).LT..001)GO TO 80
      BM=HM+DELH
      GO TO 31
32    DIF2 = ABS(DIF)
      IF(ABS(DIF2/LHS).LT..001)GO TO 80
      IF(DIF2.GT.DIF1) DELH = -.5*DELH
      BM=BM+DELH
      DIF1=DIF2
      N=N+1
      IF(N.LT.500 )GO TO 31
      WRITE(6,5)
5     FORMAT(/" ASSUMING UPSTREAM WEDGE PRESENT - USING F = 1.02")
      BM = 1.
      C=3.+4.*.02
      CC=1.-1./C
      B1=8.*Q**4*GP*C/T**3/(P*SP*LHS**3*CC**2)
      H1=SP*LHS**2*CC/(2.*Q**2*GP*C/T)
C
C     CALCULATE INITIAL VALUES OF Q,X,Y
   80 XP = XP + SI*COS(TH)
      YP = YP + SI*SIN(TH)
      B=B1*HM
      H=H1*HM
      Q = 2.0*Q/T
      THO = 90.0*THO/1.5707963
C
C
C       ASSIGN VALUES TO PARAMETERS IN SUBROUTINES OUTP AND KHPCG
      NLINE = 50
      NPAGE = 0
      PRMT(1)=SI
      PRMT(2) = SLIM
      PRMT(3) = DS
      PRMT(4) = 0.01
      DO 85 I=1,7
   85 D(I) = 0.1
      D(4) = 0.25
      D(5) = 0.25
      IST=0
C
      CALL KMPCG
C
C     WRITE AREAS WITHIN ISOTHERMS
      WRITE (6,200) (INFO(I),I=1,20)
  200 FORMAT (1H1,//////,5X,"A R E A S  OF  E X C E S S   T E M P E R A
     1T U R E   F O R      ",/,6X,20A4)
      WRITE (6,201)
  201 FORMAT (//,5X,"REL. TEMP.",5X,"AREA",/)
      DO 90 I=1,20
      TI = I
      TI = TI/20.0
         IF(T.GT.TI) GO TO 301
         WRITE(6,202) TI,AR(I)
         GO TO 90
301      WRITE(6,302)TI,AR(I),T
302      FORMAT(6X,F5.2,5X,E10.3,2X,"PARTIAL AREA - CALCULATION VALID TO
    1 T ="F5.3)
90       CONTINUE
  202 FORMAT (6X,F5.2,5X,E10.3)
  100 CONTINUE
      STOP
      END
      SUBROUTINE AREA(J)
      COMMON E,CO,CF,EH,EV,GP,DR,AK,V,AM,DSS,P,SP,S2,RE
      COMMON THO,FRO,FS,INFO(20),NLINE,NPAGE,XK1
      COMMON  Y(7), D(7), PRMT(5), AUX(20,7),A(20),YY(8),IHLF,S
      COMMON U1,S1,TIME
      EQUIVALENCE (Y(1),Q), (Y(2),T), (Y(3),TH), (Y(4),B), (Y(5),H)
      EQUIVALENCE (Y(6),XP), (Y(7),YP)
      DIMENSION  W1(20), W2(20)
C
      IF(J)GO TO 20
C
C     INITIALIZE VARIABLES A AND W1
      DO 15 I=1,20
      A(I) = 0.0
   15 W1(I) = B
      SLAST=0.
      GO TO 150
C
C     CALCULATE AREAS
   20 DS=S-SLAST
      DO 100 I=1,20
      TI = I/20.0
      IF(TI.LE.T)GO TO 40
      W2(I) = 0.0
      GO TO 50
   40 W2(I) = B*SQRT(ALOG(T/TI))
   50 A(I) = A(I) + (W2(I) + W1(I))*DS
  100 W1(I) = W2(I)
      SLAST=S
  150 CONTINUE
      RETURN
      END
      SUBROUTINE FCT
      COMMON E,CD,CF,EH,EV,GP,DH,AK,V,A,DS,P,SP,S2,HE
      COMMON THO,FRO,FS,INFO(20),NLINE,NPAGE,XK1
      COMMON  Y(7), D(7), PRMT(5), AUX(20,7),AR(20),YY(8),IHLF,S
      COMMON U1,S1,TIME
      EQUIVALENCE (Y(1),Q), (Y(2),T), (Y(3),TH), (Y(4),B), (Y(5),H)
      EQUIVALENCE (Y(6),XP), (Y(7),YP)
      CTH = COS(TH)
      STH = SIN(TH)
      VCT = V*CTH
      VST = V*STH
      FA = GP*P*SP*0.5*H*H
      DE = GP*T*H*B*P*SP
      HE = Q*Q/(H*H*B)
      FD = CD*H*VST*ABS(V)*STH/S2
      U = 2.0*(Q/(P*B*H) - VCT)
      J=2
      F=Q**2/(P*SP*GP*T*H*(H*B)**2)
C
C     IF  Q,T,TH,B, OR H ARE NEGATIVE, RETURN
      DO 5 I=1,5
      IF (Y(I)) 50,5,5
    5 CONTINUE
C
C
C     CALC HORIZONTAL AMBIENT AND JET ENTRAINMENT
      EA = EH
      QA = 3.5*P*EA*H/B
      RV = U*U + VST*VST
      QJ = SP*E*SQRT(RV)*H
      QH = QA + QJ
C
C     CALC VERTICAL AMBIENT ENTRAINMENT
      RI = GP*S2*T*H/(U+VCT)**2
      CALL RED(RI,RF)
      QA = 3.5*P*B*EV*EA*RF/H
C
C     CALC VERTICAL JET ENTRAINMENT AND INTERFACIAL SHEAR
      QJ = 0.0
      SFX = 0.0
      SFY = 0.0
      DO 25 I=1,10
      YI = I
      YI = 0.1*YI - 0.05
      YI = EXP(-2.0*YI*YI)
      RV = U*U*YI*YI + VST*VST
      RI = GP*S2*T*YI*H/RV
      CALL RED(RI,RF)
      DQ = 2.0*RF*E*SQRT(RV)*S2*H/10.0
      QJ = QJ + DQ
      RV = RV**0.375
      SFX = SFX + RV*(VST*STH - U*YI*CTH)
   25 SFY = SFY + RV*(VCT + U*YI)
      QJ = QJ + 1.77*DQ
      QV = QA + QJ
      GN = SQRT(SQRT(1./(RE*H)))*0.0206*S2*B/10.0
      SFX = SFX*GN*2.0
      SFX = CF*SFX
      SFY = SFY*GN*2.0
      SFY = -SFY*CF*STH
C
C     CALC DERIVATIVES OF Q,T,TH,B,H,X, AND Y
      D(1) = QH + QV
      D(2) = -T*(2.0*SP*AK*B + D(1))/Q
      DTH = -FD + SFY*CTH - SFX*STH
      DTH = DTH - VST*D(1)
      D(3) = DTH/(Q*U/(P*B*H) + GP*T*[illegible]*H*B*SP/2.0)
      IF(F.LT.1.0) F=1.001
      D(4)=XK1/(SQRT(B*F/H-1.0))
      DH = SFY*P*STH + SFX*P*CTH
      DB = DB + (P*VCT-2.0*Q/(B*H))*D(1)
      DH = DB - FA*H*D(2)
      DB = -DB/((QV/QH+1.0)*HE*H/B)
      D(4)=D(4)+DB
      DH=DH+Q*Q*D(4)/(B*B*H)
      DH = DH - FA*T*D(4)
      D(5) = DH/(DE-HE)
      D(6) = CTH
      D(7) = STH
   50 CONTINUE
      RETURN
      END
      SUBROUTINE RED(RI,RF)
      IF (RI.GT.0.8) GO TO 10
      E4 = EXP(-4.0)
      RF = (EXP(-5.0*RI) - E4)/(1.0 - E4)
      GO TO 20
   10 RF = 0.0
   20 CONTINUE
      RETURN
       END
         SUBROUTINE OUTP
      COMMON E,CD,CF,EH,EV,GP,DR,AK,V,A,DS,P,SP,S2,HE
      COMMON THO,FRO,FS,INFO(20),NLINE,NPAGE,XK1
      COMMON  Y(7), D(7), PRMT(5), AUX(20,7),AR(20),YY(8),IHLF,S
      COMMON U1,S1,TIME
      COMMON/IDASH/Y2LAST
      EQUIVALENCE (Y(1),Q), (Y(2),T), (Y(3),TH), (Y(4),B), (Y(5),H)
      EQUIVALENCE (Y(6),XP), (Y(7),YP)
C
C     IS NUMBER OF LINES 50.
      Y2LAST=T
      IF (NLINE-45) 11,10,10
```

```
C
C     NUMBER OF LINES IS 50 OR MORE, SKIP TO NEXT PAGE AND WRITE HEADING
   10 NPAGE = NPAGE +1
      NLINE = 0
      WRITE(6,1) (INFO(I),I=1,20),NPAGE
    1 FORMAT(1H1,///," FLOATING WARM WATER JETS --",2X,20A4,3X,"PAGE",
     1I2,//)
      WRITE(6,2)FRO,A,V,THO,AK
2     FORMAT(1X,"FRO = ",F5.1,5X,"2BO/HO =",F5.1,5X,"V/UO =",F7.3,
     15X,"ANGLE =",F5.1,5X,"SURFACE H =",E10.3/)
      WRITE(6,3)E,CD,CF,RE,EV,EH
3     FORMAT(1X,"E =",F7.4,3X,"CD =",F7.4,3X,"CF =",F7.4,3X,
     1"RE =",E10.3,3X,"EV =",E10.3,3X,"EH =",E10.3//)
      WRITE (6,4)
    4 FORMAT (5X,"S",8X,"X",8X,"Y",6X,"TH",6X,"T",6X,"U",5X,"TIME",4X,
     1"Q",7X,"HT",6X,"H",7X,"B",7X,"F ",6X,"RI",5X,"IHLF",//)
C
C     NUMBER OF LINES LESS THAN 50 , CALCULATE AND WRITE OUTPUT DATA
   11 NLINE = NLINE + 1
      CALL AREA(1)
      U = 2.0*(Q/(P*B*H) - V*COS(TH))
      F = (U*0.5 + V*COS(TH))*SQRT(SP/(GP*T*H))
      RV = U*U + (V*SIN(TH))**2
      RI = GP*T*H*S2/RV
      UVCT = U + V*COS(TH)
      TIME=TIME+2.*(S-S1)/(U1+UVCT)
      VC=TIME
      U1=UVCT
      S1=S
      THOUT= Y(3)*90.0/1.5707963
      QOUT= Q/A
      HT = QOUT*T*0.5
      WRITE (6,5) S,XP,YP,THOUT,T,U,VC,QOUT,HT,H,B,F ,RI,IHLF
    5 FORMAT (3(1X,F7.1,1X),F6.1,2X,2(F6.3,1X),1X,E7.3,1X,2(F6.3,2X)
     1 ,F5.2,1X,F7.1,2(2X,F6.3),3X,I3,3X,I3)
C
C     PUT PRMT(5)= 1.0  IF NUMERICAL INTEGRATION SHALL STOP
      IF (T .LT. 0.01) PRMT(5)=1.0
      IF (NPAGE .GT. 5) PRMT(5)=1.0
      RETURN
      END
      SUBROUTINE KHPCG
      COMMON E,CD,CF,EH,EV,GP,DR,AK,V,VV,AM,DS,P,SP,S2,RE,GPP,TPRIM
      COMMON THO,FRO,C(5,6),FS,INFO(20),NLINE,NPAGE,NOPT,IOR,XK1
      COMMON  Y(7), DERY(7), PRMT(5), AUX(20,7),A(20),YY(8),IHLF,X
         COMMON/DASH/Y2LAST
      N=1
      NDIM=7
      IHLF=0
      X=PRMT(1)
      H=PRMT(3)
      PRMT(5)=0.
      DO 1 I=1,NDIM
      AUX(16,I)=0.
      AUX(15,I)=DERY(I)
    1 AUX(1,I)=Y(I)
```

```
      IF(H*(PRMT(2)-X))3,2,4
C
C  ERROR RETURNS
    2 IHLF=12
      GO TO 4
    3 IHLF=13
C
C  COMPUTATION OF DERY FOR STARTING VALUES
    4 CALL FCT
C
C  RECORDING OF STARTING VALUES
      CALL OUTP
      IF(PRMT(5))6,5,6
    5 IF(IHLF)7,7,6
    6 RETURN
    7 DO 8 I=1,NDIM
    8 AUX(8,I)=DERY(I)
C
C  COMPUTATION OF AUX(2,I)
      ISW=1
      GO TO 100
    9 X=X+H
C
      DO 10 I=1,NDIM
   10 AUX(2,I)=Y(I)
C
C  INCREMENT IS TESTED BY MEANS OF BISECTION
   11 IHLF=IHLF+1
      X=X-H
      DO 12 I=1,NDIM
   12 AUX(4,I)=AUX(2,I)
      H=.5*H
      N=1
      ISW=2
      GO TO 100
C
   13 X=X+H
      CALL FCT
      N=2
      DO 14 I=1,NDIM
      AUX(2,I)=Y(I)
   14 AUX(9,I)=DERY(I)
      ISW=3
      GO TO 100
C
C  COMPUTATION OF TEST VALUE DELT
   15 DELT=0.
      DO 16 I=1,NDIM
      IF(Y(I).LT.0.AND.I.NE.6)GO TO 17
   16 DELT=DELT+AUX(15,I)*ABS(Y(I)-AUX(4,I))
      DELT=.06666666667*DELT
          IF(DELT.LT.PRMT(4).AND.Y2LAST-Y(2).LE..05)GO TO 19
   17 IF(IHLF-10)11,18,18
C
C  NO SATISFACTORY ACCURACY AFTER 10 BISECTIONS.  ERROR MESSAGE
   18 IHLF=11
```

```
      X=X+H
      GO TO 4
C
C  THERE IS SATISFACTORY ACCURACY AFTER LESS THAN 11 BISECTIONS
   19 X=X+H
      CALL FCT
      DO 20 I=1,NDIM
      AUX(3,I)=Y(I)
   20 AUX(10,I)=DERY(I)
      N=3
      ISW=4
      GO TO 100
C
   21 N=1
      X=X+H
      CALL FCT
      X=PRMT(1)
      DO 22 I=1,NDIM
      AUX(11,I)=DERY(I)
   22 Y(I)=AUX(1,I)+H*(.375*AUX(8,I)+.7916666667*AUX(9,I)
     X-.2083333333*AUX(10,I)+.04166666667*DERY(I))
   23 X=X+H
      N=N+1
      CALL FCT
      CALL OUTP
      IF(PRMT(5))6,24,6
   24 IF(N-4)25,200,200
   25 DO 26 I=1,NDIM
      AUX(N,I)=Y(I)
   26 AUX(N+7,I)=DERY(I)
      IF(N-3)27,29,200
C
   27 DO 28 I=1,NDIM
      DELT=AUX(9,I)+AUX(9,I)
      DELT=DELT+DELT
   28 Y(I)=AUX(1,I)+.3333333333*H*(AUX(8,I)+DELT+AUX(10,I))
      GO TO 23
C
   29 DO 30 I=1,NDIM
      DELT=AUX(9,I)+AUX(10,I)
      DELT=DELT+DELT+DELT
   30 Y(I)=AUX(1,I)+.375*H*(AUX(8,I)+DELT+AUX(11,I))
      GO TO 23
C
C  THE FOLLOWING PART OF SUBROUTINE HPCG COMPUTES BY MEANS OF
C  RUNGE-KUTTA METHOD STARTING VALUES FOR THE NOT SELF-STARTING
C  PREDICTOR-CORRECTOR METHOD
  100 DO 101 I=1,NDIM
      Z=H*AUX(N+7,I)
      AUX(5,I)=Z
C  Z IS AN AUXILIARY STORAGE LOCATION
C
  101 Y(I)=AUX(N,I)+.4*Z
      Z=X+.4*H
      CALL FCT
      DO 102 I=1,NDIM
      Z=H*DERY(I)
      AUX(6,I)=Z
  102 Y(I)=AUX(N,I)+.29697760924*AUX(5,I)+.15875964497*Z
CC
      Z=X+.4557372*H
      CALL FCT
      DO 103 I=1,NDIM
      Z=H*DERY(I)
      AUX(7,I)=Z
  103 Y(I)=AUX(N,I)+.21810038822*AUX(5,I)-3.0509651486*AUX(6,I)
     *  +3.8328647604*Z
C
      Z=X+H
      CALL FCT
      DO 104 I=1,NDIM
  104 Y(I)=AUX(N,I)+.17476028226*AUX(5,I)-.55148066287*AUX(6,I)
     X+1.2055355994*AUX(7,I)+.17118478122*H*DERY(I)
      GOTO (9,13,15,21)ISW
C
C  POSSIBLE BREAK-POINT FOR LINKAGE
C
C  STARTING VALUES ARE COMPUTED.
C  NOW START HAMMINGS MODIFIED PREDICTOR-CORRECTOR METHOD
  200 ISTEP=3
  201 IF(N-8)204,202,204
C
C  N=8 CAUSES THE ROWS OF AUX TO CHANGE THEIR STORAGE LOCATIONS
  202 DO 203 N=2,7
      DO 203 I=1,NDIM
      AUX(N-1,I)=AUX(N,I)
  203 AUX(N+6,I)=AUX(N+7,I)
      N=7
C
C  N LESS THAN 8 CAUSES N+1 TO GET N
  204 N=N+1
C
C  COMPUTATION OF NEXT VECTOR Y
      DO 205 I=1,NDIM
      AUX(N-1,I)=Y(I)
  205 AUX(N+6,I)=DERY(I)
      X=X+H
  206 ISTEP=ISTEP+1
      DO 207 I=1,NDIM
      DELT=AUX(N-4,I)+1.333333333*H*(AUX(N+6,I)+AUX(N+6,I)-
     *  AUX(N+5,I)+AUX(N+4,I)+AUX(N+4,I))
      Y(I)=DELT-.9256198*AUX(16,I)
  207 AUX(16,I)=DELT
C  PREDICTOR IS NOW GENERATED IN ROW 16 OF AUX, MODIFIED PREDICTOR
C  IS GENERATED IN Y.  DELT MEANS AN AUXILIARY STORAGE
C
      CALL FCT
C  DERIVATIVE OF MODIFIED PREDICTOR IS GENERATED IN DERY
C
      DO 208 I=1,NDIM
      DELT=.125*(9.*AUX(N-1,I)-AUX(N-3,I)+3.*H*(DERY(I)+AUX(N+6,I)+
     X  AUX(N+6,I)-AUX(N+5,I)))
```

```
      AUX(16,I)=AUX(16,I)-DELT
  208 Y(I)=DELT+.07438017*AUX(16,I)
C
C  TEST WHETHER H MUST BE HALVED OR DOUBLED
      DELT=0.
      DO 209 I=1,NDIM
  209 DELT=DELT+AUX(15,I)*ABS(AUX(16,I))
          IF(DELT.GT.PRMT(4).OR.Y2LAST-Y(2).GT..05)GO TO 222
C
C  H MUST NOT BE HALVED.  THAT MEANS Y(I) ARE GOOD
  210 CALL FCT
      CALL OUTP
      IF(PRMT(5))212,211,212
  211 IF(IHLF-11)213,212,212
  212 RETURN
  213 IF(H*(X-PRMT(2)))214,212,212
  214 IF(ABS(X-PRMT(2))-.1*ABS(H))212,215,215
  215 IF(DELT-.02*PRMT(4))216,216,201
C
C
C  H COULD BE DOUBLED IF ALL NECESSARY PRECEEDING VALUES ARE
C  AVAILABLE
  216 IF(IHLF)201,201,217
  217 IF(N-7)201,218,218
  218 IF(ISTEP-4)201,219,219
  219 IMOD=ISTEP/2
      IF(ISTEP-IMOD-IMOD)201,220,201
  220 H=H+H
      IHLF=IHLF-1
      ISTEP=0
      DO 221 I=1,NDIM
      AUX(N-1,I)=AUX(N-2,I)
      AUX(N-2,I)=AUX(N-4,I)
      AUX(N-3,I)=AUX(N-6,I)
      AUX(N+6,I)=AUX(N+5,I)
      AUX(N+5,I)=AUX(N+3,I)
      AUX(N+4,I)=AUX(N+1,I)
      DELT=AUX(N+6,I)+AUX(N+5,I)
      DELT=DELT+DELT+DELT
  221 AUX(16,I)=8.962963*(Y(I)-AUX(N-3,I))-3.361111*H*(DERY(I)+DELT
     X  +AUX(N+4,I))
      GO TO 201
C
C
C  H MUST BE HALVED
  222 IHLF=IHLF+1
      IF(IHLF-10)223,223,210
  223 H=.5*H
      ISTEP=0
      DO 224 I=1,NDIM
      Y(I)=.00390625*(80.*AUX(N-1,I)+135.*AUX(N-2,I)+40.*AUX(N-3,I)+
     XAUX(N-4,I))-.1171875*(AUX(N+6,I)-6.*AUX(N+5,I)-AUX(N+4,I))*H
      AUX(N-4,I)=.00390625*(12.*AUX(N-1,I)+135.*AUX(N-2,I)+
     X108.*AUX(N-3,I)+AUX(N-4,I))-.0234375*(AUX(N+6,I)+18.*AUX(N+5,I)-
     X9.*AUX(N+4,I))*H
      AUX(N-3,I)=AUX(N-2,I)
```

```
224 AUX(N+4,I)=AUX(N+5,I)
    X=X-H
    DELT=X-(H+H)
    CALL FCT
    DO 225 I=1,NDIM
    AUX(N-2,I)=Y(I)
    AUX(N+5,I)=DERY(I)
225 Y(I)=AUX(N-4,I)
    DELT=DELT-(H+H)
    CALL FCT
    DO 226 I=1,NDIM
    DELT=AUX(N+5,I)+AUX(N+4,I)
    DELT=DELT+DELT+DELT
    AUX(16,I)=8.962963*(AUX(N-1,I)-Y(I))-3.361111*H*(AUX(N+6,I)+DELT
   X   +DERY(I))
226 AUX(N+3,I)=DERY(I)
    GO TO 206
    END
```

REFERENCES

1. Prych, Edmund A. "A Warm Water Effluent Analysis as a Buoyant Surface Jet" Swedish Meteorological and Hydrological Institute, Series Hydroli, Nr 21, 1972.

2. Shirazi, Mostafa A., "Some Results from Experimental Data on Surface Jet Discharge of Heated Water" Proceeding of the International Water Resources Association, Chicago, 1973.

3. Stolzenbach, K. D., Harlemann, D. R. F. "An Analytical and Experimental Investigation of Surface Discharges of Heated Water." Water Pollution Control Series 16130 DJV 02/71, Feb. 1971.

4. Policastro, A. J. and Tokar, J. V. "Heated Effluent Dispension in large Lakes: State-of-the-art of Analytical Modeling Part I, Critique of Model Formulations? Argonne National Laboratory ANL/ES-11 Jan. 1972.

5. Stolzenbach, K. D., Adams, E. E. and Harleman, D. F. "A User's Manual for Three-Dimensional Heated Surface Discharge Computations" Environmental Protection Technology Series EPA-R2-73-133, Jan. 1973.

6. Koh, R. C. Y., Fan, L. N. "Mathematical Models for the prediction of Temperature Distributions Resulting from the Discharge of Heated Water into Large Bodies of Water" Water Pollution Control Series 16130 DWO 10/70, Oct. 1970.

7. Stefan, Heinz. Personal Communication.

8. Weil, J. "Mixing of a Heated Surface Jet in Turbulent Channel Flow" Report No. WHM-1, Department of Civil Engineering, University of California, Berkeley, June 1972.

9. Ellison, T. H., and Turner, J. S., "Turbulent Entrainment in Stratified Flows," Jour. of Fluid Mechanics, Vol 6, Part 3 p. 423-448.

10. Stefan, Heinz, Hayakawa N., and Schiebe, F. R. " Surface Discharge of Heated Water" Water Pollution Control Research Series 16130 FSU 12171, Dec. 1971.

*U.S. GOVERNMENT PRINTING OFFICE: 1974 546-319/442 1-3